SIMAUD 2013

San Diego CA USA

2013 Proceedings of the

Symposium on Simulation for Architecture and Urban Design

Edited by

Liam O'Brien, Burak Gunay, Azam Khan

2013 Proceedings of the

Symposium on Simulation for Architecture and Urban Design

Edited By

Liam O'Brien
Burak Gunay
Azam Khan

Cover by

Justin Matejka

Layout by

Stephen Gaebel
Michael Glueck
John Yee

Contents

Dedication 1

Preface 3

Session I

Simulating Nonlinear Nano-to-Micro Scaled Material Properties and Effects at the Architectural Scale 7
Simin Wang, Andrew Lucia, Jenny E. Sabin
College of Architecture, Art, and Planning Cornell University

The Faraday Pavilion: Activating Bending in the Design and Analysis of an Elastic Gridshell 15
Paul Nicholas, Elisa Lafuente Hernández and Christoph Gengnagel
Centre For IT and Technology, Universität der Künste

Self-Learning Algorithm as a Tool to Perform Adaptive Behaviour in Unpredictable Changing Environments – A Case Study 23
Elite Sher, Angelos Chronis, Ruairi Glynn
University College London

Choreographic Architecture: Inscribing Instructions in an Auxetic Based Material System 31
Themistocleous Theodoros, Chronis Angelos
The Bartlett, UCL

Session II

Façade Apertures Optimization: Integrating Cross-Ventilation Performance Analysis in Fluid Dynamics Simulation 41
Chrysanthi (Sandy) Karagkouni, Ava Fatah gen Schieck, Martha Tsigkari, and Angelos Chronis
UCL, Bartlett School of Graduate Studies

A Review of the Brazilian NBR 15575 Standard: Applying the Simulation and Simplified Methods for Evaluating a Social House 49
Tassia H. T. Marques and Karin M. S. Chvatal
University of Sao Paulo, Architecture and Urban Planning Institute of Sao Carlos

Thermal Reconstruction of a Crime Scene Using Calibrated Simulation 57
Nathan Brown, M. Susan Ubbelohde, George Loisos, Santosh Philip, and Ibone Santiago
Loisos + Ubbelohde, California College of the Arts, University of California, Berkeley

Beginning Session, April 9

Modeling, Analysis and Simulation of a Form-Found Civic Sculpture for Lower Manhattan 67
Zak Kostura, Erin Morrow, Ben Urick
Arup, Texas Advanced Computing Center

Visualization in 3ds Max for Cell-DEVS Models Based on Building Information Modeling 75
Victor Freire, Sixuan Wang, and Gabriel Wainer
Universidade Federal de Campina Grande, Carleton University

Session III

Evaluating the Performance Robustness of Fixed and Movable Shading Devices against Diverse Occupant Behaviors 85
William O'Brien
Carleton University

Simulating the Sensing of Building Occupancy 93
Simon Breslav, Rhys Goldstein, Ben Doherty, Dan Rumery, Azam Khan
Autodesk Research, BVN Architecture

Development of Discrete Event System Specification (DEVS) Building Performance Models for Building Energy Design 101
Huseyin Burak Gunay, Liam O'Brien, Rhys Goldstein, Simon Breslav, Azam Khan
Carleton University, Autodesk Research

Session IV

City Information Modeling (CIM) and Urbanism: Blocks, Connections, Territories, People and Situations 111
Todor Stojanovski
Traffic and logistics, KTH Royal institute of technology

A Study of the Relationship between Urban Form and Environmental Performance for Three Urban Block Typologies in Paris 119
Ji Zhang
Centre for Sustainable Asian Cities, School of Design and Environment, National University of Singapore

End-node Approach for Pedestrian Flow Simulation 129
Hiroshi Ota
Institute of Industrial Science, The University of Tokyo

Session V

Designing-In Performance: Towards Cloud Based Simulation and Multidisciplinary Design Solution Space Search 139
Shih-Hsin (Eve) Lin and David Jason Gerber
University of Southern California

From Statistical to Diagrammatic: Geo-spatial and Time- based Data Visualization through Parametric Modeling 147
Ming Tang, Chris Auffrey, Mingming Lu
University of Cincinnati

Integrated Design in the Simulation Process 153
Martha Tsigkari, Angelos Chronis, Sam Conrad Joyce, Adam Davis, Shuai Feng, Francis Aish
Foster + Partners

Session VI

Building Simulation Weather Forecast Files For Predictive Control Strategies 163
José. A. Candanedo, Éric Paradis, Meli Stylianou
CanmetENERGY, Canada

How Hot Can the University Campus Get in 2050? Environmental Simulation of Climate Change Scenarios at an Urban Neighborhood Scale 169
Chengzhi Peng, Amr F Elwan
University of Sheffield, UK

Session VII

Improving Building Performance at Urban Scale with a Framework for Real-time Data Sharing 179
Xiufeng Pang, Tianzhen Hong, Mary Ann Piette
Lawrence Berkeley National Laboratory, Berkeley, CA

Isomorphic City: A Customizable Future Scenario 183
Susannah Dickinson, David Gonzalez, Kyle Szostek
University of Arizona

A Collaborative Multi-Touch, Multi-Display, Urban Futures Tool 191
Michael van der Laan, Ron Kellet, Cynthia Girling, Maged Senbel, Tao Su
University of British Columbia

Session VIII

Solutions for Scalability in Building Information Modeling and Simulation-Based Design 197
Sixuan Wang, Gabriel Wainer, Rhys Goldstein, Azam Khan
Carleton University, Autodesk Research

Evaluation of Indoor Climate in Low Energy Houses 205
Liesbeth Staepels, Griet Verbeeck, Staf Roels, Liesje Van Gelder, Geert Bauwens
PHL University College / Hasselt University, KU Leuven, Belgium

HubPod: Integrating Acoustic Simulation in Architectural Design Workflows 213
Brady Peters, Jane Burry, Nicholas Williams, and Daniel Davis
Royal Danish Academy of Fine Arts, Royal Melbourne Institute of Technology

Session IX

Data Mining using ANN for Finding the Effects of Building Structure on Thermal Comfort Parameters 223
Lubaid Ahmed, Abdolreza Abhari
Ryerson University

A Generalized Event Driven Framework for Building Occupancy 227
Gandherva Gunathilak, Aiswarya Prasannakumar, Negin Nazarian, Homa Naeimi
Indian Institute of Technology Hyderabad, University of California San Diego

Simulation for Planning Passenger and Freight Transportation System Projects 231
Beth C. Kulick
TranSystems Corporation

Preliminary Results of Model Predictive Control of Shading Systems 235
Brent Huchuk, William O'Brien, Cynthia A. Cruickshank
Carleton University

Presenting Author Biographies **239**

Organizers **245**

Sponsors **247**

Cover Image Credits **249**

Author Index **251**

Dedication

Kevin Pratt, Cornell University

(1970-2013)

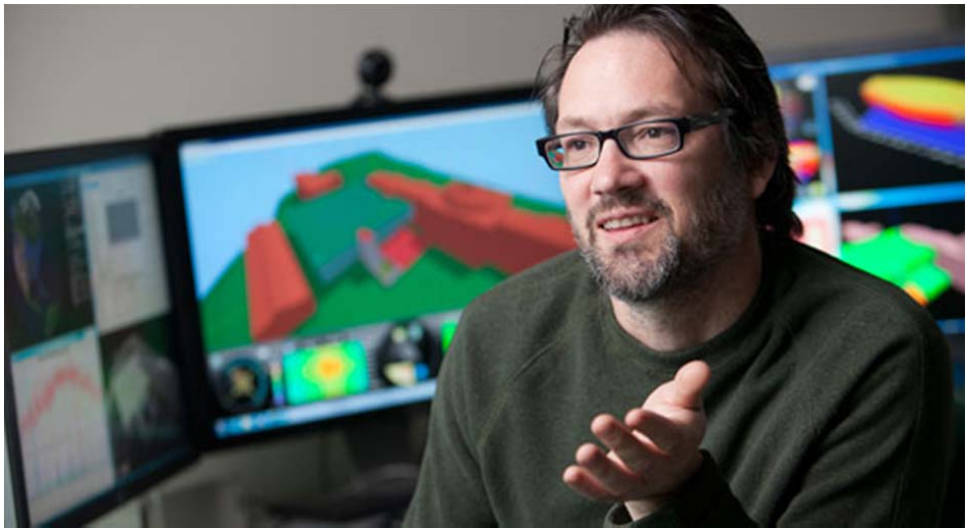

Assistant Professor Kevin Pratt in November 2011 in Rhodes Hall
(Lindsay France / University Photo)

The Symposium on Simulation for Architecture and Urban Design 2013 is dedicated to the memory of our friend Kevin Pratt. He will be dearly missed, as will his dedication and enthusiasm for sustainable design to make this a better world.

Azam Khan
SimAUD General Chair

Preface

This is the fourth Symposium on Simulation for Architecture and Urban Design (SimAUD 2013). Once again, SimAUD presents innovative cutting-edge design and engineering research from around the world from academia, industry, and government. SimAUD brings technical and non-technical researchers, designers, academics, and practitioners together under one roof for in-depth exploration of how simulation can improve our built environment. While we have diverse approaches and applications, we all use simulation to advance how buildings, cities, and landscapes are designed, built and operated throughout their life-cycle.

This year, we received papers of unprecedented quality and diversity. 54 abstracts were submitted and we accepted 30 for paper submission. These papers were carefully reviewed and useful feedback was given to all authors. It is absolutely fascinating to see the new applications of simulation applied to design, architecture, and urban problems. These range from forensic analysis of a crime scene and solar access in urban environments to modelling traffic flows and modelling complex structures and materials. This year, SimAUD saw a record number of submissions about building occupants and understanding their movement within buildings. It was consistently recognized by the authors that this major source of uncertainty provides many challenges and opportunities.

Also, on behalf of all of the past and present SimAUD Chairs and Co-Chairs: Ramtin Attar, Lira Nikolovska, Liam O'Brien and Burak Gunay, Azam Khan was awarded the SpringSim Leadership Award by The Society for Modeling & Simulation International at the opening ceremony of SpringSim 2013 for creating and building a successful domain-specific symposium within the auspices of the annual SpringSim Conference. This external recognition for the success of the SimAUD Community is a valuable asset to our community efforts.

We would like to give thanks to our hard-working committees: the Program Committee and the Technical Committee. Special thanks to Lira Nikolovska and Ramtin Attar, who provided valuable feedback about the third SimAUD. The Symposium would not have been possible without the highly-qualified reviewers. It was inspiring to see their commitment to provide unique perspectives for established researchers while having the patience to nurture up-and-coming researchers. We also thank Glenn Katz from Autodesk Education who generously provided funding for SimAUD's second Student Travel Scholarship. Thanks to John Yee, Michael Glueck, Gord Kurtenbach, and Jeff Kowalski from Autodesk Research for their ongoing hard work and support of SimAUD.

Finally, we would like to thank the authors of the submissions, without whom we would not continue to grow as a community. We look forward to a fantastic conference and to many SimAUDs to come!

Liam O'Brien
Carleton University

Burak Gunay
Carleton University

Azam Khan
Autodesk Research

All accepted papers will be published in the ACM Digital Library at the SpringSim Archive.
Sponsored by The Society for Modeling and Simulation International.

Session I

Simulating Nonlinear Nano-to-Micro Scaled Material Properties and Effects at the Architectural Scale 7
Simin Wang, Andrew Lucia, Jenny E. Sabin
College of Architecture, Art, and Planning Cornell University

The Faraday Pavilion: Activating Bending in the Design and Analysis of an Elastic Gridshell 15
Paul Nicholas, Elisa Lafuente Hernández and Christoph Gengnagel
Centre For IT and Technology, Universität der Künste

Self-Learning Algorithm as a Tool to Perform Adaptive Behaviour in Unpredictable Changing Environments – A Case Study 23
Elite Sher, Angelos Chronis, Ruairi Glynn
University College London

Choreographic Architecture: Inscribing Instructions in an Auxetic Based Material System 31
Themistocleous Theodoros, Chronis Angelos
The Bartlett, UCL

Simulating Nonlinear Nano-to-Micro Scaled Material Properties and Effects at the Architectural Scale

Simin Wang[1], Andrew Lucia[2], Jenny E. Sabin[3]

[1]College of Architecture, Art, and Planning
Cornell University
139 E. Sibley Hall,
Ithaca, NY 14850
sw629@cornell.edu

[2]College of Architecture, Art, and Planning
Cornell University
139 E. Sibley Hall,
Ithaca, NY 14850
apl73@cornell.edu

[3]College of Architecture, Art, and Planning
Cornell University
139 E. Sibley Hall,
Ithaca, NY 14850
jes557@cornell.edu

Keywords: Nano material, Micro material, Material simulation, Architectural simulation, Environmental simulation, Responsive architecture

Abstract

The problem of simulating atypical and nonlinear nano-to-micro scaled material properties at the architectural scale is untenable given the complexity of calculating such data using current rendering and simulation platforms. Though existing rendering engines enable the simulation of material optical properties such as angle dependence, transparency, translucency, and color, the unique behavior and scale of many nonlinear nano materials' angular dependence and wavelength filtering properties requires the development of new tooling methods and workflows.

eSkin—a project to develop passively responsive building façade systems—frames the larger foundation for this paper, which is narrowly focused upon our catalogue of tools where desired optical properties of nano and micro array structures are first simulated in order to extract angle- and wavelength-dependent quantitative optical data. Once calculated, these optical properties are then redeployed at the architectural scale utilizing custom written software platforms and algorithms.

1. INTRODUCTION

1.1. Background on eSkin

As part of the *eSkin* project, the work presented in this paper is one subset of ongoing trans-disciplinary research spanning across the fields of cell biology, material science, electrical and systems engineering, and architecture. *eSkin*, the full title of which is, *Energy Minimization via Multi-Scalar Architectures: From Cell Contractility to Sensing Materials to Adaptive Building Skins,* is jointly housed at the University of Pennsylvania and Cornell University. The PIs on the project are: Shu Yang, Jenny E. Sabin, Nader Engheta, Jan Van der Spiegel and Kaori Ihida-Stansbury. Andrew Lucia is Senior Personnel. This project represents a unique avant-garde model for sustainable and ecological design via the fusion of the architectural design studio with laboratory-based scientific research. In turn, this project benefits a diverse range of science and technologies, including the construction of energy efficient and aesthetic building skins and materials. Given the groundbreaking nature of this work, many of the tools we use to simulate, visualize and model nonlinear nano-to-micro scaled material properties and effects at the architectural scale must be custom written and designed. While there are commercially available software packages for optical engineering and design such as TracePro that can handle some, but not all, of our needs in terms of angular and spectral dependent properties, our interest resides in developing a design process to work with these nano to microscaled material features through the development of custom-written tools. Through the development of our own simulation tools that work directly with these optical data while also understanding the state of the art in optical engineering and design simulation, it is possible to generate a thinking space and design intuition for materiality not yet realized at the architectural scale. To this end, this paper focuses on our latest set of visualization and design tools.

Comprised of a field of low-cost sensors and passively responsive materials, eSkin is conceived to be generic and homogenously structured upon installation (i.e., laden with the full potential) but readily adaptable to local heterogeneous spatiotemporal conditions, thereby reducing the overall functioning demands upon it and ultimately

lowering overall energy consumption. In this regard, a "learning" and adaptive second skin would forgo the need for lengthy, costly, and one-time site analysis relegating ever-changing environmental analysis and response of the local and global spatiotemporal environments to its own internal/local functionality. This manner of operation not only maximizes immediate performative efficiency, but also allows for ongoing contextual adaptation.

Ultimately the goal of the eSkin project is to explore materiality from nano to macroscales based upon understanding of nonlinear, dynamic human cell behaviors on geometrically-defined substrates. Through the eSkin project, insights as to how cells can modify their immediate extracellular matrix (ECM) microenvironment with minimal energy and maximal effect are being investigated and applied to the biomimetic design and engineering of highly aesthetic, passive materials, and sensors and imagers that will be integrated into responsive building skins at the architectural scale.

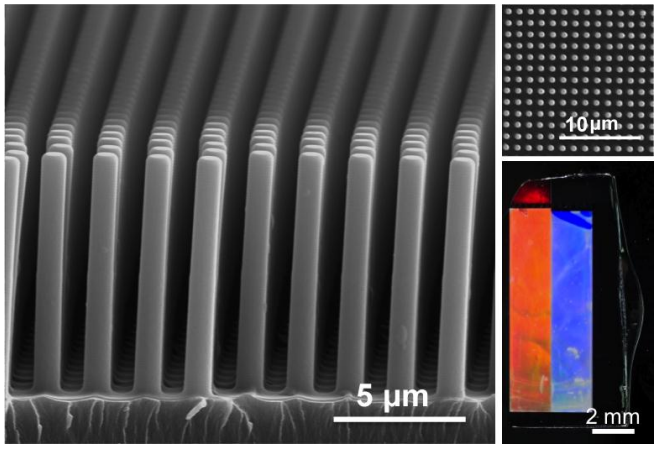

Figure 1. SEM image of square micropillar array (left). Photo Credit: Lo, C.W., Zhang, Y., and Yang, S., Univ. of Pennsylvania. SEM (upper right) and optical (lower right) images of micropillar arrays. Two different colors (lower right) result from Bragg diffraction of micropillar arrays with different periodicities (image adapted with permission from CHANDRA, D., et al. 2009. Biomimetic ultrathin whitening by capillary force induced random clustering of hydrogel micropillar arrays. ACS Appl. Mater. Interfaces. Vol. 1. No 8. 1698–1704. Copyright 2009 American Chemical Society).

1.2. Background on materials research & challenge

The particular research presented in this paper focuses on one subset of study within the eSkin project, the optical simulation and application of nano-to-micro scale PDMS pillar array substrates (Figure 1) deployed at the building scale. Specifically, these nano-to-micro scale pillar substrates, designed in the Yang lab, form the basis of this investigation. These substrates are fabricated via microlithography and softlithogragy, first requiring a negative nano/micro pattern to be etched into a substrate in which PDMS is subsequently cast, cured, and removed, thus producing a positive relief of nano/micro pillars (see for example Thompson et al. 1994, Xia et al 1998, & Zhang et al. 2006). Though these positive substrates may be cast using an array of polymers, compounds and mixtures, for the purpose of this study we are exclusively interrogating the properties of PDMS as a proof of principle.

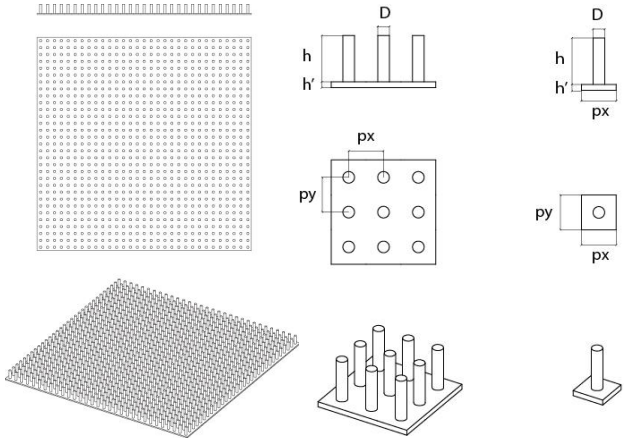

Figure 2. Left, schematic geometry of nano/mictopillar arrays. Right, schematics of nano/micropillar units.

Demonstrating unique angle-dependent and wavelength filtering optical properties of interest, these periodic pillar arrays act as passive filters of light given the specific nano-to-micro scale periodicity of their structures and the angle at which they are viewed. Because of the particular periodic spacing and geometry of these arrays existing at the nano-to-micro scale, light is absorbed via the PDMS material, but also filtered as a property of the particular wavelength of light that is allowed to pass through a particular pillar array. Depending on factors such as the diameter and the periodic distance between each pillar in an array, the visible spectrum of light, which exists between 390nm to 750nm, will be filtered out, absorbed/scattered, or reflected/refracted from the material (Figure 3).

Though these qualities can be seen by the naked eye (Figure 1), extracting their optical performance quantitatively for speculation at larger architectural scale applications is necessary, given: a) the current limitations in which these substrates can be fabricated (currently 4 inches maximum), and b) the necessity to speculate on large-scale deployments of potential materials without the need to actually fabricate. Thus, simulating the effects of larger swathes of these materials has been a goal and focus of this

research; to speculate as to the larger scale application and effect of these substrates in an architectural context.

Aside from the unique angle-dependent and wavelength filtering properties foreign to much existing architectural simulation and rendering software (exceptions discussed below), there exist more fundamental modeling and memory issues that do not allow for the explicit modeling and simulation of nano-to-micro scale materials at the architectural scale. Though it would be conceivable to geometrically model large swathes of these structures using existing software, overcoming limitations of computational memory is a major obstacle. The amount of memory necessary to deploy vast arrays of nanoscaled features in an architectural context is inconceivable and several orders of magnitude beyond current standard capabilities. For example, the memory requirement to model and distribute a cylindrical nanopillar (D = 200nm & h = 800nm) with 400nm periodic spacing of 100 x 100 units (40um x 40um total sample size) approaches 290mb in NURBS, 750mb in refined mesh, and 96mb in low-quality mesh. Extrapolating further, a 10m x 3m swath of this same modeled material would be 1.76*10^9 gigabites in even low-quality mesh. Thus, modeling large swathes of these nano materials at an architectural scale is highly impractical.

Even if this first limitation were overcome, a second limitation exists given the current state of simulation and rendering software, namely that most platforms do not take into consideration the filtering of angle-dependent wavelength data through material at the nano-to-micro scales. A few exceptions do exist, but are limited for our purposes. One robust exception to this limitation is the software TracePro by Lambda Research, which uses geometric optics as the basis for its simulations. While TracePro does take into consideration angle-dependent geometric optics for specular material, BSDF (bidirectional scattering distribution function), or a combination of both, its current capabilities do not account for sub-10 micron feature sizes or wavelength filtering at this scale, which are specific material properties of interest to our research. Maxwell, another popular and highly accurate software for design rendering, is limited for our purposes in that only colors with incident angles of 0 degrees and 90 degrees are taken into consideration. Here again, our research demands the full range of angle-dependent behavior between these poles. Another option, Radiance, can simulate angle dependent properties but is not specialized or suited for rendering complicated geometric surfaces, and only capable of rendering pure BSDF or specular material.

The unique properties generated by certain nanoscale materials, such as those we are probing, require new approaches to workflow in our tooling environments as we venture into a new era in which we are capable of actively influencing material properties at the nanoscale. Architects have always engaged materiality in the design process. Our challenge is to develop a design process and material inuition through the crafting of digital tools that simulate material properties that cannot be engaged directly with the hand or in some cases, the naked eye. In order to overcome this design and visualization challenge, we have developed a methodology and workflow by which the nonlinear optical properties of these nano materials are simulated for a small portion of an actual sample, and then distributed across vast macro areas through the use of custom written algorithms in conjunction with robust rendering engines.

2. METHODS

First, the unique physical and angle dependent optical properties of a small portion of these periodic geometric substrates are simulated in the labs of Van der Spiegel and Engheta through the use of Lumerical FDTD Solution, a material simulation software. Due to the periodic nature of the substrates in question, only a portion of these substrates need be simulated, after which the characteristics of the material would “repeat” itself. These simulations, which derive the angle dependent optical properties of the material substrates, ultimately form the basis for larger scale simulations of potential material applications within the eSkin system. At the architectural scale, speculations as to the extracted performative and aesthetic qualities of these nano/micro materials are then deployed using custom written algorithms in conjunction with the Rhinocerous (NURBS modeling) software environment.

2.1. Simulating Optical properties at the Nano-to--Micro Scale

As stated prior, the nano-to-micro scale structure tested in simulation is a periodic high-aspect-ratio (HAR) pillar array. To simulate these pillar arrays with high efficiency, a simplified geometry is necessary to begin with. First, a matrix of pillars and a continuous sheet of substrate are modeled as a NURBS surface and mesh.

As illustrated in Figures 1 and 2, the structure of the untreated pillar substrate is 2D periodic. Therefore, the

optical properties of the pillar array may be obtained by simulation of a single unit in a matrix. While neighboring units must be considered, immediate neighbors in the simulation are taken to be the same geometry in order to increase efficiency. The parameters that describe the geometry of such units are shown in Figure 2, where the aspect ratio of the micropillar is AR: AR = h/d. This periodic structure is the simplest condition of the substrate, excluding any variation or gradient across the field of pillars. Any reshaping or treatment method that destroys the periodic property of the epoxy micropillar arrays cannot be analyzed by this method, but is being considered for future investigations.

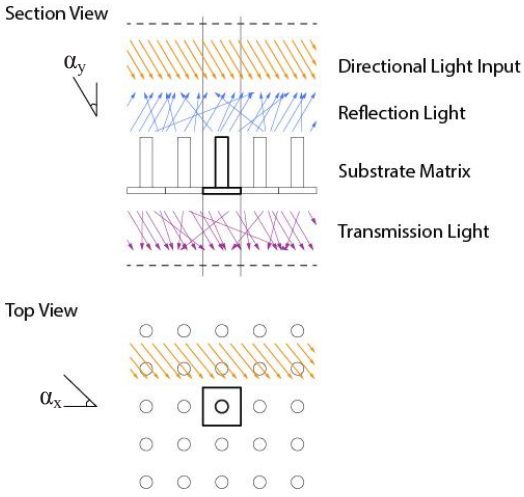

Figure 3. Two sub directions of incident light and reflection and transmission light.

To develop a digital material that reproduces the optical properties of the selected sample faithfully, its bidirectional light distribution function must first be determined in transmission (BTDF) and reflection (BRDF), so that the spatial distribution of emerging light can be identified for varying incident directions. For this simulation we use Lumerical FDTD Solution, specifically designed for determining nano-scale optical effects. The process of simulation can be described as follows: a light source with intensity, I, at given incident angle, α, is evenly distributed. Total light intensity coming from reflection by the substrate will be recorded as I_r, that from transmission is I_t. The reflection coefficient, C_r, and transmission coefficient, C_t, are:

$$c_r = I_r/I$$

$$c_t = I_t/I$$

Since the only power source is the incident light, the summation of C_r and C_t should be equal to or less than 1.

Because the scale of the pillar array nanostructure is very close to visible light wavelength, the material is highly sensitive to different light wavelengths, λ, at different incident angles, α. The variable α in this case can be interpreted as the angle between the light direction and substrate surface normal, α_y, and the angle between the light direction in the substrate surface and matrices direction, α_x. To fully understand the optical properties of the material, the incident light must be considered from different directions with different α_y, and α_x. Given the symmetrical and periodic property of the matrices, only ½ α_y and 1/8 α_x are necessary for simulation (Figure 5, a & b). Taking into consideration these varied directions with respect to a sphere, it is only necessary to calculate 1/16 of the sphere as shown in Figure 5c. Simplifying the simulation process, α_y' can be defined as the angle between the surface normal facing the light source. α_x' is the smallest angle between 2 major matrix direction lines as illustrated in the following diagram (Figure 4). The domain of α_y' is [-90°, 90°]. That of α_x' is [0°, 45°].

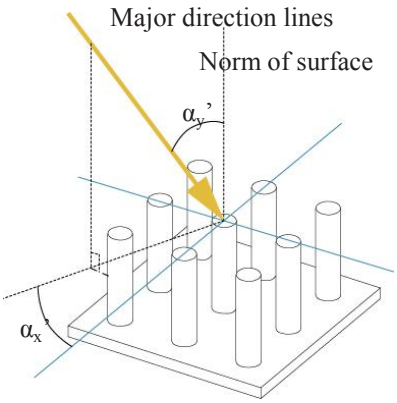

Figure 4. α_x' and α_y' incidental angles

Since the material is wavelength sensitive, it is necessary to obtain a spectral power distribution for both reflection, $I_r(\lambda)$, and transmission light, $I_t(\lambda)$, at each light angle. Given the spectral power distribution of input light, $I_i(\lambda)$ where $C_r(\lambda)$ and $C_t(\lambda)$ are reflection and transmission coefficients at a specific wavelength λ (Fairchild, 2005):

$$I_r(\lambda) = c_r(\lambda)\, I_i(\lambda)$$

$$I_t(\lambda) = c_t(\lambda)\, I_i(\lambda)$$

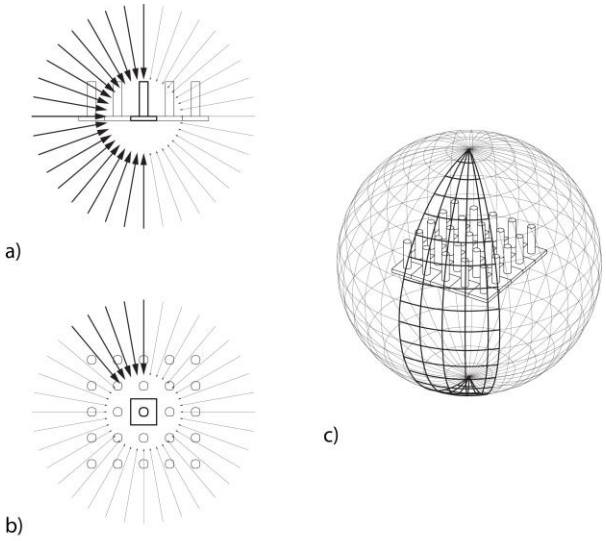

Figure 5. Simulation of the incident angle about a sphere

As opposed to conventional architectural material simulation and rendering software, the direction of reflected and transmitted light of these unique nonlinear nano/micro pillar surfaces and substrates perform neither like a conventional specular surface, nor a diffuse material. To this end, our method requires integrated spherical measurements rather than a total summation of reflection light and transmission light intensity in all directions.

From this nano/micro material simulation, we are able to obtain the reflection and transmission coefficient of the material under specific light incident angles (including α_x and α_y) given unique light wavelengths.

2.2. Interpreting the Simulation Data

Methods for interpreting large amounts of simulation data are key for simulations operating at the building scale and in understanding the optical properties of the nano/micro material in architectural contexts. Light in the natural world is almost never purely monochromatic. To analyze or simulate our virtual material substrates under polychromatic light mixtures, the following process has been developed.

2.2.1. Obtain XYZ value via color matching function

(λ) is the reflected spectral power distribution. For a single light source:

Similarly,

For multiple light sources (n), at a certain wavelength (λ), the overall reflected/transmitted spectral power distributions are:

$$\sum C$$

$$\sum C$$

Thus, through the color matching function, the reflection color, and transmission color of the substrate can be calculated (Vos, 1978 & Wyszecki, 1982). An example of the unit simulation was conducted to show the method. The unit for this test has the following parameters: D = 200nm, AR = 4, h = 800nm, Px = 400nm, & Py = 400nm. Given this, the simulation was processed from 0 to 90 degrees by 5 degree increments with a "middle resolution" mesh generated from a NURBS surface and implemented using a custom written algorithm written in Grasshopper. Figure 6 shows the reflection color and transmission color calculated by the algorithm based on the method described in 2.1 versus incident light angle.

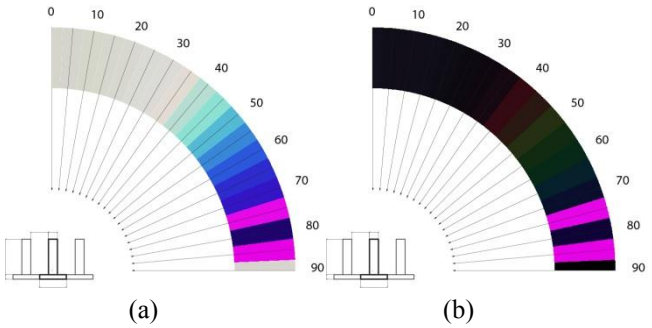

Figure 6. Reflection (a) and transmission (b) color versus incident angle (α_x) of the sample test.

As illustrated in Figure 8, visible color change for this sample happened after the 35 degree incident angle. After 75 degrees, the color of both reflection and transmission become very unstable. This issue will be addressed in future iterations. Ideally, data shown in Figure 6 should be tested for each α_y. For this paper, the discussion was limited to α_x from 0^o to 90^o. For the particular material tested in this proof of principle, given an increasing incident angle, the material tends to be more transparent /translucent.

Having interpreted the nano-to-micro scale simulation data, we may now deploy these optical and material properties at the architectural scale.

2.3. Simulation and Rendering at the Architectural Scale

Given that there is no software available to render faithfully the types of materials under consideration in this study, the large-scale deployment and simulation of these

material effects must also be a part of our custom digital tool kit. In order to overcome this, the quantitative values of simulated material properties from the above method are considered across large-scale surfaces via custom written digital tooling methods and algorithms. For the purposes of this study, these tooling methods have been carried out in Rhinocerous, utilizing the Grasshopper Plug-in. Due to shortcomings of these architectural rendering and modeling environments, however, Rhino/Grasshopper combination will not directly render the material. The level of scripting freedom embedded within tooling components in these software, however, does enable one to write custom algorithms that are close and efficient approximations of the nonlinear material properties inherent to the tested nano/micro substrates. This allows a seamless connection with modeling software, making it possible to produce real-time visualizations and ultimately prepare material for robust rendering using software such as Maxwell.

3. RESULTS

As mentioned before, a vast amount of data is obtained by simulation. Measured data is organized in the following format to be analyzed:

Λ	$C_r(\lambda)$	$C_t(\lambda)$
780	0.882837	0.11386
767.005	0.880057	0.116441
764.0299	0.87806	0.118748
761.0744	0.876797	0.120779
758.1384	0.876158	0.122527
…	…	…
380	0.712232	0.282342

Table 1: Reflection/transmission coefficient at different wavelength, C(λ), and spectral power distribution function of input color, I(λ).

For a single surface with a single light source of uniform distribution, each point on the surface has the same optical properties. Therefore, evaluation of the center point represents properties of the whole surface. With one single light, the two sides of the surface can be named as the reflection side and transmission side. After calculating the redefined incident angle (α_x'), and angle between the light source and pillar matrix direction (α_y'), a matrix of C_r and C_t at different wavelength (λ) can be obtained by interpreting the measured data. For a given light source with a specific spectral power distribution (I(λ)), reflected/transmitted spectral power distribution can be obtained by $C_r(\lambda)$ I(λ), and $C_t(\lambda)$ I(λ), so that the previously discussed method can be used to generate a XYZ color for the surface. With multiple light sources, a total reflection/transmission spectrum has to be calculated by the previous equation. Finally a color in XYZ space can be generated based on the color matching function. To represent the different behavior of both sides of surfaces, the surface was offset minimally in both directions with a small distance (Figure 7).

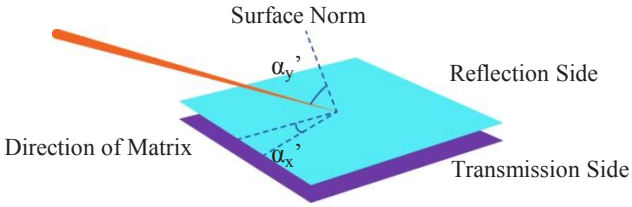

Figure 7. Incident light angle on two sides of a surface

For a curved surface and/or uneven distribution of light, the analysis of a sub-divisional surface is necessary. Having sub-divided the larger surface into a number of small discrete flat mesh sub-surfaces, we are then able to run the simulation for the vertex of each sub-divided face, and linear interpolation colors are assigned by mesh color properties to approach the overall property of the surface. As before, with the use of a flat surface, the basic logic is to turn a NURBS surface into two meshes with a small distance between each. This replicates a double-side property of the material, one for reflection and one for transmission. Furthermore, since the mesh is uniquely colored at each vertex, the process of simulation for single curved surface with uniform light has to be conducted for each sub-divided vertex comprising the whole. The following drawings show the process under a uniform directional lighting condition (Figure 8).

Having assigned a unique material property to each mesh face across the surface, the final output of this method enables a colored mesh that can be directly rendered by standard architectural/computer graphics rendering software.

For software, such as Maxwell, that does not support colored meshes; a script generates a bitmap, demonstrated in Figure 9, for rendering a diffuse map of a material and a mesh with modified texture mapping coordinates that match the bitmap (How to Render Mesh colors?, 2012).

The following example (Figure 10) shows a rendered image of a test façade, whereby the color of each panel varies passively, according to the methods described in this paper.

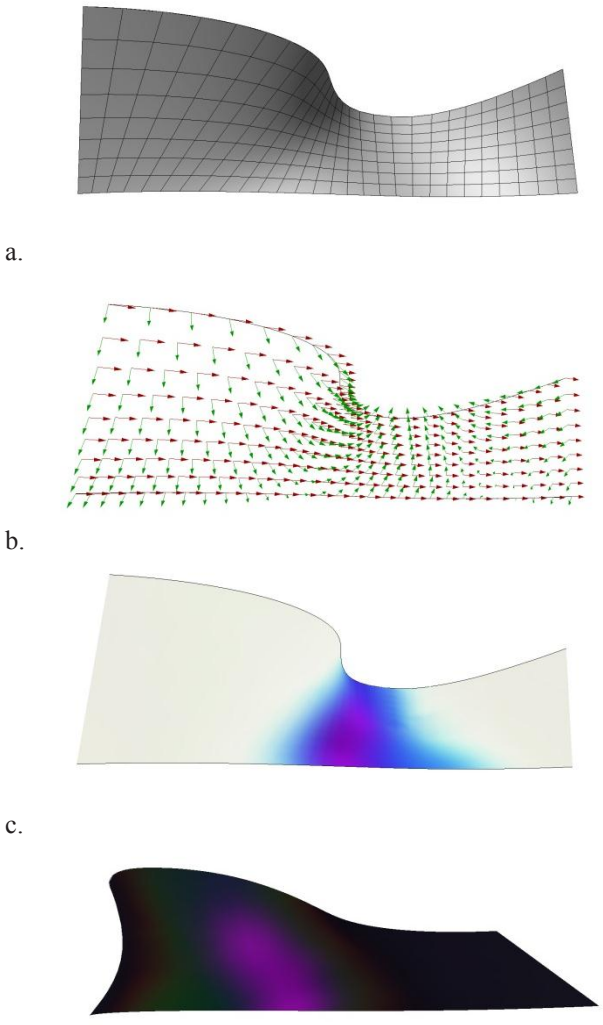

Figure 8. a) Mesh from NURBS surface; b) Direction of matrix and surface normal of each vertex; c) Colored mesh (reflection side) based on described method; d) Colored mesh (transmission side) based on described method.

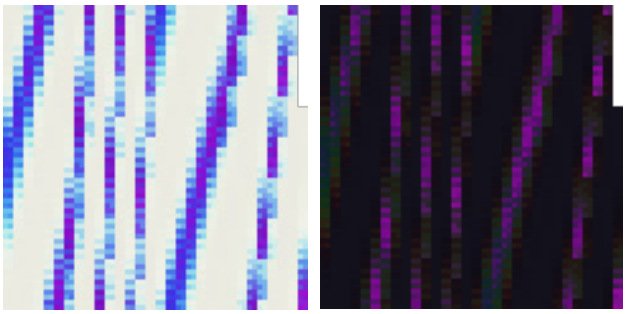

Figure 9. Bitmap for rendering material mapping to both sides of a surface, reflection side (left) & transmission side (right).

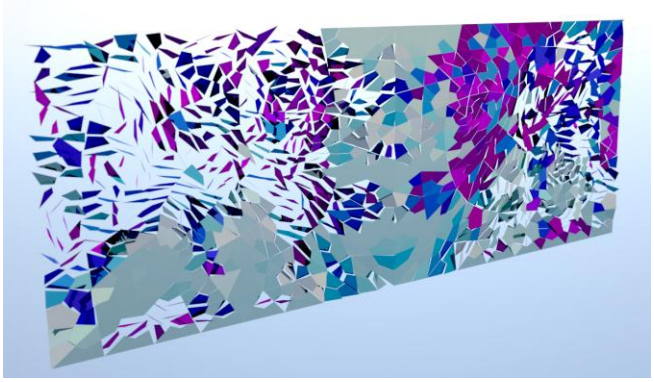

Figure 10. ColorMapping of the test facade by using the method described, and rendered in Maxwell.

4. DISCUSSION

The representation of material and material properties has long been a critical portion of the architectural design process. To illustrate or render is to convey intention behind a particular set of spatio-material ideas. From the pen to the computer, architects and designers have sought and implemented tools to aid in this visually communicative endeavor. Though advances in computer graphics have afforded the ability to speculate and render complex material environments with extremely accurate and realistic models of light based on reflection, refraction, scattering, and diffusion, these environments are, by and large, comprised of stable "architectural materials," which have until now comprised a pallet of materials whose properties one might consider consistently deployable over large swathes of surface without a deviation in their phenomenal behavior.

Through the collaborative efforts embarked on within the *eSkin* project, an identified point of impasse arose when the issue of propagating/rendering a simulation of unique observational and wavelength-dependent nano-to-micro scaled material was to be emulated and speculated upon at the architectural scale. More specifically, the materials of interest exhibit nuanced nonlinear behavior as a product of their nano and micro scale geometric structures, such as angle and wavelength dependent properties. This, in turn, led to an investigation that extracted the quality of these properties, while at the same time eliminating the need to geometrically model *ad infinitum* these nano/micro materials across an architecturally scaled application. Even if the latter were computationally possible, the current state of rendering technologies is not sufficient for simulating optical and light based properties at the fine-grained scale required of the materials in question. Save uniform material

attributes of refraction, reflection and transmission, current rendering technologies do not take into consideration many of the combined unique nanoscaled material properties queried in this paper, including surface curvature, points of observation, discrete wavelength filtering, and the effect of multiple points of incident light.

Though several issues persist as unresolved future areas of exploration within this study, the methods presented here demonstrate a working methodology for dealing with the effects of nonlinear nano/micro differentiated materials; materials whose properties are dependent on several parameters not typically associated with common macro materials. Whereas common linear materials that are mapped or "applied to surfaces" in a rendering environment devoid of a particular scale (i.e. the object is red, has x refraction, and x transmission), these nonlinear nano-to-micro scaled materials explored in this study must not only be attributed in a scale specific manner, but also with a sensitivity to the direction in which an observer may "see" the material. This also implies a unique qualitative signature that is intrinsically aligned with the morphology of a surface.

5. CONCLUSION

Advances in materials science are rapidly advancing the ways in which architects may "see" and design their material environments. Once limited to a material pallet comprised of matter that was largely conceived of and affected by consistent notions of light intensity, direction, shadow, macro-applied color, and the like, we are now forced to deal with an artificial world that no longer behaves according to well-established norms of "common" material phenomenal properties. While the interplay of light on a steadfast architectural material such as steel, brick, wood, stone, and glass, has produced incredible phenomenal results throughout history, we are now forced to deal with a new reality of a customizable and tunable material world, one in which we are capable of actively defining as architects.

The implications of current material technology advances and the speculative approach outlined in this paper not only implies, but deploys a notion that affect is generated through the articulation of form, rather than merely being applied to a shape or morphology after a "design" has been executed. The latter is the common practice of workflow given current rendering technologies and modes of design thinking. In our case, geometry, matter, and associated optical effects are embedded and contribute to the design and simulation process across multiple length scales. This is not just about overcoming technical gaps that exist in robust commercially available optical engineering and design softwares, but most importantly is about contributing to and fostering a design space saturated in materiality. By designing custom-written tools to simulate nano-to-micro scaled material properties and interfacing this related data directly, it is possible to develop design intuition for materiality not yet realized at the architectural scale. The approach outlined in this paper underscores the importance underlying the generation of affect being intrinsically linked to observation and material organization, rather than through the *ex-post facto* application of materiality and effect to predefined shapes.

Bibliography

CHANDRA, D., YANG, S., SOSHINSKY, A. A., GAMBOGI, R. J. 2009. Biomimetic ultrathin whitening by capillary force induced random clustering of hydrogel micropillar arrays. ACS Appl. Mater. Interfaces. Vol. 1. No 8. 1698–1704.

FAIRCHILD, M. D. 2005. *Color Appearance Models.* John Wiley and Sons.

FAIRMAN H.S., B. M. 1997. How the CIE 1931 Color-Matching Functions Were Derived from the Wright–Guild Data. *Color Research and Application* , 22 (1): 11–23.

How to Render Mesh colors? (2012, 08 19). RETRIEVED FROM GRASSHOPPER, GENERATIVE MODELING TOOL FOR RHINO: http://www.grasshopper3d.com/forum/topics/how-to-render-mesh-colors

MARDALJEVIC, J. 1995. Validation of a lighting simulation program under real sky. *Lighting Research & Technology* , 181–188.

THOMPSON, L. F., GRANT WILLSON, C., BOWDEN, M. J. 1994. Introduction to microlithography, 2nd Ed. Publisher: American Chemical Society.

VOS, J. J. 1978. Colorimetric and photometric properties of a 2-deg fundamental observer. *Color Research and Application* , 125-128.

WYSZECKI, G. &. 1982. Color Science: concepts and methods, quantitative data and formulae. (2nd ed.). New York: Wiley.

XIA, Y. N., WHITESIDES, G. M. 1998. Ann. Rev. Mater. Sci. 28, 153.

ZHANG, Y., LO, C., TAYLOR, A., YANG, S. 2006. Replica Molding of High-Aspect-Ratio Polymeric Nanopillar Arrays with High Fidelity. Langmuir. Vol. 22. No. 20. 8595-8601.

The Faraday Pavilion: Activating Bending in the Design and Analysis of an Elastic Gridshell

Paul Nicholas[1], Elisa Lafuente Hernández[2] and Christoph Gengnagel[2]

[1]Centre For IT and Technology
Philip de Langes Alle 10,
Copenhagen, Denmark, 1435
paul.nicholas@kadk.dk

[2] Universität der Künste
Hardenbergstraße 33,
Berlin, Germany, 10623
lafuente@udk-berlin.de

Keywords: Material activation, Computational Design, Gridshell, Bending, GFRP.

Abstract

This paper reports the architectural and engineering design, and construction, of The Faraday Pavilion, a GFRP elastic gridshell with an irregular grid topology. Gridshell structures are self-formed through an erection process in which they are elastically deformed, and the prediction and steering of this aspect becomes a central part of both architectural and engineering design processes. While there are existing architectural approaches to determining the geometry of other kinds of form-active structure, as well as new engineering approaches to the simulation of bending active structures, a fast and light-weight design approach to bending active structures is not currently developed.

In this paper, we introduce an approach to the architectural design of a bending active structure whereby the shell form and grid topology are determined by simulation. Particular features are that the grid topology is not pre-described, but rather emerges as part of the simulation, and that different calculative models relating to the material, element and structural scales are solved and synthesized by extending the technique of dynamic relaxation. Secondly, the results of this design modelling are provided as the input for a quantitative engineering simulation, where the equilibrium shape and load-bearing capacity of the elastically-bent structure is calculated with a non-linear, three-dimensional finite element model within the FEM-package Sofistik. We compare the advantages and disadvantages of both methods, which while complementary have important differences relating to the interaction with the design of the structure, differences in the definition of supports, connections and elements, the speed of calculation and the magnitude and precision of the results.

1. INTRODUCTION

The Faraday Pavilion design explores the activation of glass fibre reinforced polymer's (GFRP) high capacity for bending and strength within a connected series bending-active gridshells. It investigates the capacity of a force-based modeling approach to incorporate and nest descriptions of bending behaviour at multiple scales, to simulate the bending of a network structure within a generative design process, and to closely match bending as it occurs in the analysis and onsite assembly process. In looking to force-based models, specifically dynamic relaxation, the project investigates how the simulation of bending in structures with network topologies might be achieved using architecturally oriented design tools, as part of a more integrated design process. The larger aim was to develop an approach to design and specification that exploited the ability for digital modeling and simulation to synthesise different physical material properties at multiple scales, to achieve a more materially responsive architecture.

Taking point of departure in a brief to provide a seating and relaxation space for the 2012 Roskilde Festival, the design comprises three seating 'poles' and a series of elastic FRP gridshells with irregular mesh size. This grid is composed of two layers of pultruded 40mm diameter GRP-tubes, principally arranged in radial and transversal directions. The correlation of design and behavioural simulation developed during the project connects a top-down design intent with a bottom-up understanding of material behaviour. As a result, there is a shift in the understanding of material performance away from the absolutes of strength and lightness, with which composites have traditionally been associated, and towards the ability to negotiate a range of conditions.

2. BENDING ACTIVE GRIDSHELL STRUCTURES

Traditional building structures facilitate load bearing through a correlation of compressive and tensile forces passing loads linearly through a building envelope that is considered to have failed if it bends. In contrast, bending active structures utilize a material's capacity to bend elastically to generate 3D curved geometries from initially straight or planar 2D building elements. Bending active gridshells, in which continuous members span from support

to support and are connected at their intersections, allow large spans with very little material

Materially, bending active gridshells must be flexible enough to deform and bend easily, with the capacity to remain elastic. They also need to possess high strength, which makes their high curvature possible. Traditionally, timber has been the most commonly used material however FRP, which has a lower relation of stiffness to strength, and thus the ability to achieve higher curvatures, is now of great interest (Paoli 2007).

The geometry of a gridshell emerges from a process of transformation, where force is exerted on the flat elements to deform them into a doubly curved surface that is the equilibrium of applied shaping forces, internal bending moments and the forces transferred from one element to another (Lienhard et al 2012). This sequence begins with the definition of an initial flat grid topology that is then deformed into a smooth surface, either as a mat or incrementally, and finally locked into position through bracing and restraint at footing points. In the case of Mannheim Multihalle (Figure 1) the gridshell was built flat on the ground and then raised into position (Happold 1975), while the Downland Gridshell was built on a raised platform and bending induced via gravity and the structure's own self-weight (Dickson and Harris 2004).

Figure 1. Mannheim Multihalle (Burkhardt et al 1978)

3. MODELING BENDING ACTIVE STRUCTURES

Because gridshell structures are self-formed through an erection process in which they are elastically deformed, the prediction and steering of this aspect is a central part of both architectural and engineering design processes. Yet while architecture possesses approaches for designing forms that are driven by material characteristics, the fact that bending is absent from most building structures has meant that its description is likewise absent from architectural representation and simulation tools for form generation. In the architectural design of gridshells, the approaches that have been used include include the generation of a geometric grid, or geodesic lines, on a doubly curved 3D surface (Cabrinha 2008) and computational form-finding using physics-based modelling (Kilian and Ochsendorf 2005). This behaviour-based approach utilises dynamic relaxation in the form of mass-spring models to find funicular forms, but does not include bending, only axial forces.

In engineering, dynamic relaxation methods do include bending (Douthe et al 2006), but do not include the generation of the underlying form. Instead, a grid of fixed topology is distributed on a predefined surface, typically by equalising member lengths and angles, however alternative approaches that do not use dynamic relaxation include a geodesic approach (Pirazzi and Weinand 2006) and the optimisation of angles and member direction to achieve emergent grid geometries (Winslow et al 2008).

The approach taken for the modelling of the Faraday Pavilion sought to address the limits of architectural modelling, in seeking to develop a lightweight design oriented simulation tool that incorporated bending, as well as the limits of both architectural and engineering approaches in the prescription, prior to simulation, of a grid topology and mesh size. In this approach, which links material behavior, 3D form and the tectonics of assembly, the topology of the gridshell is not predefined but emerges from a consideration of bending behaviour. This is achieved by extending the dynamic relaxation method to incorporate material parameters at different scales, and by simulating elements in incremental stages – firstly individually and then as a structure. In this way, the placement, path and intersection of elements is determined as a negotiation between a desired target geometry and a form-finding process that incorporates the bending capacities and behavioural tendencies of GFRP tubes into a digital design model. One advantage of incorporating bending in this way is that the grid geometry that results approaches the equilibrium shape without needing to be fixed using bracing.

4. CASE STUDY: THE FARADAY PAVILION

The Faraday Pavilion provides a place for people to rest, to meet, to eat and to socialize between concerts. Three circular areas provide bench seating, and located activities such as DJs within them. From these seating elements emerge a series of gridshells, with a span of about 10m, a maximum height of 4m and a total extents of approximately 30x40m, under which people can sit, lie and picnic. While there are distinct entrances, the porosity of the gridshell allows people to enter and exit the structure where they wish. In this way the structure secures a large area,

protected from the passing festival crowds, with minimum material means.

Figure 2. The Faraday Pavilion at Roskilde Festival 2012

4.1. Design Concept

The design draws conceptually on the investigations and theories of Michael Faraday, who pioneered the empirical study of electricity and magnetism (Faraday 1852). His work introduced for the first time the notion of the field: that a space seemingly empty physically could in actual fact contain energy and momentum. To represent the field, Faraday introduced the notion of lines of force, which he believed had a real, physical manifestation. We now know that lines of force do not have a presence beyond that of representational device, but the conceit that they might have drives the design and geometric definition of the pavilion. During the design process, a computational model that calculates lines of force given a set of input points was used to develop and explore different plan configurations generated by 3 positively charged poles, the seating areas. The resultant geometry becomes the target geometry for a subsequent 3D, materially informed simulation process.

4.2. Design Modeling Sequence

The design modeling process is developed so that design, analysis and assembly all reflect an incremental approach to construction. It sequentially determines radial and then transverse GFRP elements, and then simulates the combined interaction of radial and transverse elements. Force-based modeling via a node-spring system, whereby nodal properties (position/displacement, velocity, acceleration) are altered in order to obtain an equilibrium, is used as the method of simulation. Each GFRP element is defined within the simulation by multiple nodes connected by springs and bending constraints. The springs, whose stiffness is defined as cross section (mm)*e-modulus(gpa)/total length (m) -830 for a 12m long element-act to control the length of the element, while the bending constraints impose resistance against bending in an angle defined by three nodes (Figure 3).

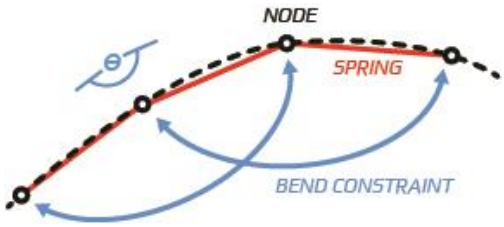

Figure 3. Definition of each element via spring and bend constraints

The bending constraints are set to a strength of 750, however this figure is not externally validated and was instead judged to be appropriate through testing. Together these constraints impart a good approximation of real-world bending behaviour (Figure 4).

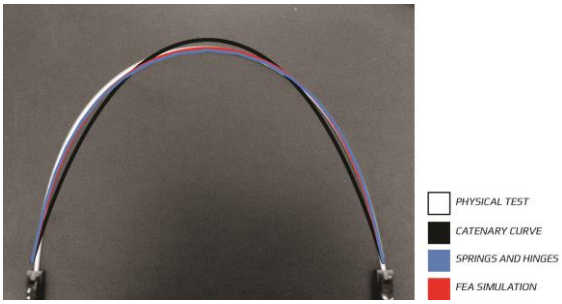

Figure 4. Comparison of physical and simulated bending: real, dynamic relaxation, finite element analysis

To match the desired target geometry, one end of each element is moved inwards, inducing bending, while the elements are locally constrained to constraint surfaces that are extruded from the 2D target plan (Figure 5). The strength of the surface constraint is dependent on the local measured bending radius, and is reduced as the bending radius approaches a minimum. Within the simulation, the geometric definition of each radial element therefore emerges from the negotiation of the element's local utilisation, its natural minimum energy bending behaviour, and the plan definition that acts as target geometry.

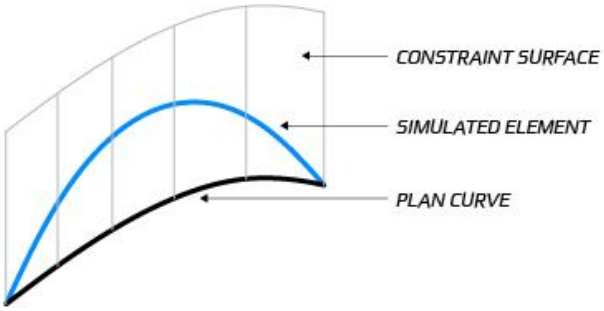

Figure 5. Radials are attracted to the target geometry via a pull to surface constraint

Once the radial elements are generated, the transverse elements are constrained to a surface defined by a loft through the radial elements, but are free to change their start and end points as well as their path across the structure, which is influenced by material bending and length parameters. In this way, the topology of the elements is not predescribed, as the intersection points vary over the course of the simulation as the structure finds an equilibrium, but instead is determined by a form-finding process that incorporates the bending capacities and behavioural tendencies of the material into a digital design model. When both the radial and transverse elements are defined, springs are introduced at each intersection point to enforce a geometric separation and connectivity that matches scaffolding joints, and the entire structure is simulated as a self-supporting network free from any artificial constraints.

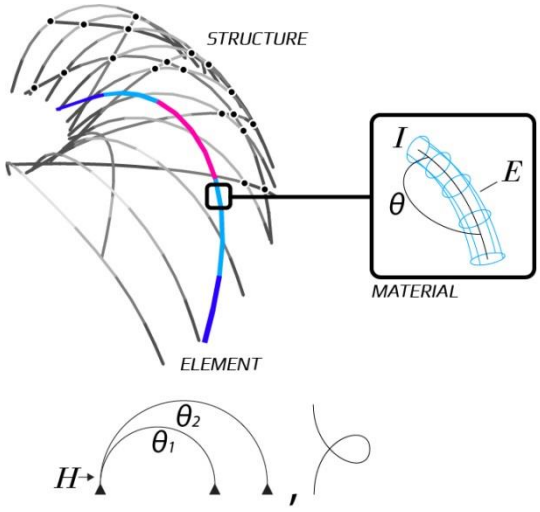

Figure 6. Material parameters inform the simulation at multiple scales

4.3. A Model for the Element Level

The behaviour of each radial and transverse element is determined by the negotiation between two bottom-up materially-oriented processes and the top-down definition of a target geometry, to which the GFRP elements are attracted. The two material considerations operating at the element level relate to the type of bending, and the amount of force required to bend and restrain each element.

Thin tubes, like the GFRP elements used in this project, bend to form what is known as an elastica, and this behaviour can be simulated using a combination of springs and bending constraints (which resist bending acting on an angle defined by 3 points) within a force-based model. The elastica, Latin for a thin strip, is the curve that most accurately describes the bending of a long thin piece of material as it tries to minimise its bending energy over its length, given specified endpoint conditions.

The bending of each FRP element requires a force that is applied and then held. On site, this occurs when members of the construction team take each end of the element and bend it by moving one endpoint towards the other, and connect that endpoint to a footing. There is a limit to the amount of force that the team of people can safely apply, and here the relationship between the length of each pole and its capacity for deflection becomes important. The longer the pole, the easier it is to deflect. The shorter it is, the more difficult is becomes for the construction team to physically push it into place.

The reaction force is calculated in a simplified manner, using the equation H = (E*I/p)/f, where f = distance apex to ground, p = radius of curvature, E = E modulus and I = second moment of area. For example, a 12m long GFRP element bent to span 6m generates a reaction force of 0.139kN, and needs to be restrained by a load that is the equivalent of carrying 14kg. A 6m long pole bent to span 3m generates a reaction force of 0.553kN, and needs to be restrained by a load that is the equivalent of carrying 55kg. One person can safely carry approximately 25 kilograms. To ensure that the relationships between length and bending within the structure allow it to be constructed without machinery, the definition of the elastica behaviour within the force based model, as described above, is extended so that the length of each element is partly determined by a non linear relationship between restraint force and element length, that acts to increase the length of the element during the simulation to keep the restraint force within a permissible range.

4.4. A Model for the Material Level

The elastic potential energy stored within a bent FRP tube is not distributed equally, but increases towards the middle as it reaches the tube's minimum bending radius. Figure 7 shows this range of bending for the shortest and longest tubes used in the project.

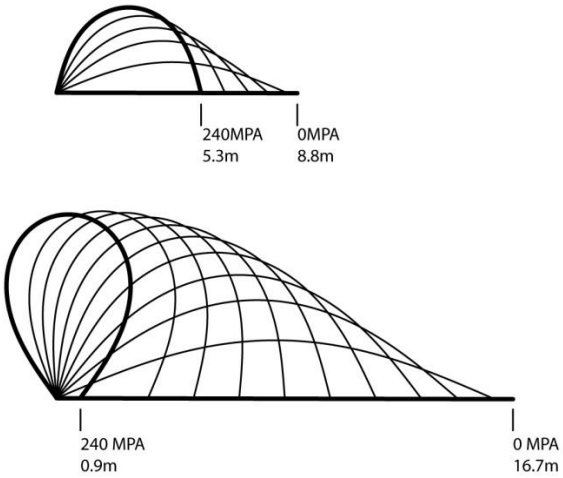

Figure 7. The shortest(8.8m) and longest(16.7m) tubes bent until reaching a bending strength of 240 MPa, considering a modulus of elasticity of 25 GPa

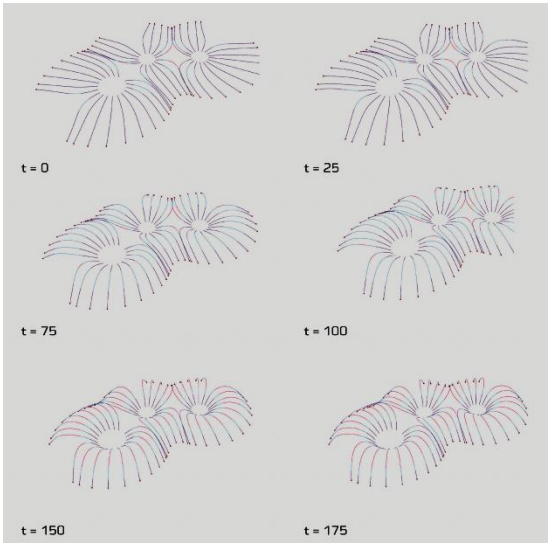

Figure 8. Sequence from simulation of radial elements

Equally, when one element is connected to other elements, the material can be locally stressed at those points in a way that exceeds the strength of the material, leading the material to break. This local material capacity can be calculated knowing the type and volume ratios of its two component materials, the glass fibre and the polymer matrix, and the tube's section and wall thickness. At each iteration within the simulation, the bending that is being generated by the springs and bending constraints underlying the elastic behaviour, the attraction of each tube towards the target geometry, and the bending that is caused by connecting the beams together, are calculated and only applied if larger than the minimum bending radius.

4.5. A Model for the Structure Level

Much like a pole vault, each of the tube elements want to return the bending energy stored within it, and when connected together as a structure also needs to deal with new bending forces induced because of the behaviour of other elements. As a result, each element stores a significant amount of energy that will potentially deform the structure, making it unstable or moving it away from the desired shape. To understand this compound behaviour qualitatively, the final phase of the force-based simulation removes all the target geometry and its associated attracting forces and simulates the behaviour of the whole structure based on the connections between elements and the forces that govern their material behaviour. To then gain a quantitative understanding of this behaviour, a three-dimensional, geometric non-linear finite element model defined with the FE-analysis software Sofistik AG was used to analyse the resulting geometry and equivalent stresses after the shaping of the gridshell. With the FE-modelling, a more accurate calculation is possible, since the real material and section properties of the tubes, modelled as beam elements, are considered and the connection and support conditions can be defined more precisely.

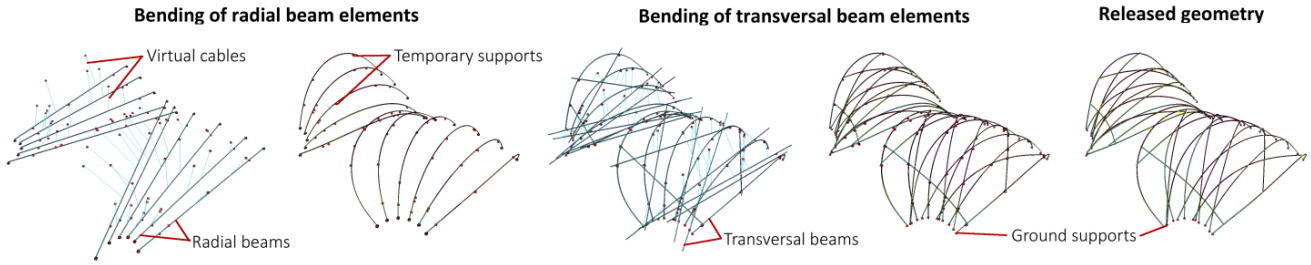

Figure 9: Finite-element-modelling of the erection process of the Faraday Pavilion gridshell

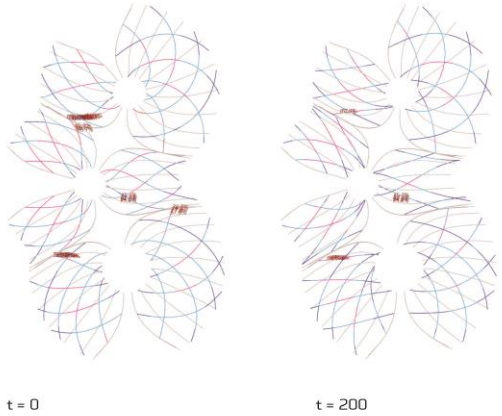

Figure 10. Sequence from simulation of transversal elements

5. METHODS FOR CALCULATING THE GEOMETRY OF BENDING ACTIVE STRUCTURES IN ENGINEERING

During the shaping of the profiles, internal forces - axial forces, bending and torsional moments - are induced on the structure so that the final equilibrium shape of the gridshell, and with it its resultant structural properties, will be attained not before fixing the edge nodes, connecting all the structural members (crossing grid profiles, stiffening elements) and removing the external shaping forces. The goal of the finite element approach is to analyse quantitatively the geometry and material stresses after the process of bending, taking into account the actual properties of the structural elements, connections and supports, all of them affecting the resulting internal, shaping and reaction forces.

The equilibrium shape and load-bearing capacity of elastically-bent structures can be calculated with non-linear three-dimensional finite elements models. The FEM-package of Sofistik was used for the modelling of the Faraday Pavilion gridshell. The structure was analysed according to the third-order theory (material and geometrical non-linearities are considered) using a modified Newton method with constant stiffness matrix. The iterative equation solver Conjugate Gradients provided good convergence. Besides, the high deformations and rotations, to which the beam elements are subjected during their shaping process, are the origin of convergence problems.

In order to avoid them, the bending of the profiles was modelled incrementally. The bending of the beam elements can be generated applying nodal displacement or using temporary virtual elements, inducing the deformation of the profiles. For the simulation of the Faraday Pavilion, the form-finding methodology for coupled active-bending structures suggested by J. Lienhard et al 2011 has been used. This methodology consists on defining virtual cable elements with reduced elastic stiffness between the start and target positions of the profiles and pre-stressing them to generate the bending of the beam elements.

The simulation of elastic gridshells starts with their deployed geometry. Their subsequent erection process depends on their grid topology. Gridshells with constant mesh size - regular gridshells - are usually shaped as an entire grid. Firstly, the straight profiles are placed on the ground and arranged in two crossing superimposed layers forming a grid. Afterwards, the profiles of the different layers are connected on the intersection points and the grid can be deformed as a whole. In the case of gridshells with variable mesh size – irregular gridshells – the grid profiles are usually bent independently from each other in a incrementally way. The profiles of the first direction are initially bent into the target geometry and independently fixed. Then, the profiles of the second direction are bent and afterwards connected to the first profiles. Figure 10 shows the simulation of the bending process of the irregular Faraday Pavilion gridshell.

5.1. Engineering Simulation Process: Case Study of the Faraday Pavilion

The structure of the Faraday Pavilion consists in three adjacent irregular gridshells, with a shape similar to a half torus and composed of elastically-bent GFRP tubes of 40mm diameter and 3mm thickness. The span length and height of the shells are about 10 and 4m, respectively. The GFRP profiles are arranged in two crossing – radial and transversal - superimposed layers. The radial elements run parallel to each other from the centre to the outside of the structures, while the transversal elements cross the radial ones in different directions and at different space intervals, forming a partially triangulated irregular mesh. Radial and transversal elements are connected through rotating scaffolding swivel joints. As the geometry of the grids is pretty homogenous, in order to simplify the FE-simulation, only a part of the structure – two adjacent modules not attached to the rest ones - has been modelled. The GFRP profiles have been defined as beam elements with tubular section and a modulus of elasticity of 25 GPa. The interlayer connections have been modelled as coupling elements. The structure has been calculated applying different support conditions and kinematic constraints to the connections to analyse their structural influences. The weight of the scaffolding joints, 1.5 kg per connection, has been considered and applied as point loads.

The simulation of the erection process of the Faraday gridshell begins with the bending of the radial elements pre-stressing virtual shaping cables. Once the radial elements have been deformed into their target shape, their extremities

are fixed and temporary supports along the profiles length are modelled in order to maintain their geometry. Then, the transversal elements are shaped, also by pre-stressing shaping virtual cables, fixed at their ends and finally connected to the radial elements. Both layers being bent in their target form and connected to each other, all temporary supports and virtual cables are removed and the released equilibrium state of the gridshells is calculated.

The following table (Table 1) presents the maximum equivalent stresses resulting after the process of bending and maximum nodal displacements after releasing the temporary bearings and shaping forces on the profiles. The profiles ends have been defined as restrained (Model 1) and hinged (Model 2) supports. In the real structure, the steel poles and swivel joints used as anchorages correspond to partially hinged bearings. The connections between radial and transversal elements have been defined as restrained in Model A, hinged in Model B and partially hinged, allowing only rotation about the x-axis of the connection as by the swivel couplers, in Model C.

Concerning the equivalent stresses resulting from the shaping process, the maximum values (138 – 143 MPa) are located in all the models at the top of the profiles. Indeed, in the geometry calculated by the force-based simulation and used for the finite-element-modelling, the shapes of the radial elements resemble the form of elastica curves, having their minimum radius of curvature in their middle. The support or connection properties do not have any relevant influence.

Concerning the deformations after releasing the structure, corresponding also to the difference with the geometry given by the force-based simulation, an increment of 56 – 68 % of the maximum nodal displacements can be noticed when using hinged instead of restrained supports. Due to the lack of reinforcement at the gridshells edges, the maximum deformations are to be found at the border profiles: by restrained connections on the adjacent tubes between the two modelled modules and by hinged connections on the outer border tubes. When partially hinged connections are used, the position of the maximum nodal displacements changes depending on the support conditions: on the outer profiles with restrained bearings and in the adjacent profiles with hinged bearings. This last model (Model 2.C) presented the maximum deformations, which constitute 388mm. In the following figure (Figure 11) its resulting equivalent stresses and nodal displacements are illustrated.

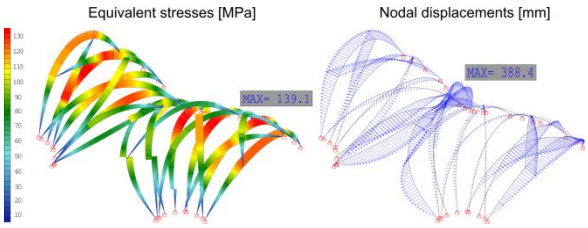

Figure 11: Equivalent stresses and nodal displacements of Model 2.C

An optimisation of the stiffness and bearing capacity of the gridshells could be achieved by connecting the transversal elements to each other – obtaining thereby a higher triangulation of the structure - or reinforcing the border beams.

6. DESIGN DOCUMENTATION AND CONSTRUCTION

All design documentation was derived from the 3D model once the geometry of the gridshell was determined by the simulation process. An underlying circular geometry embedded into the form-finding process provided the logic by which the site was surveyed and set-out points for the footings identified. Spreadsheets were used to set the correct overall length of each FRP element and to position the scaffolding joints along them, and footings and FRP elements were tagged with laser-cut identification tags to aid the location of elements. The seating elements were pre-milled and assembled on site. During the erection process, the radial elements were bent first and diagonal struts were used as lateral bracing. Afterwards the transverse elements were progressively bent and connected to the radial ones through rotating scaffolding joints. This incremental process of erection matched that of the forced-based and engineering simulations, and was completed in 3 days.

	Restrained supports		Hinged supports			
	Model 1.A	Model 1.B	Model 1.C	Model 2.A	Model 2.B	Model 2.C
Interlayer connection	Restrained	Hinged	Partially hinged	Restrained	Hinged	Restrained
max.σv (MPa)	140	143	141	138	141	139
max. v (mm)	203	236	233	340	368	388

Table 1: Maximum stresses resulting after the process of bending and maximum nodal displacement after releasing the temporary bearings and shaping forces on the profiles

7. DISCUSSION AND CONCLUSION

This paper has introduced an approach to the architectural simulation of bending active structures. This approach is based on the iterative sequence of the gridshell's physical construction, and its aim is to incorporate physical behaviour and material properties within the process of form generation, so that the found form is partially driven by material behaviour and partly by architectural intent. The simulation process constructs a feedback loop between these two aspects, drawing the geometry towards a pre-defined target but only so far as the material allows. Such an approach is possible because of the ability to inform the simulation about behaviour at multiple scales - the material, element and structure - by simultaneously solving the grid shape and topology in an integrated manner, and by the ability to change the length of elements and update the equilibrium during the simulation. As material properties are increasingly foregrounded and activated within architectural design, it is hoped that here, this paper contributes a recognition that the simulation of structures that activate these properties may require their description to be incorporated at more than a single scale, or via a single number.

While allowing for high speed simulation and therefore an iterative, exploratory design process, a possible limitation of the approach described is that only near equilibrium shapes are possible. In comparison to the FEA simulation, the simplifications used in the architectural simulation limit the definition possibilities of the sectional and structural properties of the elements, e.g. by asymmetric cross-sections or particular support and connection conditions, which have a important influence on the resulting shape, stresses and load-bearing capacity of the structure. Therefore, a complementary more accurate FEA simulation, providing more precise and relevant information for the dimensioning not only of the structural but also of the cladding elements, is essential to complete the overall design procedure of the structure. In the case study, the combination of these methods was used successfully.

In order to establish the level of correspondence between the geometric results of architectural and engineering simulations, the authors are currently working towards a direct numeric comparison.

References

BURKHARDT, B. ET AL. (EDS). 1978. IL13: Multihalle Mannheim, Institut für leichte Flächentragwerke, Stuttgart.

CABRINHA, M. 2008,Gridshell Tectonics: Digital Values Material Parameters, in Proceedings of Acadia 2008, pp.118-125

DICKSON, M & HARRIS, R. 2004. The Downland Gridshell: Innovative Design in Timber, in Ingenia, Issue 18, Feb

DOUTHE, C., BAVEREL, O. AND CARON, J.F. 2006. Form-finding of a grid shell in composite materials, in Proceedings of the International IASS Symposium

FARADAY, M. 1852. On the physical character of lines of force

FLEISCHMANN, M., MENGES, A. 2012. Physics-Based Modeling as an alternative approach to geometrical constrain-modeling for the design of elastically-deformable material systems, in Achten, H., Pavlicek, J., Hulin, J., and Matejdan, D., (eds), Digital Physicality - Proceedings of the 30th eCAADe Conference - Volume 1, Czech Technical University in Prague, September 2012, pp. 565-575

HAPPOLD, E. 1975. Timber Lattice Roof for the Mannheim Bundesgartenschau, in The Structural Engineer Vol. 53, No.3½

KILIAN, A AND OCHSENDORF, J. 2005. Particle-Spring Systems For Structural Form Finding, in Journal Of The International Association For Shell And Spatial Structures: IASS, VOL. 46 (2005) n. 147

PAOLI, C. 2007. Past and Future of Grid Shell Structures, PhD thesis, Massachusetts Institute of Technology

LIENHARD, J., ALPERMANN, H., GENGNAGEL, C. AND KNIPPERS, J. 2012. Active Bending, a Review on structures where bending is used as a self formation process, in Proceedings of the International IASS Symposium, Seoul, Korea

LIENHARD, J., SCHLEICHER, S., AND KNIPPERS, J. 2011. Bending-active Structures – Research Pavilion ICD/ITKE, in Nethercot, D.; Pellegrino, S. et al. (eds) Proceedings of the International Symposium of the IABSE-IASS Symposium 2011, Taller Longer Lighter, London, UK

PIRAZZI, C. AND WEINAND, Y. 2006. Geodesic Lines on Free-Form Surfaces - Optimized Grids for Timber Rib Shells, in Proceedings of the World Conference in Timber Engineering WCTE, Portland, USA

WINSLOW, P., PELLEGRINO, S., SHARMA, S.B. 2008. Mapping two-way grids onto free-form surfaces, in Journal of the International Association for Shell and Spatial Structures, Vol. 49, No. 2 August n. 158

Self-Learning Algorithm as a Tool to Perform Adaptive Behaviour in Unpredictable Changing Environments – A Case Study

Elite Sher, Angelos Chronis, Ruairi Glynn

University College London, Gower Street,
London, UK, WC1E 6BT
elite.sher.11@ucl.ac.uk, achronis@fosterandpartners.com, r@ruairiglynn.co.uk

Keywords: Adaptive architecture, self-learning, Genetic Algorithms, Artificial Neural Network, Structural Optimisation

Abstract

Adaptive architecture is expected to improve buildings' performance and create more efficient building systems. One of the major research areas under this scope is the adaptive behaviour of structural elements according to load distribution. In order to achieve this, current studies develop structures that adapt either by following a database of pre-calculated solutions, or by using massive computation resources for real-time calculations.

This study aims to achieve an adaptive behaviour in real time, affected by load distribution, by implementing learning abilities on a case study. This is done by applying a learning algorithm—Artificial Neural Network (ANN)—on a physical prototype. The ANN was trained by an optimised database of finite solutions, which was created by a Genetic Algorithm (GA). Through this method, complex calculations are conducted 'off-line' and the component operates in a 'decision-making' mode in real-time, adapting to a versatile environment while using minimal computational resources.

Results show that the case study successfully exhibited self-learning, and acquired the ability to adapt to unpredictable changing forces. This method can be applied over different structural elements (façade elements, canopies, structural components, etc.) to achieve adaptation to other parameters with an unpredictable pattern such as human behaviour or weather conditions.

1. INTRODUCTION

Adaptive Architecture is an expanding, multi-disciplinary research field, exploring the possibilities of buildings to change and respond with relation to various parameters (Teuffel, 2010). The need of adaptive architecture arose once the advantages of it were recognised–buildings can fit a wider range of uses, improve their performance and extend their life time (Sobek & Teuffel, 2001).

Kinetic structures–building or building elements that can change their location, move or change their shape (Fox & Yeh, 2004)–are a key aspect in adaptive architecture.

Various researchers have examined adaptive kinetic structures in an attempt to improve buildings` performance (Sterk, 2006, Senatore et. al. 2011). Currently, research relies on massive complex calculations in real-time or on a vast database of pre-calculated solutions. In order to overcome these issues, this paper offers an approach for structural adaptation by developing self-learning abilities in order to acquire adaptive behavior. This is done by examining a case study element (a canopy), which is situated in a dynamic environment that changes the element's load distribution. This simulated a structure that has to adapt to changing forces and loads such as wind, rain, snow, earthquakes etc. In order to improve its stability performance, the case study had to adapt to unpredictable changes. The case study element chosen by this paper has the potential of being duplicated and assembled as part of a bigger surface or double skin façade, as well as a single structural component, for instance.

2. BACKGROUND

Load distribution, one of the major fields of adaptive structures, deals with the manipulation of external loads and internal force distributions over a structural element, changing over time (Sobek &Teuffel, 2001). This can be carried out in two ways: either by controlling the adaptation of the structure`s shape, or by adapting its structural components' properties--stiffness or strength for instance (Sterk, 2006). A combination between the two methods is possible as well. When time is critical to fulfill the adaptation task, real-time adaptation can be carried out, by embedding computer methods in the kinetic element (Fox & Yeh, 2004).

Optimisation is one of the qualities of an adaptation process, in order to increase structures' efficiency (Sterk, 2006). This allows the structural element to exploit its properties for improving performance and also allows the object to respond to its surroundings. Two of the most commonly used methods for optimisation are Evolutionary Algorithms and Artificial Neural Networks (ANN) (Hanna et. al, 2010). Evolutionary methods, such as Genetic Algorithms (GA), attempt to achieve optimisation through the evolvement of 'generations' (each generation consisted of calculated solutions to the given problem). However, learning methods such as the ANN, enable improvement over time based on the experience gained, to reach the optimised solution (Flake, 1998).

2.1. Genetic Algorithm (GA)

GA is especially suitable for solving optimisation problems with a very large number of possible solutions. The algorithm is based on a process that mimics evolution through a population of candidates. A 'population' (creating a generation) consists of number of 'members', each with its own properties—'genes'. These members represent a possible solution or configuration for a given problem. The 'members' are ranked according to their performance in relation to the target ('fitness' criteria). Following some algorithms that mimic biological principles of natural selection (breeding, crossover and mutation), the fittest 'members' have a higher probability to reproduce and generate a 'better' generation; i.e., to create a population with a better configuration to the given problem.

The use of GAs for optimisation in the architectural field has only recently been initiated. Architectural design problems are often too complex to be simulated, and the number of parameters shaping an 'architectural' problem can make the optimisation process chaotic.

2.2. Artificial Neural Network (ANN)

The ANN can map large data sets and detect their patterns. By that, it is able to find a solution to very complex problems. The ANN algorithms are inspired by the way biological neural networks work, based on neurons and perceptrons (a type of pattern classification device based on visual perception principles) in order to achieve adaptive behaviour within machines. The ANN uses a database as a reference to learn from (known as the 'Training Set'). This database stores similar 'problems' and their known 'solutions'. By looking for patterns in these similar cases, the ANN trains to get a 'right answer' to a given problem.

The ANN consists of three layers: input (problem), hidden layer ('calculation' layer) and output (solution). All layers are connected to each other by 'neurons' that propagate the data from one layer to another. All the connections are weighted based on their relevance to the desired output, so that connections with a higher score are closer to the desired output. First, a 'problem' from the stored database is processed and the ANN gives it a solution. By comparing the suggested solution the ANN produced to the 'right known solution,' the learning process is conducted. The error (the difference between the right answer and the given one) is then calculated and the weights adjusted accordingly (Mitchell, 1997). This is done iteratively until a satisfactory training state is achieved. During that process the results converge to the right solution. Further to the training phase, there is a 'testing phase' based on a data set as well. In this testing phase, the pattern the algorithm has found is tested and verified in a similar way.

The use of the ANN algorithm is widespread in the engineering fields, mainly for purposes of pattern recognition, structures and materials behaviour prediction (Mitchell, 1997; Kota et. al., 2003).

2.3. Relevant Work

In recent years, studies in the field of structures' optimisation according to external changing parameters are well known, especially in the engineering and aerospace studies (Kota et. al., 2003). In the architectural context, however, researchers mainly focus on two fields: The first

uses optimisation as a design tool–optimising different aspects of the design during the design process. The second uses optimisation in real-time to increase the performance of a building by controlling an adaptive dynamic element. Current studies are developing kinetic elements that will perform adaptive behaviour in real-time. These methods follow two main approaches:

One approach is based on reacting according to a vast database, created in advance by detailed simulations with high accuracy. The simulations analyse the behaviour of the structure under the influence of certain static and dynamic loads, and calculate the optimised counter movements required (Details Magazine, 2012). In this method the structure can respond only to known, pre-calculated conditions. That way, the structure is strongly context-based (as the database is created according to a specific environment). Moreover, versatile and unpredictable parameters such as wind or snow, for instance, are destructive.

The second approach currently researched by Senatore et. al. (2011) is a conceptual study that examines the possibility of designing an adaptive structure to achieve improved performance and increase its structural efficiency. This method performs real time optimisation calculations and activates a large number of actuators to maximize accuracy. The complexity of many changing parameters, together with the actuation needed, requires great computational power.

3. METHODOLOGY

This research explores the potential of using adaptive structure methods, based on self-learning abilities, in order to achieve adaptation to unpredictable changing environments and prevent the canopy from buckling. By this, it aims to achieve a wider range of operation and improve its ability to survive in versatile environments.

A single-segment canopy was selected as the examined structural component. The dynamic adaptation process is carried out by controlling the components' properties: by changing the length of the canopy's columns, the column's buckling limit is changed. The case study is aimed to be as generic as possible and to have the ability to adapt to various conditions regardless of location, orientation or materials.

3.1. Research Design

In order to implement a self-learning method, the ANN algorithm was chosen, as it is an efficient learning method for sensor-based data in a constantly changing environment (Mitchell, 1997). Since the ANN requires a database of inputs and finite solutions with which it is trained, a digital simulation was created (Figure 1).

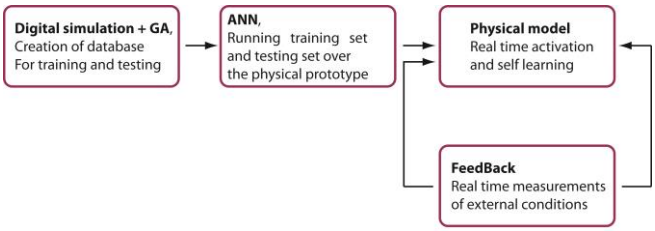

Figure 1. General course of experiment.

First, a digital model of the canopy was created and random forces were applied on it. Aiming to avoid reaching the buckling limit by changing the columns' length, a GA optimisation algorithm was applied on that model, and a database of optimized solutions was constructed accordingly. Later, the ANN algorithm was tested, using the pre-optimised GA database as its initial source of learning.

Lastly, a physical model of the canopy was built and the ANN algorithm was implemented on it. Weight sensors, integrated within its columns, measured the internal loads on each column in order to examine and analyse the acquired adaptive behavior. Linear actuators were embedded in the canopy's columns to enable the change in length of each column. Each 'answer' given by the ANN led to physical adjustments of the prototype. The new configuration was then checked by the weight sensors, in order to ensure the system indeed achieved stability. According to this feedback, the ANN algorithm continued its learning process on the physical model as well as improving its performance. By using this method the optimisation processes was conducted 'off line' (where the complex computation process is carried) and the system operated in real time, in a 'decision making' process, which does not require heavy computing.

3.2. Research Assumptions

In order to examine the feasibility of the method presented above, the system's definitions were based on an abstracted reality and the experiments were conducted under

several simplifications and assumptions (Boris & Srinivasan, 2012):

- The simulation considers the element as isolated. All applied forces and forces acting on the element due to environmental interactions are calculated as a net force: vector sum of all forces.
- Several parameters were defined in a way that allowed tolerance range for fitting the digital simulation to the physical model examined.
- Feedback loops were conducted throughout the process to ensure the goal (defined both to the digital model and the physical one) is achieved.
- Columns are taken as linear and homogeneous.
- Loads on each column are caused by forces applied over the surface. The load on the column is the criteria being examined.
- The critical column load is the buckling limit. The study's buckling threshold is set to a certain percent of the actual buckling limit value, to allow a pre-required tolerance.

The length of a column affects its buckling limit, and therefore the allowed threshold (Figure 2), according to Euler's rule:

$$F = (\pi^2 EI) / (KL)^2$$

where:

F = maximum or critical force (vertical load on column);
E = modulus of elasticity;
I = area moment of inertia;
K = column effective length factor, whose value depends on the conditions of end support of the column; and
L = length of column.

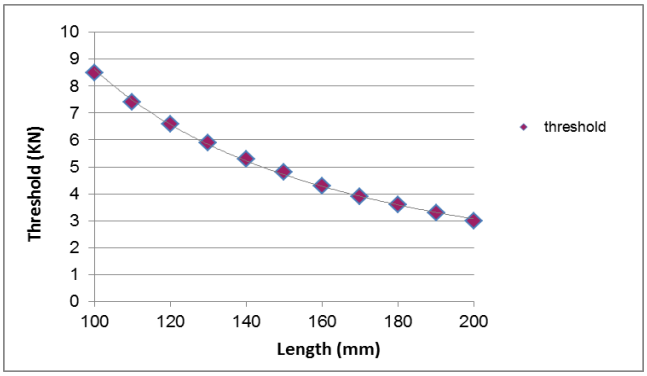

Figure 2. The change of the column's buckling limit in relation to its length.

The success of this test will be measured by measuring the load on each column, and comparing it to the columns' threshold (once adjusted by changing the column's length), so:

Current Threshold – Current Load > 0

Changing the length of one column leads to a change in the angle of the canopy`s surface and therefore a change in the load distribution on each column. There is no single combination of column lengths that avoids the buckling limit of each column; therefore there is no single solution to this problem. By applying a GA, this study got an optimised set of finite solutions.

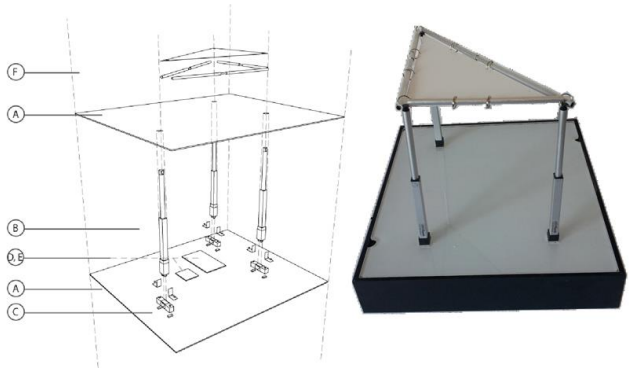

Figure 3. The physical prototype.

3.3. The Physical Prototype

The physical prototype consisted of several components (Figure 3) with inherent elements that can be adjusted and by that change the threshold level. These elements included:

- A wooden 12mm constructed box 400mm*400mm, with upper side made of 6mm Perspex.
- Actuators: 3 Pirgelli linear servos L12-100-100-6-I, with a position feedback, 6V.
- Load cells: 3 micro load cells (0-5 kg) measure the loads applied on each column within the vertical axis only.
- An Arduino board integrated into an electronic circuit operating 3 actuators.
- A PhidgetBridge 4-Input, operating 3 load cells.
- A plastic surface 2mm, attached to telescopic aluminum rods, so it can change its length.

3.4. The Digital Optimisation Process (GA)

Each possible combination of column lengths is called a 'member'. Each 'member' has 3 'genes'—the length of each one of the three columns. Each GA 'generation' is

constituted of 50 members. Each 'generation' picks the members who had the best performance in the previous generation, and uses their 'genes'. Eventually, the GA has 100 generations (as the number of generations increases, the calculated solution is better). In order to overcome the complexity of the problem and to avoid local optima (Hanna et. al. 2007), a 5% degree of randomness was added to the GA when searching for the optimal solution (through the mutation function).

The optimization goals were focused, to avoid chaotic optimisation process (Hanna et. al. 2010). The target was to achieve a stable system, where all columns are stable (load < threshold), while changing the length of each column as minimally as possible and keeping each column as long as possible. This target was set this way for several reasons:

- To avoid generic solutions in which the columns are always in their shortest position, and have the highest threshold value.
- To minimize the energy put into the actuation of the system. (A bigger change requires more power).
- This constraint represents 'Architectural' or 'programmatic' value; and can be further developed.

After setting the new length for each column, feedback loops were conducted to ensure the configuration that was chosen is 'stable' and that the loads on all the columns are indeed below the column's threshold.

In order to create a vast database the simulation ran according to the following method:

- Force applied between the range of 0 to 20N (as this is the maximum load can be carried by the columns of the physical prototype). Each simulation had 1[N] load interval.
- The angle between the surface and the force applied ranges between 0 to 90 degrees (as there is symmetry between the range of 0-90 and 90-180). The simulation ran for every 9 degrees.
- 7 different configurations of force deployments were simulated, each time the combination of the distribution of the force on the columns was changed).

This database included both a training set (1000) and a testing set (400) that were applied on the physical prototype.

3.5. The Learning Algorithm (ANN)

The ANN algorithm was implemented on the physical model using the back propagation method. The canopy reacted to real time inputs (forces applied in real-time) that were detected by the sensors. The input was the current length and the current load for each column (6 parameters in total). If at least one of the columns was above the threshold the ANN produced an output of the new length required for each column in order to avoid the threshold (3 parameters). Since the position of each column affects the other two columns, the output considered the combination of all three columns, rather than the load on a single one.

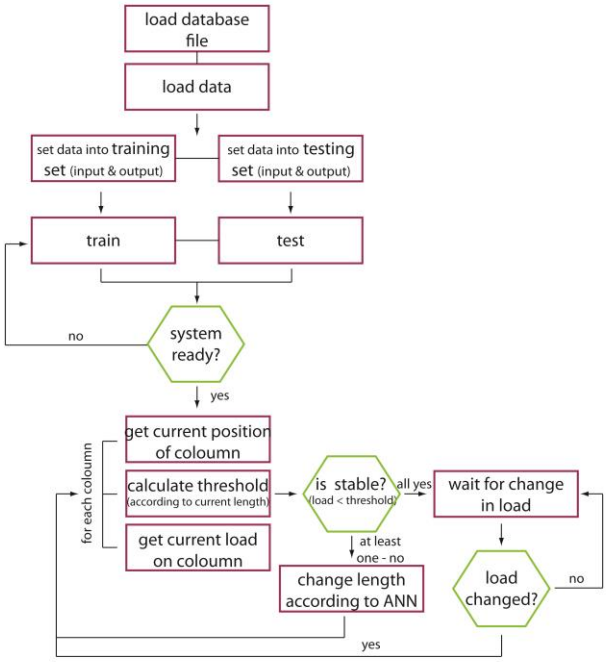

Figure 4. Code flow chart.

3.6. Implementation

All code used in this study, including the communication between Processing and Arduino, Processing and PhidgetBridge, and, the GA and the ANN, have been developed by the author in the Processing programming language.

Once the creation of the database was completed, real-time experiments were conducted in order to calibrate both simulations and model to the same range. The ANN algorithm was embedded inside the final code, including the communication code between the Arduino, Processing and the PhidgetBridge. Both the Arduino and the PhidgetBridge

were used as a feedback tool to get inputs measured in real-time. The Arduino was also used for implementing the results and controlling the physical system. The process consists of the steps as described in Figure 4.

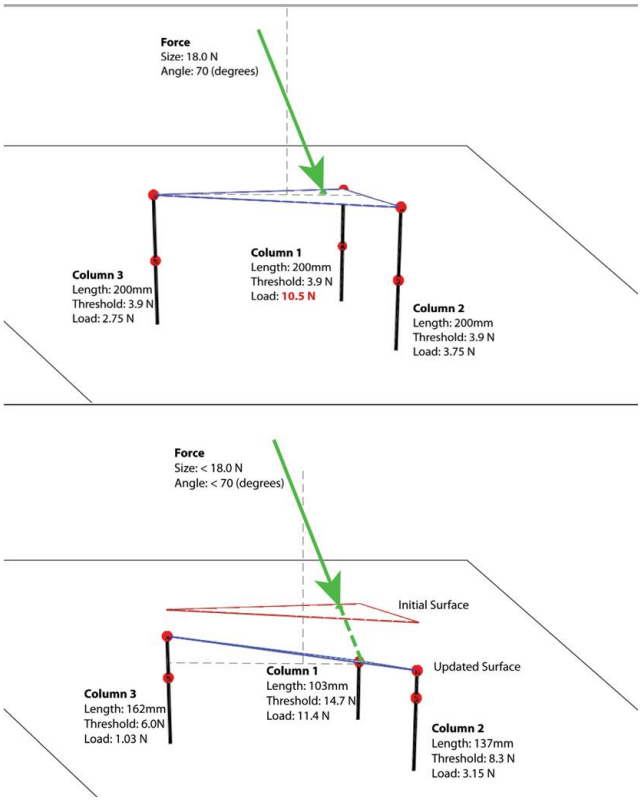

Figure 5. Digital simulation: (Top) Initial configuration – **not stable**. (Bottom) Updated configuration, after optimization – **stable.**

4. RESULTS AND DISCUSSION

4.1. Digital Simulation and the GA

Figure 5 shows an example of a single simulation, and its result. As shown in Figure 5, when the force was first applied over the initialized surface, column 1 was not stable (in 'danger') as its load was supposed to exceed its threshold. By changing the angle of the surface, i.e. by changing the length of the columns, a new setup was created. Within the updated surface position, all columns are stable.

Figure 6 shows the result of 10 (out of 1400) configurations (1 configuration = combination of lengths of the 3 columns), conducted in the simulation and optimised by the GA algorithm. Each chart presents one column. The initial state of the column was the same (length = 200 mm), and random forces were applied over the structure.

As it shows, after optimisation, the load over each column always stays below the updated threshold. The length of the column is changed when at least one of the columns is loaded above its threshold, as can be seen in configurations 1-3 for example.

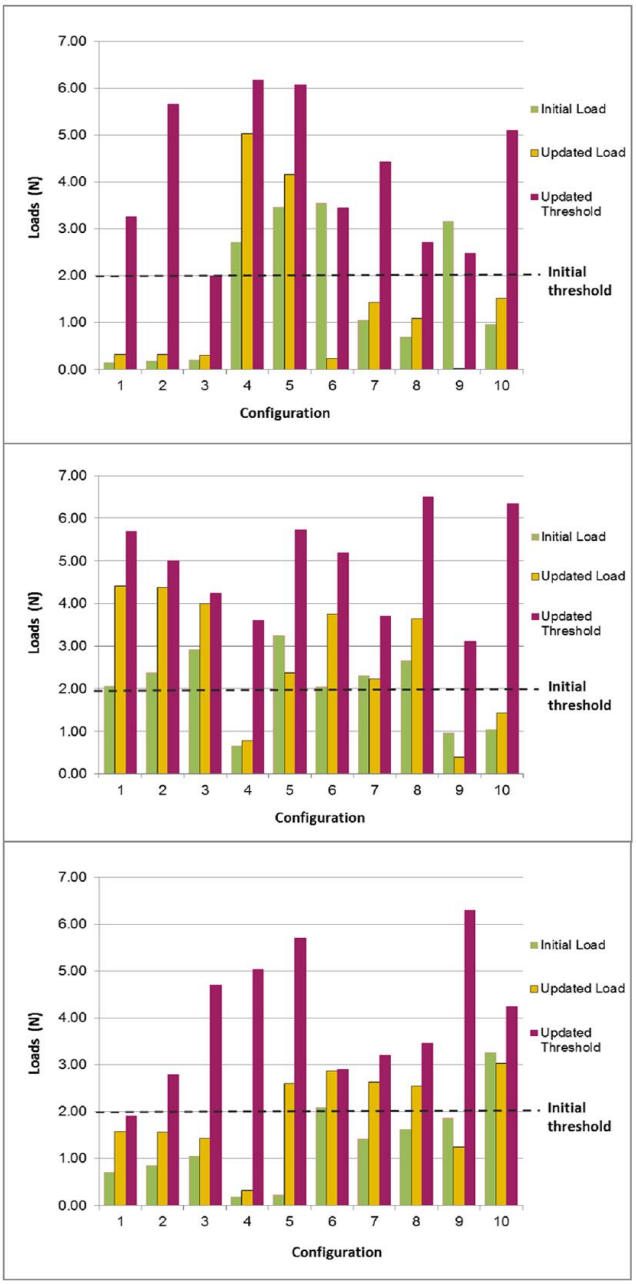

Figure 6. 10 configurations conducted by the simulation: (Top) Column no. 1; (Middle) Column no. 2; (Bottom) Column no. 3.

4.2. ANN

The figures below (Figures 7 to 9) present the results of the testing phase on the digital model. The first testing was conducted with no training before. Then the system was trained and after each training (iteration) it was tested again. 10 training phases were conducted.

Figures 7 and 8 show the results for the first 30 configurations of the testing set without training, after the first training set and after the tenth training set. The 'right answer' is the one given by the GA in the digital simulation to a similar set of inputs.

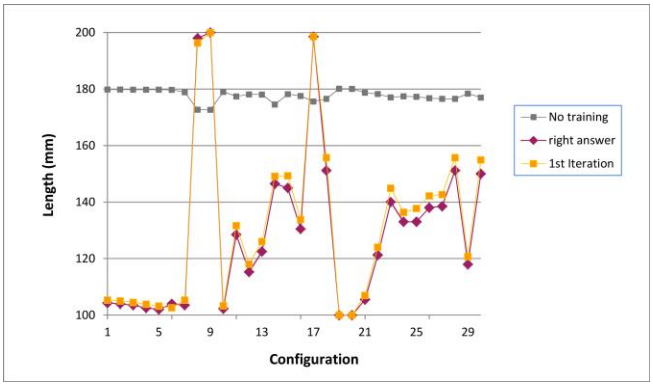

Figure 7. Length change, for a specific configuration, for the first two testing iterations, for a single column.

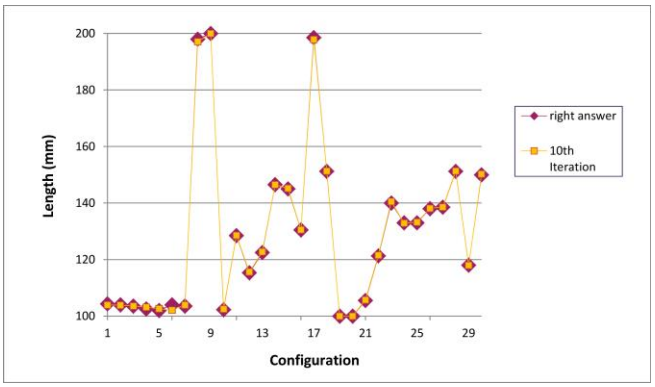

Figure 8. Length change, for a specific configuration, for the 10th testing iteration, for a single column.

Figure 9 shows the convergence of the system to the right answer by presenting the error rate. The error rate was calculated as the difference between the 'desirable length' of each column, as given in the GA database, and the length given by the ANN, for a specific set of inputs.

As can be seen in these charts, the algorithm managed to converge to the 'right solution' and successfully exhibit self-learning ability. The more iterations conducted, the bigger the improvement that is achieved by the algorithm.

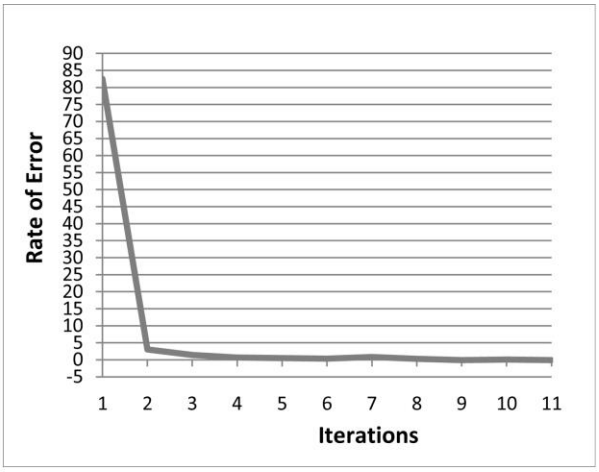

Figure 9. Error rate through the testing iterations

4.3. Physical Model

The last step of the study included an implementation of the ANN on the physical prototype. Figure 10 shows the adaptive behavior acquired by it. All measurements for these charts were in real time, as detected by the load cells and the position feedback of the linear actuator (the column). As Figure 10 shows, in all the examined configurations the system reached its target.

5. CONCLUSION

In this study the potential of a structural component to exhibit self-learning in order to adapt to an unpredictable changing environment was explored and successfully achieved using a case study. An ANN algorithm, trained by a set of optimised finite solutions created by a GA, was applied on a prototype.

The objective of this study focused on the potential for creating an adaptive structural element. The case study successfully presented self-learning abilities: the physical structure reacted to various forces, and managed to learn how to change its position in order to avoid buckling. These structural problems are often too complex to have one absolute solution. Thus, several assumptions and simplifications were made, as described above. These simplifications do not affect the results of these tests, as the main aim of this study was achieving an adaptive behaviour and by that to improve its performance. This goal was achieved and considered as proof of the study's aim. This

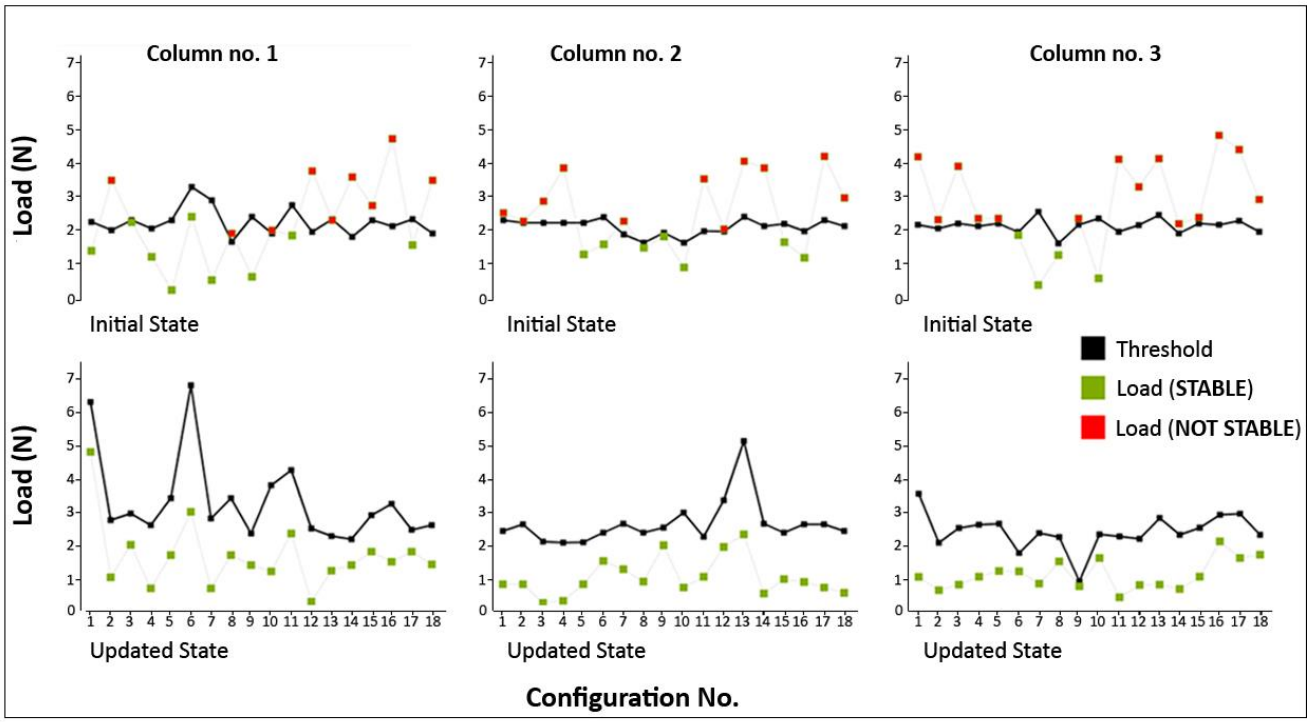

Figure 10. Configurations conducted on the physical prototype. Initial load / Initial threshold – Updated load / Updated threshold

method has a potential for further development and can be applied over different structural elements (façade elements, canopies, and structural components etc.) as well as to adapt to other parameters with an unpredictable pattern (human behaviour, weather conditions, combination of different parameters that will cause unpredicted patterns, etc.).

References

BONVIN, D., SRINIVASAN, B. (2012), 'On the use of models for dynamic real time optimization'. Available in: http://focapo.cheme.cmu.edu/2012/proceedings/data/papers/052.pdf [Accessed 01 September 2012].

DETAIL online-magazine, (2012). Available in: http://www.detail-online.com/architecture/news/maximum-load-carrying-capacity-with-minimum-material-input-018603.html. [Accessed 01 September 2012].

FLAKE, G. W. (1998), The computational beauty of nature: computer explorations of fractals, chaos, complex systems, and adaptation', Cambridge, MIT Press.

FOX, M., YEH, P. (2004), 'Intelligent kinetic system', available in: http://kdg.mit.edu/Pdf/ iksov.pdf [Accessed 01 September 2012].

HANNA, S., (2007). 'Inductive machine learning of optimal modular structures: estimating solutions using support vector machines', Artificial Intelligence for Engineering Design, Analysis and Manufacturing, vol. 21, No. 1, pp. 351-366.

HANNA, S., HESSELGREN, L., GONZALEZ, V. & VARGAS, I. (2010), 'Beyond Simulation: Designing for Uncertainty and Robust Solutions', in Proceedings of the Symposium on Simulation for Architecture and Urban Design at the 2010 Spring Simulation Multiconference, April 2010, Orlando, USA.

KOTA, S., HETRICK, J., RUSSELL, O., PAUL, D., PENDLETON, E., FLICK, P., TILMANN, C. (2003), 'Design and Application of Compliant Mechanisms for Morphing Aircraft Structures, Smart Structures and Materials 2003: Industrial and Commercial Applications of Smart Structures Technologies', Eric H. Anderson, Editor, Proceedings of SPIE Vol. 5054.

SOBEK, W., TEUFFEL, P. (2001). 'Adaptive Structures in Architecture and Structural Engineering'. In the proceedings of the Symposium on Smart Structures and Materials, at March, 2010. Newport Beach, CA, USA.

SENATORE, G., DUFFOUR, P., HANNA, S., LABBE, F., WINSLOW, P. (2011). 'Adaptive structure for whole life energy savings'. Intelligent Environments (IE), 2011 7th International Conference.

STERK, E. de T. (2006). 'Shape control in responsive architectural structures – current reasons and challenges'. In Proceedings of the 4th World Conference on Structural Control and Monitoring, San Diego, CA, USA, July 2006.

TEUFFEL, P. (2010). 'Architectural engineering and beyond'. In the 50th Symposium of the International Association for Shell and Spatial Structures. In the proceedings of 'Evolution and Trends in Design, Analysis and Construction of Shell and Spatial Structures.' Valencia, 2009. Proceedings. Editorial de la Universitat Politécnica deValencia.

Choreographic Architecture: Inscribing Instructions in an Auxetic Based Material System

Themistocleous Theodoros, Chronis Angelos

[1]The Bartlett, UCL
14 Upper Woburn Place West,
London, UK, WC1H 0NN
theo@theothem.com

Keywords: Kinetic Architecture, Morphing Structures, Simulation, Auxetics, Optimization, Systems Design.

Abstract

This paper presents the development of an SLS 3D-printed auxetic structure actuated to a predefined form by an embedded pneumatic network through an iterative process of feedback between digital simulation and physical testing. This feedback process is critical to the development of a more accurate predictive model and to compose the geometry of the suggested structure. An approach based on the emergence of final structure from the convergence of the behavior of sub-structures has been introduced from the beginning and a methodology based on the analysis and synthesis of the simplest sub-system is the core of this research. The results indicate a promising simulation environment and a novel methodology for the design and fabrication of auxetic structures with embedded pneumatic actuation. This exploratory research suggests a fertile research space within the field of adaptive architecture and kinetic design.

1. INTRODUCTION

The motivation of this research lies in designing and creating a morphing auxetic structure, actuated from an embedded pneumatic network and fabricated with additive layer manufacturing as a design opportunity for the means of kinetic architecture. Therefore, the research question first related to the synthesis of the geometry of the structure and second to its application in kinetic architecture through a simulation environment. The research procedure is following an iterative process of design through making (Sheil 2005) and simulation through testing and observing. Methodologically, this is achieved through the manufacturing and testing of components of the system, which creates a knowledge base for the next steps. Then, a simulation environment is suggested for the implementation of the structures in the field of kinetic architecture based on an approach that creates hierarchies between sub-systems analyzed with the Direct Stiffness Method. Finally, the construction of the method is following a bottom-up procedure with iterative steps of experiments, observations, and reformulations.

2. KEY COMPONENTS

The work of Hanna and Haroun Madhavi (2004) in relation to the optimization of stiffness in structures in order to control the compliant behavior—and the work of Lu and Kota (2002) about compliant behavior—initialized the idea of the ability of monolithic morphing structures to shape shift under load. In these systems, the optimization of their materiality could create predicted shape shift when actuated.

For the purpose of this research, *auxetic structures* have been selected for the base geometry of the study. They are cellular structures with negative Poisson ratios, and they also have the ability to form synclastic surfaces. Furthermore, according to Evans (1991), *"By varying the cell geometry of auxetics it is possible to produce different combinations of curvatures,"* which is understood as a way to optimize the behavior of the structure by changing its geometrical composition.

The cellular geometry of the auxetic structure also inspired the implementation of an *embedded pneumatic network* responsible for the self-actuation of the structure; an actuation method to exploit the cellular geometry of auxetics and the properties of fluids to transform itself. This proposal forms a novel approach in relation to current studies on materiality in architecture as pathetic systems (Oxman 2012), and it proposes to design the materiality of

architectural artifacts for the creation of kinetic morphing structures in architecture.

For the study of these new opportunities in architecture, the advances in digital fabrication have a fundamental role. The creation of monolithic auxetic structures with conventional methods (molding) is an expensive and time-consuming procedure with limited potential of producing a variety of geometries (Bianchi et al. 2011). Therefore, *digital fabrication* (3D printing) breaks new ground in the development and creation of optimized cellular auxetic structures.

3. BACKGROUND

The composition is of an ordered geometry that will be based on the basic cell introduced by Masters and Evans (1996). A study of the unit cell suggests that its implementation with pneumatics can be done in the form of bellow actuators.

Figure 1. Re-entrant cell proposed by Masters and Evans (1996)

The mechanism governed the axial expansion of a bellow type air muscle based on the geometry of the convolutions and on the pressure/thrust (F = p.Aeff) (Figure 2).

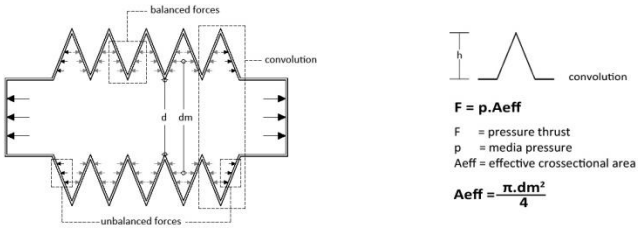

Figure 2. Diagram of the engineering physics of bellow

While the internal pressure is known and is homogeneous, it is proved from the equation of pressure/thrust that in order to create eccentricity, it should be changed to Aeff, and therefore, the ratio of h1 divided by h2 should not equal one and is explained in the diagram below (Figure 3).

There are many methods to study the deformation of a structure (Kaminakis and Stavroulakis, 2012), and most of them are related to numerical methods and non-linear analysis (Kirk 2001), particularly in the case of Real Time Deformations (RTD). However, in this research, it is suggested that RTD could be solved by analytical methods and, specifically, by using the Direct Stiffness Method (DSM). DSM is a method of linear structural analysis based on matrices, and according to Carlos Felippa (2004), it is the most common implementation of the Finite Element Method to all commercial software.

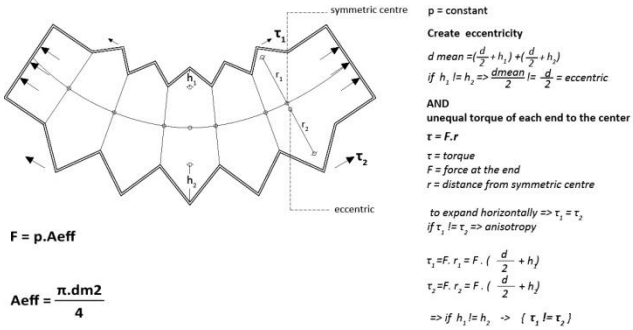

Figure 3. Diagram of the engineering physics of bending bellow

Generative algorithms are mimicking the evolution in the physical world, and they are used in computation for optimization procedures. In this research, the evolutionary algorithm will "search for paths to goals" (Mitchell 1998) and will be implemented for the optimization of digital structure according to the behavior of a physical model.

4. RESEARCH METHOD

As the final geometry of the structure was unknown, the simplest way to begin the research was considered the analysis of the simplest functional sub-component of the system. This approach to the unknown was the beginning of a research methodology based on sub–systems analysis and synthesis. The whole system was split into sub-systems and, consequently, into a smaller hypothesis, where the testing of sub-hypothesis, the observation of their weaknesses, and the reformulation of the initial hypothesis accordingly will structure an adequate solution step-by-step.

4.1. Tests of Unit Cell and Materiality

The first experiments explored the basic properties of the material and the behavior of the unit cell to evaluate the structure of the actuator, the size of the actuator, and the maximum deformation before its failure. The first physical bellows had been designed with a rectangular section and with wall thickness of 0.7 mm (Figure 4). Accordingly, three models were fabricated with the same properties

(length, number of convolutions, width and wall thickness) except the ratio of upper to lower convolutions, which had a different value from one to the other.

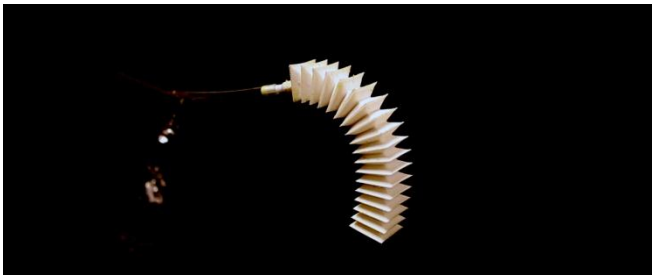

Figure 4. Actuated bending bellow with convolution ratio 0.29 (2/7)

During tests, the three structures bent with a different maximum curvature under the same maximum pressure (Figure 5). Therefore, it has been concluded that with similar bellows, the maximum bending is related to the ratio of convolutions, and it could be predictable.

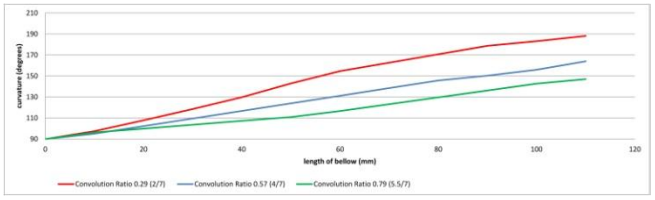

Figure 5. Diagram of curvature (degrees) to length (mm) of fabricated bellows.

4.2. Digital Model

DSM was implemented for the development of the simulation environment. The physical model was translated into a mathematical representation based on pin-joined trusses, while the internal pressure represented as forces—vectors acting on nodes (Figure 6). During the first digital tests, an unusual deformation to the length and the ends of the digital bellow was observed. The first response to correct this problem was to stiffen specific areas to prevent partial deformation.

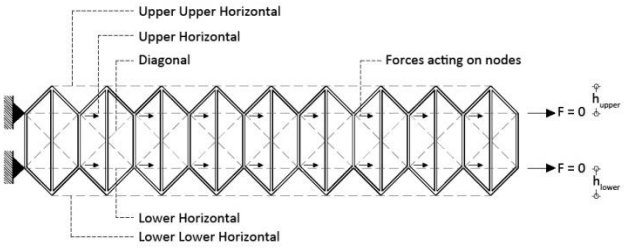

Figure 6. Mathematical model of continuous 2D bellow structure used in simulations

4.3. Reformulation

The reinforcement of the mathematical model was achieved through two different procedures. First was the increase of triangles by adding more elements, and second, the change of the elasticity of individual elements in the areas that exhibited higher values of deformation. After some tests with manual optimization, it was realized that a huge number of parameters had to be adjusted simultaneously in order to achieve the fittest result. To overcome this problem, a goal-oriented evolutionary algorithm was introduced.

Having measured the mean curvature of the physical model, the Generative Algorithm optimized the digital model in order to correlate its mean curvature with that of the physical one. By minimizing the distance between sampling points on the two curves, the correlation was achieved. For this optimization, the fitness function was based on a critical review of the research of LU and Kota (2002), which suggested to set a multi-objective fitness function to define the fittest from the sum of the fitness of each sampling point; the less the sum, the fitter the offspring (Figure 7). The optimization with generative algorithms successfully concluded that it is possible to optimize the digital model to behave like the physical model (in terms of curvatures), but it's impossible to achieve a correlation to their overall shape deformation.

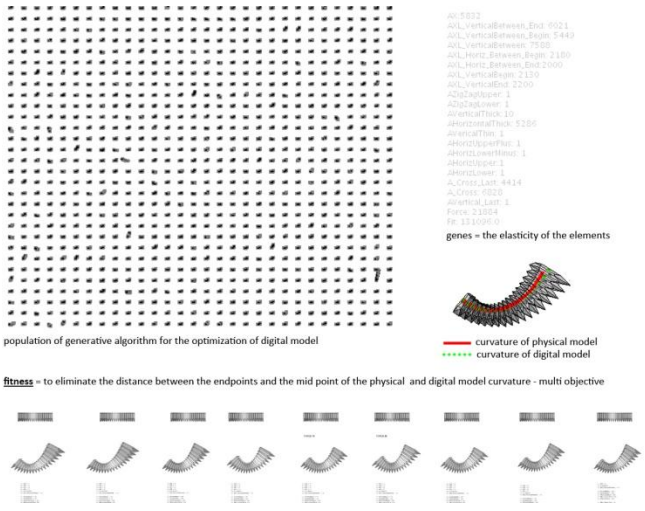

Figure 7. Generative algorithms to optimize the digital model according to the physical

4.4. Digital to Physical

The next step was testing the hypothesis of the actuator's anisotropic deformation using several values to the ratio of convolutions. This would also test the adequacy of the method to predict the behavior and eventually to become a design tool for kinetic structures of this type (Figure 8).

Generally, it was concluded that by changing the geometry of every unit cell, it was possible to force a bellow to bend while the mean curvature of bending is proportional to the ratio of the heights of convolution. The prediction of its mean curvature through a simulation environment using a continuous mathematical model and DSM is possible, but its accuracy depends on the optimization of the mathematical model. Finally, it was observed that even if the correlation of their mean curvatures has been achieved in a high degree, the overall deformation of the digital model never correlates with using this method. However, for the purpose of this research, the results have been considered acceptable since the aim was to predict the relation of convolution's ratio to mean curvature.

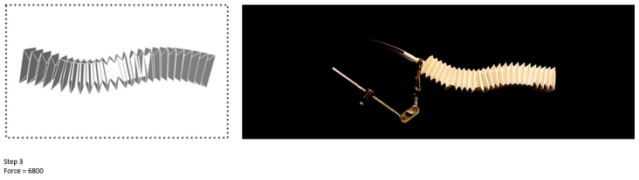

Figure 8. Physical model of anisotropic bellow during tests

4.5. Auxetic Structures

Having achieved adequate results, the next step was to test its performance in auxetic-based structures in an inverse procedure. Using the knowledge gained in previous experiments, the digital analysis and synthesis of the geometry was attempted prior to the fabrication and test of the physical artifacts. Specifically, it was suggested that the unit cell of the tested bellows could form auxetic structures in a certain geometrical composition. Thus, the following experimental procedure was an attempt to define and simulate a possible auxetic geometry based on the properties of bellows. The auxetic unit cell proposed (Figure 9) was a polar array of four bellow convolutions with a 90^{o} angle offset between them. The final auxetic structure was as a rectangular array of those unit cells.

The research then led to the development of a three-dimensional digital auxetic model having all possible triangulations in every unit. The model worked in small dimensions and in a small number of cells during the digital tests. When the number of cells increased, the simulation became very slow due to the huge number of equations it had to resolve. The above method of simulation proved insufficient for use with complicated auxetic structures due to the large size of the resultant stiffness matrix. The fact that a digital environment for simulation should be fast and flexible stimulated the introduction of a new hypothesis for the simulation of this kind of structure, which stated that “an algorithmic analysis and synthesis of sub-systems could be the base for the simulation of a complex system using linear analysis." This hypothesis was the aftermath of the procedure followed previously to define geometrically a bellow from the determination and composition of its sub-components after analysis.

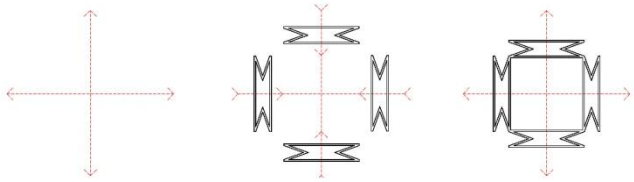

Figure 9. Hypothesis for the cell and the geometry of cellular auxetic structure

4.6. Reformulation of the Algorithm Based on Sub - Systems Analysis

According to the above argument, the hypothesis stated that the structure should be discretized in sub-systems, and the structural behavior of each sub-system should be solved separately following a hierarchical procedure. The hierarchy of analysis and synthesis should be based on the connections between the components. Starting from solving a sole element in the first iteration, the second iteration of elements to be solved should include all the components connected to the first one. The second iteration should be solved using the known displacements of the connection nodes of the first element as boundary conditions. Following this procedure to solve the structural behavior of all the elements and a transformation matrix to combine them together, the algorithm resulted in the simulation of the behavior of the whole system.

To test the new hypothesis of the mathematical model, it was suggested to test it first in a bellow as it was a simpler model, and then in an auxetic structure.

(1) First phase of the algorithm - discretization and solution (Figure 11):

A component nodes = **B** component nodes = …… = **N** component nodes **A** component -> **Solve** = **A'** component = **A1**, **A2**+$\mathbf{A_{u2}}$, **A3**, **A4**+$\mathbf{A_{u4}}$ => Displacements of the **nodes 2**, **4** are $\mathbf{A_{u2}}$ + $\mathbf{A_{u4}}$.

From the discretization of the structure, the initial reentrant cell was derived. Each cell has an equal number of nodes, and in a two-dimensional representation as in Figure 10, there are 4 nodes. Nodes 1 and 3 have zero degrees of freedom (DOF), and therefore, these nodes could have prescribed displacements (Felippa 2004). Starting from the first cell, in every iteration, a cell is being solved, inscribing in its DOF nodes 1 and 3 the resolved displacements of the connections nodes from the previous cell (boundary conditions).

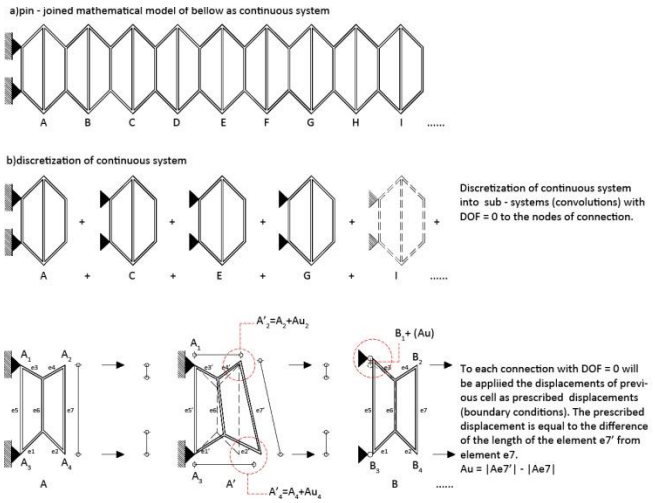

Figure 10. Diagrammatical description of first phase of component-based algorithm

(2) Second phase of the algorithm (Figure 11)

During the second phase of the algorithmic procedure, a rotation matrix R ($\vec{w}$) and a transformation T are applied to each element after structural analysis S in order to combine the digital model in its final shape (Figure 12) (connect elements).

$$\sum_{i=0}^{n} \{S(C_i)\} + \{S(C_{i+1} + |u_i|).TR_{i+1}(\vec{w}_i)\} + \ldots + \{S(C_n + |u_{n-1}|).TR_n(\vec{w}_{n-1})\}$$

S = structural analysis, C = component, u = prescribed displacements, $(T + R)(\vec{w})$ = (Transformation) matrix) of unit vector w

Figure 11. Proposed component-based algorithm for bellow structures

The proposed algorithmic method has been successful in simulating the bending, and from the comparison of the curvatures of the two models derived, the conclusion is that the physical bellow has a viscoelastic behavior. Also, a derivative was that the viscoelastic factor has a different rate in the first half of the bellow, which could be described by a sine curve, in comparison to the last half, which can be described by a cosine curve.

From the above observations, the addition of viscoelasticity to the mathematical model was suggested by changing the magnitude of force in relation to the length of the structure as the deformation is related to elasticity and force (F=((E×A)/L)×Dx)). The proposed force acted along the structure from the beginning to its centre in a sine function, while it decreased from the centre to the end in a cosine function.

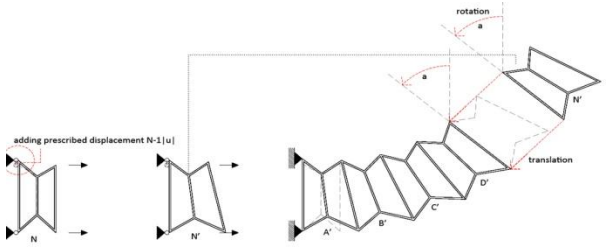

Figure 12. Diagrammatical description of first phase of component based algorithm

After several tests, it was defined that the correlated mathematical model was successful in simulating fabricated bellows. From the results, it was proved that by simplifying the mathematical model, it is possible to simulate the behavior of a fabricated pneumatically actuated bellow accurately and faster.

4.7. Auxetic Structure: Final Digital Model and Algorithm

To test the algorithmic process with an auxetic structure, it was suggested that a sub-system geometry derived from the diagonal separation of four sub-elements (Figure 11), which has four auxetic units, would be able to transform the component in four directions. The proposed algorithm (Figure 13) for this approach used three types of components in relation to the hierarchy of connections with their neighbours (Figure 14). The first component (C1) had four rectangular connection-faces (CF) with fixed lower nodes. The second component (C2) had four fixed nodes at the upper and lower corners of its rectangular CF, and the third component (C3) had two rectangular CF with eight fixed nodes at the upper and lower corners of each face. The

first component (C1) was positioned in the centre and was constructed only once at the beginning. After its structural analysis, the displacements of the edges of its CF were applied as prescribed displacements to the fixed nodes of the CF of the components C2, which were connected to the four CFs of the component C1. During the third iteration, a component C3 was positioned between two components C2 after the displacements of the two CFs of neighbouring C2s were applied to the edges of the CFs of C3. The last two steps were repeated proportional to the size of the auxetic structure.

$$\sum_{j=1}^{n} j = \{S(C1)\} + \sum_{i=1}^{2^2=n} \{S(C2_i + |u1|).TR_i(\{\vec{w}1\})\} + \sum_{i=1}^{4} \left\{S(C3_i + |u2_{i-1}| + |u2_{i+1}|).TR_i(\frac{\overrightarrow{w2_{i-1}} + \overrightarrow{w2_{i+1}}}{2})\right\}$$

S = Structural analysis, Ck = Component k , uk = prescribed displacements derived from component k,
$TR(\vec{w})$ = (Transformation) + (Rotation matrix) of unit vector w

Figure 13. Final algorithm for the simulation of an auxetic structure

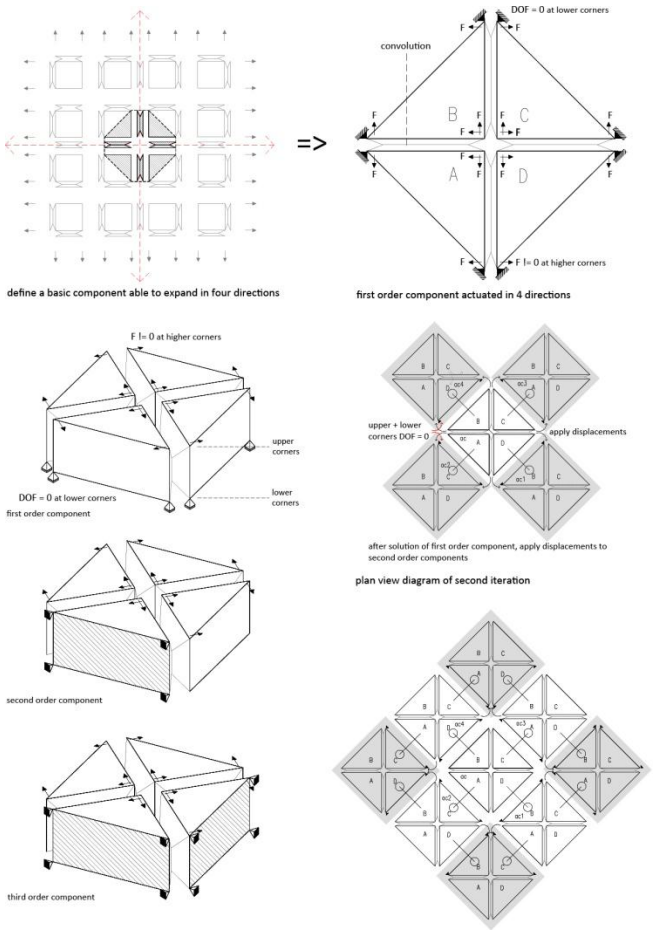

Figure 14. Diagram of the mathematical model and basic steps of final algorithmic process

4.8. Results from digital model simulation

According to the measurements, the simulation algorithm and the geometry of structure proved able to transform the structure and to form synclastic bending when the ratio of the heights of convolutions was not equal to one (Figure 15). Therefore, the curvature of the structure could be optimized according to the ratio of convolutions, and as the algorithmic method and the geometry were considered adequate, the next step was to proceed with the physical model's tests.

Figure 15. Simulation of auxetic-based structure in processing

4.9. Fabrication (SLS 3D Printing) and Final Test of Auxetic Structure

The physical model performed as was suggested and simulated, exhibiting an auxetic behavior and forming synclastic geometries (Figures 16, 17). The transformations of the physical model were analyzed from a Kinect camera's point cloud, where the auxetic behavior of the physical model was observed. The forces acted internally from the pneumatic actuation that had produced the expansion of the structure in two perpendicular axles and, therefore, had created the auxetic behavior. The fabricated auxetic structure had a similar viscoelastic behavior along its axis with fabricated bellow structures. The application of "viscoelastic force" to the mathematical model also created also viscoelastic behavior and a high degree of correlation (Figure 18).

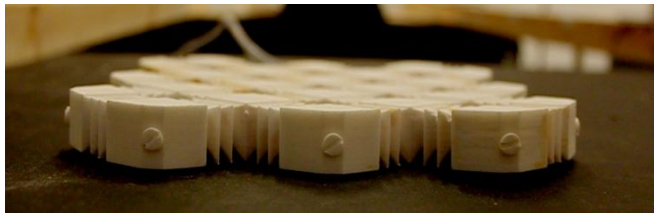

Figure 16. Relaxed 3D-printed (SLS) auxetic structure

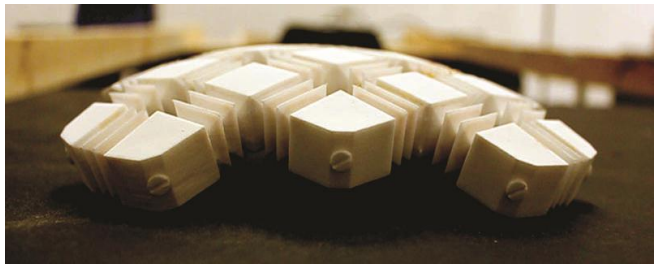

Figure 17. Actuated 3D-printed (SLS) auxetic structure

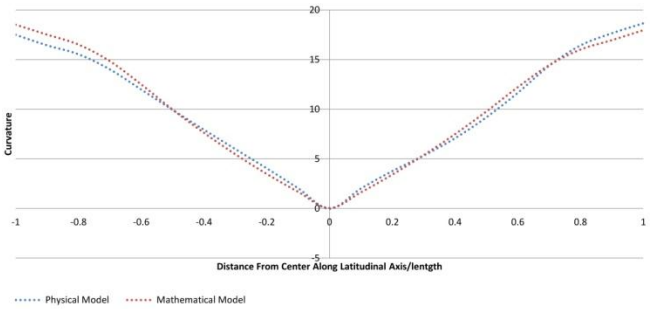

Figure 18. Comparison of curvatures of mathematical and fabricated models with ratio 0.29 along their latitudinal axis

5. DISCUSSION

5.1. Method

The approach of researching by design, in combination with theoretical backgrounds, constituted a successful method in conceptualization, design, fabrication, and simulation of a kinetic system. The combination of physical and digital models and the iterative experimenting process proved adequate in the creation of the hypothetical system and to the acquisition of its properties in a digital environment. Additionally, the approach of sub-system analysis and synthesis had a fundamental role in the development of the research, to the development of an auxetic structure, and also for the development of an adequate algorithm that simulated its behavior.

5.2. Algorithm

The discretization of the geometry in the simpler units made possible the use of linear analysis for the simulation of the geometry. The solution came through the creation of hierarchies and dependencies between unit cells. The final algorithm was responsible for creating the hierarchies between unit cells, beginning from a centre cell and growing the structure in a *"circular"* array. Starting from a centre cell with four links, the geometry expanded by connecting four other cells to the unit cells. By applying the boundary conditions to the connection nodes and using translation matrices achieved the right alignment and deformation of the actuated cells and, therefore, simulated the behavior of the whole.

5.3. Conclusion

The methodology, based on an iterative process (hypothesis, test, and feedback), succeeded to define an adequate method of creating, simulating, and optimizing the behavior of an auxetic monolithic cellular structure. Following this procedure, both the digital and physical systems were constructed. By understanding and manipulating the micro-behaviors of the auxetic sub–components, it was possible to design, optimize, and simulate the emergent macro-behavior of the whole.

The possibilities of a dialogue between physical and digital models were explored and led to a bridging of the gap between the material and immaterial world. The potential of control of change by inscribing instructions in the topology of structures and by exploiting the properties of the materials led to results that would otherwise be almost impossible to reach. The implementation of digital techniques in design, simulation, and fabrication of auxetic-based pneumatically actuated structures breaks new ground for research and creates new possibilities in the field of responsive kinetic architecture.

Acknowledgements

I would like to thank Ruairi Glynn and Sean Hanna for their inspirational feedback and valuable advice regarding this research, held during my MSc AAC at Bartlett, UCL, UK.

References

SHEIL, B., 2005. Design Through Making: An Introduction. Architectural Design, 75(4), pp. 5-12.

EVANS, K.E., 1991. The design of doubly curved sandwich panels with honeycomb cores. Composite Structures, 17(2), pp. 95-111.

BIANCHI, M., SCARPA, F., BANSE, M. AND SMITH, C.W., 2011. Novel generation of auxetic open cell foams for curved and arbitrary shapes. Acta Materialia, 59(2), pp. 686-691.

LU, K. & KOTA, S., 2002. Compliant Mechanism Synthesis for Shape - Change Applications Preliminary Results, Smart Structures and Materials 2002 : Modeling, Signal Processing, and Control, Vittal S. Rao, Editor, Proceedings of SPIE Vol. 4693

MASTERS, I.G. AND EVANS, K.E., 1996. Models for the elastic deformation of honey-combs. Composite Structures, 35(4), pp. 403-422.

KAMINAKIS, N.T. AND STAVROULAKIS, G.E., 2012. Topology optimization for compliant mechanisms, using evolutionary-hybrid algorithms and application to the design of auxetic materials. Composites Part B: Engineering, 43(6), pp. 2655-2668.

KIRK, M., 2001. Non-linear Structural Analysis as Real-Time Animation Borrowing from the Arcade, Proceedings of the Ninth International Conference on Computer Aided Architectural Design Futures, 8-11 July 2001 2001, pp. 643-656

FELIPPA, C., 2004. INTRODUCTION TO FINITE ELEMENT METHODS. Boulder, Colo-rado 80309-0429, USA: Department of Aerospace Engineering Sciences and Center for Aerospace Structures University of Colorado. [Online]. Available : http://www.colorado.edu/engineering/cas/courses.d/IFEM.d/edn.

Session II

Façade Apertures Optimization: Integrating Cross-Ventilation Performance Analysis in Fluid Dynamics Simulation 41
Chrysanthi (Sandy) Karagkouni, Ava Fatah gen Schieck, Martha Tsigkari, and Angelos Chronis
UCL, Bartlett School of Graduate Studies

A Review of the Brazilian NBR 15575 Standard: Applying the Simulation and Simplified Methods for Evaluating a Social House 49
Tassia H. T. Marques and Karin M. S. Chvatal
University of Sao Paulo, Architecture and Urban Planning Institute of Sao Carlos

Thermal Reconstruction of a Crime Scene Using Calibrated Simulation 57
Nathan Brown, M. Susan Ubbelohde, George Loisos, Santosh Philip, and Ibone Santiago
Loisos + Ubbelohde, California College of the Arts, University of California, Berkeley

Façade Apertures Optimization: Integrating Cross-Ventilation Performance Analysis in Fluid Dynamics Simulation

Chrysanthi (Sandy) Karagkouni, Ava Fatah gen Schieck, Martha Tsigkari, and Angelos Chronis

UCL, Bartlett School of Graduate Studies
14 Upper Woburn Place
London,WC1H 0NN
sandy.k.x@gmail.com, ava.fatah@ucl.ac.uk, mtsigkari@fosterandpartners.com, achronis@fosterandpartners.com

Keywords: Parametric Design, Generative Design, Building Performance Simulation, Wind-Induced Ventilation, Multiple Criteria Optimization.

Abstract

Performance-oriented design has as a primary aim to introduce spaces that achieve acceptable levels of human comfort. Wind-induced airflow plays a significant role in improving occupants' comfort in a building. This paper explores the extent to which simulation of natural airflow can potentially be a contributing parameter in the conception of performance-aware designs. To test the natural ventilation performance of a pavilion, the study employs a Fast Fluid Dynamics simulation. A performance analysis is conducted, whereby an array of automated feedback loops carried out by a genetic algorithm can produce a number of acceptable solutions in regard to the optimization of the facades' openings. The experimentation conducted proves the ability of the model to yield design instances that fulfill a number of environmental criteria related to airflow and human comfort. In this light, the paper suggests that the aforementioned method can be used as an experimentation platform to influence the direction a designer may take when considering a design proposal.

1. INTRODUCTION

Performance analysis in the field of architecture allows designers to become aware of buildings' behavior in regard to their relationship with the environment. Researchers focus on different ways to predict the interaction of a designed proposal with natural elements, towards a more comfortable built environment that achieves, in parallel, low levels of energy consumption. Moreover, building engineering aims to solve everyday problems, such as providing sufficient day lighting and indoor air circulation. As a result, a great amount of knowledge in the territory of natural elements, such as sun and wind, is now available. It is in the designers' remit to integrate this knowledge into their plans, but as a common practice it is not until the last phases of the design process that they engage with such issues. This study focuses on wind, which is a dynamic phenomenon that can exhibit complex behavior in relation to built forms. Therefore the question arises of how the building skin may respond to it. In this study, an exploration is carried out regarding the shaping of façade openings as they get informed about the state of wind around them.

In recent years, mechanical ventilation has been preferred to natural ventilation, as it can provide stable air conditions and resolve airflow problems triggered by inadequacies in design (Cowell 2012). Nevertheless, heating, ventilation and air conditioning systems (HVAC) are complex and need a large number of components to operate. In addition, this kind of technology consumes a great amount of energy, whilst not always managing to deliver the desired indoor climate (Kleiven 2003).

Consequently, architects propose the integration of natural ventilation techniques in order to create functional buildings (Mendez 2012). In this case, computational achievements like Computational Fluid Dynamics (CFD) and evolutionary algorithms which were investigated during the development of this paper can be proven as potentially useful techniques to design, taking into account performance analysis.

Natural phenomena simulated in computer models require a skilled expert user. Wind engineers are employed for the interpretation and operation of such complex simulations (Malkawi 2004). Moreover, powerful computer

processors and a great amount of time are needed until the simulation model converges with an accurate result. Recently in the field of fluid dynamics, a less accurate but adequately informative model was presented. This model is Fast Fluid Dynamics (FFD), first presented by Stam (1999), and this has been the model used for the tests conducted in this research.

The main objective of this paper is to highlight the architectural consequences and possibilities as formed by the integration of wind analysis in the design process. The goal of the simulation model presented is to provide optimum airflow rate and distribution in the building's interior. How can we design a façade that allows the appropriate amount of air to circulate through the internal space? In addition, the study presents an exploration of natural ventilation in combination with the forced opening and closing of façade components that imply random movement of people through the building envelope.

2. BACKGROUND

Hensel and Menges (2008) argue that in considering the performance of a design during early stages, both the morphology of the structure and its environmental performance is important. In this light, form generation and environmental analysis become equal factors to the decision-making process. Thus, performance-driven design can take place even from the conception phase. The scope of such a strategy is not to gather specific and accurate information about energy performance, but rather observe and manipulate the "*tendencies or patterns*" of the design's behavior in accordance to natural forces (Hensel and Menges 2008).

2.1. Natural Ventilation Principles and Comfort Levels

Utilisation of the natural driving forces for the purpose of ventilation has for several decades provided the desired thermal comfort and air quality for people. In the traditional architecture of southeast Asian countries, porous structures (i.e. screenwalls) were widespread as a way of providing good comfort levels for the inhabitants (Hensel et al 2008; Hensel 2008). The performance analysis of these structures can prove their efficiency to achieve high rates of air exchange due to the availability of air, passing through the perforated building envelope (RIBA 2011).

Natural ventilation is a method to deliver air into buildings and replace the existing stale air with fresh air, using the force of wind (Cheung and Liu 2011; RIBA 2011). The most common type of use of this method is the stack effect, enabled by wind towers and cross-ventilation, enabled by openings on opposite sides of the buildings (RIBA 2011). The second is the case examined in this study. The wind is the driving force of the whole system. The way to allow this force to move through indoor spaces and also control its distribution is to design openings that affect the circulation of air and channel it to specific directions. The parameters that define the requirements of airflow depend on the comfort level standards (ASHRAE-55 2010; ISO 2005).

It has been studied and estimated that the way people perceive their comfort satisfaction levels depend on parameters such as the air temperature, the mean radiant temperature, the air velocity and the relative humidity of the space they live in. Apart from these comfort level parameters, one should also consider the local climate to draw some conclusions in regard to the applicability of natural ventilation in each case. The above parameters should be considered before implementing the model presented in this paper.

2.2. Simulations of Fluid Dynamics

Computational Fluid Dynamics are models used to predict air distribution using mathematical equations to solve the flow of air in spaces (Awibi 1989). Carillho de Graca et al (2002) have implemented CFD simulation to assess the air circulation performance in indoor spaces in specific countries. Suga et al (2010), focused on the design of windows, taking into account wind-flow. Also, Cheng and Liu (2011) examined the patterns created by air around buildings, with the objective to optimize the void space among them. These studies used the CFD model as an evaluation analysis only for orthogonal rooms or buildings and typical rectangular windows.

Stam proposed a different way to approach the simulation of fluids. The FFD model, which he proposed, was initially introduced for the game industry (Stam 2003). Chen and Zuo (2007) validated the model for several situations, among which indoor ventilation can be found. In a more recent study, the conclusions that are drawn apart from the accuracy of the model also prove that it is a much faster solution in comparison to conventional CFD models (Chen and Zuo 2009). Computing time is considered an important factor when trying to implement a methodology

during the conceptual phase of design.

To date there is a limited number of studies that aim to prove the applicability of this model in building engineering. Such an approach has been proposed by Chronis (2010) and Chronis et al (2011) as a form-finding method. This method is not environmental, but an effort to find forms that are informed by the wind load. Hence, this model has not yet been used for wind-induced indoor ventilation that can provide human comfort by investigating the transformations of the apertures of a façade, as is the case presented in this paper.

In the studies discussed above, it is a usual practice to couple fluid simulations with genetic algorithms. This model has been used extensively by Malkawi, who also noted the importance of visualization during the optimization process (Malkawi et al. 2005). This enables the designer to visually evaluate the good solutions carried out by the algorithmic process, providing an opportunity to select from a number of good solutions for air simulation (Malkawi et al 2005). Malkawi's studies focus on mechanically ventilated systems. The coupling of FFD and GA have also been recently realized and proved to be an effective strategy (Chronis 2010).

The space tested in this research exhibits similarities with previous studies. These similarities include the fluid simulation and main principles of the genetic algorithm (Chronis 2010), as well as the setting of the space and the placement of openings on windward and leeward side (Malkawi et al 2005; Cheung and Liu 2011). On the contrary, a different approach is suggested for the geometry of the façade's openings, which is non-orthogonal, and the optimization for natural ventilation using FFD as the evaluation method.

3. METHODOLOGY

This paper proposes a simulation model that aims to give the designer insight into the natural ventilation performance of a built form. Such a methodology can be considered useful for architectural projects located in countries with climate that exhibits high temperature and moderate or high humidity. Although there is not a specific brief to be fulfilled, an assumption for the parameters that would appear in such a case was made.

3.1. General Setup and Simulation Environment

As an initial step to set up the context for the experimentation, specific assumptions were made in respect to human-related and environmental parameters. The calculations are made for an unfurnished room and the space is considered to be a communal space. Hence, the metabolic rate of the occupants is 1.2, which implies sedentary activity (ISO 2005). The clothing insulation that influences the human comfort levels is 0.7. Using the above values it is possible to have as an output the desired air velocity, which in this case is in a range between $0.4ms^{-1}$ and $0.8ms^{-1}$ (ASHRAE-55 2010).

When cross-ventilation is the objective, it is a common practice to place openings on the windward and leeward side of the building. Using a wind rose diagram from Rome as a reference, the apertures are placed accordingly (Figure 1). Due to the hot climate in this city, it is considered a suitable case study for a natural ventilation system.

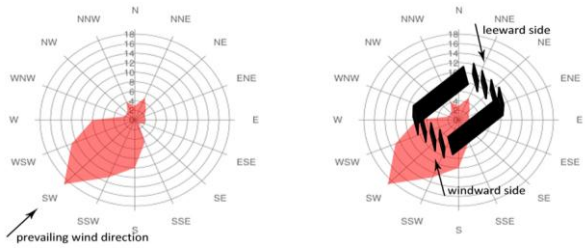

Figure 1. The space tested placed on the wind rose diagram.

Other parts of the structure (the remaining walls, the ceiling and the floor) are given a flat shape, creating an orthogonal volume of fixed area in order to eliminate the complexity of the system. Moreover, the objective of the investigation is to optimize the apertures' form and not the overall shape of the building envelope.

This paper engages with curved openings and their optimization for natural airflow, as they are formed by a series of louvres. In order to evaluate the performance of the model, testing was implemented on an existing type of louvres' geometry. Specifically, the properties of the louvres were based on the façade of the Thematic pavilion at Expo 2012 in Yeosu, Korea. For this project, Soma architects and Knippers Helbig developed a series of elastic fins that can perform complex deformations (Knippers and Speck 2011). The building shell of Nebuta house in Japan, realised by Molo, was also taken as reference for the form of the louvres. In both cases an array of fins creates variations in

the sizing of the openings due to the ability to bear torsion.

The model is implemented in Processing and allows three-dimensional free-form geometries to be presented. The whole configuration of space is divided in two categories: static elements and moving elements. The static elements consist of the ceiling, the floor and two lateral walls; while moving elements are proposed for the two remaining sides of the space which are also the windward and leeward sides (Figure 2). In the above described design it is suggested that the moving elements will replace the role of doors and windows, if it is thought of as a real building. The overall volume occupied by the simulated model is characterized by its width (4.8m), length (6.15m), and height (3.9m).

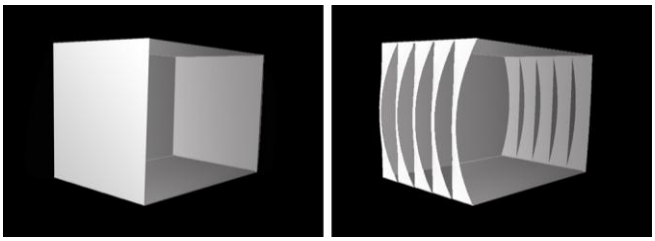

Figure 2. The louvres closed (left) and open (right).

Each louvre in the simulation environment is a non-uniform rational B-spline (NURBS) surface. Trying to simulate the behavior of the elements found on the façades mentioned (Soma pavilion, Nebuta house), the louvres should perform a certain range of movements. In both projects the property of twisting is prevalent. For this to be achieved, a Gaussian distribution was incorporated into the NURBS algorithm. Creating a Gaussian function is a simple way to achieve the expected type of relation between the adjacent control points (Figure 3).

3.2. Implementation of Fast Fluid Dynamics

FFD has already been used in a number of studies (Stam 1999; Chen and Zuo 2007; Chronis 2010). The algorithmic model used is based on an implementation, in three-dimensional space, of Stam's model (1999) by Ash (2006), which was later coded in Processing by Chronis (2010).

The fluid solver runs iteratively to define the fluid movement that will take place in every time step. The model is grid-based, which in three-dimensional space consists of uniform voxels. The visualization of the whole scheme is exclusively based on a range of colours that represent the value of velocity in each voxel, using a mapping function. Furthermore, the behavior of the system relies on the initial velocity forced into the system to stimulate the fluid. While the research focuses on natural ventilation, this velocity represents the wind. Throughout the simulation, the first row of voxels in the y direction is prescribed to have a specific velocity. This implies that the wind is blowing continuously with a specific direction and velocity.

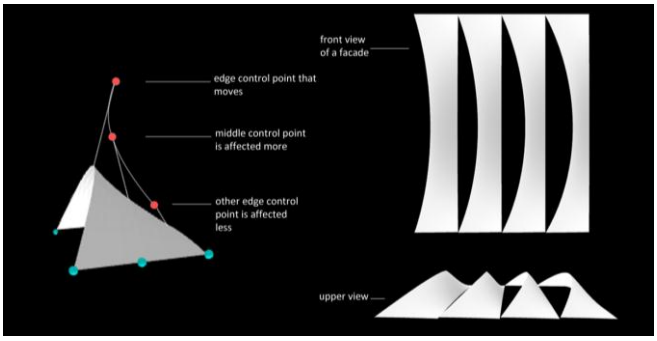

Figure 3. The louvres simulated as NURBS surfaces.

As a further step, a three-dimensional vorticity confinement function was incorporated into the algorithm. This was based on a two-dimensional scheme (Mckenzie 2004). The specific extension aims to reduce the numerical dissipation that exhibits the FFD model. By creating small swirling flows commonly found in smoke simulation, the velocity field is influenced (Fedkiw et al 2001).

It is also worth mentioning that a visual representation of the information that the fluid simulation can provide was created. Trying to visualize the indoor condition of the airflow, a function in Matlab was used to create a 3D graph from the given velocities (Matlab 2012). For every test, a memory structure was created where the velocity value of each cell located at height equal to 1.5m was kept. These values were later parsed by a Matlab function and a 3D graph was created where the velocity component specified the colour and height of each part of the surface (Figure 4).

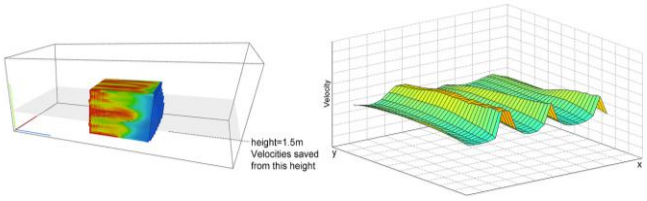

Figure 4. From left to right: FFD domain, Visualization of velocities in 3D space using the surface function in Matlab.

The fluid solver, as with the majority of CFD programs, is voxel-based. The NURBS surfaces, and the remaining elements that confine the room, were incorporated into the

fluid solver using a parametrization technique, which subdivides each surface into discrete voxels. The voxels that depend on the shape of the NURBS are enabled to change their state, according to the displacement of the surface, while the remaining voxels are static, and unaltered for each test. These voxels represent the internal boundaries of the fluid solver, redefined in every time step. The size of the fluid domain for all the tests on the x, y, and, z axes was set to 76, 150 and 50 respectively. In total, 57 x10^5 voxels were simulated and their size was uniform. Size values between 2 and 5 were tested and 3 was chosen as the voxel size that would be used in the final tests (Figure 5).

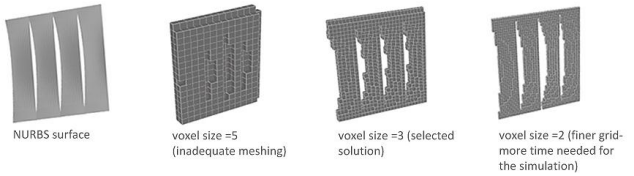

Figure 5. The meshing of the surfaces as it occurs due to different voxel size.

The simulated room occupies 34x10^3 voxels. Numerically the space that can possibly be occupied by people is taken in a distance of 0.6cm from the lateral walls and 1m of the ceiling. This region was used for the calculations that took place, in order to evaluate the performance of the room for natural ventilation. This is a common practice, since in the periphery of a room the condition of the air does not affect considerably human comfort (ASHRAE-55 2010; Malkawi et al 2005).

3.3. Genetic algorithm

An evolutionary method was implemented along with the FFD scheme to enable an automated evaluation of a large group of possible design solutions. The algorithm implemented relies on an example created by Turner (2010). Specifically, the genetic algorithm (GA) is based on a standard number of population members that are evaluated by a fitness function. Each member consists of a possible instance of the design. The differentiation between each instance depends on the genes, as they are encoded. In the case presented, the genes determine the displacement of the control points for each louvre on the x and z direction. These genes, random initially, are assigned with a range of values, and the pace according to which these values can be incremented. The possible values are discrete from 0 to 5. The lower limit of this range means that the louvre is completely closed and the displacement is 0°, while the upper limit means that the louvre, at the height of 1.5m, is open at 50°. The pace of the inclination is 10° (figure 6).

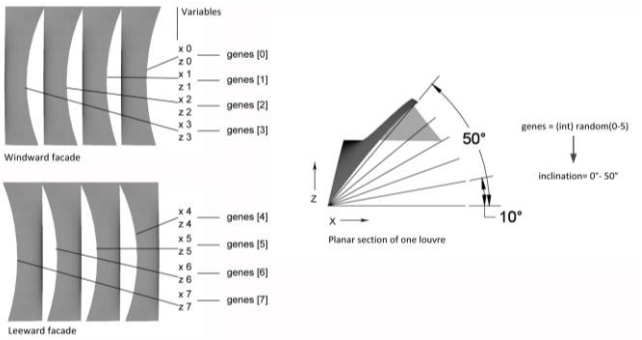

Figure 6. Representation of the GA scheme and the possible values of the genes.

A fitness function, related to natural ventilation, determines the effectiveness of each solution. Afterwards the whole population is sorted from the less to the most fulfilling option. The next step is the mutation and crossover of the possible values of the genes. Two instances are selected and a percentage of their genetic elements is passed to a new instance, while there is also a probability of new solutions to occur. The resultant solution is then evaluated, replacing the less effective member of the existing population (figure 7).

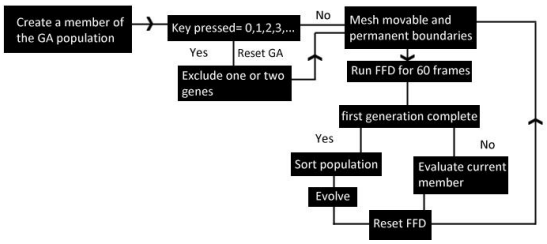

Figure 7. Flowchart of the GA scheme**.**

3.4. Multiple criteria fitness function

The fitness function elaborates the objectives of the problem into an algorithmic process. In the case presented, the airflow is adjusted due to the transformations of the façade elements, until an appropriate airflow pattern is met. The main parameter that influences the airflow is the velocity of air in the occupied space. In this light, velocity is used to recognise the behavior of the wind indoors.

Although the velocity component was the only key element used for the evaluation scheme, it was used in a number of ways that could provide adequate information concerning the indoor conditions. Four different functions

were incorporated into the fitness function, creating multiple criteria for the evaluation process. These required the calculation of the average velocity, the air exchange rate, the standard deviation and the maximum velocity.

The average velocity of the values found in the occupied space should fall into a range where the fitness increments. The upper limit for the average velocity was $0.8ms^{-1}$ and the lower $0.4ms^{-1}$. If the values did not fall into this range the fitness would be influenced negatively.

Furthermore, since the aim is to achieve a great degree of air exchange, to replace the stale air with fresh, the calculation of volumetric range exchange was adapted. Examining the voxels located in the interior side next to inlet openings, the area they occupy was multiplied by the average velocity found in their centres. This equation is commonly found in environmental studies for air (Autodesk 2011). The higher value of the volumetric rate, the better the resulting fitness.

Additionally, in order to achieve a uniform distribution of air indoors, one more function was introduced. This function was formulated for eliminating the deviation from the mean velocity. Standard deviation increments in a high degree when a great difference from the average value is found, and respectively the fitness decreases. As stated in previous studies, it is considered as an effective way to achieve a better distribution of uniform air velocities (Malkawi et al 2005).

Moreover, the maximum velocity found indoors was also integrated into the fitness function. A high value for maximum velocity affects inversely proportionally the fitness value. As this function also influences the evaluation part of the GA, the solution space was further constrained.

The above values are considered integral parameters that affect the effectiveness of a natural ventilation system. Thus, it was decided to elaborate them in a way that they could equally affect the fitness of a solution. In this respect, all the values as they are computed by each function were mapped to numbers raised to the power of -1.

4. TESTS AND RESULTS

The first test consisted of the ventilation performance analysis of a room with orthogonal openings so as to provide a set of measurements. These values provide the study with a performance benchmark in order to compare the effectiveness of the proposed façade that consists of louvres, to a convetional type of façade that consists of common windows and doors (figure 8). The second test examined the possible transformations of 8 louvres, so as to provide sufficient wind-induced ventilation. For the rest of the tests, one or two louvres on the windward façade, were left open throughout the simulation as if people were allowed to pass from the open louvres.

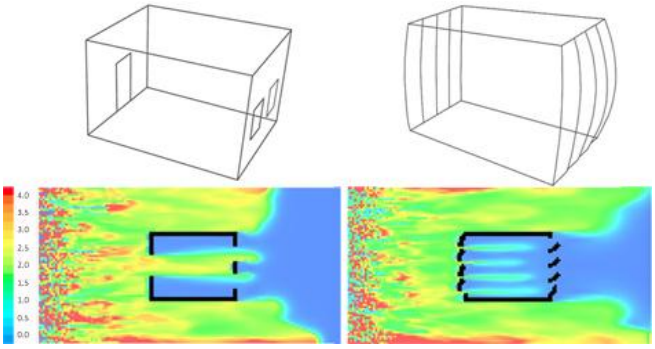

Figure 8. Diagrammatic representation of the rooms tested and their respective planar sections, across the x and y axis, for z=1.5m during the fluid simulation.

The most effective way to introduce sufficient airflow indoors is the creation of inlets that are slightly smaller than the outlets (RIBA 2011). This design principle for cross-ventilation appeared in the solutions presented in this study, proving that the solution follows the general guidelines of designing for natural ventilation. In addition, the coupling of FFD and the optimization method is effective and sufficiently creates solutions that can be considered acceptable, as we can also visually evaluate from the 3D representation of the air velocity distribution found in the room (Figure 9). Thus, the model generates solutions that could provide informative insight during the process of decision making, even for complex façade configurations as the one implemented in the present experimentation.

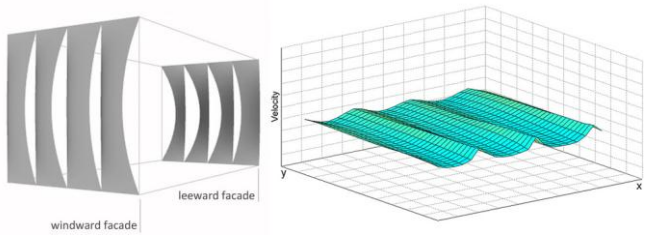

Figure 9. The optimized form of the openings and 3D representation of the velocity values found indoors that exhibit good distribution.

Moreover, the tests that factor in human circulation, where a number of louvres have openings with inclination set at 50°, enabling the remaining louvres to be optimized, achieved a convergence of acceptable solutions in regard to human comfort levels. Among the successful tests, a specific pattern of the configuration of louvres came up in the solutions. Firstly, once more the sizing of inlets and outlets roughly matched. Secondly, the pattern that emerged indicated an interaction between the louvres of the windward and the leeward façades. As a general overview, the louvres placed in opposite positions between the two sides exhibited inversely proportional inclinations, creating a better distribution of air (Figure 10). This shows a trend towards a solution of the addressed problem, converging in an optimal form of the two opposite façades.

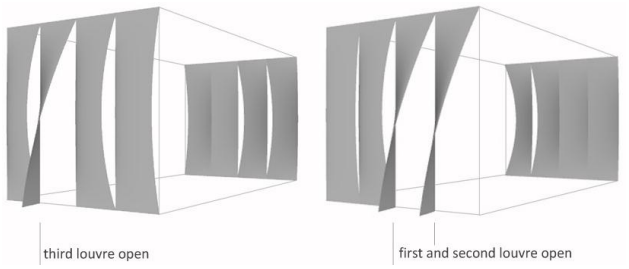

Figure 10. Two examples that depict the trend appears between the windward and leeward facades in the optimized solutions.

As presented in this paper, the method of computing the fitness combined four different functions. In this light, a system of multiple layers was created for the evaluation process. This method provided the study with a complete set of criteria with the aim to create a robust methodology that allows an accurate evaluation method. However, this method added extra complexity to the optimization problem, resulting in a high level of difficulty towards the convergence of one solution. The four calculations taken into account were conflicting. For example, throughout the optimization process a satisfactory result should exhibit average velocity that falls into a specific range of low values and low maximum velocity but high volumetric rate exchange, which are contradictory attributes. Although the problem was complex throughout the majority of the tests, the genetic algorithm managed to converge in solutions that achieve the required standard conditions.

The coupling of FFD and GA is a computationally demanding scheme, however. For every design instance to be evaluated, the fluid simulation should run across the whole domain, creating a time consuming performance analysis method where approximately 6 hours are needed until the GA converges in a solution. The complexity appears visually in the fitness graph of the tests where two louvres in a row should remain open and thus a great amount of air was introduced indoors. In these cases the optimization process remained steady in local optima, for about 100-200 generations, until a better solution was found (Figure 11). Hence, a refinement of the optimization algorithm so as to integrate a hybrid-heuristic model is proposed for further investigation.

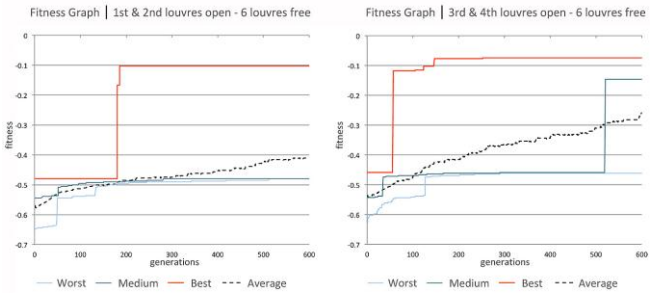

Figure 11. Improvement over generations of three population members (optimization process).

5. CONCLUSION

The paper presented the extent to which simulation of natural airflow can potentially be a contributing parameter in the conception of performance aware designs. A specific case study, where two façades consisting of elastically deformable vertical louvres, was implemented to enable experimentation. A set of fulfilling design instances that have been analysed for their ventilation performance have been generated. The coupling of fluid dynamics simulation and genetic algorithm have proved an effective way to design, taking into account wind-induced ventilation. The aftermath of integrating such a methodology could be the choice of passive cooling systems instead of mechanical air conditioning systems, which are more popular in architectural concepts to date. Providing a platform for experimentation, this paper aims to stimulate a reciprocal conversation between performance and shape. As a general overview, this paper underlines that the form of a structure can be enriched by the information provided from its performance attributes. This way a structure will be able to

exhibit inherent performative qualities from the initial stages of its creation.

Acknowledgements

This research was supported by the State Scholarships Foundation of Greece. In addition, the first author would like to express her gratitude to Anna Mavrogianni, Vagelis Giouvanos and Petros Koutsolampros for their suggestions on critical points of the study.

References

ASHRAE-55 (AMERICAN SOCIETY OF HEATING). 2010. Refrigerating and Air-Conditioning Engineers. ANSI/ASHRAE Standard 55-2010 Thermal Environmental Conditions for Human Occupancy. Atlanta: ASHRAE.

ASH, M. 2006. Fluid Simulation for Dummies, [online] Available at: <http://mikeash.com/pyblog/fluidsimulation-for-dummies.html> [Accessed 1 June 2012].

AUTODESK (Autodesk Education Community). 2011. Sustainability Workshop: Wind ventilation. [online] Available at: <http://sustainabilitywork shop.autodesk.com/fundamentals/wind-ventilation> [Accessed 15 June 2012].

AWIBI, H., D. 1989. Application of Computational fluid Dynamics in Room Ventilation, Building and Environment, 24(1), pp. 73-84.

CHEN, Q. AND ZUO, W. 2009. Real time or faster-than-real-time simulation of airflow in buildings, Indoor Air, 19 (1), pp. 33-44.

CHEN, Q. AND ZUO, W. 2007. Validation of fast fluid dynamics for room airflow, Proceedings of the 10th International IBPSA Conference Building Simulation, pp. 980-983, Beijing, China.

CHEUNG, J., AND LIU, C. 2011. CFD simulations of natural ventilation behaviour in high-rise buildings in regular and staggered arrangements at various spacings, Energy and Buildings, 43, pp. 1149-1158.

CHRONIS, A. 2010. Generative Fluid dynamics, Integration of fast fluid dynamics and genetic algorithms for wind loading optimization of a free form surface. Diploma thesis. MSc AAC. UCL.

CHRONIS, A., TURNER, A., TSIGKARI, M. 2011. Generative Fluid Dynamics: Integration of Fast Fluid Dynamics and Genetic Algorithms for Wind-Loading Optimisation of a Free Form Surface, Proceedings of the Symposium on Simulation for Architecture and Urban Design at the 2011 Spring Simulation Multi-conference, Boston, USA, pp. 79-86.

COWELL, R. 2012. Seminar Review: The Natural Ventilation of UK School Classrooms, UCL, October 2011. Natural Ventilation News, 5, CIBSE Natural Ventilation Group Management Committee, London, pp.7-8.

FEDKIW, R., STAM, J., AND JENSEN, H., W. 2001. Visual Simulation of Smoke. In SIGGRAPH 2001 Conference Proceedings, Annual Conference Series , pp. 15-22.

GARRILHO DA GRACA G., CHEN Q., GLICKSMAN L. R., NORFORD L. K. 2002. Simulation of wind-driven ventilative cooling systems for an apartment building in Bejing and Shangai. Energy and Buildings, 34. pp.1-11.

HENSEL, M. 2008. Performance oriented design, precursors and potentials. Architectural design, (78) 2, Wiley Academy, London. pp.48-51.

HENSEL M. AND MENGES A. 2008. Inclusive performance: Efficiency versus effectiveness towards a morpho-ecological approach for design. Architectural Design, 78 (2), Wiley Academy, London. pp. 54-63.

HENSEL, M., HENSEL, D., S., GHARLEGHI, M., AND CRAIG, S. 2008. Towards an architectural history of performance. Architectural Design, 78 (2), Wiley Academy, London. pp. 25-37.

ISO (INTERNATIONAL STANDARDS OFFICE). 2005. ISO 7730-2 Ergonomics of the thermal environment. Analytical determination and interpretation of thermal comfort using calculation of the PMV and PPD indices and local thermal comfort criteria. Geneva: ISO.

KATO, S. AND MURAKAMI, S. 1985. Three-dimensional numerical simulation of turbulent air flow in ventilated room by means of 2-equation model. International Symposium Computation Fluid Dynamics, Tokyo.

KLEIVEN, T. 2003. Natural ventilation in buildings. Architectural concepts, consequences and possibilities. Phd Thesis. Norwegian University of Science and Technology.

KNIPPERS J. AND SPECK T. 2011. Design and construction principles in nature and architecture. Bioinspiration and Biomimetics, 7.

MALKAWI A. M. 2004. Developments in environmental performance simulation. Automation in Construction, 13(4). pp.437-445.

MALKAWI A. M., SRINIVASAN R. S., YI Y. K., AND CHOUDHARY R. 2005. Decision support and design evolution: integrating genetic algorithms, CFD and visualization. Automation in construction, 14. pp.33-44.

MATLAB (WEBSITE). 2012. Surface and mesh creation. [online] Available at: <http://www.mathworks.com/help/matlab/ref/surf.html > [Accessed 30 July 2012].

MENDEZ, G. 2012, Barriers for natural ventilation in the UK. Natural Ventilation News, 5, CIBSE Natural Ventilation Group Management Committee, London, pp.3-5.

RIBA (ROYAL INSTITUTE OF BRITISH ARCHITECTS). 2011. Sustainability Hub. Natural ventilation stuck ventilation. [online] Available at:< http://www.architecture.com/SustainabilityHub/Designstrategies/Air/Air.aspx >, London: RIBA. [Accessed 9 June 2012].

STAM J. 2003. Real-fluid dynamics for Games. In Proceedings of the Game Developer Conference, March 2003.

STAM, J. 1999. Stable Fluids, In SIGGRAPH 99 Conference Proceedings, Annual Conference Series, pp.121-128.

SUGA, K., KATO, S., HIYAMA, K. 2010. Structural analysis of Pareto-optimal solution sets for multi-objective optimization: An application to outer window problems using Multiple Objective Genetic Algorithms, Building and Environment, 45, pp. 1114-1152.

TURNER, A. 2010. Genetic Algorithm. [online] Available at:< http://www.openprocessing.org/sketch/3101>. [Accessed 5 July 2012]

A Review of the Brazilian NBR 15575 Standard: Applying the Simulation and Simplified Methods for Evaluating a Social House Thermal Performance

Tassia H. T. Marques1 and Karin M. S. Chvatal1

[1] University of Sao Paulo, Architecture and Urban Planning Institute of Sao Carlos
400 Av. Trabalhador Saocarlense
Sao Carlos, Sao Paulo, Brasil
tassia.marques@usp.br

Keywords: Housing Thermal Performance Simulation, NBR 15575 Standard, Thermal Performance Regulation.

Abstract

The new Brazilian ABNT NBR 15575 Standard (the "Standard") recommends two methods for analyzing housing thermal performance: a simplified and a computational simulation method. The aim of this paper is to evaluate both methods and the coherence between each. For this, the thermal performance of a low-cost single-family house was evaluated through the application of the procedures prescribed by the Standard. To accomplish this study, the *EnergyPlus* software was selected. Comparative analyses of the house with varying envelope U-values and solar absorptance of external walls were performed in order to evaluate the influence of these parameters on the results. The results have shown limitations in the current Standard computational simulation method, due to different aspects: weather files, lack of consideration of passive strategies, and inconsistency with the simplified method. Therefore, this research indicates that there are some aspects to be improved in this Standard, so it could better represent the real thermal performance of social housing in Brazil.

1. INTRODUCTION

The Brazilian NBR 15575 Standard - Residential buildings - Performance (ABNT 2012), establishes performance requirements for residential buildings. Among the requirements to be met, one of them refers specifically to the thermal performance of buildings. It is worth mentioning that this Standard is expected to be approved by March 2013.

In general, the thermal performance as established by the NBR 15575 Standard seeks to meet the comfort needs of residents in their homes. There is not any mention of heating or cooling systems. It considers that the housing thermal performance depends only on the interactive behavior between external walls, roof and floor. It allows the thermal performance to be evaluated for external walls and roof independently, or for the building as a whole, defining requirements according to the bioclimatic zone where the building is located. The eight Brazilian bioclimatic zones are prescribed by ABNT NBR 15220 (ABNT 2005).

The Standard establishes two procedures: simplified normative—list of pre-requirements to be fulfilled—and the evaluation method through computer simulation, offered as an alternative, in case the building does not meet the requirements by the simplified method. Figure 1 below outlines the evaluation of thermal performance recommended by the Standard.

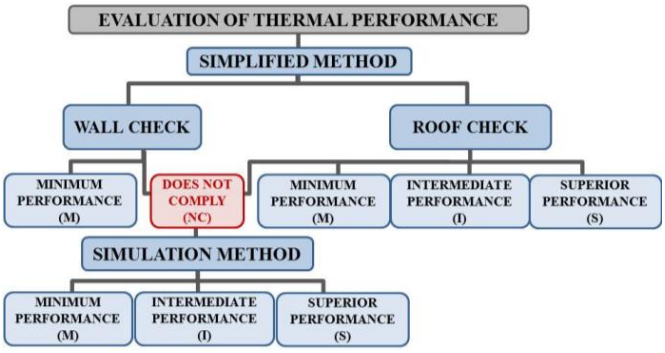

Figure 1: Thermal performance evaluation procedure according to the NBR 15575 Standard.

In the simplified procedure, the sole requirement is that thermal transmittance (U), solar absorptance (α) and heat capacity (C) of external walls and roof have to be below certain limits. Values corresponding to the bioclimatic zone 4, where the city analyzed in this paper is located, are placed in Table 1. It can be noted that according to the Standard's logic, better performance levels are related to lower U-values and solar absorptance (α).

			α ≤ 0.6	α > 0.6
Walls (Minimum Performance/M)	U (W/m².K)	M	≤ 3.7	≤ 2.5
	C (KJ/m².K)		≥ 130	
Roofs (Minimum/M, Intermediate/I or Superior/S Performance)	U (W/m².K)	M	≤ 2.3	≤ 1.5
		I	≤ 1.5	≤ 1.0
		S	≤ 1.0	≤ 0.5
Notes: Walls are classified just as minimum performance/M or it does not comply/NC				

Table 1: Thermal properties of walls and roofs according to NBR 15575 Standard.

The method of evaluation by simulation recommends using software validated by ASHRAE Standard 140 (ASHRAE 2004). The building should be modeled following the guidelines shown in Table 2. Basically, the simulation has to be performed for the house with no occupation and windows and doors closed.

Climate file	Summer and Winter design days
Solar Orientation	According to the project, or: a) Summer: bedroom or living room window to the west (another wall to the north, if possible) b) Winter: bedroom or living room window to the south (another wall to the east, if possible)
Internal gains	No internal gains
Infiltration	1 air change / hour (ACH)
Shading	Consider shading elements, if they are provided in the building
Envelope absorptance	Walls and roof color specified in the project. If wall color is not defined, use three absorptance values 0.3, 0.5 and 0.7
General observations	Each room has to be considered as one thermal zone If the building does not meet the minimum performance in the summer, consider one of the options below: a) adoption of external or internal solar protection, reducing at least 50% of the direct solar radiation b) ventilation rate of 5 ACH c) Combination of the two previous strategies

Table 2: Guidelines for simulations according to NBR 15575 Standard.

Comparisons are made between the outdoor air temperature and the maximum or minimum indoor air temperatures in longer permanence rooms (bedrooms and living rooms) for Summer and Winter design days, based on the following performance levels (Table 3).

	Performance level	Temperatures required for Bioclimatic Zone 4
Summer	Minimum/M	$T_{i,\,max} \leq T_{o,\,max}$
	Intermediate/I	$T_{i,\,max} \leq (T_{o,\,max} - 2\ °C)$
	Superior/S	$T_{i,\,max} \leq (T_{o,\,max} - 4\ °C)$
Winter	Minimum/M	$T_{i,\,min} \geq (T_{o,\,min} + 3\ °C)$
	Intermediate/I	$T_{i,\,min} \geq (T_{o,\,min} + 5\ °C)$
	Superior/S	$T_{i,\,min} \geq (T_{o,\,min} + 7\ °C)$
Notes $T_{i,\,max}$ is the indoor maximum air temperature, in degrees Celsius, during the Summer design day $T_{o,\,max}$ is the outdoor maximum air temperature, in degrees Celsius, during the Summer design day $T_{i,\,min}$ is the indoor minimum air temperature, in degrees Celsius, during the Winter design day $T_{o,\,min}$ is the outdoor minimum air temperature, in degrees Celsius, during the Winter design day		

Table 3: Minimum, intermediate and superior thermal performance according to NBR 15575 Standard.

This Standard has been causing a great impact in the national civil construction industry. Considering its significance in the actual scenario, it is worth analyzing if its procedures would really lead to better residential building thermal performance. There are still few studies that analyze the NBR 15575. Loura, Assis e Bastos (2011) compare this Standard with other Brazilian housing energy efficiency regulation; Brito et al (2012) analyze the limits prescribed by the simplified method for one bioclimatic zone (the hot and humid zone number 8) and Sorgato et al (2012) analyze some aspects of the Standard text and justify the need for a better consideration of the effect of shading and ventilation. Thus, this paper aims to evaluate the simplified and simulation methods prescribed by the Standard and the coherence between each other. This paper focuses on social housing, due to the general lack of quality usually found in this type of building and the large housing deficit in Brazil.

2. METHODS

The thermal performance of a social housing model was analyzed. The analyses were performed according to the simplified and simulation procedures as described in the Standard, regardless of whether the building had fulfilled the simplified method requirements or not. The simulations followed the recommendations shown in Table 2. The selected computer program for simulating thermal-energy performance was the *Energy Plus* (EERE, 2012). To evaluate the coherence between the two methods, the simulations were accomplished considering different external walls and roof thermal transmittance and solar absorptance, and the same thermal capacity. The values were chosen to cover all ranges considered in Table 1.

The analyzed model corresponds to a single-family and single-storey two-bedroom residence (Figure 2). It represents a typical model of social housing, obtained from a major housing funding agency in Brazil. The simulations were performed for the city of São Carlos, State of São Paulo, latitude 22°01'S and longitude 47°53'W, which represents a subtropical climate, with mild and dry winters and hot and humid summers (Table 4). This city belongs to Brazilian bioclimatic zone four.

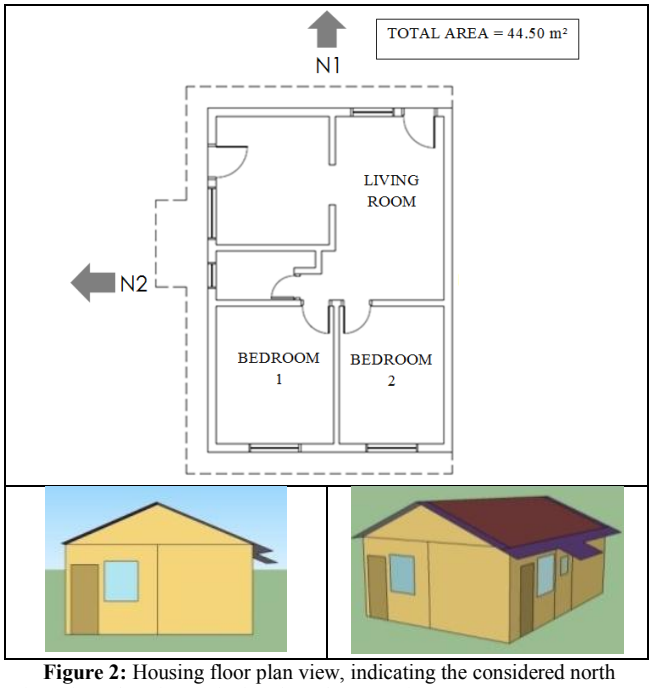

Figure 2: Housing floor plan view, indicating the considered north orientations; housing main façade and perspective.

In addition to the verification of design days, recommended by the NBR 15575 Standard, an analysis was carried out based on the building's annual performance. The EPW climate file was obtained from a national database (Roriz 2012). Annual heating and cooling degree-hours were obtained for the rooms of longer stay (living-room and two bedrooms). The limits of 18 °C for heating and 26 °C for cooling were considered.

Month	Max T (°C)	Min T (°C)	AverUR (%)
January	26.3	18.3	76.6
February	27.5	18.5	74.5
March	26.5	17.6	73.7
April	25.5	16.6	75.7
May	22.7	12.7	71.1
June	23.1	13.1	70.5
July	24.4	12.0	53.2
August	26.1	14.8	57.9
September	26.0	13.8	59.0
October	27.9	17.6	65.2
November	27.8	17.0	68.5
December	27.4	17.4	70.7
Average	25.9	15.8	68.1

Max T- monthly average maximum air temperature
Min T- monthly average minimum air temperature
AverUr- monthly average relative humidity

Table 4: Climate data for Sao Carlos, SP.

Table 5 summarizes the main input data for the simulations and their variations. With the exception of solutions defined for walls and roofs, the other fixed parameters correspond to the most common values for this type of housing in Brazil.

3. RESULTS

3.1. Comparison between Simulation and Simplified Procedures

In the analysis corresponding to the simplified procedure, the U-value, the absorptance and the heat capacity of the walls and roof must comply with certain limits (Table 1). That is, by the simplified procedure only the requirements for walls and roofs are evaluated. In the studied cases (Table 6), it can be noted that if the walls or the roof show absorptance above 0.6 (dark colors) and that the thermal transmittance is above 2.5 (for the walls) or 1.5 (for the roofs), the minimum performance is not met. These three cases are highlighted in the two first columns of Table 6. When this occurs, the simulation procedure has to be done, when the performance of housing is evaluated as a whole. Otherwise, it is not necessary to simulate the building.

Variable parameters			
Solar Orientation (Figure 2)	N1 - analysis of the Winter design day and by the degree-hour method[1] N2 - analysis of the Summer design day		
α_w[2]	$\alpha_w1 = 0.30$	$\alpha_w2 = 0.56$	$\alpha_w3 = 0.72$
α_r[3]	$\alpha_r1 = 0.30$	$\alpha_r2 = 0.90$	
Construction solutions for the external walls (W) (Material order from outside to inside)	W1 Solid brick (10cm) uncoated U = 3.70 W / m². K and C = 149 kJ / m². K		
	W2 Mortar (2.5 cm) + expanded polystyrene insulation (0.5 cm) + solid brick (10cm) U = 2.40 W / m². K and C = 149 kJ / m². K		
	W3 Mortar (2.5 cm) + expanded polystyrene insulation (1cm) + solid brick (10cm) U = 1.85 W / m². K and C = 149 kJ / m². K		
Construction solutions for the roof (R) (Material order from outside to inside)	R1 Mortar (2.5 cm) + insulation (expanded polystyrene) 0.5 cm + concrete slab 10cm + mortar 2.5cm U = 2.30 W / m². K and C = 270 kJ / m². K		
	R2 Fiber cement tile (slab and cover) (0.8cm) + expanded polystyrene insulation (0.5 cm) + concrete slab (12cm) U = 1.61 W / m². K and C = 264 kJ / m². K		
	R3 Fiber cement tile (slab and roof) (0.8cm) + expanded polystyrene insulation (1cm) + concrete slab (12cm) U = 1.34 W / m². K and C = 264 kJ / m². K		
Fixed parameters			
Window glass type	Clear glass 4 mm Solar transmittance at normal incidence: 0.84		
Percentage of window area	window area/ wall area bedrooms: 19.3% living room: 16.3%		
Construction solution for the internal walls	Mortar (2.5 cm) + hollow concrete block 9 cm + mortar (2.5 cm) U = 2.27 W / m². K, C = 206 kJ / m². K		
Internal gains	No internal gains		
Air infiltration	1 ACH in each room and in the attic		
Notes [1] A reference house, with usual walls and roof constructions was simulated in various solar orientations and the N1 orientation resulted in the maximum heating plus cooling degree-hours (considering the sum of the three rooms). [2] α_w= Solar absorptance of the external surface of the walls [3] α_r = Solar absorptance of the roof			

Table 5: Main parameters of the simulations.

Alternative simplified methods to simulation can be pointed to by standards in order to facilitate the analyses of building models that have typical features. Thus, the performance of less elaborate buildings can be quickly evaluated. The simulation analysis, a way to assess more accurately the housing performance, could be used only when necessary. Therefore, coherence between these methods is expected, so that the simplified method represents a reliable building performance. Or, if the model is simulated, its performance has to be equal or superior to the evaluation provided by the simplified method. This consistency between both methods was always observed when the building performance did not comply with the simplified procedure requirements (highlighted cases in Table 6: (g), (m) and (n)). It can be noted that in these three cases, when the buildings were simulated, two distinct situations were found:

1) in the Summer, the performance continued to not meet the criteria and in the Winter, minimum performance was achieved. This happened in cases (g) and (m);

2) minimum performance was achieved both in the Summer and Winter. This happened in case (n).

Moreover, there are other situations in which the coherence between the methods was not observed. In such cases, highlighted in Table 6 (cases (d), (h), (l) and (o)), the performance requirements were met according to the simplified method, and later it was shown that the performance requirements were lower or unmet according to the simulation method. This type of result, also observed in other situations (Brito et al. 2008), indicates that there are problems in the Standard's simplified method. It is believed that the evaluation of a home building solely by the thermal properties of its environment, without considering other factors influencing the thermal performance is, in principle, one form of flawed analysis. Even in the case of social interest housing, which meet very limited standards and have very similar architectural features. After all, these results regarding very simple low-cost housing, show that the limits set by the simplified method do not consistently represent what happens in the simulation. Furthermore, it is important to highlight that the NBR 15575 Standard is valid for any type of residential building, in which the performance differences due to other factors, such as the percentage of glass area, could lead to greater inconsistencies.

Envelope thermal properties Walls and Roof (U, α)	Evaluation by Simplified Procedure		Evaluation by Computer Simulation Procedure	
	Performance		Performance	
	Walls[1]	Roofs	Winter	Summer
(a) W1, α_{w1} + R2, α_r1 (3.7, 0.3) + (1.61, 0.3)	M	M	M	M
(b) W2, α_w1 + R2, α_r1 (2.4, 0.3) + (1.61, 0.3)	M	M	M	M
(c) W3, α_w1 + R2, α_r1 (1.85, 0.3) + (1.61, 0.3)	M	M	M	I
(d) W1, α_w2 + R2, α_r1 (3.7, 0.56) + (1.61, 0.3)	M	M	M	NC
(e) W2, α_w2 + R2, α_r1 (2.4, 0.56) + (1.61, 0.3)	M	M	M	M
(f) W3, α_w2 + R2, α_r1 (1.85, 0.56) + (1.61, 0.3)	M	M	M	M
(g) W1, α_w3 + R2, α_r1 (3.7, 0.72) + (1.61, 0.3)	NC	M	M	NC
(h) W2, α_w3 + R2, α_r1 (2.4, 0.72) + (1.61, 0.3)	M	M	M	NC
(i) W3, α_w3 + R2, α_r1 (1.85, 0.72) + (1.61, 0.3)	M	M	M	M
(j) W2, α_w1 + R1, α_r1 (2.4, 0.3) + (2.3, 0.3)	M	M	M	M
(k) W2, α_w1 + R2, α_r1 (2.4, 0.3) + (1.61, 0.3)	M	M	M	M
(l) W2, α_w1 + R3, α_r1 (2.4, 0.3) + (1.34, 0.3)	M	I	M	M
(m) W2, α_w1 + R1, α_r2 (2.4, 0.3) + (2.3, 0.9)	M	NC	M	NC
(n) W2, α_w1 + R2, α_r2 (2.4, 0.3) + (1.61, 0.9)	M	NC	M	M
(o) W2, α_w1 + R3, α_r2 (2.4, 0.3) + (1.34, 0.9)	M	M	M	NC

[1] According to the Standard, in the simplified procedure, walls are classified just as minimum performance or it does not comply (NC).

Minimum performance not achieved by the simplified method or the simulation method

Performance by simplified method superior to performance by simulation

Table 6: Compliance to the simplified and simulation methods according to NBR 15575 Standard.

3.2. Evaluation by the NBR 15575 Standard Simulation Procedure (Design Days) and by the Annual Simulation

3.2.1. Walls with different U-values and absorptances

Figures 3 and 5 show the results according to the Standard simulation procedure, which considers the Summer (Figure 3) and Winter (Figure 5) design days. Figure 3 shows in the y-axis the $T_{i, max}$ in bedroom 1 during the Summer design day (warmest room in the summer, with the worst sun exposure). Figure 5, the $T_{i, min}$ in bedroom 2 during the Winter design day (the coolest room in the winter, also with the worst sun exposure). The U-value of the external walls is shown in the x-axis and each line corresponds to distinct solar absorptances of the house walls. In all combinations shown in these graphs, the roof was maintained with U = 1.61 W / m². K and α = 0.3. The performance levels that the house would have according to the Standard's criteria, presented in the Introduction, are indicated on the graph.

Figures 4 and 6 show the results for the same simulations, run for a typical year. The annual cooling (Figure 4) and heating (Figure 6) degree-hours are represented on the y-axis. They are the sum of the annual degree-hours of the longer permanence rooms. In this case, there are no performance levels, as this is not a method regulated by the Standard.

Figure 3 shows that the minimum performance was not reached in the case of higher values of absorptance and U-value. These results follow the same pattern of the simplified method table (Table 1), where only walls with a U-value below certain limits are accepted and these limits decrease as the solar absorptance increases. However, the limits found for this situation differ somewhat from those established by the Standard, which led to the incompatibility between the simplified and the simulation methods presented in the previous item (Table 6). The results for the typical year simulation (Figure 4) present the same graphic pattern.

In Figure 5 it was found that the minimum performance was reached in all cases analyzed. Similar to the Summer, walls with higher U-value show the worst performance (lower temperatures in the Winter). Nevertheless, with respect to solar absorptance, the result was the opposite of that observed for the Summer: the higher the absorptance, the better the performance. That is, for the situations above,

it is more difficult to achieve minimum performance in the Summer than in the Winter. Similar results were obtained by the annual analysis method (Figure 6).

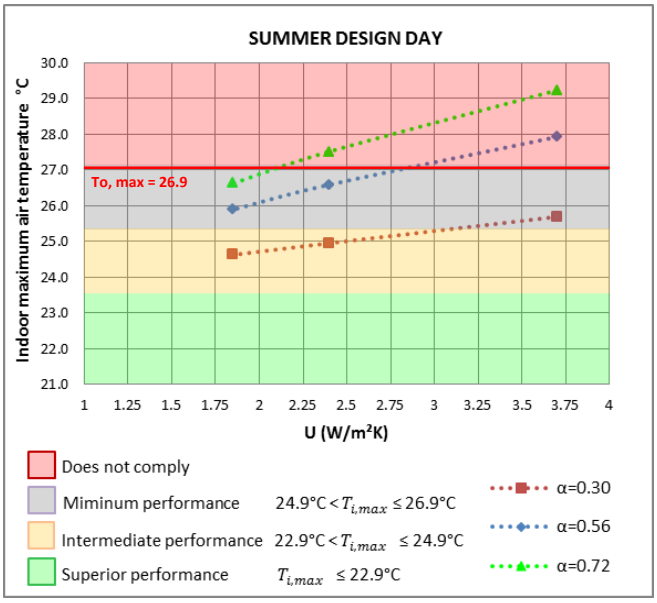

Figure 3: Indoor maximum air temperature during the Summer design day, for the house with various external walls U-value and solar absorptance. Roof with U = 1.61 W / m². K and α = 0.3.

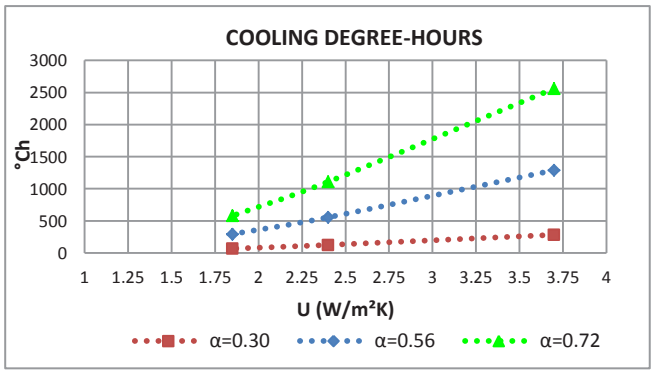

Figure 4: Cooling degree-hours during a typical year for the house with various external walls U-value and solar absorptance. Roof with U = 1.61 W / m². K and α = 0.3.

3.2.2. Roofs with different U-values and absorptances

Similarly to the walls, Figures 7, 8, 9 and 10 refer to the results for Summer and Winter design days (Figures 7 and 9) and for the annual simulation (Figures 8 and 10), considering distinct roof U-values and solar absorptances. In such cases, the wall was maintained with U=2.4 W / m². K and α = 0.3 for all combinations.

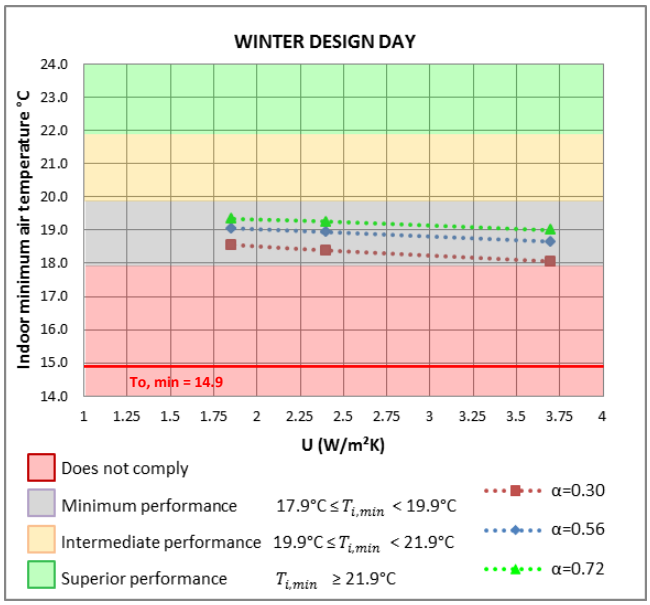

Figure 5: Indoor minimum air temperature during the Winter design day, for the house with various external walls U-value and solar absorptance. Roof with U = 1.61 W / m². K and α = 0.3.

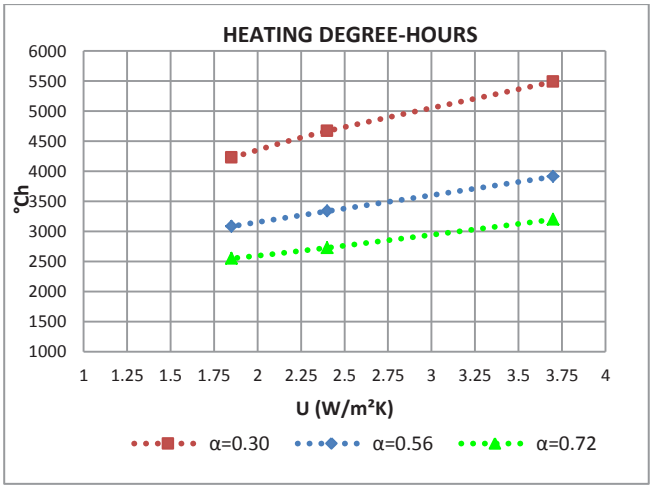

Figure 6: Heating degree-hours during a typical year for the house with various external walls U-value and solar absorptance. Roof with U = 1.61 W / m². K and α = 0.3.

The results for the Summer design day (Figure 7) are very similar to the ones previously shown in Figure 3: the higher the absorptance and the U-value, the worse the performance. Also, in a similar way, these results follow the same logic of the simplified method (Table 1), but the limits do not correspond exactly to those established by the Standard, resulting in the incompatibilities already mentioned in the previous items (3.1 and 3.2.1). The typical year simulation (Figure 8) shows the same pattern of results.

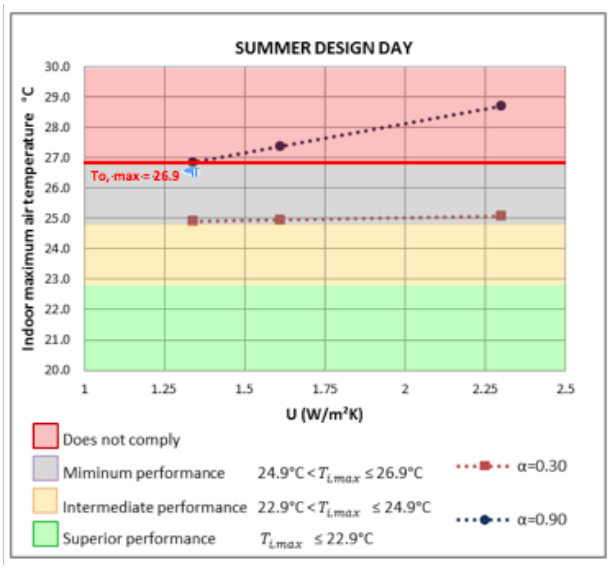

Figure **7:** Indoor maximum air temperature during the Summer design day, for the house with various roof U-value and solar absorptance. External walls with U = 2.40W / m². K and α = 0.3.

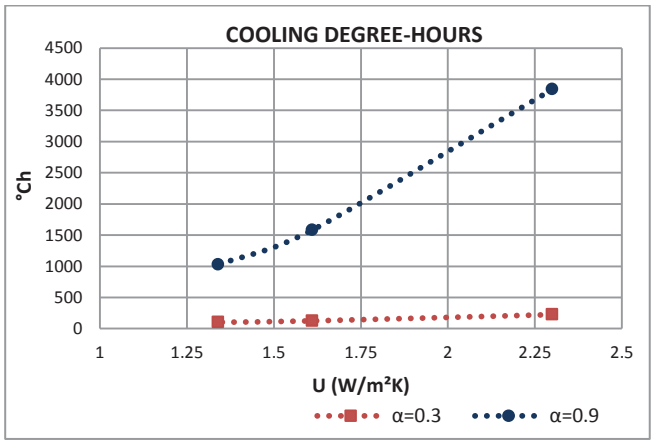

Figure 8: Cooling degree-hours during a typical year for the house with various roof U-value and solar absorptance. External walls with U = 2.40W / m². K and α = 0.3.

Regarding the Winter, all cases are classified with the minimum performance (Figure 9). Again, the results follow the same pattern already mentioned in 3.2.1, when thermal properties of walls were varied. And also, achieving the desired performance for Summer requires more of the envelope than for Winter. The typical year simulation showed the same type of results (Figure 10).

3.3. General Remarks on the Simulation Method

When applying the simulation procedure, some aspects that could be improved were observed and they are listed in the sequence.

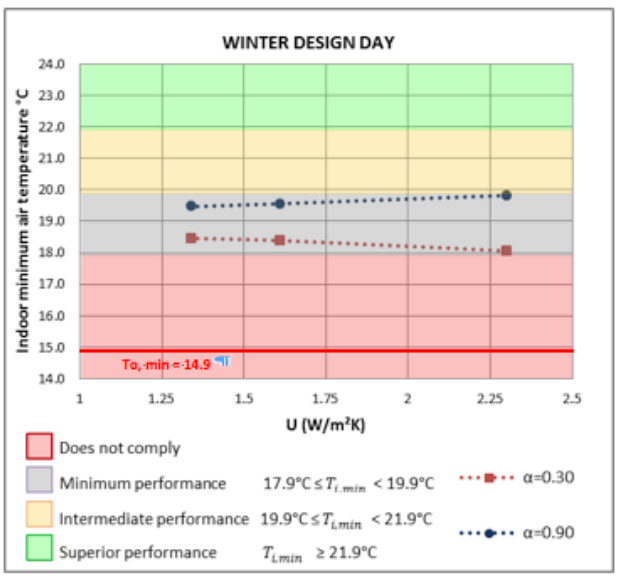

Figure 9: Indoor minimum air temperature during the Winter design day, for the house with various roof U-value and solar absorptance. External walls with U = 2.40W / m². K and α = 0.3.

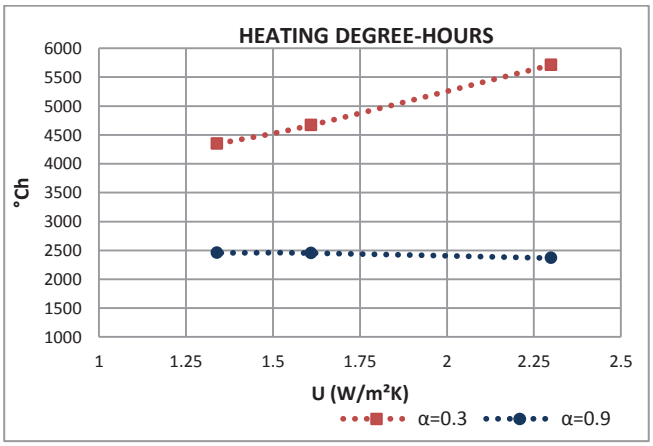

Figure 10: Heating degree-hours during a typical year for the house with various roof U-value and solar absorptance. External walls with U = 2.40W / m². K and α = 0.3.

1) Definition of Summer and Winter design days. Climate data for these days have to be based on the Standard, which provides this information only for state capitals, and even then the data is incomplete. This indicates the need of interpretation by the user, which may lead to misunderstandings.
2) Lack of consideration of important aspects that influence the building performance and may change its final evaluation. The simulation procedure does not consider the building with internal gains—people, equipment, lighting—

which would change the results, and better reflect the thermal performance of the housing in interaction with its users (as it occurs, for example, in another national standard that assesses home energy efficiency, the RTQ-R (INMETRO 2010)). Also, the NBR 15575 Standard disregards the use of passive strategies for thermal comfort, such as natural ventilation and shading. These resources are widely used in this type of building in Brazil, where the use of artificial conditioning systems has a high cost. As evidenced by Sorgato et al. (2012), these aspects significantly influence the building performance and should be considered more thoroughly by the Standard.

4. CONCLUSION

The NBR 15575 Standard has been widely discussed in the academy and civil construction industry. With its approval, a great impact in the construction market is expected. However, this research indicates that there are some aspects to be improved. This Standard presents simplified and simulation procedures to verify the thermal behavior of buildings. The simplified method is important because it provides general guidelines for easy verification, requiring no special knowledge, as in the case of the simulation method. Nevertheless, in the results analyzed in this research, incoherence was found between the two methods presented in the Standard. In four studied situations, performance requirements were met according to the simplified method, and later it was shown that they were lower or unmet according to the simulation method. In addition, the simplified method sets limits for the envelope thermal properties that do not take into account the equilibrium between different needs for Summer and Winter. Moreover, evaluating a building only by its opaque surface is a limited assessment. There are other aspects, such as the glass area, that should also be considered. It is also important to highlight that these results are limited to Sao Carlos (Brazilian bioclimatic zone number four). The analysis of other climate zones would contribute to improving NBR 15575.

Acknowledgements

This research is supported by FAPESP (Sao Paulo Research Foundation).

References

ABNT - ASSOCIAÇÃO BRASILEIRA DE NORMAS TÉCNICAS. 2005. NBR 15220: Desempenho Térmico de edificações. Rio de Janeiro.

ABNT - ASSOCIAÇÃO BRASILEIRA DE NORMAS TÉCNICAS. 2012. NBR 15575: Edificações habitacionais – Desempenho. Rio de Janeiro.

ASHRAE - AMERICAN SOCIETY OF HEATING, REFRIGERATING AND AIR-CONDITIONING ENGINEERS. 2004. ANSI/ASHRAE Standard 140: Standard method of test for the evaluation of building energy analysis computer programs. Atlanta.

BRITO, A. C. ET AL. 2012. Contribuições para o aprimoramento da NBR 15.575 referente ao método simplificado de avaliação de desempenho térmico de edifícios. In: ENCONTRO NACIONAL DE TECNOLOGIA DO AMBIENTE CONSTRUÍDO, XIV, 2012, Juiz de Fora. Anais... Juiz de Fora: ENTAC.

EERE -DEPARTMENT OF ENERGY EFFICIENCY AND RENEWABLE ENERGY. 2012. EnergyPlus. Version 7.1.0.012. US: Department of Energy Efficiency and Renewable Energy, Office of Building Technologies.
Available at: <http://apps1.eere.energy.gov/buildings/EnergyPlus/>. Accessed: 22 June. 2012.

INMETRO - INSTITUTO NACIONAL DE METROLOGIA, NORMALIZAÇÃO E QUALIDADE INDUSTRIAL. 2010. RTQ-R - Regulamento técnico da qualidade para o nível de eficiência energética em edificações residenciais. Rio de Janeiro.

LOURA, R. M.; ASSIS, E. S.; BASTOS, L. E. G. 2011. Análise comparativa entre resultados de desempenho térmico de envoltórias de edifício residencial gerados por diferentes normas brasileiras. In: ENCONTRO NACIONAL DE CONFORTO DO AMBIENTE CONSTRUÍDO, XI, 2011, Búzios. Anais eletrônicos... Búzios: Associação Nacional de Tecnologia do Ambiente Construído, 2011. 1 CD-ROM.

RORIZ, M. 2012. Arquivos Climáticos de Municípios Brasileiros. ANTAC – Associação Nacional de Tecnologia do Ambiente Construído. Grupo de Trabalho sobre Conforto e Eficiência Energética de Edificações. Relatório Interno. Available at: <http: www.labeee.ufsc.br/downloads/arquivos-climaticos>. Accessed: 12 May 2012.

SORGATO, M. J. ET AL. 2012. Nota técnica referente à avaliação para a norma de desempenho NBR 15575 em consulta pública em 2012. Florianópolis: LabEEE. Available at: <http://www.labeee.ufsc.br/sites/default/files/publicacoes/notas_tecnicas/NT_15575_FINAL.pdf>. Accessed: 20 Nov. 2012.

Thermal Reconstruction of a Crime Scene Using Calibrated Simulation

Nathan Brown[1,2], M. Susan Ubbelohde[1,3], George Loisos[1], Santosh Philip[1], and Ibone Santiago[1]

[1]Loisos + Ubbelohde
1917 Clement Ave, Bld 10A,
Alameda, CA, 94501
nathan@coolshadow.com
susan@coolshadow.com
george@coolshadow.com
santosh@coolshadow.com
ibone@coolshadow.com

[2]California College of the Arts
1111 8th St,
San Francisco, CA 94107
nbrown@cca.edu

[3]University of California, Berkeley
College of Environmental Design,
230 Wurster Hall #1820
Berkeley, CA, 94720
subb@berkeley.edu

Keywords: Energy Model Calibration, Energy Model Accuracy, Free Floating Energy Simulation, Legal Application of Thermal Simulation.

Abstract

This study utilized energy simulation in support of a forensic pathology time of death analysis for a corpse discovered in a single family residence two years prior to the study. In order to produce an accurate estimate of the interior temperature profile at the time of death, a thermal model was constructed using EnergyPlus and calibrated using environmental monitoring data from the site.

The thermal model was able to predict the temperature in the room of interest within 1.4°C (2.5°F) with 90% confidence. This model was then altered to account for known differences between the monitoring period and the period of interest, and used to predict what the temperature profile had been at the time of death.

This study adds to a small body of work that compares simulated to measured performance data for unconditioned spaces, which should have a growing relevance as building energy performance simulation (BEPS) tools are used to model passive strategies.

1. INTRODUCTION

This project began with an unlikely telephone call from an attorney seeking expert advice for a homicide trial. Two years prior, a body had been discovered in the closet of a two-story home in the greater Sacramento area (Figure 1), and a suspect had been arrested. With the trial imminent, the attorney's question to us was, would we be able to determine the temperature in the closet in the specific building during the few days prior to the discovery of the deceased? Crime scene photographs showed that the building's HVAC system was off at the time the corpse was discovered. The temperature of the environment was a critical component of the time of death analysis, the findings of which might help the jury determine the verdict.

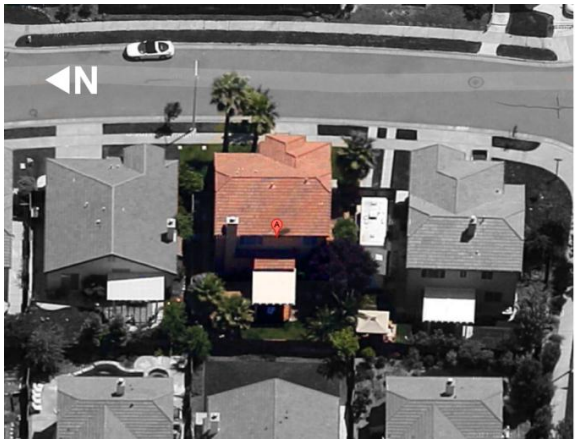

Figure 1. The two-story house in question.

Because the findings would need to withstand courtroom scrutiny, the accuracy and defensibility of this study were critical. While we did not find a precedent for such a forensic study in the literature, there is a body of work that seeks to accurately predict thermal conditions in buildings for design and operation using building energy performance simulation (BEPS).

In order to increase the accuracy of a BEPS model, studies have shown that a process of calibration can be used to "tune" a model. Many published calibration studies focus

on HVAC system energy use; relatively few published studies show a process for calibrating a BEPS model of an unconditioned space or building. As an initial phase of a project to form a process for comparing measured and simulated building energy performance data, Maile and colleagues built a BEPS model of a typical zone of the San Francisco Federal Building, installed a series of environmental sensors, and then used the monitored data to adjust modeling assumptions so that simulated and measured temperatures were similar (Maile 2010b). Pereira and Ghisi built a calibrated model of a ventilated and otherwise unconditioned single-family house to investigate the impact of thermal envelope properties on occupant comfort (Pereira and Ghisi 2011).

However, even if a BEPS model of the house is calibrated with perfect accuracy for the current time period, there may have been conditions that existed immediately before and after the homicide that deviate from the assumptions in the calibrated model. The goal of this study was not only to create an accurate calibrated simulation of the house, but also to make assumptions explicit and meaningful in terms of their effect on the final predicted temperature profile.

Through a court order, we were able to gain access to the specific house in question, which had just been vacated by the previous tenant. We designed a thermal model and an environmental monitoring plan to address the goals of the study. We used monitored data gathered on site to calibrate the thermal model, and then adjusted assumptions to account for known differences between the calibration period and the period of interest at the time of the homicide.

2. THERMAL MODEL

In order to build an accurate thermal model of the house, we selected EnergyPlus as the BEPS platform. EnergyPlus provided a few key advantages for this study:

- sub-hourly calculation and explicit zone temperature reporting, allowing direct comparison to high-resolution monitored temperature data.
- accurate representation of thermal mass effects
- ability to explicitly control model geometry through Open Studio, and assumptions through a text editor

The published validation reports for EnergyPlus (version 7.0.0.036) include a suite of tests described by the BESTEST methodology. For this study, a series of four envelope tests was especially relevant. As with most of the tests published, each test result is compared with results of other BEPS models of the same zone. The report then identifies if the EnergyPlus results are within the approved range (defined by Min and Max in Table 1 below). We note that EnergyPlus (E+) simulation results are within the acceptable range for all cases. However, we also note that the EnergyPlus value is an average of 1.4°C (2.4°F) above the minimum, and an average of 1.2°C (2.2°F) below the maximum. The range indicates acceptance of some internal error in BEPS in general. Since the report is not an empirical validation, it may or may not indicate how closely EnergyPlus might simulate actual measured results.

	Average Hourly Zone Temperature (°C)			
	BESTEST			
Test case	**Min**	**Ave**	**Max**	**E+**
Low mass building	24.2	25.3	27.4	26.2
High mass building	24.5	25.5	27.5	26.4
Low mass, ventilated	18.0	18.9	20.8	18.9
High mass, ventilated	14.0	14.5	15.3	14.6

Table 1: EnergyPlus BESTEST validation results for free floating zone temperature models (Henniger and Witte 2011)

In order to recreate the crime scene of the past using BEPS and also describe our confidence in the result, an accounting of the potential errors was required. In general, we grouped these errors into problems with

- the accuracy of the BEPS platform algorithms,
- the ability of the BEPS platform to accurately represent site conditions, or
- the accuracy of BEPS user inputs (weather, shading, building envelope properties, internal gains, incorrect simulation settings, etc).

The first and last were described as internal vs external error types, respectively, by NREL researchers who completed research to systematically test for internal error types (Judkoff and Neymark 1999). The Building Energy Simulation Test (BESTEST) methodology that they developed formed the basis for the current ANSI/ASHRAE 140-2007 standard for testing for BEPS accuracy. ANSI/ASHRAE 140-2007, Standard Method of Test for the Evaluation of Building Energy Analysis Computer

Programs (ANSI/ASHRAE 2007), specifies a series of analytical tests to determine if a BEPS platform produces results in line with theoretical results as well as with other BEPS platforms.

The ANSI/ASHRAE 140-2007 standard tests for accuracy using a simplified, geometrically pure model. Errors may also be introduced due to the approximations, assumptions, and simplifications required for building a BEPS model of an actual building, such as simplification of geometry, the assumption that zone air is perfectly mixed, or the simplification of foliage shading (Maile 2010a).

2.1. Input Model

We designed the input model with particular attention to the downstairs closet (the space of interest) and zones adjacent (see Figure 2 below). All zones in the house were modeled, although we grouped rooms into a single zone for spaces that were not adjacent to the downstairs closet. While we constructed the initial model carefully, we did not spend too much time working out fine details, since we were working with initial instincts about what parameters might be critical. We anticipated that the calibration process would reveal any critical, inaccurate assumptions.

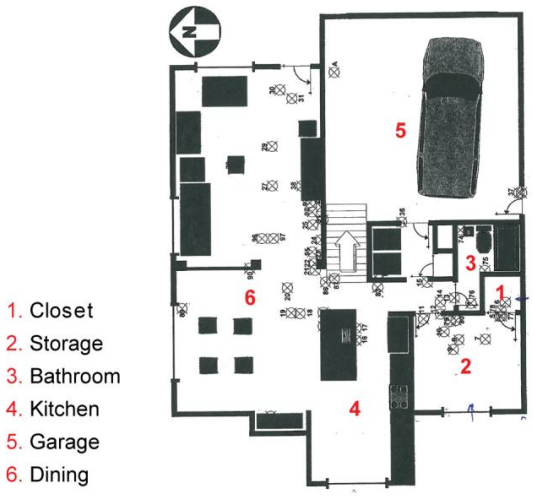

Figure 2. First floor plan of house, showing spaces referenced. The body was discovered in the closet.

The energy model consists of 9 thermal zones, representing the downstairs closet, adjacent storage room, bathroom, kitchen, garage, dining room/foyer, the southwest bedroom, its closet, the rest of the upstairs, and the attic. Site shading objects were modeled for buildings and trees adjacent to the house (Figure 3).

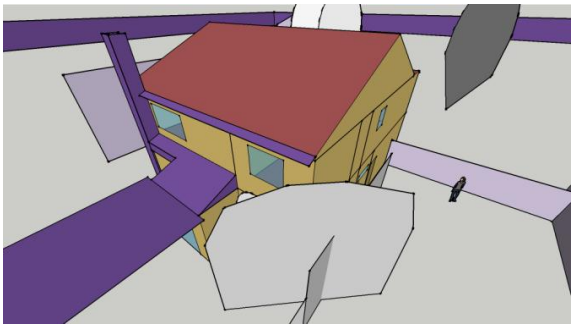

Figure 3. Screen capture of the energy model geometry. Note that two-dimensional purple and white objects are providing shade, while orange and red objects define thermal zones.

The thermal model was built using building materials and processes most likely to be used at the time of the house construction (1999). This was further informed by regulatory research regarding the Title 24 (California Energy Code) requirements in effect at the time. In addition we performed thorough non-invasive observations at the building at the time of the monitoring equipment installation.

To estimate internal loads, we considered possible ways that energy can be added to the house other than through the building enclosure or through the HVAC system. These included the presence of people, the use of lights, the use of electronics, and heat from miscellaneous installed equipment. Up until the last 36 hours, it was assumed the house energy use was typical as indicated by monthly energy bills. Energy usage for the month prior was an average of 18.1 kWh/day, which increased to an average of 18.8 kWh/day for the period of interest. While this use would not in reality be constant, we started this analysis with the assumption that the energy use was consistent, or about 765 W on average. While this may have introduced errors associated with daily patterns (ie, day vs night), it should accurately represent heat balance due to electric loads over the course of a multiple day period as long as daily patterns did not vary significantly.

In order to assign these electrical loads to appropriate thermal zones in the house, we referenced police photographs. These indicated a variety of appliances in the kitchen and adjacent laundry area. On the second floor, each

bedroom contained some electrical devices, but the main electric load upstairs was the home entertainment system in the living area. This would be a significant draw on electricity: our research on the model of television in the second floor living area indicated that it would have been drawing over 200W when it was on. Electricity use for lighting would also have been distributed throughout the house. Lastly, the HVAC system energy for operating the heat pump would be present in the attic space. Our rough approximation is that the power was distributed as follows: 50W in the attic, 500 W upstairs (of which 100W was placed in the southwest bedroom), and 200W in the kitchen.

The use of natural gas would also have contributed to internal loads through hot water heating and cooking. For an unoccupied time period, we estimated the hot water heater energy use to be about 80W on average (ie, the rate at which energy dissipates from the system to the space regardless of the actual use of hot water).

The model contained no interzonal airflow. This was a characteristic we initially expected to change in the calibration process, but did not for two reasons. First, the closet and its adjacent storage room were connected to the rest of the house through a door that the police report described being approximately 1 inch open. Since infiltration was the only other potential source of air movement, we did not expect to find significant interzonal airflow in these two critical spaces. Second, the calibration process yielded effective ventilation areas far smaller than our initial assumptions, as well as closely matching temperature profiles without assuming interzonal airflow.

3. ENVIRONMENTAL MONITORING

For the site monitoring, we deployed a series of sensors throughout the house to track temperature conditions in the first floor closet, as well as in the adjacent zones: the adjacent storage room, bathroom, kitchen, dining room, garage, southwest bedroom, and southwest bedroom closet.

We studied the police photographs from the crime scene and police reports in order to configure components of the house as close as possible to how they were found when the body was discovered. The door between the downstairs closet and storage room was approximately 7 inches ajar, and the door between the storage room and kitchen was about 1 inch ajar. The downstairs bathroom window was partially open, as was the window to the bedroom above the storage room. The storage room window was closed. Interior blinds on upstairs windows were also adjusted. The HVAC system was turned off.

The sensors used were HOBO U12-012 dataloggers. These dataloggers were configured to record simultaneous measurements at 10-minute intervals for a period of approximately 5 weeks, starting February 8, 2012. We monitored air temperature in all rooms and also monitored globe temperature and insulated surface temperatures in the downstairs closet and adjacent storage room.

3.1. Weather Data

We identified two sources of weather data in the general area: Sacramento International Airport (KSMF) and the Sacramento Municipal Utility District Rotating Shadowband Radiometer (SMUD RSR). We found that these stations would have data available for the calibration period as well as at the time of the homicide.

To ensure that the data from the nearby weather stations was comparable, we also collected weather data on site to confirm that the weather data collected from the nearby stations would accurately represent the conditions on site. We used an industry-standard weather station (a HOBO H21 weather station) to monitor temperature, humidity, wind speed and direction, and solar radiation.

The outdoor temperature profile at the site was very similar to the temperature profile recorded at the airport. The solar radiation was a very close match between the global horizontal radiation measured on site compared with the global horizontal radiation measured at the SMUD RSR (Figure 4). Clear days show a nearly identical profile, while

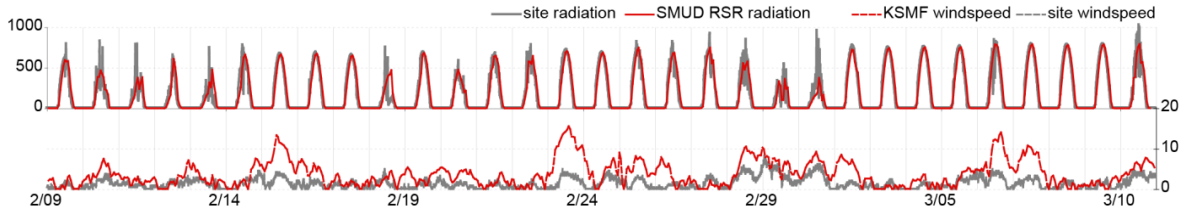

Figure 4. Comparison of solar radiation (left axis, W/m2) and wind speed (right axis, mph) between local and site weather stations.

cloudy days show a similar overall pattern despite discrepancies due to passing clouds. The comparison of wind speed shows the most variation between site and KSMF data (Figure 4). This is due in part to differences in the boundary layer profile between the open, unobstructed airport site and site monitoring station surrounded by obstacles such as houses and trees. Note that while the magnitude of the wind speed does not match, the variation is similar. This means that the speed of wind at the site can be approximated by applying a boundary layer correction factor to the airport wind speed, a correction that is taken into account in EnergyPlus.

Finally, the frequency distribution of wind direction shows a similar general trend: winds tended to come from either the north or the S/SE. During southerly wind patterns, the airport has a tendency to show winds more from due south, while the site winds veer slightly to the east. The weather stations report a wind direction of 0, or North, when wind is calm.

In preparation for the use of weather data in an EnergyPlus simulation, the EnergyPlus weather file (EPW) for Sacramento Metropolitan Airport was modified. For the weather file dates that corresponded to the monitoring period, the temperature, humidity, dewpoint, wind speed, and wind direction were replaced with data from KSMF, and the global horizontal radiation, diffuse horizontal radiation, and direct normal radiation were replaced with data gathered from SMUD RSR.

4. MODEL CALIBRATION

The process of model calibration was iterative. Each iteration was configured to generate subhourly air temperatures for each zone. Data visualization was utilized to graph all simulated zone temperatures with the monitored data, which initially did not match well (Figures 5 and 6). We began the process by exercising parameters to assess the effect on overall results (insulation, ground temperature calculation parameters, thermal mass, and ventilation) and performing elimination parametrics where major thermal drivers were eliminated in turn (no solar gain through

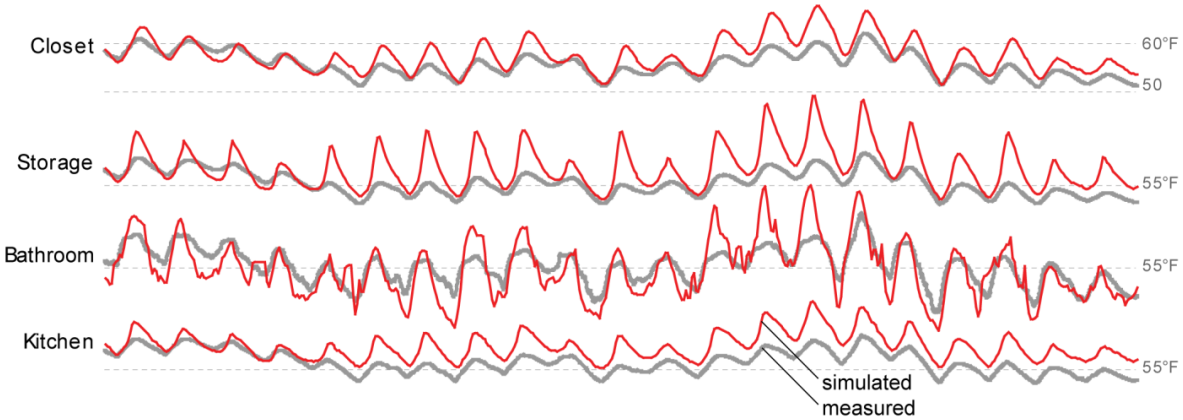

Figure 5. Before calibration: time series visualization of simulated and measured zone air temperatures for first 3 weeks of monitoring period.

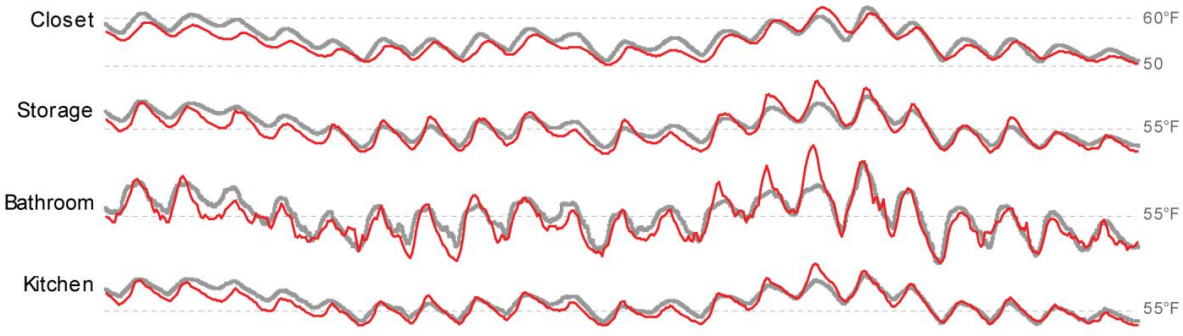

Figure 6. After calibration: time series visualization of simulated and measured zone air temperatures for first 3 weeks of monitoring period.

windows, no solar gain on opaque surfaces, no wind). This helped us develop intuition about which parameters were driving the system.

Then, the model was tuned to produce results that matched the measured temperatures more closely. For each iteration, a hypothesis was developed for differences observed between simulated and actual results, and how differences varied across different zones. Ultimately, measured and simulated results matched closely (Figure 6).

We ran the energy model simulation using the weather file modified for the calibration period. We then compared the conditions predicted by the energy model with the actual conditions measured on site. The iterative calibration process resulted in simulated data that much more closely matched the measured data (calibrated assumptions are shown in Table 2). The following are a number of notable alterations made to the model in the calibration process:

- removed scheduled occupancy that was erroneously included in the model
- fine tuned interior space temperature parameter of slab temperature pre-processor
- reduced ventilation opening areas by an average of 73%
- fine tuned foliage shading objects
- slightly increased thermal mass in walls
- increased shading coefficient of storage room window screen based on photograph of weave

In addition, we noted that Energy Plus reported a spike of transmitted solar radiation entering the storage room when the sun was at a very large angle of incidence upon the storage room window. Our back of the envelope calculations of transmitted solar radiation for that moment in time indicated that this was likely an internal EnergyPlus error that could not be completely corrected in the calibration process.

Ultimately, we found that a model with the parameters listed in Table 2 generated the closest fit for all zones, and the downstairs closet in particular. These assumptions constitute the calibrated model. Comparing the modeled results to the actual conditions measured results in predicted temperatures that vary from the actual recorded by less than 2.5°F (1.4°C) 90% of the time; the average difference was 1.1°F (0.6°C). The quality of fit for the model is shown in Figure 6 above.

Lights and Equipment	Lights off; 80W from water heater in garage	
Site Shading	Buildings, 8 palm trees, a tall hedge to the south, a deciduous tree to the southwest, and an orange tree near the storage room window (as shown in Figure 3 above)	
Building Shading	Various overhangs	
Infiltration	Effective Leakage Area calculation as described by Title 24 legacy building calculation methods	
Ventilation	Effective open areas for airflow due to wind and stack effect for the bathroom (0.04 m^2), garage (0.04 m^2), southwest bedroom (0.03 m^2), and attic (0.186 m^2) zones	
Internal Mass	Closet, Storage, Bedroom, Bedroom Closet : none Kitchen : counter tops, millwork, interior walls	Bathroom : fixtures Dining, upstairs : interior walls
Exterior Roof	U-Factor with film = 1.965 W/m^2-°K	
Attic Walls	U-Factor with film = 0.851 W/m^2-°K	
Exterior Walls	U-Factor with film = 0.472 W/m^2-°K	Thermal Mass = 32mm gypsum inside insulation
Exterior Windows	U-Factor = 3.979 W/m^2-°K	Solar Heat Gain Coefficient (SHGC) = 0.70
Attic Floor	U-Factor with film = 0.162 W/m^2-°K	
Ground Floor	Uninsulated concrete slab, with wood finish in closet and storage	
HVAC System	Off during calibration period, but set to heating mode at 68°F prior to calibration period	

Table 2: Calibrated model settings

5. TEMPERATURE PROFILE PREDICTION

Even though the BEPS model and the monitoring configuration were designed to match the configuration of the house at the time of the homicide, there were differences that could not be recreated and therefore could not be calibrated. During our study of crime scene photographs and police reports, we maintained a list of differences between the calibrated model and the model that would be used to simulate the time period around the homicide (Table 3).

The model was changed to take these assumptions into account, and then it was run with a weather file constructed from the time period of the homicide. We ran two predictive models to assess a range of potential scenarios for HVAC system use, since there was some uncertainty regarding when the HVAC system was switched off. While police photographs indicated that the system was off when the body was discovered, the client indicated that the system could have been on or off prior to Saturday at 1:30 PM. We therefore ran two models to simulate each scenario.

The energy model run with calibrated parameters and the addition of the assumptions described above showed that the temperature in the closet varied during the time period of interest as shown in Figure 7, for each HVAC scenario. A 90% prediction interval is shown, based on the error observed in the calibration process.

5.1. Potential Sources of Error

We acknowledge three potential types of error: inaccurate simulation, non-representative sampling for calibration boundary conditions, and inaccurate assumptions regarding conditions in the prior period. The inaccuracy of the simulation is evidenced by the error between modeled temperatures and measured temperatures. Our selection of a 90% prediction interval accounts for this error.

Lights and Equipment	attic: 50W, kitchen:200W, upstairs:400W, bedroom:100W
Site Shading	Include foliage of deciduous tree to the southwest
Internal Mass	Addition of objects in various zones: furniture, boxes, etc
People	1 person with a typical residential occupancy for all spaces except closets and attic, up to Saturday, at 1:30 pm, and 0 people after that
HVAC System	Unconditioned: System set to 68°F up until two weeks before the body was found
HVAC System	Partially conditioned: System set to 68°F up until Saturday at 1:30 pm

Table 3: Additional assumptions for prediction.

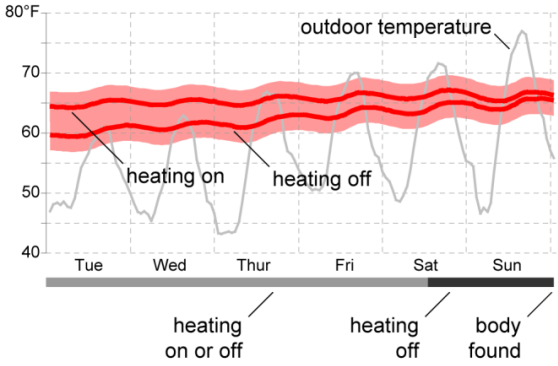

Figure 7. Projected temperature variation in the downstairs closet during the time period of interest.

Because the study occurred during a slightly different season, the boundary conditions present in the calibration period differed from those during the time period of interest. Ideally, the study would have been conducted during the same dates to obtain a more representative sample of boundary conditions, but even this approach will not generate a perfectly representative sample.

Finally, our list of assumptions for differences in the thermal model may have contained inaccuracies. Rather than exhaustively study the impacts of varying these assumptions, we instead provided the list of potential errors. For each, we made a preliminary, directional estimate about the effect that the potential error would have on the results. For instance, Table 4 shows the effect of two potential errors in estimating the Lights and Equipment load (a complete list was provided to the client). We proposed further analysis to study sensitivity to any of these assumptions if any became points of contention in the trial.

Error: Energy use for Lights and Equipment was much higher than typical during or prior to the period of interest. *Effect:* Reduce system energy use during system operation, and slightly increase temperatures when system was off.
Error: Energy use for Lights and Equipment was much lower than typical during or prior to the period of interest. *Effect:* Increase system energy use during system operation, and slightly decrease temperatures when system was off.

Table 4: Example of two potential errors between calibration period and period of interest.

6. DISCUSSION

This study presents a framework for calibrating a BEPS model to address a specific question relating to interior environmental quality. If the question had changed, the method of calibrating the model would also likely have changed. For instance, the zoning and detail in the energy model would have been distributed quite differently had the deceased been discovered in a different room. Similarly, the particular set of data available to us influenced the course of the study. With available data from SMUD RSR, we did not have to estimate the three components of solar radiation used in the EPW files. Had we less information about the crime scene or about the house, our confidence interval would have been larger, or our potential sources for error between the time periods would have become more problematic.

A number of findings may be significant relative to the field. First, we note that just as ventilation has been a significant calibration adjustment in prior EnergyPlus calibration studies (Pereira and Ghisi 2011, and Maile et al 2010b), so too was it a significant adjustment in this study. Our finding that we needed to reduce ventilation area by 73% is consistent with a finding that a 75% reduction in airflow was needed to achieve calibrated results for an unconditioned San Francisco Federal Building (Maile et al 2010b). This may indicate a tendency for the theoretical airflow models in EnergyPlus to not account for the complexity of dynamic airflow in actual buildings.

Second, the ability of EnergyPlus to closely match measured data in unconditioned buildings is not represented well in the literature. This study indicates that EnergyPlus is able to reproduce such conditions within a reasonable tolerance. As BEPS is used to study passive conditioning strategies, this finding should be pertinent.

7. CONCLUSION

We were ultimately able to provide an estimate for the temperature profile in the space of interest, along with quantitative and qualitative assessments of potential error. This was due to the availability of BEPS software capable of representing space at a sufficient level of detail, the availability of data, access to the property for monitoring and the process of calibrating the model.

In future studies, one significant tool that could be brought to bear to potentially improve the accuracy of the result is automated parametric optimization. Rather than tuning variables by eye, a parametric search algorithm could be employed to search for a set of parameters that minimizes the error between simulated trend lines and measured trend lines. We believe that optimization tools can complement the framework presented in this paper, but that they could not replace the prioritization or sequence of comparisons. Parametric analysis can only help identify issues with the handful of initially selected parameters; knowing which parameters to study and change was a result of studying subsequent iterations.

Finally, we note that the findings of our study were in the end not presented in court, for reasons not known to us. However, the importance of the accuracy of this study is underscored when considering that the accused has been convicted and is currently serving a life sentence for the homicide.

Acknowledgements

The authors would like to thank Michael Martinez for his help setting up environmental monitoring equipment on the site, as well as the public defender's office for the opportunity to perform this research. Lastly, the authors would also like to thank Brendon Levitt, who fielded the initial call for the project and did not hang up the phone.

References

ANSI/ASHRAE 2007. Standard 140-2007, Standard method of test for the evaluation of building energy analysis computer programs. American Society of Heating, Refrigerating and Air-Conditioning Engineers. Atlanta, GA.

HENNINGER, R.H, AND WITTE, M.J. 2011. EnergyPlus testing with building thermal envelope and fabric load tests from ANSI/ASHRAE Standard 140-2007, EnergyPlus Version 7.0.0.036, downloaded from United States Department of Energy website, accessed Dec 26, 2012.

MAILE, T., FISCHER M., HAYMAKER, J., AND BAZJANAC, V. 2010a Formalizing approximations, assumptions, and simplifications to document limitations in building energy performance simulation. Stanford University, CIFE Working Paper WP126.

MAILE, T., FISCHER M., AND BAZJANAC, V. 2010b A method to compare measured and simulated data to assess building energy performance. Stanford University. CIFE Working Paper WP127.

PEREIRA, C.D., AND GHISI, E. 2011. The influence of the envelope on the thermal performance of ventilated and occupied houses. Energy and Buildings 43, 3391-3399.

Beginning Session, April 9

Modeling, Analysis and Simulation of a Form-Found Civic Sculpture for Lower Manhattan 67
Zak Kostura, Erin Morrow, Ben Urick
Arup, Texas Advanced Computing Center

Visualization in 3ds Max for Cell-DEVS Models Based on Building Information Modeling 75
Victor Freire, Sixuan Wang, and Gabriel Wainer
Universidade Federal de Campina Grande, Carleton University

Modeling, Analysis and Simulation of a Form-Found Civic Sculpture for Lower Manhattan

Zak Kostura[1], Erin Morrow[2], and Ben Urick[3]

[1]Arup
77 Water Street,
New York, NY, USA, 10005
zak.kostura@arup.com

[2]Arup
2 Bloor Street East,
Toronto, Canada, M4W 1A8
erin.morrow@arup.com

[3]Texas Advanced Computing Center
10100 Burnet Road (R8700),
Austin, Texas, USA, 78758
benurick@tacc.utexas.edu

Keywords: Cable Net, Nonlinear Analysis, Performance Based Design, Public Sculpture, Vector Algebra.

Abstract

Analysis and design of an 8-storey cable net sculpture for a new transit center in Lower Manhattan required its designers to adopt a highly integrated computational approach. This approach combined aspects of structural analysis, form-finding, and 3D and parametric modeling to achieve the artistic objectives of the sculptural form while ensuring desired performance of the extensive tensile system.

This paper presents an overview of the artistic and functional objectives of the cable net and describes in detail the design approach of the project team, including software integration, nonlinear analysis, geometric modeling, documentation, and construction administration. It outlines a partial approach toward performance-based design for a system with strong aesthetic objectives and a collaborative approach to construction administration to manage risk amogst the various stakeholders.

1. INTRODUCTION

Eleven lines of the New York City subway system converge at or near the corner of Fulton Street and Broadway, one block east of the World Trade Center site and two blocks south of City Hall Park. Despite their dense tangle, these lines have evaded efficient connection for nearly a century: a legacy of disparate planning and construction practices common to the era of competitive, privatized transit operation. The eleven lines around Fulton Street, which were unified under a state agency in 1968, serve as a hub for more than 300,000 transit riders each day.

Figure 1. Project rendering of central public space, showing cable net and oculus.

In the aftermath of September 11, 2001, the Metropolitan Transportation Authority enacted plans to redevelop this hub into an efficient transfer point between nearby subway lines. They began a project to replace the labyrinthian corridors retroactively constructed to link existing lines with an efficient system of pedestrian mezzanines, concourses and underpasses to link platforms

of the eleven transit lines. At the corner of Broadway and Fulton Street, the MTA planned a spacious multi-story pavilion structure to crown the new underground pedestrian network and serve as an iconic gateway to Lower Manhattan.

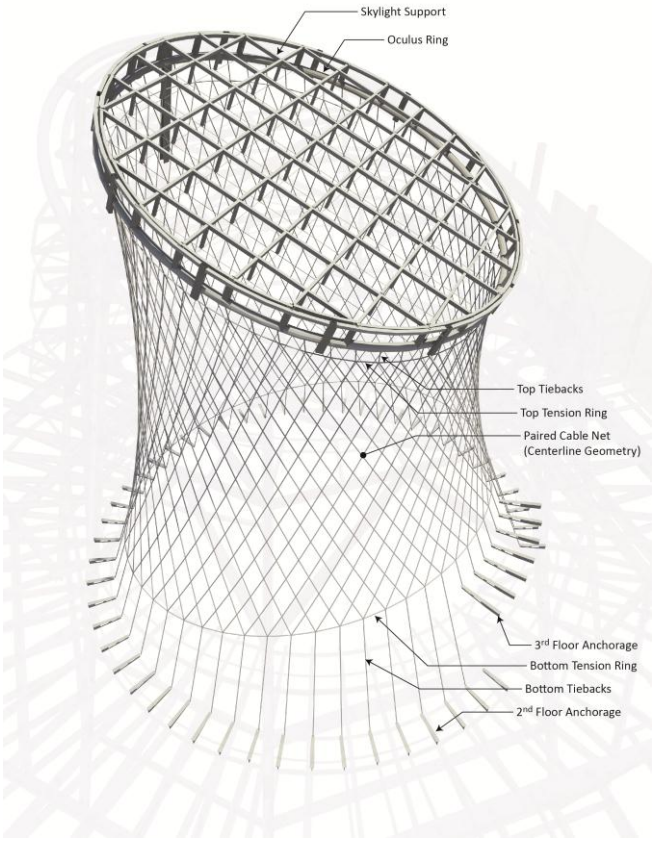

Figure 2. Cable net components and boundary support.

Arup has served as the prime consultant for the project, called the Fulton Street Transit Center, and has offered a wide range of multidisciplinary design services as well as overall planning and project management. Architectural design services for the transit center superstructure have been provided by Grimshaw, whose building concept included a three-storey glazed pavilion set around a centrally located, 8-storey dome structure. Topped with an inclined, circular skylight measuring 50 feet in diameter referred to as the oculus, this large central space marks the focal point of the extensive project and serves to collect and redirect natural sunlight through the building to the exhumed sublevels below.

The central space beneath the dome and oculus offer a unique opportunity for a large-scale artistic installation, to further add character to the space and extend the architectural objective of repurposing incident sunlight to illuminate subterranean spaces. The MTA held a public art competition to find a concept for an installation.

Submitted by artist James Carpenter, the winning entry called for a metal lining offset from the interior of the dome that would provide diffuse reflection of incident sunlight into the spaces below. Through a collaborative process with the design team, the concept was refined into a steel cable net structure supporting nearly 1,000 coated aluminum infill panels using flexible, universal node connection assemblies.

2. DESIGN

The cable net extends the full height of the central public space. It is suspended from 56 connection points around the compression ring of the oculus and anchored to as many cantilevered beams at levels 2 and 3. The form of the cable net is that of a skewed hypar. Unlike a regular hypar, this form has double curvature. Moreover, the skewed form has only one axis of symmetry. As a consequence, the shape of each four-sided infill panel is unique. Its shape is set out by the lengths and intersecting angles of cable segments adjacent to each side.

The reflective infill panels are comprised of 1/8” aluminum substrate with a high performance coating applied to the interior faces. They are perforated with a regular circular pattern to control the quantity of light reflected, reduce loading on the cable net, and permit the passage of interior air currents. The panels are linked to the cable net at each corner by cruciform connectors affixed to the nodes of the net.

The strategy for securing each panel follows conventional cladding practice. The panel is suspended from its top corner by a pin fed through a standard hole in the corresponding connector. The angle and position of the panel in space is established at the bottom corner, where a pin is fed through a vertically slotted hole that allows for correct positioning with a minimum amount of restraint. Holes in connector arms at the left and right corners are oversized to allow for independent movement of the net due to changes in temperature across the 8-storey net or air pressure caused by large air intake grills located at its midpoint.

The net is comprised of 112 stainless steel cable pairs. The cables, which are ¼" in diameter, are mechanically swaged at each node. Swages are through-bolted with cruciform connectors arranged in between the opposing cable pairs. Stainless steel rods are used for top and bottom ties as well as ring elements.

2.1. Form-Finding

An initial visual assessment of the skewed hyperbolic form proposed by the artist indicated that a form-found tensile system could be developed to fit the desired geometry. This was enabled through the use of swages at the cable net nodes that tightly grip the cables, allowing each cable segment to carry a unique tensile force and dramatically broadening the range of geometric forms achievable using a purely tensile system.

As the desired final form was known, the "form-finding" process entailed ascertaining the relative magnitude of tensile force required in each cable segment to achieve that form. Arup developed a computational model of the desired cable net geometry, including the position of all nodes. It was first run with a uniform 900-pound tensile force in each cable pair. The resulting found form varied significantly from the initial, desired geometry due to the generalized prestress force. Where the force entered was larger than the true prestress, the cable segment shortened. Where the force was smaller, the cable segment lengthened.

These geometric shifts from the initial geometry, while undesirable in principle, result in a redistribution of the generalized initial prestress. The shortening of segments that were overstressed, for example, leads directly to a reduction in the force in the element following form finding and prestress redistribution. Put simply, the prestress redistribution inherent in the form-finding process is self-correcting.

These redistributed forces were again applied to the desired architectural geometry. The resulting node displacements were smaller than those observed in the first iteration, and the redistribution of prestress resulting from this second form-finding routine further approached the correct prestress values for each cable segment.

The engineers at Arup then developed a custom subroutine using Microsoft Visual Basic for Applications, which automatically ran subsequent iterations, each time applying the redistributed loads to the original geometry and performing a form-finding routine. The routine terminated once convergence indicators were met, following the 113th iteration. The resulting prestress distribution pattern exhibited maximum average values of 906 pounds at the top and bottom rows and minimum average values of 886 pounds at mid height.

2.2. Geometric Analysis

In order to achieve this level of flexibility, the design team developed a comprehensive mathematical model of the cable net, using linear algebra to represent each one-dimensional linear component (e.g. cable segments, armatures, fold lines) as a unique vector in Euclidean space. This effort was carried out in Microsoft Excel with the assistance of Microsoft Visual Basic for Applications. These vector representations were then used to perform geometric checks to test the need for flexibility in the connection assemblies. Mathematical representations and sample geometric checks are illustrated in Figure 2 below.

Cartesian coordinates of nodes from the initial form-finding model were used as the basis for mathematical model generation. Vector equations were developed to represent each cable segment. Four adjacent vectors can be used to define the shape of a single infill panel, as illustrated in Figure 3a. Due to the three-dimensional shape of the net, the four nodes that define a single panel are not co-planar. Each four-sided panel was thus treated as a compound shape derived from two three-sided polygons sharing a common side. That common side was defined as the "fold line" and denoted $\vec{F}$, a vector oriented by the left and right corner nodes of the infill panel.

Cable segment equations were then used to check the corner angles (θ) for all panels (Figure 3b). From the tabulated data, the maximum and minimum panel angles for the entire system were readily extracted. Once known, the range of panel angles was used to establish panel edge details such as corner radii and perforation patterns.

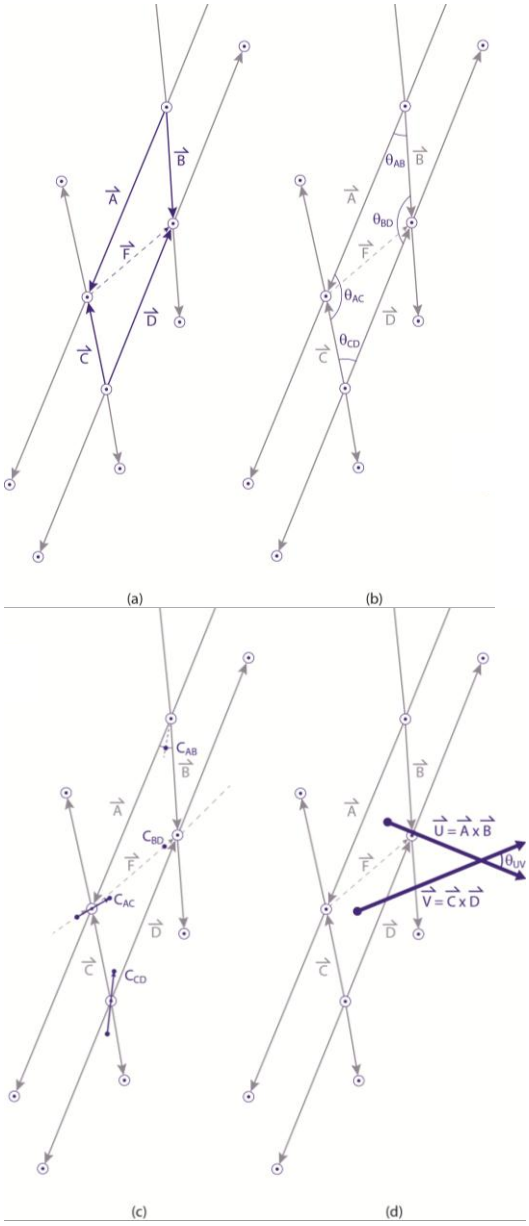

Figure 3. Mathematical model of cable net geometry.

The horizontal and vertical armatures of each connector were likewise modeled as vectors with fixed length. These vectors were set out using the location of connector bolt holes on each panel (Figure 3c). The top and right bolt holes were set out first, located a fixed distance from the nearest cable node and aligned respectively on the panel angle bisector and the fold line. As the armatures are effectively straight, vectors were drawn from these bolt holes to the nearby cable node and subsequently projected a fixed distance beyond into adjacent panels, to set out bottom and left bolt holes. This tabulated data was used to confirm that all bolt holes were suitably spaced from panel edges, and to obtain the range of angles between horizontal and vertical armatures required of a flexible universal assembly, as shown in Figure 4.

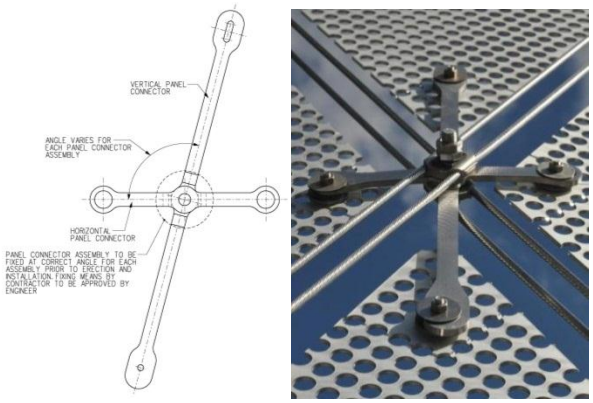

Figure 4. Perforated infill panels and universal node assemblies, with cruciform armatures and cable swages.

Figure 3d illustrates a geometric check of the angle between triangular components of a single four-sided panel. This check was necessary in order to ascertain whether planar panels could be produced, or if connector tolerances required each panel to be bent about its fold line. Analysis ultimately revealed that bending was necessary; however the range of fold angles was sufficiently slight to allow all panels to be bent to a single, averaged fold angle, thus generalizing an otherwise unique characteristic of each panel.

Numerous other geometric checks were carried out on the mathematical model of the cable net in order to fully quantify the geometric byproducts of the skewed hypar shape. Taken as a whole, these checks enabled the Arup design team to develop a range of flexible, universal assembly components that capitalized on the economies of mass production to control costs associated with the fabrication and installation of the cable net system.

2.3. Understanding Movements

The form-finding analysis performed to establish a suitable strain distribution pattern was predicated on several assumptions about the net's real-world environment. First, it assumed uniform ambient temperature and no loading from internal air pressure. Additionally, the analysis assumed an exact match between the prescribed prestress distribution and that which would be applied to the system in the field.

In reality, the 8-storey space will inevitably have thermal gradients, as warm air collects near the oculus and cool, conditioned air is diffused within the occupied space below. The ventilation strategy for the building relies on the development of air currents that must pass through the panels of the net, resulting in pressure drops across the perforated surface created by infill panels and generating loads that will influence the shape of the net.

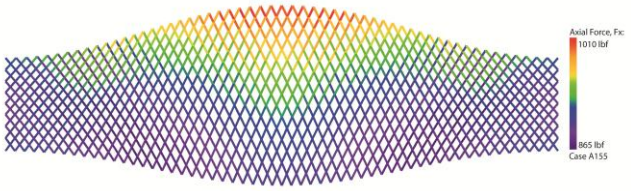

Figure 5. Axial force in cable pairs under nominal panel loading and prestress.

A realistic take on the process of tensioning the net must involve an acknowledgment of errors inherent in the final values. A review of industry standards suggested variations in applied tension loads on the order of ±20%.

Because of its scale, the cable net must be viewed as a dynamic structure, one that at any time assumes a unique form that corresponds to the sum total of loads applied. Those loads, which include the weight of panels, thermal strains, air pressures and applied prestress forces, will vary over time. Consequently the position of each cable net node will also vary. Put another way, each unique combination of loads yields a corresponding unique cable net shape.

It is essential to understand and quantify the maximum conceivable movements in the nodes of the cable net under all realistic environmental conditions. Were any of these movements to result in the transfer of tensile forces to the infill panels, such forces would quickly overwhelm the delicate aluminum elements. The cruciform connector arms thus hold each panel in place with minimal restraint in order to allow for unrestrained movement of adjacent cable net nodes.

These degrees of freedom are provided by the slotted and oversized holes in the connector arms on the left, right and bottom corners of each panel. The dimensions of these non-standard holes must be coordinated with the maximum conceivable movements in order to provide sufficient freedom of movement and avoid the transfer of force into the aluminum panels.

Arup engineers studied each environmental characteristic and developed various realistic scenarios to cover the range of corresponding loading conditions. To determine the magnitude of air pressures generated by interior air currents, a computation fluid dynamic model was developed in ANSYS. The program identified the pressure drop across panels given the known volumetric flow of intakes and diffusers throughout the building and the degree of permeability in each area of the cable net.

The scenarios for each environmental characteristic were then superimposed to generate 815 unique load combinations, each with a presumed unique cable net shape. A static non-linear analysis was conducted for each of the 815 load combinations. A custom subroutine was written to interrogate the position of each node under each load case and determine the largest changes to the support conditions of each panel. An increase in the distance between left and right corner supports was referred to as a “panel width change”; the peak value implied the required dimensions of the oversized holes at these support points. Correspondingly, an increase in the distance between top and bottom corner supports was referred to as a “panel height change”, which provided information on the necessary dimensions of the vertically slotted hole at the bottom connection point.

Analysis revealed that the largest resolved movement of any node under any perceivable load combination is approximately 2 1/16”. Broken into its components, however, this maximum movement results in a change of only 0.23” in panel width and 0.08” in panel height. The dimensions of oversized and slotted holes were correspondingly set to accommodate these movements in addition to acceptable construction tolerances of 0.25” in either direction.

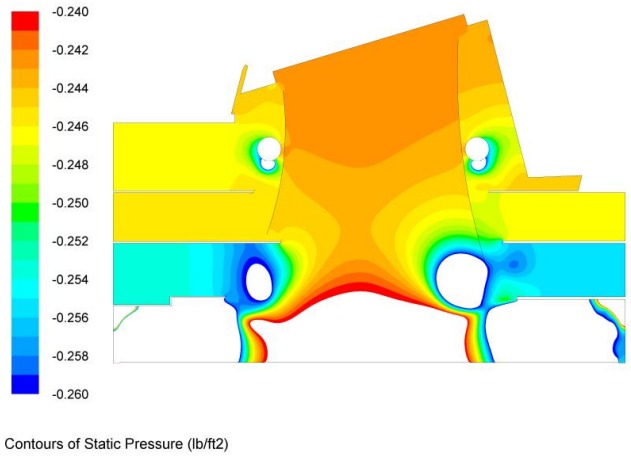

Figure 6. A computational fluid dynamic (CFD) model was generated to determine air pressure incident on each panel.

2.4. Modeling a Universal Connector

In conjunction with the project architects, Arup developed a universal cruciform connector to provide adequate panel support in the variety of configurations that result from the skewed hypar shape. Each connector is comprised of a horizontal and vertical armature, linked by a bolt at their midpoints and set between swaged cable pairs. All elements are free to rotate about the bolt axis.

This rotational freedom is needed to allow the connector armatures to conform to the various required configurations. The armatures, which are nominally 1/4" in thickness, taper to 1/8" at their midpoints to minimize the effective thickness of the armature assembly, and the corresponding eccentricity between opposing cable pairs.

The process of designing the universal connector armature required the selection of geometry that incorporated the space-saving taper while facilitating the free rotation of armature elements to accommodate the various panel configurations.

Arup developed a parametric model in Digital Project to assess the performance of various connector armature designs. Each connector component, including the armatures, bolt and swages, were individually modeled as discrete parts and subsequently assembled into a single component. That assembly was instantiated into a global model containing the 896 cruciform connector nodes.

Set-out instruction intrinsic to each connector instance facilitated the rapid configuration of each, given the position of adjacent nodes in all directions. A separate clash detection program was then used on the solids to confirm the rotational adequacy of the universal part design.

Limitations to computing power available at the time led to instantiation routines that took days to complete. The design team observed that the instantiation of solid components to be by far the most time consuming; points and lines that established the location and orientation of the components, on the other hand, were much faster to instantiate.

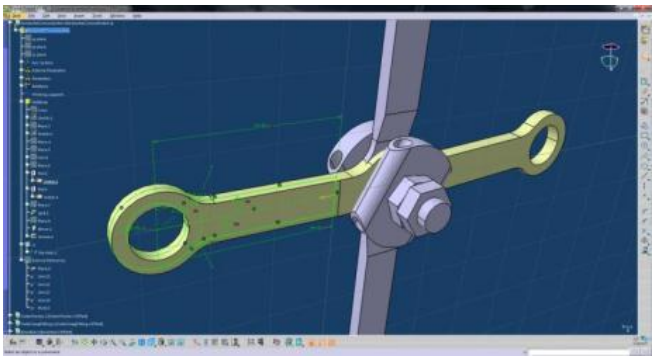

Figure 7. Parametric definition of horizontal armature.

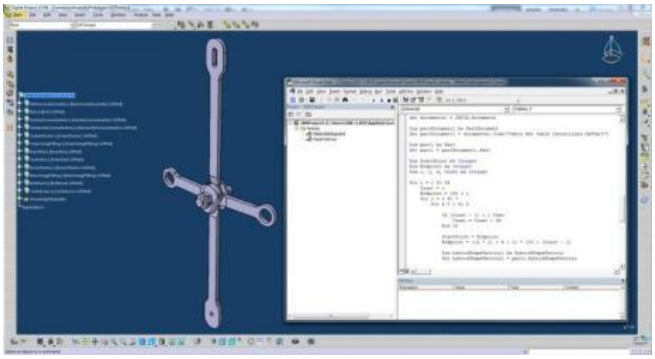

Figure 8. Custom routines instantiate the connector prototype throughout the node cloud.

In order to accelerate the process of studying each armature design, solid components were removed and only set-out lines were instantiated. A custom script was written to interrogate the relative angles between each armature pair, and the most severe angles were then modeled using the solid components to test their suitability. This modified approach to parametric modeling proved exceptionally fast, and instantiation of armatures on all 896 points was completed in a matter of seconds.

The geometry of the armatures for the universal connector was optimized for visual and performance criteria through the parametric model, and the final design was extracted from the individual part models and presented as simple 2-dimensional sections and elevations in contract drawings.

3. DOCUMENTATION AND CONSTRUCTION

The design team employed a hybrid approach to documentation, largely embracing prescriptive design but thoughtfully integrating performance criteria to ensure the selection of a specialty subcontractor knowledgeable and experienced in the construction of such a system. In addition, Arup was motivated to bring in performance requirements in order to facilitate a productive dialog with the contractor that would allow the designer to more effectively monitor and observe the contractor's coordination, shop drawing preparation, fabrication and assembly of the cable net. The resulting working environment promoted open dialog on potential construction issues and a balanced approach toward project risk management.

Construction of the transit center superstructure and fit-out of the area bounded by its enclosure and foundation beneath were packaged into a single construction contract that was awarded to a joint venture comprised of Plaza and Schiavone (PSJV) in August of 2010. The complex and unconventional nature of the cable net compelled the general contractor to bring on several specialist subcontractors to fabricate and install the tensile structure. Coordination of the cable net was managed by Enclos, the subcontractor also selected to provide façade components for the pavilion enclosure and the oculus. Cables and custom connection elements, such as the cruciform armatures, were provided by TriPyramid Structures, Inc. The anodized aluminum infill panels were provided by Durlum out of Schopfheim, Germany. Along with the steel fabrication and erection subcontractor STS Steel, these members of the construction team exhibited skill and expertise that added to the value of the design through open collaboration. Performance-based provisions in the contract documents, which were intended to incite discourse among members of the design and construction teams, brought about fruitful if occasionally intense discussion over elements of the design and strategies for its execution.

Fabrication of the cable net cables, connectors and panels are currently underway by suppliers and subcontractors. Installation of the tensile structure, which has an estimated construction cost of $3.8M, is scheduled to begin in April of 2013.

4. CONCLUSION

The Fulton Street Transit Center cable net is a powerful example of the capacity of a large tensile structure to define a landmark public space. A comprehensive understanding of the system geometry across the form, assembly and subcomponent levels was necessary in order to ensure that cost-effective, universal components embodied the necessary flexibility to accommodate the complete range of aconnection arrangements and patterns. This understanding was achieved through the development of a complete mathematical model of the system to facilitate rapid geometric checks throughout the component detailing phase, and a live parametric model of universal components to ensure a final design informed by system needs across a broad range of design disciplines.

Acknowledgements

The authors would like to thank Ricardo Pittella, P.E. (Associate Principal), John Batchelor (Director), and Craig Covil and Markus Schulte (Principals) at Arup for their supervision and guidance during the entire project. We would also like to thank James Carpenter, Richard Kress, Cameron Wu, and Torsten Schlauersbach at JCDA and Grimshaw Architects, PC, New York for their collaboration on the project. Special thanks are extended to the MTA, in particular Uday Durg, Raj Desai and Virginia Borkoski. All images courtesy of MTACC/NYCT and Arup. All images © MTACC/NYCT.

References

ANSYS, 2012. Fluent. ANSYS, Incorporated, Canonsburg, PA.

BENTLEY SYSTEMS, INCORPORATED, 2012. Microstation, V8i. Bentley Systems, Incorporated, Exton, PA.

MICROSOFT, 2012. Visual Basic for Applications. Microsoft, Redmond, WA.

OASYS LIMITED, 2012. GSA Analysis, Version 8.6. Oasys Limited, Newcastle-Upon-Tyne, UK.

ROBERT MCNEEL & ASSOCIATES, 2012. Rhinoceros 3D, Version 4.0. Robert McNeel & Associates, Seattle, WA.

Visualization in 3ds Max for Cell-DEVS Models Based on Building Information Modeling

Victor Freire[1], Sixuan Wang[2], and Gabriel Wainer[2]

[1]Dept. of Systems and Computing,
Universidade Federal de Campina Grande
Rua Aprigio Veloso, 882, Campina Grande
PB 58429-900, Brazil
victor.freire@ccc.ufcg.edu.br

[2]Dept. of Systems and Computer Engineering,
Carleton University
1125 Colonel By Dr. Ottawa
ON K1S 5B6, Canada
{swang, gwainer}@sce.carleton.ca

Keywords: DEVS, Cell-DEVS, Building Information Modeling (BIM), 3ds Max, 3D Visualization

Abstract

Building Information Modeling (BIM) increasingly benefits from modeling, simulation and visualization techniques. 3D visualization can provide a better way to obtain visual simulation results in BIM authoring tools. In this paper, we focus on improving interoperability, traceability, reusability and visibility of 3D visualization. We employ the DEVS (Discrete Event Systems Specification) formalism and its cellular extension Cell-DEVS, providing a method for visualizing Cell-DEVS models based on moving entities. We used this technique to develop a 3ds Max visualization plug-in for Cell-DEVS models based on BIM. This tool can show different animation models and allows designers to filter the building for visibility. We also show two case studies applying this tool for evacuation and occupancy simulation.

1. INTRODUCTION

Building Information Modeling (BIM) plays a significant role in the whole design lifecycle in the Architecture, Engineering, and Construction (AEC) industry. BIM is a modern way to create, document, manage and exchange information about buildings. BIM uses 3D real-time object-oriented building modeling to achieve accurate AEC projects with minimized costs, improving the way architects-contractors and fabricators work (Hardin 2009). BIM authoring tools capture a rich set of digital data, including 3D geometry (instead of 2D), properties and relationships between objects.

Modeling and simulation (M&S) has been employed in BIM applications to analyze and evaluate the performance of building designs using an iterative process with several cycles through alternative simulations (Jiang et al. 2012). Each cycle can be divided into small sub-phases (e.g. pre-design, main design, detail design). In order to evaluate the performance or find the optimal solution, at the end of each sub-phase, the designers test, analyze and refine their solutions with different simulation scenarios. Related simulation tools cover different domains, such as energy consumption, CO2 emissions, occupancy management, and evacuation planning (Wang et al. 2012).

We are interested in the interoperability of BIM and generic simulation models. In particular, we are exploring the use of the Discrete Event Systems Specification (DEVS) formalism, a popular systems theoretical approach that allows the definition of hierarchical modular models, composed by behavioral (atomic) and structural (coupled) components (Zeigler et al. 2000). Also, Cell-DEVS, which extended DEVS for modeling discrete-event spatial systems (Wainer 2009), can be used with this purpose. Here, we focus on generic 3D visualization in Autodesk 3ds Max for Cell-DEVS models. The provided tool can get information from IFC file automatically, parse the simulation results into 3ds Max and provide different options in our GUI. This tool allows designers to hide different building floors and filter models for visibility, as well as different animation features of models (the realistic model for real body movement and the arrow model for pointing the moving direction).

The following sections will present the results of this effort. We first introduce the related work about visualization techniques. Then, we present the general idea for visualizing Cell-DEVS models based on moving entities. The following section describes our implementation. We employed this tool in two case studies: Building Evacuation and Occupation model of Copenhagen House. The results have shown its higher reusability and extensibility. This kind of application brings better visualization of simulation results, enabling the designers to check building

performance, compare between different solutions and find flaws for future improvement.

2. RELATED WORK

Modeling, Simulation and Visualization has been employed in BIM applications to analyze and evaluate the performance of building designs using an iterative process with several cycles through alternative simulations (Jiang et al. 2012). 3D visualization provides a more intuitive way to obtain visual simulation results in BIM authoring tools. From 3D visualization, at the end of each sub-phase, the designers can observe, analyze and refine their solutions with different simulation scenarios. Numerous related simulation and visualization tools cover different domains, such as indoor climate, energy consumption, CO2 emissions, occupancy management, and evacuation planning (Wang et al. 2012). However, most of the tools support limited 3D visualization using BIM or Cell-DEVS, in terms of interoperability with IFC, traceability of data, reusability of model and visibility options of GUI.

There are a number of applications in BIM using spatial lattice to analyze the quality and performance of building designs during the AEC projects life cycle. For example, a space representation of work zones for resources management was represented with small grid units that take irregular shapes (Elbeltagi et al. 2004). A BIM-ISEE (Immersive Safety Engineering Environment) was developed, focused on the realistic virtualization in their immersive environment for integrating fire and evacuation simulation with BIM tools (Ruppel and Abolghasemzadeh 2009).

Advanced 3D visualization for simulation has attracted much attention. Bijl and Boer (2011) provided a 3D visualization tool for discrete event simulation using game technology. In (Guo et al. 2012), the authors proposed a Flight Data 3D visualization for an entire fight quality analysis. In (Zhange et al. 2010), they represented a platform of tunnel construction process in a distributed simulation environment. However, these advanced techniques are not applied in BIM authoring tools.

In recent years, different AEC projects with DEVS and Cell-DEVS have been developed. Cell-DEVS models were introduced for construction sites, to deal with the construction performance, conflict analysis and visualization of work site (Hammad and Zhang 2011). A Cell-DEVS simulation of Diffusion Limited Aggregation (DLA) was used to model the growth of mold in building walls, using Autodesk Revit for Data collection (Ahmed et al. 2010). An integrated framework was introduced for combining BIM and Cell-DEVS, in which a simulation of evacuation planning in a multi-floor building was used (Wang et al. 2012). However, the tool mentioned above usually supports well 1D or 2D visualization, with limited 3D visualization.

Besides, there are other efforts to 3D visualization focusing on Cellular Automata (CA). Capow (Rucker and Ostrov 1997) is a program for visualizing CAs. The user can control color, selecting view type and 3D view details. CASim (Freiwald et al. 2001) is an environment for simulating 3D cellular automata, allowing users to design states, transition rules, colors and icons. However, most of them only enable displaying the surface of the 3D graph, which cannot present realistic moving entities.

3. VISUALIZING CELL-DEVS MODELS IN 3D

In this section we show how to interface moving entities and Cell-DEVS models. The key idea in tracking the entities is to keep a record of the direction and position of each entity while parsing the simulation results. When a cell becomes empty, the position of the entity is set as the cell its direction was pointing to. This information can be extracted from the simulation. The visualization system extracts the *position* and *state* of a cell at a certain *time*. The following UML activity diagram (Figure 1) shows the overall architecture of the proposed solution.

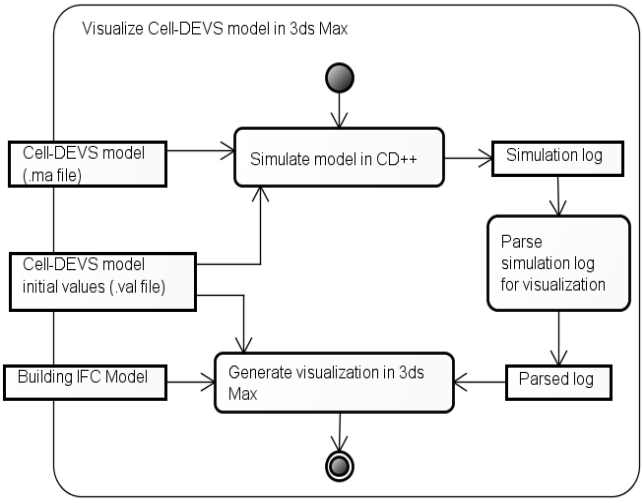

Figure 1. Activity diagram of the implementation

First, the Cell-DEVS model is simulated in CD++ and a simulation log obtained. A parsed log is provided to the 3ds Max visualization plug-in along with the file containing the

initial values of the Cell-DEVS model and the IFC model of the building.

The simulation is parsed before being passed to the visualization plug-in. This preprocessing phase facilitates the reuse of the visualization plug-in code, simplifies the plug-in code and speeds up the generation of visualization data. Reusability is accomplished by hiding details of the Cell-DEVS model from the visualization plug-in. (In the case studies to be presented in the following section, the sizes of the parsed logs were less than 5% of the original ones.) The parser extracts from the simulation log the position and state of each cell at every simulation time.

In order to generate the visualization, the plug-in needs to know the size and boundaries of the building, the number of cells in the model and the size of each cell. This information is extracted from the building model in the IFC format during the creation of the Cell-DEVS simulation. We chose to use the IFC standard to represent the building, because most BIM authoring tools support these files for collaborative development and interoperability, and it facilitates the extraction of the needed information. Figure 2 shows a part of the IFC-EXPRESS standard (buildingSMART 2012) focusing on the entity *IfcWall,* which represents the walls of the building. *IfcWall* contains the coordinate information needed to determine the size and boundaries of the building, the number of cells in the model and the size of each cell.

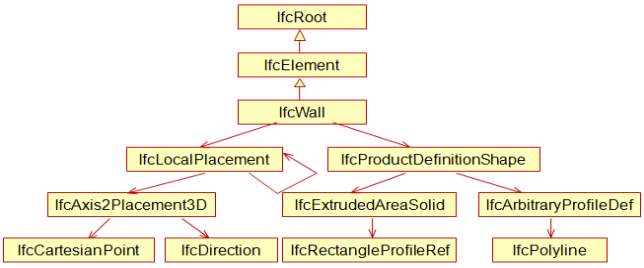

Figure 2. *IfcWall* in the IFC hierarchy

To collect this information, we used the open API from BIMServer.org for querying that the needed IFC elements are used (BIMServer.org 2012). Using this, we can obtain (*Xmin*, *Ymin)* and (*Xmax, Ymax)*, the points which constitute the bounding box of the building. Based on this box, the designers can define the size of each cell and the number of cells in each dimension.

4. IMPLEMENTING A VISUALIZATION PLUG-IN

3ds Max supports building plug-ins written in C++ or in MAXScript (a native programming language). The performance of MAXScript is lower than C++, however it is more productive and it enables faster prototyping since it is more abstract than C++ (Autodesk 2012a).

Figure 3 shows a UML class diagram of the overall architecture of the plug-in, which is based on the Model-View-Controller design pattern (Krasner and Pope 1988). The view is implemented by the *3DGui* class and 3ds Max objects; the controller is *CDVizController*, and the remaining classes are the model. Some of the model's logic is inside *CDVizController*, and it could be refactored in the future to improve understanding of the software.

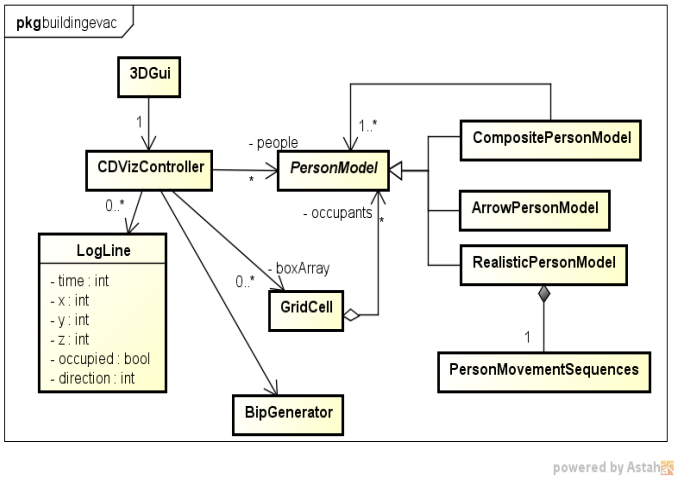

Figure 3. Class diagram of the visualization plug-in

The *LogLine* class represents a line from the parsed log and it is responsible for extracting the data from that line. *CDVizController* processes the simulation and, at each simulation timestep, sets the position of all people according to the log. The simulation grid is represented by an array of *GridCell* objects, which keep track of which person is in that cell, and each person in the simulation is represented by an instance of *PersonModel*. *GridCell* behaves like a queue, and it reports that the person at the top of the queue is the one occupying the cell. An array of *GridCell*s is used instead to prevent data being lost during the processing of the simulation (since the log is processed sequentially).

In order to allow a person to be represented graphically in one or more different ways simultaneously while abstracting this from the rest of the program, the Composite pattern was used in *PersonModel* (Gamma et al 1995). Our

implementation allows people to be represented as cones and/or 3D models that look like people.

4.1. Cone models

Cone models are implemented in the class *ArrowPersonModel*, and they allow a user to see a person's position and direction. The plug-in makes use of 3ds Max key framing ability for animations; the position and direction of the cone are set each time they change, and 3dsmax interpolates all the data producing a smooth transition between the key frames.

4.2. Realistic models

Realistic 3D person models are implemented in the class *RealisticPersonModel*. This graphical representation is not as straightforward to implement as cones and a rigged 3D model and movement animation files are needed. The *Motion Mixer* component of 3ds Max (Autodesk 2012b) was used to mix all the animations for each person in the visualization. In the Mixer, we define when each animation occurs and the order of the animations (the interaction with the Motion Mixer API is in the *PersonMovementSequences* class).

The most important feature of the Mixer for this application is the interpolation of positions between animations. Each instance of a walking animation must make the character start moving from its current position. Without interpolation, if a walking forward animation clip A is added, followed by clip B, clip B will start the animation from the starting position of the character (and not the position at the end of A). The plug-in inserts an empty animation file in the Mixer when gaps are needed.

We create an on-the-fly version of each animation for each floor, each with the Z coordinate of the corresponding floor. The Z positions of all characters are set to the Z of the top floor and then, according to the floor where the character is in, a different version of the animation is added to the Mixer. The solution is implemented by the *BipGenerator* (the cost of generating these animations increases with the number of floors of the building).

4.3. Visibility selection

The plug-in GUI lets the user select which parts of the building are shown, so that the user can have a better view. This is implemented in the *CDVizController* class.

Hiding and revealing the building constituent objects is performed by applying the *hide* or *unhide* MAXScript functions on a range of objects that fall within a certain boundary. For instance, to hide a floor, the *hide* function is applied on all objects that lie between the floor to be hidden and the next floor above. The problem of using the *hide* and *unhide* functions for is that they do not consider 3ds Max animation time. For example, if the current animation time is X and *hide* is applied on a certain object Y, this object is hidden for all the animation (not just at or after time X). If Y is a person on the second floor at time X and on the first floor at time X + 100, and the second floor was hidden by a call to *hide* at time X, then if 3ds Max is set to show time X + 100, Y will still be hidden. The consequence is that the user has to click the *Refresh Visibility* when changing the current displayed animation time to see the objects.

4.4. Grid coordinates conversion

To convert the Cell-DEVS coordinates of a cell in the simulation grid to the corresponding coordinates in the building model, an affine transformation matrix is used. This was done by first applying a scaling transformation, and then a coordinate system transformation to the grid rectangle. The scaling transformation matrix is calculated as follows (Shirley et al. 2009):

$$\begin{pmatrix} \frac{c1-c0}{a1-a0} & 0 & 0 & 0 \\ 0 & \frac{d1-d0}{b1-b0} & 0 & 0 \\ 0 & 0 & 1 & 0 \\ 0 & 0 & 0 & 1 \end{pmatrix}$$

Here *(a0, b0)* is the bottom-left corner of the grid rectangle, *(a1, b1)* is the top-right corner of the grid rectangle, *(c0, d0)* is the bottom-left corner of the building model and *(c1, d1)* is the top-right corner of the building model. Also, *(c0, d0)* is *(Xmin, Ymin)*; *(c1, d1)* is *(Xmax, Ymax)*, *a1 – a0* is *CellsX* and *b1 – b0* is *CellsY*. Therefore, the 4x4 scaling transformation matrix becomes:

$$\begin{pmatrix} \frac{X_{MAX}-Xmin}{CellsX} & 0 & 0 & 0 \\ 0 & \frac{Ymax-Ymin}{CellsY} & 0 & 0 \\ 0 & 0 & 1 & 0 \\ 0 & 0 & 0 & 1 \end{pmatrix}$$

The coordinate system transformation matrix depends on the coordinate system of the building model and examples of it can be seen in the Case Study section. The final transformation matrix for converting grid coordinates to building model coordinates is given by multiplying the

scaling transformation matrix and the coordinate transformation matrix. This matrix is generated once in the *CDVizController* class before processing the parsed simulation log.

5. CASE STUDIES

5.1. Building Evacuation

The visualization system was applied to a Cell-DEVS model of the occupancy of a building model with three floors. The objective of the model is to help determine the maximum occupancy for the building that allows a reasonable emergency evacuation time (Wang et al. 2012).

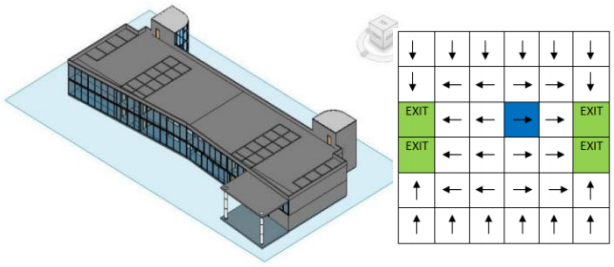

Figure 4. (a) Building for evacuation and (b) pathway

The building (shown in Figure 4a) contains three floors connected by two stairwells. There are exit doors on the first floor (in the lower right corner). In the case of emergencies, people try to evacuate along the pathway on each floor (Figure 4b), go down the stairwell, and finally get out the building through exits. This multi-level evacuation Cell-DEVS model is defined in CD++. The behavior of each cell depends on its current state whose value is determined by a set of rules after satisfying a precondition of his neighborhood. It contains different groups of rules (describes in Wang et al. 2012). For instance, to model someone entering into an unoccupied cell the rule is as follows:

rule : 4 100 { (0,0,0) = 3 and ((0,1,0) = 10 or (-1,0,0) = 4 or (0,-1,0) = 6 or (-1,0,0) = 14 or (1,0,0) = 14 or (0,1,0) = 14 or (0,-1,0) = 14)}

The parser for this model extracts the following properties from each simulation log: the *time* a change occurred, the *position* of the cell if it is now *occupied* or empty (a 3D tuple [x, y, z]) and its *direction*. Then, it builds a human-readable text line with this using the following format:

time position_x position_y position_z occupied direction

All duplicate lines are removed, and the remaining lines are sorted according to its time and outputted. The GUI allows the user to select which floors will be displayed. To obtain the height of each floor, the plug-in iterates through all the objects whose name starts with the prefix "floors" and adds their height to a list that does not allow duplicate values. The height of a floor is calculated by adding the Z coordinate of the position of the floor to the height of its bounding box. After the list is filled, it is sorted and then it contains the height of each floor in a bottom to top order.

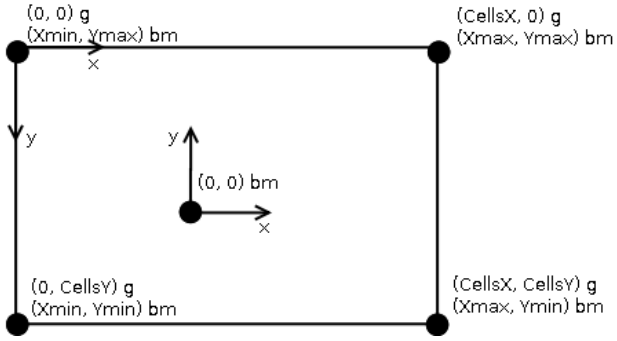

Figure 5. Diagram showing how the two coordinate systems differ.

The grid coordinate system uses the Cartesian system with an inverted Y axis in relation to the building model coordinate system. The diagram below shows how the two coordinate systems differ. The notation *(x, y) g* represents a point in the grid coordinate system and *(x, y) bm* represents a coordinate in the building model coordinate system. The rectangle represents the boundaries of the building, as seen in Figure 5.

The following matrix was used to convert from the grid coordinate system to the building model coordinate system:

$$\begin{pmatrix} 1 & 0 & 0 & 0 \\ 0 & -1 & 0 & 0 \\ 0 & 0 & 1 & 0 \\ Xmin & Ymax & 0 & 1 \end{pmatrix}$$

In the test machine (Intel Quad Core Q8200, 8GB DDR3, Geforce GTX 560 Ti 448), the realistic visualization took about 1 minute to load and the average visualization playback rate was 0.5 frames/s. Using cones in the same machine, the visualization takes on average 15 seconds to load and a maximum playback rate defined for the visualization of 10 frames/s is achieved.

5.2. Occupation model of Foster's Elephant House

The visualization system was applied to a Cell-DEVS model of the occupancy of Foster's Elephant House at the Copenhagen Zoo (Figure 6a). The objective of the model is to bring designers to understand different building

properties in order to facilitate the occupancy management or design suggestions for future improvement (e.g., door locations, number of stairs, rush/slash hours (Wang et al. 2013)).

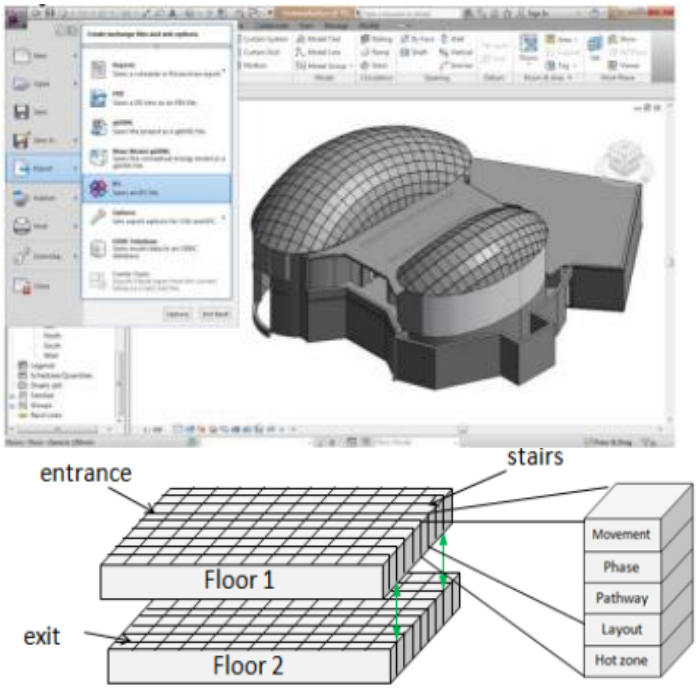

Figure 6. (a) Elephant House Building and (b) Cell states

This occupancy model simulates people's behavior for occupancy analysis. People walk in from the main *entrance* on *floor1*, go downstairs to *floor2* and then leave the house through the *exit*. People can move in different directions (which is simulated using a random selection) and they wait randomly when visiting in the two floors of this building.

This occupancy Cell-DEVS model is defined in CD++, similarly as in the model in Section 5.1. The cells of this building change their values according to a set of rules. As shown in Figure 6b, each cell has five state variables: *Movement*, *Phase*, *Pathway*, *Layout*, and *Hotzone*. The most important variable is *Phase*, which is divided into four sub-phases: *intend*, *grant, wait* and *move*. They occur sequentially in that order every 400ms: e.g., if an *intend* phase happens at time X, *grant* happens at time X+100, *wait* phase at time X+200, *move* phase at time X+ 300, the *intend* phase at X+400 and so on. The time is used to identify to which of these phases the event belongs to. For an occupied cell, a visitor chooses a direction randomly at the *intend* phase. If the target cell accepts it, it changes to *get grant*; otherwise, it turns to *get rejected*. If granted, the visitor would *wait* for some time randomly according to the hot zone where the visitor is standing at, and then *empty* the cell at the *move* phase. For the purpose of visualization, the only relevant information comes from the *intend* and *move* phases.

One rule in the *intend* phase is used to choose the intended direction of an occupied cell at random, and is defined as follows (Wang et al. 2013):

rule : {~movement := uniform(0,1); ~phase := 1.1}
100 { (0,0,0)~phase = 1 and (0,0,0)~movement=1 and (0,0,0)~pathway>=5}

The events of an intend-grant-wait-move sequence actually happen at the same time but are separate in simulation time for ease of modeling. The parser groups each intend-grant-wait-move sequence. The parser output will denote that events from intend phase at time X and events from move phase at time X+300 both happened at time:

$$Y = \left\lfloor \frac{X-1}{400} \right\rfloor * 100.$$

For instance, events from intend phase at 500 and move phase at 800 will be outputted as having occurred at time 100.

The parser output lines, which denote events from *intend* and *move* phases, are in the following format:

- *Intend* event:
  real_time x y z direction
- *Move* event:
  real_time x y z "m"

The lines are ordered first in increasing order by real_time and secondly by type with *intend* events coming before *move* events since the direction of the person must be set before it moves.

The GUI allows the user to hide each floor, the roof, and the side walls. The height of each floor is obtained as described in the previous case study and the position of the side walls is obtained manually and typed into the plug-in code.

The grid coordinate system is rotated by 90 degrees and transposed by $(Xmax, Ymin)$ in relation to the building model coordinate system (Figure 7):

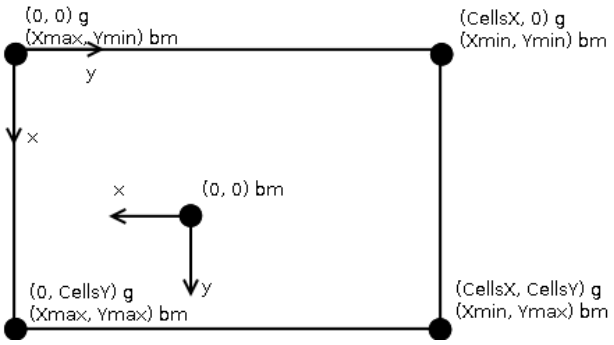

Figure 7. Diagram showing how the two coordinate systems differ.

Thus, the following matrix was used to convert from the grid coordinate system to the building model coordinate system:

$$\begin{pmatrix} 0 & 1 & 0 & 0 \\ -1 & 0 & 0 & 0 \\ 0 & 0 & 1 & 0 \\ Xmax & Ymin & 0 & 1 \end{pmatrix}$$

The plug-in helped locate several bugs in the Cell-DEVS model, as the 3D visualization is an effective way to find errors in these types of Cell-DEVS models. These errors were detected because the plug-in works with people not cells, therefore assumptions about the behavior are made: e.g., when a cell that does not represent an exit becomes empty, it means the person who was in that cell is now in an adjacent cell. Examples of the types of errors detected were people disappearing from the simulation and people being duplicated.

These errors would manifest as 3ds Max error messages while the plug-in generated the visualization, or as visual errors with people models being displayed in incorrect places. The stack trace shown in 3ds Max error messages would pinpoint the time where the simulation was behaving wrongly and for the visual errors the name of the person model would show the time when it was created.

The performance of realistic models for this case study was very similar to the previous case study. A snapshot of the simulation visualization can be seen in Figure 8.

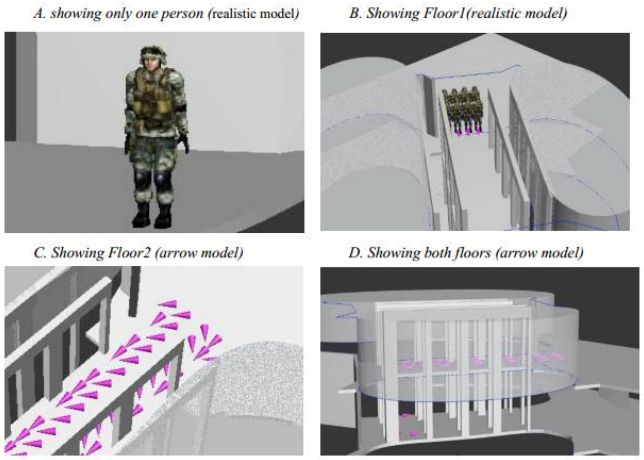

Figure 8. Screenshots of the visualization plug-in for the model of Foster's Elephant House.

6. CONCLUSION

The case studies provided evidence that the tool does solve the issues present in similar tools discussed in Section 2. The tool in both case studies: showed people moving continuously from one cell to another; was integrated into a BIM authoring tool (Autodesk 3ds Max 2012); was easily adapted to each model; and displayed specific models (cone and realistic models) that allowed the user to see easily extra information about each person, namely, where they were facing and intending to move to.

The reusability of the tool could be further improved if a uniform interface between the parser and the visualization plug-in was created. With this interface, the plug-in would not need to be changed for different underlying Cell-DEVS models. That is, only the parser would need to be changed for different applications of BIM.

The Elephant House case study suggests 3D visualization can be effective in verifying Cell-DEVS models based on moving entities. Hence, this could also be a subject for future research.

Since the performance of the realistic models was found to be unsatisfactory in the test machine, improving it in future work would be helpful to users of the tool.

Acknowledgements

We would like to thank Vinu Subashini Rajus for creating the building model used in the case study of Foster's Elephant House and the company Mixamo for making a rigged 3D person model freely available on: http://www.turbosquid.com/3d-models/free-fbx-model-soldier-military-character-rigged/516949.

References

Autodesk 2012, MAXScript Help: The SDK and MAXScript, http://docs.autodesk.com/3DSMAX/15/ENU/MAXScript-Help/index.html?url=files/GUID-C0F38270-F5DD-4356-AFFF-B037D97F0017.htm,topicNumber=d30e3671. Accessed December 14th, 2012.

Autodesk 2012, 3ds Max Reference: Motion Mixer http://download.autodesk.com/us/3dsmax/2012help/index.html?url=files/GUID-A4F4A6A6-27A9-482C-9A95-853B1ADC68C-1251.htm,topicNumber=d28e256342. Accessed December 14th, 2012.

Bijl, J. L., and Boer, C. A. 2011. Advanced 3D visualization for simulation using game technology. In Simulation Conference (WSC), Proceedings of the 2011 Winter (pp. 2810-2821). IEEE.

BIMServer.org. 2012. http://bimserver.org/buildingSMART. Accessed Nov 6. 2012.

IFC2x3. http://www.buildingsmart-tech.org/ifc/IFC2x3/ Accessed Nov 6 2012.

Elbeltagi, E., Hegazy, T., and Eldosouky, A. 2004. Dynamic Layout of Construction Temporary Facilities Considering Safety. Journal of Construction Engineering and Management. 130(4):534-541

Freiwald, U., Weimar, J. 2001. JCASim - a Java system for Simulating Cellular Automata, Theoretical & Practical Issues on Cellular Automata (ACRI 2000), S. Bandini and T.Worsch (eds.), Springer Verlag, London.

Friendly, M., and Denis, D. J.. 2012. Milestones in the history of thematic cartography, statistical graphics, and data visualization. Accessed Nov 6.

Gamma, E., Helm, R., Johnson, R., AND Vlissides, J. M. 1995. Design Patterns: Elements of Reusable Object-Oriented Software. Addison-Wesley. ISBN 0-201-63361-2. pp. 395

Guo, H., Pang, J., Han, L., and Shan, Z. 2012. Flight Data Visualization for Simulation & Evaluation: A General Framework. InComputational Intelligence and Design (ISCID), 2012 Fifth International Symposium on (Vol. 1, pp. 497-502). IEEE.

Hammad, A., and Zhang., C. 2011. Towards Real-time Simulation of Construction Activities Considering Spatio-temporal Resolution Requirements for Improving Safety and Productivity. In Proceedings of the 2011 WSC, AZ. 3533-3544.

Hardin, B. 2009. BIM and Construction Management: Proven Tools, Methods, and Workflows. Wiley.

Jiang, Y., Ming, J., Wu, D., Yen, J., Mitra, P., Messner, J. I., and Leicht, R. 2012. BIM Server Requirements to Support the Energy Efficient Building Lifecycle. In Proc. 2012 ASCE international conference on computing in civil engineering.

Khan, A., Wainer, G. A. 2005 Advanced Visualization of DEVS and Cell-DEVS Models in CD++/Maya. Proceedings of SISO Fall Interoperability Workshop, San Diego, CA. U.S.A - 2005

Krasner, G. E., Pope, S. T. 1988, A Description of the Model-View-Controller User Interface Paradigm in the Smalltalk-80 System, http://www.itu.dk/courses/VOP/E2005/VOP2005E/8_mvc_krasner_and_pope.pdf. Accessed Nov 6, 2012.

Malinowsky, B., and Kastner, W. 2010. Integrating Process Communication in Building Information Models with IFC and LON. 8th IEEE International Workshop on Factory Communication Systems.

Rucker, R., Ostrov, D. 1997. Continuous-Valued Cellular Automata for Non-Linear Wave Equations, Complex Systems 10 (1196) 91-119.

Ruppel, U., and Abolghasemzadeh, P. 2009. BIM-based Immersive Evacuation Simulations. In 18th In-ternational Conference on the Application of Computer Science and Mathematics in Architecture and Civil Engineering. Weimar, Germany.

Shirley, P., Marschner, S., Ashikhmin, M., Gleicher, M., Hoffman, N., Johnson, G., Munzner, T., Reinhard, E., Sung, K., Thompson, W. B., Willemsen, P., Wyvill, B. 2009. Fundamentals of Computer Graphics. AK Peters 3rd ed ISBN 978-1-56881-469-8. pp.132

Wainer, G., 2009. Discrete-event Modeling and Simulation: a Practitioner's Approach. CRC/Taylor & Francis.

Wainer, G., Poliakov, E., Hayes, J., and Jemtrud, M. 2007. A Busy day at the SAT building. In Proceedings of the International Modeling and Simulation Multiconference Buenos Aires, Argentina.

Wang, S., Schyndel, M.V., Wainer, G., Subashini, V., and Woodbury, R. 2012. DEVS-based Building Information Modeling AND Simulation for Emergency Evacuation.bIn Proceedings of the 2012 Winter Simulation Conference. Berlin, Germany. IEEE.

Wang, S., Wainer, G., Rajus, V.S., and Woodbury, R. 2013 (accepted). Occupancy Analysis Using Building Information Modeling and Cell-DEVS Simulation. Symposium on Theory of Modeling and Simulation. TMS'13. San Diego, USA

Venhola, W., and Wainer, G. 2006. DEVSView: A tool for visualizing CD++ simulation models. SIMULATION SERIES, 38(1), 133.

Zeigler, B.P., H. Praehofer, and T.G. Kim. 2000. Theory of Modeling and Simulation. Academic Press

Zhang, Y., Moghani, E., AbouRizk, S. M. and Fernando, S. 2010. 3D CAD modeling and visualization of the tunnel construction process in a distributed simulation environment. In Simulation Conference (WSC), Proceedings of the 2010 Winter (pp. 3189-3200). IEEE.

Session III

Evaluating the Performance Robustness of Fixed and Movable Shading Devices against Diverse Occupant Behaviors 85
William O'Brien
Carleton University

Simulating the Sensing of Building Occupancy 93
Simon Breslav, Rhys Goldstein, Ben Doherty, Dan Rumery, Azam Khan
Autodesk Research, BVN Architecture

Development of Discrete Event System Specification (DEVS) Building Performance Models for Building Energy Design 101
Huseyin Burak Gunay, Liam O'Brien, Rhys Goldstein, Simon Breslav, Azam Khan
Carleton University, Autodesk Research

Evaluating the Performance Robustness of Fixed and Movable Shading Devices against Diverse Occupant Behaviors

William O'Brien

Carleton University
1125 Colonel By Drive,
Ottawa, Ontario, Canada, K1S 5B6
liam_obrien@carleton.ca

Keywords: Robust Building Design, Occupant Behaviour, Building Performance Simulation, Stochastic Occupant Modelling, Occupant Comfort

Abstract

Given the diverse operating conditions, weather conditions, space users, and occupant preferences of buildings, it is commonplace to provide occupants with multiple means to adapt their immediate indoor environment. However, numerous studies have shown that occupants sub-optimally use such controls to improve comfort during times of significant discomfort, but are much more passive when the source of discomfort is alleviated. Occupant-related building performance simulation (BPS) models continue to use very simple and rigid rules when a building's performance is predicted, despite the topic's complexity. This is likely an artifact of envelope load-dominated buildings, whose energy use is mostly dependent on their ability to isolate the indoor environment. But as envelopes and HVAC become more efficient, occupants are playing an increasingly important role in building performance; especially for highly efficient building (e.g., net-zero energy buildings). Traditionally the associated uncertainty of these effects has been excused for the designer and isolated during design by focusing on energy performance relative to a reference building. This paper proposes a method using a combination of probabilistic occupant models and explicit models of adaptive comfort to gain an improved understanding of robust building design. Results are presented of an example of a yield of 45% lighting energy savings if a fixed shading device is present.

1. INTRODUCTION

In the past decade, the uncertainty from occupant-related behaviour and habits in buildings has been widely recognized as playing an increasingly significant role in building performance (Hoes et al. 2009; Haldi and Robinson 2010). A number of occupant actions—, including use of appliances, lighting, operable windows, thermostats, and window shades—have all been shown to have a considerable effect on energy performance and the indoor environment. At least as notable and complex is the diversity of occupant preferences and adaptive measures, including clothing level, consumption of hot and cold drinks, and tolerance for cool or warm temperatures.

Consider the end use energy use breakdowns for residential and commercial buildings in Canada (similar to US figures), shown in Figure 1. Occupants have direct control over between three and five of the categories of energy shown, depending on their access to controls. The biggest category, space heating, which has traditionally been considered one of the most predictable categories because of its strong affiliation with building envelope and the HVAC system, has also been shown to be among the most uncertain because of occupant behaviour. Gram-Henssen (2010) found a 350% variation – between 4000 and 14,600 kWh for heating energy – among five identical houses, owing to attitudes about heating and energy use, thermostat control habits, use of operable windows in the heating season, and typical occupancy schedules. Buildings whose occupants are not motivated to reduce their energy by economic incentives, as is the case for commercial building dwellers and bulk-metered apartment dwellers - tend to use even more energy.

Navigant Consulting (2012) studied nearly 4000 apartment units in Ontario, Canada and found that units whose residents directly pay for their exact energy use consumed about 30% less than those who paid a fixed fee.

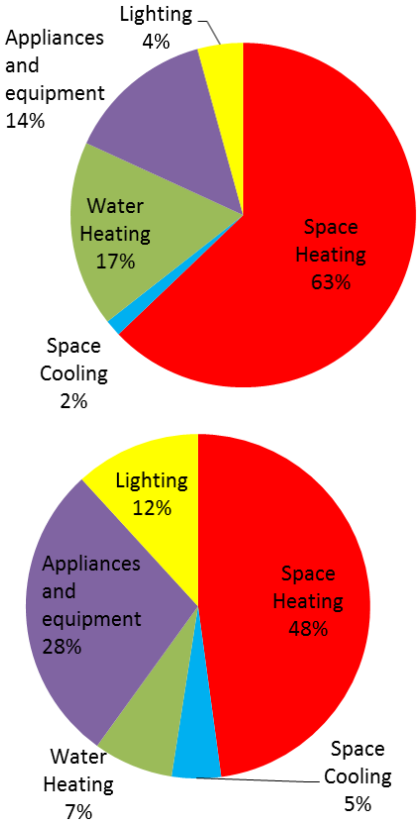

Figure 1: Energy use in residential (top) and commercial (bottom) buildings in Canada. (NRCan, 2008)

The other major categories of energy use—appliances and equipment, water heating, and lighting—are generally considered to be even more sensitive to occupant behaviour since they can usually be directly controlled by occupants. Needless to say, occupants play a substantial role in building performance, and this has yet to be well-characterized.

Recent years have seen a surge in publications that focus on the stochastic nature of occupants. The most common areas of study include window opening (Rijal et al. 2007), electric lighting (Boyce 1980), shades (Rubin et al. 1978; Inoue et al. 1988), or some combination of these (Pigg et al. 1996; Reinhart and Voss 2003). Others studies have examined thermostat use (Karjalainen 2009), clothing changes, consumption of hot/cold drinks (Haigh 1981), and position in a space (Reinhart and Wienold 2011; Veitch 2011). A common conclusion to these studies is that behaviour is stochastic; not deterministic (Nicol and Humphreys 2002). The result is that occupants' decisions to take action are quite complex and somewhat random (e.g., Figure 2).

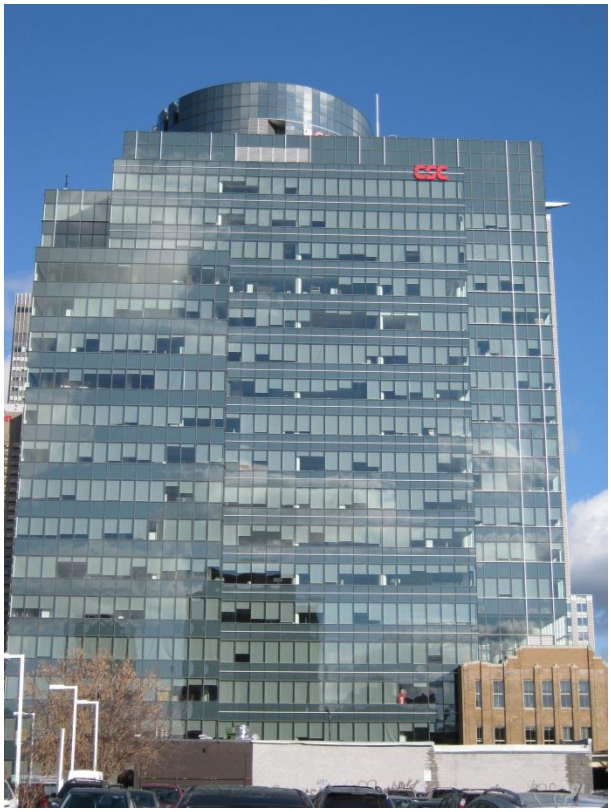

Figure 2: Typical shade deployment levels of a south-west facing office building façade in the winter.

The emphasis of stochastic occupant behaviour modelling research to date has been on improving the accuracy at which building performance has been predicted. However, little attention has been given to how accurate knowledge of occupant behaviour can be used to improve building design (Hoes, Hensen et al. 2009). This paper proposes robust building design: the notion that buildings can be designed "off line" to provide greater comfort while relying less on occupants to adapt their environment and themselves. A simple example is provided to demonstrate that the presence of an overhang reduces the probability of glare and actually decreases lighting energy because occupants are less reliant on window shades.

2. THE ROBUSTNESS CONCEPT

About three decades ago, Genichi Taguchi proposed the idea that the quality of manufactured goods could be improved by designing them to be more resistant or *robust* against a wide variety of operating conditions (Phadke 1995). Taguchi suggested that designers should minimize the signal-to-noise ratio. That is, the resulting variability in product performance should be minimized relative to the magnitude of the deviations from nominal operating conditions.

In the current context of occupant-building interactions, robust design means we do not want to attempt to control occupants and their adaptive actions, but instead we want to design buildings that are less sensitive—more robust—to diverse occupant behaviour and weather conditions (noise). In fact attempting to modify occupant behaviour has shown to yield only modest returns (Abrahamse et al. 2005).

Rather than naively assume that BPS will yield accurate predictions in absolute terms, we must recognize that it is primarily valuable in relative terms and that results should be expressed in probabilistic terms, accordingly. Figure 3 shows the energy performance results of two designs: one that has greater robustness (lower standard deviation) and also a lower mean energy use than the other.

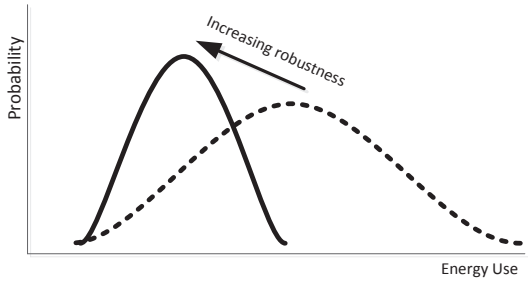

Figure 3: Illustration of the robustness concept: lower mean and standard deviation of building performance

Hoes et al. (2009; 2011) are the only researchers, to the author's knowledge, to explicitly apply Taguchi's robust design method to buildings and their performance. In their first paper, they varied several parameters such as thermal mass and glazing area. They used the occupant blind algorithm from Lightswitch-2002 which dictates that blinds are closed by occupants if solar radiation on the façade exceeds 50 W/m^2 and it "hits the work place" (Reinhart 2004). For their second paper Hoes et al. optimized a simple building with multi-objective optimization (comfort and energy use) and BPS engine ESP-r to establish a Pareto front. Using a "relative standard deviation" indicator, which is essentially the signal-to-noise ratio, they suggested that designers should select the most robust of the building designs among those on the Pareto front.

The important feature of the currently proposed methodology is that it considers that the response of occupants is directly tied to the design of the building and the conditions that result from it (see Figure 4). An important feature for future occupant models used for robust design is that they are sufficiently generalizable for the entire range of building design features being considered.

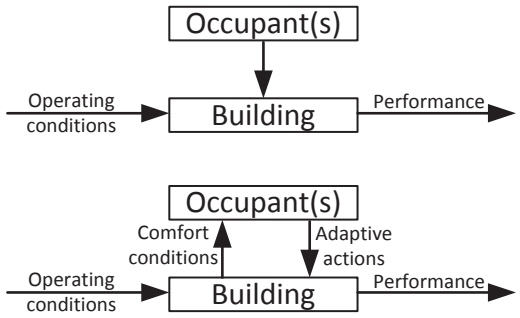

Figure 4: Robustness model: without considering influence of building on occupants (top) and with direct influence of building design on occupants (as discussed in this paper; bottom).

The key phenomenon that is being addressed here, by robust building design, is that occupants are known to attempt to adapt their environments at times of discomfort, but do not respond nearly as quickly when the source of discomfort is alleviated—especially if an alternate (often energy-consuming) option is available. For example, occupants often close window shades quite promptly to protect themselves from severe glare. But if a building has electric lighting, then the occupants remain relatively comfortable, insofar that they can still function because there is adequate illuminance. Thus, their only motivation to re-open shades would be to admit daylight or enable views to the outside. Because many low-energy building strategies rely on weather conditions—which are often cyclical—this phenomenon of prompt discomfort alleviation but slow system restoration is quite common. Thus, the goal here is to minimize the frequency at which

the 'crisis of discomfort' (Bordass et al. 1994) events occur. An excellent example of this is by Rijal, Tuohy et al. (2007) who found that addition of thermal mass and fixed horizontal solar shading (i.e., an overhang) to an office reduces the fraction of time when occupants rely on open windows for reducing overheating by about 85%. Thus the potentially negative effects of leaving windows open (e.g., loss of useful solar gains and noise from outside) are avoided. Meanwhile, less effort is required from the occupant to maintain comfort.

Many of the popular passive strategies that are used to achieve low energy in buildings encounter periods of discomfort, including:

- Daylight: glare, high levels of incident solar radiation on occupants
- Passive solar: overheating, high/low radiant surface temperatures
- Natural ventilation: drafts, noise.

One final example of robust design is the National Renewable Energy Laboratory (NREL) Research Support Facility (RSF) (Guglielmetti et al. 2010). It uses windows whose upper portions have fixed light louvers that are specifically designed to redirect beam solar radiation up onto the ceiling – regardless of solar altitude - thereby protecting occupants from glare. The result of this design is that movable shades are not needed, thus not requiring occupant interference. It should be noted that light louvers operate best under sunny conditions, which this Colorado building has plenty of, and on the south-facing façade.

Figure 5: Exterior of NREL RSF space showing fixed shading (lower portion) and light louvers (upper portion).

Eventual building simulation models should include greater awareness of uncertainty since virtually all inputs have some uncertainty and express predicted performance not as a single definitive value but as a probability distribution (Figure 6). This includes building materials and construction quality, climate, occupant behaviour, space uses, etc.

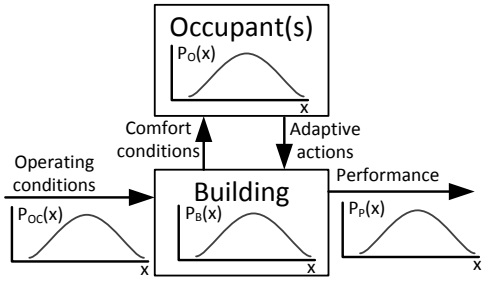

Figure 6: High-level modelling methodology for robust building design, whereby one or more inputs is provided to the BPS engine as a stochastic process rather than deterministic or absolute value.

3. CASE STUDY

To demonstrate the concept of robust building design, a quasi-stochastic window shades model was implemented in EnergyPlus V7.2. The building model is a single 3-meter cube office in Toronto with a south-facing window (window-to-wall ratio of two-thirds), and fixed shading device as shown in Figure 7. The fixed shading device is designed to completely block the direct solar radiation from hitting the workplane during the six warmest months of the year. It extends far in the east-west directions to simulate a long row of identical offices. The office is assumed to be occupied from 9 to 5 o-clock on all weekdays. The office is modelled to be equipped with motion sensors and a daylight sensor that turns the electric lights off if workplane illuminance in the centre of the office exceeds 500 lux.

The top-down roller shade (visible transmittance 5%) is assumed to be manually controlled in the following way.

1. Start simulation year with shade open.
2. If workplane illuminance exceeds I_{max} and there is direct solar radiation on the workplane, close it and keep it closed for $t_{inactive}$ days.
3. Re-open if $t_{inactive}$ days have elapsed and an occupant is present (i.e., 9-5 weekdays).

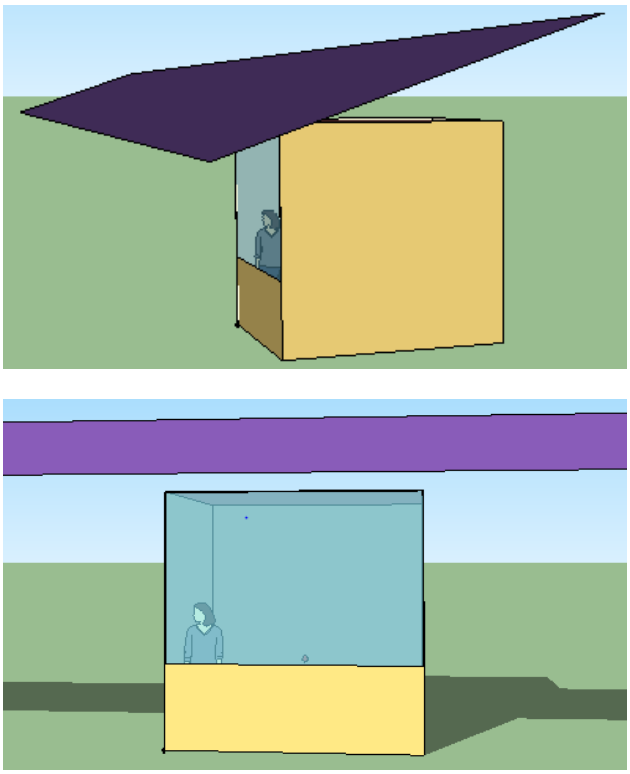

Figure 7: Screenshots in SketchUp/OpenStudio showing the south-facing single-occupancy office and fixed shading device.

Where I_{max} and $t_{inactive}$ are determined at the beginning of each simulation year by randomly obtaining a value from the two normal distributions in Figure 8 and Figure 9. The values are based on reasonable values provided by the literature (Reinhart 2004; O'Brien et al. 2012), but do not follow any particular model; they are intended primarily for illustrative purposes. The mean threshold for beam solar radiation on the exterior of the window of 50 W/m^2 is based on Lightswitch-2002 (Reinhart 2004). Values under this indicate a particularly sensitive occupant or an office which is prone to glare (e.g., large monitors). Values above the mean would correspond to a more tolerant occupant, a space use which is not prone to glare, or a shared office in which there is a diffusion of responsibility regarding closing the shades, for example.

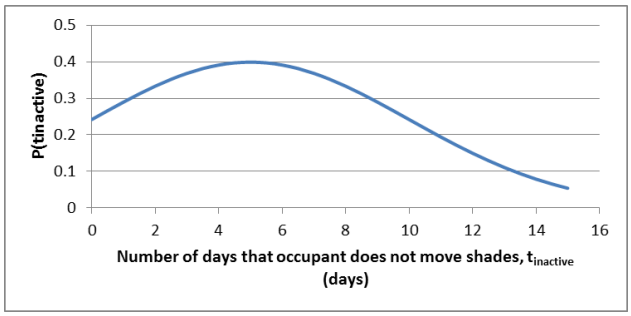

Figure 8: Probability distribution for the number of days (rounded to nearest integer) for number in inactive days after a shade closing event.

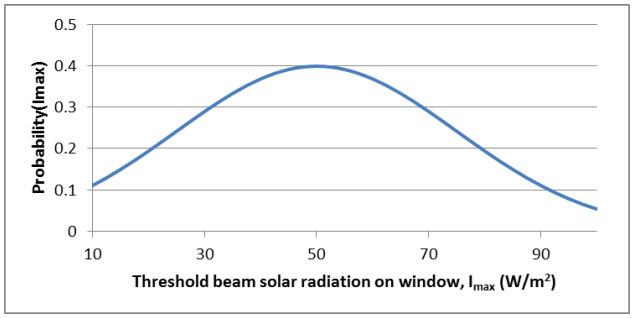

Figure 9: Probability distribution for the threshold of solar radiation on the window, above which the occupant closes the shade.

One of the major limitations of most of the existing field studies on shade movement behaviour is that the movement is often studied as a direct function of exterior weather conditions. This reduces the universality of results because of the unique nature of many buildings (Haldi and Robinson 2010). Thus, the interior conditions, those that *actually* prompt shade adjustment, are unknown (or at least unpublished). Many of the simulations based on field studies exaggerate the level of responsiveness of occupants by eliminating the passive occupants. Most field studies upon which stochastic models are based use a method to screen out inactive users or increase movement (O'Brien, Kapsis et al. 2012). For instance, Inoue, Kawase et al. (1988) assumed that if a shade remained unmoved all day that the occupant must not be present. This amounted to 60% of all occupants! Reinhart (2004) introduced the notion of different occupant types and divided the population equally among four types (due to lack of literature on a more appropriate distribution). The current case study uses a different approach to achieve the same thing: a stochastic function regarding the number of days a shade remains closed after the initial closing event. Using this method, the resulting mean occlusion for the simulated office with no fixed solar

shading device is 86%, which is consistent with measured values for south-facing facades (like for the building in Figure 2) (O'Brien et al. 2010). It should be noted that intermediate shade positions were not considered; only completely open or closed.

The shade control algorithm was implemented using EnergyPlus' Energy Management System (EMS), which allows users to write some code to be executed at runtime. A limitation to this approach was that the random number generator obtains its seed from the simulation time, not computer clock time. This resulted in identical random numbers for each simulation. To resolve this, the EnergyPlus simulation was called from a MATLAB script which randomly selected the seed.

To study the behaviour of multiple occupants (e.g., in a large office tower), 100 simulations were run for each of two cases: the office with and without the fixed shading device. This is essentially Monte Carlo simulation with random selection.

The results from this case study are quite profound **(**Figure 10). They show that the building with fixed shading uses approximately half the energy, on average and with considerably less variation, than the building with no fixed shading. From the logic of the model, this occurs because the conditions required to close the shades are rarer with fixed shading. The mean shade occlusion of the office with the fixed shading is 27% versus that for the office without fixed shading (86%). In human terms, the occupant in the office with fixed shading was confronted with glare much less frequently than the occupant without it. Because the window is quite large and even a moment of glare can cause occupants to close shades and leave them closed for many days, this is quite detrimental to daylighting.

If the shades were left open all year (or did not exist), the lighting energy use would be just 15.9 kWh/year. Similarly, if they were left closed all year, the lighting energy would be 157.5 kWh/year. Both these values assume no fixed shading. Note that there is only a very small probability (and none of the 200 simulations indicated it) that the unshaded office performance exceeds that of the office with fixed shading. Theoretically, a "hyperactive" occupant can always beat the case with fixed shading by constantly adjusting the shade to optimize daylighting while avoiding glare. However, because the minimum allowed delay between closing and opening the shade was set to one day, this cannot occur.

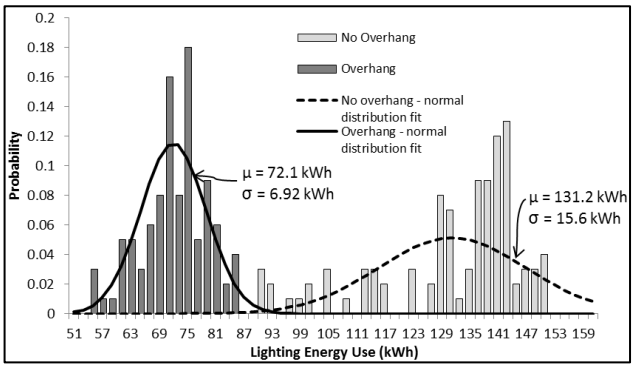

Figure 10: Probabilities distributions and normal distribution fits for the lighting energy use for an office with and without a fixed shading device.

It should be noted that considerable effort (trial and error) was required to design a shading device that adequately avoided glare while not significantly reducing the number of possible daylit hours. This research woud benefit from overhang optimization (e.g., (Marsh 2003)). Furthermore, this exercise would be significantly more difficult for east- and west-facing windows, which are notoriously difficult to shade with fixed shading because of the low solar altitudes. This exercise was somewhat impeded by the coarseness of EnergyPlus' built-in daylighting methods (Ramos and Ghisi 2010). Incorporation of more detailed lighting simulation engines, such as RADIANCE, into a growing number of BPS tools will facilitate greater design freedom. For instance, using fixed shading devices to redirect diffuse daylight into the space would likely further advance robust design of shading devices.

4. CONCLUSION AND FUTURE WORK

This paper introduced the concept of robust building design—the notion that good fixed design can help eliminate or significantly reduce some sources of occupant discomfort, resulting in a lower frequency of adaptive measures by occupants. This is important because many of the current intended and invented adaptive measures cause buildings to use more energy than expected. Furthermore, and at least as important, every action that an occupant has to take to improve their comfort decreases their satisfaction with the building. Although providing occupants with the perception of

control is very important and can trump quality of the indoor environment itself (Paciuk 1989), a building that minimizes periods of discomfort by its use of geometry and materials is highly desirable.

While, robust design can be largely tackled using traditional building design models, including rules of thumb, pattern guides, and case studies to guide new building design, BPS provides a cost-effective and quantitative method that surpasses all other methods. However, occupant behaviour models are currently in their infancy, with only a handful having evolved from research-stage to a level at which they are incorporated into publicly available BPS tools. There is a need for BPS tools to incorporate both occupant variation and adaptive measures taken by occupants. The most promising and popular method in the literature for understanding occupant behaviour is stochastic modelling; but it is not without limitations, including:

- Lack of generalizability: stochastic models are mostly based on a single field study of specific buildings, climates, cultures, and technologies. It is known that subtleties such as motorization of window shades has a profound effect on frequency of movements. Variations in research methodologies have further contributed to the difficulty of establishing universal occupant models.
- Difficulty in implementing: stochastic modelling requires some knowledge of statistics, and furthermore most BPS tools do not readily allow it. To the knowledge of the author, EnergyPlus is among the few BPS tools that readily enables development of new features without the need to compile source code.
- Lack of standards: due to the infancy of the research base, industry and government have not adapted stochastic modelling. As previously noted, the industry is accustomed to making very conservative assumptions about occupants in order to mitigate the risk of undersizing HVAC equipment.

Future research is required in robust building design, including:

- Incorporation of a more comprehensive occupant model that includes as many adaptive occupant measures as possible.
- Use of more accurate specialized models (e.g., RADIANCE) to assess glare.
- Formalized robust design methodology and incorporation into tools and design guides.

In closing, this paper proposes occupant-focusing design on “robust” features that function well and provide comfort under diverse conditions. Only after such opportunities are exploited, should automated adaptive controls with manual overrides be used. Relying on occupants to provide comfort, and particularly to avoid discomfort, should be avoided for the sake of building performance certainty, as depicted in Figure 11.

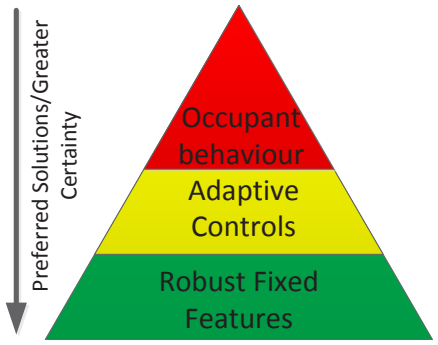

Figure 11: Preferred order of building design features that provide occupant comfort.

Acknowledgements

The author would like to thank Burak Gunay and Costa Kapsis for fruitful discussions about the underlying robustness concept. The National Renewable Energy Laboratory’s new Research Suppport Facility in Golden, Colorado is also acknowledged as providing inspiration for this research.

References

ABRAHAMSE, W., STEG, L., VLEK, C. AND ROTHENGATTER, T. (2005). "A review of intervention studies aimed at household energy conservation." Journal of Environmental Psychology 25(3): 273-291.

BORDASS, W., LEAMAN, A. AND WILLIS, S. (1994). Control strategies for building services: the role of the user. Chartered Institute of Building Conference on Buildings and the Environment, Building Research Establishment, UK.

BOYCE, P. (1980). "Observations of the manual switching of lighting." Lighting Research and Technology 12(4): 195.

GRAM-HANSSEN, K. (2010). "Residential heat comfort practices: understanding users." Building Research & Information 38(2): 175-186.

GUGLIELMETTI, R., PLESS, S. AND TORCELLINI, P. (2010). On the Use of Integrated Daylighting and Energy Simulations To Drive the Design of a Large Net-Zero Energy Office Building. SimBuild Conference, New York City, NY.

HAIGH, D. (1981). User response to environmental control. The Architecture of Energy. D. Hawkes and J. Owers. Bath, UK, The Pitmen Press**:** 45-63.

HALDI, F. AND ROBINSON, D. (2010). "Adaptive actions on shading devices in response to local visual stimuli." Journal of Building Performance Simulation 3(2): 135-153.

HOES, P., HENSEN, J. L. M., LOOMANS, M. G. L. C., DE VRIES, B. AND BOURGEOIS, D. (2009). "User behavior in whole building simulation." Energy and Buildings 41(3): 295-302.

HOES, P., TRCKA, M., HENSEN, J. AND BONNEMA, B. H. (2011). Optimizing building designs using a robustness indicator with respet to user behaviour. Building Simulation, Sydney, Australia, November 14-16.

INOUE, T., KAWASE, T., IBAMOTO, T., TAKAKUSA, S. AND MATSUO, Y. (1988). "The development of an optimal control system for window shading devices based on investigations in office buildings." ASHRAE transactions 94: 1034-1049.

KARJALAINEN, S. (2009). "Thermal comfort and use of thermostats in Finnish homes and offices." Building and Environment 44(6): 1237-1245.

MARSH, A. (2003). Computer-optimised shading design. Building Simulation.

NATURAL RESOURCES CANADA (NRCAN) (2008). Energy use data handbook tables (Canada). Office of Energy Efficiency (OEE).

NAVIGANT CONSULTING INC. (2012). Evaluation of the impact of sub-metering on multiresidentail electricity consumption and the potential economic and environmental impact in Ontario.

NICOL, J. F. AND HUMPHREYS, M. A. (2002). "Adaptive thermal comfort and sustainable thermal standards for buildings." Energy & Buildings 34(6): 563-572.

O'BRIEN, W., KAPSIS, K. AND ATHIENITIS, A. K. (2012). "Manually-operated window shade patterns in office buildings: a critical review." Building and Environment.

O'BRIEN, W., KAPSIS, K., ATHIENITIS, A. K. AND KESIK, T. (2010). Methodology for quantifying the performance implications of intelligent shade control in existing buildings in an urban context. SimBuild 2010. New York City.

PACIUK, M. (1989). The role of personal control of the environment in thermal comfort and satisfaction at the workplace, University of Wisconsin-Milwaukee.

PHADKE, M. S. (1995). Quality engineering using robust design, Prentice Hall PTR.

PIGG, S., EILERS, M. AND REED, J. (1996). Behavioral aspects of lighting and occupancy sensors in private offices: a case study of a university office building. ACEEE 1996 Summer Study on Energy Efficiency in Buildings. Pacific Grove, CA.

RAMOS, G. AND GHISI, E. (2010). "Analysis of daylight calculated using the EnergyPlus programme." Renewable and Sustainable Energy Reviews 14(7): 1948-1958.

REINHART, C. F. (2004). "Lightswitch-2002: a model for manual and automated control of electric lighting and blinds." Solar Energy 77(1): 15-28.

REINHART, C. F. AND VOSS, K. (2003). "Monitoring manual control of electric lighting and blinds." Lighting research & technology 35(3): 243.

REINHART, C. F. AND WIENOLD, J. (2011). "The daylighting dashboard–a simulation-based design analysis for daylit spaces." Building and environment 46(2): 386-396.

RIJAL, H., TUOHY, P., HUMPHREYS, M., NICOL, J., SAMUEL, A. AND CLARKE, J. (2007). "Using results from field surveys to predict the effect of open windows on thermal comfort and energy use in buildings." Energy and Buildings 39(7): 823-836.

RUBIN, A. I., COLLINS, B. L. AND TIBBOTT, R. L. (1978). "Window blinds as a potential energy saver-a case study." NBS Building Science Series 112.

VEITCH, J. (2011). "The physiological and psychological effects of windows, daylight."

Simulating the Sensing of Building Occupancy

Simon Breslav[1], Rhys Goldstein[1], Ben Doherty[2], Dan Rumery[2], Azam Khan[1]

[1]Autodesk Research
210 King St. East, Toronto, Ontario, Canada, M5A 1J7
{firstname.lastname}@autodesk.com

[2]BVN Architecture
255 Pitt St, Sydney, NSW, Australia, 000
{Firstname_Lastname}@bvn.com.au

Keywords: occupancy simulation, sensor simulation, DEVS

Abstract

Accurate building occupancy information can be beneficial in minimizing energy use by improving the intelligence of a Building Automation System (BAS) and helping designers predict the effect of different design options on occupant behavior. However, current occupancy measurements are quite inaccurate due to limitations in sensing technology and the resulting discrepancies between sensor data and what actually happens. In this paper we explore the use of simulation to model occupant behavior in combination with motion sensors to be able to study the relationship between known and measured occupant behavior. An extensible occupancy model, influenced by computational cognitive science and implemented using established modeling conventions is presented along with a simple experiment comparing the effects of different sensor density levels.

1 INTRODUCTION

It is very difficult to predict the rich tapestry of activity performed by building occupants through their day-to-day actions. As a result of this difficulty, lighting, heating, air-conditioning, and many other devices are left activated to consume power even when people are absent. Benefits of power-saving technology cannot be quantitatively assessed due to these large unknowns related to occupant behavior. Furthermore, it is difficult to compare different design options for their probable impact on occupant satisfaction, comfort, presence in various rooms, and use of water and electricity. These are tremendously important issues, since building operations account for the largest portion of global energy consumption and greenhouse gas emissions (US EIA, 2008).

Instrumenting our built environment with sensors and collecting detailed occupant data can address these issues, but this is complicated by the unavoidable discrepancy between sensor data and what actually happens. For example, a very common sensor technology for detecting occupancy is Passive Infrared (PIR) motion sensing. For this kind of sensor the discrepancy between sensed and real data occurs when certain areas are not covered by the sensors, since they have a limited range and obstacles such as furniture can interfere with proper detection. Also, even if the person is within the range of the sensor, if the person remains too still the sensor may not detect the person's presence. Treating occupant sensor data as a truthful representation of actual occupant presence could be detrimental to an intelligent Building Automation Systems (BAS) and to a designers' understanding of human behavior in buildings.

In this paper we present work towards the use of simulation to study the relationship between actual occupant behavior and occupant behavior measured by sensor networks in buildings. The simulation encompasses a building with different rooms that have sensors within them. Occupants of the building possess high level goals such as drinking water and checking email, which they satisfy by walking around a building and performing actions. As occupants walk around the building they trigger motion sensors. In our experiment we focus on evaluating different configurations of PIR-based motion sensors by comparing actual occupancy within each room to occupancy sensed by sensors.

A major goal of our work is to establish a framework to be used in future research. To set a solid foundation in that direction, the organization of the occupancy model has influences from computational cognitive science research. And most importantly, we have adopted a simulation convention called Discrete Event System Specification (DEVS) (Zeigler et al., 2000) to set a solid theoretical foundation and allow for better extensibility and future improvement of our simulation models. Throughout the paper we will point out some of the positive effects that adherence to the DEVS conventions has provided.

2 BACKGROUND

There has been a large volume of work on occupant simulation in different fields of research, including computer graphics, architecture, and energy modeling, to name a few. However, in practice, these simulations are rarely utilized for energy-efficient building design. Instead, fixed occupancy profiles are used for most building energy models. These fixed profiles are often based on large-scale metering data from utility companies or building energy codes and standards (Chiou, 2009). Such fixed profiles are not sufficient to realistically capture the relationship between a building's energy consumption and individual occupants' behavior, since

no distinction is made between individual occupants, no interaction occurs between groups of occupants, and there is little day-to-day variability. To fully understand the consequences of individual choices that occupants make, more detailed occupant models are needed.

There are many applications of occupant simulation in the field of computer graphics such as film, video games, training, and emergency evacuation. Virtual Crowds (Pelechano et al., 2008) surveys work in this area, establishing a baseline of techniques and requirements for simulating large-scale virtual populations of seemingly sentient beings that possess both crowd and individual goals. We hope to build from this computer animation perspective to achieve a greater understanding of human behavior as it relates to comfort and energy consumption in buildings.

In architecture, there has also been some push to use computer-aided design tools to look at how space is used by occupants, instead of just looking at architecture only in terms of geometrical form. As stressed in the Space Re-Actor thesis (Narahara, 2007), computational design tools need to go beyond visualizations of light, materials and geometry, and help people study and understand designed spaces as they are to be inhabited. In his thesis Nagukura presents a system where agents display different behaviors in reaction to architectural elements, such as glass, perforations, and furniture.

When it comes to behavior models, the most interesting and advanced models are being developed in computational cognitive science in an effort to merge neuroscience, artificial intelligence, and cognitive psychology to produce models of human cognition (Vernon et al., 2007). While our occupant model is not a direct implementation of any of the existing cognitive architectures, we are inspired by the current work in the field, and hope to integrate more aspects of these systems in the future.

Using more advanced occupant models instead of fixed profiles in the context of building energy modeling can have a significant impact on energy consumption predictions. For example, (Bourgeois et al., 2005) showed that energy use predictions changed by 62% in an office building when the simulated occupant had the ability to manipulate heating, cooling, and lighting controls. Another example by Hoes et al. (2009), showed that the use of a detailed occupant model can have a significant effect on both heating and cooling energy demand predictions.

To study the relationship of actual occupant behavior, and behavior collected by sensors, we need to integrate sensor networks into our agent framework. Modeling sensors and occupants in combination to find relationships between these two aspects has not received much attention in the context of building design and operation. Sensor networks are an important aspect of surveillance systems, traffic control, and healthcare monitoring, and there has been a number of papers on automatic sensor placement (Becker et al., 2009; Hengel et al., 2009; Garaas, 2011). This previous work focuses on finding ways to fully cover the geometric space with camera sensing. In our work, on the other hand, we are interested in evaluating, and understanding the relationship between sensor placement and accuracy of occupant measurement. To achieve that kind of understanding, we need an advanced occupant behavior model where people are able to perform actions such as walking around the building along paths for sensors to monitor, and in the next section we will discuss the details of creating such a model.

3 MODEL

The goal of our experiment is to study the relationship between actual occupant behavior within each room and occupant behavior measured by motion sensors within a building. To achieve that, our simulation involves occupants walking around a building performing actions to satisfy their goals, while motion sensors detect occupant presence. To understand the mechanism of the simulation, in Section 3.1 we will introduce the overall process in terms of its basic elements and output behavior. Then, in Section 3.2, we present the details of our occupant model. We conclude with ways we have used DEVS conventions for the model in Section 3.3.

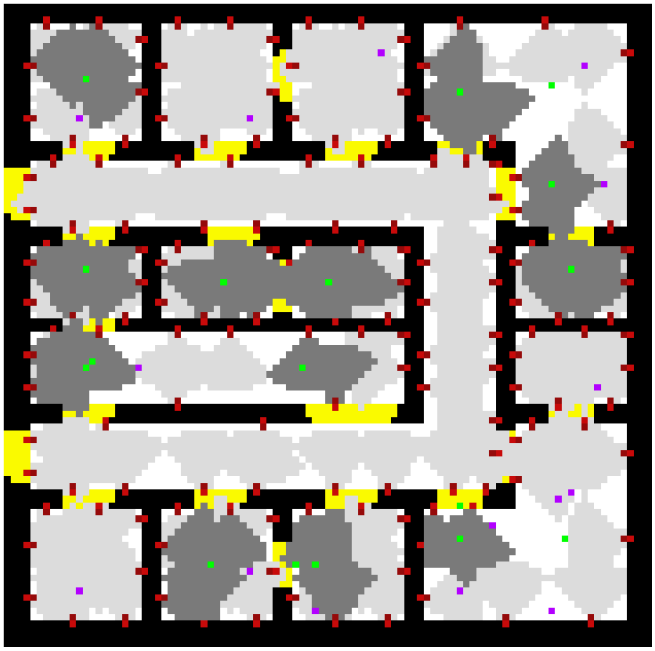

Figure 1: Grid-based floor plan. Green dots are occupants, purple dots are waypoints, red dashes are sensors with the direction of the line indicating the orientation. Light gray areas on the floor indicate the area monitored by the sensor, and dark gray areas indicate that there is an occupant within that sensed area. Doors are in yellow.

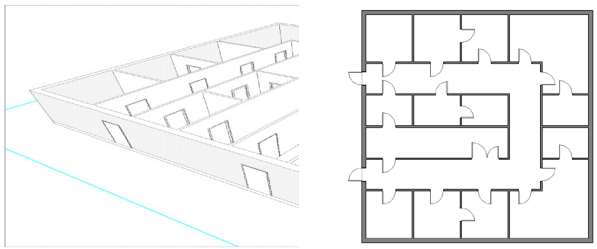

(a) (b)

Figure 2: Input building geometry, where (a) refers to the original 3D floor plan, and (b) to the extracted 2D floor plan.

3.1 Building Model

The main elements of the building model are the space layout, the occupants, and the sensors. The space layout remains fixed throughout the simulation while occupants move around it. As an occupant walks into a detection area of a sensor, that sensor gets activated, and when the person leaves the detection area, the sensor is de-activated.

Our space layout is represented as a discrete 2D grid of cells (see Figure 1). To create such a grid, a 2D floor plan (see Figure 2b) is extracted from a 3D building (see Figure 2a) which is discretized into cells. Different cells represent different elements, such as open areas, obstacles, doors, sensors, occupants, and others. The cells are colored based on their element type (Figure 1). People move from cell to cell based on the rules described in their behavior model. We have adopted a grid-based space layout representation for a number of reasons, such as to increase computational speed and to simplify the programming of the model. Alternative ways to represent the space layout, such as full 3D geometry, may be explored in future work. To generate the grid-based representation from an Autodesk Revit model of the building, we used the Spatial Analysis and Query Tool (SQ&AT). SQ&AT is a Revit plugin that affords the interactive analyses of circulation patterns of buildings (Doherty et al., 2012).

Besides the space layout data, *Waypoints* are an important input for the simulation. A *Waypoint* is a reference point in the building used for purposes of navigation. In our simulation we restrict occupants to move between these *Waypoints*, reflecting the observation that in most rooms, occupants tend to spend time at certain positions. These locations are manually authored during the design of the building, and would normally coincide with furniture or electronic devices used by the occupant. In Figure 1 they are illustrated with purple dots.

The occupant behavior is driven by high level goals such as reading an email, drinking water, or eating lunch. To achieve a high level goal, an occupant breaks the goal down to actions that she can perform. In our simulation all goals break down into at most two actions; first walking to the location where the goal can be satisfied, and second, actually performing the action necessary, e.g. drinking water. The locations at which the goal can be satisfied is picked by the selection of a random *Waypoint*. In future experiments we intend to make both of these procedures much more involved and context dependent. In Section 3.2, we will describe the *Occupancy* model in more detail.

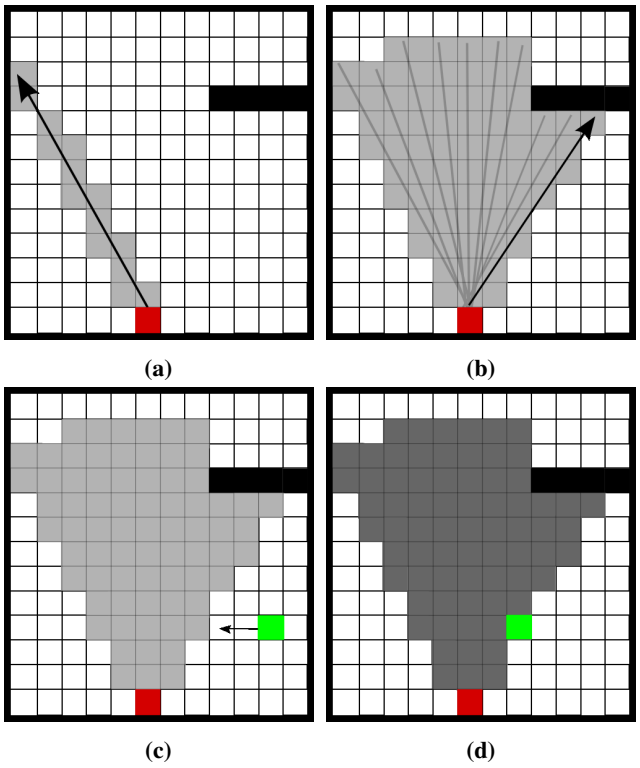

(a) (b) (c) (d)

Figure 3: Sensor Detection Process. (a) A ray is shot from the sensor (red cell), and as the ray travels through the grid space, grid cells are marked as belonging to the sensing area (gray cells). The ray stops if it hits a wall or if it reaches maximum range. (b) The process repeats for a number of rays to form a cone shaped area. (c) When an occupant (green cell) is outside the sensing area, the sensor is inactive. (d) When an occupant is inside, the sensor becomes active and the sensed area turns dark gray.

PIR-based motion sensors detect occupant presence by sensing the difference between infrared light emitted by moving people and the background. We have modeled each PIR sensor as an emitter of rays at a given location and direction. The term passive in this instance refers to the fact that PIR devices do not generate or radiate any energy for detection purposes. However, for computational and implementation efficiency, instead of modeling walls and occupants as sources of radiation, we trace rays from the sensors outwards. In Figure 1 sensors are illustrated using red line with the direction of the line indicating the orientation of the sensor, with all of the sensors being mounted on the walls. To find the sensed area

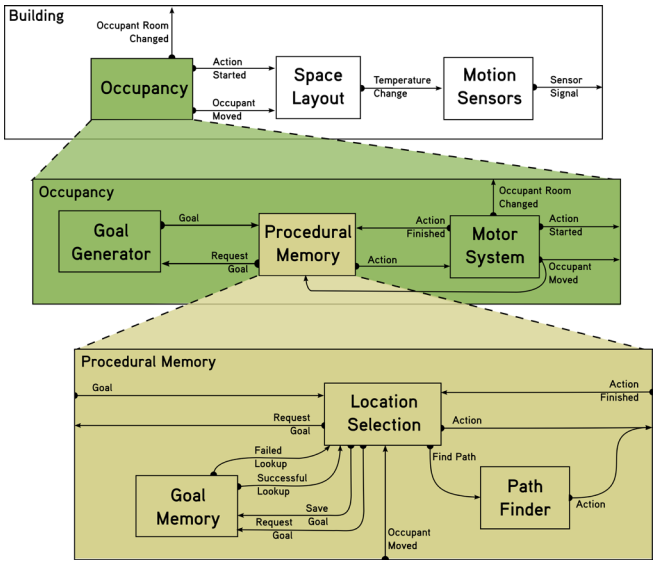

Figure 4: *Building* Simulation Model.

for a given sensor, rays are sent out using a fast grid-based ray tracing algorithm (Amanatides and Woo, 1987). See Figures 3a and 3b for the illustration of this process. Ray casting is necessary to make sure that sensors are blocked by walls and other obstacles. In practice, we perform the ray casting only once, during the initialization of the simulation, and cache the results in a reference grid for the whole building. This caching allows for fast lookup if an occupant passes within the detection range of the sensor. An important parameter for the *Motion Sensor* model is the sensor's range which includes the distance (8 meters) and horizontal angle range (90°) at which the sensor can perform detection. The process of sensing the occupant is illustrated in Figures 3c and 3d.

3.2 Occupant Model

Our overall goal in designing the *Occupancy* model was two fold; first, keeping it as simple as possible to achieve the desired simulation, and second, to set a clear foundation for future extension to more complicated behavior. Similar to other agent-based work (Yu and Terzopoulos, 2007), our occupant model is composed of different conceptual components. To talk about these components in a way that clearly communicates their purpose, we use fundamental cognitive psychological themes consistent with work in computational cognitive science (Vernon et al., 2007).

The submodels of our *Occupancy* model fall under the following themes:

Motivation A *Goal Generator* model creates a goal for the occupant to perform. An example of a goal is to satisfy hunger or thirst. A goal has an associated duration for the goal to be satisfied. Currently, this duration is a random time drawn from an exponential distribution with a mean of 10 minutes.

Motor System is responsible for controlling movement and is represented by a submodel called *Motor System*. It knows how to walk and execute various actions such as drink and eat.

Procedural Memory is memory for how to perform actions. In our model the responsibility of *Procedural Memory* is to take a high level goal and translate it to low level actions that the motor system can understand and perform.

Short-Term Memory is memory that can hold information for a short period of time. *Goal Memory* is responsible for keeping track of future goals that the occupant needs to satisfy. It is implemented using a simple queue. For example, if an occupant's goal is to drink water in room 8, but she is located in room 7, the *Goal Memory* would save the goal of drinking water in room 8, while the occupant walks there.

Spatial Memory is the part of memory responsible for information about one's spatial location and orientation. In our simulation two models fall into this theme, *Location Selection* and *Path Finder*. *Location Selection* is a model responsible for selecting the location of a given goal. In our simulation we simply pick random *Waypoints* from the building. One can imagine extending this to pick only locations depending on the goal at hand, for example, washing hands should only be done at a sink. However, for our experiment, such extensions were not necessary. *Path Finder* is a model which returns the shortest path between two points, respecting all the walls and obstacles in the building. This model uses the A* Algorithm (Hart et al., 1968) for finding the shortest path, which is very popular in the computer game industry due to its flexibility in a wide range of contexts by offering a tradeoff between speed and accuracy. It also allows different areas of the building to have different costs associated with them, to allow encouragement or discouragement of occupants from going one way or another. For example, areas in a hallway right against a wall might have a higher cost value than areas in the middle of the hallway, or an elevator might have a different cost than stairs. The biggest downside of the current implementation is that all the paths are pre-computed at the initialization of the simulation. In the future we hope to expand the simulation to use more adaptive pathfinding.

As described, our occupant behavior is missing crucial pieces of the human cognitive cycle such as perception, attention, emotions, and decision making capabilities to name a few. However, even with these limitations it does satisfy

our goals for the experiment, where an occupant is capable of generating a goal and is able to walk around the building to satisfy that goal. This set of models is also sufficient to set up the framework for future research where each psychological theme can be further expanded.

3.3 DEVS Hierarchy

DEVS is a set of conventions for specifying simulation models. The conventions promote modular models that allow for better extensibility. There are two types of models that are defined by DEVS, *atomic* and *coupled*. *Coupled* models are created by linking or coupling other models, while the *atomic* models are indivisible. A *coupled* model can be composed of many *atomic* and other *coupled* models, without needing to know if the models within are *atomic* or *coupled*. One of the important benefits of support for *coupled* models is that it allows one to break the simulation model into a hierarchical set of models. This gives rich flexibility to abstract complicated behavior behind intuitive sets of modules.

Please refer to Figure 4 for the illustration of the *Building* simulation model hierarchy, showing all the models that make up the *Building* and the *Occupancy* model. The links in the diagram represent the pathways of information flow. For example, a Goal is sent from *Goal Generator* to *Procedural Memory*, and within the *Procedural Memory* model it travels to *Location Selection*. *Location Selection* in turn may translate the goal into an Action, and send it out to its parent model, *Procedural Memory*, who will pass it to *Motor System*. However, if an occupant is not at the right location to perform the action, *Location Selection* will send the goal to *Goal Memory* instead, for temporary storage, and will request *Path Finder* to find a path to the desired location. It will send an Action to walk to that location and *Procedural Memory* will delegate the walk Action to Motor System. Motor System will update the occupant's location and send out all the messages regarding the changes internally to *Procedural Memory* and to the parent Occupant model who will delegate the message onward to *Space Layout*. *Space Layout* will then send a message to the *Motion Sensors* model.

In designing our *Occupancy* model, we have created a hierarchy based on cognitive models to stress the idea that the model represents a general behavior of occupancy instead of individual occupants. Thus, an important property of the model is that it represents all the occupants in the building. This approach implies that input and output messages must contain occupant IDs and that some internal variables have to contain structures indexed by this occupant ID (e.g. a dictionary or an array) instead of a single variable. A possible alternative to support multiple occupants is to be take advantage of Dynamic Structure DEVS (Barros, 1995), which gives one the ability to define a network of models that can undergo structural changes during a simulation so that each instance would be a new model.

Using DEVS in designing our models allowed us to isolate the responsibility of different aspects of the simulation, where each model does not have to know anything about any other models. This is very convenient, since often the models have to be adjusted or changed. If different models have high dependency on each other, this would be hard to achieve. When models sends out messages, they know nothing about the recipients of those messages, and thus stay independent from the surrounding models. This property of reconfiguration is crucial in the context of occupant behavior, since as our understanding of cognitive processes evolve and new computational models for different aspects of the mind are developed, we will be able to adjust accordingly.

4 EXPERIMENT

To better understand the discrepancy between occupancy data collected by sensors and true occupancy, the goal of our experiment is to investigate how sensor configuration influences accuracy of occupancy detection. Specifically, our experimental variable is per-room sensor density. Sensor density is the degree at which a given room is sensored, high density implies lots of motion sensors in a room, while low density having few sensors. Refer to Figure 5 for examples of how the density maps to the degree of sensing of the space layout.

To create the full 100% sensor density placement for a given room, each wall segment was instrumented with two sensors. The placement along the wall is chosen by parameterization the wall on a $[0,1]$ interval, and placing the sensors at 0.2 and 0.6 locations. This can be seen in 5f, where sensors are represented as red dashes. While this simple sensor placement schema will not scale well for more complicated building plans, it is sufficient for our basic experiment. To produce the sensor density of 10%, for each room, 10% of the sensors are randomly used from all the sensors that were initially placed. Then, to produce 25% density, more sensors are added on top of the ones that were previously added when creating the 10% density configuration. This procedure ensures that sensors that were present in the 10% density trial are also present in the 25% density trial.

For each density (10%, 25%, 40%, 60%, 100%) a trial was run for 8 simulated hours. As the simulation is running, occupants walk around the space layout to get from one *Waypoint* to another, activating and deactivating sensors in the process. The number of occupants in the building is a parameter initialized to generate 30 people. When an occupant gets to their *Waypoint* of interest, they perform an action (e.g. drink water). The time it takes to perform the action is randomly drawn from an exponential distribution with a mean of 10 minutes. This mean time is also an input parameter for the simulation set during the initialization phase.

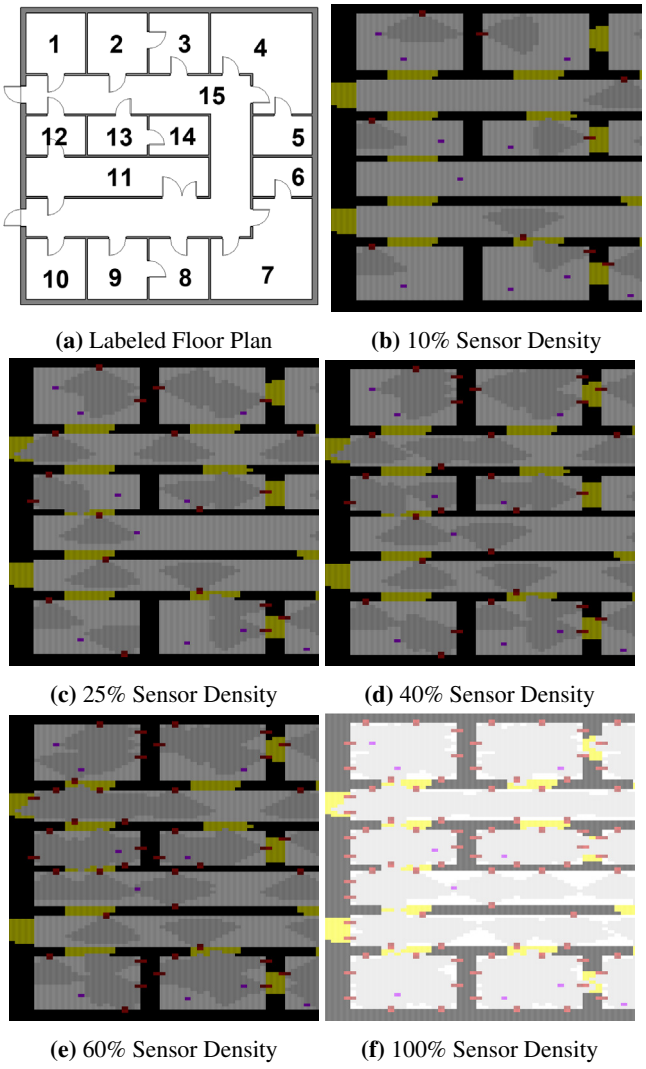

(a) Labeled Floor Plan **(b)** 10% Sensor Density

(c) 25% Sensor Density **(d)** 40% Sensor Density

(e) 60% Sensor Density **(f)** 100% Sensor Density

Figure 5: Floor Plans with different sensor densities. Red dashes are sensors with the direction of the line indicating the orientation. Light gray area on the floor indicates the sensed area.

To calculate both the sensed and actual occupancy in each room, we look at times when occupants walk in and out of sensor coverage and enter and exit rooms. According to the sensor network, a room is considered occupied whenever at least one sensor in the room is active. Based on actual occupant behavior, a room is considered occupied whenever there is at least one occupant in that room. The Relative Error between sensed and actual occupancy of each room is given by $\frac{O_{true}-O_{sensed}}{O_{true}}$, where O_{sensed} is the percentage of time the room is occupied according to the sensor network and O_{true} is the percentage of the time the room is actually occupied.

All simulation runs were performed using DesignDEVS, a simulation tool we created for developing and testing DEVS models. The results of our experiment for Room 15, which is a hallway, can be seen in Figure 6. In the plot, observe that as the density of sensors is increased, the error rate decreases in a very smooth trend. However, note that as sensor density goes to 100%, the Relative Error does not go to zero. To understand the reason behind this, see Figure 5f, using Figure 5a to identify Room 15. There are a few areas of the hallway (outside of Room 8, 9, and 10) which are not covered by sensors. These unsensed areas explain the discrepancy.

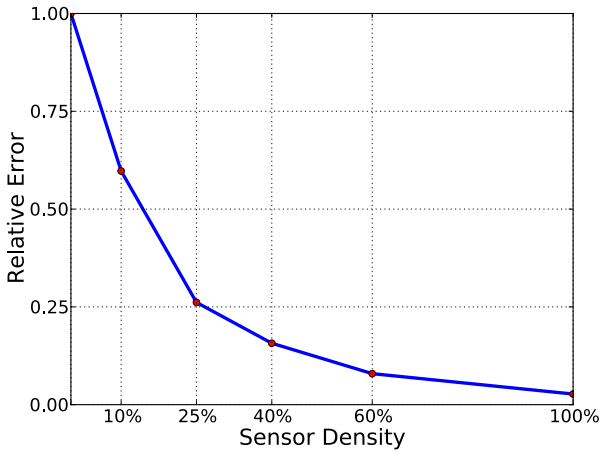

Figure 6: Error Plot for Room 15, the hallway.

The distinction between a hallway and the rooms is the fact that rooms have *Waypoints* where occupants stop to perform actions, while a hallway is simply a circulation area where occupants pass through to get to the rooms. Since *Waypoints* may fall outside of the sensed area, the whole time an occupant spends at that location would count towards increasing the Relative Error between sensed and actual occupancy. The resulting error for the rooms can be seen in Figure 7. As an example, see the error plot for Room 5 where the error stays high until 25% density, and then plunges nearly to 0 at 40% density. To understand what happened, see Figure 5b, using Figure 5a to identify Room 5. Observe that the *Waypoint* (a purple dot) is outside of the sensor's range. As we increase the density to 25% (Figure 5c) the *Waypoint* continues to be outside of the sensed area, and finally at 40% density (Figure 5d) we can see the *Waypoint* being inside the sensing area of one of the sensors. Similar relationships between the Relative Error plots and sensor coverage can be seen in other rooms. A slight loss of sensor coverage in an important area can result in a significant error in occupancy measurements. Although the model is simplified, the variability of the plots in Figure 7 is a good reflection of the complication of sensing occupants in real buildings.

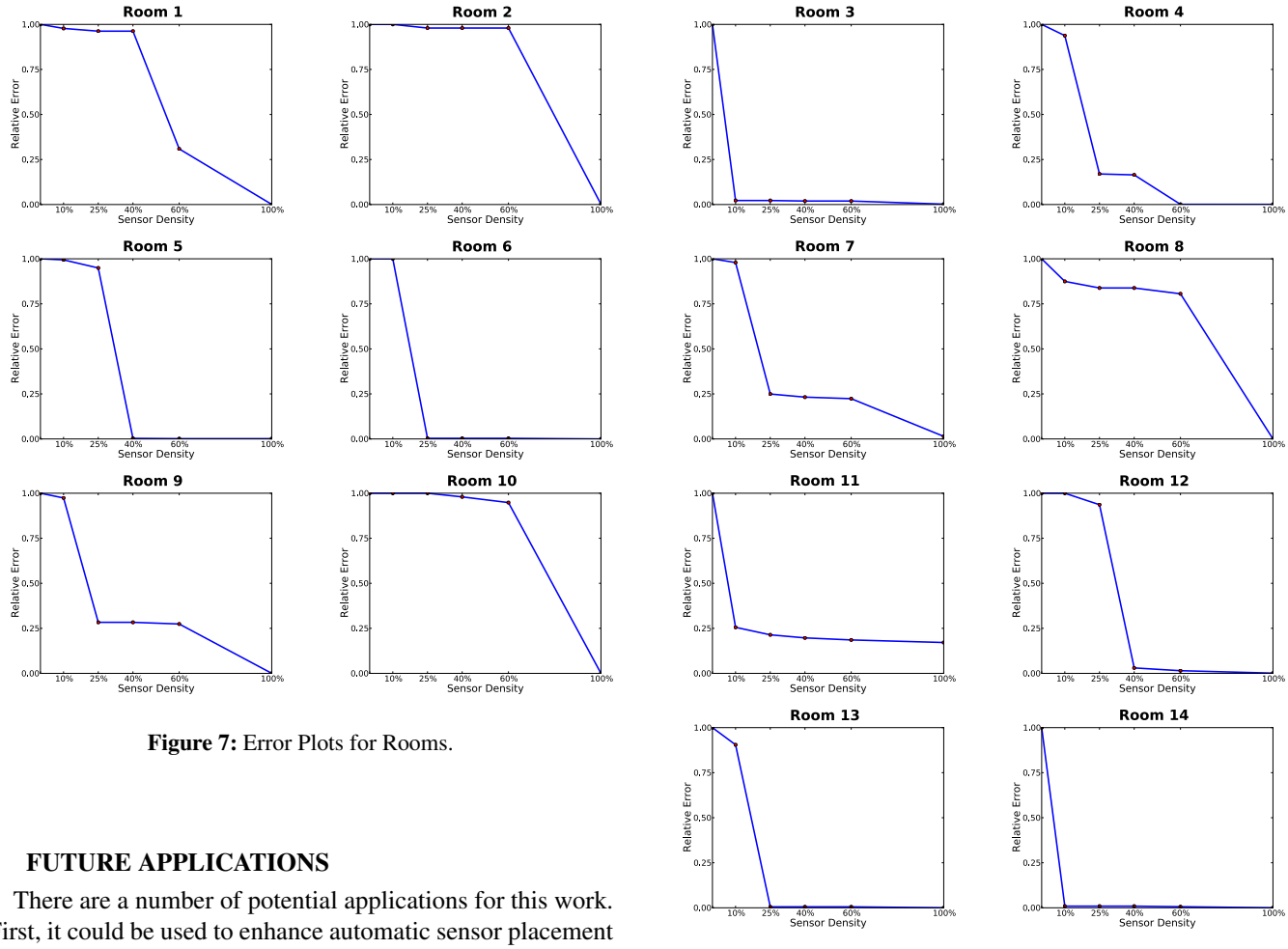

Figure 7: Error Plots for Rooms.

5 FUTURE APPLICATIONS

There are a number of potential applications for this work. First, it could be used to enhance automatic sensor placement tools to account for dynamic occupant behavior. Second, with additional models for occupancy sensing technologies based on pressure and ultrasound, the work could support the design of accurate and cost efficient occupant monitoring systems. Simulation models of building occupants and sensors could be integrated with thermal, lighting, and air flow models to improve energy use predictions. They could also support emergency evacuation experiments. To get to the point where such applications are possible, we anticipate a number of necessary enhancements.

For some of these applications, our current occupant behavior is not detailed enough, and new aspects of behavior need to be modeled. Since all our models adhere to the DEVS convention, it is straightforward to replace one model for another. For example, we can easily replace our *Location Selection* model with work by Goldstein et al. (2011), which would help make location selection favor nearby rooms, or steer the occupants away from rooms that are overcrowded. As the occupancy model evolves to account for more enviromental factors, we envision omitting both waypoints and the explicit distinction between rooms to start examining emergent occupant behavior. This would introduce a need to dynamically adjust navigation paths, requiring enhancements to the *Path Finder* model. For example, we could use a geometrical navigation mesh (Doherty et al., 2012) instead of the grid based navigation to allow for greater freedom of movement. Also, it is easy to replace an existing atomic model with a more complicated hierarchical one. For example, instead of using a simple *Goal Memory* model for the memory, we can adopt a more advanced hierarchical model like Atkinson and Shiffrin (1968), which would have three sub-models: short-term, long-term, and sensory memory.

To expand the simulation to different domains, such as adding thermal and energy models, DEVS allows us to easily add new models adjacent to existing models and connect them using links. For example, for modeling energy consumption we might want to add an *Appliances*, an *HVAC* system, and a *Lighting* model that connects to our *Space Layout* model. Similarly, if we want to expand the occupancy model to support perception of the environment, interaction with the environment, and decision making, we can add new models inside

of the occupancy model, and easily adjust the way submodels are connected. Connecting all these different pieces into one simulation allows us to ask new questions about correlations between different aspects of our environment and occupant behavior.

6 CONCLUSION

In this paper we have contributed a hierarchical model of occupant behavior inspired by cognitive research and an experiment that studies how sensor density influences effectiveness of occupancy detection. We have found that the effectiveness of sensors increases as the density of sensors increase, with hallways having a predictable Relative Error, while other room's Relative Error being more variable. By adhering to the DEVS conventions, we have established a foundation for extending our simulation model to support more advanced human behaviors and set a path for future research in our understanding of human behavior in the context of building performance. This research path may help in creating more intelligent Building Automation Systems and increasing designers' understanding of human behavior in buildings.

References

Amanatides, J. and A. Woo (1987). A Fast Voxel Traversal Algorithm for Ray Tracing. In *In Eurographics '87*, pp. 3–10.

Atkinson, R. and R. Shiffrin (1968). Human memory: A proposed system and its control processes. *The psychology of learning and motivation 2*, 89–195.

Barros, F. J. (1995). Dynamic structure discrete event system specification: a new formalism for dynamic structure modeling and simulation. In *Proceedings of the 27th conference on Winter simulation*, WSC '95, Washington, DC, USA, pp. 781–785. IEEE Computer Society.

Becker, E., G. Guerra-Filho, and F. Makedon (2009). Automatic sensor placement in a 3d volume. *Proceedings of the 2nd*.

Bourgeois, D., C. F. Reinhart, and I. A. Macdonald (2005). Assessing the total energy impact occupant behavioural response to manual and automated lighting systems.

Chiou, Y. (2009). *An Occupant-Driven Integrative Household System For Residential Building Energy Simulation*. Ph. D. thesis, Carnegie Mellon University.

Doherty, B., D. Rumery, B. Barnes, and B. Zhou (2012). A spatial query & analysis tool for architects. In *Proceedings of the 2012 Symposium on Simulation for Architecture and Urban Design*, SimAUD '12.

Garaas, T. W. (2011). Sensor placement tool for rapid development of video sensor layouts. In *Proceedings of the 2011 Symposium on Simulation for Architecture and Urban Design*, SimAUD '11, San Diego, CA, USA, pp. 134–137. Society for Computer Simulation International.

Goldstein, R., A. Tessier, and A. Khan (2011). Space layout in occupant behavior simulation. *IBPSA-AIRAH Building Simulation*, 1073–1080.

Hart, P., N. Nilsson, and B. Raphael (1968). A Formal Basis for the Heuristic Determination of Minimum Cost Paths. *IEEE Transactions on Systems Science and Cybernetics 4*(2), 100–107.

Hengel, A., R. Hill, and B. Ward (2009). Automatic camera placement for large scale surveillance networks. *Workshop on Applications of Computer Vision (WACV)*.

Hoes, P., J. L. Hensen, M. G. Loomans, B. de Vries, and D. Bourgeois (2009). User behavior in whole building simulation. *Energy and Buildings 41*(3), 1–22.

Narahara, T. (2007). The space re-actor: Walking a synthetic man through architectural space. Master's thesis, Massachusetts Institure of Technology.

Pelechano, N., J. Allbeck, and N. I. Badler (2008). *Virtual Crowds: Methods, Simulation, and Control*. Morgan & Claypool Publishers.

US EIA (2008). *Assumptions to the Annual Energy Outlook*. U.S. Energy Information Administration, Washington, D.C.

Vernon, D., G. Metta, and G. Sandini (2007). A survey of artificial cognitive systems: Implications for the autonomous development of mental capabilities in computational agents. *Evolutionary Computation*.

Yu, Q. and D. Terzopoulos (2007). A decision network framework for the behavioral animation of virtual humans. *Symposium on Computer Animation*.

Zeigler, B. P., H. Praehofer, and T. G. Kim (2000). *Theory of Modeling and Simulation* (2nd ed.). San Diego, CA, USA: Academic Press.

Development of Discrete Event System Specification (DEVS) Building Performance Models for Building Energy Design

Huseyin Burak Gunay[1], Liam O'Brien[1], Rhys Goldstein[2], Simon Breslav[2] and Azam Khan[2]

[1]Carleton University
1125 Colonel by Drive,
Ottawa, ON, Canada, K1S 5B6
{firstname_lastname}@carleton.ca

[2]Autodesk Research
210 King Street East,
Toronto, ON, Canada, M5A 1J7
{firstname.lastname}@autodesk.com

Keywords: DEVS, modular BPS, stochastic occupant models, energy simulation in building design

Abstract

The discrete event system specification (DEVS) is a formalism for describing simulation models in a modular fashion. In this study, it is exploited by forming submodels that allow different professions involved in the building design process to work independently to create an integrated model. These submodels are the *building*, the *HVAC system*, and the *occupant*. In this study, a coupled DEVS building energy model of a generic office space is presented to demonstrate the viability of the DEVS formalism for BPS based design. Results indicate that the DEVS formalism is a promising way to improve poor interoperability between models of different domains involved in building performance simulations.

1. INTRODUCTION

Approximately 40% of the total energy produced in North America is consumed by residential and commercial buildings (DOE 2009). More importantly, it is reported by NRCan (2006) that nearly 60% of the total energy consumption of buildings in Canada can be attributed to space heating and cooling.

Building performance simulation (BPS) is a powerful design tool for predicting buildings' energy performance and thermal comfort. It represents significant potential for optimizing design such that substantial energy and operating cost savings can be achieved with little, if any, additional capital cost. Clarke (2001) estimated these savings as high as 50-75% in new buildings and 30% in existing buildings relative to 2000 levels; however, NRCan (2006) reported that the change in energy use per unit area is stable between 2000 and 2005. This indicates that conventional BPS based design techniques have not yet been adapted efficiently by the building industry to the integrated design process.

Integrated design, a process by which all building design team members (architects, mechanical engineers, civil engineers, electrical engineers, consultants, etc.) work together and share a common data model, is very uncommon. Instead, the same data is manually input by multiple designers, leading to redundant work, a slower design process, and possibly errors. The cost of poor interoperability between designers and software has been conservatively estimated at $15.8-billion annually (Gallaher et al. 2004).

The Discrete Event System Specification (DEVS) formalizes the description of simulation models in such a way as to provide benefits in the areas of collaboration and software development, which together, provide scalability. First, models are completely independent of the simulator. That is, a generic DEVS simulator can be created without any knowledge of the domain being simulated. Consequently, models do not contain any simulation management functionality, and so are typically much simpler to program. Secondly, models may be composed in a hierarchical manner without knowing whether the submodels are themselves compositions. For example, a building energy model may be composed of a building model, an HVAC model, and an occupant model. Each of the submodels may be initially created as simple atomic models but may be refined later to include submodels without affecting the rest of the simulation. Finally, models with no explicit references to one another can be coupled to

communicate via input and output messages. Detailed information about the theory and application of DEVS can be found elsewhere (Zeigler et al. 2000, Wainer 2009).

It is the ability to couple independently developed models that makes DEVS a promising option for supporting collaboration between experts of different domains. For example, state-of-the-art building performance models require a background in math and physics for heat transfer, expertise in mechanical engineering for heating, ventilation, and air-conditioning (HVAC) systems, and the use of statistics and psychology for occupant behavior. Using DEVS, the idea is that various teams can each focus on developing a model in a single domain that addresses both the scalability issues of whole building simulation and the practical needs of designers. By combining these submodels, the resulting coupled model may capture interactions between domains such as the effect of an HVAC system on indoor temperatures, the effect of temperature on occupant comfort, and the effect of an occupant's actions on windows, shades, and thermostat set-points.

Building and HVAC system simulations involve the simultaneous solutions of systems with varying time constants ranging from seconds to hours for continuous differential equations. Therefore, solvers that impose a common time step for all submodels introduce considerable redundancy for domains associated with relatively large time constants. Cellier and Kofman (2006) explained a new way of approximating differential equations by replacing time discretization by quantization of the state variables. Moreover, modeling of the occupant involves stochastic decision making processes such as opening the windows, changing the clothing level, adjusting the blinds, drinking a hot/cold beverage and/or changing the thermostat setpoint. Incorporation of such adaptive behavior into conventional BPS tools designed to solve continuous differential equations is rare and restricted to predefined time periods due to the way time advancement is handled. For example, Rijal et al. (2007) demonstrated window opening behavior in ESP-r using Humphrey's window opening algorithm in 1 hour time steps. In reality, the occupant undertakes such adaptive measures at random time intervals rather than fixed multiples of given time steps.

DEVS inherently supports the variable time steps needed for the alternative numerical integration techniques and stochastic behavior described above. A DEVS model's time delay is recalculated after every state transition regardless of whether these delays vary or remain fixed. State transitions are described by an *external transition* function for cases in which the model receives an input message, or by an *internal transition* function for cases in which the model generates an output message. The *time advance* function gives the delay before an internal transition occurs. The delay is recalculated if an input triggers an external transition before the original delay elapses. Understanding external and internal transition functions as well as the time advance function is the key to understanding indivisible, or atomic, DEVS models. The other type of DEVS model is the coupled model, which links submodels of either type.

This paper presents a DEVS building energy model of a generic office space to demonstrate the viability of the DEVS formalism for BPS-based design. A DEVS-based simulation prototype (Autodesk DesignDEVS v.0.4.1) was used in this study. To illustrate the actual workflow of each design group, a *building submodel*, a *HVAC system submodel*, and a stochastic *occupant submodel* were developed independently as atomic models. These submodels were then linked with each other by defining the input/output relationships to demonstrate the overall response of the coupled DEVS building energy model.

2. BUILDING MODEL

A thermal network model of the north facing office shown in Figure 1 is established. This thermal network model is used to solve for the first-order approximation of the heat conduction equation. In a thermal network model, a building is represented as an electrical network. Thermal masses, which include both indoor air volumes and physical elements like walls, windows, and slabs, become nodal points in the network. They are each assumed to have a uniform temperature in the same way that nodal points in an electrical network are each associated with a single voltage level. Adjacent thermal masses may be linked by a time-dependent thermal resistance —the reciprocal of thermal conductance— through which heat flows like current in an electrical network (Clarke 1986). A thermal network model consists of lumped thermal mass (J/^{o}C), lumped conductance elements (W/^{o}C), and heat sources (W). Detailed information about thermal network models can be found elsewhere (Athienitis 2000).

A central finite difference formulation is used to solve for the thermal network model explicitly as follows:

$$\{T_{i+\Delta t}\} = \overbrace{\left([U_i]_{nxn}\{T_i\}_{nx1} + \{Q_i\}_{nx1}\right)\Delta t./\{C\}_{nx1}}^{\Delta T_i} + \{T_i\} \qquad [1]$$

where the conductance matrix U_i (W/°C), the temperature array T_i (°C), and the heat source array Q_i (W) at a given time are used to determine the heat flow in the thermal network model. The time step Δt (s) and the thermal mass array (J/kg) are then used to determine temperature variations ΔT_i (°C) due to the heat flow in the thermal network model. The summation of ΔT_i and T_i are then used to determine the temperature in the next time step $T_{i+\Delta t}$.

While discrete time solvers use fixed time steps, discrete event solvers may vary the time step according to how fast the system is changing state. As mentioned, the quantization of state variables is one way to determine Δt (Cellier and Kofman, 2006). The building model presented here determines Δt by limiting the temperature change per time step for all thermal masses. Therefore, during the simulation, when abrupt temperature changes are expected due to occurrences such as opening the window or turning the HVAC unit on, the model chooses a smaller Δt but during tranquil regions of the simulation such as night time, the model chooses a larger Δt. The internal time advancement in the building model is carried out as follows:

$$\Delta t = \Delta T \ \min\left|\{C\}_{nx1} / \left([U_i]_{nxn}\{T_i\}_{nx1} + \{Q_i\}_{nx1}\right)\right| \qquad [2]$$

where ΔT (˚C) is the maximum temperature change (e.g. 1˚C change in temperature at any of the nodal points). The function determines the scheduled time advance so that a ΔT change can happen at any of the nodal points. It should be noted that Δt is a real number and its variation depends on the physics of the problem. This internal scheduling can be interrupted with an external input being received at anytime. For example, if the occupant opens the window; the time advance stops, the model is modified accordingly with the change in physics, and then proceeds.

The *building model* starts with the transformation of the weather data (i.e. dry-bulb temperature, diffused solar radiation, normal solar radiation, and solar luminance) to the environmental loads (i.e. solar-air temperature, solar gains, window temperature, indoor daylight), as shown in Figure 2. This transformation is achieved using input parameters such as window area, latitude, orientation, daylight factor (Simons and Bean 2001), solar heat gain coefficient (SHGC), and absorptivity. The *building model* receives inputs from (1) the environmental loads (i.e. solar-air temperature, solar gains, window temperature, indoor daylight), (2) the *occupant model* (i.e. blind closing, window opening, light turning, and occupant presence), and (3) the *HVAC system model* (i.e. heat input).

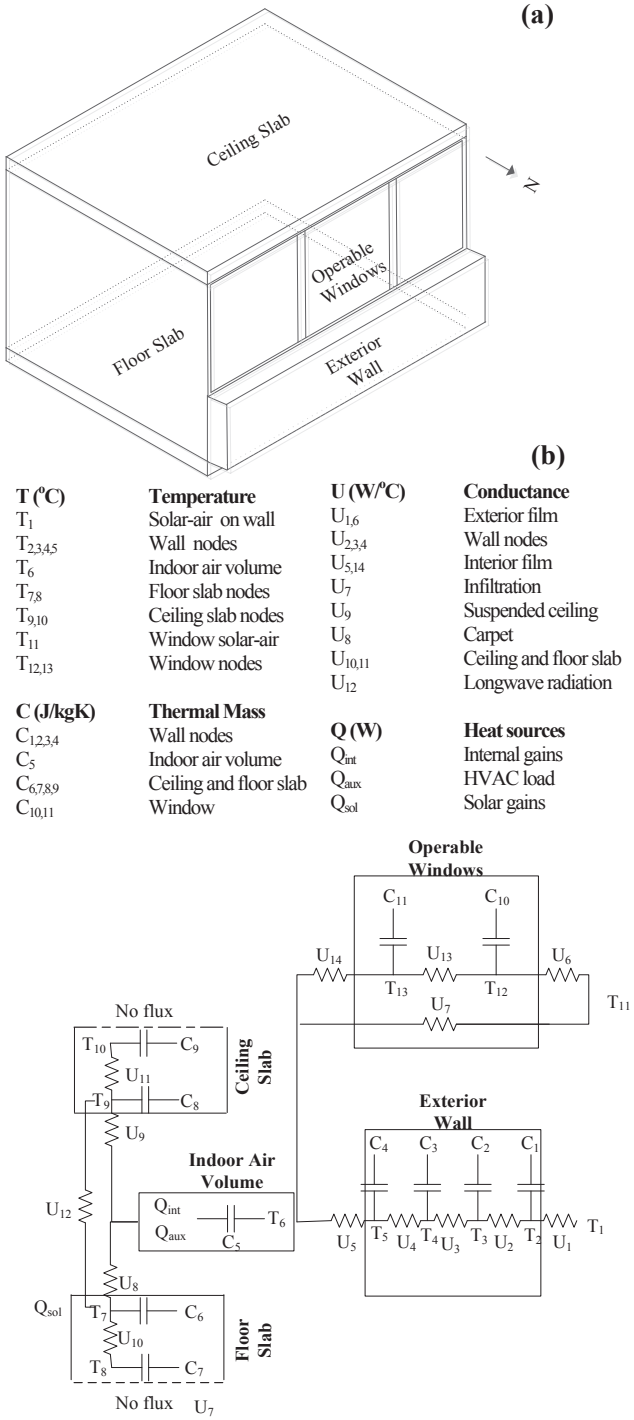

Figure 1: (a) Analysis domain and (b) thermal network model

Subsequently the *building model* calculates the temperature at each of the nodal points and outputs the air temperature of the zone and the mean radiant temperature using the parameters defined in Figure 2. The *building model*, in absence of the *occupant model* and the *HVAC system model*, reveals the passive building response, as shown in Figure 2. It should be noted that both mean radiant temperature and the indoor air temperature are higher than the outdoor temperature. This occurs as the windows are transparent for the shortwave radiation (solar radiation), while opaque for the longwave radiation from building surfaces.

The physical impacts of the occupant adaptive behaviors and the HVAC loads are defined in the *building model*. The primary physical implication of the window opening behavior is the airflow between the indoor and outdoor environment which is adapted as 8 L/s/person from ASHRAE (2009) and CIBSE (2006). This is with 4 occupants ~27 times larger than the air infiltration rate (0.3 ach) assumed in this study. Infiltration conductance in the conductance matrix, U_7 is modified accordingly, if the window is opened. The secondary implication of window opening behavior is that the reflected portion of the shortwave irradiation from the glazing incidents directly on the floor. Moreover, some of the longwave radiation emitted by the slab incident on the window opening leaves the room. This is implemented in the *building model* by changing the solar heat gain coefficient (SHGC) from 0.58 to 1 and by defining a conductance between the ambient air and the slab surface to take into account the radiation emitted from the slab surface through the window opening.

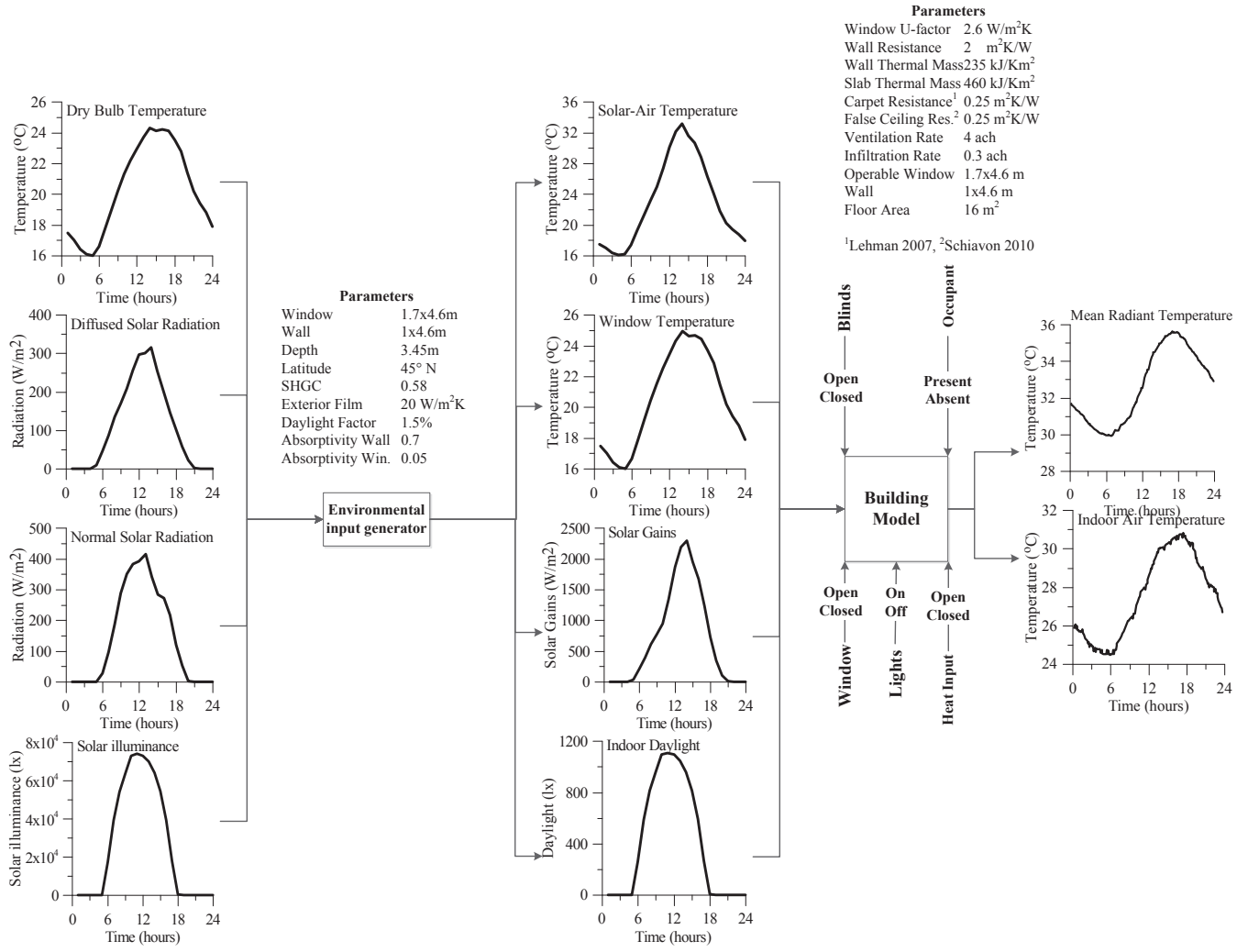

Figure 2: Parametric input/output relationships to the building model

Similarly, the primary physical implication of closing the blinds is reducing the transmitted solar irradiation. The roller blinds are assumed to reduce the transmitted solar irradiation on the slab surface to 10% of the incident solar radiation (Kuhn et al. 2000). The secondary implication of having blinds closed is that 20% of the incident solar energy is absorbed quickly by the blinds and due to its low thermal mass is emitted quickly into the air space (Kuhn et al. 2000).

Physical impacts of the occupant presence and lighting are defined as a heat gain of 100 W/person (ASHRAE 2009) and 32 W/bulb for 3x32T8 light bulbs (DiLouie 1967), respectively. The physical effect of the heat input from the HVAC unit is defined as a conditioned air flow into the air space. This is implemented in *building model* as follows:

$$Q_{aux} = \dot{m} C_{air} (T_{zone} - T_{dif}) \quad [3]$$

where $\dot{m}$ (kg/s) is the mass flow rate of conditioned air through the diffuser, C_{air} (J/kgK) is the specific heat of the air, and T_{zone} (K) and T_{dif} (K) are the air space temperature and the conditioned air temperature by the diffuser, respectively.

3. HVAC SYSTEMS MODEL

A simple model of a packaged air handling unit is formed using a set of mass and energy balance equations at each component. The *HVAC systems model* is composed of a mixing box, a cooling coil, a humidifier, and a reheater, as shown in Figure 3 (Clarke 2001). For simplicity, each component is represented as a single node. At the mixing box the return air (indoor air volume temperature) (80%) and the outdoor air (20%) is mixed prior to entering the cooling coil (Sugarman 2007). Then, the cooling coil extracts the heat from the ventilation air. Humidifier and reheater components maintain the humidity of the ventilation air. The conditioned ventilation air is then supplied to the zone. Each component in the *HVAC systems model* introduces a thermal inertia that lags the output of the model. The *HVAC systems model* needs to receive input messages (HVAC decision, outdoor and indoor air temperatures) to invoke its internal transition function that solves for the output message (heat input). To demonstrate this input/output relationship, a few input messages are left on the *HVAC systems* simulation time grid, as shown in Figure 3. Initially HVAC decision (input) state is defined as false, thus the heat input to the zone (output) is 0. The indoor and the outdoor air temperature is defined at time=31 min. Once the HVAC decision state is changed to true, the internal state transition function is invoked and solves for the heat input as follows:

$$\underbrace{\begin{cases} \text{Energy Balance} \begin{cases} \dot{m}_o c_{air}(T_o - T_1) + \dot{m}_r c_{air}(T_r - T_1) = T_1 C_1 \Delta t \\ \dot{m}_2 c_{air}(T_1 - T_2) + Q_2 = T_2 C_2 \Delta t \\ \dot{m}_3 c_{air}(T_2 - T_3) = T_3 C_3 \Delta t \\ \dot{m}_4 c_{air}(T_3 - T_4) = T_4 C_4 \Delta t \end{cases} \\ \text{Mass Balance} \quad \{\dot{m}_2 = \dot{m}_3 = \dot{m}_4 = \dot{m}_o + \dot{m}_r \end{cases}}_{Q_{input} = (T - T_r)\dot{m}_4 c_{air}} \quad [4]$$

where $\dot{m}_i$ (kg/s) represents mass flow rate between the component nodes, $\dot{m}_o$ (kg/s) and $\dot{m}_r$ (kg/s) are the outdoor and return air flow rates, c_{air} (J/kg-K) is the specific heat of air, Q_2 (W) is the capacity of the cooling coil, Q_{input} (W) is the heat input rate to the zone and C_i (J/K) is the thermal mass of the component nodes. It is evident that the Q_{input} (2.75kW) is different than the cooling coil capacity (i.e. 3kW). This can be explained with the thermal mass induced time lag for the HVAC system to reach its capacity.

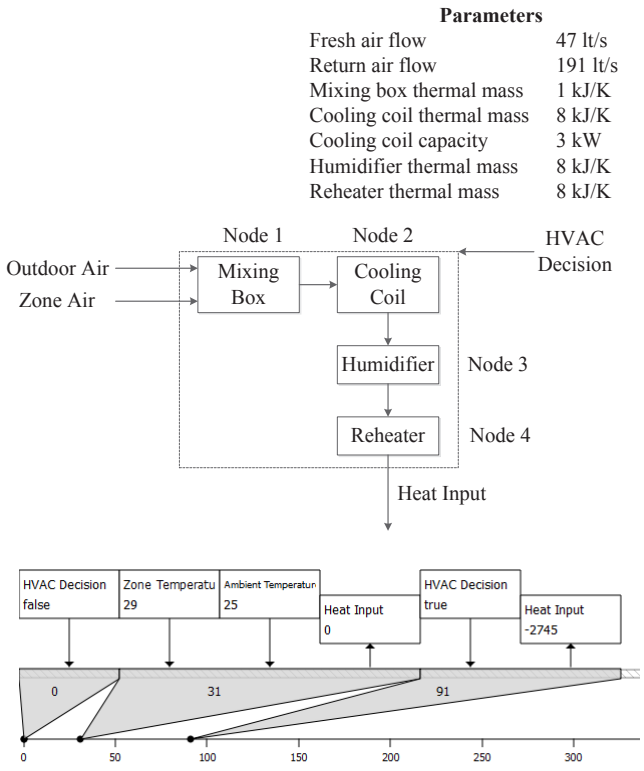

Figure 3: Parametric input/output relationships to the HVAC systems model

4. OCCUPANT MODEL

The *occupant model* is a set of decision making processes related to the way an occupant satisfies his/her thermal comfort. These involve actions to adapt both personal (clothing, drinking) and environmental (windows, blinds, HVAC) characteristics (Haldi and Robinson 2008). This study adapts the experimental results acquired by Haldi and Robinson (2008) to establish the *occupant model*. The model receives inputs such as the operative temperature (average of the indoor air temperature and the mean radiant floor temperature), the indoor luminance, and the occupant's schedule and outputs decisions about the blind state, clothing state, drinks state, lights state, window state, and HVAC state, as shown in Figure 4.

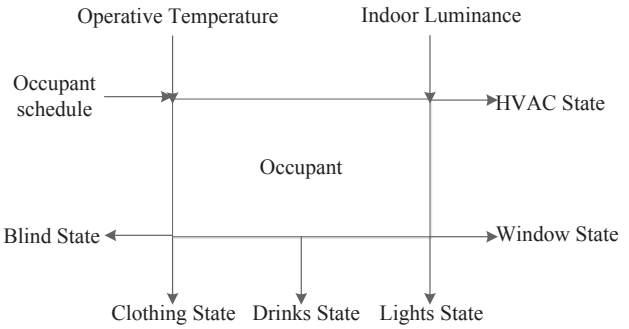

Figure 4: Parametric input/output relationships to the HVAC systems model

The cumulative distribution functions (CDFs) of these decisions are presented in Figure 5.a. The uniform pseudo-random number generator is transformed to a Gaussian probability density function using the Box-Muller algorithm which satisfies these CDFs (Box and Muller 1958). The flowchart shown in Figure 5.b. shows the decision making process of the occupant. For example, whenever an input message indicating a change in the operative temperature (weighted average of the air and the mean radiant surface temperature) is received, a cloth state (S_{cloth}) change temperature (T_{cloth}) is generated with a 24.6℃ mean (μ) and a 6℃ standard deviation (σ). If T_{cloth} exceeds the operative temperature, the occupant reduces his/her clothing level by 0.2 clo or 0.0155 m^2K/W (ASHRAE, 2010). This gives an occupant with 100W of metabolic energy generation an additional 1.5℃ (ΔT_{cloth}) tolerance. If the operative temperature exceeds the window opening temperature (μ=25.6℃ and σ=6℃), the window state (S_{win}) is changed to 'true'. If the operative temperature exceeds the beverage drinking temperature (T_{drink} μ=28.6℃ and σ=6℃), the

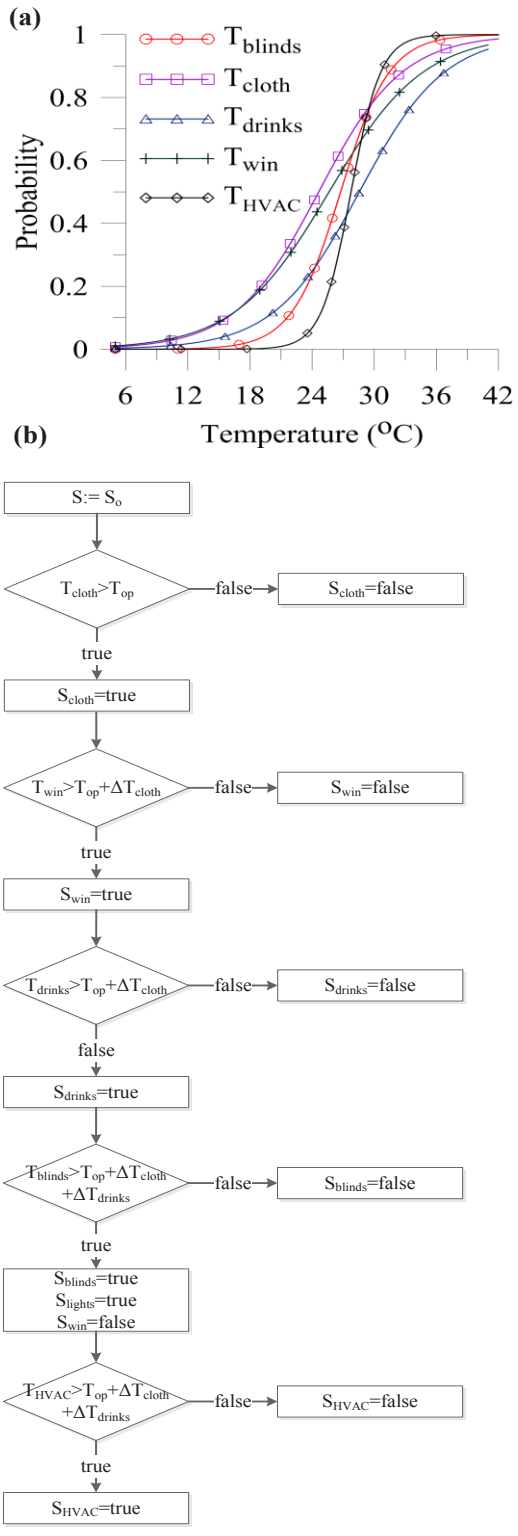

Figure 5: (a) CDFs for decision making temperatures and (b) flow of stochastic adaptive actions undertaken by an occupant

occupant drinks 500mL of a cold beverage at 5℃. This gives the 70kg occupant an additional 0.3℃ (ΔT_{drink}) tolerance. If the operative temperature exceeds the blind closing temperature (μ=26.8℃ and σ=2.5℃), the blind state (S_{blind}) is changed to 'true'. The light use decision (S_{light}) is undertaken when the indoor day light falls to less than 300 lx or when the blinds are closed. The blinds are assumed to block the airflow substantially, therefore the window is closed when the blinds are closed. If the occupant, after attempting all available adaptive actions, is not thermally satisfied and the HVAC decision temperature (μ=26.3℃ and σ=1.5℃) is reached; the HVAC unit state (S_{HVAC}) changes to 'true'.

5. DEVS BUILDING ENERGY SIMULATION MODEL

Three domains of the building energy simulation problem (i.e. *building, HVAC systems,* and *occupant models*) have been separately modeled. A coupled DEVS building energy model is formed as shown in Figure 6.

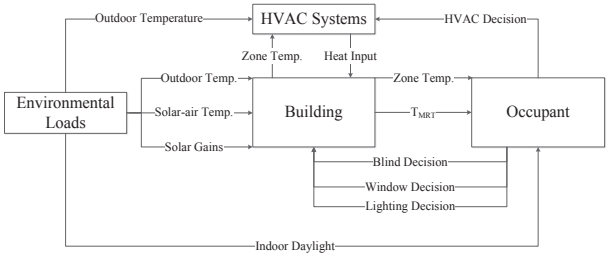

Figure 6: Coupled DEVS building energy model

The simulation of the coupled model starts as the weather data is transformed to the environmental loads such as outdoor temperature, solar-air temperature, and solar gains. These environmental loads are received by the building model and the air and mean radiant temperatures are sensed by the occupant. Subsequently, the occupant, in order to satisfy his comfort, undertakes personal (clothing, drinking) and environmental actions (blinds, window, HVAC). The environmental actions invoke the *building model,* the *HVAC systems model* or the *occupant model* (e.g. closing blind leads to a decision change on the lighting use or HVAC use leads to a decision change on the window state).

Figure 7 shows the operative temperature and cooling loads estimated by 5 repeated simulations of the coupled DEVS building energy model. The steady-periodic temperature data fluctuates between 26℃ and 32℃ where it increases until the occupant begins to adjust his/her personal perception and/or his/her environment. Due to the stochastic nature of the *occupant model*, results of the simulations vary. The temperature and the cooling load data are scattered over a range of a 2-3℃ and 500-1000 W between the simulations, respectively. The design day cooling load is estimated as 11, 11.5, 10, 10, and 14 kWh for the 5 repeated simulations. Thus, the mean cooling load can be estimated as 11.5 kWh with a standard deviation of 1.5 kWh.

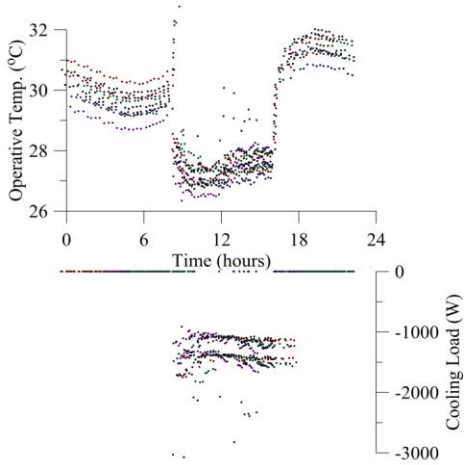

Figure 7: Operative temperature and the cooling load calculated using a coupled DEVS building energy model with repeated 5 simulations

6. DISCUSSION

The major advancement of using the DEVS formalism in *building model* development is that the developers can incorporate the physics of an external output without considering when, why, and how this external event occurs. The developer would rather be concerned with what happens physically, if it occurs. For example, the developer of the *building model* can incorporate the physics of the window opening without being overwhelmed with the processes leading to the window opening action (e.g. adaptive actions undertaken prior to the window opening action or the probability of the window opening behavior). Similarly, the *HVAC systems model* developer is solely concerned with the mechanical component modeling and the developer of the occupant model is just preoccupied with capturing the decion making process behind this adaptive action. In other words, opening the window is not a heat and mass transfer problem for the *occupant model* developer, it is a statistical reflection of a behavioral psychology problem. Thus, DEVS, by introducing modularity can enhance the interoperability of the different professions

involved in the integrated design process. However, the modularity may also cause a limitation about performing isolated testing on the submodels. Figure 3 illustrates an isolate testing procedure for the *HVAC systems model* by leaving input messages. The reliability of such submodel testing is restricted by the artificial inputs in absence of other coupled submodels.

Traditional BPS-based design of a real-size building involves the assembly of matrices with a few thousand rows and columns (Clarke 2001). The interaction amongst different domains (i.e. building and HVAC) are sustained at a few overlapping regions, while the occupant decisions are distributed within the solver code. The modularity of the DEVS formalism, rather than challenging the existing building simulation algorithms, suggests a more organized code structure which will make models more flexible, transferable, and reusable. Moreover, degree of freedom of the problem increases as the number of occupants and the number of available adaptive actions that each occupant can undertake increase. This cannot be easily accomodated in traditional BPS tools, as the occupant decisions are distributed within the solver code. The Modelica modeling language, described in the context of BPS by Wetter (2009), addresses many of the same issues as DEVS. It keeps models separate from the simulation process and provides a framework for connecting these models. Modelica, however, features a non-traditional equation-based modeling approach. DEVS does not involve a universal differential equation solver. Multiple solvers, typically implemented by users in imperative code, may be embedded in the submodels.

7. CONCLUSIONS

The modular nature of the DEVS formalism is exploited in this study by forming submodels that allow domain experts to develop simulation techniques independently and later combine their work. These submodels are the *building*, the *HVAC system*, and the *occupant.* The *DEVS building energy* model shows the viability of the formalism in building energy simulation and indicates a promising way to enhance the interoperability amongst different professions involved in the integrated building design process.

Acknowledgements

This research was funded by a research grant provided by Natural Sciences and Engineering Research Council (NSERC) of Canada and Autodesk Inc., which is gratefully acknowledged.

References

ASHRAE, 2009. ASHRAE handbook fundamentals. Atlanta: American Society of Heating, Refrigerating and Air-Conditioning Engineers.

ASHRAE, 2010. Standard-55 Thermal environmental conditions for human occupancy, Atlanta: American Society of Heating Refrigerating and Air-conditioning engineers.

ATHIENITIS, A. AND SANTAMOURIS, M., 2000. Thermal analysis and design of passive solar buildings. 1st ed. Montreal: James and James Science.

BOX, G. E. AND MULLER, M. E., 1958. A note on the generation of random normal deviates. Annals of Mathematical Statistics, 29(2), pp. 610-611.

CELLIER, F. AND KOFMAN, E., 2006. Continuous system simulation. 1st ed. New York: Springer.

CIBSE, 2006. Environmental Design Guide. London: The Chartered Institution of Building Services Engineers.

CLARKE, J. A. "Simulation of building energy systems." Proc. 5th CIB symp. on Energy Conservation in the Built Environment. Bath, 1986.

CLARKE, J. A., 2001. Energy simulation in building design. London: Butterworth and Heinemann.

DILOUIE, C., 2005. Advanced lighting controls: energy savings, productivity, technology and applications. Florida: The Fairmont Press.

DOE, 2009. Building energy data book, Washington: U.S. Department of Energy.

GALLAHER, M. P., O'CONNOR, A. C., DETTBARN, J. L., AND GILDAY, L. T., 2004. Cost Analysis of Inadequate Interoperability in the U.S. Capital Facilities Industry , Maryland: National Institute of Standards and Technology.

GOLDSTEIN, R. AND KHAN, A., 2010. Introducing DEVS for collaborative building simulation development, SIMAUD, Orlando.

HALDI, F. AND ROBINSON, D., 2008. On the behaviour and adaptation of office occupants. Building and Environment, Volume 43, pp. 2163-2177.

KUHN, T. E., BUHLER, C. AND PLATZER, W. J., 2000. Evaluation of overheating protection with sun-shading. Solar Energy, Vol. 69, pp. 59-74.

NRCAN, 2006. Energy use data handbook, Ottawa: NRCan.

RIJAL, H. B., TUOHY, P., HUMPHREYS, M.A., NICOL, J.F., SAMUAL, A., AND CLARKE, J., 2007. Using results from field surveys to predict the effect of open windows on thermal comfort and energy use in buildings. Energy and Buildings, 39(7), pp. 823-836.

SIMONS, R. H., AND A. R. BEAN. Lighting Engineering Applied Calculations. Oxford: Butterworth-Heinemann, 2001.

SUGARMAN, S., 2005. HVAC Fundamentals. Florida: Fairmont Pr.

WAINER, G. Discrete event modeling and simulation: A practicioner's approach. 1st ed. Florida: Taylor and Francis, 2009.

WETTER, M., 2009. Modelica-based modelling and simulation to support research and development in building energy and control systems. Journal of Building Performance Simulation, 2(2), pp. 143-161.

ZEIGLER, B. P. AND PRAEHOFER, H., KIM, T. G., 2000. Theory of Modeling and Simulation. 2nd ed. California: Academic Press

Session IV

City Information Modeling (CIM) and Urbanism: Blocks, Connections, Territories, People and Situations 111
Todor Stojanovski
Traffic and logistics, KTH Royal institute of technology

A Study of the Relationship between Urban Form and Environmental Performance for Three Urban Block Typologies in Paris 119
Ji Zhang
Centre for Sustainable Asian Cities, School of Design and Environment, National University of Singapore

End-node Approach for Pedestrian Flow Simulation 129
Hiroshi Ota
Institute of Industrial Science, The University of Tokyo

City Information Modeling (CIM) and Urbanism: Blocks, Connections, Territories, People and Situations

Todor Stojanovski[1]

[1]Traffic and logistics, KTH Royal institute of technology,
Brinnelvägen 32,
11428 Stockholm, Sweden.
todor.stojanovski@abe.kth.se

Keywords: City, Information Modeling, Urbanism, Blocks, Territories.

Abstract

The urban theory is a voluminous body of knowledge. There is a kaleidoscope of urban definitions and standpoints, but there are no tools that capture the variegated viewpoints and representations in urbanism. In this article I look at different urban theories, discourses and representations in architecture, sociology, geography, economy, transportation, and computer science, in order to conceptualize city information modeling (CIM). CIM is conceived and discussed as a system of *blocks* with dynamic relations or *connections* that define and redefine *territories*. The urban life today is a sequence of temporally inhabited and interconnected spaces, movable or fixed. The *connections* between spaces inspire or inhibit contacts and interactions between people. They bend time and continuously shape and reshape spaces, sociabilities and situations. In architecture there was an evolution from computer-aided design (CAD) to building information modeling (BIM), but in urbanism, where the geographic information systems (GIS) dominate, there is no such analogy.

1. INTRODUCTION

Cities are "the greatest artworks of humanity" (Mumford 1938:5), artifacts that we inherit and inhabit, hate or cherish. They store, fossilize and convey wordless messages and stories, witnessing and withstanding the turbulences of many generations and societies. Within their timeless monumentality, they safeguard the everydayness and the spectacle, the mundane and extraordinary. They inspire and depress, mystify and enlighten. Each city has "unique individuality, own life and physiognomy" and it is a "complex individual" (Reclus, 1905:385) entangling buildings, communities and neighborhoods. There is "a plethora of fragmentary theoretical formulations" (Harvey, 1973/2009:195), a kaleidoscope of urban definitions and standpoints, but we lack tools that capture the variegated viewpoints and representations in urbanism. Can we integrate the fragmentary urban definitions, representations and conflicting ideological positions and join these discourses into one tool? Can we unveil and represent the unique individuality and complexity of cities, the urban mundane and extraordinary? What should we include and emphasize? What are the prospects and limitations? Here I transplant the French meaning of urbanism as umbrella for urban studies, theory and analysis, design and planning. Urbanism in the English language has much narrower meaning, emphasizing the "way of living" in cities (Wirth 1938; Gregory et al. 2009:791). It "describes the distinctive features of the experience of everyday life in cities" (Bridge 2009:106), or "sets of social relationships" (Harvey 1973/2009).

2. DISCOURSES ON CITIES

Urban theory is a voluminous body of knowledge where some formulations are "very particularistic, while others are clearly mutually incompatible" (Harvey 1973/2009:195). Urbanism is fragmented and transmitted through schools, often through hybridization and intermixing of theories. It is taught as urban sociology, urban planning and design, urban geography, urban transportation, urban economy, etc. Here I juxtapose several urban discourses, schools or even ideologies of urbanism into one definition, where none of them is exclusive. They coexist together. The city joins together and stores incompatibilities, since they complete the urban representation.

2.1. The city as artwork of political struggle

Cities are constituted by charter, political decision or by fiat (Kostoff 1991). They are artworks accomplished by

clearly defined people and groups in historical conditions (Lefebvre 1996:101), products of political struggle, or struggle for control over the rights of the city (Soja 1989:49). The city is a stage where different interests, individuals, social groups or classes struggle for the right to develop the city. The city at the same time is an artifact, a monument to political clashes in the past. The conflict is not only between the actors of today, but also with the successful endeavors from the past and expectations for the future.

Urbanism partly reflects the prevailing ideology of the ruling groups and institutions in society and partly it is fashioned by capitalism and the dynamics of market forces (Harvey, 1973/2009:310). Lefebvre (1996:83-85) writes instead about tendencies in urbanism (technocratic, of the "people of good will" who advocate "human scale" and developer who is in pursuit of profits), whereas Hall (1980) extracts bureaucrats, politicians and the community as a "concert of actors" that shapes the city through a political struggle.

2.2. The city as mosaic

The city in urban morphology is a mosaic of urban areas or spaces. Urbs are "any groupings of buildings in which various families live" (Cerdà and Soria y Puig, 1867/1999). The city is defined as a "complex individual" of different urban quarters or neighborhoods (Reclus 1905:385) or "a mosaic of little worlds that touch, but do not interpenetrate" (Park 1925:40). It is an agglomerate of clearly differentiated urban spaces (Ahlmann at al. 1934:7).

2.3. The city as agglomerations of flows

The geographers clash about whether the city is physical or social space. Physical geography focuses on territorial or areal differentiation (Harvey 1969:3), whereas the social view includes territories and territoriality, rights of the city, social relationships and justice. Territories are produced and reproduced social spaces that cannot be defined absolutely or permanently (Raffestin 2012). Cities are an "extraordinary agglomeration of flows" (Ash and Thrift 2002:42), not only as people on the move, but as other forms of mobility like flows of information, capital, values, norms, habits and lifestyles. Their urban realm is worldwide, endless and interweaved with digital technology—brought into existence by massive globally extended sets of systems and infrastructures (Graham 2004:7-13).

2.4. The city as localization and aggregate of individuals

The city is a "relatively permanent, compact settlement of large numbers of heterogeneous individuals" and we can formulate it through the relationship between: (a) population numbers, (b) density of settlement, (c) heterogeneity of inhabitants and group life (Wirth 1938). Wirth saw urban systems through variables, relationships and prepositions (Gottdiener and Hutchison 2000:115). His algebraic approach is deeply rooted today in urban modeling and regional science, urban economy and transportation. The focus is on agglomeration of agents, and spaces as locations defined by urban activity and land use. In this discourse the city is "a permanent localization, relatively large and dense, of socially heterogeneous individuals" (Castells 1977:77). It is an aggregation of N individuals that interact in n-dimensional space, a phenomena captured by simulations and matrix algebra (Chadwick 1971).

2.5. The city as mental image and feeling

Cities and cityscapes are deeply engraved mental images in the human mind. They give a feeling of enclosure or sanctuary. If the planet Earth is our "original geographic prison, the city is our constructed or produced derived prison" (Raffestin 2012). It traps and emprisons, but also protects. (*ur*) means *roof*, *to shut* or *protection* in Sumerian (http://psd.museum.upenn.edu) and *roof* (ur) or *enclose* is found throughout Indo-European languages and even in the Chinese sign 市 (shi) for city. City is (*iri*, *eri*, *uru*) in Sumerian (http://psd.museum.upenn.edu), पुरं (*pur*) in Sanskrit (http://www.sanskrit-lexicon.uni-koeln.de/), *uru* in Hittite, *paru* in Old Persian, *urbs* in Latin, *baurgs* in Gothic, *bær* in Old Norse, *gradu* in Old Slavonic from *gherd* (*enclose*), (http://www.utexas.edu/cola/centers/lrc/eieol/).

3. REPRESENTATION OF CITIES

The city is conceived either as physical space or as socially or mentally constructed space. These three spaces interrelate and overlap (Soja 1989:79, 120), but traditionally economy links systems with physical form and ways of living; architecture and geography claim domain over physical form or systems, psychology over cognition and mental images, sociology and politics over ways of living, social associations and spaces, whereas, each discipline utilizes and improves its own methods of representation, such as writing, rhetorics and language, drawing, sketching and illustrating, photography, algebra and geometry, or programming.

3.1. Stories, pictures and songs (image and feeling)

Urbanism has its own grammar, language, expressions, and schemata, which easily translate through other verbal or visual arts. Travelers, artists, painters, musicians, historians, anthropologists, journalists, geographers and sociologists describe the city with words, pictures or sounds. These representations are incredibly heterogeneous and capture urban images and feelings in their qualities (figure 1).

Figure 1. Transformation of Stortorget in Stockholm (Christmas market)

3.2. Legislation and policies (regulating an image)

The lawmakers and politicians write agendas or enact strict regulations and guiding procedures that are executed and controled by bureaucrats and administrators. The legislation reflects the political struggle or societal endeavors. The urban codes constitute and control the right to develop the city. Sometimes there are rigid regulatory details that design cityscapes to meticulous city image, where parts of the city are uniformed by rules, parts are conserved and mummified.

3.3. Maps and plans (2D graphics)

Architects, urban designers and geographers use 2D graphics or 2D geometric models, graphs and symbols to depict the city as accurate maps and plans or as thematic allegorical illustrations or diagrams.

Physical geographers are concerned with the Earth's surfaces, and there are two fundamental ways of representing physical geography (Longley et al. 2005:65-83). The Earth's surface is continuous and heterogeneous. The first way is to superpose the Earth with an orthogonal grid, tessellated into cells. Each cell or area in the Earth's mosaic is differentiated, categorized and attributed with one variable. The second way is to pin discrete objects on the Earth's surface or reference them with geographic information and position. The discrete objects are represented by 2D shapes (points, polylines and polygons) and are attributed with multiple variables. The discrete objects and the variables are organized in attribute tables as rows and columns. These two geographic representations in GIS and in 2D computer graphics are known as raster and vector graphics (Figure 2).

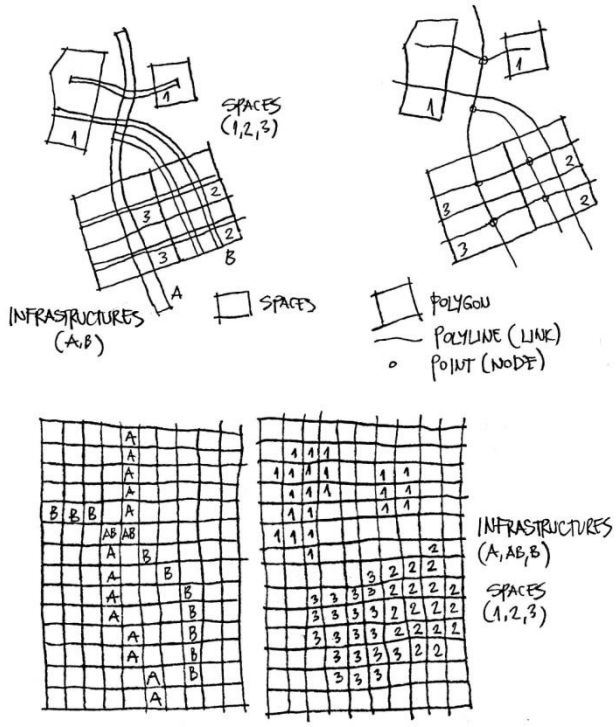

Figure 2. Raster (below) and vector (upper right) graphics as 2D representation in GIS

Architects use 2D graphics to represent 3D. They use geometry, projections and various transformation methods from 3D to 2D to draw urban plans, sections and elevations. Architecture manifests itself through mass and surface, which are determined by plan. The "plan is generator" of architecture and cities and "geometry is the foundation" (Le Corbusier 1931/1986:26, 1929/1987:xxi). Computer-aided

design (CAD) today uses almost the same toolbox of geometry with 2D objects and symbols, which is displayed on the first page of Le Corbusier's book "Urbanisme".

3.4. Perspectives and models (3D graphics)

Architects often look at and study urban detail, and design urban spaces, in 3D. They draw perspectives and make scale models or maquettes of buildings and cities. Scale modeling and 3D computer modeling are common techniques in the architects' toolboxes. The 3D computer graphics use the same method and visualization techniques as our mental processes. We see images and we transform them into 3D objects by triangulation. We cannot really see or make 3D objects in space if they are are not enclosed. The empty space deludes us. Our perception of space is predominantly photographic, or rather cinematographic. In 3D computer modeling the 3D objects are polygons or edges that are mapped with textures or images. The photorealism depends on image processing and texture mapping to the 3D mesh, rather than on the detail of the 3D model. 3D modeler programs like the CAD programs use a geometric toolbox of 3D objects and modifiers, and this toolbox is much more complicated and deterring.

Architects also generalize and reduce 3D to 2D symbols (or *blocks* in AUTOCAD). That knowledge was integrated and systemized in ArchiCAD as building information modeling (BIM). BIM allows work with 3D using a much simpler modeling toolbox. Each symbol, *block* or object consists of 3D model and 2D symbols for any projection (plan or elevations). That makes it possible to work 3D in plan and in one view. It is better than 3D modeling, which is done in at least two views. The 3D objects are interactive (windows and doors are part of walls, walls are trimmed by roofs, etc.) and have attributes.

3.5. Models and simulation (urban systems and agents)

The city and its urban spaces are represented by variables, models, formulas and matrices in urban economy and transportation, urban modeling, systems planning and regional science. The spaces are reduced to points and links, *centroids* or activity centers and the relationships between them (Figure 3). Different models and matrices define the variables in the centroids and links, and the relationship between centroids and between centroids and links. The activities in the centroids and on the links are simulated on an aggregated level as variables, or by assigning agents that interact. Urban modeling ranges from large-scale land use-transportation (LUT) models and macrosimulations of regions to agent-based models (ABM), cellular automata (CA) and microsimulations (Batty 2009). CA is a hybrid with 2D raster graphics where the physical structures and agents are represented by *cells*, or as space matrixes.

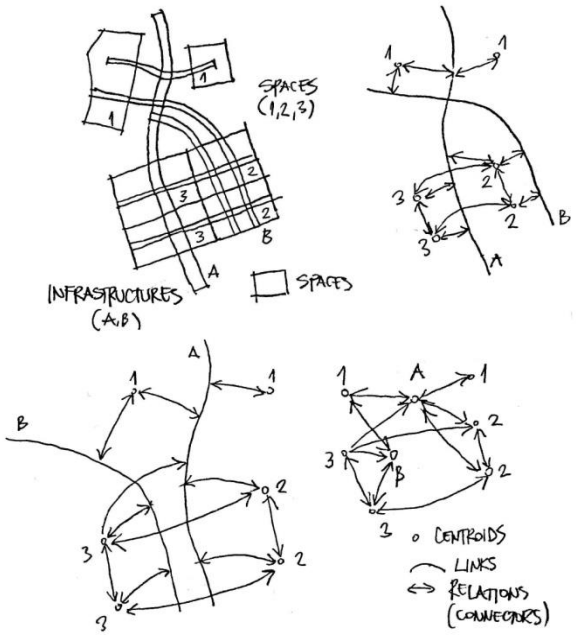

Figure 3. Relational representation of spaces

4. CITY INFORMATION MODELING (CIM)

CIM is a BIM analogy in urbanism. It is a system of urban elements represented by symbols in 2D space and the 3D spaces within. It is also conceived as 3D expansion of GIS (3DIS or 3D information system) enriched with multilevel and multiscale views, designer toolbox and inventory of 3D elements with their relationships.

4.1. *Blocks* and *territories*, connections and access

The city is an urban system of *spaces* and *channels*, *activities* and *communications*. The *activities* are linked by *communications* and they occur and recur in *adapted spaces* and *channels*. The *communications* are described by *origins and destinations,* whereas *spaces* are defined by *location* and *boundaries*. Other characteristics of *space* are *type* and *quality of adaptation and improvement* (McLoughlin 1969). The *adapted spaces* and the *flow system* (Lynch and Rodwin 1958) define the physical form of cities as *spaces for people and activities*, *spaces for vehicles and communications* and *shared spaces* (Boverket 1991).

CIM emphasizes this mosaic definition of urban morphology. The city is a 3D mosaic of *blocks*. The *blocks* are 3D atoms, undividable spaces in CIM. A *block* is a 3D object defined by a 2D symbol on different levels (like ground or 0, underground 1 or -1, elevated 2 or -2), *location* on the level, *boundaries* and *connections* to other *blocks*. The *boundaries* are edges and exits and entrances to other *blocks* as anchoring points of the *block* as 2D symbol, shape with anchoring points as location in 2D space and 3D object with anchoring points in 3D space. Most people have significant social contact only on the urban block and with friends around the city. The neighborhood plays a minor role (Gans 1968:12-24). The social life is strong within a "social field of vision" (Gehl 1987:67) up to 100 meters. The urban spaces that are broader than 200 meters are not regarded as near, enclosed or even "urban". The *blocks* in CIM are a scale within this "social field of vision".

The *blocks* are both 2D symbols and 3D spaces. There are two viewpoints on cities (broadened from Cecchini and Rizzi 2001), within or inside (the perspective), or from the top (the plan). To make a 2D representation of 3D space I joined plan and perspective in one representation to represent specific *blocks* in CIM. To illustrate through example, I made a top-within perspective of Stortorget in Stockholm. Stortorget is one *block*. It has objects: the fountain, for example, or for part of the year the Christmas market. These objects are represented by plan and only one elevation. Similarly only the edges of the *block* are represented, with the façades of the buildings distorted in top perspective to get a 3D perception (Figure 4).

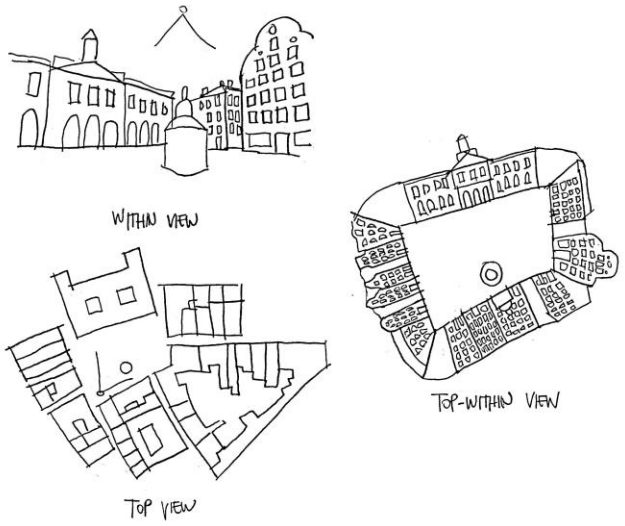

Figure 4. Within, top view and top-within view of Stortorget in Stockholm.

The *blocks* in CIM are interconnected and represented as sequences. Exit from one connected *block* to enter another. It should be possible to walk through in CIM only by looking at top perspectives of the different blocks in the city and clicking on the exits between the buildings.

The *blocks* are cognitive spaces. Within a *block* we locate impermeable edges and exits or entrances to the other *blocks*. We remember the façades as images. In the end we add the *block* in the mental map of the city and visualize *territories*. We make relations between *blocks* and join contiguous *blocks* in wider *territories;* for example, take Gamlastan, the old urban core of Stockholm. "Territories" are geographic spaces defined by administrative borders, by social structures like neighborhoods, or by distinctive or recognizable landmarks that evoke character (Lynch 1960). Each *block* has a set of extensions or overlaying *territories* in CIM, represented as sets of hollow blocks. The fixed *territories* show administrative borders and they have the same "edge, entrance and exit" logic as the *blocks*, but in 2D. They are 2D objects defined by edges and interconnected by exits and entrances as anchoring points (Figure 5).

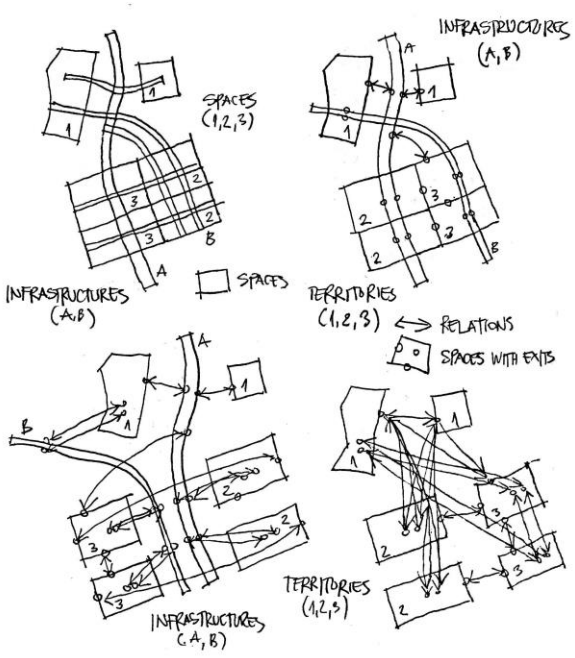

Figure 5. Representation of territories as edges, exits and entrances and their relations

The fluid *territories* depend on the *transport modes* for means of communications. These modes are graph representations of networks of *blocks*. The connections are sequences of *blocks* and accessibility, as travel times and costs can be calculated by matrices and adjusted by congestion in *blocks* using the representation from transportation. Each transport mode has a different graph. I made a simplified graph representation of Stortorget (Figure 6) to illustrate accessibility as the number of exits between the surrounding blocks. In the network of territories we are usually interested in one number in the matrix (from 1 as origin to 6 as destination for example) and it is 1 exit and x minutes walk.

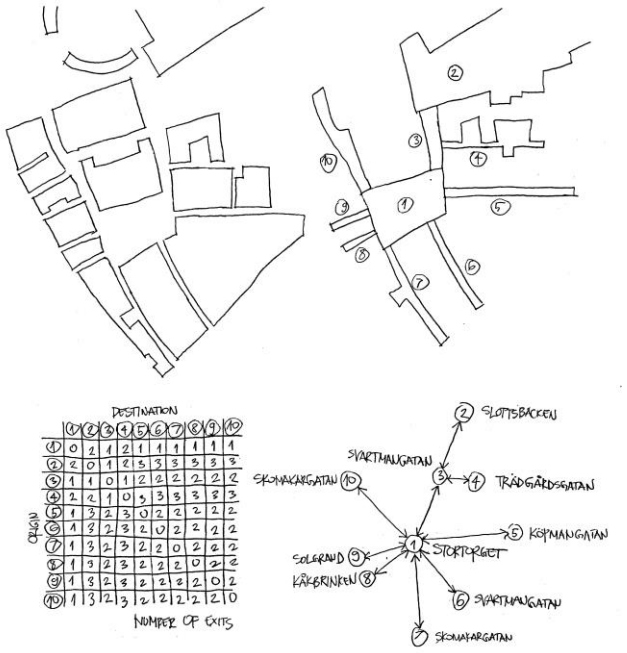

Figure 6. The development from edges, to blocks, to graphing (clockwise) in Stortorget, resulting in a matrix showing number of exits between the different origins and destinations

4.2. Blocks and territories, connections and access

The social life in a city is seen through a series of layers: the house, the block, the neighborhood and the politically defined community. The people socialize either within the block or within the wider *territory* (Gans 1968), often defined by its accessibility by automobile, walking or transit. CIM structuralizes these as tags. Just imagine that someone lives in block 1 and is interested in the lunch restaurants or art galleries in block 10. There is ongoing research and initiatives for tagging data on specific places in cities that coincide with *blocks*. Web 2.0 and smart phones are used to attach data to things and places. Web 2.0 is technology that enables interaction on Internet, among other adding tags and new information besides only accessing the presented information (Web 1.0). CIM is conceptualized as a stage for situational Web 2.0 information (events, stories, pictures and sounds). Its *blocks* and *territories* are ideal tags or keywords to sort the urban information.

5. DISCUSSION

5.1. Why CIM?

I see CIM not only as conceptualization, but also as introduction to a debate about urban theories, definitions and representations that we conceive and tools that we use as architects, urban designers, planners, geographers, sociologists, economists, psychologists, or transport planners and engineers. The kaleidoscope of urban representations today is too fragmented and in a digitizing world of sensors and databases the fundamental questions are often forgotten: How to analyze spaces, connections and flows? How to capture the urban flows and liquidity? Do urban borders and edges change and how do they change? The physical geography fails in the city today, because urban life is mobile. The *block* and *territory* are important social spaces that can be captured only by relational geography, graphs and matrices. The GIS data is predominantly 2D. That destroys the 3D detail of the *block* and freezes the liquidity and dynamics of the *territory*.

5.2. CIM as evolution of GIS and its applications

The geography in GIS is represented as geographically referenced chessboard matrices or layers of shapes with IDs and attributes. While each cell in the raster has one attribute, and each discrete object has one ID and many attributes in the vectors, each *block* as an urban element in CIM has its own attribute table and a 3D space with its own coordinate system with 2D projections in the city (or *territory)*. At any one time, every *block* as urban element exists with its ID in the attribute tables of the other *blocks* or urban elements. Let us consider Stortorget in Figure 6 as one discrete object or urban element in CIM. In a vector representation of GIS, Stortorget is a feature with 1 as assigned ID in an attribute table. It is one feature in a layer of polygons that has 10 features. In CIM, Stortorget has its own table with 10 IDs and its own 2D representation (see the block representation in Figure 6, top right) of 3D space (top-within view on Figure 4). The number of exits from Stortorget as origin is a

row, but in the CIM attribute table it is a column. If there were also columns with attributes such as number of supermarkets or commercial area of supermarkets in square feet or meters and walking distances as time traveled between blocks, it would then be very easy to calculate other features, such as accessibility to supermarkets by walking.

CIM is conceived as an evolution of GIS, an evolution from physical to relational geography and an evolution from discrete objects listed in an attribute table to discrete objects in relation to other discrete objects. Even though GIS has representation as discrete objects, they are not 3D and there are no direct and visible connections between them. There are already signs of change away from physical towards relational geography; for example in online maps. Google Maps uses relational geography when representing Stockholm's transit. The bus stops are connected directly, neglecting the physical geography of the bus routes, which are distorted in the online map. There is a need to upgrade GIS to better understand these space-time convergences in cities and other relations between spaces as urban elements. Subjects like urban agglomeration, connectedness between urban spaces, urban detail versus flow or intensification of urban activities and flows are becoming fundamental, and they are covered by the relational and top-within perspective of CIM.

5.3. Limitations and prospects of CIM

Urbanism revolves around sensing and interpreting urban information, interaction, communication and action. Carlo Ratti illustrates the process through a cycle of sensing and actuating (Figure 7, upper left) and he revives and transliterates surveying and planning in the emerging information society. Patrick Geddes, In his book, "Cities in Evolution", Patrick Geddes similarly uses surveying and planning as cycles in urbanism. But the change in words is more refined. It is a change from plan to action. To define the place of CIM in urbanism, I overlaid and enriched Ratti's cycle with an upgraded diagram of urban action (Figure 7, bottom right) originally conceived by John Turner (Figure 7, upper right). He argues that action is generated by previous action and administration, information, theory and norms, either as legislation or regulations (Turner 1976:159-60). Information and theory belong to the scientific sphere, in contrast to action and regulation, which are in the political sphere.

The resultant of the overlay (Figure 7, bottom) is a cycle that includes the city and representation as intermediate steps in sensing and actuating cities. The representation, with analysis and theory as background, is within the scientific sphere and it is where CIM is positioned. The city has a political sphere and its centre has shifted from design to negotiation in today's urbanism. CIM is only a background for the political sphere, but the *blocks* and *territories* are conceived as stages for political debates where CIM is conceived as a database of situational information in a system. The *blocks,* as tags, link stories, advertisements, business, events, happenings and other situations. The *blocks* are visible in their *territories*. This thinking is deeply inspired and biased by the outlook tower in "Evolution of cities" (Geddes 1915), which is a stage where citizens are experts and experts are citizens. The outlook tower is also a database of the past, present and future of cities.

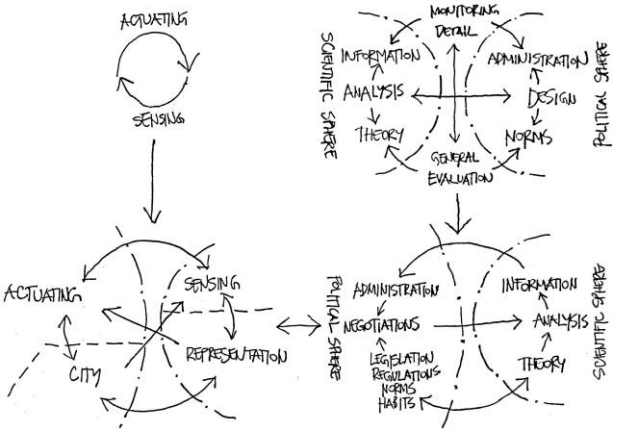

Figure 7. Carlo Ratti's sensing and actuating cycle (upper left) and John Turner's original (upper left) and modified (bottom right) scientific and political spheres and the resultant (bottom left), a simplified overlay of Ratti's cycle and Turner's spheres.

Enormous efforts are made in GIS to develop very accurate and detailed geographic representations, which are not always needed in urbanism. The scientific goal in GIS is accuracy and perfect correspondence between the city and its representation. Descartes (1627/1965:30) argues that we imagine objects (for example, the triangle) that probably do not exist anywhere, but demonstrate intrinsic properties, such as the sum of a triangle's three angles are equal to two right angles. Urbanism is multifaceted. It is sometimes important to pursue symbolic and simple representations that convey very practical information instead of perfect representations. CIM is about structuring *blocks* and

territories and making simple representations with complex relationships. Our everydayness is entangled within *blocks* and their *territories*. Within this structure of elements and relations, 3D in 2D, it is easier to look at interconnectivity and details of urban spaces. Many win when the distorted urban geography—its paths within and its scale, the urban flows and choices—is visible.

References

AHLMANN, H. W. (ED.) 1934. Ekonomisk-geografisk undersökning av nutida Stockholm med förorter. Stockholms inre differentiering. Stockholm: Geografiska institutet vid Stockholms högskola.

ASH, A., AND THRIFT, N. 2002. Cities: reimagining the urban. Malden: Polity.

BATTY, M. 2005. Cities and complexity: understanding cities with cellular automata, agent-based models, and fractals. Cambridge, Massachusetts: M.I.T. Press.

BOVERKET. 1991. TRÅD -92: Råd för planering av stadens trafiknät och trafik i sammanhållen bebyggelse. Karlskrona: Boverket.

BRIDGE, G. 2009. "Urbanism". International Encyclopedia of Human Geography. Oxford: Elsevier, pp. 106-111.

CASTELLS, M. 1977. The urban question. London: Edward Arnold.

CHADWICK, G. 1971. A systems view of planning. Oxford: Pergamon press.

CECCHINI, A., AND RIZZI, P. 2001. "Is urban gaming simulation useful?". Simulation and gaming. Vol. 32, No. 4. pp. 507-521.

CERDÀ, I., AND SORIA Y PUIG, A. (ED.), 1867/1999. Cerda: the five bases of the general theory of urbanization. Madrid: Electa.

DESCARTES, R. 1627/1965. Discourse on method, optics, geometry, and meteorology. Indianapolis: Bobbs-Merrill.

GREGORY, D., JOHNSTON, R., AND PRATT, G. (EDS.) (2009). Dictionary of Human Geography fifth edition. Hoboken. New Jersey: Wiley-Blackwell.

GANS, H. 1968. People and Plans: Essays on Urban Problems and Solutions. New York: Basic Books.

GEDDES, P. 1915. Cities in evolution: an introduction to the town planning movement and to the study of civics. London: Williams & Norgate.

GEHL, J. 1987. Life between buildings. New York: Van Nostrand Reinhold.

GOTTDIENER, M., AND HUTCHISON R. 2000. The new urban sociology, second edition. McGraw-Hill.

GRAHAM, S. (ED.) 2004. The cybercities reader, London: Routledge.

HALL, P. 1980. Great planning disasters. Berkeley: University of California press.

HARVEY, D. 1973/2009. Social Justice and the City (Revised Edition). Athens, Georgia: University of Georgia Press.

HARVEY, D. 1969. Explanation in Geography. London: Arnold.

KOSTOF, S. 1991. The city shaped: urban patterns and meanings through history. London: Thames and Hudson.

LE CORBUSIER. 1929/1987. The city of to-morrow and its planning. New York: Dover publications.

LE CORBUSIER. 1931/1986. Towards a new architecture. New York: Dover publications.

LEFEBVRE, H. 1996. Writings on Cities, Oxford: Blackwell

LONGLEY, P. A., GOODCHILD, M. F., MAGUIRE, D.J., AND RHIND, D. W. 2007. Geographic information systems and science. Chichester: Wiley.

LYNCH, K., AND RODWIN, L. 1958. "A theory of urban form", Journal of the American institute of planners. Vol. 24, No. 4.

LYNCH, K. 1960. The image of the city. Cambridge, Massachusetts: M.I.T. Press.

MCLOUGHLIN, B. 1969. Urban and regional planning: a systems approach. London: Faber and Faber.

MUMFORD, L. 1938. The culture of cities. New York: Harcourt, Brace and Company.

PARK, R., BURGESS, E., AND MCKENZIE, R. 1925. The city. Chicago: University of Chicago Press.

RAFFESTIN, C. 2012. "Space, territory, and territoriality". Environment and Planning D: Society and Space. Vol. 30, pp. 121-141.

RECLUS, E. 1905. L'homme et la terre, tome cinquième. Paris: Librarie universelle.

SOJA, E.W. 1989. Postmodern geographies: the reassertion of space in critical social theory. London: Verso.

TURNER, J.F.C. 1976. Housing by people. London: Marion Boyars.

WIRTH, L. 1938. "Urbanism as a way of life". American journal of sociology. Vol. 44, No. 1, pp. 1-24.

A Study of the Relationship between Urban Form and Environmental Performance for Three Urban Block Typologies in Paris

Ji Zhang[1]

[1]Centre for Sustainable Asian Cities, School of Design and Environment, National University of Singapore
SDE1, #02-24, Architectural Drive, NUS, Singapore, 117566
hope.zh@gmail.com

Keywords: Urban Form, Environmental Performance, Daylight Potential, Solar Radiation, Sky Exposure Factor, Sky View Factor, Total Floor Area Normalized Performance Indicator, Open Block.

Abstract

This study explores the relationship between urban form and environmental performance by analyzing three representative urban street block typologies proposed for Paris at various periods in her urban history. The performances of these typologies in terms of daylight potential, annual insolation, exposure to the sky, and potential to produce urban heat islands were simulated and compared. The implications of the results on 1) the importance of appropriate performance indicators to be used in comparative studies, and 2) the relationship between urban form, density, and environmental performance are discussed.

1. INTRODUCTION

Cities stand at the forefront of the global sustainability agenda, as more than half of the global population is living in urban areas now, and cities are the major consumers of energy and resources. For architects and urban planners, one of the key research questions regarding urban sustainability concerns the relationship between urban forms and their environmental performances. This question is based on the understanding that the same built density can be achieved through adopting different building typologies and various spatial arrangements (Rogers & Urban Task Force, 1999, p.62), and the resulting urban morphological configurations may lead to different environmental performance, in addition to affecting urban dwellers' physiological comfort, psychological wellbeing, and overall urban energy consumption to various extents.

Previous studies have addressed this research question from different perspectives via various approaches (Ratti et al, 2003; Compagnon, 2004; Ratti et al, 2005; Cheng et al, 2006; Robinson, 2006; Montavon et al, 2006; Kämpf et al, 2010a, 2010b; Zhang et al, 2012a, 2012b).

Regardless of the forms being tested and performance areas being examined, a key issue in exploring the relationship between urban form and environmental performance concerns the appropriate performance indicators to be used to compare across various built form cases under investigation.

In the diagram shown below (Figure 1), the two unobstructed buildings are identical in terms of the overall external form and envelope area, and their daylight and insolation performance as indicated by average amount of daylight receivable on building facade and annual solar radiation receivable on building envelope, respectively, for the two buildings are identical as well. However, due to the difference in total usable floor space, the implications of the facade-level daylight quantity to interior-level daylight distribution potential, and the implication of envelope-level solar radiation incidence quantity to solar radiation heat gain for unit floor space are obviously quite different.

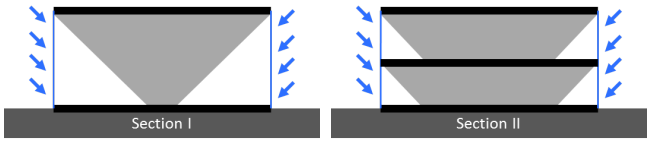

Figure 1. Sections for two buildings in the same shape but with different total floor space

In Figure 2, two unobstructed buildings of the same height have an identical building perimeter length and, therefore, total facade area. So, it might be concluded that their daylight performances in terms of average facade daylight incidence are the same. However, under the same assumptions of a window-head height of 3m and depth of daylit area of 6m, the floor-level daylight penetration

potential as indicated by the ratio of daylit area to overall floor space is different for the two buildings due to the difference in their usable floor space.

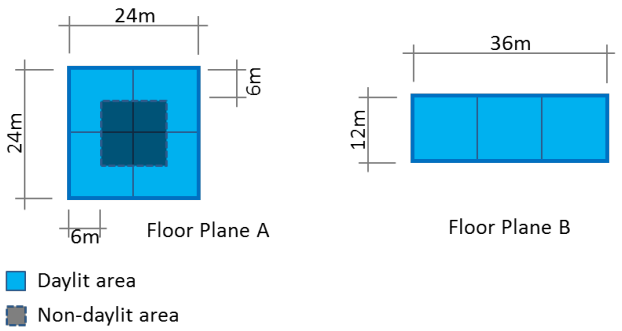

Figure 2. Planes for two buildings with the same perimeter length but different total floor space.

The two examples suggest that daylight/insolation availability on building facade as performance indicator may lead to wrong conclusions in comparative studies if the research objective is to understand the relative difference in the daylight penetration potential or implication in solar radiation heat gain for various building forms. As discussed in a previous study (Zhang et al, 2012b), "in urban scale analysis the quantity of an environmental variable … as aggregated or averaged for building surfaces may only capture one aspect of the story about the overall environmental performance of urban forms. In order to obtain the first level of understanding on the implications of facade-level environmental quantity to interior-level environmental potential by taking into account the built density, accumulated environmental quantity on facades as shared by usable floor spaces may need to be measured for different urban forms". In short, total-usable-floor-area-weighted performance indicators might provide better estimates than average-value-based performance indicators, a conclusion consistent with what has been applied in previous studies conducted by Compagnon (2004).

Other than understanding the relative performance across various urban forms regarding a given environmental variable, the formal characteristics that might affect environmental performance may also need to be addressed. This is no less important in that the geometric factors can be adjusted by planners and architects in the early stage of a design process to achieve certain preset performance objectives.

2. THREE REPRESENTATIVE URBAN BLOCK TYPOLOGIES OF PARIS

Throughout the urban history of Paris, various urban planning ideologies and architectural approaches have been tested or proposed in response to their respective contemporary prominent urban problems. Three representative urban form typologies for Paris were chosen for this case study to demonstrate the analytical process in addressing the relationship between urban form and environmental performance.

It should be noted that a critical review of the success and failure of the three urban design approaches from a history-and-theory point of view is beyond the scope of this study. Instead, it seeks to examine from a building science quantitative analytical perspective and compare the environmental performance across the three typologies against what were claimed or promised to be the advantages of the designs.

2.1. Traditional Parisian Street Block

As a result of the Haussmann's urban interventions in the 19th century, which super-imposed hierarchical grids radiating from multiple centers that cut through the urban fabric (Salat et al, 2011, p.78), the traditional Parisian street blocks are characterized by compact buildings of 5 to 7 stories densely packed over the entire plot with small courtyards distributed across the site acting as light wells or service areas. Bounded by and aligned along the surrounding roads and usually narrow pedestrian walkways, the traditional Parisian street blocks are the result of an urban design ideology that serves primarily a neat and tidy public street space, with less concern for the quality of life for the people living within the block. The FAR (Floor Area Ratio) of this type of urban block ranges from 3.5 to 5, which is relatively high in the European context. The compact urban form is said to be preferable in terms of reducing heat loss during the winter season. However, it may lead to poor daylight quality for a large proportion of the floor spaces.

Figure 3. Traditional Parisian Urban Block (Source: Google Maps)

2.2. La Ville Radieuse

Le Corbusier's "Contemporary City of Three Million Inhabitants" master plan, originally proposed during the 1920s and further developed into "La Ville Radieuse (The Radiant City)" in the 1930s, depicted an urban landscape which is radically different from the traditional Parisian urban fabric. In response to the over-crowded and non-hygienic living environment of the Parisian urban block, Le Corbusier proposed to replace the Paris urban fabric with a new grid of mega-structures composed of cross-shape skyscrapers and low-rise perimeter residential blocks submerged in vast green open spaces in between buildings organized according to the modernist functional urban planning rationale. The design intention was to free up the compact urban fabric and allow more access to daylight and a view for most of the residents.

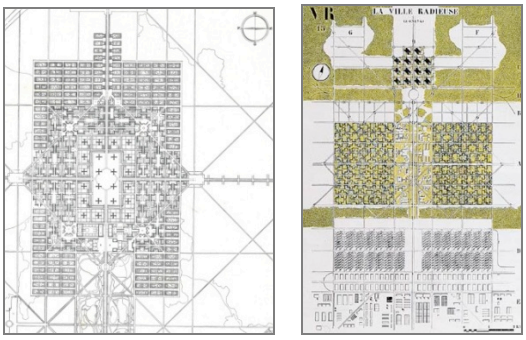

Figure 4. The plans for the "Contemporary City of Three Million Inhabitants" and "La Ville Radieuse (The Radiant City)"

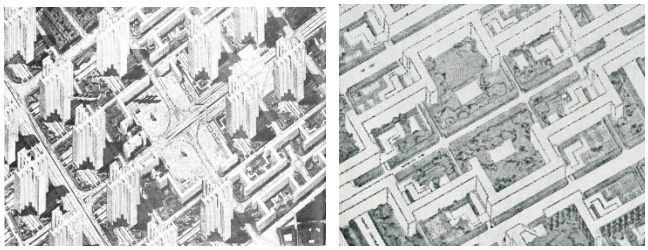

Figure 5. The skyscrapers and the "setback" type of urban block

2.3. Open Block

French architect and planner Christin de Portzamparc's Open Block concept represents the contemporary exploration for urban design strategies that attempts to break away from the formal characteristics of the traditional European urban fabric while maintaining the integrity of the urban spaces. The Open Block is an urban design framework rather than a specific formal style, through which the interaction between public and private and that between building mass and open space are specified as 3D urban design guidelines. Both Le Corbusier and Portzamparc's designs were proposed as an objection to the traditional Parisian street blocks, which were criticized for being unable to meet the requirements and expectations for quality of modern urban life. While Le Corbusier proposed high-rise tower blocks to absorb most of the built density, leaving vast open spaces for the development of landscaped gardens and low-rise low-density residential blocks, Portzamparc instead proposed to break up the enclosed and introverted volumes of the traditional street blocks by distributing the built density via median-rise building blocks with small-scale open spaces scattered in between the building masses in a carefully coordinated way on an urban design level, while maintaining spatially a clearly defined street space, striking a rare balance between diversity and coherence. Allowing more daylight and breeze to penetrate into the center of the site and providing outward views towards the gardens and streets for all the residents are some of the primary environmental objectives of the Open Block design strategies (Portzamparc, 2012, p.159).

Figure 6. The Open Block urban design strategies as implemented in the Messena district in Paris (Source: Portzamparc, 2012)

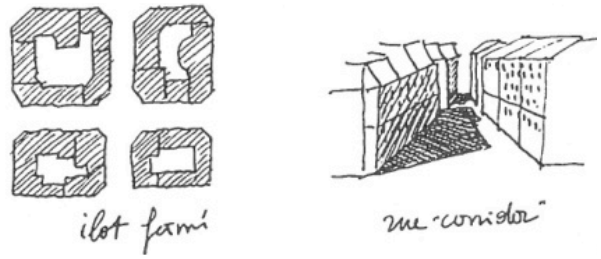

a) The traditional enclosed perimeter block

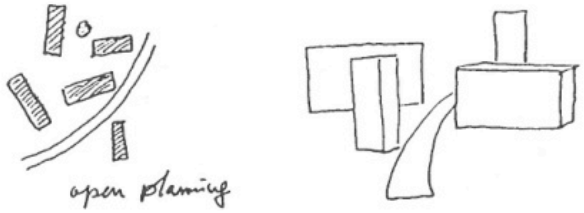

b) The modernist free-standing buildings detached from the street

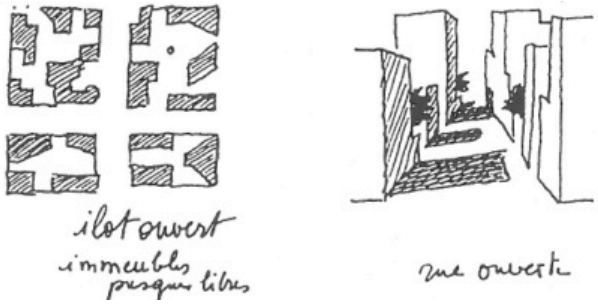

c) The Open Block

Figure 7. The Open Block concept (http://www.chdeportzamparc.com)

3. METHOD

3.1. The Representative Urban Blocks

To put the three types of urban forms to test, representative urban blocks/buildings were chosen for each of the three urban design "ideologies", and thirteen relatively precise 3D building massing models were created with reference to several sources (Portzamparc, 2012; Le Corbusier, 1947; Le Corbusier et al, 1947; Salat et al, 2011).

Three compact traditional Parisian urban blocks (PA1-3) were selected and modeled with the variation in roof forms and building facades been simplified. Two different versions of the skyscrapers by Le Corbusier proposed in "La Ville Radieuse" were modeled: the "plain" design, (CT1: 176m in length and 33m in depth) and the "convoluted" design, (CT2: 200m in length and 36m in depth). The "cellular" (CC1: 350x100x15m) and two versions of the "setback" block (CS1 and CS2: 15m and 18m in depth, respectively) were also modeled. Five blocks from the Messena district in Paris (ME1-5) were also modeled in simplified building masses. The key planning information for each of the forms tested is summarized in Table1.

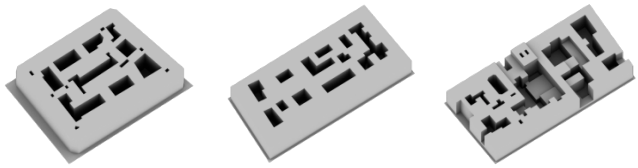

a) The traditional Haussmannian Parisian Compact Blocks (PA1-PA3)

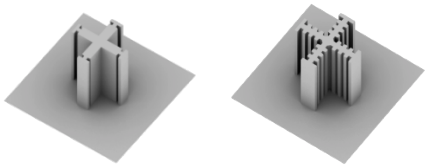

b) Le Corbusier's cross-shaped Tower Blocks (CT1, CT2)

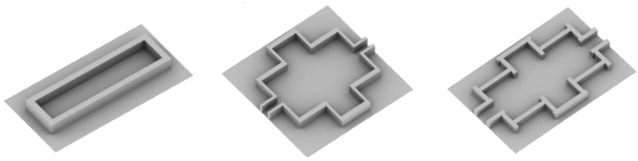

c) Le Corbusier's Perimeter Blocks: Cellular (CC1) & Setbacks (CS1, CS2)

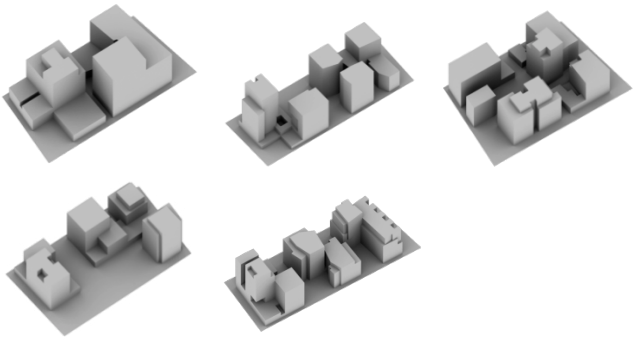

d) Portzamparc's Open Blocks selected from the Messena district (ME1-5)

Figure 8. The 3D models for the eleven urban blocks (in different scales)

Name	Gross FAR*	Site Coverage	Site Size**	No. Stories
PA1	3.74	63.6%	113x84m	7
PA2	4.53	73.3%	158x80m	7
PA3	3.53	70.3%	139x71m	1-7
CT1	4.24	6.4%	400x400m	73
CT2	4.79	7.3%	400x400m	73
CC1	1.58	21.9%	400x200m	10
CS1	1.05	11.5%	400x400m	10
CS2	1.43	17.4%	600x400m	10
ME1	3.02	57.7%	93x47m	2-11
ME2	2.51	43.8%	129x51m	2-13
ME3	2.69	42.6%	109x70m	1-12
ME4	2.38	42.7%	124x70m	2-12
ME5	2.63	48.4%	128x51m	1-13

*Gross FAR: Total Floor Area / Site Area (including half of the surrounding roads)
**Site Size: measured from the centre lines of the surrounding roads

Table 1: Key planning information of the thirteen urban blocks modeled.

3.2. Theoretical Homogeneous Context

Each urban form being tested was surrounded by two layers of replications of itself. In this regard, a theoretically homogenous context was created, composed of the same form and the same spatial layout unique for that typology. The theoretical environmental performance for the center block (highlighted in yellow in the images below) in this theoretical context was thus simulated and compared (Ratti, Raydan, and Steemers, 2003; Zhang et al, 2012a, b).

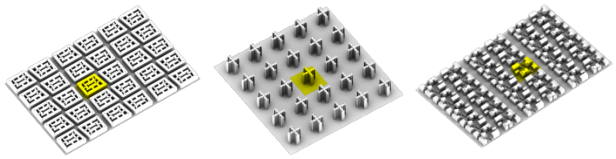

Figure 9. Example of the theoretically homogenous context created

3.3. Performance Indicators and Geometric Variables

Vertical Daylight Factor (0-50%) was calculated for building facade as a measure of the amount of light receivable on facade. The facade's Vertical Daylight Factor per Gross Floor Area (VDF/GFA) was used as indicator for daylight potential (Zhang et al, 2012b). VDF/GFA was calculated as area-weighted total facade VDF divided by Gross Floor Area (GFA). The larger the value, the greater the daylight potential for interior spaces. The percentage of facade surfaces that receive 10klx or more "average hourly illuminance"[1] was also calculated for each form to show that the use of this indicator may lead to wrong conclusions in any comparative study.

[1] Assuming standard office hours from 8am to 6pm, the annual daylight hours are calculated as 11*365=4015h. The average hourly illuminance for a given point is calculated as its annual total irradiance multiplied by 179 (luminance efficacy) and then divided by 4015.

Using a similar rationale, the performance of the urban forms tested in terms of the impact of insolation on solar radiation heat gain for the entire building volume was indicated by area-weighted total building envelope insolation (kWh/m^2/year) per unit floor area (Insolation_en/GFA) (Compagnon, 2004). Two additional sets of threshold values from Compagnon's study (p.324) were adopted to evaluate the potential to utilize solar radiation for the urban forms tested in terms of their overall potential to implement photovoltaic systems (the percentage of building surfaces that can receive $800kWh/m^2$ and $1000kWh/m^2$ or more insolation annually for facade and roofs, respectively) and solar thermal collectors (the percentage of building surfaces that can receive $400kWh/m^2$ and $600kWh/m^2$ or more insolation annually for facade and roofs, respectively). The larger the value, the greater the potential for solar radiation heat gain.

Sky Exposure Factor (SkyEF) (Zhang et al, 2012a), which is calculated as the ratio of the total solid angle subtended by visible sky patch/patches to that of the unobstructed sky hemisphere, was used to measure the degree of openness for any given point on the building facade (0-0.5) or on the ground (0-1). Total facade SkyEF per unit floor area (SkyEF_f/GFA) and area-weighted average SkyEF for unbuilt ground areas (aw-avg SkyEF_g), respectively, were used as the performance indicator of perceived openness on urban scale.

Sky View Factor (SVF), which is the ratio of the irradiance for a given point on the surface to that of an unobstructed point (0-1), is obtained for unbuilt ground spaces as an indicator of the intensity of urban heat island effect (Oke, 1981). Since SVF is concerned with the longwave radiation exchange between urban geometries and the sky, area-weighted average SVF for ground open spaces (aw-avg SVF_g) was calculated as the performance indicator. The smaller the value, the less the potential for the urban geometry to generate a nocturnal urban heat island.

Several geometric variables were also calculated for each urban form to summarize their form characteristics. These variables were used for correlation analysis with the calculated performance indicators in order to understand the key geometric factors affecting performance. Average Area to Perimeter Ratio (avg APR), calculated as the ratio between floor area to floor perimeter length, was an indicator of building depth; Compacity, calculated as the

ratio of building envelope area to "building volume to the power of 2/3" (Adolphe, 2001, p.191), was used as an indicator of the compactness of building volume. Open Space Ratio, calculated as the ratio of areas of unbuilt ground open spaces to total floor area, was used as an indicator of the open space shared for each unit of floor space (Berghauser Pont & Haupt, 2004).

3.4. Simulation Workflow

A simulation workflow was established by using the 3D animation software HoudiniFX (www.sidefx.com) as an integrated simulation and visualization platform. Digital Assets, or user-defined tools as called in Houdini, were customized to 1) retrieve 3D model information and pass it to simulation software in the format required, 2) adjust simulation settings and execute simulation, and 3) retrieve simulation results generated and bring them back to Houdini for visualization. The Radiance (Ward & Shakespeare, 1998) and GenCumulativeSky (Robinson & Stone, 2004) programs were used for the calculation of Vertical Daylight Factor, annual insolation, Sky Exposure Factor, and Sky View Factor. Paris' local weather file (www.energy.gov) was used as input for the two simulation programs to construct a cumulative sky radiation distribution for Paris. A 3x3m subdivision grid was applied to building envelope surfaces, and virtual sensors were placed at the centroid of each individual polygon. Simulation results obtained for a given sensor were thus treated as the average value for the individual polygon surface the sensor represented.

4. RESULTS

4.1. Daylight

Vertical Daylight Factor as simulated on building facade for four of the thirteen cases is illustrated in Figure 11. The results of daylight potential as indicated by both VDF per unit floor area and percentage of facade (>10klx) are shown in Figure 12.

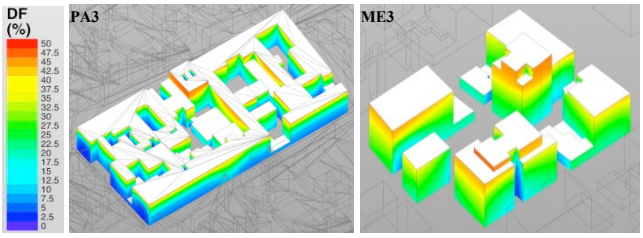

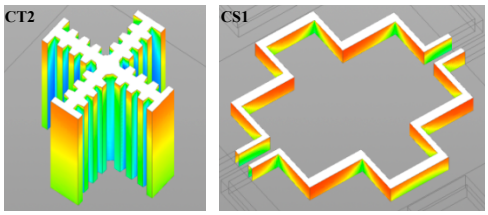

Figure 11. Facade Vertical Daylight Factor as simulated

The results suggest that the Open Blocks of Messena as a group perform the best with their VDF for unit floor area ranging from 15.43% to 19.76%. Le Corbusier's low-rise perimeter blocks also perform relatively well but with larger variation of the performance indicator (13.56% to 20.14%). The three Parisian blocks have relatively poorer daylight performance (7.3% -11.4%), and the two cross-shape skyscrapers from Le Corbusier have the poorest performance (8.15% and 8.47%), which is only slightly better than one of the very compact Parisian blocks. However, the slightly better performance for the "convoluted" tower (CT2) suggests that the facade convolution design strategy as proposed by Le Corbusier seems to have improved the daylight penetration potential for the interior spaces by providing more surface areas for daylight access. In comparison, the indicator of percentage of facade (>10klx) seems to give a wrong evaluation of the relative performance across these typologies.

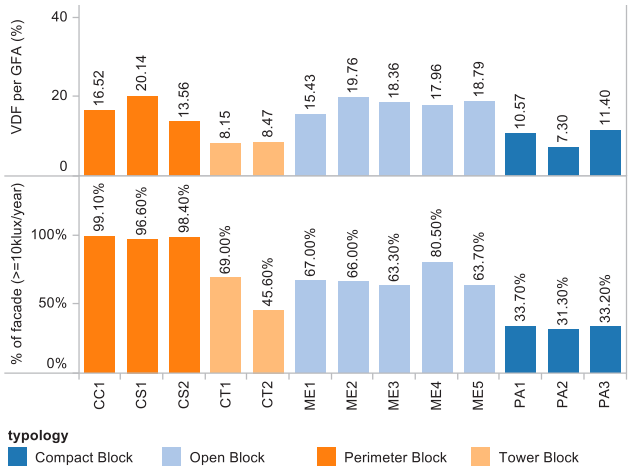

Figure 12. Daylight performance by different indicators

4.2. Insolation

The cumulative envelope insolation as simulated is illustrated in Figure 13.

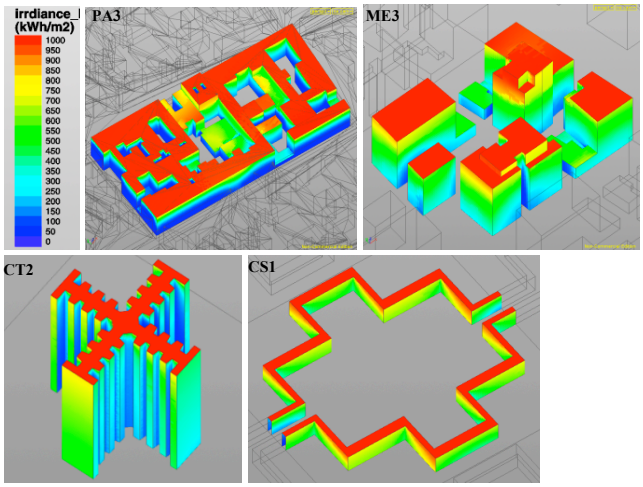

Figure 13. Envelope annual insolation as simulated

The two Le Corbusier skyscrapers have, surprisingly, the lowest cumulative irradiance shared for unit floor area (or unit volume, as the floor-to-ceiling height is fixed at 3m). This is followed by the compact Parisian blocks, the low-rise perimeter blocks, and the Open Blocks (Figure 14.). The performance ranking might be attributed to the relatively smaller ratio of roof to envelope area for the skyscrapers regardless of their relatively large amount of surface exposure. Consistent with the daylight performance, the convoluted skyscraper design incurred a slightly higher amount of insolation per GFA.

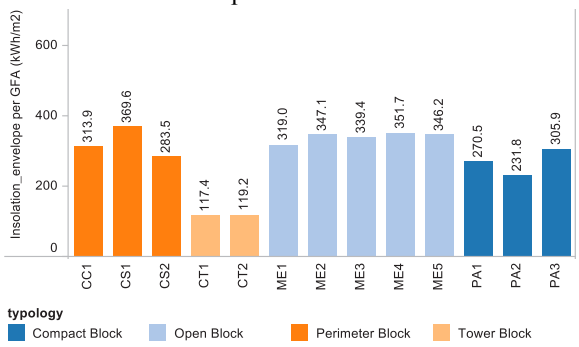

Figure 14. Insolation performance for the entire building envelope.

Since building roofs are usually well insulated and covered by other facilities, and therefore the impact of roof solar radiation heat gain to the building volume underneath is minimized, another performance indicator—cumulative insolation on facade per unit floor area—was calculated as well and compared (Figure 15). It seems that skyscrapers still perform relatively better than the Parisian, the low-rise perimeter, and the Open Blocks. The larger spacing between buildings and shallower building depth of the Open Blocks and the Setback perimeter blocks may have contributed to their relatively poorer performance; that is, more solar radiation heat gain for every unit floor space.

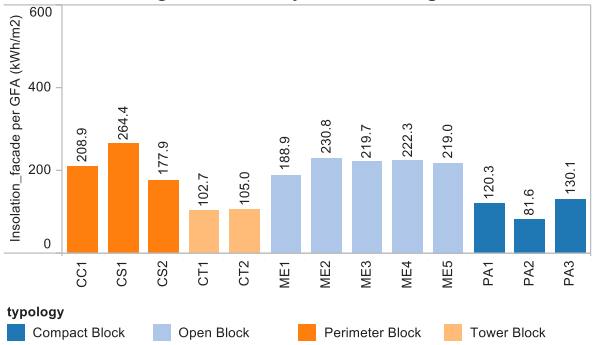

Figure 15. Insolation performance for building facade only

Alternatively, area-weighted average insolation was also calculated for envelope and facade, respectively (Figure 16), and the relative performance derived accordingly seems to be suggesting misleading implications on the relative impacts of solar radiation heat gain for the building forms tested.

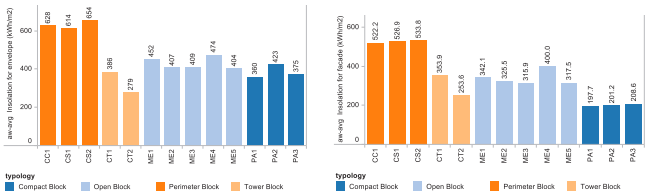

Figure 16. Alternative insolation performance indicator for envelope and facade, respectively

As for the potential to apply PV systems on building facades, the low-rise perimeter blocks perform far better than the other groups (Figure 17, left). The self-shading caused by facade convolution for the serrated skyscraper design reduced the PV application potential by almost a half as compared with the "plain" design. The PV potential for the five Open Blocks varies a lot, ranging from 1.5% to 3.5%, as compared to that for the Parisian blocks (1.6% to 2%).

Due to absence of obstruction in their respective theoretically homogenous simulation contexts, the roofs for the perimeter blocks, the skyscrapers, and two of the Parisian blocks can be fully utilized for PV panels (Figure 17, right). Shading caused by the variation of building heights may have resulted in the relatively lower potential for the roofs of the Open Blocks and one of the Parisian blocks to install PV.

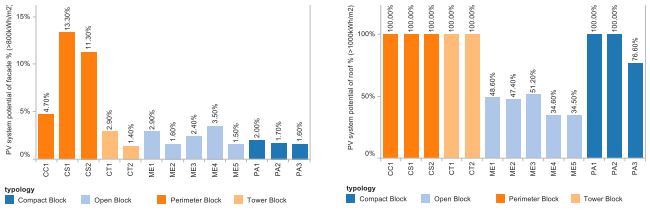

Figure 17. Facade (left) and roof (right) PV system implementation potential

On the other hand, the Corbusier perimeter blocks have the highest potential for facade solar thermal collector installation, followed by the Open Blocks, the skyscrapers, and the Parisian blocks (Figure 18, left), and similarly, the Open Blocks and one of the Parisian blocks have less than 100% potential for rooftop solar thermal collector implementation due to their variations in building height (Figure 18, right).

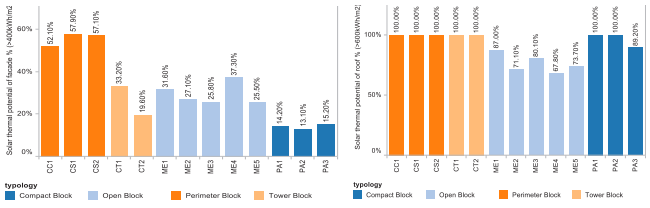

Figure 18. Facade (left) and roof (right) solar thermal collection potential

4.3. Sky Exposure

The Sky Exposure Factor as simulated on facade and ground is illustrated in Figure 19.

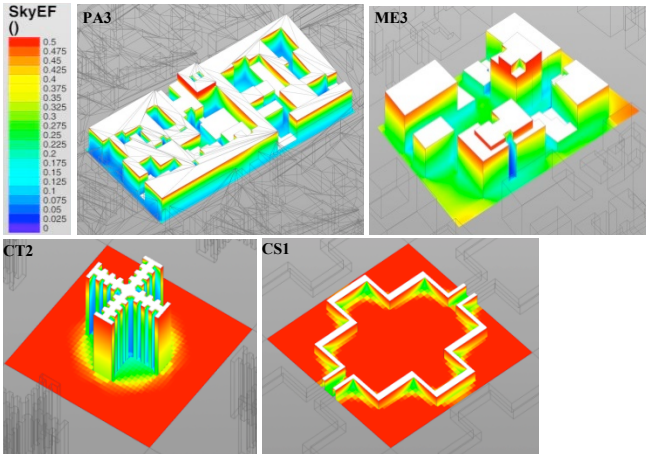

Figure 19. Facade and ground Sky Exposure Factor as simulated

For facade sky exposure performance, taking into account the usable floor spaces associated with a given form, the Open Blocks outperform the other typologies with their GFA normalized SkyEF ranging from 0.16 to 0.21, beating even the low-rise perimeter blocks (Figure 20, above). The Corbusian skyscrapers, however, have the worst performance regardless of the generous spacing between their tower blocks. Area-weighted average facade SkyEF was also calculated as a measure of the average level of openness to the sky as perceived from facade. The perimeter blocks achieve the highest performance, understandably, and the Open Blocks performance is better than the scattered tower blocks and compact Parisian blocks (Figure 20, below).

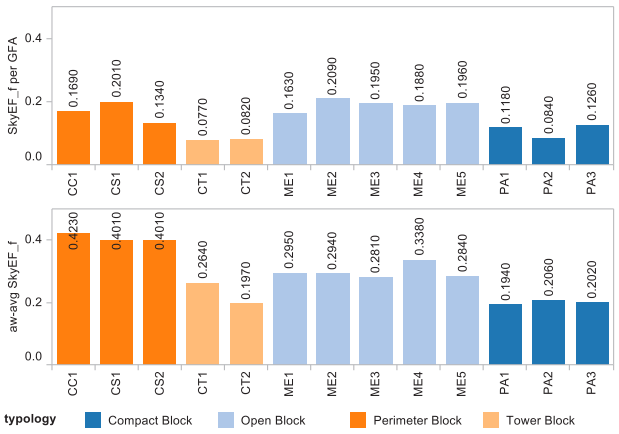

Figure 20. Facade Sky Exposure performance

The perimeter blocks and the skyscrapers have far greater ground level openness as indicated by area-weighted average ground SkyEF than the Open Blocks and the Parisian blocks (Figure 21). This seems to be directly related to the site coverage for each form (Table 1).

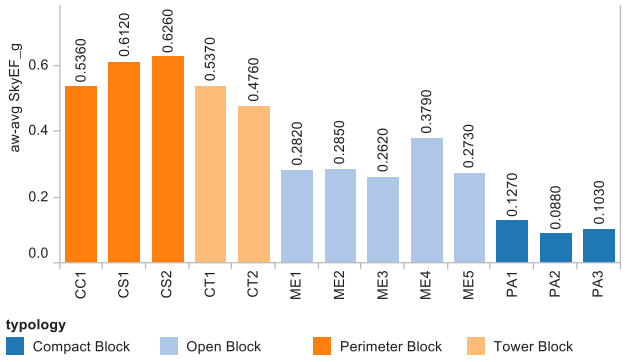

Figure 21. Ground Sky Exposure performance

4.4. Sky View Factor

The Sky View Factor as simulated for unbuilt ground areas is illustrated in Figure 22.

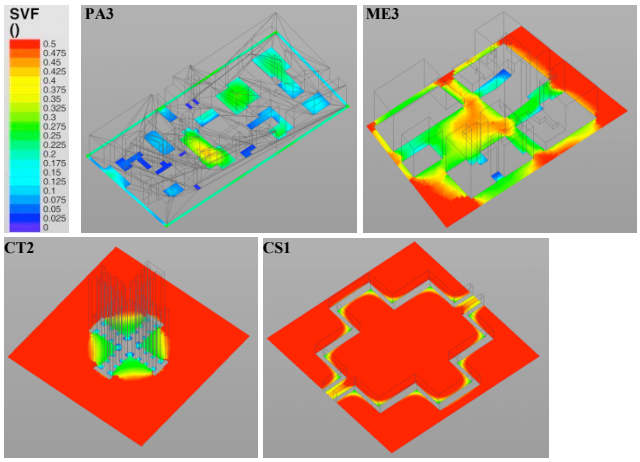

Figure 22. Ground Sky View Factor as simulated

The area-weighted ground level SVF also seems to be directly related to site coverage (Figure 23). The perimeter blocks and the skyscrapers, which have large spacing between buildings, have the highest SVF, followed by the Open Blocks and the Parisian blocks. This suggests that the compact Parisian blocks will have a greater tendency to induce nocturnal urban heat island effect.

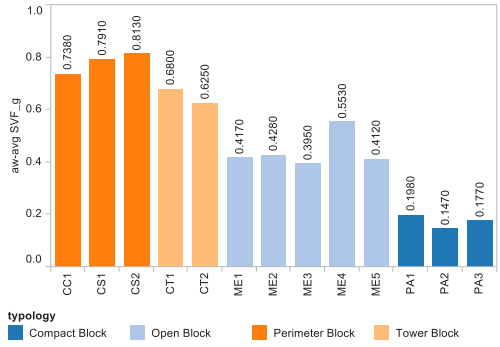

Figure 23. Ground Sky View Factor performance (or potential to minimize Urban Heat Island Effect)

4.5. The Impacts of Density and Geometry

Generally speaking, the environmental performance in terms of daylight, openness to sky, and tendency to incur urban heat island effect are negatively correlated with density, whereas the potential to reduce envelope solar radiation heat gain is positively related to density (Figure 24).

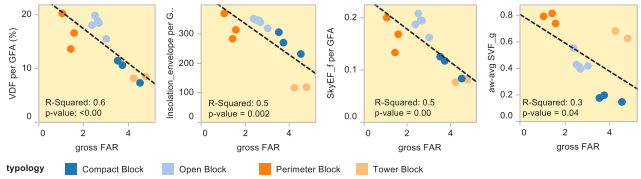

Figure 24. Relationship between density (FAR) and performance

The geometric variables tested in this study are summarized in Table 2. It was found that average area-to-perimeter ratio (avg APR) and Open Space Ratio (OSR) have significant impacts on some of the performance indicators (Figure 25). The larger the building depth (avg APR), the better the ground level sky exposure, the less the tendency to induce nocturnal urban heat island, the more solar radiation heat gain through the building envelope, and the lower ground level openness to the sky. On the other hand, it was found that the more the ground open space as shared by unit floor space, the higher the ground level openness to the sky, the lower the tendency to generate urban heat island, and the greater the potential to implement PV systems and solar thermal collectors on the facade. Compacity, a variable to measure the potential of heat lost or gain, was found to have no significant impact on all the performance indicators tested.

name	Compacity	avg APR	OSR
PA1	11.630	4.932	0.082
PA2	10.084	7.046	0.052
PA3	12.778	3.525	0.079
CT1	12.827	10.344	0.222
CT2	18.808	7.249	0.195
CC1	12.051	7.500	0.535
CS1	15.986	5.904	0.849
CS2	14.603	8.833	0.599
ME1	7.892	5.151	0.113
ME2	10.411	4.137	0.183
ME3	10.625	4.146	0.181
ME4	9.690	5.112	0.205
ME5	10.521	3.929	0.163

Table 2: Key geometric variables of the thirteen urban blocks modeled.

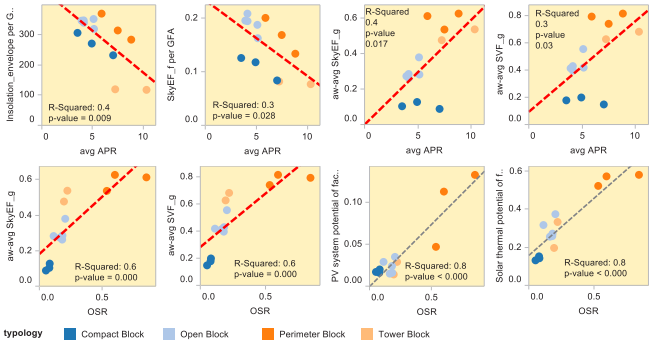

Figure 25. Significant relationships between geometric variables and performance indicators

5. CONCLUSIONS AND DISCUSSION

This study emphasizes the importance of adopting appropriate performance indicators in any comparative study on urban scale, and of understanding the geometric characteristics that may affect environmental performance of urban forms of different typologies.

The results of testing 13 urban blocks representing four different urban form typologies applied in or proposed for Paris suggests that the total floor space normalized performance indicator can help to reveal minor differences in performance evaluation.

It seems the Open Blocks do outperform the other typologies in terms of daylight potential and openness to the sky as claimed by the originator of this urban design concept, Christin de Portzamparc. This might be regarded as a testimony of the effectiveness of the Open Block design strategies: distributing the building masses and open spaces in a checkerboard pattern to provide more daylight and view access for the total usable floor spaces they serve. On average, this design also seems to provide greater potential for implementing solar energy harvesting systems on facade as compared to the other typologies (if the low-rise perimeter blocks are excluded from the comparison due to their low built densities).

Contradicting Le Corbusier's claim, the daylight performance of the skyscrapers proposed in La Ville Radieuse is no better than that of the traditional Parisian block, although they didn't seem to fall behind the compact Parisian block that much as indicated by a previous study (Montavon et al, 2006). The insolation performance of the tower blocks is surprisingly better than other typologies. This might be attributed to their relatively large building depth as compared to that of the other forms.

While revealing the general trend in terms of the relationship between built density and environmental performance, the results of the study also highlight how geometric variables such as average area-to-perimeter ratio and Open Space Ratio can be used in urban planning and architectural design to address environmental performance of urban form in significant ways.

Future studies could look into the variation of performances for the urban forms tested in response to heating and cooling seasons, and examine the performances of potential hybrid urban block and building typologies generated based on the observations obtained in this study.

Acknowledgement

The author would like to thank Dr. Patrick Janssen in the Department of Architecture in the National University of Singapore who originally initiated the Houdini-based simulation workflow to which the simulation tools newly created by the author for this study have referred.

References

Adolphe, Luc. (2001). A simplified model of urban morphology: application to an analysis of the environmental performance of cities. Environment and Planning B: Planning and Design, 28(2), 183–200

Berghauser Pont, Meta, & Haupt, Per. (2004). Spacemate : the spatial logic of urban density. Delft: Delft University Press.

Cheng, Vicky, Steemers, Koen, Montavon, Marylene, & Compagnon, Raphaël. (2006). Urban Form, Density and Solar Potential. Paper presented at the 23rd Conference on Passive and Low Energy Architecture, Geneva, Switzerland.

Compagnon, Raphaël. (2004). Solar and daylight availability in the urban fabric. Energy and Buildings, 36(4), 321-328.

Ward, Greg & Shakespeare, Rob. (1998). Rendering with Radiance : the art and science of lighting visualization. San Francisco: Morgan Kaufmann.

Kämpf, Jérôme Henri, & Robinson, Darren. (2010a). Optimisation of building form for solar energy utilisation using constrained evolutionary algorithms. Energy and Buildings, 42, 807-814.

Kämpf, Jérôme Henri, Montavon, Marylène, Bunyesc, Josep, & Bolliger, Raffaele. (2010b). Optimisation of buildings' solar irradiation availability. Solar Energy, 84, 596-603.

Le Corbusier. (1947). The city of tomorrow and its planning. London: Architectural P.

Le Corbusier, Jeanneret, Pierre, & Boesiger, Willy. (1984). Oeuvre complete. Zurich: : Les Editions d'Architecture.

Montavon, Marylène, Steemers, Koen, Cheng, Vicky, & Compagnon, Raphaël. (2006). *'La Ville Radieuse' by Le Corbusier: Once again a case study*. Paper presented at the PLEA2006 - The 23rd Conference on Passive and Low Energy Architecture, Geneva, Swizerland.

Oke, T.R. (1981). Canyon geometry and the nocturnal urban heat island: comparison of scale model and field observations. *Journal of Climatology, 1*(3), 237-254.

Portzamparc, Christian De. (2010). *The Open Block*. Bruxelles, Belgium: Archives d'Architecture Modern.

Ratti, Carlo, Raydan, Dana, & Steemers, Koen. (2003). Building form and environmental performance: archetypes, analysis and an arid climate. *Energy and Buildings, 35*, 49-59.

Ratti, Carlo, Baker, Nick, & Steemers, Koen. (2005). Energy consumption and urban texture. *Energy and Buildings, 37*(7), 762-776

Robinson, D., & Stone, A. (2004). *Irradiation modelling made simple: the cumulative sky approach and its applications*. Paper presented at the The 21st Conference on Passive and Low Energy Architecture (PLEA), Eindhoven, The Netherlands.

Robinson, Darren. (2006). Urban morphology and indicators of radiation availability. *Solar Energy, 80*, 1643-1648.

Rogers, Richard George, & Urban Task Force. (1999). *Towards an urban renaissance: final report of the Urban Task Force*. London: Department of the Environment Transport and the Regions.

Salat, Serge, Labbé, Françoise, Nowacki, Caroline, & Laboratoire des morphologies urbaines. (2011). *Cities and forms on sustainable urbanisme*. Paris: Hermann.

Zhang, J., Heng, C. K., Malone-Lee, L. C., Hii, D. J. C., Janssen, P., Leung, K. S., & Tan, B. K.. (2012a). Evaluating environmental implications of density: A comparative case study on the relationship between density, urban block typology and sky exposure. *Automation in Construction, 22*(0), 90-101.

Zhang, J., Heng, C. K., Malone-Lee, L. C., Huang, Y. C., Janssen, P., Hii, D. J. C., & Ibrahim, N. (2012b). *Preliminary Evaluation of A Daylight Performance Indicator for Urban Analysis: Facade Vertical Daylight Factor per Unit Floor Area*. Paper presented at the SimBuild 2012, Madison, Wisconsin, USA.

End-node Approach for Pedestrian Flow Simulation

Hiroshi OTA

Institute of Industrial Science,
The University of Tokyo
4-6-1 Komaba Meguro-ku,
Tokyo Japan #153-8505
otah@iis.u-tokyo.ac.jp

Keywords: Street Network, Queueing Network, Building Node, Multi-Agent Simulation

Abstract

Studies on urban networks mostly focus on street systems, such as streets as links and junctions as nodes. This paper proposes an evaluation model with "building-nodes", to examine how buildings may contribute to the whole urban network. Firstly, by evaluating the total floor area of building nodes in the calculation process of betweenness centrality, the paper proposes a "potential pedestrian flow" that has an acceptable correlation coefficient with the pedestrian flow in the actual street network. Secondly, the paper explores an approach in regard to the urban network as a queueing network where "end-node congestion controls" are possible. For a general understanding of the methodology, the simulation in this paper principally focuses on the effect of changes in building clusters where the elements are all defined as end-nodes, and the advantage of a change to decentralized clusters was confirmed.

1. INTRODUCTION

1.1. Background of Street Network Study

Notions that regard the city as a network have been tried many times in history. For example, Georges E. Haussmann used the term "réseau" (network) when he re-designed Paris in the late 19th century with boulevards as links, and magnificent architecture as nodes. In the 20th century, Kevin Lynch identified paths and nodes as elements constituting the city of Boston and used network theory terminology to describe sequences of events in cities. In the recent regeneration project in Birmingham (UK), the city has been expanding its "Activity Nodes and Pedestrian Links" from 1990, and succeeded in reconstructing the fragmented city structure (Tibbault et al. 1990).

However, the discussion of urban networks often ignores the most important node elements: namely, the buildings, which are the places from which people leave to start walking, and the destinations where people arrive. For example, the well-known assessment method of "Space Syntax" (Hillier and Hanson 1984) doesn't include buildings in their evaluation of urban networks, and the recent studies of "Multiple Centrality Assessment (MCA) also highlights the network structure without including buildings (Porta 2006). Recently, a remarkable attempt to link buildings' attributes with street networks was done by Sevstuk, but the cartographic approach for extended urban networks is not shown yet (Sevstuk, Mekonnen 2012). This paper starts the discussion with a methodology to prepare the basic network data to include the nodes of buildings and streets, and thereafter discusses the methodology of simulation.

2. DATA SET WITH BULIDING NODES

2.1. Preparation of Data for a Building-Street Network

As a preparatory step in the development of a simulation method, the author produced an extended network data set that included buildings. The primary network data of street centerlines was imported from free open source software, Open Street Map (www.openstreetmap.org), with the author's modification on ArcGIS for better accuracy. As for the building node data, such as building locations, number of stories, and floor area, a dataset from Zmap Town II 2008/2009 (Shape version) was used. The data processing program was created on a Java platform, with GeoTools 2.1.0 for GIS toolkits and Processing 1.5 for visualization.

As for the target survey area, the Ginza, a district 1.5 km × 1.5 km in central Tokyo, was chosen. The specifications for the primary data set from Open Street Map and ZmapTown II are shown in Table 1, and Figure 1 shows the area's well-balanced distribution of various building sizes.

Number of Nodes	Number of Links	Number of Buildings	Mean Length of Links	Mean Volume of Buildings
858	3,822	4,545	50.2m	1,915.6m^2

Table 1: Specifications for primary network data set

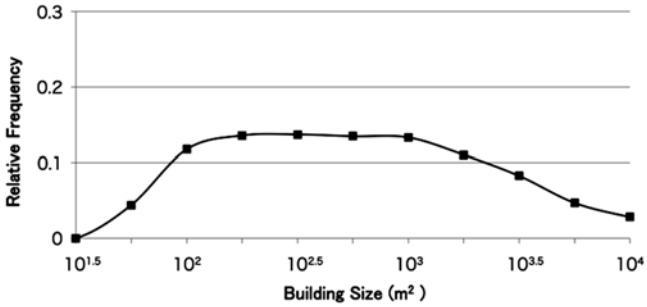

Figure 1. Well-balanced distribution of building sizes in Ginza area

With this data set, the extended network data was generated as shown in Figure 2. In the list of specifications in Table 2, "1. Intersection" and "3. Building" are the nodes imported from the primary data set. The nodes under "2. Branch" were newly created by the author. These Branch nodes are the points on streets nearest to the centroids of buildings, which are connected with building nodes by newly added links. Hereafter, the extended network model will be referred to as a "building-street network".

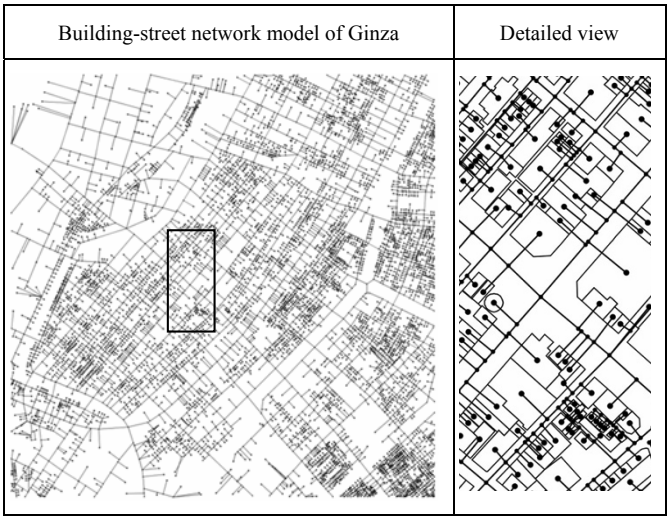

Figure 2: Generated building-street network and its details

Node Type and its numbers			Total Number of Nodes	Number of Links
1.Intersection	2. Branch	3. Building		
858	9,653	4,545	9,225	9,653

Table 2: Specifications for building-street network

2.2. Weighted Betweenness Centrality and Potential Pedestrian Flow

The advantage of the building-street network model is that it can include the valuable properties of buildings by assigning weights to building nodes. In this paper, the total floor area of the buildings is used for calculation of the betweenness centrality of the weighted network, and this calculation shows an acceptable correlation coefficient with the actual pedestrian flow.

Betweenness centrality is an index often used in the field of complex network and social network studies, to define the importance of a link or node in the network. Its definition generally includes the following formula:

$$C_i^B = \frac{1}{(N-1)(N-2)} \sum_{j=1;k=1;j\neq k\neq i}^{N} \frac{n_{jk}(i)}{n_{jk}} \quad (1)$$

The value of $n_{jk}(i)$ is 1 when the route node i appears in the shortest route between node j and node k , or 0 when it doesn't. The factor $n_{jk}(i)$ is the total number of the shortest routes between node j and node k, which is always 1 in the network with Euclidean distance. Therefore, the C^B of node i shows the frequency of appearance in all shortest routes between any two nodes of the network.

While C^B shows the indices of nodes or links in an unweighted network, C^{BW}, the weighted betweenness centrality, shows the importance of the nodes or links between node j and node k by assigning certain weights. Following the formula (1), this paper adopts the definition as follows:

$$C_i^{BW} = \frac{1}{(N-1)(N-2)} \sum_{j=1;k=1;j\neq k\neq i}^{N} n_{jk}(i) \times \left(\frac{W_j}{\sum_{i=0}^{N} W_i} \times \frac{W_j}{\sum_{i=0}^{N} W_i} \right) \quad (2)$$

W_j and W_k represent the weights of node j and node k respectively, and their products are added when the node i appears in the shortest route between node j and node k. In this paper, W_j and W_k are their total floor area, which are provided by GIS data.

Figure 3 shows the difference between the distribution of C^B and C^{BW} over the same area. C^B (on the left) shows higher centrality in the dense area with smaller buildings in the lower right of the area pictured. C^{BW} shows the

supplemented distribution of centrality affected by the larger buildings in the upper left of the area pictured.

Figure 3: Distribution of C^B (Left) and C^{BW} (Right)

If we assume all buildings have equal population density over their floor areas, C^{BW} can be interpreted as the frequency of interaction between the populations of building j and building k, and the distribution of C^{BW} is the possible interaction of all shortest routes between any two nodes in the network. This suggests to us that C^{BW} can be interpreted as the possible number of passages when interaction is represented as a direct trip between two buildings by their populations. To examine this, the distribution of C^{BW} and the data of the actual pedestrian flow survey in Ginza (Tokyo Metropolitan Government, 2001) are compared in Table 3. To confirm the effectiveness of the method, similar C^{BW} data for the Shimokitazawa area in Tokyo is also compared with pedestrian flow (Setagaya City Hall, 2002).

		Surveyed points	C^B	C^{BW}
Ginza	Weekday	20	0.344	0.596
	Holiday	20	0.375	0.561
Shimokitazawa	Weekday	92	0.068	0.595
	Holiday	92	0.078	0.554

Table 3: Correlation coefficient between C^B / C^{BW} and pedestrian flow

Though their correlation coefficient is not significantly high, C^{BW} values around 0.6 are acceptable because they are derived simply from the network structure and its building nodes. Considering the enormous effort and cost of conducting an actual pedestrian flow survey, the distribution of C^{BW}, which shows all the trips between any two buildings, can be useful to measure the "potential pedestrian flow" in a building-street network. Hereafter, this paper will utilize this measure of potential pedestrian flow for further simulation procedures.

2.3. Clustering of Building Nodes by the Girvan-Newman Algorithm

The number of building nodes in the survey area totaled over four thousand. For a smaller sample, this paper examines forty to fifty clusters of building nodes for which prior knowledge exists of the general character of their building-street network model. The network clustering was performed using the Girvan-Newman algorithm (Girvan and Newman 2004), one of the most well known algorithms in complex network studies, and the result is shown in Figure 5, with the identification of 46 clusters.

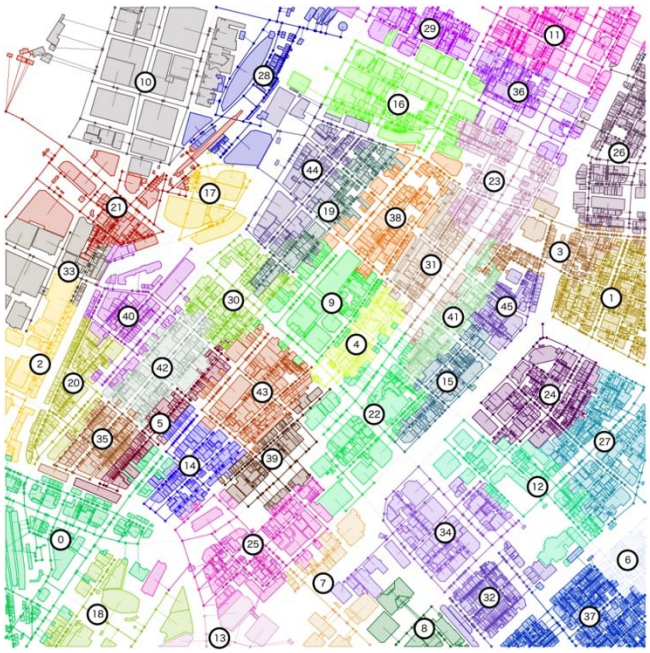

Figure 4. Result of Girvan-Newman Clustering Method (46 clusters)

Using these clustered building-street networks, the methodology for multi-agent simulation is developed in the following sections.

2.4. Simulation model for discrete event simulation

A characteristic of the buildings in an urban network is that they are a place where pedestrians stop and stay. This means the simulation model must handle stationary states, along with the length of time of the stay and the capacity of the building. The most explored field for this approach is the queueing network model, which is used for the analysis of hospital planning (Cheah and Smith 1993) or theme parks where each attraction generates waiting queues (Kawamura et al. 2004). Simulation that involves the use of a queueing model is generally known as "discrete event simulation" and

it is used to analyze traffic networks, production systems, and supply chains. However, it is important to note that in the context of this paper's analysis, the discrete event simulation focuses on events occurring continuously, and the software is designed to represent a succession of chained events, as shown in Figure 5.

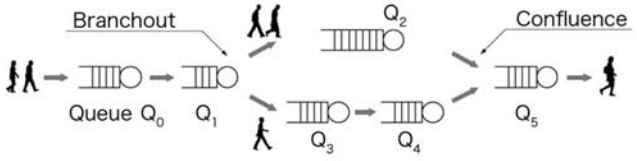

Figure 5. The model for discrete event simulation.

To focus on the contribution of buildings in urban networks, a novel approach will be to treat buildings as start points, as queues, and as end points. If the queueing network model were capable of addressing only the waits and congestion along a path, the modeling elements would be limited only to intermediate nodes, such as intersections and plazas. Considering this, the network model in this paper should have the buildings serving as the start and end nodes in queues, and intersections and plazas will not necessarily be considered as queues, as shown in Figure 6.

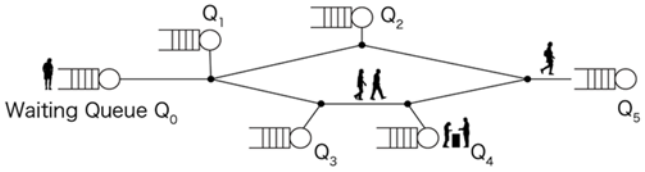

Figure 6. The model for building node simulation.

2.5. End-node Congestion Control in Protocol Research

There already exists a field of study in which researchers give more attention to the start and end nodes than the intermediate nodes. It is the research field of congestion control in computer networks, and this field evaluates protocols used by "end-node" servers to transfer data over networks. For example, the most famous protocol, TCP/IP, requires the server to start data transmission at a low transmission rate and allows gradual increase in the rate until congestion on the transmission route on the network is detected. This approach to enhance the ability of servers is distinguished from the study of data transmission in intermediate gateways or routers, which are called relay nodes. In this paper, this idea of congestion control at end nodes is used when analyzing the roles of building nodes in urban networks. As shown in Figure 7, urban networks are comparable to telecommunication networks; in this context, buildings are comparable to servers, and the movement of people and materials is comparable to the flow of data.

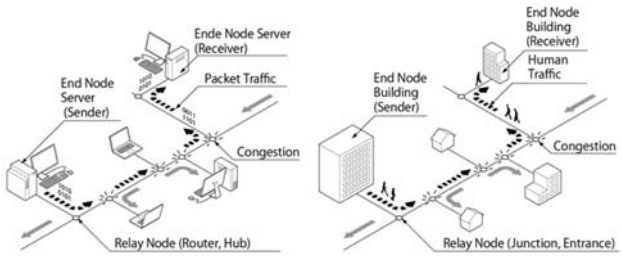

Figure 7. Comparison between networks of servers and buildings.

3. DEVELOPMENT OF SIMULATION SOFTWARE

As mentioned, discrete event simulation software, capable of simulating a queueing network, is widely in use. However, available systems have difficulty simulating a network having thousands of nodes and cannot import GIS data. Therefore, the author developed software for multi-agent simulation on building-street networks, using Java. The network data is stored in XGMML format, the network description language, and loaded into the program together with the routing information and building outline data.

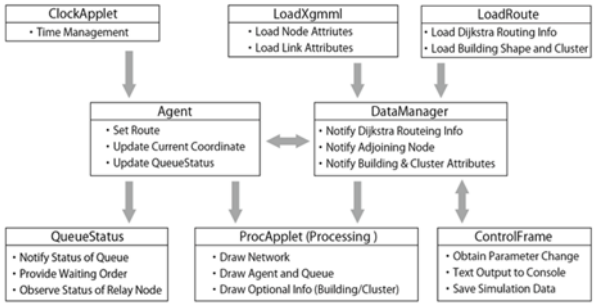

Figure 8. Structure of simulation program.

As mentioned in Section 2-4, only the building nodes acting as end nodes are assigned a queue attribute in the context of this study. The program, however, is also designed to allow the assignment of a queue to all nodes. Therefore, it will be possible in the future to study congestion at relay nodes by assigning a queue to them. Waiting queues are assumed to be of M/M/c/c type (see Cheah, Cruz), with which the arrival of agents is represented by a Poisson distribution and the required service time by an exponential distribution; the number of service counters and

the maximum queue length inside the building are set constant.

The queueing theory is the method of analysis on a crowding or congestion model, originating from research on the telephone by Erlang. In the illustration in Figure 9 below, λ represents the arrival rate—the number of people who arrive in the queue per unit of time—while μ represents the service rate—the service units per unit of time. For the condition where service is provided at a single counter, the traffic intensity ρ, which means the amount of congestion, is described as follows.

$$\rho = \lambda / \mu \tag{3}$$

Using ρ *and* λ, the waiting time W in the queue and the length of the queue are described as follows:

$$W = \rho / (1 - \rho) \tag{4}$$

$$L = \lambda W \tag{5}$$

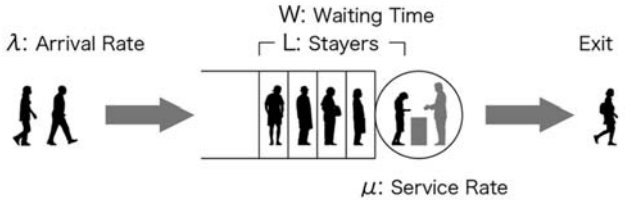

Figure 9: Illustration of waiting queue expressions.

The typical graphic representation of a single waiting queue is shown in Figure 6. Figure 10, on the other hand, shows a number of service counters with a queue; the spiral represents each queue in the simulation. This spiral illustrates a situation where up to 35 persons are queueing for services provided at 10 counters. The four diagrams, numbered 1 through 4, depict four steps in a series of events.

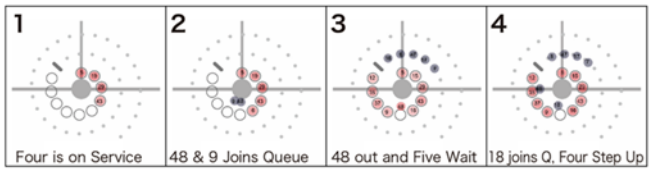

Figure 10. Presentation of events in a queue with ten counters.

Figure 11 shows a screen displayed by the simulation program. In this example, 40,000 agents are strolling around urban networks, and some of them are queueing at 4,545 building nodes.

Figure 11. Simulation screen showing waiting queues in buildings

As discussed later, the number of service counters is proportional to the building's total floor area in this simulation. The figure shows a long queue as a spiral representing a large building in the left part of the screen.

The following process, shown in Table 4, is the definition of agent behavior: the route to the destination is derived from the route information (generated in advance by calculations using the Dijkstra method), and when the agent reaches the target destination, the next destination is selected using a random number generator. The random number follows the probability of the destination building's service rate μ (discussed later). The walking speed is calculated as 1 meter per second (3.6 km per hour).

Process	Behavior
1. Selection of start point	Selected according to μ
2. Selection of destination	Selected according to μ
	Fetching of route information
3. Walking	Giving of pass-through information to relay nodes
4. Arrival	Fetching queue information and joining the queue
	Back to Process 2

Table 4: Definition of agent behavior

4. SIMULATION OF BUILDING-STREET NETWORK

4.1. Basic Characteristics of Random Walking

As an indicator used in connection with the queueing theory, μ represents the number of people served per unit of time, multiplied by the number of service counters.

Variations in the service time and/or the surpassing of μ by the actual customer arrival rate λ will result in a queue of customers. In the first simulation, the number of service counters was assumed to be proportional to the building's total floor area, and the service time was assumed to be 10 minutes in all cases. Since the simulation results were given in terms of the total number of persons who passed through nodes, the coefficient of the proportional relationship between the building's total floor area and the number of service counters does not affect the simulation results. Nevertheless, it was assumed that there existed one service counter per every 40 m^2 to ensure that even the smallest buildings could be assumed to have at least one service counter. Random walks were repeated until the total number of persons who passed by intersection nodes and branch nodes amounted to 10,000,000. The distribution of passages is illustrated in Figure 11.

The map shows greater traffic in the area of Hibiya and Marunouchi, where large-sized buildings are concentrated (the top left corner of the map) and Ginza central area where mid-sized commercial buildings are concentrated (the center of the map). Because the simulation is based on the definition of agent behavior shown in Table 4, and because the destination which is randomly given is proportional to service rate μ, or total floor area of the buildings, the distribution of passages is assumed to be one of betweenness centrality, or the potential pedestrian flow defined in Section 2.3.

4.2. Correlation between the Number of Service Counters and Service Time

The above discussion concerned the distribution of traffic given by a simulation with a weighted destination in which the service rate μ was considered. As discussed in Section 3, the service rate μ is defined as "*the number of agents served per time* × *the number of service counters*." Therefore, doubling *the number of agents served per time* vs. doubling *the number of service counters* would both be expected to be equivalent in terms of their impact on the distribution of passing agents; they both result in the doubling of μ at the given building node. This is similar to the equivalence between the strategy to double the size of transferred packets vs. the strategy to double the transmission rate. However, as shown in Figure 15, even though the service rate is kept the same for the two cases, a greater number of service counters will result in more stays in the building, while a limited number of service counters would require agents to stay out of the building and remain on the street. This means any change in the service rate will affect the distribution of agents in the whole network.

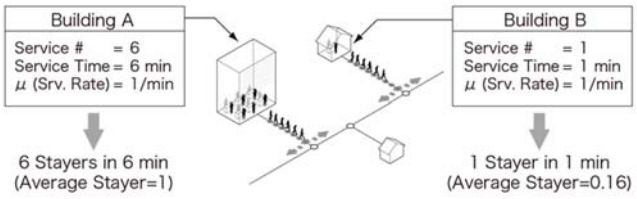

Figure 12. Relation between service rate and numbers of stays in the building.

If all buildings are given one counter for every 100 m^2 of floor area to provide 60 minutes of service, the total number of service counters in 4,545 buildings will be 85,485. With these conditions, the simulation shows the average proportion of agents staying in the building will be 49.2%. When the service time and the number of counters are both doubled to 120 minutes and 170,234 (one counter for every 50m^2 floor area), the service rate μ is kept the same, but the simulation shows the proportion of agents staying inside the buildings rises to 66.9%. Table 5 and Figure 13 show the variation of changes on service time and number of counters, and the simulation results show how the percentage of pedestrians inside the buildings decreases proportionally to the square root of service time.

Service time	Total number of service	Percentage of pedestrians
120 min.	170,234	66.9%
60 min.	85,485	49.2%
30 min.	42,806	39.8%
15 min.	22,002	28.5%
7.5 min.	12,163	21.9%

Table 5: Changes in the proportion of agents inside/outside of buildings

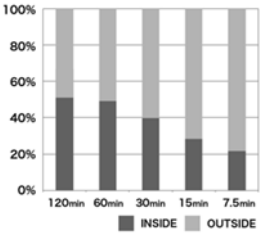

Figure 13: Agents inside/outside of buildings

4.3. Simulation Concerning the Effect of Modifying Specific Building Clusters

The previous section described the results of a simulation in which the queueing attributes were modified for all the 4,545 building nodes inside Ginza area. This section discusses the results of simulations in which the service rate μ of building nodes is doubled only within one or two clusters out of 46 clusters (see Section 2.4). As service rate μ is proportional with total floor area in this paper, the question can be asked as *"what are the effects on the city when the floor area is doubled in certain building clusters?"* As shown in Fig. 14, the author chose Case A: only one cluster (# 9) at the center, and Case B: two clusters

(#5 & #26) decentralized by a considerable distance, and studied the impact of doubling the service rate μ at building nodes inside the chosen cluster or clusters. As shown in Table 6, the total floor area to be examined is approximately the same for Case A and Case B.

Figure 14. Clusters to double μ: Case A (left) and Case B (right)

	Cluster	Number of buildings	Total floor area	Service rate μ
Case A: Centralized	#39	136	194,856 m^2	60 min. per 50 m^2
	The rest	4,409	8,683,980 m^2	60 min. per 100 m^2
Case B: Decentralized	#5 & #12	379	220,082 m^2	60 min. per 50 m^2
	The rest	4,166	8,658,754 m^2	60 min. per 100 m^2

Table 6: Specifications of Case A and Case B

The conditions were defined as shown in the above table for the two simulation cases, and the simulations were repeated with the service time sampled at 120 minutes, 60 minutes, 30 minutes, and 15 minutes for the building nodes in the selected cluster or clusters (similar to Section 4.2) to observe the agent traffic through relay nodes and the proportion of agents inside and outside buildings within each cluster.

4.4. Simulation Results and Observations

Figure15 illustrates the results of simulations performed under the conditions described above. First, as to the number of node visits, both simulation cases showed major changes in the traffic through nodes around the selected cluster or clusters. However, in Case B, the traffic increased most at nodes situated along the shortest route between the two selected clusters, and the results show a wider effect at the center of the map. This effect is caused by an increase in the probability that the route between the two new clusters will be selected, resulting in a doubling of the service rate at building nodes in these clusters. A longer service time would be expected to decrease the proportion of agents inside buildings, but the impact of this variable was too small to produce a significant change in the general pattern—although the simulation did predict some decreases in Case B.

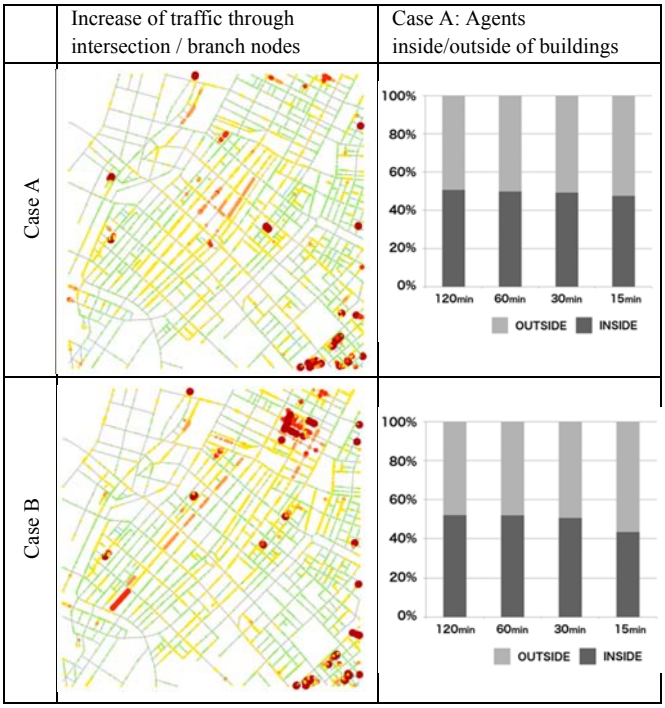

Fig. 15: Increase of traffic (left) and proportion of agents (right)

Next, we shall see how changes in the service time affect the surrounding area. Figures 16A and 16B show the rate of increase in the proportion of agents inside buildings in each cluster when service time is decreased from 120 minutes to 15 minutes within the selected cluster(s).

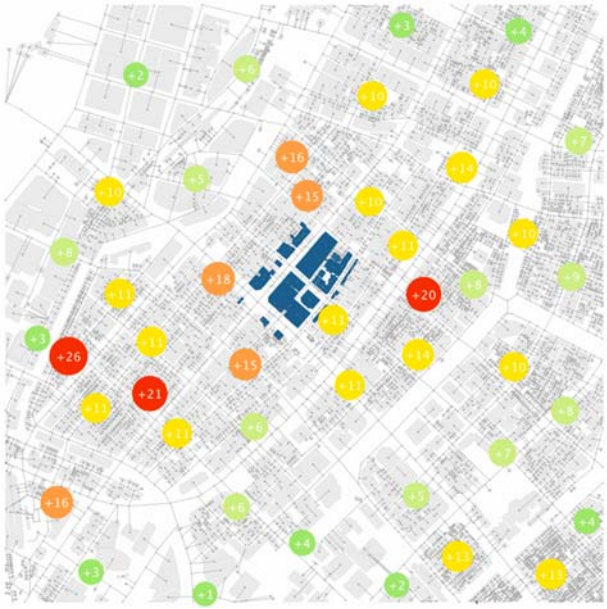

Fig. 16A: Increase in the proportion of agents inside buildings (Case A)

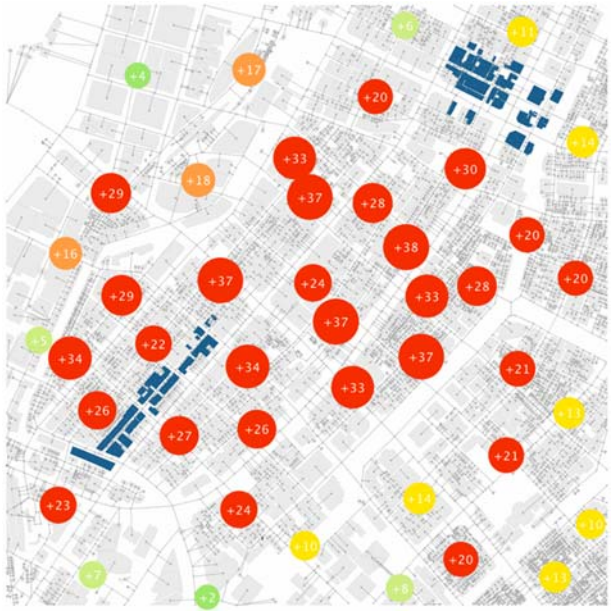

Fig. 16B: Increase in the proportion of agents inside buildings (Case B)

In the simulation performed for Case A, the proportion of agents inside buildings increased mostly within clusters around the selected cluster. However, as illustrated, the cluster in which this proportion increases the most is not located close to the cluster in which the service time was shortened but exists at a certain distance from it. In the simulation performed for Case B, the proportion of agents inside buildings changed in the whole area. As shown in Table 6, the one cluster selected in Case A is roughly equivalent to the two clusters selected in Case B in terms of total floor area, and therefore, the number of agents who flow out of buildings due to the shortening of service time in the selected cluster or clusters is expected to be approximately the same for the two cases. However, the simulation performed for Case B demonstrated changes in the proportion of agents inside buildings in the whole area. This seems to indicate the greater effectiveness of the decentralized approach.

5. CONCLUSION

This paper described a study on building-street networks using the approach of queueing networks, informing the readers of the theoretical basis, the method used for the preparation of data, the simulation technique, and simulation results.

The study yielded the following conclusions, confirming the validity of the methodology used:
(1) The control of congestion in the street network was achieved by manipulating service rate μ at building nodes, by changing the number of service counters and amount of service time.
(2) Decentralizing manipulations of existing building clusters more effectively diffuse impacts to wider areas.

In future studies, the author intends to perform a finer analysis on smaller areas to study the contributions of individual buildings within a cluster.

References

BLANCHARD P., VOLCHENKOV D., 2008, Exploring Urban Environments By Random Walks,Stochastic and quantum dynamics of biomolecular systems, 183 - 203, Bernido CC, Springer

CHEAH J.Y., SMITH M., 1993, Generalized M/G/C/C state dependent queueing models and pedestrian traffic lows, Queueing Systems 15, pp.365-386

CRUZ F.R.B., SMITH J.M., 2007, Approximate analysis of M/G/c/c state dependent queueing networks, Computers & Operations Research 34, pp.2332-2344

GIRVAN M., NEWMAN M.E.M., 2002, Community structure in social and biological networks, Proceedings of the National Academy of Sciences, Vol.99, No.12, pp.7821-7826

HILLIER B., HANSON J., 1984, The Social Logic of Space, Cambridge University Press

KAWAMURA ET AL., 2004, Investigation of Global Performance Affected by Congestion Avoiding Behavior in Theme Park Problem, IEEJ Transactions on Electronics, Information and Systems, Vol. 124 (2004) No. 10, pp.1922-1929

PORTA S., CRUCITTI P., LATORA V., 2006, The network analysis of urban streets: A dual approach, Physica A 369, p.853

SEVTSUK A., MEKONNEN, M. 2012. Urban network analysis: a new toolbox for measuring city form in ArcGIS. Proceedings of the 2012 Symposium on Simulation for Architecture and Urban Design (SimAUD '12). Society for Computer Simulation International, San Diego, CA, USA, 10 pages.

SETAGAYA CITY HALL, 2002, Traffic Survey Report for Shimokitazawa Station Renewal, Setagaya City Hall Publication

TIBBALDS COLBOURNE KARSKI WILLIAMS, 1990, City Cnetre Design Strategy, The City of Birmingham

TOKYO METROPOLITAN GOVERNMENT, BUREAU OF INDUSTRIAL AND LABOR AFFAIRS, 2001, Survey of commercial districts in Tokyo

Session V

Designing-In Performance: Towards Cloud Based Simulation and Multidisciplinary Design Solution Space Search 139
Shih-Hsin (Eve) Lin and David Jason Gerber
University of Southern California

From Statistical to Diagrammatic: Geo-spatial and Time- based Data Visualization through Parametric Modeling 147
Ming Tang, Chris Auffrey, Mingming Lu
University of Cincinnati

Integrated Design in the Simulation Process 153
Martha Tsigkari, Angelos Chronis, Sam Conrad Joyce, Adam Davis, Shuai Feng, Francis Aish
Foster + Partners

Designing-In Performance: Towards Cloud Based Simulation and Multidisciplinary Design Solution Space Search

Shih-Hsin (Eve) Lin[1] and David Jason Gerber[1]

[1]University of Southern California
School of Architecture,
Watt Hall 204, Los Angeles, CA90089
shihhsil@usc.edu, dgerber@usc.edu

Keywords: Conceptual Energy Simulation, Early Stage Design Decision Making, Performance-Based Design Process, Multidisciplinary Design Optimization, Genetic Algorithm.

Abstract

This research is built upon a previously established multidisciplinary design optimization (MDO) framework and further explores the impact of this framework on the early stages of design. Specifically, this paper addresses the potential of introducing a cloud-based approach to tackle geometrically complex design problems and to facilitate early stage design exploration. To address these interests, two experiment sets are presented and then discussed in the context of the application of cloud-based computing. First presented is a hypothetical scenario possessing complex geometry to understand how the existing established framework assists in the exploration of complex geometric design problems. Second, a pedagogical benchmark case allowing for the observation of the human versus automated decision-making process. By comparing these processes the impact of the established MDO approach on "designing-in performance" and the potential impact of applying cloud-based computing to the MDO framework can be revealed and discussed.

1. INTRODUCTION & OBJECTIVE

Computer-Aided Design and Engineering (CAD/CAE) tools enable architects and engineers to design higher performance buildings by simulating many different aspects of building performance. However, due to tool interoperability, design cycle latency, domain expert disconnection, design cognition limitations, and fundamental research requirements into the impacts of simulation on the design process—these performance feedback CAD/CAE tools rarely support decision making during the early stage of the design phase where design decisions have a long-term impact on overall building performance. Recent research has explored the use of multidisciplinary design optimization (MDO) methods to automate the visualization of geometry in conjunction with Pareto-ranking and quantification of performance feedback as a potential solution to facilitate the performance feedback loop. However, the application of preliminary energy performance feedback to support the exploration of complex geometry has not been fully developed. In response, an MDO design framework was developed in conjunction with a prototype tool (named the H.D.S. Beagle), which combined parametric design and a Genetic Algorithm (GA) based multi-objective optimization with specific interest in energy, spatial programing compliance, and finance by the research team (Gerber et al. 2012). The established platform specifically selects a cloud-based energy simulation engine, with the intent that this approach can further facilitate the MDO application in the early design stage of the design process.

In this paper, the research presents the potential of this cloud-based approach to tackle higher degrees of geometric complexity, as is the contemporary architectural need, and how the approach can further facilitate the early-stage design process. To address this issue, the research started with problem definition and a literature review to isolate the requirements to provide a "designing-in energy performance" environment and reveal the current gaps. "Designing-in" refers to the notion of bringing energy performance to the foreground in early-stage design processes. The research then follows up by conducting two experiments to understand how the established MDO design framework, which is empowered by a cloud-based approach, can further enable the performance feedback

decision-making process. The first experiment is to explore the capability of the Beagle to process complex geometry and to assist in the yielding of complex geometric solutions with measurable improved performance. The second experiment is to compare the established design framework process with the human-based decision-making process though a benchmarking pedagogy. During these two experiments, the established MDO design framework's benefits, limitations and impact on the current design process are explored and discussed. The further potential of our cloud-based system and computational approach is also revealed.

2. BACKGROUND & REVIEW

In this section, the research presents the current issues and obstacles between the design and energy simulation domains while synthesizing the need to provide a "designing-in performance" environment. The research then reviews precedents, potential solutions, summarizes gaps in current attempts, and provides our current point of departure.

2.1. Problems and Needs between the Design and Energy Simulation Domains

While the overall performance of buildings is greatly impacted by design decisions made during the early design stages (Bogenstätter 2000), unfortunately design professionals are often unable to adequately explore design alternatives and their impact on energy consumption up front (Crawley et al. 2008). In order for designers to integrate these engineering-oriented analysis tools, model conversion and expert domain knowledge are required to produce usable results. However, the model conversion process is not well supported by existing design tools and typically requires expert translation and interpretation of generated data (Augenbroe et al. 2004). Other issues, such as tools interoperability among different expert domains, intensive analysis time requirements, limitations of design cognition and complexity, can all be considered as contributing factors to design uncertainty, poor performing designs and design cycle latency (Augenbroe 2002). Consequently, performance assessments are typically made after the initial design phase, where the analysis is performed on a very limited set of design alternatives rather than to support early stage design decisions where a broader range of possible more optimal solutions may exist (Hensen 2004). Furthermore, design decisions are never made for one design objective alone, as there are competing objectives in which a designer must find the best fit through understanding of tradeoffs (Aish and Marsh 2011). In order to overcome the obstacles of current design and energy simulation domains, and to enable designers to design with performance feedback in mind, a design framework and tool should provide 1) rapid generation of design alternatives; 2) rapid evaluation of design alternatives; 3) tradeoff study against competing criteria; and 4) a search method to identify design alternatives with better fit performance. These requirements speak directly to the essence summarized by Augenbroe and can represent the trend of recent efforts regarding the domain of design and performance feedback.

2.2. Precedent Research of Potential Solutions

Recently, multidisciplinary design optimization (MDO) approaches have drawn the attention of the AEC industry as potential solutions to overcome obstacles existing between design and other performance analysis domains. MDO refers to an approach that uses optimization methods to solve design problems that have several objective functions and a number of disciplines (Coello Coello et al. 2007). This approach has been successfully adopted by the aerospace industry (AIAA 1991) and has begun to be explored in its applicability to the AEC field. In the MDO design framework, there are two essential components that directly address the four previously identified needs of current performance-based design: parameterization and optimization.

The use of parametric design is becoming increasingly common in the AEC due to the acknowledged advantages and inherent ability to quickly generate design alternatives through the parameterization of geometry (Burry and Murray 1997; Gerber 2009). With the predefined and pre-rationalized requirements of the parameterization process, once a parametric model is formed, design alternatives can be rapidly generated and explored rigorously through parameter value manipulations, thereby further facilitating the exploration process by adopting an automation rule (Menges 2011). The automation of the design exploration process can shorten design exploration cycle time (i.e. latency), as demonstrated in the work of Aish and Woodbury (2005). Furthermore, the automation of the parametric exploration process provides the opportunity for relationally incorporating performance criteria as part of the process, and thereby eliciting more extensive feedback by

which to evaluate and identify potentially optimal design alternatives.

Besides the benefits of parametric design—which increase the generation of design alternatives, reduce necessary exploration time, and enable the automation process—another critical component of the MDO design framework is the use of an optimization method that provides the automation rules to identify design alternatives that meet desired goals. The concept of optimization can be described as the ability "to attain what is Best once one knows how to measure and alter what is Good or Bad" (Beightler et al. 1979). While there are various optimization methods and algorithms, they all contain the definition to measure, and the method to determine, good or bad. Within the complexity of the building design field, design problems generally are considered as 'ill defined' (Simon 1973) and are often understood as not having a singular optimum, but rather optimality is found through the understanding of tradeoffs (Aish and Marsh 2011). Therefore, among various optimization approaches, Genetic Algorithms (GAs) are considered a more efficient means for handling complex design problems where Pareto front candidates can be evolved and tradeoffs can be explored (Gero et al. 1983). A representative precedent was developed by John Frazer, with his influential evolutionary architectural theory and application of GAs in building design and complex geometry (Frazer 1995). More recently, Caldas and Nordford use a GA to solve for the thermal and lighting performance optimization of a design solution (Caldas and Norford 2002).

2.3. Gap Analysis and Point of Departure

Research precedents have demonstrated the potential of adopting MDO to provide a performance feedback loop for supporting early design stage decision-making (Flager et al. 2009). However, precedents exploring MDO in the AEC field have typically employed simplified geometry (Flager et al. 2009), while precedents involving more complex geometry have limited themselves to single domain optimization (Yi and Malkawi 2009). The few precedents which have explored both MDO and complex geometry have not included the energy performance domain as a domain of interest nor the use of cloud-based computing for the automating of the solution space (Turrin et al. 2011). Where the energy performance domain has been included for optimization, the relationship between design form and energy performance has been largely excluded. Instead, the optimization process has focused on mechanical systems (Pantelic et al. 2012) and simple geometric modifications such as window sizing and placement (Hamdy et al. 2011). Furthermore, the application of these precedents' subject of interest to the overall design process remains largely unexplored.

In response to this gap in existing research, an MDO design framework was developed that could incorporate both conceptual energy analysis and exploration of complex geometry for the purpose of providing early stage design performance feedback. Subsequently, the established MDO design framework was applied to the overall design process, where its impact could be observed inclusive of cloud-based computing solutions. The established MDO design framework utilizes a prototype tool (H.D.S. Beagle) which enables the coupling of parametric design with multi-objective optimization (Gerber et al. 2012). The developed framework specifically enables the exploration of varying degrees of geometric complexity with energy simulation feedback. Also provided are spatial programing compliance and financial performances for consideration in performance tradeoff studies. The framework has demonstrated the ability to reduce design cycle latency, automate design exploration, automate analysis and the evaluation process, and provide improving performance design alternatives (Gerber and Lin 2012a; Gerber and Lin 2012b). In addition, the established MDO framework is being tested in pedagogical and practical design process settings.

This paper proceeds to explore the application of the established MDO framework to the overall design process, which addresses the potential for utilizing a cloud-based approach to tackle higher degrees of geometrically complex design problems, and explores how this approach could continue to facilitate the early-stage design process.

3. RESEARCH METHOD

For the purpose of understanding how the established MDO design framework, empowered by the cloud-based approach, could further enable the performance feedback decision-making process, two experiment sets were gathered. The first experiment set utilized a hypothetical design problem developed in a design studio setting. This scenario represents the potential complexity and forms of interest to designers. In addition, due to the aforementioned existing obstacles between the design and energy simulation domains, the energy performance analysis for this type of

complex geometry could hardly be conducted by the designer. The first step needed was the formulation of the design problem into a parametric model recognizable by the Beagle before engaging the MDO design framework to test the scenario. By exploring this scenario, the capability of the Beagle to process complex geometry and to assist in the yielding of complex geometric alternative solutions can be measured and discussed. The second experiment set compares the established MDO framework process with a benchmarking pedagogical design process. In this case the same design problem was provided to the MDO framework and to a group of human users. The benchmark case was designed to have the same objectives as the MDO framework, but through manual use of the same tool platforms as the Beagle by these different student designers. The Benchmark process differed from the H.D.S. Beagle process in that users were required to manually manipulate the parametric values to explore design alternatives. In addition, the users were required to manually calculate the three objective functions as used by the Beagle before manually evaluating and implementing subsequent design decisions accordingly. The two processes utilized by these experiment sets are illustrated in **Figure 1.**

For both experiment sets, three categories of quantitative measurements were recorded: 1) Design Problem Complexity; 2) Design Process Time; and 3) Design Product Quality. Design Problem Complexity is measured according to the surface count of the scenario's initial energy model and the number of parameters explored. Design Process Time is the measurement of the times recorded to obtain analysis results. The Design Product Quality measures the resulting solution spaces' performance by the range in terms of the defined objective scores and the number of the Pareto solutions in the respected ranking of the overall solution pool. After the analysis and observation of these two experiment sets, the established MDO design framework's current benefits, limitations and impact on the current design process can be identified and discussed. Following this discussion, the further potential of the MDO design framework empowered by the affordance of the cloud-based computational approach can be ascertained.

4. H.D.S. BEAGLE

In order to realize the proposed framework, selection of the platforms by which to implement GA-based multi-objective optimization (MOO) algorithm was needed. To this end, a prototype tool (H.D.S. Beagle) was developed as a plugin for Autodesk® Revit®. The plugin integrated Autodesk® Green Building Studio® (GBS) and Microsoft® Excel® to generate the desired automation and optimization routine. **Figure 2** illustrates H.D.S. Beagle's automation loop developed through C# as a plug-in for Revit, using Revit API, Excel API and GBS SDK.

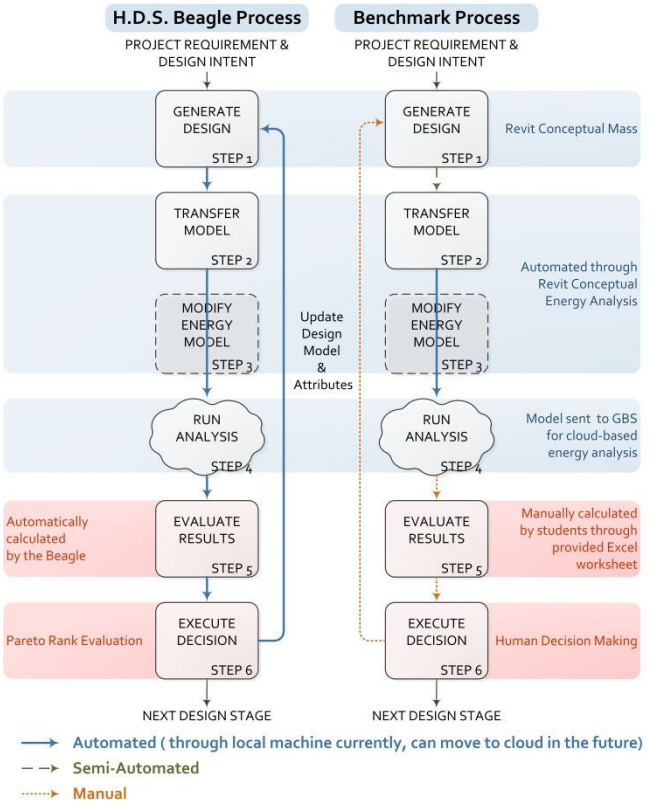

Figure 1. Comparative simulation process maps between the automated Beagle and the manually implemented pedagogical benchmark experiment set.

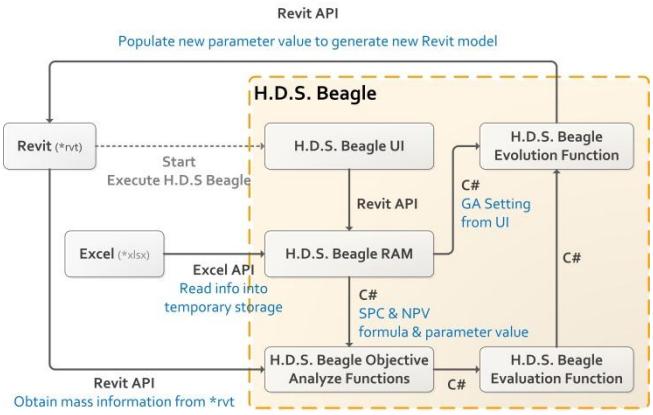

Figure 2. H.D.S. Beagle automation loop developed through C# as a plug-in for Revit, using Revit API, Excel API and GBS SDK.

Autodesk® Revit® is a building information modeling platform with parametric capabilities enabling designers to define their geometry while providing a series of parameters that impact the development of varying geometric configurations. This platform also serves as an insertion point for the energy settings necessary for a conceptual energy analysis through Autodesk® Green Building Studio® (GBS). This approach avoids the hurdle of geometry and parameter translation between the design and energy simulation domains. GBS is a cloud-based energy analysis service that serves as the energy simulation engine for the prototype. Microsoft® Excel® 2010 not only provides a means of containing the financial parameters and formula, but also serves as a user interface proxy in which designers can set up design parameter ranges of interest, constraints, spatial program parameters, and the spatial programing compliance formula.

After the determination of the integrated platform, H.D.S. Beagle was developed to complete the automation routine by utilizing a GA-based multi-objective optimization algorithm. This automation and optimization is conducted on a multi-core cloud-based system architecture. The three objective functions can be formulaically expressed as follows:

$$S_{obj} = Max.SPC$$
$$E_{obj} = Min.EUI$$
$$F_{obj} = Max.NPV$$
$$where$$
$$S_{obj} = Spatial\ Programing\ Compliance\ Objective\ Function$$
$$E_{obj} = Energy\ Performance\ Objective\ Function$$
$$F_{obj} = Financial\ Performance\ Objective\ Function$$
$$SPC = Spatial\ Programing\ Compliance\ Score$$
$$EUI = Energy\ Use\ Intensity$$
$$NPV = Net\ Present\ Value$$

A more detailed description of the adopted method, which drives the overall framework, can be found in previously published research (Gerber et al. 2012).

5. CASE STUDIES

5.1. Hypothetical Case: Twisting Tower

The first scenario, with a twisting double tower, was selected due to its geometric complexity, in order to observe the performance of the established framework when confronted with a more geometrically complex problem. This scenario was modeled after an existing design studio project in order to reflect the type of geometrically complex problems that might be encountered with real-world design applications. This hypothetical scenario was defined as possessing a twisting double tower divided by a wind canyon atop a shared plinth. In order to translate the design problem into a Beagle readable format the design problem needed to be redefined as a series of parameters consisting of driving, fixed, and driven properties. The resulting parametric model is illustrated in **Figure 3**. The final parametric model is composed of four program space types, parking, retail, office, and hotel, along with 9 geometric driving parameters.

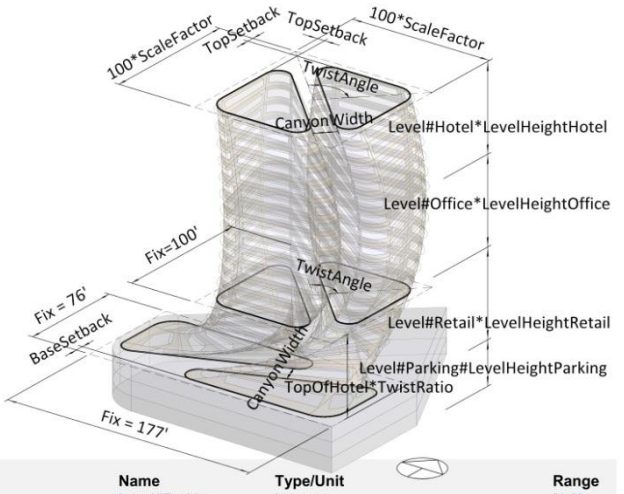

	Name	Type/Unit	Range
Driving Parameters	Level#Parking	Integer	[1,3]
	Level#Retail	Integer	[4,6]
	Level#Office	Integer	[4,6]
	Level#Hotel	Integer	[4,6]
	TwistAngle	Angle/°	[0,90]
	TopSetback	Length/ft	[1,10]
	BaseSetback	Length/ft	[6,15]
	ScaleFactor	Number	[0.8,1.25]
	CanyonWidth	Length/ft	[12,30]
Fixed Parameters	TwistRatio	Number	0.3
	LevelHeightParking	Length/ft	10
	LevelHeightRetail	Length/ft	10
	LevelHeightOffice	Length/ft	10
	LevelHeightHotel	Length/ft	10
Driven Parameters	TwistHeight =	BuildingHeight * TwistRatio	
	ScaleTop =	ScaleFactor * 100'	
	TopOfRetail =	Level#Retail * LevelHeightRetail	
	TopOfOffice =	TopOfRetail + Level#Office * LevelHeightOffice	
	TopOfHotel =	TopOfOffice + Level#Hotel * LevelHeightHotel	
	BottomOfParking =	Level#Parking * LevelHeightParking	

Figure 3. Resulting parametric model and ranges as translated from the original hypothetical design studio problem for the twisting tower scenario as used in the hypothetical case study by the Beagle.

After the design problem was formally defined, the initial model is then used by the Beagle to generate and breed design alternatives. Parameters available for exploration include not just the defined 9 driving geometry parameters, but also window opening percentage, shade depth and skylight percentages. The average time needed to obtain the analysis results for a single design alternative was

approximately 28.64 minutes. This measurement includes the time required for updating the geometry, sending the updated geometry to the cloud-based GBS server for energy analysis, receiving the requested energy analysis results, extracting necessary data from the updated geometry, and calculating the 3 objective scores based on the analysis results and extracted data. After a 20-generation run, the measured improvement in the performance of the solution space from the initial design model can be observed as the following: the NPV improved from $440 to $514 million dollars, the EUI improved from 66 to 55 kBtu/sqft/yr, and the SPC improved from 44% to 99% compliance. At the end of the run a total 63 Pareto solutions were identified out of the 250 generated design alternatives during the 120 hours of active runtime.

Figure 4. An example of a sub-set of the solution space for the twisting tower scenario in which the multi-objectives –EUI, NPV, and SPC- are calculated, ranked, and visualized for ease of manual decision making.

These results demonstrate that the Beagle can provide the opportunity for designers to explore a broader range of alternatives with data and performance feedback support than conventionally available. **Figure 4** provides a sampling of the solution space generated with Pareto designated solutions enlarged and highlighted. While the selection of a particular design alternative for the final scenario may not be based solely on the optimized performance for any or all of the three objectives, H.D.S. Beagle provides an opportunity for understanding the impact of a particular decision on the overall expected performance of a design. As a result, complex geometric design alternatives can be analyzed both aesthetically and by their performative properties through the Beagle.

5.2. Pedagogical Experiment Comparative Study

In this experiment, the initial parametric model was provided to 27 students. Students were instructed to only manipulate 9 predefined parameters by which to explore potential design alternatives, with 5 parameters driving the overall building geometry and 4 built-in energy parameters available through the Revit conceptual energy analysis platform illustrated in **Figure 5**. In addition to the initial design, students were also provided an Excel worksheet by which to calculate and record the objective scores of their generated design alternatives. Students were also asked to record their progress and times necessary for designated steps. These records were used later to measure the students' search methods and exploration process.

During the pedagogical experiment, students averaged 16.4 minutes per iteration compared to the Beagle's 6 minutes per iteration. The average exploration time recorded by students was 3 hours, with approximately 5 generated iterations. Therefore, for qualitative comparison purposes the Beagle was given the same time period in which to generate results for the same design problem. However, in the interest of exploring the capability of the Beagle when given an extended period of time, the Beagle was also given a 7-hour period, and also asked to reach 6 generations in separate runs. For comparison purposes there are two result sets of interest. The first is in comparing the student generated solution space with the Beagle generated solution space within the designated 3 hrs time period. The second set is between the solution spaces generated by the Beagle during the 3 hours, 7 hours, and 6th generation runs. **Table 1** provides a summary of the performance ranges of the solution pools generated by these experiments.

With regards to the Beagle versus the student-generated solution pool under the same time constraints, the Beagle was able to provide a solution pool with a 26.8% increase in the measured NPV and a 13.7% reduction in the calculated EUI. However, the pedagogical solution pool was able to provide a 22.2% more compliant spatial programming set. Overall, when ranked according to their performance for all three objectives, 36.7% of the design alternatives generated by the Beagle were

designated as Pareto optimal solutions while only 26.9% of the students generated design alternatives received this designation.

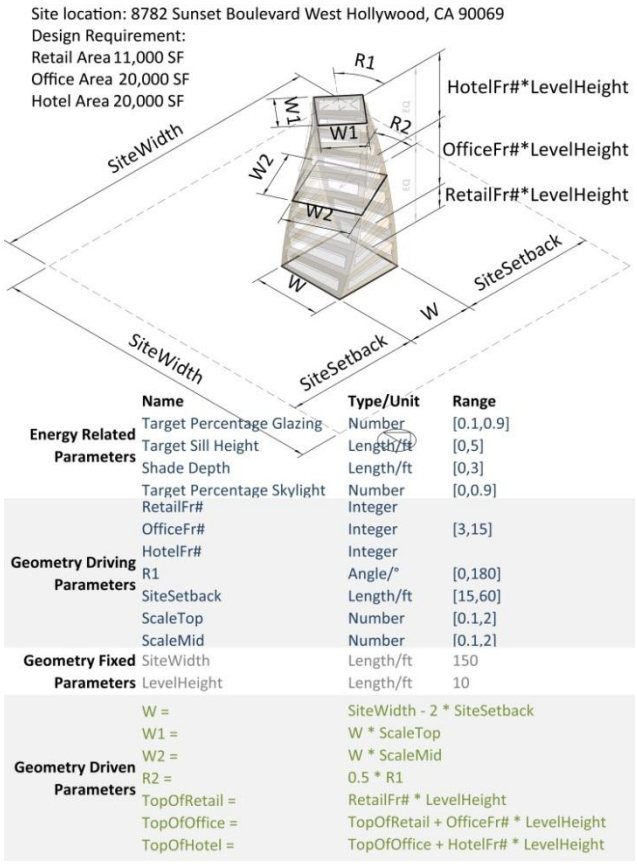

Figure 5. The provided parametric model and ranges for the pedagogical benchmark experiment and comparative Beagle studies.

		SOLUTION SPACE			
		Students	H.D.S. Beagle		
			3 HRS	7HRS	6th Gen
NPV (Million$)	MIN.	-48	-41	-41	-41
	MAX.	341	432	584	835
Initial: -41	Improved	382	473	626	875
EUI (kBtu/sqft/yr)	MIN.	67	59	59	56
	MAX.	292	233	233	233
Initial: 174	Improved	107.0	115.1	115.1	117.8
SPC	MIN.	-151	-134	-266	-404
	MAX.	99	81	83	88
Initial: 10	Improved	90	72	73	78
Pareto (%) (Students/ Beagle)	3 OBJ		26.9/ 36.7	22.4/ 40.0	19.4/ 37.2

Table 1. Performance comparison of the solution space generated by the pedagogical experiment and the Beagle after completed runtimes of 3 hours, 7 hours, and 6 generations. Improvement is measured by comparing with the initial objective score.

The quantity of iterations and generations available during a specified time period is directly dependent on the capacity of the hardware, software, Internet, and simulation engine used. Therefore another point of interest is to see if there was observable improvement over extended generations, as will become available during the same time period with improvements in computational affordances. For this purpose, the Beagle was asked to run for the extended time period of 7 hours and then again to reach the 6th generation. The Beagle was able to continue to improve the performance of the solution space through increased generations. For example, with regards to maximizing the NPV, the 6th generation reached $835 million while the 7 hours solution pool reached only $584 million and the 3 hours solution pool only reached $432 million. Improvements in this fashion are observable across all 3 objectives. Therefore, we conclude, with increases in computational affordances through our cloud-based approach, the measurable improvements on the solution pool provided by the established MDO design methodology within a designated time period will continue to expand.

6. CONCLUSION

This research uses the previously established MDO design framework to run two experiments with the intent of observing the framework's ability to tackle complex geometric exploration, discernable impact on the early stage design process, and potential empowerment through increased computational affordance, i.e. cloud computing.

Through the hypothetical case study the framework demonstrated an ability to provide performance feedback via the generated solution space with improved performance over the initial design for a geometrically complex design problem. While noticeable improvement in the solution space was observed, computational time constraints limited the effectiveness of the results. However, during the pedagogical experiment the Beagle was able to demonstrate superior results under the same time constraints as human users, and further improved results when given extended time. With the application of cloud-based computing, the framework would gain the ability to run design scenario analyses in parallel through apportionment of increased computational resources. This would result in significantly reduced time requirements to acquire the desired analysis results. Given that time typically dominates early design exploration, with the incorporation of cloud-based computing it can be extrapolated that the reduction in computation time necessary to generate desired results would further acclimate the framework to the early stage design process. Cloud-based computing requires formal definitions of objectives and procedures. While the established MDO framework has not fully explored the direct application of cloud-based computing, these requirements have been met.

The applicability of this framework during the early stage design process and the impact of this framework on the overall

design process are still in need of further research. Subjects regarding the translation of design problems into parametric models, for example, require additional research. Also in need of supplementary study is the impact of the results generated by the framework on a design problem's final design, thereby examining the framework's effectiveness in supporting early design decision making.

Assuming Moore's Law holds true, current computing power affordance can be expected to continue to grow exponentially. Combined with cloud-based computing as previously demonstrated, the quality of the framework's generated solution space can also be expected to improve. This expansion of computing power and of solution space analysis will lend itself to the augmenting of the MDO framework to enable designing-in performance at early stages where time and seeing is tantamount for the designer.

Acknowledgements

The work was in part supported by funding from the USC School of Architecture Junior Faculty Research Fund and in part by Autodesk, Inc. The authors thank the USC Dean of Architecture Qingyun Ma; Ms. Bei "Penny" Pan our initial lead software developer; Junwen Chen, Ke Lu, Shitian Shen, Yunshan Zhu for their continued software development; Prof. Kensek and her class; Laura Haymond for her review and participation; and Autodesk Inc. for their generous support within the IDEA Studio program.

References

AIAA. 1991. Current State of the art on multidisciplinary design optimization (MDO). Washington D.C., USA, American Institute of Aeronautics and Astronautics.

AISH, R. and MARSH, A. 2011. An integrated approach to algorithmic design and environmental analysis SimAUD 2011, Boston, MA, USA.

AISH, R. and WOODBURY, R. 2005. Multi-level interaction in parametric design. Smart Graphics. A. Butz, B. Fisher, A. Krüger and P. Olivier, Springer Berlin / Heidelberg. 3638**:** 924-924.

AUGENBROE, G. 2002. "Trends in building simulation." Building and Environment 37(8-9): 891-902.

AUGENBROE, G., DE WILDE, P., MOON, H. J. and MALKAWI, A. 2004. "An interoperability workbench for design analysis integration." Energy and Buildings 36(8): 737-748.

BEIGHTLER, C. S., PHILLIPS, D. T. and WILDE, D. J. 1979. Foundations of optimization, Prentice Hall.

BOGENSTÄTTER, U. 2000. "Prediction and optimization of life-cycle costs in early design." Building Research & Information 28(5-6): 376-386.

BURRY, M. and MURRAY, Z. 1997. Computer aided architectural design using parametric variation and associative geometry. 15th eCAADe Conference: Challenges of the Future, Vienna, Austria, Österreichischer Kunst- und Kulturverlag.

CALDAS, L. G. and NORFORD, L. K. 2002. "A design optimization tool based on a genetic algorithm." Automation in Construction 11(2): 173-184.

COELLO COELLO, C. A., LAMONT, G. B. and VAN VELDHUISEN, D. A. 2007. Evolutionary algorithms for solving multi-objective problems. New York, Springer.

CRAWLEY, D. B., HAND, J. W., KUMMERT, M. and GRIFFITH, B. T. 2008. "Contrasting the capabilities of building energy performance simulation programs." Building and Environment 43(4): 661-673.

FLAGER, F., WELLE, B., BANSAL, P., SOREMEKUN, G. and HAYMAKER, J. 2009. "Multidisciplinary process integration and design optimization of a classroom building." Information Technology in Construction 14(38): 595-612.

FRAZER, J. 1995. An evolutionary architecture. London, Architectural Association.

GERBER, D. J. 2009. The parametric affect: Computation, innovation and models for design exploration in contemporary architectural practice. Cambridge, MA, Harvard Design School.

GERBER, D. J. and LIN, S.-H. E. 2012a. Designing-in performance through parameterisation, automation, and evolutionary algorithms: 'H.D.S. BEAGLE 1.0'. CAADRIA 2012, Chennai, India.

GERBER, D. J. and LIN, S.-H. E. 2012b. Synthesizing design performance: An evolutionary approach to multidisciplinary design search. ACADIA 2012 - Synthetic Digital Ecologies San Francisco, California, USA.

GERBER, D. J., LIN, S.-H. E., PAN, B. P. and SOLMAZ, A. S. 2012. Design optioneering: Multi-disciplinary design optimization through parameterization, domain integration and automation of a genetic algorithm. SimAUD 2012, Orlando, Florida, USA.

GERO, J. S., D'CRUZ, N. and RADFORD, A. D. 1983. "Energy in context: A multicriteria model for building design." Building and Environment 18(3): 99-107.

HAMDY, M., HASAN, A. and SIREN, K. 2011. "Applying a multi-objective optimization approach for Design of low-emission cost-effective dwellings." Building and Environment 46(1): 109-123.

HENSEN, J. L. M. 2004. Towards more effective use of building performance simulation in design. 2004 DDSS, St.Michielsgestel, The Netherlands.

MENGES, A. 2011. Integrative design computation: Integrating material behaviour and robotic manufacturing processes in computational design for performative wood constructions. ACADIA 2011 - Integration through Computation Banff, Alberta.

PANTELIC, J., RAPHAEL, B. and THAM, K. W. 2012. "A preference driven multi-criteria optimization tool for HVAC design and operation." Energy and Buildings(0).

SIMON, H. A. 1973. "The structure of ill structured problems." Artificial Intelligence 4(3-4): 181-201.

TURRIN, M., VON BUELOW, P. and STOUFFS, R. 2011. "Design explorations of performance driven geometry in architectural design using parametric modeling and genetic algorithms." Advanced Engineering Informatics 25(4): 656-675.

YI, Y. K. and MALKAWI, A. M. 2009. "Optimizing building form for energy performance based on hierarchical geometry relation." Automation in Construction 18(6): 825-833.

From Statistical to Diagrammatic: Geo-spatial and Time-based Data Visualization through Parametric Modeling

Ming Tang[1], Chris Auffrey[2], Mingming Lu[3]

[1]University of Cincinnati
SAID, College of DAAP
Cincinnati, OH. 45221
tangmg@ucmail.uc.edu

[2] University of Cincinnati
SOP, College of DAAP
Cincinnati, OH. 45221
auffrec@ucmail.uc.edu

[3] University of Cincinnati
SEEBME, College of Engineering
Cincinnati, OH. 45221
lumg@ucmail.uc.edu

Keywords: Parametric, Diagrammatic, Geo-spatial, Visualization.

Abstract

The paper describes experiential learning outcomes in the application of geospatial data to generate diagrammatic representations. It also focuses on models and animations used in engineering, architecture and urban planning to visualize specific urban issues such as urban health, education, crime, and air pollution, as they are currently being confronted in major cities such as Cincinnati. The paper discusses how to reconstruct geospatial and time-based data into various representations. It describes the process of visualizing and representing databases with emerging parametric modeling and animation tools. Starting with statistical data, parametric design tools are used to decode and recode the social, cultural, economic and environmental complexity within the parametric equation. Computational tools for architects and urban designers—such as Geographic Information Systems (GIS), Excel, Maya, Rhino and the Grasshopper plugin—are used to build platforms that allow parametric control of the rendered outcome.

1. INTRODUCTION

With the abundance of data visualization technology developed over the last few years, infographic techniques have evolved from simple charts and maps to sophisticated 3D models, animations and interactive media. As for designers, it is crucial to identify the appropriate visualization for the data set by investigating graphical features as well as their roles in the data representation. This paper examines the result of an ongoing collaborative interdisciplinary research project on geospatial data visualization involving faculty and students from School of Architecture and Interior Design (SAID), School of Planning (SOP), and School of Energy, Environmental, Biological and Medical Engineering (SEEBME) at University of Cincinnati.

Several student projects used parametric modeling methods to determine spatial patterns, clusters, networks, hierarchies, as well as the changing typology over time. Yet, the essential goal of this research is not constructing a mathematical model for the original data set, but rather applying a diagrammatic model and translating the complex data set into an abstract form. The geospatial data used, for factors such as air pollution, health, population, housing and employment, are presented through three dimensional and time-based media.

1.1. What is the statistical data visualization?

For architects and urban designers, a design process usually starts with data mining and site analysis. It is essential to collect geospatial information and visualize it in a meaningful way to stimulate design solutions. Although the data format might be different, the essential nature of various geospatial data at this stage is usually expressed as statistical distribution. The statistics, such as mean, median and outliers, need to be computed at the associated geographic unit (e.g. parcel, block, neighborhood, city, etc). Typically two possible distributions are compared by graphing quantities against each other and then studying the generated patterns. This allows viewers to see whether the plot values are similar and if the two distributions are related.

There are a variety of conventional methods for data presentation and infographics techniques, such as tables, histograms, pie charts and bar graphs. However, architects and urban designers are always interested in finding alternative methods to visualize data from a designers'

mindset. There are a growing number of creative design-related methods for visualizing data using the emerging digital tools in the built environment design field. Many of these new data representations are generated by directly feeding the statistical data into the digital design tools.

Figure 1: In order to integrate population density into parametric modeling tools so as to construct an urban model parametrically, the population density is visualized by the height of each block. Created by student Jesse Larkins.

1.2. What is diagrammatic urban model?

Parametric modeling is increasingly implemented in genetic computing to create 3D models with a high degree of complexity, such as the parametric urbanism by Patrick Schumacher, *City Engine* by Pascal Mueller and urban ontology by José Beirão. Beirão described the process of using shape grammar and pattern to study the "topological relations between object classes, object types with specific topologies and attributes to condition their behavior and relationships" (Beirão 2008). Inspired by their theories and research, as well as data-driven urban modeling techniques, a graduate course was developed to utilize a set of visualization principles to generate abstract urban models driven by a variety of datasets. The goal is to represent the statistical information, such as population census data, with new methods, and explore the relationships among urban elements such as crime, pollution and various social parameters. "The geospatial database can provide a rich resource to optimize urban forms with respect to ecological performance criteria. The demographic, traffic and economic data from GIS provides the trace of activity and event parameters of the urban life process" (Tang 2011). In an experimental project based in the Cincinnati area, the population density data is defined as the only rule to control the height of each parcel (Figure 1). Although the generated model does not reflect any real typology in this area due to its singular parameter, it does allow the viewers to observe complex 3D urban patterns that communicate the information clearly. This is similar to how contour lines and digital elevation models (DEM) are used to represent 3D topography. These types of translations deliver meanings by manipulating data across various formats and structures, which allow points, lines, surfaces and masses to be interpreted as the diagrammatic objects. In this modeling approach, an abstract urban model is parametrically constructed by various inputs, which are not normally associated with any urban design vocabulary.

There are two approaches that can be used to visualize urban data within a parametric model. First, 2D maps can be used to generate a 3D diagrammatic model. These thematic maps contain GIS data for zoning, population, transportation, and other spatial information. Parametric tools such as Maya or Grasshopper can read the 2D information embedded in the GIS maps based on the RGBA value of each pixel and apply corresponding modeling operations. The resultant model inherits all the geographical, social, demographic and design information from the GIS maps. Integrating multiple 2D GIS maps allows modeling of changes in data over time. This change can be effectively displayed as a continuously played video clip (Figure 2).

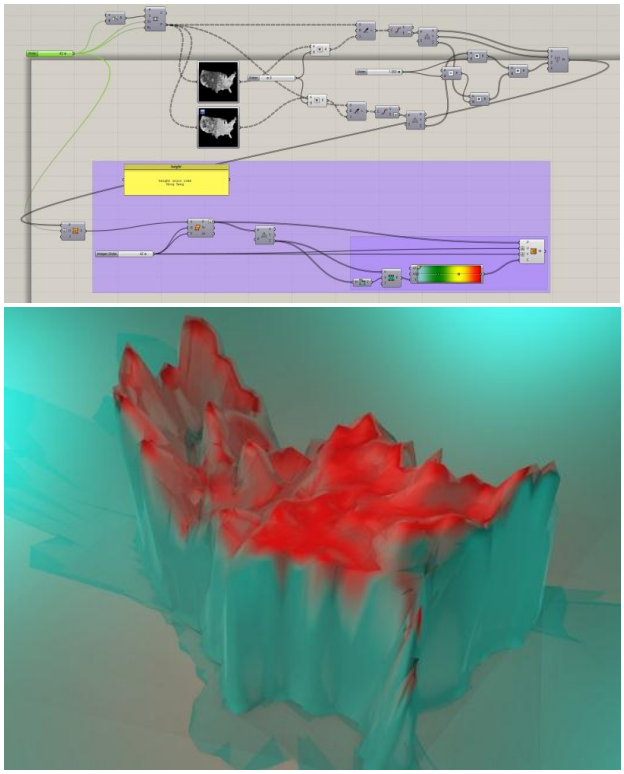

Figure 2: Population change of United States. Animated 3D form. Created by student Kuang Li.

The second approach involves using script to stream an Excel database directly to execute parametric modeling operations automatically and thus replacing more labor-intensive approaches. Designers only need to import the database, observe and evaluate the 3D result, and optimize the result by manipulating a limited number of variables. Because this process only uses text format data, the processing time from an Excel table to animation is easily manipulated back and forth, though it is less intuitive compared with previous mapping approaches (Figure 3).

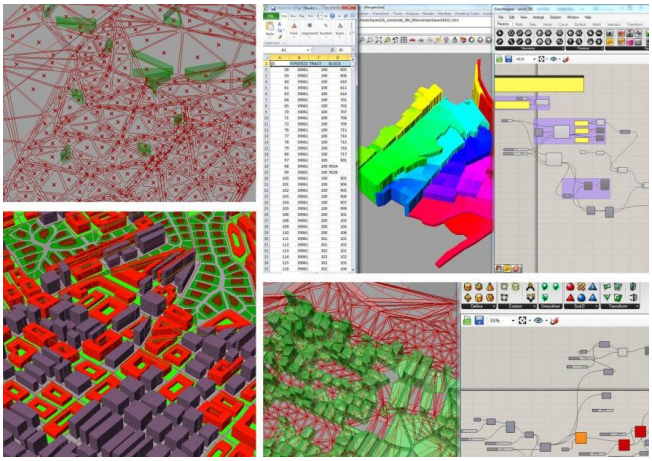

Figure 3: Excel files were streamed into parametric modeling process.

2. THE PARAMETRIC CONNECTION BETWEEN STATISTICAL DATA AND DIAGRAMMATIC URBAN MODEL

One of the objectives of connecting statistical data to a diagrammatic model is to create an engaging experience that allows designers to control the final form in a dynamically changing interface. This permits designers to visualize a large numbers of representation options in a relatively short period of time. As the parametric model is generated very quickly, it is advantageous for the designers to be aware of the following essential categories of visualization.

2.1. From time based data to animated form

The computational method is extended by exploring, collecting, analyzing, and visualizing urban information and interactively representing the information through digital technologies. As mentioned previously, a diagrammatic model allows complex conditions to be represented in a simplified form so that it might be more easily understood and managed. For instance, the designers would be able to read certain correlation patterns over a period of time.

Time-series data is frequently used in data visualization. Index charts and stacked graphs are the conventional ways to illustrate the relative changes over time. However, it is difficult to accurately interpret trends over a complex spatial pattern. An alternative way is to use morphing forms so the overall trends can be more easily interpreted. The 3D animation can become very powerful when it is used to illustrate geospatial data within a defined coordination system. The animated objects can be constructed based on the geographical geometries such as parcels, blocks, counties or states. Animation becomes a natural way to represent the changing data. Time and space can be depicted through the use of lines, shapes, colors and other visual elements. For instance, the animated magnetic field encodes data through the attractors within a geographical region (Figure 4).

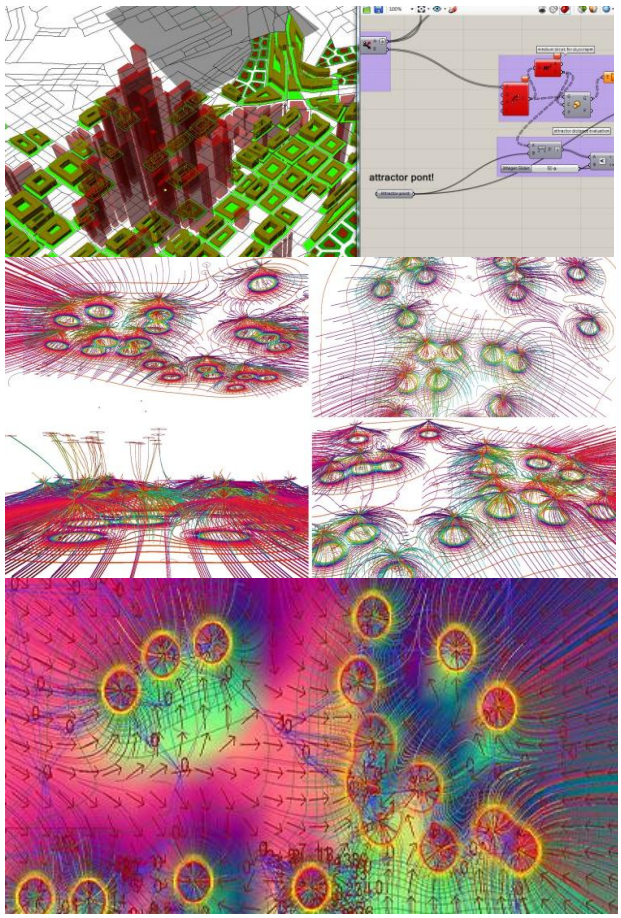

Figure 4: 3D field generated based on census data over time.

Using a variety of data, whether from a map sequence or multi-column Excel database, the resulting animation allows for a larger number of dimensions to be represented.

2.2. Hierarchy and networks

Simple lines with added values can be interpreted into many possible spatial features, such as transportation networks or social connections, depending on their positions in the hierarchy. Geospatial data can be organized into polygon-based or line-based hierarchies. States, counties, tracts, blocks and parcels are common polygon hierarchies for data organization. Streams and transportation networks are common line-based hierarchies. One can also use space-filling variants such as point density to generate new hierarchies. Instead of generating hierarchies based on geographic organization, a large number of spatial nodes can be drawn as a point cloud and grouped based on their adjacency or distance. For instance, a Delaunay mesh grid can be constructed based on a group of points. This new hierarchy can be used to connect points into a web-like network to represent spatial linkage. Each point on the web has a (x,y,z) value, as well as its neighboring nodes' index values. By using color and saturation instead of text, values associated with the links can be perceived visually (Figure 5).

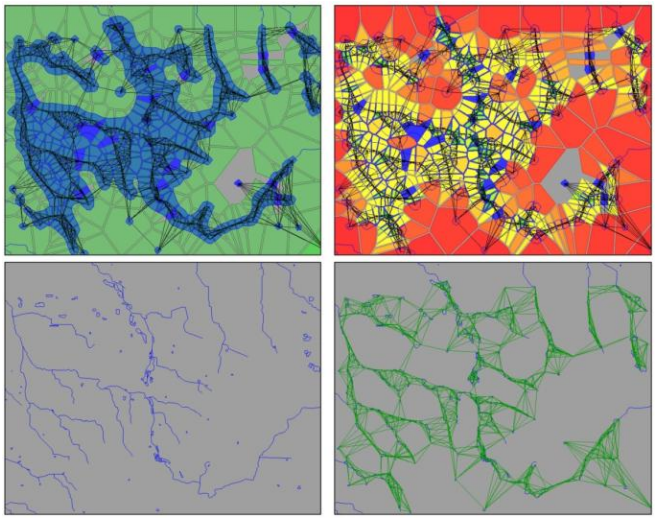

Figure 5: Spatial hierarchies of polygons, lines and points.

3. PROJECTS

Based on a course taught at the University of Cincinnati in 2012, the authors investigated methods for integrating three disciplinary perspectives (Architecture, Planning and Environmental Engineering) within the context of data visualization and analysis. Students used theories, models and methods of modeling and visualization to examine various data representation. The course encouraged students to question the role of parametric design for integrating visualization as a diagrammatic instrument for inspiring hybrid conceptualizations of logical urban forms.

3.1. Project: Gender & education

Students started by collecting data about the educational attainment level by gender within one county based on U.S. Census data. Students were able to use GIS to symbolize the data as a dot density map, with each dot representing five persons. Students then used GIS data of educational attainment level in the dot density map and extracted the center point of each dot into a Rhino program. Students defined point fields based on the clusters of points and extracted centroids from these clusters. Finally, a magnetic field was created in Grasshopper (Figure 6). At each level of education attainment, the magnetic field defined by the points changes from negative to positive. The fields move as the points move from the original educational level to the next education level.

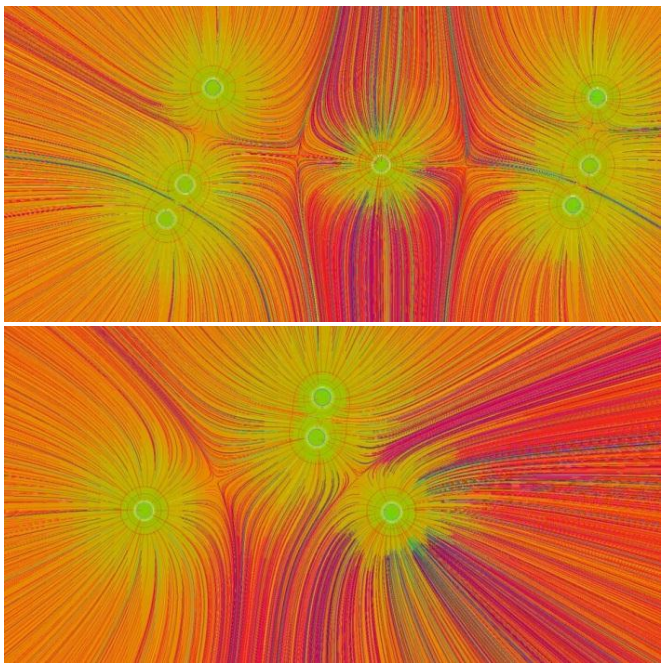

Figure 6: Changing field based on education level. Female, vs. male. Created by student Sarah Kusuma.

Students created two videos: one using data for female educational attainment, and the other using data for male educational attainment. In each video, students animated progressively from no school completed to doctorate degree

using the following increments: nursery school to fourth grade, fifth to sixth grade, seventh to eighth grade, ninth grade, tenth grade, eleventh grade, twelfth grade with no diploma, high school graduate (and equivalency), some colleges with less than one year completed, some college with more than one year but no degree, associate's degree, bachelor's degree, master's degree, and professional degree.

3.2. Project: Urban crime

Students first located point-based crime data for the City of Cincinnati. Data for Hamilton County was downloaded as Excel files for 2007, 2008, and 2009. Excel was then used to compile and format the data for geocoding. Geocoding is the process of assigning each instance of reported crime to a point in space (on a map). This was done through a custom address locator, based on the street grid layer, which matches the street, house number, city and zipcode in the original crime table with a physical, real address existing in Hamilton County. Subsequently, only points occurring within the City of Cincinnati were selected and plotted. This data was used to calculate the incidence (density) of crime by type. Students then performed a basic kernel density analysis, examining and charting statistically significant clusters of the point-based data. To ensure an accurate and unbiased (to the extent possible) analysis of the clusters, the displayed properties of the resulting raster were of utmost importance. The 1/4 standard deviation settings were used, which resulted in 14 classes of clustering, with the first class (0-.00000019) being omitted for graphical clarity. The resulting raster images were exported and brought into Rhino and Grasshopper to construct a 3D morphing surface to represent changes in crime over time and space. This 3D surface was compelling and effectively displays spatial changes in crime over the years. The final result was rendered as several videos (Figure 7).

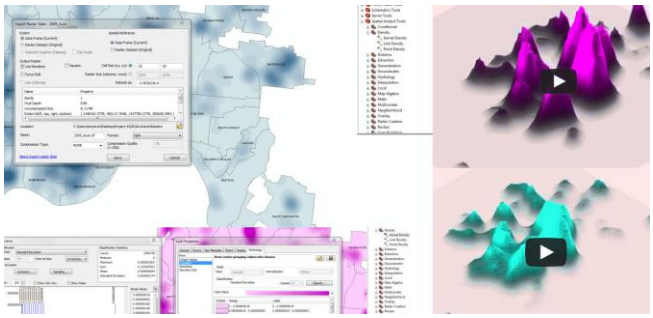

Figure 7: Crime data in Cincinnati, 2002 to 2010. Created by student Craig Moyer.

3.3. Project: Air pollution

In this project, students modeled air pollution in southwest Ohio using data collected from five air quality monitoring stations. The original PM2.5 air pollution data over the past 5 years was formatted as an Excel file. Students geocoded each monitoring station. Then the Excel data was streamed to control five spatial nodes in Rhino. By using one slider, the students manipulated the reading of the Excel file to drive the Z value of these nodes based on daily PM2.5 levels. By combining these spatial nodes, the students created a Grasshopper script to form a 3D surface. The surface became the representation of air pollution across the entire area. The next task was to communicate the PM2.5 daily values by adding a color code to the surface. Students reconstructed another recognizable form for the gradient color script, and created a sequence of stacking contours with darker on the top and lighter at the base. Animated texts were added to highlight values over a one year timeline. In the end, the time parameter was animated to load daily data and compiled as an animation (Figure 8).

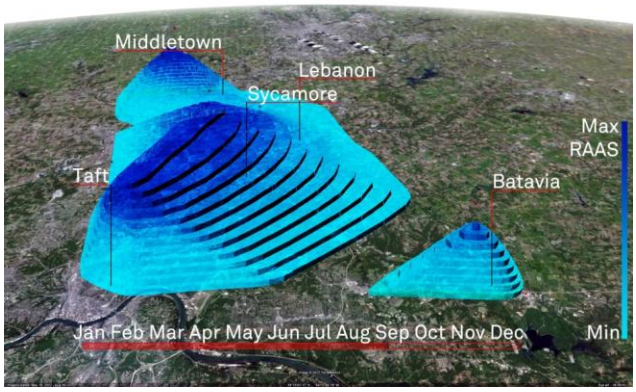

Figure 8: Daily PM5 Particle level in Cincinnati. Animation. Created by student Alexis Payen.

4. CONCLUSION

In all the experiments, social and environmental data from the U.S. Census Bureau were used to develop diagrammatic visualizations based on its geospatial information. The information was streamed and visualized as 3D animations with various shapes and colors to represent the quantifiable values in the database. Customized Grasshopper scripts, as well as advanced modeling tools such as Maya and Rhino, were used to construct 3D diagrammatic models from the parameters. Also, information was extracted with image sampling

processes and then used to drive the animation in the advanced rendering programs. As a result of the continuous transformation and representation, the visualization presented by the database, 2D maps and 3D models empowered each other.

Parametric modeling in the urban visulization field has allowed designers and planners to observe patterns and analyze spatial relationships. The gap between the abstract data and the graphical content is narrowing due to the increasing availability of digital tools for constructing interactive models based on input parameters. “It created an interesting notion to the parametric urbanism practice and further exploited the idea that design practice begins with the information” (Tang 2011). Incorporating variables from urban demographic, social and environmental data into parametric equations allows for a broader range of information to be integrated into 3D and animation formats. This new parametric procedure has worked as an interactive learning tool for assisting students to better visualize and understand complex urban environments and also serves as an efficient way to transfer the collected data into urban patterns and forms.

Acknowledgements

Participating students from the School of Architecture and Interior Design (SAID) at University of Cincinannati were: Alexis Payen, Anjali Patel, Craig Moyer, Dylan Fischer, Jesse Larkins, Kuang Li, Richard Huizenga, Melissa Long, Michael Rogovin, Nabi Hamdi Mortan, Ross Battoclette, Sarah Kusuma.

References

Beirão, José; Duarte, José; Stouffs, Rudi. Structuring a Generative Model for Urban Design: Linking GIS to Shape Grammars. Education and research in Computer Aided Architectural Design in Europe Confrence (Ecaade) 2008

Tang, M. City Generator: GIS Driven Genetic Evolution in Urban Simulation, Proceeding of the 96th ACSA Conference

Tang, M., Anderson, J. Information Urbanism---Parametric urbanism in junction with GIS data processing & fabrication. 2011 Annual Architectural Research Centers Consortium (ARCC) Spring Research Conference. Detroit, MI.

Integrated Design in the Simulation Process

Martha Tsigkari, Angelos Chronis, Sam Conrad Joyce, Adam Davis, Shuai Feng, Francis Aish

Foster + Partners
Riverside, 22 Hester Road,
London, United Kingdom, SW11 4AN
mtsigikar, achronis, sjoyce, addavis, sfeng, faish @fosterandpartners.com

Keywords: Integrated Design, Integrated Practice, Simulation, Fast Feedback, Optimization, Environmental Analysis, FFD, Structural Analysis, View Analysis, Speed-Accuracy Trade-Off, Custom Interfaces, Multidisciplinary Team, Tool Development.

Abstract

During the past decade the construction industry has been witnessing a constant shift in the way it operates. The advances of technology have made possible the adaptation of a more direct, performance-driven design approach based on multi-objective—and sometimes contradicting—criteria of environmental, structural, economic and aesthetic impact. As a consequence, the various teams of consultants involved in the process no longer inform it consecutively, forcing various changes at different stages of the design. Instead, building projects increasingly comprise numerous design issues that can be delegated to small groupings of architects, engineers, and consultants to be resolved simultaneously, in parallel. In the light of this new *status quo,* the significance of new customized simulation tools and interfaces, capable of providing near real-time feedback and driven by multiple input criteria, looms as a potential game changer to the industry. This paper outlines the advances implemented by the authors to support these new integrated workflows.

1. INTRODUCTION

Building design is informed by diverse professions and criteria, most of which are vital in the way buildings perform, are perceived and are experienced. Continuous advances in technology have allowed for digital simulation and verification of processes that until recently were based on manual calculations and rules of thumb. Consequently, contemporary software can accurately calculate the performative impact of various criteria, which enables quantitative and qualitative comparisons.

Although the *idea* of a performance driven design process is straightforward, its actual implementation is rather less so. There are various problems in achieving a seamless design process that can operate under the aforementioned premises. How do all the disciplines come together in an integrated fashion? How can inputs so varying, and in cases contradicting, be presented, be understood and drive the process of design? How can this happen in a timely fashion and, furthermore, in the context of extremely fast design cycles, when most of the aforementioned simulations are so time-consuming that by the time they finish they have become obsolete due to the projects' progression and fast pace? How can the dialogue be facilitated by legibly expressing the trade-off between multiple criteria in increasingly complex design briefs?

This paper attempts to demonstrate how answers to the above questions were sought in the context of a project within an integrated practice. It will analyze the type of multi-disciplinary problems in hand, and how performance-driven design based on multi-objective criteria can be achieved with the aid of fast-feedback tools and interfaces. It will argue for the need for customization and programmatic capability. This is in order to achieve near real-time analysis and simulation, which can accommodate rapid design cycles, by taking into advantage a speed-accuracy trade off. Finally, it will discuss the ways by which Research & Development becomes a facilitator in the process of obtaining, analyzing, quantifying and explaining the impact of different parameters in design, and thus enhancing integration within a multidisciplinary industry.

2. INTEGRATION, SIMULATION AND INTERACTIVE INTERFACES

The challenges designers often face are usually characterized by the following aspects:

- the diversity of the problems in hand, where the multiplicity of the input parameters makes divergence to an optimal solution non-intuitive
- the rapid turnaround of the design cycles that requires fast-feedback analyses, usually not available from off-the-shelf software packages
- the intricacy of interpreting overlaying analytical results, their interaction and how they ultimately affect the design

The above aspects can be overcome within the context of an *integrated practice*, where new tools can be developed in order to provide near-real time analysis and simulation and innovative custom interfaces can assist in the interpretation of the results.

2.1. Context

This performance-driven design process is presented in the development of a residential project in Bangalore, India, undertaken by an international integrated practice (Figure 1). The design brief along with the complex constraints of the site posed a number of different challenges to which the design team had to respond. Specific goals included:

- Increase the potential for natural ventilation
- Maximise daylight to facades and covered public space
- Maximise views of greenery
- Minimise overlooking
- Minimise material usage in structural performance

This diverse set of goals required a multi-disciplinary response to inform design decisions at early conceptual stages. Moreover, space planning constraints and aesthetical considerations were also important drivers that informed the design response.

Figure 1. Artist's Impression of Project

2.2. Design Complexity and the Need for a Multilayered Response

The need for better building performance, as driven by increasingly demanding regulations, is inevitably raising the complexity of the design solutions that are sought by contemporary practices. The cross-disciplinarity of the objectives of an overall optimally performing solution calls for new approaches that exceed the current professional capabilities. The fragmentation of professional responsibilities and the segmentation of the design process are considered to pose significant limitations in achieving these new levels of building performance (Cantin et al 2012). In many cases the analytic approach and the juxtaposition of different technical expertise creates a complex and often conflicting field. The benefits of the integration of building performance simulation tools at early design stages has very often been argued for but still remains a challenge (Attia and De Herde 2011). Despite the continuous effort to tackle this challenge, through the development and incorporation of simulation methods in conceptual stage tools, the complexity of current architectural projects often renders impossible an analytic approach (Hanna et al 2010).

This evolving design complexity, with which the current architect is confronted, requires a higher level of overview of the various aspects of each design problem and as well a better integration of the relevant disciplines in the design process. Arguably the effort to incorporate more '*architectural friendly*' simulation tools, through the development of more efficient interfaces and interoperable

models, greatly facilitates this goal (Attia et al 2009). However, in order to allow the architectural ingenuity to thrive and incorporate intuition back in the equation, current practice requires a more integrated approach.

2.3. Integrated Practice

The definition of an integrated practice is still very much developing, as more practices have adopted this approach as a means to improve the delivery of their projects. However what is common in most examples of such practices is an attempt to reduce the barriers and hurdles for communication between disciplines. This can be literal in terms of having team members of different professions in the same building working on the same design. It can also mean having more inter-disciplinary meetings with communal goal setting and exploration rather than parallel studies and results sharing. This is especially relevant at the conceptual stage where many fundamental but often less well founded decisions are made. Integral, of course, to this model is the commercial alignment of the various disciplines by them being in the same company, with the intended consequence that they are working towards the same goals.

2.4. Simulation as a Decision Maker – Speed Accuracy Trade Off

Simulation is a key tool used by engineers and consultants in order to analyze and interpret the effect that various conditions have not only on a building, but also at the urban scale. Although simulation is very powerful, there are some drawbacks that make it hard to use as a driver on fast design cycles. First of all, many off-the-shelf simulation tools are limited by the amount of time they require in order to run a simulation. Secondly, the results are often difficult to interpret by the non-specialist in the particular domain analyzed. The latter becomes even more prominent when various simulations processed for different criteria are seen in conjunction with each other.

But based on the assumption that modeling and simulation of building physics phenomena entails a certain amount of complexity and uncertainty as it depends on noisy and often conflicting input data (Hong 2000) we could see the potential of a trade-off between speed and accuracy when running simulations to accommodate the need for quick results, especially at the initial stages of the design process. On this premise, results accurate enough can be acquired much faster and drive the scheme by helping the designers make more informed decisions, especially during the initial stages of a project. To accommodate the above considerations, an array of innovative, fast feedback analysis and simulation tools was developed.

3. PERFORMANCE DRIVERS

The authors of this paper are part of an interdisciplinary research and development team within the architectural practice. Their professional backgrounds in architecture, engineering, art and computer science allowed them to both understand and evaluate the inputs provided or required by the different parties within an integrated practice spectrum. On that aspect, they developed tools that helped the engineers and consultants run fast analyses and simulations and present them to all interested parties in a way that could become drivers in the scheme design process.

3.1. Fast Fluid Dynamics

The assessment of the wind conditions in an urban scale using computational fluid dynamics (CFD) simulations is traditionally time consuming; thus their application is mostly restricted to the final stages of the design process. CFD simulations have yet to fully meet the expectations of designers despite the development of novel methods and the constant increase in computational resources (Chen 2009). This complexity of the physics involved largely justifies this resource cost, but in many cases it is argued that a compromise in accuracy might be required to inform design decisions at early stages. In CFD literature it is generally suggested that the accuracy of the CFD simulation needs to be leveled against the turnaround time requirements of its application and the level of detail needed by the task at hand (Lomax et al 2001).

To overcome the time requirements of standard CFD packages in order for them to meet the design cycle timeframes, the authors have incorporated a less accurate but much faster CFD solver. The FFD (Fast Fluid Dynamics) solver is based on a less accurate numerical solver, introduced by Stam (1999) to the computer graphics industry. Despite its numerical dissipation, the solver's accuracy has been assessed as adequate for certain cases (Zuo and Chen 2010) and has been already used in a number of studies (Chronis et al 2011, Chronis et al 2012). Its turnaround time far exceeds typical CFD applications, therefore allowing for quick feedback of design iterations.

The FFD solver was used to simulate the airflow around the massing for the two prevailing wind directions in 3D. The simulation and interface tools were custom developed to allow for quick interoperability with the design platform used. In conjunction with the speed of the FFD solver, this could enable a CFD study for every new cycle of the design process. The simple interface that was developed allowed the design team to directly interact with the results, thus giving them a better understanding of the effect of the different design options on wind flow.

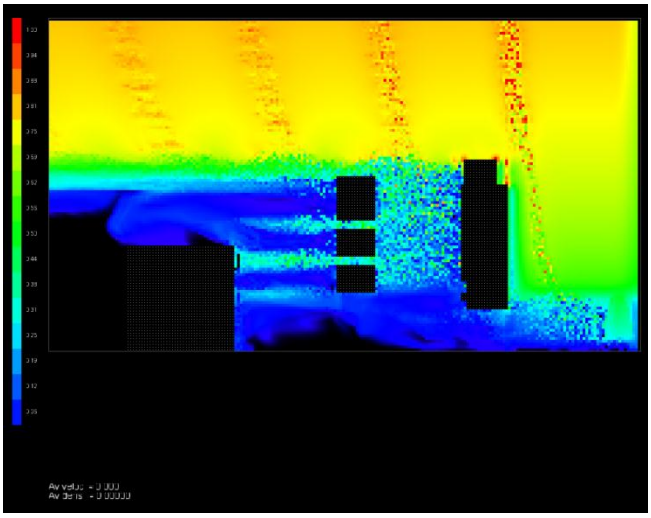

Figure 2. CFD Analysis viewed via a customized interface

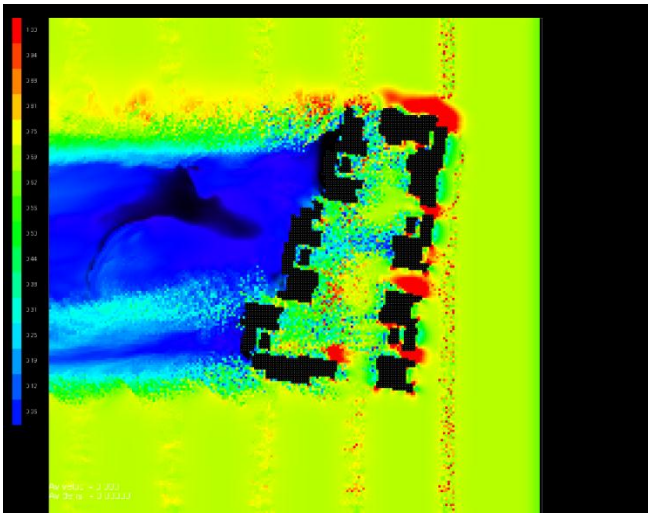

Figure 3. CFD Analysis viewed via a customized interface

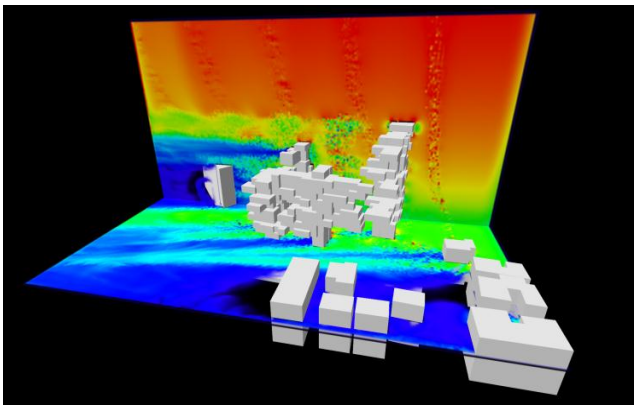

Figure 4. CFD Analysis viewed via a customized interface

3.2. Solar and Daylight Analysis

It has been argued that more precise solar design tools actually help to broaden the range of architectural form (Otis 2011). But research has shown that while there is a growing number of practitioners who dedicate a significant amount of time to daylighting, most have but a couple of days per project to spend on this topic. Their reasons for not using simulations were mostly linked to time and budget constraint (Galasiu and Reinhart 2008). Furthermore, the time needed to run many existing environmental software tools is increased due to poor interoperability, which requires timely file conversions to adequate formats for analysis. Based on this aspect, a need was identified for a new and powerful tool that can provide accurate and fast solar and daylight analysis within the software platform used in-house.

This new near-real-time solar and daylight analysis software (called RadIO for Radiance I-O) was developed using the Radiance ray trace engine (Ward and Shakespeare 1998; Mardaljevic 1995), as was Diva before it (Lagios et al. 2010). The GenCumulativeSky method (Robinson and Stone 2004) was also used. RadIO is capable of calculating seasonal radiation maps, daylight factor and vertical sky component (Chronis et al 2012). Furthermore, a set of extra capabilities were exposed in a user-friendly manner, such as the calculation of sunlight hours relative to different local codes. This tool offers tremendous performance gains, as it is orders of magnitude faster than other commercial software (Chronis et al 2012).

Using the RadIO tool, many massing options could be run natively in the office design platform (Microstation), and very quickly provide comparative feedback. It proved very powerful in comparing completely different options

and ranking them against each other. It demonstrated that the more complex massings were performing better than simpler ones, a fact that was somewhat counter-intuitive and hard to prove otherwise (Figures 5, 6).

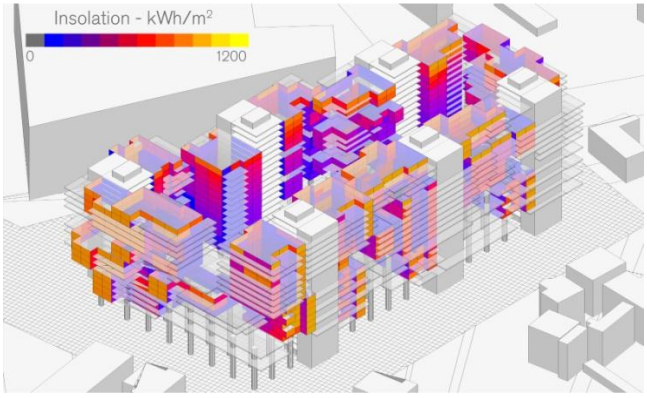

Figure 5. Insolation Analysis run inside Microstation via RadIO

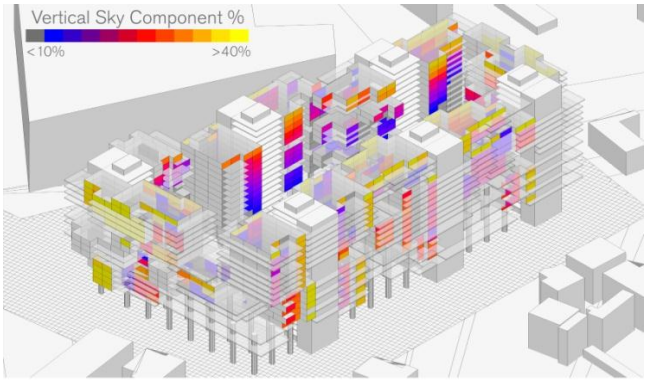

Figure 6. VSC Analysis run inside Microstation via RadIO

3.3. Reflection and Soffit Analysis

In certain situations analytical processes come to bridge the disconnection between conceptual ideas and their realization within the specific site and economic constraints. Within an integrated design process, not only engineering and optimization aspects can be integrated into decision making, but moreover key improvements on the design concept can be implemented through comprehensive parametric strategies.

Under that spectrum, and progressing from the general daylight potential analysis, the next challenge was the development of a soffit that would emerge into a tree-like pattern, recalling the memory of the local forest while providing extra performances such as shading, reflective lighting and even evaporative cooling. The design task was initially incarnated into a conceptual drawing, from which the soffit of the building would generatively emerge in a standarized and performative manner. The general idea incorporated the use of a finite number of standardized reflective tiles that can create a tree pattern on the soffit, with the columns as their notional trunks.

For the development of the parametric analytical tool, the emphasis was on reflectivity of the pattern, as well as buildability and standardization of the components, promoting economy in material and construction costs. That was a response to the architects' expectation of a trade-off between an aesthetically driven pattern generation process, and affordability of locally available traditional handcraft techniques.

The analytical approach of the tool can be understood both in the pattern input selection (which is then tessellated based on standard components) as well as its diffuse light capability performance. On the one hand, it leaves enough flexibility in terms of pattern inputs. Research undertaken, together with the architects, delivered a selection pool of appropriate local tree canopy patterns which represent the appeal delivered through the architectural conceptual drawings. On the other hand, the patterns' arrangement study has progressed alongside to provide valid light reflection paths in relation to the locations of the 'reflectors' that have been housed underneath the soffit, such as highly reflective ground tiles and water ponds.

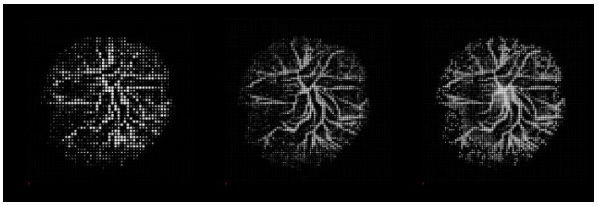

Figure 7. Parametrically Generated Soffit Patterns

Eventually, a process of pixelation was introduced to rationalize the complexity of the pattern selected (Figure 7). During this process, the study of the light reflection paths was taken into consideration, providing differentiated distributed densities of the mirror components in order to facilitate a better reflected lighting environment underneath the soffit. Throughout the rationalization process, the feedback from the architects was taken into account. This is demonstrated in the flexibility left for the properties of the mirror components, such as their sizes, shapes, thicknesses, numbers of types of gradient transitions, and positive or

negative physical attributes. Visualization of one of the options can be seen in Figure 8.

Figure 8. Suggested customised standard tiling of reflective soffit

3.4. Structural Analysis

When looking to engineer a design that is influenced by the many interacting factors as outlined above, it was thought that a flexible method of generating the structural arrangement that provided meaningful feedback was required. It was important not simply to produce structural analysis, but actually to go beyond this to give an indication of the effective sizes of columns and the placement of shear walls to allow the team to access impactful feedback on the structural scheme. The goal being, that based on the initial configuration an approximate but working structural scheme could be returned for appraisal alongside the other design considerations.

The task was divided into two optimization problems working at different resolutions. The first problem was the configuration of the cross-bracing, and the second the sizing of the members. The building being a basic framed grid with supporting shear wall bracing able to be placed anywhere in that grid, it presented a high number of possible bays to brace and thus an even higher number of possible combinations of walls. For this reason, a genetic algorithm approach was applied similar to that outlined in Evins, Joyce et al (2012). The coding genome of the design was a binary on/off of the cross bracing in the planar slice of the structure considered—essentially a 2D grid. The objective function to be optimized was linked to the output of the second optimization problem. For the second optimization a method was applied similar to that outlined in Joyce, Fisher et al (2011) where members were sized relative to their stresses in an iterative fashion. This method provided a figure for the weight of the material required for the cross-bracing configuration considered by the first optimization to not structurally fail. This tonnage could then be passed back to the objective function of the first optimization and combined with terms to penalize overuse of cross-bracing, which it was decided was disadvantageous to the overall design. The first optimization, then, after a number of generations produced optimized configurations of cross-bracing, still retaining the thickened structural elements from the second optimization. The output was presented for fast appraisal as a simple compression and tension diagram with the elements having exaggerated thickness to show the variation in thickness (Figure 9). This enabled designers to interpret the result quickly, especially the means of spanning and placement of thickened members which were the primary designed part of the structure. Using this approach, comparisons both quantitative (material volume) and qualitative (aesthetic) could be made between the different amounts of cross-bracing used.

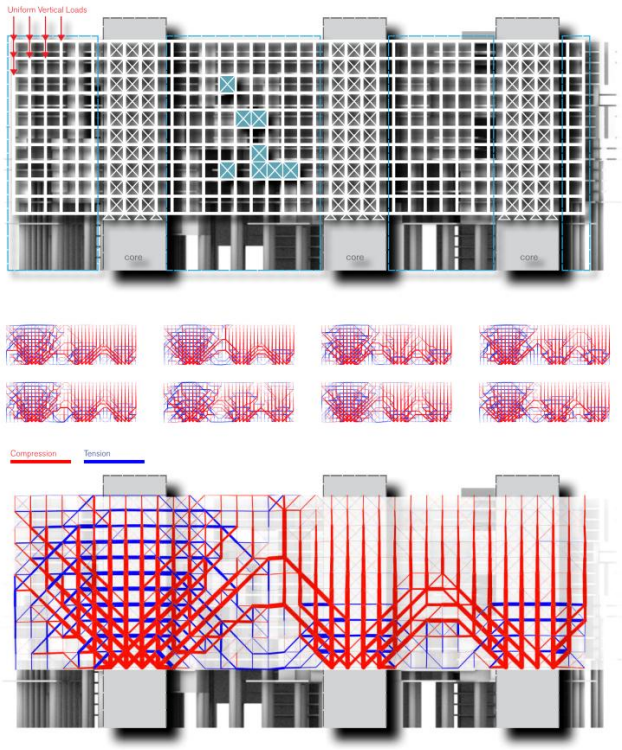

Figure 9. Structural Optimization through Evolution: An example of a optimized planar structure section for given boundary conditions

3.5. View Analysis

As the scale of an architectural project increases, so does the complexity of the issues that have a bearing on the visual apprehension and appreciation of the environment. Designers need to consider the effects of different schemes with regard to such criteria as views of varying depths, the effect of obstruction— and conversely, framing—of views of interest, and the visibility of 'natural' landscape elements (water, vegetation) if possible.

There is scant literature to establish any of these issues in such a way as to make them amenable to computational analysis based on objective criteria. Some of the authors of this paper are currently engaged in research seeking to establish perceptual bases for judgments about the visual environment. A first step in this is simply measuring the visibility of subjects of interest (landscape, landmarks) and disinterest (nearby windows, where privacy may be a concern). Secondly, it is possible using image analysis techniques to understand something of the composition of a view: how segmented is the view of a landmark or of rolling hills in the distance? Given the orientation of a window, is a point of interest centered or oblique in the field of view?

In the context of the residential scheme that is the subject of this paper, it was important to assess the availability of views of green space and vegetation—surrounding landscape, courtyard garden, and vegetated elements of facades within the scheme. Scenes were rendered from the facade of each apartment. Features of interest were extracted from these scenes and measured for the amount of area they occupied proportional to the total field of view. This metric of prevalence in the visual field is proposed to be a suitable reflection of view quality at least insofar as it reflects potential availability of features of interest in the scene. In the same way that the vertical sky component measures potential daylight for a given facade area, this metric of view quality represents availability of interesting scene features on a facade. (Figure 10). Views from within architectural space have considerable qualitative importance, yet objective quantitative metrics can also be established that allow for design iterations to be analysed and optimised numerically, much like the other types of analysis discussed in this paper.

Figure 10. Quality of View Analysis for the Bangalore scheme

4. CONCLUSION

The implication that we find might pertain to our work in building design and analysis can be summed up—perhaps ironically—by the decades-old mantras of UNIX system programmers:

- Write programs that do one thing and do it well
- Write programs to work together

Our experience suggests that 'doing it well' means producing results rapidly, to the level of precision appropriate to the stage of design. Large-scale, monolithic applications still have their place when evaluating a relatively static proposal over the course of days or weeks, but early-stage design requires agility on the part of decision-makers and the analysis tools available to them.

We find that composing modular tools that work in this fashion improves the ability of our software and our designers and analysts to work together. This allows not only for standard user-initiated analysis workflows, but also for computer-controlled routines such as optimization loops between different types of analysis. It also allows for assessment to be conducted regularly, as it is easy to evaluate the simulation data at any stage in the design and analysis process, rather than waiting for many batches or iterations to run before any judgement can be made.

Acknowledgements

We would like to thank our colleagues in the design and engineering teams with whom we collaborated on thids case study project.

References

ATTIA, S. AND DE HERDE, A. 2011. Early design simulation tools for net zero energy buildings: a comparison of ten tools, International Building Performance Simulation Association, November 2011, Sydney, Australia.

ATTIA, S., BELTRÁN L., DE HERDE, A, HENSEN, J. AND DE HERDE A. 2009. "Architect Friendly": a comparison of ten different building performance simulation tools, International Building Performance Simulation Association, July 2009, Glasgow, UK.

CANTIN, R., KINDINIS, A. AND MICHEL, P. 2012. New approaches for overcoming the complexity of future buildings impacted by new energy constraints, Futures, Volume 44, Issue 8, October 2012, Pages 735-745.

CHITTKA, L., SKORUPSKI, P. AND RAINE N.E. 2009. Speed–accuracy tradeoffs in animal decision making. In Trends in Ecology & Evolution, vol. 24 (7): 400-407.

CHRONIS, A., TURNER, A. AND TSIGKARI, M. 2011. Generative Fluid Dynamics: Integration of Fast Fluid Dynamics and Genetic Algorithms for wind loading optimization of a free form surface. Proceedings of the Symposium on Simulation for Architecture and Urban Design at the 2011 Spring Simulation Multiconference, Boston, USA.

CHRONIS, A., TSIGKARI, M., DAVIS A. AND AISH, F. 2012. Design Systems, Ecology + Time. Proceedings of ACADIA at the 2012 ACADIA Conference, San Francisco, USA.

EVINS R, JOYCE S, POINTER P, SHARMA S, VAIDYANATHAN R, WILLIAMS C, 2012. Multi-objective design Optimization: getting more for less Proceedings of the ICE - Civil Engineering, Volume 165, Issue 5, 01 May 2012 , pages5 –10

GALASIU A. AND C. REINHART. 2008. Current Daylighting Design Practice: A Survey. In Building Research and Information, Vol. 36 (2), 159-174. London: Routledge

HANNA, S., HESSELGREN, L., GONZALEZ, V. AND VARGAS, I. 2010. Beyond Simulation: Designing for Uncertainty and Robust Solutions. Proceedings of the Symposium on Simulation for Architecture and Urban Design at the 2010 Spring Simulation Multiconference, Orlando, USA.

HONG, T., CHOU, S.K. AND BONG T.Y. 2000. Building simulation: an overview of developments and information sources. In Building and Environment, vol 35 (4): 347-361.

JOYCE S, FISHER A, WILLIAMS C, SHARMA S. 2011. Towards Ubiquitous Structural Frame Design Tools, IASS IABSE Conference 2011, London, UK.

LOMAX, H., PULLIAM, T. H., ZINGG, D. W., PULLIAM, T. H. AND D. W. ZING. 2001. Fundamentals of computational fluid dynamics. Berlin: Springer.

LAGIOS, K., NIEMASZ, J. AND REINHART, C.F. 2010. Animated Building Performance Simulation (ABPS) - Linking Rhinoceros/Grasshopper with Radiance/Daysim. Proceedings of SimBuild 2010. New York.

OTIS T. 2011. Solar design a straightjacket for architecture? Proceedings of PLEA Conference 2011. Boston: Passive and Low Energy Architecture.

MALKAWI, A.M. 2004. Developments in environmental performance simulation. Automation in Construction 13(4). Pages 437-445.

MARDALJEVIC, J. 1995. Validation of a Lighting Simulation Program under Real Sky Conditions. In Lighting Research & Technology, vol 27(4): 181-188.

ROBINSON, D. AND A. STONE. 2004. Irradiation modeling made simple: The cumulative sky approach and its applications. Proceedings of PLEA Conference 2004: 1-5. Eindhoven: Passive and Low Energy Architecture.

STAM 1999. Stable fluids in Proceedings of the 26th annual conference on Computer graphics and interactive techniques, August 1999, Los Angeles, USA, 121-128.

ZUO, W. AND CHEN, Q. Y. 2007. Validation of fast fluid dynamics for room airflow, Proceedings of the 10th international IBPSA conference Building Simulation 2007, September 2007, Beijing, China.

WARD, G. AND R. SHAKESPEARE. 1998. Rendering with RADIANCE, The Art and Science of Lighting Visualization. San Francisco: Morgan Kaufmann Publishers.

Session VI

Building Simulation Weather Forecast Files For Predictive Control Strategies 163
José. A. Candanedo, Éric Paradis, Meli Stylianou
CanmetENERGY, Canada

How Hot Can the University Campus Get in 2050? Environmental Simulation of Climate Change Scenarios at an Urban Neighborhood Scale 169
Chengzhi Peng, Amr F Elwan
University of Sheffield, UK

Building Simulation Weather Forecast Files For Predictive Control Strategies

José. A. Candanedo[1], Éric Paradis[2] and Meli Stylianou[3]

[1]CanmetENERGY-Varennes, NRCan
1615 Lionel Boulet Blvd
Varennes, Québec, Canada, J3X 1S6
jose.candanedo@nrcan.gc.ca

[2]CanmetENERGY-Varennes, NRCan
1615 Lionel Boulet Blvd
Varennes, Québec, Canada, J3X 1S6
eric.paradis@nrcan.gc.ca

[2]CanmetENERGY-Ottawa, NRCan
1 Haanel Drive - Building 5A,
Ottawa, Ontario, Canada, K1A 1M1
meli.stylianou@nrcan.gc.ca

Keywords: Predictive Control, Weather Forecast, EPW Files, Building Simulation.

Abstract

Model-Based Predictive Control (MPC) has received significant attention in recent years as a tool for load management in buildings. MPC is based on predicting the response of a system based on knowledge of future inputs, such as weather and occupancy. Despite the availability of online weather forecasts, there is a lack of software tools enabling the use of weather forecast information in building modelling. This paper describes a "proof of concept" approach to the creation of EnergyPlus Weather (EPW) files containing weather forecast information. These EPW files, updated at periodic intervals, also contain up-to-date recorded measurements, thus permitting initial conditions to be established by applying "warm up" simulations. The combination of recorded data and expected weather allows the use of these files in predictive control. This approach can be readily reproduced for different weather file formats and other locations.

1. INTRODUCTION

The main objective of this paper is to present and describe a procedure to create EPW files (the weather files used by the EnergyPlus simulation software) that include both measured and forecast weather data. This procedure is intended as a proof of concept for the incorporation of weather forecasts for model predictive control in buildings. Model Predictive Control (MPC) is the generic name given to a group of control techniques that use a model of a system and a forecast of disturbances (i.e., non-manipulated input variables) to choose a set of actions to optimize system performance (Camacho and Bordons 2004). The application of predictive controls to buildings has received significant attention in recent years (Gyalistras and OptiControl Team 2010; Ma et al. 2010). In buildings, the non-manipulated variables are the weather and internal load forecasts; this information is thus essential in the implementation of MPC. This paper focuses on the weather forecast aspect.

Although the idea of using weather information in building controls is several decades old, the lack of tools facilitating the integration of weather forecasts into building modelling and/or building automation systems has been one of the obstacles to the deployment of MPC in buildings. Different strategies have been put in place to overcome this limitation. For example, a strategy that has been investigated is the use of Markovian stochastic chains with transition probability matrices based on recent measurements (Scartezzini 1986; Scartezzini et al. 1987). This methodology had the advantage of implicitly dealing with prediction uncertainty. Another approach is the introduction of weather data obtained from public bulletins. For example, models for predicting exterior temperature and solar irradiance based on qualitative weather forecasts available in local newspapers were developed in the early 1990s, assigning weights to "shape factors" based on historical records, current temperature trends and the weather forecast (Chen and Athienitis 1996). More recently, different "homemade" forecast models were developed and compared (Florita and Henze 2009). These forecasts were mainly data-driven (as opposed to being based on physical models of weather), and relied on on-site measurements and the subsequent determination of trends. In recent years, the OptiControl project has undertaken a serious effort towards integrating weather forecasts in advanced control strategies, in a collaborative project linking control engineers, building experts and modelling experts (Stauch et al. 2010). Despite these advances, there is still a lack of standardized tools

enabling the use of weather forecasts to predict the response of a building and its systems.

The procedure described in this paper originated as part of a project on MPC carried out at our institution. While a significant part of the project focused on the development of optimal control algorithms using simplified building models, a rule-based MPC scheme was also considered. In this scheme, an EnergyPlus model of the building is used to determine the required cooling load for the next day with EPW files including weather forecasts. These files, created automatically at periodic intervals, incorporate recorded data *and* forecast data. The resulting cooling load estimation can then be used to manage an ice-storage system and avoid the higher electricity costs associated with running the chiller during the day. The EPW weather file can be used: (a) To run "warm-up" simulations to reproduce the current conditions of the building (i.e., the initial conditions); (b) to calculate the cooling load over the next 24 hours, since this information is required for the rule-based approach.

2. OVERVIEW OF EPW FILES

A thorough description of the EPW files can be found in the EnergyPlus documentation, and will therefore not be provided here (DOE 2010). However, a brief overview of the EPW format helps to illustrate its use and the challenges encountered when creating these files from different data sources.

An EPW file has 34 columns (35, if a column with text indicating the data source is included). Each file has 8,760 rows, corresponding to each hour of the year. The data is preceded by 8 header lines presenting: location, design conditions, typical extreme periods, ground temperatures, holidays and daylight saving times, two lines of comments, and data periods.

Essential variables in an EPW file (i.e., those required in EnergyPlus calculations) are shown in Table 1. Other variables in an EPW file, such as "days since last snowfall" or "liquid precipitation depth", have mainly an informative purpose.

Table 1: EPW Weather Variables.

Col. #	Variable	Col. #	Variable
2-5	Month, day, hour, min	15	Diffuse horizontal radiation
6	Dry bulb temperature	20	Wind direction
7	Dew point temperature	21	Wind speed
8	Relative humidity	23	Opaque sky cover
9	Atm. Pressure	26	Present weather observation
12	Horizontal infrared radiation	27	Present weather codes
14	Direct normal radiation	33	Liquid precipitation depth

3. METHODOLOGY

Building simulation files for predictive control should include both historical measurements and forecast information. The main difficulties in creating these files consist of: combining different data sources (on-site measurements, publicly accessible records, and online meteorological services); having different file formats covering different time periods; and having different time resolutions and time-stamps. Finding all the information required by building simulation weather files can be quite challenging: for instance, temperature or humidity values are more easily found than variables like snow depth or global horizontal illuminance. Finally, information gaps attributable to software glitches, hardware malfunction or instrumentation faults are common in weather data.

However, the abovementioned issues can be satisfactorily addressed. First, since the variables in a weather file are not equally important for a building simulation, some "default" or "placeholder" values may be used without major detrimental consequences. Interpolation can be used to address the problem of different time resolution. Some values may be used to find good approximations of others. For instance, global horizontal radiation can be used to estimate diffuse and direct solar radiation (Duffie and Beckman 2006).

The EPW file will include "past" data (records from the previous year), "present" data (recent measurements) and "future" (forecast), as shown in Figure 1. The information from the different data sources slightly overlaps near the current time.

The procedure described in Sections 3.1 through 3.3 corresponds to the particular requirements and information for our project, and is presented here to illustrate the general approach. The procedure to be followed in any location will depend on the available information and the objectives. The building is located in the vicinity of Montréal (Canada).

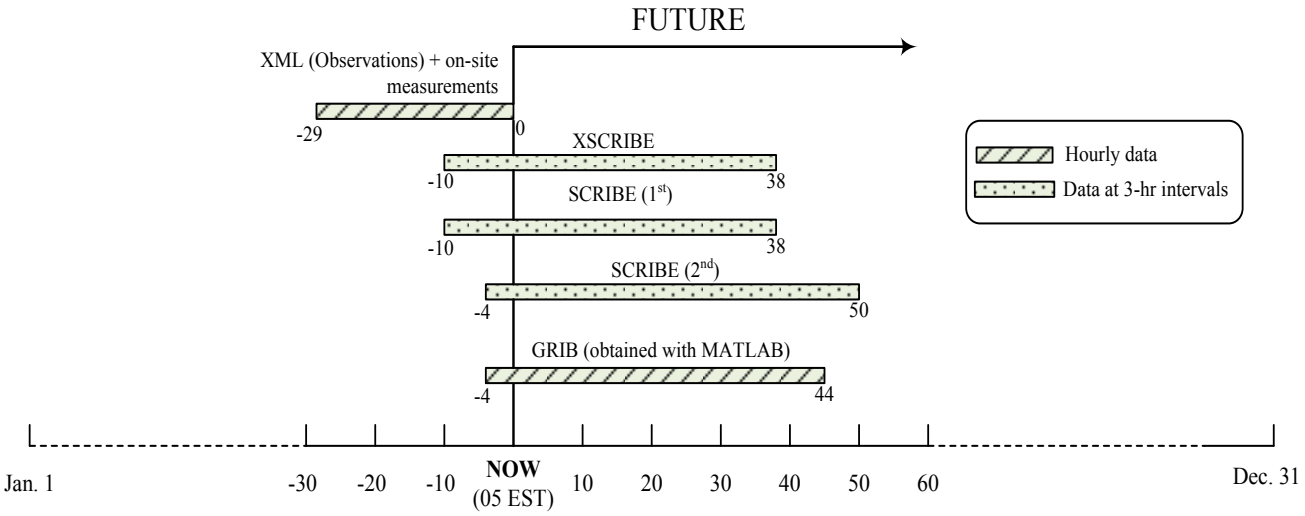

Figure 1. Time span covered by each of the weather files.

3.1. EPW file template and previous year data

Every day at about 17:15 (local time), an EPW file with historical measurements is received by email. This file, created by the Laboratoire des Technologies de l'Énergie (LTE) a research agency of the local electric utility (Hydro-Québec) in the context of their development of the SIMEB simulation software (Millette et al. 2011), corresponds to hourly measurements of weather variables, at the station nearest to the building site, for the entire previous year. For example, if an EPW file is received at 17:00 on June 27th, 2011, the information it contains corresponds to the measurements taken from the first hour of June 26th, 2010 to the last hour of June 26th, 2011.

Although historical records are also available (Environment Canada 2011c), the information received from the LTE is already in the EPW file structure, which serves as a substrate for the rest of the information. Forecast values can then be replaced in the appropriate columns. The time stamp in the EPW files corresponds to the local time (Eastern Standard Time, EST, for this particular case). EPW files contain cumulative values for each hour (e.g., Wh/m^2 rather than average W/m^2). Therefore, data lines are enumerated from 1 to 8760, where the first line corresponds to mean values obtained from 0:00 to 1:00, the second line to values between 1:00 and 2:00, and so forth.

3.2. Recent measurements

As the first priority, measurements collected at the building site—particularly those corresponding to temperature and solar radiation—can also be included at this point. For most of the other weather variables, the most recent weather measurements are obtained in XML format from Environment Canada's "observations" files (Environment Canada 2011b). They correspond to the 29 hours before the current time. A script written in Java is then used to add this information to the EPW files received from LTE. Care is taken to ensure that data is inserted into the right line according to timestamps.

Finally, in case data is still missing, SCRIBE files which contain data from recent forecasts, not measurements, can be used (more details on SCRIBE files are provided in the next section). In summary, in descending order of priority, recent records are based on on-site measurements, XML observations, and "few-hours-old" SCRIBE forecasts.

3.3. Forecast information

3.3.1. SCRIBE and XSCRIBE matrices

SCRIBE is a tabular format developed to facilitate the production of forecast bulletins. SCRIBE matrices are only available for a limited number of locations. SCRIBE

matrices contain some of the most relevant variables for building simulation, such as dry bulb temperature, relative humidity and wind speed (Environment Canada 2011d). In a SCRIBE matrix, the character "I" is used as the delimiter between columns. The data in a SCRIBE matrix is listed at 3-hour intervals (Figure 2). SCRIBE matrices are used to fill out the forecast information corresponding to most variables (wind speed, cloud cover, etc.) in the EPW file at 3 hour intervals.

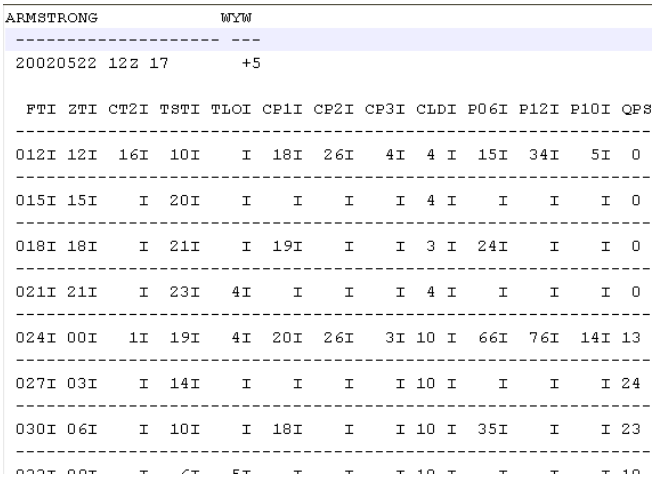

```
ARMSTRONG             WYW
--------------------- ---
20020522 12Z 17        +5

 FTI ZTI CT2I TSTI TLOI CP1I CP2I CP3I CLDI P06I P12I P10I QPS
-------------------------------------------------------------
012I 12I  16I  10I    I  18I  26I   4I  4 I  15I  34I   5I  0
-------------------------------------------------------------
015I 15I    I  20I    I    I    I    I  4 I    I    I    I  0
-------------------------------------------------------------
018I 18I    I  21I    I  19I    I    I  3 I  24I    I    I  0
-------------------------------------------------------------
021I 21I    I  23I   4I    I    I    I  4 I    I    I    I  0
-------------------------------------------------------------
024I 00I   1I  19I   4I  20I  26I   3I 10 I  66I  76I  14I 13
-------------------------------------------------------------
027I 03I    I  14I    I    I    I    I 10 I    I    I    I 24
-------------------------------------------------------------
030I 06I    I  10I    I  18I    I    I 10 I  35I    I    I 23
-------------------------------------------------------------
```

Figure 2. SCRIBE matrix format.

Two kinds of SCRIBE matrices, containing different information, are available: regular (SCRIBE) and supplementary (called XSCRIBE), which include solar radiation data. In Figure 1, the labels "1st" and "2nd" refer to the times when the SCRIBE files are issued.

The time stamp of SCRIBE matrices corresponds to Coordinated Universal Time (UTC) (approximately equivalent to Greenwich Mean Time). For example, the line designated as 015 actually corresponds to 10:00 a.m. for EST. During the daylight saving time period (EDT), local time is one hour ahead (EDT = EST+1).

SCRIBE matrices can display the output of global or regional weather models (i.e., simulations at a planetary or regional scale), or ensemble forecasts (the result of statistically combining several weather models). A description of the meaning of the fields in SCRIBE matrices can be found in (Environment Canada 2011d). SCRIBE matrices are posted online every 6 hours with a 48-hour prediction horizon (Environment Canada 2011a).

Attention has been paid to ensuring agreement between units and data format. For example, the SCRIBE matrix lists "dew point depression" (DPD) instead of dew point temperature. The following correction was applied:

$$T_{\text{dew point}} = T_{\text{dry bulb}} - \text{DPD} \tag{1}$$

Given that the data from SCRIBE files is available at 3-hour time steps, a linear interpolation is applied to calculate intermediate values. While the main purpose is to make the data usable in the EPW file, the application of more sophisticated interpolation techniques (probably taking into account other factors) is worth considering.

3.3.2. GRIB files

The most relevant data for calculating the cooling load—namely global horizontal radiation, dry bulb temperature and relative humidity—is obtained from a GRIB file released by Environment Canada, at hourly intervals for a 48-hour time horizon. GRIB files are binary files containing output information of weather models in a relatively "raw" format, which is not easily accessible. A MATLAB program was used to access the information contained in the GRIB files and create a CSV (comma-separated values) table.

The direct and diffuse horizontal radiation components, corresponding to columns 14 and 15 of the EPW file, can be calculated with the global horizontal radiation (I_{gh}) from the GRIB file. The correlation by Erbs et al (Erbs et al. 1982) is then used to calculate the diffuse fraction of the global horizontal radiation (I_d/I_{gh}) as a function of the hourly clearness index k_T:

$$\frac{I_d}{I_{gh}} = \begin{cases} 1.0 - 0.09k_T & \text{, if } 0 \le k_T \le 0.35 \\ 0.9511 - 0.1604k_T + 4.488k_T^2 & \\ \quad -16.638k_T^3 + 12.336k_T^4 & \text{, if } 0.35 < k_T \le 0.75 \\ 0.165 & \text{, if } k_T > 0.75 \end{cases} \tag{2}$$

When the information corresponding to historical records, recent measurements and forecasts is integrated, the EPW is ready to be used in simulations. The procedure followed in the creation of the EPW files is summarized in Figure 3.

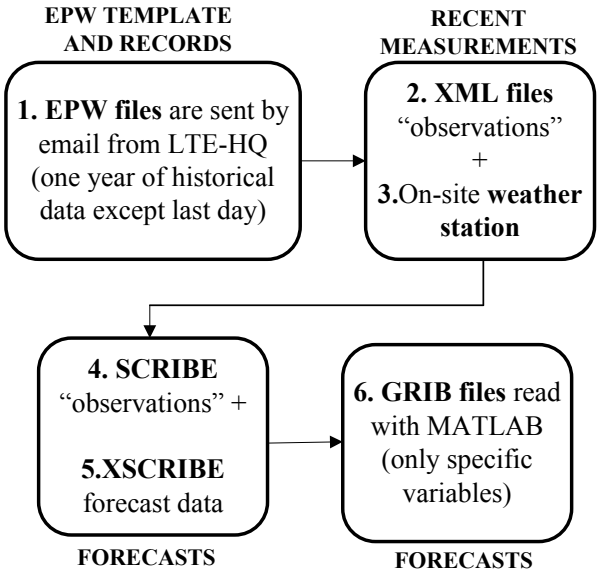

Figure 3. Summary of the procedure for the creation of EPW files with forecast information.

4. DISCUSSION AND CONCLUSIONS

This paper has discussed a proof-of-concept procedure for the creation of building simulation weather files (EPW files) that include both historical records and weather forecast information so that they can be used in the study of predictive control strategies. The procedure presented here illustrates the variety of problems one might encounter when creating these files. This paper does not attempt to provide a general methodology; instead, its purpose is to show the potential pitfalls when creating weather files for building simulation, and discuss strategies to overcome these pitfalls.

This paper has emphasized the importance of combining recorded measurements with forecast information, so that appropriate initial conditions are used. This is an essential requirement in predictive control.

As expected, when creating the weather files it is important to "match" the different time-stamps in order to insert the data into the right lines. This is no easy task, as attention must be paid to the time when forecasts are released, the time zone used in the time stamps (GMT or EST) and the time intervals. Information is often fragmentary in weather forecasts: a key issue has been how to proceed when information is missing. The solutions proposed in this article are not the only possible ones, but they are sufficient to make the file work for its intended purpose. It is also essential to identify which weather variables have the most significant impact on building performance. Creating weather files, in summary, requires a thorough understanding of the format of weather files used in building simulation tools, some knowledge of numerical weather simulation and solar radiation modelling, and a dose of common sense to find practical strategies to deal with incomplete information.

This project has covered the creation of EPW files for a set of particular conditions. Future extensions include applying a similar procedure to other weather file formats (e.g., TMY2 files) and for other locations. The development of an automatic, flexible and user-friendly software tool for the generation of forecast files for control studies with building simulation tools remains an interesting project. Moreover, more research is needed for the validation of the generated weather files.

Acknowledgements

The advice of our colleague Sophie Pelland is gratefully appreciated. We would like to thank Simon Sansregret from Hydro-Québec's LTE, as well as Miguel Tremblay and Lewis Poulin from Environment Canada. We thank Danielle Monfet, Jacques Martel and Vahid Raissi-Dehkordi for their valuable comments. This work has been funded by the Clean Energy Fund of the Office of Energy Research and Development (OERD) of Natural Resources Canada.

References

CAMACHO, E., and BORDONS, C. 2004. Model Predictive Control. London, UK: Springer.

CHEN, T.Y., and ATHIENITIS, A.K. 1996. Ambient temperature and solar radiation prediction for predictive control of HVAC systems and a methodology for optimal building heating dynamic operation. ASHRAE Transactions, 102(1), 26-35.

DOE. 2010. Weather Converter Program. In Auxiliary EnergyPlus Programs (EnergyPlus Documentation). 45-54.

DUFFIE, J.A., and BECKMAN, W.A. 2006. Solar Engineering of Thermal Processes. Hoboken, New Jersey: John Wiley & Sons.

ENVIRONMENT CANADA. 2011a. Index of /model_gem_regional/matrices/land_regions (Regional SCRIBE Matrices). http://dd.weatheroffice.ec.gc.ca/model_gem_regional/matrices/land_regions/. Retrieved on October 2011.

ENVIRONMENT CANADA. 2011b. Index of /observations/xml/QC/hourly (recent hourly data in XML format).

http://dd.weatheroffice.gc.ca/observations/xml/QC/hourly/. Retrieved on October 2011.

ENVIRONMENT CANADA. 2011c. National Climate Data and Information Archive. http://climate.weatheroffice.gc.ca/climateData/canada_e.html . Retrieved on September 2011.

ENVIRONMENT CANADA. 2011d. SCRIBE Definition. http://collaboration.cmc.ec.gc.ca/cmc/cmoi/product_guide/product-pages/alpha_glb_scrib_scribe-documentation_gen_e.html. Retrieved on September 2011.

ERBS, D.G., KLEIN, S.A., and DUFFIE, J.A. 1982. Estimation of the diffuse radiation fraction for hourly, daily and monthly-average global radiation. Solar Energy, 28(4), 293-302.

FLORITA, A.R., and HENZE, G.P. 2009. Comparison of Short-Term Weather Forecasting Models for Model Predictive Control. HVAC & R Research, 15(5), 835-853.

GYALISTRAS, D., and OPTICONTROL TEAM. 2010. Final Report: Use of Weather and Occupancy Forecasts for Optimal Building Climate Control (OptiControl). In Zürich, Switzerland: ETH Zürich.

MA, Y., BORRELLI, F., HENCEY, B., COFFEY, B., BENGEA, S., and HAVES, P. 2010. Model predictive control for the operation of building cooling systems. In 2010 American Control Conference. Baltimore, Maryland, USA.

MILLETTE, J., SANSREGRET, S., and DAOUD, A. 2011. SIMEB: Simplified interface to DOE2 and EnergyPlus -a user's perspective- case study of an existing building. In Building Simulation 2011 (12th Conference of IBPSA). Sydney, Australia.

SCARTEZZINI, J.-L. 1986. Application des Méthodes Stochastiques à l'Étude des Systèmes de Captage de l'Énergie Solaire. Ph.D. Thesis, École Polytechnique Féderale de Lausanne.

SCARTEZZINI, J.-L., FAIST, A., and LIEBLING, T. 1987. Using Markovian stochastic modelling to predict energy performances and thermal comfort of passive solar systems. Energy & Buildings, 10(2), 135-150.

STAUCH, V., HUG, C., SCHUBIGER, F., and STEINER, P. 2010. Weather Forecasts, Observations and Algorithms for Building Simulation and Predictive Control. In Zürich: MeteoSwiss.

APPENDIX

In Equation (2), the hourly clearness index k_T is calculated by dividing the global horizontal radiation I_{gh} by the extraterrestrial horizontal radiation (H_o). The latter value is obtained by calculating first the beam extraterrestrial radiation I_{on} (i.e., solar radiation above the atmosphere) and then multiplying by the sinus of the solar altitude angle α_s:

$$I_{on} = I_{sc}\left(1 + 0.033\cos\left(\frac{2\pi n}{365}\right)\right) \quad (3)$$

$$H_o = I_{on}\sin\alpha_s \quad (4)$$

where I_{sc} is the solar constant (1361 W/m^2) and n is the number of days from the beginning of the year.

The solar altitude angle (α_s) is calculated by following the method described in (Duffie and Beckman 2006). First, the equation of time (ET) is used to calculate the difference between the local standard time (LST) and the apparent solar time (AST). Four minutes are also included to account for the difference between the local standard meridian (LSM, the meridian used as a reference for the time zone) and the geographical longitude of the location (LON). Again, following (Duffie and Beckman 2006):

$$\mathrm{ET} = 9.87\sin\left(4\pi\frac{n-81}{364}\right) - 7.53\cos\left(2\pi\frac{n-81}{364}\right) - 1.5\sin\left(2\pi\frac{n-81}{364}\right) \quad [\mathrm{min}] \quad (5)$$

$$\mathrm{AST} = \mathrm{LST} + \mathrm{ET}\,[\mathrm{min}] + \left(4\frac{\mathrm{min}}{\mathrm{deg}}\right)(\mathrm{LSM} - \mathrm{LON}) \quad (6)$$

The hour angle accounts for the time past since solar noon:

$$h = \left(15\frac{\mathrm{deg}}{\mathrm{hr}}\right)(\mathrm{AST} - 12) \quad (7)$$

The declination angle (δ) corresponds to the seasonal changes in the sun's trajectory. This angle, (zero at both equinoxes), is approximately given by:

$$\delta = 23.45°\sin\left(2\pi\frac{284+n}{365}\right) \quad (8)$$

Finally, the solar altitude angle α_s is given by:

$$\alpha_s = \arcsin\begin{pmatrix}\cos(\mathrm{LAT})\cos(\delta)\cos(h)\\ +\sin(\mathrm{LAT})\sin(\delta)\end{pmatrix} \quad (9)$$

How Hot Can the University Campus Get in 2050? Environmental Simulation of Climate Change Scenarios at an Urban Neighborhood Scale

Chengzhi Peng and Amr F Elwan
University of Sheffield, School of Architecture, Sheffield, UK

University of Sheffield,
School of Architecture,
Arts Tower, Western Bank,
Sheffield S10 2TN, UK
{c.peng;a.elwan}@sheffield.ac.uk

Keywords: Environmental Simulation, ENVI-met, Ecotect, CCWorldWeatherGen, Climate Change Conscious Urban Neighborhood Design, 3D Virtual Neighborhood.

Abstract

Based on the results from simulating a case study neighborhood design to be built in New Cairo, Egypt, a conceptual framework and an environmental simulation workflow towards Climate Change Conscious Urban Neighborhood Design (C3UND) is proposed. Coupling neighborhood outdoor and building indoor simulations, the C3UND workflow is further applied to a neighborhood site at the Sheffield University campus in England with weather data representing the 2010s and 2050s. We describe how the ENVI-met platform can be applied to contextualize Ecotect building simulations, taking into account the present day as well as future simulated urban micro-climatic conditions. This study suggests that environmental simulation of climate change scenarios at an urban neighborhood scale is currently achievable but not without considerable gaps. The lessons learned and areas for further research are discussed.

1. INTRODUCTION

Urban dwelling in hot-arid or hot-humid climates has a greater need to inhabit the space between outdoor and indoor environments (Ali-Toudert et al. 2005; Chalfoun 2003; Fahmy and Sharples 2009). This state of interconnectedness needs to be considered in sustainable design such that the dwellers are enabled to gain optimal environmental comfort while minimizing energy consumption in cooling, heating, ventilation, lighting, etc. However, the developments and applications of environmental simulation software have been rooted mainly in how city dwelling is understood in temperate climatic zones. Hence, software-based urban outdoor and building indoor environmental simulations have always been performed independently of each other. Using Autodesk® Ecotect® Analysis (Ecotect in short thereof) as a standalone simulation package, for instance, most college students are now able to simulate detailed environmental performance of a building. The main variant in Ecotect simulation of two contemporary city buildings—say, one in Cairo, Egypt, and the other in Sheffield, UK—is the weather data files loaded. Given that very little is known about how Ecotect actually deals with the urban conditions of Cairo vs. Sheffield, one would query the accuracy of such simulations. In a recent study reported by Vangimalla and co-workers on their validation of Ecotect accuracy for thermal and daylighting simulations through field measurements, Ecotect has been found to consistently underestimate the building's thermal load (Vangimalla et al. 2011). If the level of accuracy of simulation for present day weather is called into question, it is less likely that one will continue simulating building performance under future climate change scenarios to inform current decision-making. Therefore, we are particularly interested in investigating if it makes any difference conducting building performance simulation within an urban neighborhood context that takes into account simulated local urban micro-climatic conditions. ENVI-met was chosen for this investigation. Developed by Michael Bruse and team at the University of Mainz, ENVI-met is one of the first computational models to simulate the

main processes in the atmosphere affecting micro-climates using computational fluid dynamics and thermodynamics. The latest release ENVI-met 3.1 has been extended to model an even wider range of thermal interactions in built environments (Bruse et al. 2011). The results from our study are presented as follows: (1) A case study of an urban neighborhood design proposed for a site in New Cairo, Egypt, under present day and future climate change scenarios; (2) A conceptual framework and simulation workflow towards *Climate Change Conscious Urban Neighborhood Design* (C3UND); (3) Applying the C3UND approach to an existing campus neighborhood at the University of Sheffield, England; and (4) The lessons learned from the two urban neighborhood climate change simulations and the areas identified for further investigation.

2. CASE STUDY OF A NEIGHBORHOOD DESIGN IN NEW CAIRO, EGYPT

Starting with an exploratory case study, we first looked at a small part of a new town development scheme proposed by DAMAC Properties for a site in the city of New Cairo, Egypt (Figure 1).

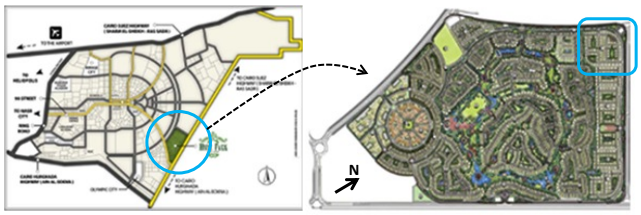

Figure 1. Master plan of New Cairo – the blue box indicates the scope of the case study neighborhood (Original drawings courtesy of DAMAC Properties, 2009).

This particular residential neighborhood compound was designed to provide around 120 housing units. The main purpose of the case study was to experiment with an approach to environmental simulation that takes into account (a) urban dwelling in a city located in hot-arid climates such as Cairo where outdoor and indoor living is much more interconnected; and (b) the climate change scenarios as understood and projected by today's meteorological experts. The experiment was expected to give us a direct view into the current software capabilities of environmental simulation of an urban neighborhood design that includes both the outdoor spaces of the neighborhood and the interiors of the buildings located within the neighborhood. Our simulation of the New Cairo neighborhood design case study took the following steps as summarized below.

2.1. Single building unit Ecotect simulation

Ecotect 2011 was used to model one of the building units based on the CAD drawings and the basic constructional and operational specifications outlined in Table 1. The default weather data provided within the Ecotect package (Cairo, present day) was first used. We believe this data originated from the weather station at the Cairo International Airport, about 30km west to the neighborhood site. The thermal comfort (mean radian temperature) outputs for the two building unit floors indicate a temperature range of 29ºC to 41ºC (Figure 2).

Parameter	Constructional and Operational Specs
Total area	540m^2
No. of floors	2 floors
Ext. walls	0.25m brick 20mm plaster inside and outside
Int. walls	0.25m brick 20mm plaster inside and outside
Floor height	3.2m
Orientation	North to south
Roofing	20 tiles 20 mortar 50 sand 150mm concrete
Glazing	6mm single glass
Zoning	Multiple thermal zones
Lighting	12w/m^2
Occupancy	2 families with average 5 persons per family

Table 1: The basic constructional and operational specifications of the building unit of Type A with a larger total floor area.

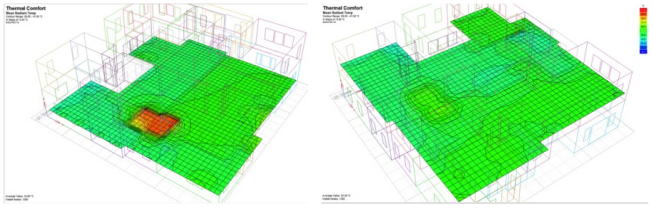

Figure 2. Ecotect Thermal Comfort output from the building unit simulation of present day Cairo International Airport weather data (Left: Ground Floor; Right: First Floor).

2.2. Neighborhood micro-climate ENVI-met simulation

By setting up the Configuration and the Area Input files (Figure 3.a) according to the ENVI-met input requirements (ENVI-met 2011), we obtained a large volume of outputs from the neighborhood simulation which can be further extracted and visualized in the LEONARDO module included in ENVI-met 3.1. Figure 4 shows an assembly of four such visualized outputs.

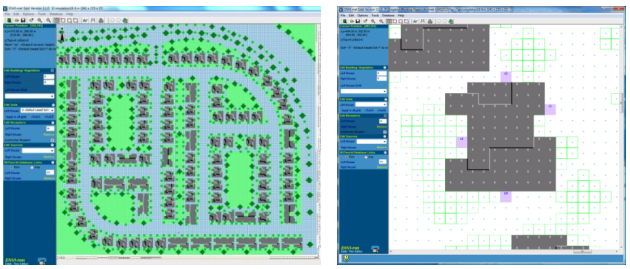

Figure 3. Constructing the Area Input file in ENVI-met's graphic editor: (a, left) The entire neighborhood; (b, right) The four instances of ENVI-met *Receptor* placed around the building unit selected for Ecotect analyses.

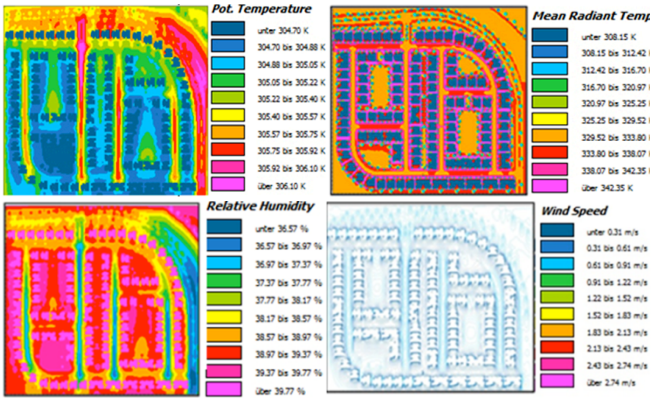

Figure 4. ENVI-met outputs rendered in LEONARDO from case study simulation of present day Cairo International Airport weather data.

2.3. Contextualized building unit simulation

In ENVI-met, the "Receptor" construct can be initiated to produce simulated urban micro-climatic conditions specific to any locations of the described input area (i.e., the entire neighborhood, in our case study). We find that by placing instances of Receptor around a specific building (Figure 3.b), localized weather data files can be generated specific to that building's immediate urban surroundings. We then loaded the ENVI-met simulated weather data to repeat the Ecotect building unit simulations. Our results

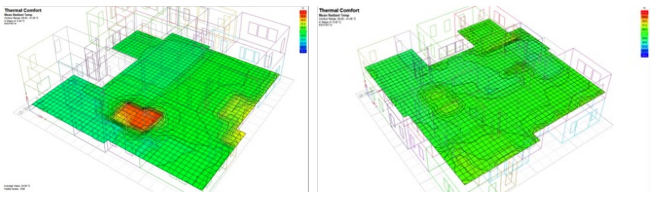

Figure 5. Ecotect Thermal Comfort output from the building unit simulation of present-day with ENVI-met simulated weather data (Left: Ground Floor; Right: First Floor).

show that there is +0.29ºC on the Ground Floor and +0.57ºC on the First Floor when the weather data generated with ENVI-met receptors is loaded (Figure 5).

2.4. Generating future weather data files

To perform simulation of climate change scenarios, we used the CCWorldWeatherGen tool provided by the UK Climate Impacts Programme (UKCIP). Central to the design of CCWorldWeatherGen is the 'morphing' methodology for climate change transformation of TRY/DSY weather files (Belcher et al. 2005). By selecting from four UKCIP02 climate change scenarios related to greenhouse gas emissions (Low, Medium-Low, Medium-High, High Emissions), users can generate weather data files projected for the 2020s, 2050s, 2080s, and so on. In our case study, we used the ENVI-met simulated neighborhood weather data as input to CCWorldWeatherGen (High Emissions) in generating weather data for the 2050s and 2080s.

2.5. The neighborhood under climate change scenarios

The New Cairo neighborhood design case study was concluded with an assembly of the outputs from the ENVI-met and Ecotect coupled simulations over the timeframes of Present Day, 2050s and 2080s (Figure 6 and Figure 7).

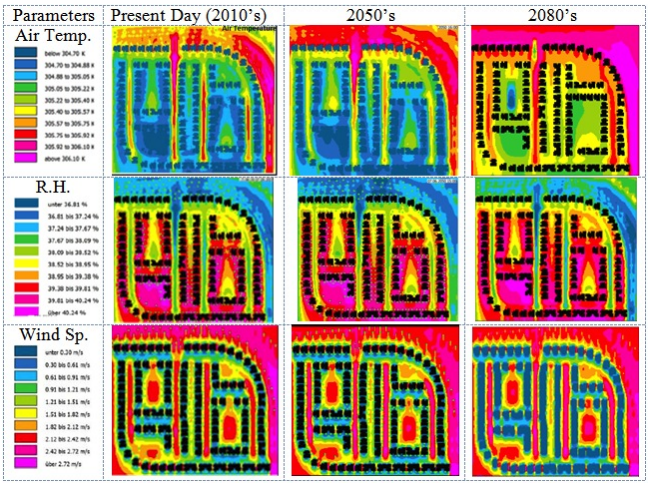

Figure 6. An aggregate of ENVI-met outputs rendered as LEONARDO maps (on the hottest day of the year, for 2010, 2050, and 2080). Top to bottom: Air Temperature, Relative Humidity, Wind Speed.

3. C3UND: A PROPOSED ENVIRONMENTAL SIMULATION FRAMEOWRK

The New Cairo case study shows that it is feasible to conduct climate change simulation at an urban neighborhood scale with the software tools and weather datasets currently available. We consider it essential to be

able to perform such simulation at the two interconnected levels of Neighborhood and Building such that it reflects the pattern of urban dwelling in the space between outdoors and indoors. Assuming the validity of current combined software capabilities, the differences as predicted by the present day and future climate change simulations could provide highly valuable information to guide sustainable neighborhood design and climate change adaptation. To conceptualize, we proposed an environmental simulation framework for climate change conscious urban neighborhood design (C3UND) (Figure 8).

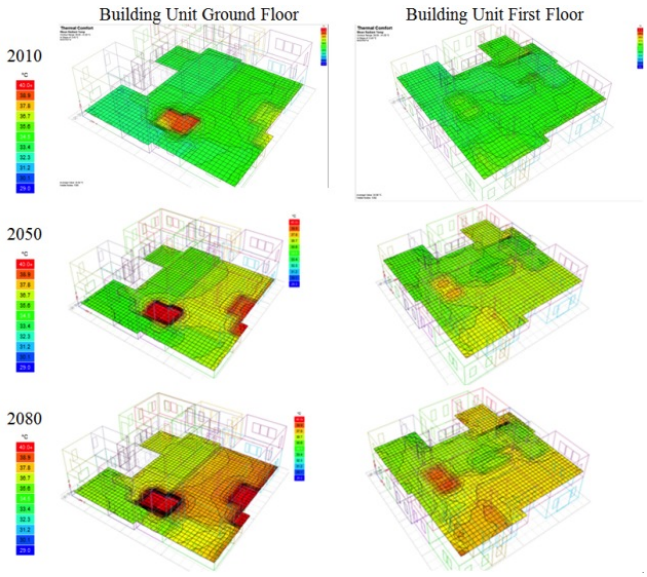

Figure 7. An aggregate of Ecotect simulations of the building unit's indoor air temperatures (hottest day of the year, for 2010, 2050 and 2080) all based on the ENVI-met simulated neighborhood weather data files. Temperature range: 29.0ºC – 40.0+ºC in steps of 0.4ºC.

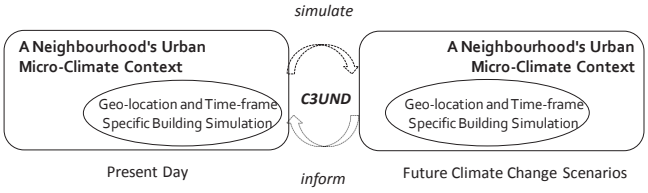

Figure 8. A proposed environmental simulation framework for climate change conscious urban neighborhood design (C3UND).

Working through the case study, we also identified the set of software tools with which we were able to build up a digital simulation workflow (Figure 9). Although there are gaps in the current dataflow which require substantial manual-based data editing, the objective of C3UND can be broadly achieved via an iterative application of the workflow to the weather data of present day and of projected future climate change scenarios. Future versions of the outdoor-indoor coupled environmental simulation workflow could be replaced with other software packages such as DesignBuilder (DBS 2012), and VE-Pro (IES 2012). Well-developed alternatives to ENVI-met are yet to be found.

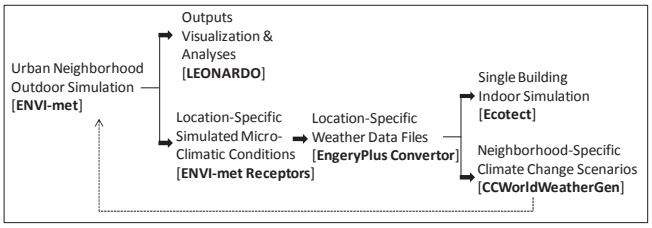

Figure 9. A workflow to implement C3UND with existing software tools: ENVI-met, LEONARDO, EnergyPlus Convertor, Ecotect and CCWorldWeatherGen.

4. APPLYING C3UND TO A SHEFFIELD UNIVERSITY CAMPUS NEIGHBORHOOD

Following the New Cairo case study, we further applied the C3UND framework and workflow to a different climatic zone by simulating a Sheffield University campus site in northern England. This larger simulation of present day (2010s) and 2050s was carried out in the Spring semester of 2012 while working with a group of 16 postgraduate students at the Sheffield School of Architecture. Prior to this simulation experiment, a 3D virtual campus model, developed previously through the weCAMP-uCampus project (Peng 2011), was introduced to define a campus neighborhood for the urban micro-climate ENVI-met simulation. Four large university buildings within the neighborhood were selected for Ecotect analyses. Due to limited space, only two building simulations are reported below.

4.1. ENVI-met simulation of the campus neighborhood

A smaller special task group was formed to generate the input required for ENVI-met simulation, including the Configuration and Area Input files. Figure 10 shows the campus neighborhood site drawn in ENVI-met's graphic editor. The area input model specifies the buildings' 2D outlines and heights, vegetation species, soil types, and placement of receptors around the buildings selected for Ecotect analyses to be performed later by the student groups (see Figures 12.b and 14.b).

The weather data collected from the Finningley weather station, being nearest to the site about 30 miles north east, was used to set up the configuration file required by ENVI-

met. It took about 20 hours for an average PC workstation to complete the simulation with the present day (2012) weather data. Using the "Climate Change Weather File Generator for UK Weather Data" tool (CCWeatherGen V1.1.2), the 2050 weather data was generated from the Finningley dataset (again, in High Emissions) to run another ENVI-met simulation with the same area input model. We then compiled a visual comparison of the 2010s and 2050s ENVI-met outputs (Figure 11). The neighborhood results were then used in the Ecotect building simulations.

Figure 10. The campus neighborhood site and four university buildings selected for climate change simulation (an area of 150m X 100m, 1: Arts & Humanities Building, 2: Music Department; 3: Social Sciences Faculty; 4: Computer Science Department).

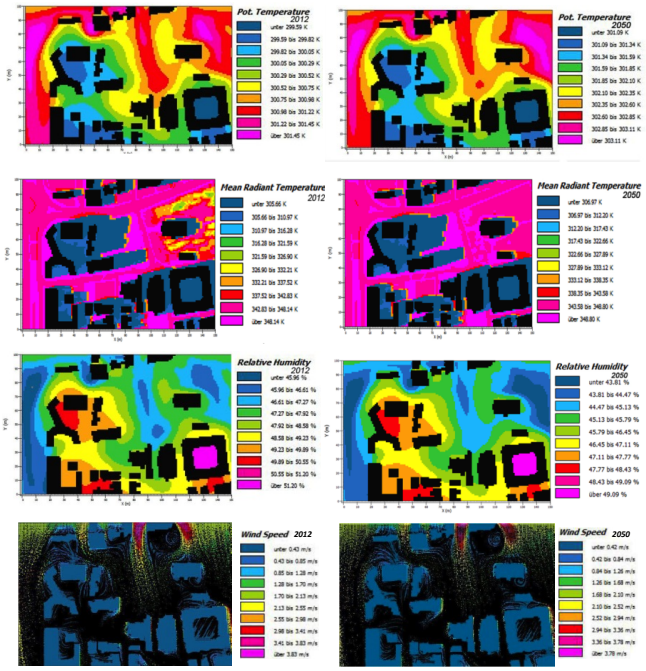

Figure 11. A visual comparison of the ENVI-met outputs of the campus neighborhood simulation for 6th July, the hottest day of the year (Left column: 2012; Right column: 2050. Top to Bottom: Air Temperature, Mean Radian Temperature, Relative Humidity, Wind Speed).

4.2. Ecotect analyses of the Social Sciences Building

Based on the principle of passive solar design, the Social Sciences Faculty Building (opened in November 2004) is naturally ventilated with a high thermal mass and fully glazed north- and south-facing façades (Figure 12.a). During the ENVI-met neighborhood simulation stage, in order to generate localized weather data for running Ecotect building simulations, a set of seven receptors was placed around the building envelope (Figure 12.b). For conducting Ecotect simulations of the building, four sets of weather data files were prepared: Finningley 2012, ENVI-met simulated 2012, Finningley 2050 (generated by CCWeatherGen), and ENVI-met simulated 2050 (with reference to Finningley 2050 in setting up the ENVI-met configuration file).

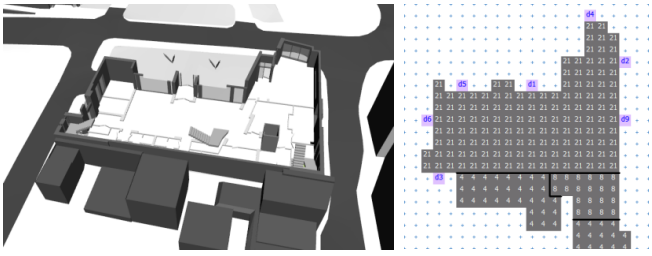

Figure 12. (a) A view of the X3D model of the Social Sciences Faculty Building on uCampus; (b) Placement of 7 receptors around the building when setting up the ENVI-met area input model.

Figure 13 shows the Ecotect Thermal Comfort analyses of the Social Sciences Building under the four different weather data scenarios. In terms of average air temperature, the simulation shows about +0.1°C [Finningley 2012, ENVI-met simulated 2012]; +1.7°C [Finningley 2012, Finningly (CCWeatherGen) 2050]; and +1.6°C [ENVI-met simulated 2012, ENVI-met simulated 2050].

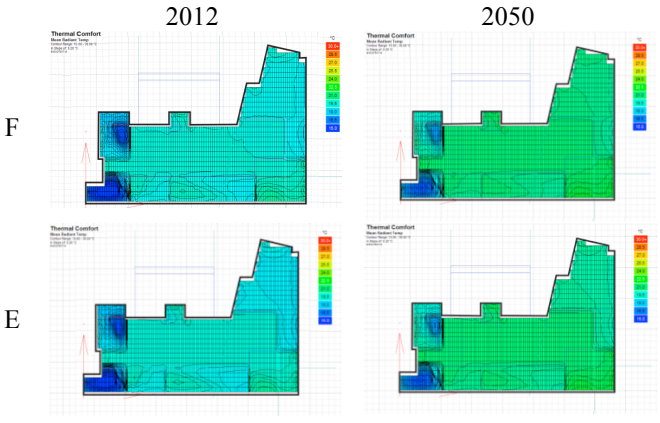

Figure 13. Ecotect thermal comfort analyses of the Social Sciences Faculty Building under four weather data scenarios (F: Finningley weather station; E: ENVI-met simulated).

4.3. Ecotect analyses of the Computer Science Building

Opened in 1993, the Computer Science Building has a large square central courtyard. It is a 5-storey structure with a basement car park and is surrounded by similar high buildings on 3 sides along the enclosing streets (Figure 14.a). The building receives a limited amount of direct solar radiation on all facades all year round due to its shadow-casting context. Due to the size and typology of the building's footprint, 20 receptors were deployed in the ENVI-met area input model with 8 receptors attached to the courtyard sides and 12 to the outer skin of the quadrangle (Figure 14.b). As described in the Social Sciences Building simulation, the 20 receptor outputs were used to calculate the four sets of weather data files for Ecotect simulations.

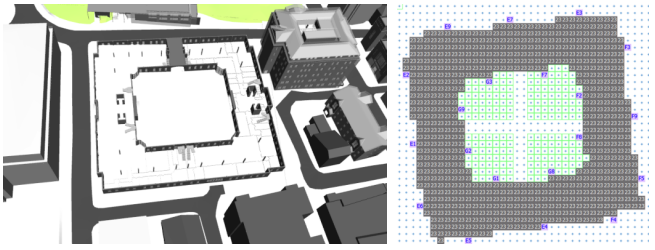

Figure 14. (a) A view of the X3D model of the Computer Science Building on uCampus; (b) Placement of 20 receptors around the building when setting up the ENVI-met area input model.

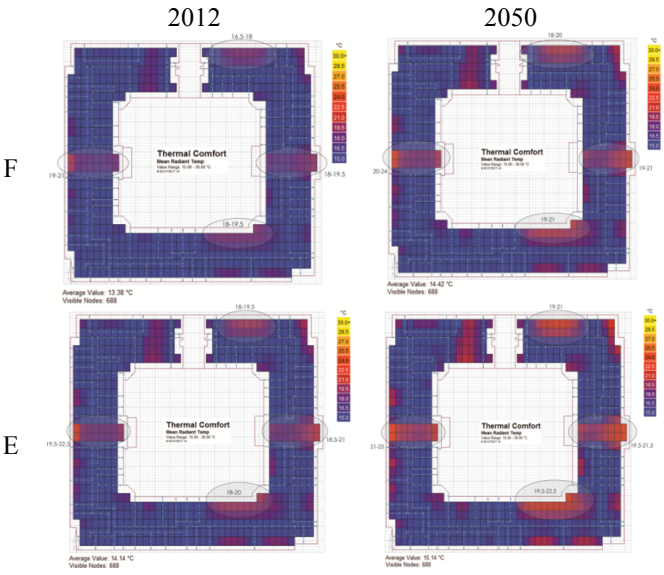

Figure 15. Ecotect thermal comfort analyses of the Computer Science Building under four weather data scenarios (F: Finningley weather station; E: ENVI-met simulated).

Figure 14 shows the Ecotect Thermal Comfort analyses of the Computer Science Building under the four different weather data scenarios. In terms of average temperature values, the Finningley 2012 and 2050 simulations show +1.04°C (13.38°C–2012; 14.42°C–2050); while the ENVI-met simulated 2012 and 2050 simulations show +1.0°C (14.14°C–2012; 15.14°C–2050). There is +0.76°C between Finningley 2012 and ENVI-met simulated 2012, and +0.72°C between Finningley 2050 and ENVI-met simulated 2050.

5. BRINGING OUTDOOR AND INDOOR TOGETHER ON UCAMPUS

During the New Cairo case study simulations and the Sheffield University campus neighborhood simulations as reported above, we introduced and applied the outdoor-indoor coupling approach to modeling climate change scenarios. At present, we have to work with both ENVI-met and Ecotect, because neither of them is able to handle all the simulation tasks alone. A comprehensive urban neighborhood simulation therefore always ends up with two distinct sets of output, which are not yet brought together to convey both the simulated urban neighborhood and the buildings in a unified visual presentation scheme. To this end, we have experimented with a *virtual neighborhood* modeling approach based on the aforementioned uCampus platform which is an X3D model server developed for 3D interactive on-line visualization and navigation of the Sheffield University campus.

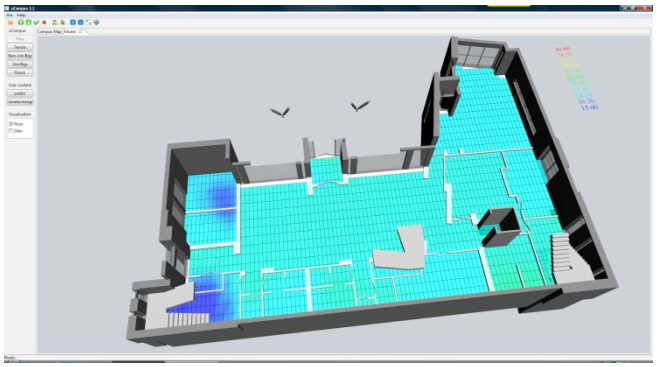

Figure 16. Ecotect thermal comfort map (with ENVI-met simulated 2012 weather data) overlaid onto the Social Sciences Building Ground Floor model on uCampus.

The idea here was to use the 3D virtual campus models, which include detailed floor models of key university buildings, as the common geospatial reference framework for piecing together the ENVI-met/LEONARDO and Ecotect graphic outputs. The neighborhood outdoor and building indoor simulation maps were first texture-mapped

onto the uCampus models in a 3D CAD package such as 3D Studio Max. The results were then converted into the X3D format and uploaded to uCampus. Figure 16 shows an example of an Ecotect thermal comfort analysis overlaid onto the Social Sciences Building's Ground Floor model.

For the campus neighborhood climate change simulation project, an account was registered on uCampus as a common repository for hosting all geo-positioned ENVI-met and Ecotect outputs. Student users can access the uCampus account to construct model overlays according to certain simulation themes. Figure 17 shows examples of bringing outdoor and indoor together in a single unified display. Once assembled on uCampus, users can freely navigate the 3D models with an X3D viewer such as BS Contact (Bitmanagement 2012) (Figure 18).

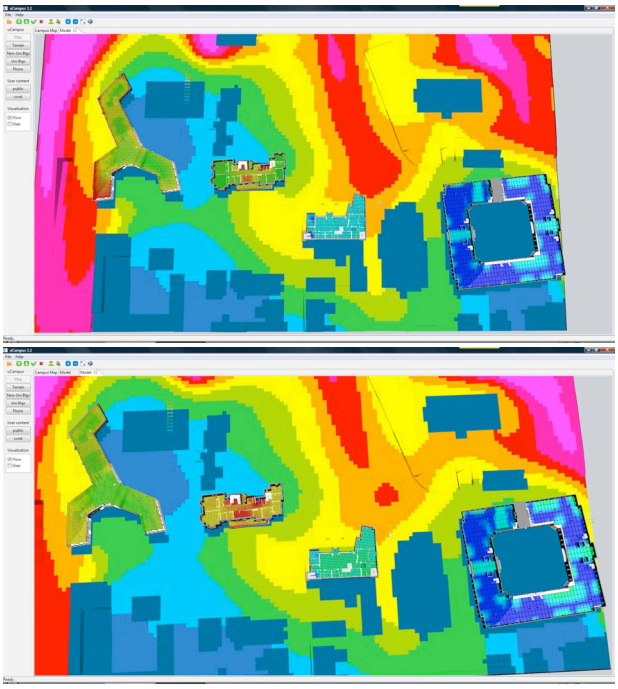

Figure 17. Bringing ENVI-met/LEONARDO and Ecotect outputs together in a single unified display on uCampus: (top) Air Temperature and Thermal Comfort under ENVI-met simulated 2012; (bottom) Air temperature and Thermal Comfort under ENVI-met simulated for 2050.

Similarly, the virtual neighborhood approach was applied to the New Cairo case study results. Again, the purpose here is to bring the coupled neighborhood outdoor and the building unit's indoor simulations together into a single common visual display (Figure 19). User-centered 3D navigation of the virtual neighborhood also allows reading of the climate change simulations in a context-rich immersive mode, making cognitive connection to viewers' sense of dwelling (see, e.g., Cuba and Hummon 1993).

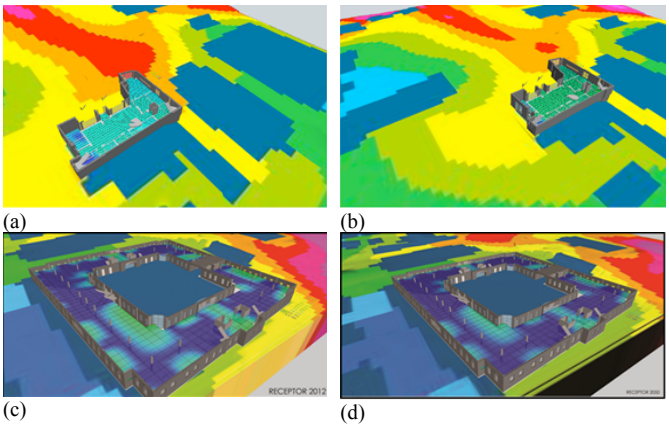

Figure 18. X3D-based navigation of various assembled neighborhood models: (a) Social Sciences Building in context (ENVI-met simulated 2012); (b) Social Sciences Building in context (ENVI-met simulated 2050); (c) Computer Science Building in context (ENVI-met simulated 2012); (d) Computer Science Building in context (ENVI-met simulated 2050).

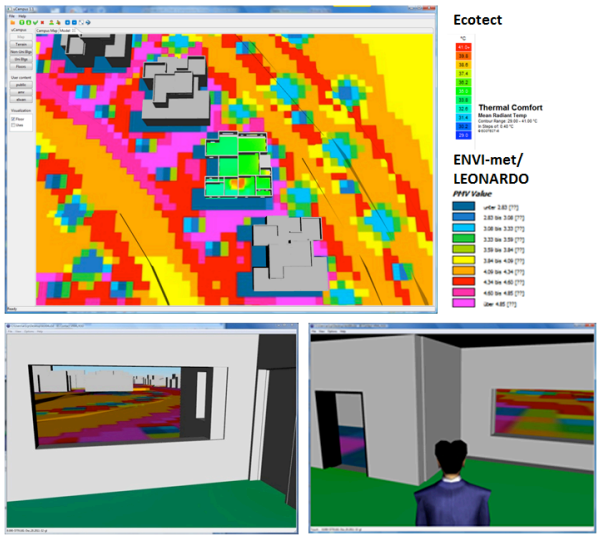

Figure 19. Bringing the ENVI-met and Ecotect outcomes from the New case study together into an X3D-based virtual neighborhood model hosted on uCampus (Top: A bird's eye view of the building unit; Bottom: Two views from standing inside the building unit).

6. CONCLUSION AND AREAS FOR FURTHER RESEARCH

We have presented two attempts at environmental simulation of future climate change scenarios at an urban neighborhood scale that includes both outdoor and indoor environments. A conceptual framework and a simulation workflow are proposed for achieving what we call Climate Change Conscious Urban Neighborhood Design (C3UND). Drawing on the outcomes from the New Cairo

neighborhood design case study and the Sheffield University campus modeling, we consider it is feasible to conduct environmental simulation for C3UND based on existing software tools and weather datasets. In particular, we have identified ENVI-met/LEONARDO, Ecotect, and CCWorldWeatherGen (or, CCWeatherGen for UK climate change projection) as the key capabilities to build up the simulation workflow.

In both the New Cairo and Sheffield cases, we have shown how ENVI-met can be used to contextualize Ecotect building simulations, taking into account simulated urban micro-climates of present-day and future scenarios. For present-day weather data, all contextualized Ecotect simulations predict higher indoor air temperatures compared with running the simulations with the default city-based weather settings. For the moment, we attribute the differences to the possible effects of the buildings being situated in an urban heat island that may have been captured by ENVI-met in generating neighborhood-specific weather data through the deployment of receptors.

There are several areas to be further investigated: (1) Further outdoor and indoor field measurement studies are required to validate the potential correlations between urban neighborhood micro-climate simulation and the accuracy of contextualized building simulation. (2) In searching for a more effective visual communication, we saw initial results from the 3D virtual neighborhood modeling approach to bringing ENVI-met/LEONARDO and Ecotect outputs together into a single common display. To promote more holistic understanding of building simulation in its neighborhood context through evoking viewers' sense of dwelling, further real user testing is needed to advance the design of the virtual neighborhood display such that more precise and consistent visual communication of the simulation outputs can be achieved as a Web application. (3) Currently, the data-flow from converting the ENVI-met receptor outputs to weather data files acceptable for running Ecotect is not without considerable gaps. New software is required to automate the tedious and potentially error-prone manual editing processes. (4) Perhaps most challenging, we need to invest in new system architecture capable of supporting *interactive* C3UND. The current implementation of ENVI-met takes up days' computing time to complete a simulation cycle when tackling the scale and complexity of an urban neighborhood. Designers and engineers are less likely to engage with C3UND if they are unable to make informed design decisions effectively with reference to the feedback from the climate change simulation cycle.

Acknowledgements

The second author is supported by a doctoral scholarship awarded by the Ministry of Defence, Arab Republic of Egypt. Thanks to the postgraduate students who undertook the ARC6700-2012 course and collaborated on climate change simulation of the University of Sheffield campus neighborhood.

References

ALI-TOUDERT, F., DJENANE, M., BENSALEM, R., MAYER, H. 2005. Outdoor thermal comfort in the old desert city of Beni-Isguen, Algeria, Climate Research, 28(3): 243-256.

BELCHER, S.E., HACKER, J.N., POWELL, D.S., 2005. Constructing design weather data for future climates. Building Services Engineering Research and Technology. 26 (1): 49-61.

BRUSE, M., AND ENVI-MET TEAM, 2011. ENVI-met Version 3.1 BETA V (incl. LEONARDO 3.75). Latest Build: 04-Oct-2010. <http://www.envi-met.com/>. Date accessed: 25/12/2012.

CCWEATHERGEN. Climate Change Weather File Generator for UK Weather Data. <http://www.serg.soton.ac.uk/ccweathergen/index.html>. V 1.1.2. Date accessed: 25/12/2012.

CHALFOUN, N.V. 2003. Sustainable Urban Design in Arid Regions: Integrating Energy and Comfort. Collaborative Symposium: Urban Design in Arid Regions. The University of Arizona and The Pontificia Universidad Catolica De Chile, May 2003.

CUBA, L., HUMMON, D.M. 1993. A Place to Call Home: Identification with Dwelling, Community, and Region. SOCIOLOGICAL QUARTERLY. 34(1): 111-131. DESIGNBUILDER SOFTWARE LTD. 2012. DesignBuilder. <http://www.designbuilder.co.uk/>. Date accessed: 25/12/2012.

ENVI-MET 2011. A1. The Configuration File .CF: Overview. <http://www.envi-met.com/htmlhelp/hs40.htm>. Accessed: 25/12/2012.

FAHMY, M., SHARPLES, S. 2009. On the development of an urban passive thermal comfort system in Cairo, Egypt, Building and Environment, 44, 1907–1916.

IES (INTEGRATED ENVIRONMENTAL SOLUTIONS LIMITED), 2012. VE-Pro. <http://www.iesve.com/software/ve-pro>. Date accessed: 25/12/2012.

PENG, C. 2011. uCampus: Can an open source 3D interactive virtual campus modeling platform support institutional learning and innovation? International Journal of Architectural Computing. 9(3): 303-324.

UKCIP. Climate Change World Weather File Generator for World-Wide Weather Data. V 1.7. <http://www.serg.soton.ac.uk/ccworldweathergen/index.html >. Date accessed: 25/12/2012.

VANGIMALLA, P., OLBINA, S., ISSA, R., HINZE, J. 2011. Validation of Autodesk Ecotect Accuracy for Thermal and Daylighting Simulations. Proceedings of the IEEE 2011 Winter Simulation Conference (S. Jain, R.R. Creasey, J. Himmelspach, K.P. White, and M. Fu, eds.): 3383-3394.

Session VII

Improving Building Performance at Urban Scale with a Framework for Real-time Data Sharing 179
Xiufeng Pang, Tianzhen Hong, Mary Ann Piette
Lawrence Berkeley National Laboratory, Berkeley, CA

Isomorphic City: A Customizable Future Scenario 183
Susannah Dickinson, David Gonzalez, Kyle Szostek
University of Arizona

A Collaborative Multi-Touch, Multi-Display, Urban Futures Tool 191
Michael van der Laan, Ron Kellet, Cynthia Girling, Maged Senbel, Tao Su
University of British Columbia

Improving Building Performance at an Urban Scale with a Framework for Real-time Data Sharing

Xiufeng Pang, Tianzhen Hong*, Mary Ann Piette

Lawrence Berkeley National Laboratory
1 Cyclotron Road
Berkeley, CA 94720, USA
*Corresponding author email: thong@lbl.gov

Keywords: Building Performance, Energy Efficiency, Energy Modeling, Optimal Operation, Urban Scale.

Abstract

This paper describes work in progress toward an urban-scale system aiming to reduce energy use in neighboring buildings by providing three components: a database for accessing past and present weather data from high quality weather stations; a network for communicating energy-saving strategies between building owners; and a set of modeling tools for real-time building energy simulation.

1. INTRODUCTION

Many well-developed energy efficiency measures and emerging technologies to reduce energy use in buildings have been available for years. However, adoption of many of these technologies is slow. The reasons include unmotivated building owners, high implementation costs, and operational difficulties.

Due to the relatively low utility costs in the U.S., most building owners are not motivated to improve building energy efficiency as long as comfort can be maintained. Based on the authors' experience, most energy efficiency projects are initiated as a result of some sort of mechanical system failures or degradations in buildings that cause issues related to discomfort. There is a need for a marketing mechanism to inspire building owners to go beyond energy and cost savings to implement energy efficiency.

When a building owner starts an energy efficiency project, the implementation can be costly, including hardware upgrades and labor costs. Most available measures and technologies require hardware that is of higher quality than today's standard practice. For example, the standard sensors used in today's systems cannot provide the required accuracy and reliability of outdoor air temperature and humidity measurement for implementing an enthalpy economizer or an outdoor wet-bulb temperature-based cooling tower control strategy. These high-quality sensors cost much more than the standard sensors and require significant routine costs to maintain and calibrate. The implementation of an energy efficiency project is also labor intensive. An energy efficiency project typically has three phases: energy audit and planning, implementation, and Measurement and Verification (M&V). Each phase involves heavy labor investment from both the on-site staff and the service provider. There is a need to reduce the implementation cost to make any energy efficiency project more appealing to building owners.

At completion of the energy efficiency project, the facility management team takes over the building. However, they usually do not have a deep understanding of the energy efficiency measures and technologies that were implemented. Often, they turn controls back to the original settings they are familiar with when any comfort complaints arise. As a result, the energy savings diminish over time. There is a need for a tool to inform the facility management team about the degradation of the achieved energy savings and provide them with operational suggestions.

To address the three challenges described above, we suggest that any solution at the individual building level will be expensive and not scalable. A more effective way to scale up energy efficiency would be to promote it on the urban scale.

On the urban scale, buildings are close to each other and share many common features such as microclimates, building functions, and occupancy patterns. Some energy efficiency measures taken for a single building may work

for multiple other buildings nearby. Weather measurements from one station, taken with high accuracy by well-maintained sensors, can be shared, in contrast to today's systems where each building takes its own poor-quality weather measurements.

The potential to reduce energy consumption by harnessing the competitive spirit of the occupants has been proven in residential buildings and college dormitories (Behavioural Insights Team 2011; Petersen et al. 2007). The same strategy can be applied to the commercial sector to motivate building owners. If building owners compared the energy performance of their buildings with that of their neighbors, a competition would be naturally triggered, which could help accelerate the deployment of new advanced building technologies.

In this paper, we introduce a framework to promote large-scale energy efficiency by motivating building owners, reducing implementation costs through data sharing, and improving operations through cloud-based real-time building energy simulation.

2. THE FRAMEWORK

Figure 1 shows the proposed framework. It consists of a server, a weather station network, and client software and the Energy Management and Control System (EMCS) at each individual building. The three components are connected through the internet.

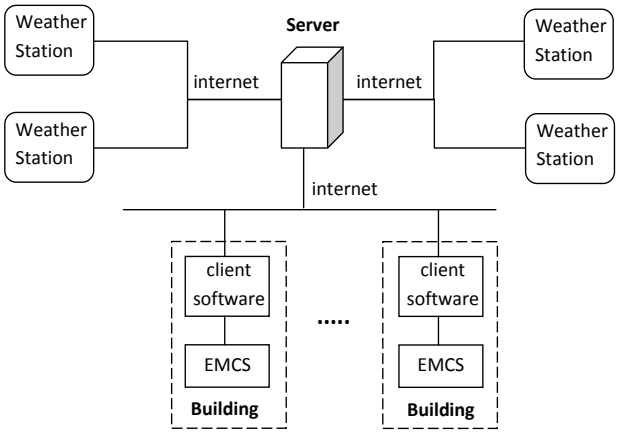

Figure 1. The proposed framework for urban scale energy efficiency

The high quality weather station network provides measurements for the complete list of weather parameters that are needed for energy efficiency measures and emerging low energy technologies. All of the weather measurements are sent to the server through the internet in real-time.

The server provides three main functions: 1) a database to collect and store data, including weather measurements, smart meter data from building owners or utility companies, and building information provided by the owners; 2) a user interface to take user input and display the data; 3) a computational engine to create building energy models, run the simulation in real time and provide the building operators with operational suggestions.

The client software running in each building serves as a gateway to allow the EMCS to access data from the server in real-time: for example, weather data, the predicted building performance, and optimal operational suggestions.

2.1. Weather station network

The idea of integrating real-time weather data into the EMCS through the internet is not new (Stunder et al. 2003; Kok 2007; Madsen 2009). However, the current solutions do not provide the measurement accuracy and reliability required by the building industry. Most importantly, none of the existing weather station networks provide all the necessary weather parameters. The emerging low-energy technologies and urban energy systems—such as radiant heating/cooling, demand response, district heating/cooling, and renewable energy—require more weather measurements—such as global horizontal solar, direct and diffuse solar, wind speed and direction—to ensure their proper operation. In addition, the controls of the emerging technologies and the urban systems mentioned above also need predicted weather parameters to deliver optimal operation strategies. The existing weather forecast technology can predict the temperature, humidity, rain and snow very well, but the forecast model for solar radiation, especially direct and diffuse solar radiation, needs further development.

The weather station network should not only be able to accurately measure outdoor air temperature, relative humidity, direct solar, diffuse solar, global horizontal solar, wind speed and direction, CO_2 concentration, and indication of rain and snow, but also be able to predict these weather parameters for at least 24 hours ahead. So far, there is no single product that can measure all the parameters mentioned above. Lawrence Berkeley National Laboratory (LBNL) had a proof-of-concept demonstration project for

the Department of Defense (DOD). For that project, a weather station was assembled to measure the above parameters except for CO_2 and rain/snow (Pang et al. 2012). This prototype can be further improved to address these needs.

Once we have the weather station, the remaining challenge is to determine how many weather stations are needed for a given city and where these weather stations should be installed.

2.2. Data sharing

The building owners log on to the server and create their user profile by providing the detailed building characteristics, such as the year built, the location, the square footage, the building type, the occupancy density and schedule, the HVAC system type, low-energy technologies used, and energy efficiency measures. Once logged in, the building owners can generate a detailed whole building model by using an online wizard, and download the model to their local computers. This energy model is based on the user input, which represents the design intent of the building.

The building owners can also view their neighbor's information and compare their own energy consumption with that of their neighbors. Based upon this comparison, the building owners can refer to the energy efficiency measures or the low-energy technologies adopted by those neighbors whose energy consumption is lower than their own. The server also serves as a computational engine to provide real-time building energy simulation and optimal continuous operation improvement suggestions. The design intent model takes the weather data as real-time input and reports the predicted building performance which is used for the comparison with the actual building performance. Based on the comparison between the measured and predicted building performance, a whole building diagnostic algorithm will be used to provide continuous operation improvement suggestions.

2.3. Client software

Commercial solutions using the internet have been developed to access weather data in real time. One company has developed a communication driver, based on industry software standards (OPC Data Access), for the purpose of accessing weather station and forecasting data for use in the EMCS. Data is then available for use by EMCS software that is OPC Standard compliant, such as Automated Logic, Honeywell, Invensys, Johnson Controls, and Siemens.

3. ENERGY MODELING AND REAL-TIME ENERGY SIMULATION

To address the operational challenges faced by the facility management team, LBNL developed and demonstrated a technique that allows a comparison of actual building performance and expected performance in real time (Pang et al. 2012). When significant differences between the measured and predicted performance are observed, the system can inform the building operator about the presence and location of the degradation. The proposed framework leverages this effort to benchmark buildings against optimal performance and provides operational suggestions.

Optimal building performance is typically represented by the design intent or the state of the art. In order to evaluate how a building performs, as opposed to its optimal performance, a building energy model that represents the optimal performance is needed. There are two approaches for building energy modeling: a forward model and a data-driven model. The forward model utilizes first principles, such as conservation of mass, energy and momentum, while the data-driven model relies on experimental data or simulated data from a physical model to train an empirical or black-box model. For the purpose of whole building performance monitoring and optimization, the data needed for a data-driven model typically does not exist. Therefore, only the forward model approach or the data-driven model based on simulated data generated by a forward model would work in this context.

Most current simulation programs (for example, EnergyPlus), use the forward model approach. EnergyPlus is a detailed whole building energy simulation program that calculates building heating and cooling loads, and disaggregates energy end use as well as many other simulation details that are necessary to verify that the simulation is matching the measured performance of the actual building (Crawley et al. 2001). Because of its comprehensive features and extensive development and verification process, EnergyPlus is selected for the proposed framework.

The key effort in creating an EnergyPlus model is the generation of a geometry model and a building mechanical system model. The modeling process is typically time

consuming and it's unrealistic to build the energy model for every building in a city from scratch. A technique will be developed for rapid building energy modeling on the urban scale. The main idea behind this technique is to extract the common features from building blocks and develop the parameterized building models for different building types, such as large office buildings, shopping malls, small retails, hospitals, schools, and fast-service restaurants. With the development of templates based on the common features, the modeling process is reduced to modifying the free parameters according to the user's input, which is accomplished by an online wizard. Once the model is created, an automatic model validation process will be executed to make sure that the created model is within the allowed tolerance.

Once a reference model is established, it can be used for the building's continuous operation improvements. The real-time energy simulation technology developed at LBNL is used for this purpose. This technology is able to compare the predictions of a reference building model to the measured performance and analyze the difference to infer potential operational degradations that might be causing the discrepancies (Pang et al. 2012). Middleware software acquires the relevant inputs from the server and passes them to EnergyPlus at each time step. The EnergyPlus model runs in real-time and reports the predicted building performance at each time step. Figure 2 shows the architecture of the technology.

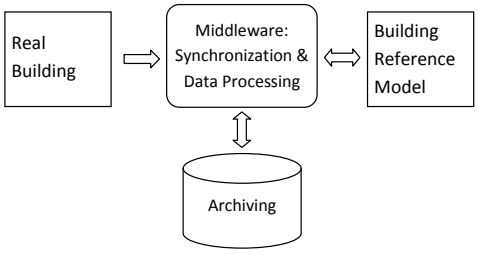

Figure 2. The architecture of real-time energy simulation

4. DISCUSSION

This paper presents a framework that can potentially improve building operations and thus reduce energy use at the urban scale. The keyword for this technology is "share". Building automation systems share high-quality and well-maintained weather measurements. The building owners share their building information, such as energy use and efficiency measures employed in their buildings. It can be challenging to motivate building owners to share their building information, but recent developments in regulations to encourage or require building owners to disclose energy use data will definitely help.

The success of the proposed system could lead to game-changing effects on the building industry, not only on energy savings, but also on the infrastructure of building operations in general. The system is an effective method to lead to energy savings on the national scale with minimal investment. The proposed system can: 1) improve energy performance of buildings; 2) promote low-energy buildings; 3) facilitate the national energy goal of achieving net-zero energy buildings.

References

PANG, X., WETTER, M., BHATTACHARYA, P AND HAVES, P. 2012. A framework for simulation-based real-time whole building performance assessment. Building and Environment 54. 100-108.

STUNDER, M., SEBASTIAN, P., CHUBE, B. AND KOONTZ, M. 2003. Integration of real-time data into building automation systems. Technical Report, Geomet Technologies, Inc, January 2003.

KOK, R. 2007. Weather on demand - a new way for building automation to leverage real-time weather information. http://www.automatedbuildings.com/news/sep07/articles/kepware/070827030303kepware.htm.

MADSEN, J.J. 2009. Integrate weather data into building automation. http://www.buildings.com/tabid/3334/ArticleID/6841/Default.aspx.

BEHAVIOURAL INSIGHTS TEAM. 2011. Behaviour change and energy use. Cabinet Office, London. http://www.cabinetoffice.gov.uk/resource-library/behaviour-change-and-energy-use

PETERSEN, J.E., SHUNTUROV, V., JANDA, K., PLATT, G. AND WEINBERGER, K. 2007. Dormitory residents reduce electricity consumption when exposed to real-time visual feedback and incentives. International Journal of Sustainability in Higher Education 8. 16-33.

CRAWLEY, D.B., LAWRIE, L.K., WINKELMANN, F.C., BUHL, W.F., HUANG, Y.J., PEDERSEN, C.O., STRAND, R.K., LIESEN, R.J., FISHER, D.E., WITTE, M.J. AND GLAZER, J. 2001. EnergyPlus: creating a new-generation building energy simulation program. Energy and Building 33. 319-331

Isomorphic City: A Customizable Future Scenario

Susannah Dickinson[1], David Gonzalez[2] and Kyle Szostek[3]

[1]University of Arizona
1040 N. Olive Road
Tucson, AZ, USA 85721
srd@email.arizona.edu

[2] University of Arizona
1040 N. Olive Road
Tucson, AZ, USA 85721
davidg8@email.arizona.edu

[3] University of Arizona
1040 N. Olive Road
Tucson, AZ, USA 85721
kszostek@email.arizona.edu

Keywords: Collective Intelligence, Parametric Urban Design, E-topias, Live Data, Programmable Matter.

Abstract

This paper discusses a future city design and research project for Tucson, Arizona, USA. The project, *Isomorphic City*, set in the year 2087 develops a truly customizable and ever-adapting computational approach to the existing built environment. Part of the challenge was to design digital methodologies that could simulate this scenario in as live a way as possible, incorporating real-time, live data into the equation, ranging from environmental criteria to social media information. Form was the result of inputted parameters versus the making of form in a traditional object-like fashion. The project anticipates a shift from simulating the urban condition with a rule-based set of criteria to a more human agent-based approach based on collective intelligence and social behaviour patterns.

1. INTRODUCTION

Making our urban environments sustainable, environmentally and socially, is a key design issue today. William Mitchell, in *E-topia*, wrote that, because of the digital revolution of *bits*, traditional urban models are no longer valid. He defined the new urban condition as "lean, green cities that work smarter, not harder. Their basic design principles may be boiled down to five points: 1. Dematerialization, 2.Demobilization, 3.Mass customization, 4.Intelligent operation and 5.Soft transformation" (Mitchell, 2000). Our current urban conditions are obviously a long way from these principles.

The following project, *Isomorphic City*, was an attempt to holistically incorporate Mitchell's design criteria into a proposal which would anticipate what the future may hold, while researching and testing the latest available digital methodologies that can aid in this simulated process. The project was originally part of an undergraduate options architecture studio which had input from some graduate planning students in a related geodesign seminar led by Dr. Ryan Perkl of the University of Arizona. The project developed beyond the studio as an independent research course to allow more time to create live interfaces and make the digital model work in a way in which it had been originally hypothesized. An existing city, Tucson, Arizona, USA was chosen as the base urban condition. This existing city allowed the vision to incorporate real environmental and social media data. Tucson is currently facing several challenges that impede its ability to be truly sustainable. One is the large amount of urban sprawl which puts a social strain on the urban core and aggravates several environmental issues, in a place where several key resources, e.g. water, are already low. The existing extreme climate is also a condition that cannot be avoided in any future solution that attempts to be smart and green. These apparent negative existing criteria were seen as a positive to show how the city could be transformed and modeled in the future.

2. FUTURE VISION

Mitchell's design principles are very pertinent today as they recognize the huge change that digital technologies have had on society. They are also relevant to environmental issues which are becoming more and more of a pressing concern. His criteria defined a model that is more akin to a dynamic, ecological model (like the natural world), which is alive and constantly changing and adapting. The history of this more dynamic approach to urban design is a topic in itself and not part of the scope of this paper. Of particular interest though, beyond Mitchell, were the ideas

of Yona Friedman and the Metabolist movement, who saw the metropolis as a living organism. Some of their objectives were to create structures that could expand infinitely. For *Isomorphic City* part of the challenge was balancing this desire for a dynamic model with the growth constraints of the existing resources.

Conventional land use is rigid and lacks the ability to adapt and transform in the way that Mitchell deemed necessary. In *Isomorphic City* the proposed relationship of physical and digital space allows for a dynamic environment that could adapt to meet the direct needs of the inhabitants, in real-time, during the course of each day. Many dynamic/responsive systems incorporate sensors and are generally fairly technically complex in order to make parts that can adapt and change. For this particular scenario, set in the year 2087, *programmable matter* was utilized as the building block for the community, (digitally) creating form-finding aggregation (Figure 1).

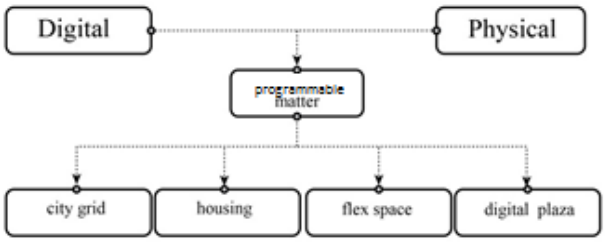

Figure 1. Main organizational diagram.

"Programmable matter" is a term coined by Toffoli and Margolus (1991). There has been extensive research in programmable matter in the biological and physical realms (Griffith, 2004). In this scenario we are referring to one of the more advanced areas of research, that of *claytronics*—reconfigurable nano-scale robots that have the ability to move around and change shape and color as needed. The use of this evolving material meant that the project would remain in virtual reality as a theoretical project. Architecture is not only what is built, or what can be built at a given time, but it is also about a conceptual trajectory. Although the project was theoretical in nature we wanted to explore the relationship of the digital to the physical. Connecting to a real environment, i.e. an existing city, was crucial to the digital simulation process as we could be specific about a given set of environmental criteria and data. These digital methodologies, which were obviously set in the present, were seen as a tool to enable us to reach this smarter, greener vision faster. Certain applications are very applicable today, particularly the live linking of environmental and social data into a digital model.

With the complexity of both cities and sustainability, it was important not just to focus on digital tools in a reductionist, performative way. For true sustainability, environmental, social, economic and political issues are all interrelated. Students were encouraged to bring together all three of these concepts of sustainability in order to articulate a liveable community where the quality of life of the inhabitants is paramount. This meant that they needed to question the status quo of our current economic system, and to hypothesize and design alternative systems. These systems would hopefully inspire more equality and diversity, which seem necessary if future increased populations are going to survive cooperatively on this earth together in a positive fashion. This was obviously a cursory analysis, but is still a valid pedagogical tool to start understanding the inter-connectedness of all these issues.

In this particular scenario, it was anticipated that an incentive- and resource-based economy would emerge. The team hypothesized that the primary capital resource of the city would be programmable matter for use in housing, transportation, communication, and entertainment (Figure 2).

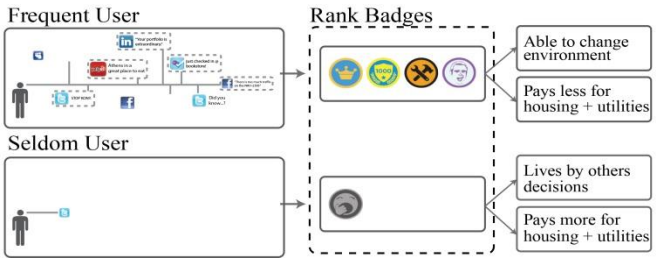

Figure 2. Diagram showing proposed city incentive program.

The vision predicts that digital designers, programmers, developers, architects, and environmental experts would constitute the main demographic work force required to maintain the city (Figure 3).

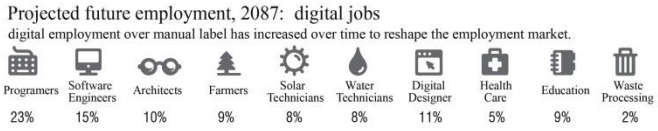

Figure 3. Projected future city employment areas.

It was anticipated that programmable matter will become autonomous (create itself), yet designers and programmers will be needed to shape the matter, generate spaces and manifest the visions of the city inhabitants on a personal level. Food production, energy generation, water, and human waste management will be overseen by a workforce of environmental experts who will utilize haptic and health data, fed directly from city inhabitants, to optimize the efficiency of these resources. The hyper-advanced interface of programmable matter has the ability to reshape to accommodate water storage for future use, as well as generate power from every surface exposed to the sun through a skin of electrically super-conductive nano-graphene. Mitchell wrote that "If you want adaptability, responsive software beats reconfigurable hardware…it is no longer the architectural programmer who controls space use, and thereby expresses power; it is now the software programmer" (Mitchell, 2003).

One of the keys to a successful city is having a diversity of programs and people. The proximity of home, work, and communal space in *Isomorphic City* allows for this life, plus reduces commuting time. The project anticipates that, as internal combustion technology declines, a more advanced form of transportation will emerge with the utilization of automated programmable matter vehicles for transport (Figure 4).

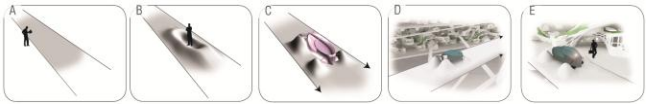

Figure 4. Proposed transportation diagram.

Traditional streets take up space and damage the environment. Roads within the *Isomorphic City* will recalibrate and manifest as they are needed, and their matter will be repurposed when not in use. The digital plaza, which is the social and cultural centre of the city, allows for virtual and surrogate travel (Figure 5). This eliminates the need for long distance travel as local space is connected to long distance digital space—thus lowering the ecological footprint of residents.

Cities are among the most complex human-designed systems on the planet so it is imperative to study them in at least three or four dimensions to understand their complexity as much as possible. It is also important to study as many elements in a connected way so that one can see the

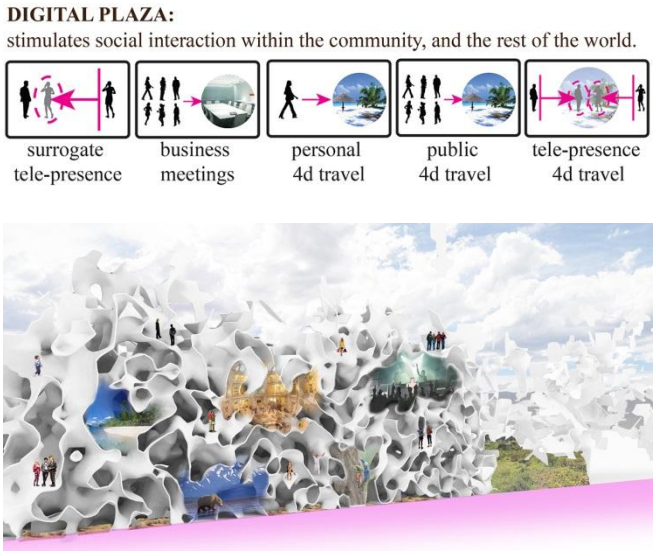

Figure 5. Image showing Digital Plaza and its various functions.

issues more holistically. Most parametric design approaches use virtual data sources or simulated data. Live information sources as direct input parameters are gaining more and more prominence as technology increases and designers seek faster and more performative solutions to their design criteria. Real-time input from the web or the environment can be integrated into the digital design model as part of the form finding process. This can be achieved as a live simulation to select models that 'fit' best with the designer's criteria or can be seen as a continuous stream that allows models or environments to adapt and change as the input alters. The project researched various digital methodologies and software applications in order to facilitate as live a simulation process as possible.

In order to be socially sustainable it is necessary to incorporate input from individuals rather than rely on more rigid top-down approaches. Shin et al (2011) have claimed that the incorporation of direct participation of citizens, in this case via social networking data, creates a shift from rule-based simulation to a human agent-based approach.

3. DIGITAL METHODOLOGY

Live digital models can still be fairly complex and clunky because of the need usually to interface several platforms together. In this instance Rhino Grasshopper was selected as the main design interface, in part because of its NURBS-based logic, but also because of all the plug-ins, which are being developed daily, that allow this interface to connect with others in live ways (Figure 6)

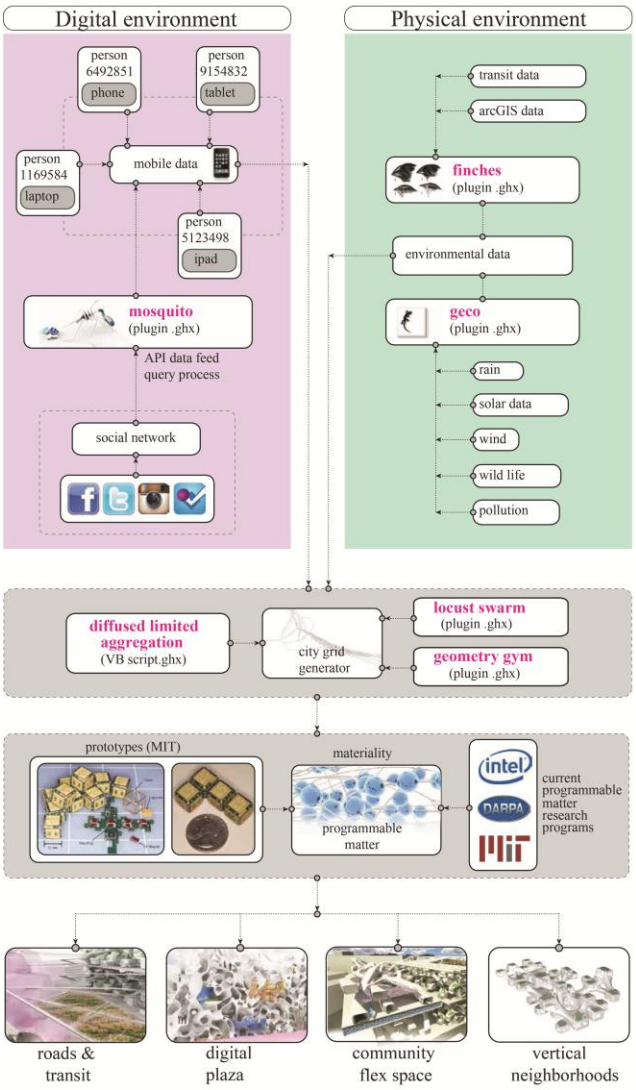

Figure 6. Digital methodology diagram.

Initially the existing city environment was developed with the Elk plug-in for Grasshopper. This plug-in has the ability to generate major map and topographical surfaces from OpenStreetMap.org. This is a fairly simple and fast generating tool, but with the drawback that the existing building fabric is not included. So, the preferred approach was to connect GIS data with the Finches plug-in developed by Nicholas de Monchaux at the University of Berkeley, California. This allowed for a much larger amount of existing city data to be incorporated into the digital model in a more dynamic fashion.

With regard to the social networking component of the project, it was noted that Salim et al (2010) referenced a project, Tweetform, that connected specific keywords and hashtags from Twitter accounts to a parametric model in Rhino. Since *Isomorphic City* was a more site-specific project concerned with environmental issues, there was the desire to incorporate geotag information from Twitter too. This would inform where the various social hotspots of the city were, in a live manner. Initially the project created a simulated data cloud with a script using the Locust plug-in for Grasshopper, created by Robert Cervellione. Locust generated a swarm-logic point cloud capable of control under various parametric behavioral criteria—e.g., avoid, seek, and alignment (Figure 7). The swarm points were studied for their association to human circulation patterns, and were later replaced by actual Twitter geotag data. The three dimensional form of the digital plaza and transportation networks were generated with the Geometry Gym plug-in created by Jon Mirtschin. The housing typologies within the vertical neighborhoods were generated from geotag points that were in closest proximity to one another, and were sorted into groups, metaphorically associated as people with similar interests. The individual unit sizes were determined based on an assortment of predetermined unit types, according to statistical family size data in Tucson collected from www.city-data.com. The units were generated according to the geotag points, and the Weaverbird plug-in for Grasshopper was used to generate a mesh that linked the housing units together in a minimal surface configuration (Figure 8).

Ultimately the initial Locust simulated data was replaced by live geotag data from Twitter accessed through the Mosquito plug in, created by Carson Smuts of Studio Nu. A Diffuse Limited Aggregation System (DLA) was used to digitally generate a new street grid from this live geotag point cloud—in effect, to digitally generate a new flexible city grid. This simulated the way in which we anticipated the programmable matter would perform. DLA is an application derived from fractal geometry, by Witten and Sanders in 1981. Chen-Wei and Mao-Lin (2000) presented

how DLA is appropriate to illustrate the distribution of urban space. In this example, a specific DLA script created by Daniel Piker (2010) was used to work with an adaptive boundary and gravitational pull to bring particles into a cluster. Specific Arc GIS information (e.g., water sources, key geographical information and infrastructure) was used for the boundary conditions (Figure 9). At the macro scale the DLA changed the grid and made the large environmental moves (e.g. agricultural zones near water sources) while at the micro scale it helped create the smaller housing communities and the digital plaza.

Climate data was linked into the Grasshopper model with the software program Ecotect by Autodesk via the GECO plug-in created by [uto], http://www.utos.blogspot.com.

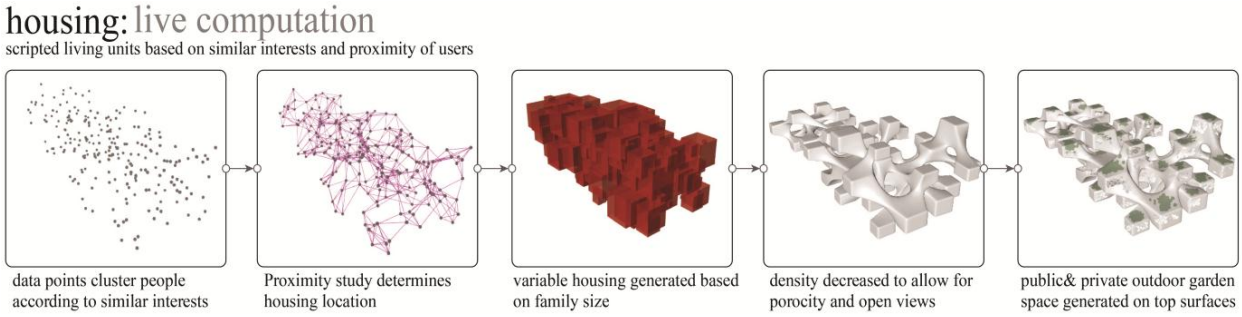

Figure 7. Diagram showing behavior parameters with locust plug-in.

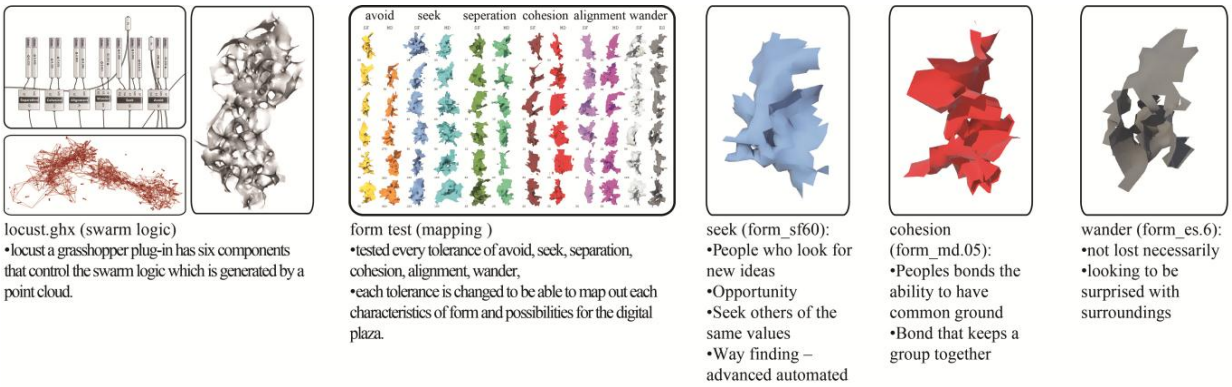

Figure **8**. Housing digital methodology

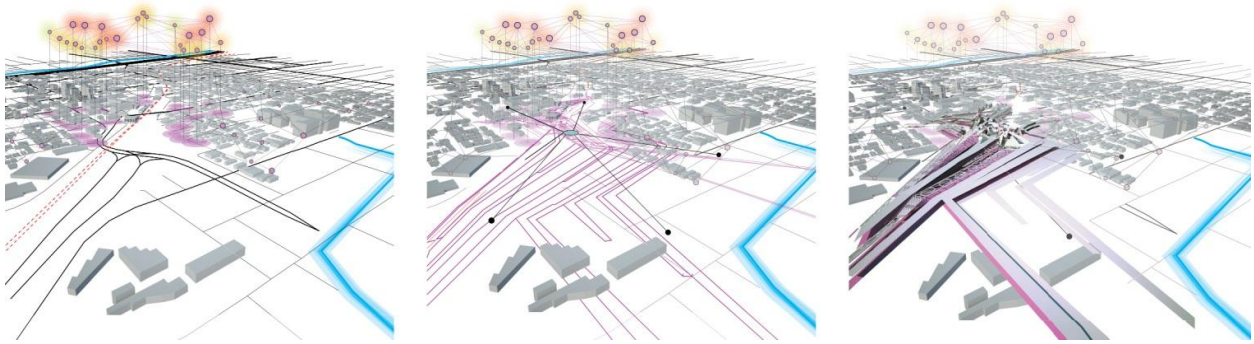

Figure 9. Image showing city growing.

4. FINDINGS

To get maximum potential from online data, the data generally needs to be refined and processed before it can be analysed or used in an effective way. This means that plug-ins or processing scripts need to be created. Although the number of Grasshopper plug-ins are increasing daily, it is imperative for designers and researchers to have the ability to customize these tools themselves. For architectural professional degrees, there always seems to be new tools that are vying for time in an ever increasingly crowded curriculum. This can be another reason to work more collaboratively with other disciplines. We have just started connecting with the computer science department on our campus in order to get more scripting knowledge and to find out how we can be smarter computationally with our model and possibly store future and past data.

Waste, as a concept, was created by human beings. In this future scenario, the thought and ideology of waste will be transformed. Resources, energy, and water use by the city inhabitants will be directly monitored and will limit potential population growth within areas of the city. Cities would grow more akin to historic cities in areas of maximum natural resources, but only to a size that can be supported—i.e., density is related to the area's carrying capacity. This carrying capacity calculation determined the supportable population and was directly proportional to the amount of water and other available necessities in the given ecosystem. The process for determining the specific carrying capacity of Tucson began by calculating the available resources in their given site. Then students evaluated standard norms of per-capita consumption evaluating these against potential (per-capita) improvements based on designs that encouraged less automobile usage and more developed attitudes to resource consumption generally. The future goal would be that city dwellers will have direct control over the programmatic function of their city, but the environment will set parameters that limit excessive and negligent use of resources, allowing the city and its inhabitants to become symbiotic within the natural ecosystem of the desert.

5. CONCLUSIONS / FUTURE DIRECTIONS

It was apparent that trying to realize William Mitchell's criteria for an E-topia was a complex task on multiple levels. The project became a future vision set in the year 2087, incorporating future technologies, but was paradoxically digitally simulated with present day technologies. This leap of faith made sense: whether the specific predictions are realized or not, it is apparent that the push for live 4D digital models, with the ability to adapt, change and incorporate multiple levels of data, is paramount today. Only in this way will we be able to design and understand our built environment more effectively, on a large scale, with any sense of specificity to place.

To create this digital model, which would incorporate live, real-time data, was complex in terms of its methodology and had high requirements in terms of computational power. To continue this study more effectively we will need more computational support. The various plug-ins worked as described earlier, but these need to be refined and customized so that we can filter inputs to just get the information that we want. Apart from needing more geotag data we would want the ability to sort and store the information from social and climate databases so we can add more layers of information for this and future studies. We also plan to link to the live weather feed at the university so we can study the project over a year-long period. This would enable the model to update in a live way to the current weather conditions. Since the concept of carrying capacity was integral to this project, at some point it would be crucial to link this data more fluidly to the live model to ensure that the growth/limits of the city were thoroughly incorporated too.

The incorporation of social data and philosophies beyond the typical architectural realm was also a key step towards more balance between bottom-up and top-down design philosophies. Even though at times these were fairly superficial, it was an important part of the process in aiding the ability to think holistically and realize how inter-connected everything is.

"A phenomenological model is tentative, malleable and always in flux, never attaining absolute isomorphism with the world. It is expressed, tested and revised in the creation or manipulation of entities in the world. Except in a utopia, which precludes creativity by refusing to differ from its description, this is the definitive aspect of the human condition…It is becoming increasingly necessary, and increasingly possible, for the form-maker to re-immerse himself in the form-giving dialogue" (Frazer, 1995).

Figure 10. Rendering of Isomorphic City

References

CHEN-WEI, C., MAO-LIN, C. 2000. A Simulation Study of Urban Growth Patterns with Fractal Geometry *CAADRIA2000,* Singapore, 55-64.

FRAZER, J. 1995. AN EVOLUTIONARY ARCHITECTURE. LONDON, UK: THE ARCHITECURAL ASSOCIATION PRESS.

GRIFFITH, S. 2004. Growing Machines, PhD Dissertation, MIT.

MITCHELL, W. 2000. E-TOPIA: 'urban life Jim – but not as we know it,' CAMBRIDGE, MA: MIT Press.

MITCHELL, W. 2003. ME ++: The Cyborg Self and the Networked City, CAMBRIDGE, MA: MIT Press.

SALIM, F., MULDER, H., JAWORSKI, P. 2010. Demonstration of an Open Platform for Tangible and Social Interactions with Responsive Models *ACADIA2010,* New York, USA 227-233.

SHIN, D., MULLER, S., SCHMITT, G. 2011. A Crowdsourcing Urban Simulation Platform Using Mobile Devices and Social Sensing *CAAD Futures 2011,* Liege, Belgium 233-246.

A Collaborative Multi-Touch, Multi-Display, Urban Futures Tool

Michael van der Laan, Ron Kellet, Cynthia Girling, Maged Senbel, Tao Su

University of British Columbia
2260 West Mall,
Vancouver, BC, Canada, V6T 1Z4
mt.vanderlaan@gmail.com

Keywords: Visualization, Simulation, Decision Support Tools, Urban Design, Collaborative Environments.

Abstract

Recent technological advances in multi-touch, multi-display computing interfaces and networking software have enabled the integration of all three of these roles into a single collaborative work space. This paper describes the development of one such application focused at carrying out complex urban design exercises through simple, transparent, and interactive means. Constructed through a federated system architecture, the system connects three independent applications: Google Earth, a Building Information Model (BIM) database, and an Indicators Dashboard (ID). The goal of this work is to provide a diverse group of stakeholders with a better understanding of the environmental impact and tradeoffs associated with a range in potential urban futures.

1. INTRODUCTION

Over the last decade, our understanding of how urban form influences energy consumption has increased substantially. In particular, transportation patterns and building energy demand are all impacted by the distribution and shape of a city's infrastructure (Norman, J., MacLean, H., and Kennedy, C. 2006, for example). In recent years, tools and frameworks have become prominent components in the measurement of existing and future urban conditions (e.g. Cherubini, F., Bargigli, S., and Ulgiati, S. 2008; Codoban and Kennedy, 2008; Kellett *et al.,* 2012). The tools that effectively educate the diverse group of stakeholders involved in planning will elevate the needed policy changes to align future development with goals.

In parallel, the way in which we engage with the city has drastically changed over the last decade (e.g. Crang and Graham, 2007; Wilken, 2009). Cities are now information landscapes, actively gaining and distributing information, adapting to new technologies and networks that arise. Utilization of this information is crucial to developing tools that adapt to evolving means of human interaction.

A number of tools targeted at engaging participants in the urban planning process exist—including those targeted at non-professionals. For example, online tools such as UrbanGuage and UrbanSim aim to balance local community concerns with planning objectives. A number of tools also exist that streamline urban planning tasks, as described by Geertman and Stillwell (2004). These Planning Support Systems (PSS) can evaluate planning alternatives through the integration of data, models and visualization. In parallel, collaborative multi-touch surfaces are increasingly available to stakeholders. This virtual venue offers promise in providing a compelling and educational work environment (Antle et al., 2011, for example). In the hopes of increasing understanding of multi-touch exercises, user interface guidelines have been proposed; of the eight outlined by Scott et al. (2003), three are most relevant for collaborative urban design exercises: supporting fluid transitions between activities, considering user arrangements, and supporting simultaneous user actions**.**

The integration of a multi-touch collaborative system with a PSS forms the basis of this paper. The application described below is used in studies that attempt to help community residents and planners visualize the energy and emissions implications of different urban form configurations through collaborative exercises with immediate design performance feedback.

2. METHODOLOGY

2.1. The Application

The PSS described by Fernquist (2010) and later by Su (2011), has been advanced for the purposes of this research. This touch-table based PSS is constructed through a federated architecture, allowing communication between

multiple components involved in measuring and visualizing neighbourhood designs (Figure 1). A federated architecture describes the exchange of information among semi-autonomous de-centrally organized nodes.

In a live design exercise, the touch-table accommodates four participants, each with their own case palette and menu (Figure 2, bottom). The case palette contains buildings, streets and open spaces. From this casebar, participants can drag a case onto an aerial view of the study area. Once in play on the tabletop, a case can be arranged and visualized according to design preferences. Accordingly, cases are indexed and live information about the study area is provided as feedback to design particpants (Figure 1: top). This paper will focus directly on the development of the Indicator Dashboards (ID), the component that relays study area information to design participants.

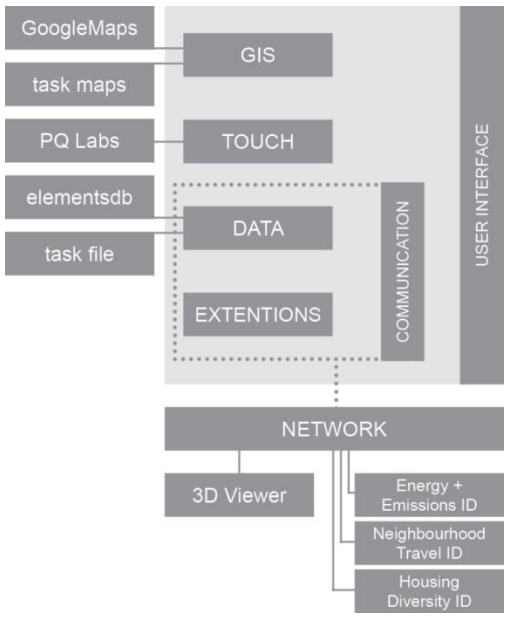

Figure 1. Shows a schematic of the touch-table system architecture.

2.2. The Indicators Dashboard

The Indicators Dashboard (ID) exists through the interaction of three components: the **task file, live metrics**, and a **dynamic infographic**.

The **task file** is broken into three sections: *basic task information, resource layers, and calculation parameters*. The *basic task information* includes general information (i.e., where to center the map, at what resolution to display the map, and which cases to make available). The *resource layers* describe the location of any additional maps (e.g., land use information, study area boundaries, environmental information and infrastructure). Lastly, the *calculation parameters* describe any variables needed for the ID calculations that ultimately generate performance indicators for the evolving design.

The **live metrics** are actively sourced data from the touch-table exercise. As each case is dragged out from the case selection bar it carries with it associated information. This information includes 3D models and quantitative data from an online BIM database. The database includes case attributes such as floor area by use, dwelling numbers, number of occupied floors, street set-backs, and pervious land surface area (http://elementsdb.sala.ubc.ca/).

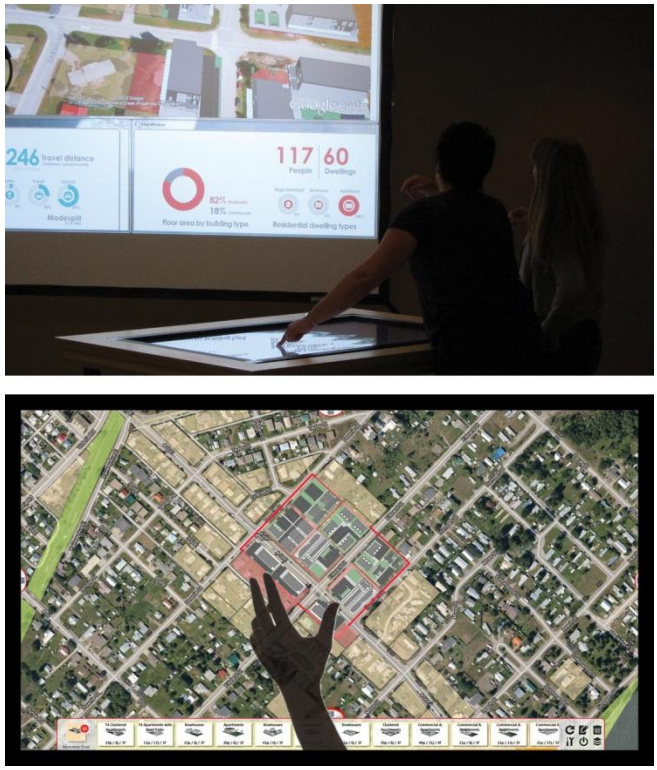

Figure 2. Top: Touch-table and external display configuration. Bottom: View of touch-table interface with study area in center.

The **dynamic infographic** consists of an HTML web page with an embedded Flash infographic. Through JavaScript, information is gathered from the **task file** and combined with **live metrics** to form the input used by the ID

calculations. The calculation output is in turn picked up by the web page through ActionScript3 and dynamically displayed as an infographic. The presentation of the ID information includes donut charts, numeric values, iconography, and goal-oriented thresholds (Figure 3).

In total, three IDs were created to quantify progress towards the City's climate change goals. These were the **Energy and Emissions ID**, **Neighbourhood Travel ID**, and **Housing Diversity ID**.

2.2.1. Energy and Emissions ID

The **Energy and Emissions ID** was developed in two steps: down-scaling municipal data to the neighbourhood study area, and developing a suite of indicators.

Taking inventory of municipal greenhouse gas emissions has been an ongoing initiative by the Province of British Columbia since 2007. This municipal-scale data, along with census information, formed the baseline for each study area. This data was down-scaled to individual buildings following a similar approach to van der Laan (2011). Following this, statistics on each study area were then input as *calculation parameters* into a **task file** prior to the design exercise—providing a context-sensitive baseline. Included in the *calculation parameters* were: building energy use intensity, average vehicle fuel efficiencies, fractional use by fuel type, fractional use of thermal energy, and emissions factors for each energy type.

Once the task file was defined, a large number of context-sensitive energy and emissions information could be quantified and visualized by the ID. However, an effective means of communicating results to non-experts involved determining which indicators were most important and how to best visualize those chosen. Household and individual level indicators were ultimately chosen, as they have been shown to be an effective means of communicating complex urban planning information to non-experts (Davis et al., 2006). The final **Energy and Emissions ID** indicators were: annual household energy cost, per capita emissions, and the viability of a district energy system for the proposed design (Figure 3, top).

2.2.2. Neighbourhood Travel ID

The **Neighbourhood Travel ID** was developed in two steps: constructing a neighbourhood-scale transportation model, and developing an engaging suite of indicators.

It is well understood that the built environment influences an individual's travel choices (Ewing and Cervero, 2010). However, the degree to which the built environment influences travel patterns is a topic of ongoing research. Following the comprehensive review by Ewing and Cervero, and given the constraints over what could be inventoried during a design exercise, two neighbourhood attributes were accounted for in the model: density (population), and diversity (population and jobs mix). Baseline travel patterns were derived from a local trip diary (travel mode, daily trips per person) and Community Energy and Emissions Inventory (annual vehicle kilometers traveled per person) documents. These variables, along with the **live metrics** for density and design, formed the model input that utilized elasticity values outlined by Ewing and Cervero.

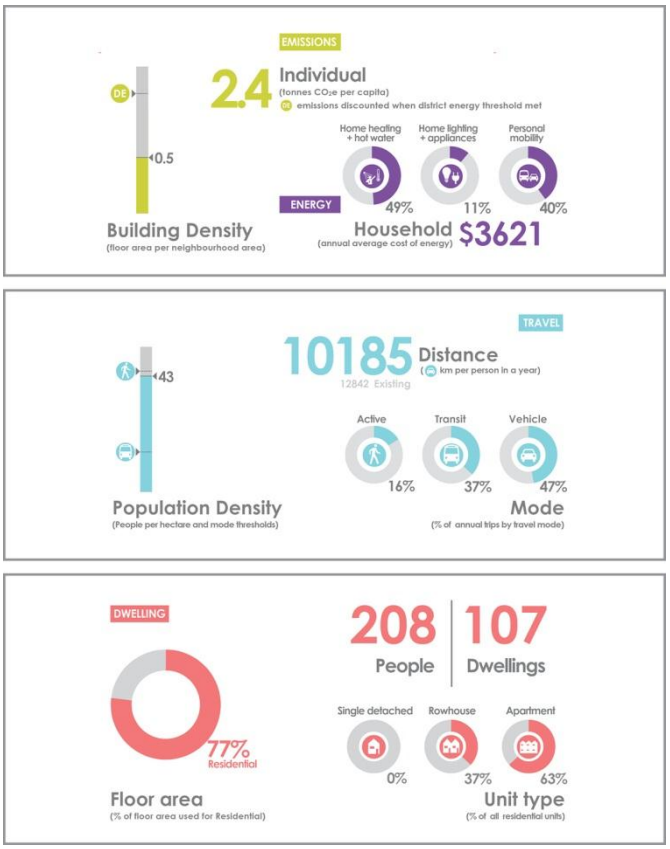

Figure 3. This figure shows static representations of the Indicator Dashboards (ID). From the top: Energy + Emissions ID, Neighbourhood Travel ID, Dwelling Diversity ID.

Three different indicators ultimately formed the visualization for the **Neighbourhood Travel ID**: 1) travel

mode, described by daily trips dedicated to active, public, and vehicle transport, 2) annual vehicle kilometers travelled per person, and 3) active and public transit viability of the proposed neighbourhood design (Figure 3: middle).

2.2.3. Housing Diversity ID

The development of the **Housing Diversity ID** was relatively straightforward, as the desired indicators were already contained within the online database (elementsdb). The database contains comparably modeled and measured cases, including information such as dwelling type and floor area by use. This information is indexed and combined with previously defined *calculation parameters* (e.g., census-derived population density per dwelling type, and floor area per job estimates) to provide the needed input for the **Housing Diversity ID** calculations. The final suite of indicators were: percentage of detached, attached, and stacked dwellings, floor area by land use type, and the total number of people and jobs in the neighbourhood design.

3. DISCUSSION

The development of a touch-table planning support system with an infographic dashboard has been described in this paper. The challenges associated with development were communicating complex urban planning principles to non-professionals and sourcing reliable data to properly define model parameters. For example, relationships between the built environment and emissions have been studied in large metropolitan areas and adapting these findings to small communities remains untested. Furthermore, the indicators chosen for this project are targeted to specific exercises and the degree to which they were understood awaits further study.

4. NEXT STEP

Through this research we hope to gain a better understanding of whether similar engagement exercises cultivate greater acceptance of land use planning that targets emissions reductions. In particular, we hope to track and evaluate if and how individual values evolve when participants are provided with explicit information linking built form, land use, transportation and a City's emissions. Further steps are needed to validate the model and legibility of graphical output. In particular, comparing model results to empirical data will form the basis for improving model accuracy. Lastly, we hope to interrogate the legibility of the Infographic Dashboards to the intended audience.

References

Antle, A. N., Bevans, A., Tanenbaum, J., Seaborn, K., & Wang, S. 2011. Futura : Design for Collaborative Learning and Game Play on a Multi-touch Digital Tabletop. Proceedings of the fifth international conference on Tangible, embedded, and embodied interaction. 93–100.

CHERUBINI, F., BARGIGLI, S., AND ULGIATI, S. 2008. Life cycle assessment of urban waste management: Energy performances and environmental impacts. The case of Rome, Italy. Waste management 28.12: 2552-2564.

CODOBAN, N., AND KENNEDY, C.A. 2008. Metabolism of neighborhoods. Journal of urban planning and development 134.1: 21-31.

CRANG, M., AND GRAHAM, S. 2007. Sentient Cities: Ambient intelligence and the politics of urban space. Information, Communication & Society 10.6: 789-817.

Ewing, R., and Cervero, R. 2010. Travel and the Built Environment: A Meta-Analysis. Journal of the American Planning Association 76.3: 265-294.

Fernquist, J. 2010. A collaborative planning support system for a multi-touch tabletop. Master's thesis, The University of British Columbia.

Kammeier, H.D. 1998. A computer-aided strategic approach to decision-making in urban planning: an exploratory case study in Thailand. Cities 15.2: 105-119.

Kellett, R., Christen, A., Coops, N., van der Laan, M., Crawford, B., Tooke, R., Olchovski, I. 2011. A systems approach to carbon cycling and emissions modeling at an urban neighborhood scale. Landscape and Urban Planning. 45.33:6057-6069.

Norman, J., MacLean, H., and Kennedy, C. 2006. Comparing high and low residential density: Life-cycle analysis of energy use and greenhouse gas emissions. Journal of Urban Planning and Development. 132.1: 10-21.

Scott, S., Grant, K., and Mandryk, R. 2003. System guidelines for co-located, collaborative work on a tabletop display. Proceedings of the 2003 ECSCW. 159–178

Su, T. 2011. A multi-display collaborative urban planning system with a federated architecture. Master's thesis, The University of British Columbia.

van der Laan, M. 2011. Scaling urban energy use and greenhouse gas emissions through LiDAR. Master's thesis, The University of British Columbia.

Wilken, R. 2008. Mobilizing place: Mobile media, peripatetics, and the renegotiation of urban places. Journal of Urban Technology 15.3: 39-55.

Session VIII

Solutions for Scalability in Building Information Modeling and Simulation-Based Design 197
Sixuan Wang, Gabriel Wainer, Rhys Goldstein, Azam Khan
Carleton University, Autodesk Research

Evaluation of Indoor Climate in Low Energy Houses 205
Liesbeth Staepels, Griet Verbeeck, Staf Roels, Liesje Van Gelder, Geert Bauwens
PHL University College / Hasselt University, KU Leuven, Belgium

HubPod: Integrating Acoustic Simulation in Architectural Design Workflows 213
Brady Peters, Jane Burry, Nicholas Williams, and Daniel Davis
Royal Danish Academy of Fine Arts, Royal Melbourne Institute of Technology

Solutions for Scalability in Building Information Modeling and Simulation-Based Design

Sixuan Wang[1], Gabriel Wainer[1], Rhys Goldstein[2], and Azam Khan[2]

[1]Dept. of Systems and Computer Engineering,
Carleton University
1125 Colonel By Dr. Ottawa
ON K1S 5B6, Canada
{swang, gwainer}@sce.carleton.ca

[2]Autodesk Research
210 King St. East, Toronto
ON M5A 1J7, Canada
{firstname.lastname}@autodesk.com

Keywords: Scalability, IFC, MDA, DEVS, Remote Simulation

Abstract

Simulation-based design can enable a number of advanced architectural and engineering applications, such as energy modeling, occupant behavior prediction, or structural integrity analysis. To help make simulation-based design practical, scalability in terms of data and computation is needed. By using a Model-Driven Architecture (MDA) approach—together with the RISE (RESTful Interoperability Simulation Environment) web interface—a generic scalable simulation design framework is presented. In our system, Building Information Modeling (BIM) data is represented in the Industry Foundation Classes (IFC) open standard from which Domain Specific Models (DSM) may be extracted for particular applications. The open RISE interface to a DEVS (Discrete Event System Specification) simulation provides computational scalability. We present a case study in which our system is applied to an evacuation model of a multi-floor building. We also show a 3D visualization of the simulation results to support further decision making. By enabling designers to extract information automatically from IFC and run simulations remotely, this kind of scalable system makes simulation a viable part of the design process.

1. INTRODUCTION

Buildings are multidisciplinary endeavors that cover many specialties, including architecture, engineering, construction, and operations. Therefore, building simulation has also been specialized into a number of areas, such as lighting, thermodynamics, occupancy, advanced control systems, computational fluid dynamics, structural finite element methods, and other modeling domains. Historically, independent efforts have led to simulation solutions appropriate for each individual domain. However, recent research has examined methods for integrating prior work for whole building simulation (Hensen 2002). Several important benefits may result from this systems perspective, such as the handling of interactions between solvers (Wang et al. 2012). For example, an occupancy solver may feed into a simulated building control system that also senses the radiant heating effects from a thermodynamics solver to provide an analysis of occupant comfort.

A key challenge in adopting a systems approach is scalability (Duboc et al. 2012) in terms of the size and complexity of the models that supply building simulations with site-specific information, the computational requirements of simulations involving multiple building domains, and the feasibility of integrating whole building simulation into the design process. Addressing these challenges will require a change in the technologies and techniques currently used to perform simulation-based design. First, the use of a file-based Building Information Model (BIM) usually impedes collaboration between designers due to its complication and redundancy (Won and Lee 2011; Hetherington et al. 2011). Second, current simulation tools do not adequately address the discrepancy between comprehensive BIM standards such as the Industry Foundation Classes (IFC) and the input data that is actually required by simulation models of individual building domains (Hitchcock and Wong 2011; Jiang et al. 2012). Third, running simulations on single-user workstations fails to take advantage of high performance server-based computing, thin clients and web services technology (Ribault and Wainer 2012; Al-Zoubi and Wainer 2010). Fourth, the separation of design tools and analysis tools

denies designers the interactivity required to fully benefit from building simulation results (Wang et al. 2012).

In this paper, we demonstrate solutions to each of the four scalability issues listed above. We first propose a generic process framework for integrating all the solutions in the simulation-based design cycle. As an alternative to file-based BIMs, we explore the database approach of BIMserver.org as a tool for simulation-based design. To address the discrepancy between IFC and the domain specific information required by simulation models, we adopt the Model-Driven Architecture (MDA) approach from the field of software engineering. As an alternative to running simulations on single-user workstations, we use web services technology to exploit computing resources on remote servers. Finally, we demonstrate how visualizations of simulation results can be implemented within existing BIM authoring tools. These solutions can enable designers to extract information selectively from a standard IFC file into a specific simulation model, run the simulation remotely, and then visualize the 3D simulation results for making decisions or planning a next design iteration.

A variety of methods can be used to develop Modeling and Simulation (M&S) applications. Among them, we are interested in exploring the use of the Discrete Event System Specification (DEVS) formalism (Zeigler et al. 2000) for building discrete event systems with models composed of behavioral (atomic) and structural (coupled) components. Cell-DEVS (Wainer 2009) extends DEVS by supporting cellular models in a spatial lattice. For remote simulation, we reuse the RISE (RESTful Interoperability Simulation Environment) (Al-Zoubi and Wainer 2010) as a simulation middleware to support RESTful-CD++ web services for remote simulation.

The integration of building information collection from BIM, simulation with Cell-DEVS, and visualizations of simulation results in BIM authoring tools have been presented in previous work (Wang et.al. 2012). Here, we demonstrate these solutions in conjunction with the MDA approach and RISE remote simulation, which are the primary contributions of this paper. The model-driven architecture (MDA) proposes a development paradigm to handle the increasing complexity of the building models. MDA is based on developing both platform independent and specific models from which executable code can be generated in an automatic/semi-automatic way (Sanchez et al. 2008). MDA uses multilayer meta-models with different abstraction levels for interoperability. In the context of building information modeling, MDA involves the use of a separate Domain Specific Model (DSM) for each building simulation domain. There are also many model transformation techniques which can automatically/semi-automatically generate models between upper models or DSMs (Wang et al. 2011). A comprehensive IFC representation of a building is transformed into each DSM, a process that filters out irrelevant data and resolves inconsistencies between IFC and simulation-specific building representations. An emergency planning example is presented to illustrate this transformation of data, and to highlight the role of all four solutions in a design workflow.

We begin with the literature review. Then we represent the generic scalability BIM&S framework, followed by details of each step, focusing on how to extract information and build DSM simulation model. Section 5 illustrates a case study of evacuation simulation.

2. LITERATURE REVIEW

BIM technologies have been widely adopted in the Architecture, Engineering, and Construction (AEC) industry for 3D-rendering, drawing extraction, estimation of cost, and emergency detection (Eastman et al. 2008). At present, there are numerous BIM software applications, including Autodesk Revit Architecture, Autodesk 3Ds Max, Bentley Architecture, and Graphisoft ArchiCAD. Striving for interoperability and standardization between different domains, various BIM standards have been created, such as DSF, STEP, IFC, gbXML, and SAT. IFC, proposed by buildingSMART International, enables different users to build models for lighting, shading, HVAC engineering, and various other AEC domains. The IFC hierarchy covers the core project information such as building elements, geometric and material properties of building products, and so on (Fu et al. 2006). The current popular standard is Ifc2x3 (the next version Ifc2x4 is in development). Ifc2x3 has 653 entities, 317 property sets and 164 enumerations (Hetherington et al. 2011).

Existing simulation processes are not fully integrated into the design life cycle. Various scalability issues have arisen when integrating standard BIM tools and simulation software. Firstly, the standard BIM file is too complicated and too highly redundant to understand and query (Lipman 2010; Hetherington et al. 2011). Take IFC as an example; it

intends to connect all design domains into one file, which covers a vast amount of information from various project participants. To make the standard BIM file consistent and reliable, lots of implicit information is added. The size of the IFC file grows and it needs more time to manipulate. Because each individual participant usually requests partial information (Won and Lee 2011), less experienced designers need more time to learn the structure of the IFC file for finding the exact information needed. Though some BIM tools allow users to select, edit or trim the IFC model (e.g. SimpleBIM, Model Checker, or BIMsight), IFC data is often file-based and hard to parse or query (Beetz et al. 2011). We still need an automatic and scalable way to reduce and query the IFC file efficiently.

Furthermore, the integration process lacks explicit support for specific simulation information (Malinowsky et al. 2010; Jiang et al. 2012). Simulations for different scenes are mostly domain-specific, which normally have different syntax, structure, and semantics compared with the standard files. Even when standards are broad, any single file does not cover all the special tasks during the simulation process. Besides, people tend not to support standards that might affect their existing implementation or threaten their dominant market positions (Wainer et al. 2010). In fact, building design and simulation are two independent domains. To solve the first two issues, in (Fu et al. 2006), the authors introduced a concept of "3D to nD Modeling", encouraging designers using multi-issues (specific domains) of design information to reduce the uncertainties and realize true "what-if" analysis. One solution is to use Model View Definitions (MVD) to facilitate automated querying from the IFC model, which is a subset of IFC (Lipman 2010). However, MVD is dependent on its implementation, and an IFC model may not cover all needed simulation information. Alternatively, in (Jiang et al. 2012; Beetz et al. 2011), the authors suggest using an MDA to parse the IFC file into its own pre-defined data structure DSM based on the Eclipse Model Framework (EMF). We can use XML and meta-models to manage the IFC data using MDA tools, then easily load, query and filter the IFC data.

Most modeling and simulation methods run on single-user workstations (Ribault and Wainer 2012), which normally require too much time for installation and configuration of all the software and dependencies needed for simulation. It is better to remotely access simulation resources with web services (Jiang et al. 2012), improving scalability (e.g., accessibility, availability and interoperability). In this way, users can reuse and share simulation resources on site without worrying about the capability of their local machine CPU or memory. Plus, with distributed simulation technologies, simulations can be executed on distributed computers via communication networks, which can further speed up the execution time (Al-Zoubi and Wainer 2010). SOAP-based Web Services use the Remote Procedure Call (RPC) to allow two distributed heterogeneous systems to call the functions of each other; but this exposes the implementation details and lacks scalability (Al-Zoubi and Wainer 2010). Another choice, RESTful Web Services, can solve these issues. Access to RESTful Web Services is through Web resources (URIs) and XML messages using uniform HTTP operations (GET, PUT, POST and DELETE). Based on these ideas, in (Al-Zoubi and Wainer 2010), the authors presented the RESTful Interoperability Simulation Environment (RISE) middleware. The main objective of RISE is to support interoperability and mash-ups of distributed simulations regardless of the modeling formalism, programming language, or simulation engine.

3. GENERIC SCALABLE BIM&S FRAMEWORK

The design phase has several iterative cycles through alternative simulations. In order to increase scalability, we propose the Generic Scalable BIM&S Framework, which is shown in Figure 1. The IFC file acts as a core information repository, whilst DSMs act as a bridge between the standard IFC model and the specific simulation demands.

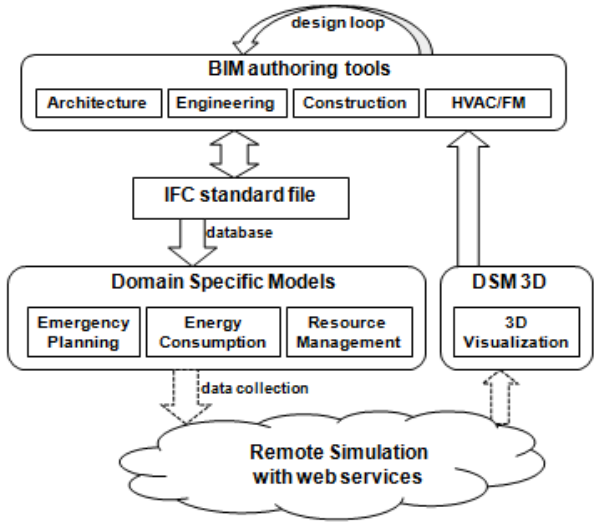

Figure 1. Generic Scalable BIM&S Framework

Generally, the process is as follows: 1) At the beginning of each cycle, various design teams collaborate and share multidisciplinary design information. They use a number of BIM authoring tools for CAD drawings, which are object-oriented, attribute-driven with 3D geometric information. 2) These BIM authoring tools support the use of an IFC standard file that acts as a core information repository for collaborating and communicating. Nowadays, several BIM tools support this step for sharing and collaboration. BIMserver.org is a model-driven open-source server that adopts EMF to represent the IFC data. In this paper, we use it to manage and query the IFC file. 3) The IFC standard file then is parsed by EMF using the MDA approach and stored in a relational database. EMF includes a meta-model (Ecore) for describing models and runtime support (e.g., XMI serialization, efficient query API, etc.). This characteristic of manipulating EMF objects generically allows us to build DSMs for specific simulation demands. A DSM can contain different syntax, structure, and semantics than the corresponding IFC file. 4) After collecting data from the DSM, all the necessary inputs are uploaded to remote simulation resources with web services. Then users can retrieve the results after simulation completion. Here we use RISE (RESTful Interoperability Simulation Environment middleware). 5) Then, the simulation results are parsed to a DSM model for 3D visualization, with special visualization features developed in the BIM authoring tools.

4. IFC & DEVS REMOTE SIMULATION

Figure 2 shows the concrete steps for integrating IFC and DEVS remote simulation by employing the proposed Generic Scalable BIM&S Framework.

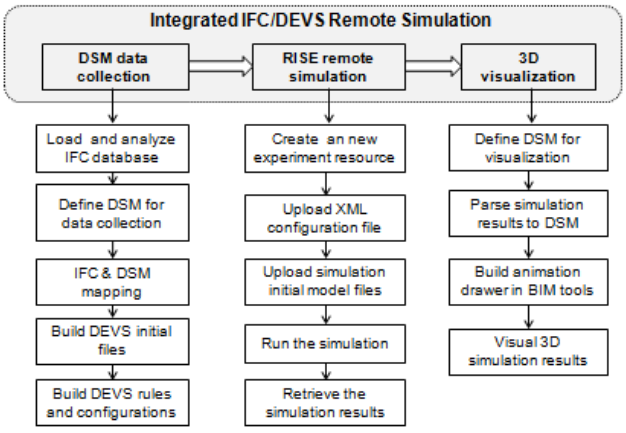

Figure 2. Integrated IFC and DEVS remote simulation

It is composed of three phases: DSM data collection, RISE remote simulation, and DSM visualization. These phases constitute a subset of the design cycle, with detailed operations shown in Figure 1. In the DSM data collection phase, we load and analyze the IFC database, define our DSM for a certain specific simulation, then find the mapping between IFC and the DSM and build initial files for the remote simulation. Then we follow the API of RISE, creating resources, uploading files, executing the simulation, and retrieving results. Next, we parse the simulation results and visualize them back in certain BIM authoring tools. Here we will elaborate on the most important operations in this process.

4.1. Industry Foundation Classes (IFC)

The IFC hierarchy covers the core project information, such as building elements, the geometric and material properties of building products, and so on (Fu et al. 2006). The most abstract entity in the IFC model is *IfcRoot*, which is in the kernel and provides attributes for the identification, ownership, and self-description of all sub-entities. Figure 3 is a hierarchical diagram of a part of the Ifc2x3 EXPRESS standard under *IfcRoot*, which is also similar to Ifc2x4.

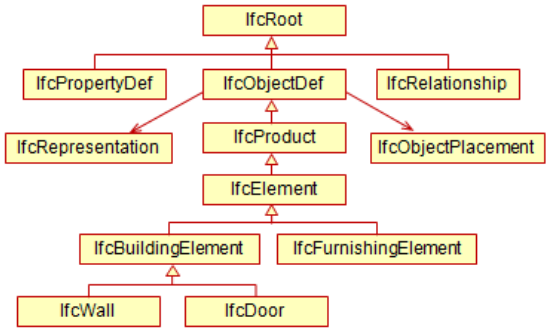

Figure 3. Part of the IFC hierarchy under IfcRoot

As we can see, *IfcRoot* is the parent for three subtypes, *IfcObjectDef* (generalizing any object or process), *IFcPropertyDef* (defining characteristics to entities), and *IfcRelationship* (describing relationship between entities). All these elements are identified from the super-class *IfcObjectDef*. The building elements category has fifteen groups of elements (e.g., walls, doors, stairs, beams, columns, etc.). Each element inherits attributes from all of its parent entities, such as geometric representation information (*IfcObjectPlacement* and *IfcRepresentation*). *IfcObjectPlacement* stores the placement information of an object. It contains the coordinates (x,y,z) which could be

absolute (relative to the global coordinate system), relative (relative to the *IfcObjectPlacement* of another object), or constrained (relative to the grid axes). *IfcRepresentation* stores the shape representations of an object. There are two geometric shape representations: 1) the explicit geometric representation of the shape (i.e., points, curves, surfaces, and solid boundaries; for example, a wall could be defined with 8 points, 12 edges and 6 surfaces.); and 2) the attribute-driven representation of the shape (i.e., extruded profiles, directions, length, and width; for example, a wall could have length, width and height).

Each specific element could have particular attributes inherited from *IfcObjectPlacement* and *IfcRepresentation*, such as *IfcWall* presented in Figure 4.

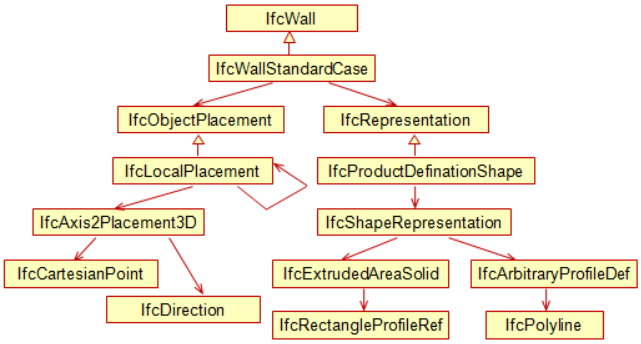

Figure 4. Building element example IfcWall

Inherited from *IfcWall*, *IfcWallStandardCase* contains the standard information of each wall. *IfcWallStandardCase* contains *IfcLocalPlacement* and *IfcProductDefinationShape* (the subclass of *IfcRepresentation*). *IfcLocalPlacement* could have not only the attribute of *IfcAxis2Placement3D* with *IfcCartesianPoint* (coordinates) and *IfcDirection* (the trend of spreading) that are relative to the global coordinate system, but also could have the reference of another *IfcLocalPlacement* with relative coordinates. *IfcProductDefinationShape* contains *IfcRectangleProfileRef*, with length, width and height, and *IfcPolyline,* with boundary points. In other words, *IfcLocalPlacement* represents the starting point, while *IfcProductDefinationShape* indicates where we can place it (in which way and how far). Assume a wall with length, width and height of (8"x2"x4") starts from (3, 2, 1) towards the direction of the Y axis with its length, the X axis with its width and the Z axis with its height. The point diagonally opposite the starting point would then be (x-width, y+length, z+height) = (1, 10, 5).

4.2. Domain Specific Models (DSM)

From the above analysis, we can see the generality and complexity of IFC, which might not cover all the requirements of a specific simulation. More importantly, there may be inconsistencies of syntax, structure and semantics. Hence, we propose the use of the MDA approach to represent the model for specific simulations and to extract/map/build DSMs from IFC data. Figure 5 shows an example of a DSM for this purpose.

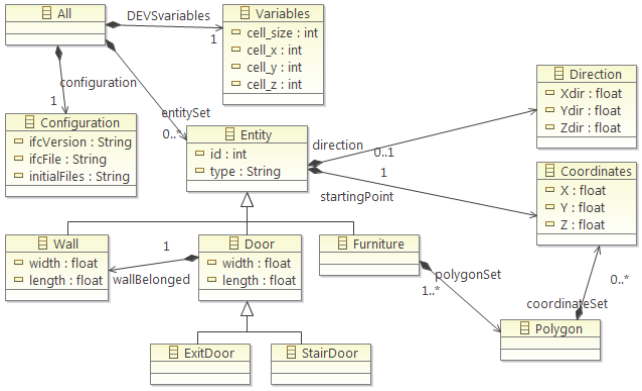

Figure 5. An example of DSM for simulation

This particular DSM is meant for tracking simulated occupants as they move through a building. Using a Cell-DEVS model, the simulated occupants move along a lattice of cells that facilitates pathfinding and collision avoidance. The class *All* consists of *Configuration*, *Variables* and *Entities*. *Entity* is the super-class for all other sub-entities, consisting of attributes of ID (sequence number), type (e.g., materials, size) and references to a direction and a starting point with absolute coordinates. *Entity* can generalize *Wall*, *Door* and *Furniture*. Apart from inherited attributes, both *Wall* and *Door* have width and length attributes. *Door* has two subclasses of *ExitDoor* and *StairDoor*. Due to the irregularity of *Furniture*, it can have a set of *Polygon*s with the coordinates of turning points. *Configuration* and *Variables* are specific information for DEVS/Cell-DEVS simulations, like ifcVersion, ifcFile, initialFiles, numbers and units of lattice cells, etc.

In order to collect the necessary data, we need to find the mappings of elements from IFC to the entities of the DSM, shown in Table 1. As we can see, they look similar but they have differences of syntax and semantics. The DSM is more compact and smaller. The class names are similar but not exactly the same (*Wall* vs. *IfcWall*), and attributes of these

classes are not identical; for example the Wall in the DSM is a subset of the combination of *IfcWall* (ID and type) and *IfcRectangleProfileRef* (width and length). One of the biggest differences is between *Direction* and *Coordinates*. In DSM all attributes are absolute to a global coordinates system, while in IFC there are different levels of relative coordinates, which require converting from relative coordinates to absolute coordinates.

DSM	IFC
Entity	IfcElement
Wall	IfcWall, IfcRectangleProfileRef
Door	IfcDoor, IfcRectangleProfileRef
Furniture	IfcFurnishingElement, IfcPolyline
Direction	IfcLocalPlacement, IfcCartesianPoint
Coordinates	IfcLocalPlacement, IfcDirection

Table 1: Mappings examples between DSM and IFC

In current implementation, Figure 6 illustrates the main classes of this DSM Data Collection tool (for clarity, the data model classes are not presented, i.e., the IFC elements in Figure 3 or DSM entities in Figure 5).

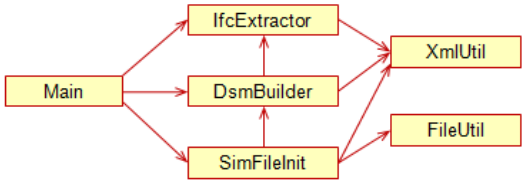

Figure 6. Part of Class Diagram of DSM Data Collection

Main takes control of the data collection process. As mentioned before, MDA technologies can parse the IFC file into a database with a UML class hierarchy based on EMF, from which we can query and filter more easily. *IfcExtractor* uses related APIs in the open source BIMServer.org. It loads the IFC data model into a database for extracting necessary information (e.g., wall, doors, furniture). *DsmBuilder* is responsible for constructing the defined DSM instance based on the extracted information and mappings list in Table 1. For example, to construct the *Wall* in DSM, we query ID and type from *IfcWall* and width and length from *IfcRectangleProfileRef*. Then, *DsmBuilder* serializes this DSM with the XMI (or, more general, XML) format for scalability and simplicity by calling *XmlUtil*. *SimFileInit* enables us to build the initial files for the specific simulation automatically. The macro variables could be calculated with size/number of cells and coordinate boundaries. The basic idea of initializing the state of each cell is to include all needed elements according to their type priorities (e.g. wall, furniture, stair, door). For each type, we find all elements belonging to it; for each element, we calculate all passing coordinates according to its starting coordinates and attributes (e.g. directions, length, width). Finally, we assign the state value to the cells that hold these coordinates.

In reality, IFC and other DSMs could have lots of many-to-many relationships or semantic inconsistencies that make it difficult to find mappings. To accommodate a DSM that represents the real world in a fundamentally different way than IFC, this work could be expanded using existing model transformation techniques in MDA. In (Roman et al. 2010), a semi-automatic framework is presented to build mappings of two meta-models and perform run-time model transformation automatically. In (Wang et al. 2011), a platform-independent approach towards semantic interoperability is proposed to analyze various kinds of semantic inconsistencies (type, scale, precision, synonym, homonym, granularity, and coverage), and address many-to-many mappings using heuristic similarity analysis.

4.3. Restful Interoperability Simulation Middleware

As discussed in previous sections, RESTful Web Services can further increase the scalability in terms of the plug-and-play interoperability and availability. In (Al-Zoubi and Wainer 2010), the authors presented the first existing RESTful Interoperability Simulation Environment (RISE) middleware. RISE is accessed through Web resources (URIs) and XML messages using HTTP methods. Implementations can be hidden in resources, which are represented only via URIs. Users can run multiple instances as needed, which are persistent and repeatable by specific URIs. The HTTP methods are typical four types: GET (to read a resource), PUT (to create or update a resource), POST (to append data to a resource), and DELETE (to remove a resource). An interface between RISE and CD++ allows running DEVS/Cell-DEVS distributed simulations. RISE API likes a classic URL http://www.example.com/cdpp/sim/workspaces, attached with the following services:

- **../{userworkspace}/{servicetype}/{framework}** allows interacting with a framework (including the simulation's initial files, configuration and src code).
- **../{userworkspace}/{servicetype}{framework}/simulation** interacts with the simulator execution.
- **../{ userworkspace}/{servicetype}/{framework}/results** contains the simulation outputs.

For a specific simulation, we can realize the remote simulation by using these URIs with HTTP methods. For example, after getting initial model and configuration files for simulation, we use PUT to create a framework with the configuration file and POST to upload these initial model files to this framework. Then, this newly created simulation environment can be executed by using PUT to *{framework}/simulation*, then we wait for the simulation to finish and GET the simulation results files from *{framework}/results*.

4.4. 3D Visualization

3D visualization provides a way to obtain visual simulation results in BIM authoring tools, enabling the designers to check the performance of the current design, find the flaws, and redesign for a next iteration cycle. The main reason for using 3D rather than 2D is that it is more intuitive and attractive. Most BIM authoring tools support full-featured 3D visualizations of buildings. Among them, Autodesk 3ds Max is a powerful BIM tool for its animation and rendering ability for 3D visualization. The IFC file can be easily imported into 3ds Max, what we want is to view the simulation results superimposed on the building model. To do this, we continue using MDA technologies, by parsing the results into a DSM that contains necessary but minimal information about changes to cells locations and values. Then we build a GUI written in MAXScript, enabling the user to load the parsed file and Cell-DEVS model. Finally we visualize it in 3ds Max using our advanced plug-in with different animation models.

5. CASE STUDY: EVACUATION PLANNING

In this section, we show a case study of evacuation planning by employing the proposed framework. We adapted and updated our previous work (Wang et al. 2012). In recent years, studying emergency evacuation has become an important design step for successful construction projects, which aims to analyze bottlenecks in order to minimize evacuation time. To do so, we applied the integration method proposed in this paper. It uses a Cell-DEVS model of the evacuation process of a multi-floor building. The current implementation uses the CD++ toolkit as the Cell-DEVS modeling environment, RISE as the remote simulation middleware, Autodesk Revit Architecture and Autodesk 3ds Max for the BIM tools, and BimServer.org for IFC data management and MDA. When an iteration cycle starts, designers from different domains could use BimServer.org to share their collaboratively developed IFC model. They could find the newest version of the IFC and load it into Revit, as shown in the left side of Figure 7.

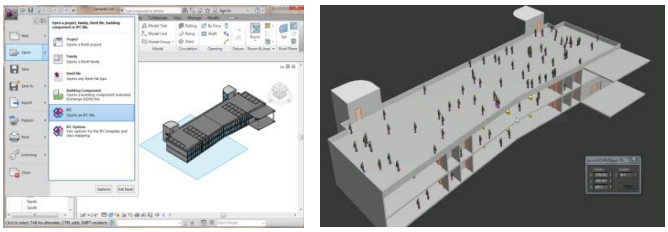

Figure 7. IFC loading in Revit (left) and 3D in 3ds Max (right)

Then analysts load the IFC file into an EMF database and extract data from it into a DSM model using our developed tool, which is currently specific to multi-floor evacuation. Figure 8 shows a part of the results of a DSM XMI file (an instance of the DSM presented in Figure 5) after the data extracting from IFC. It consists of all needed simulation information from the building. As we can see, it records the information for configuration (e.g., *ifcVersion*, *ifcFile* and *initialFiles* names), DEVS variables (e.g., *cell_size* with 24, the number of cells in dimensions of 109x43x3), and all needed entity information (e.g. *Wall, Door, Furniture*). For example, the Wall shown in Figure 8 has *id* (19564), *width* (0.67), *length* (12.0), *startingPoint* (-48.3, 20.3, 24.0) and *direction* (-1.0, 0.0, 0.0, which means its length is oriented towards the negative X axis).

```
<?xml version="1.0" encoding="ASCII" ?>
- <EVA:All xmi:version="2.0" xmlns:xmi="http://www.omg.org/XMI"
    xmlns:xsi="http://www.w3.org/2001/XMLSchema-instance" xmlns:EVA="http://eva/1.0"
    xsi:schemaLocation="http://eva/1.0 DSM.ecore">
    <configuration ifcVersion="Ifc2x3" ifcFile="eva.ifc" initialFiles="eva.val; eva.inc; eva.ma" />
    <DEVSvariables cell_size="24" cell_x="109" cell_y="43" cell_z="3" />
  - <entitySet xsi:type="EVA:Wall" id="195643" type="Basic Wall:Generic - 8":249" width="0.6666667"
      length="12.0">
      <startingPoint X="-48.333332" Y="20.333334" Z="24.0" />
      <direction Xdir="-1.0" Ydir="0.0" Zdir="0.0" />
    </entitySet>
  - <entitySet xsi:type="EVA:Door" id="181862" type="36" x 84"" width="0.0" length="3.0">
      <startingPoint X="4.9112697" Y="-5.993986" Z="12.0" />
      <direction Xdir="-1.0" Ydir="0.0" Zdir="0.0" />
    - <wallBelonged>
        <startingPoint X="4.577936" Y="19.4317" Z="12.0" />
        <direction Xdir="0.0" Ydir="-1.0" Zdir="0.0" />
      </wallBelonged>
    </entitySet>
  - <entitySet xsi:type="EVA:Furniture" id="181832" type="96" x 96"">
    - <polygonSet>
        <coordinateSet X="-36.333336" Y="-11.833333" Z="2.5" />
        <coordinateSet X="-36.333336" Y="-9.833333" Z="2.5" />
        <coordinateSet X="-33.333336" Y="-11.833333" Z="2.5" />
      </polygonSet>
    + <polygonSet>
    </entitySet>
</EVA:ALL>
```

Figure 8. DSM instances of evacuation simulation after IFC extracting

Based on the DSM XMI file, the tool can initialize the files for the remote simulation, including *.val (initial values of each cell) and *.inc (macro variables). With the RISE server, we can use the PUT method to create a

framework for the evacuation simulation, and the POST method to upload the initial model files. We can run this simulation by using PUT to *evacuation/simulation*. We wait until the simulation finishes, then GET simulation results files from *evacuation/results*. Finally, after parsing the simulation log file into a DSM for the specific 3D visualization, we can load the same version of the IFC file in 3ds MAX and visualize the simulation animations with the help of its GUI. The right part of Figure 7 shows how the 3D visualization would look. According to the performance observed from 3D visualization, all steps are scalable and easily repeated for multiple design iterations.

6. CONCLUSION

To solve the scalability issues that arise when integrating BIM and simulation, we have proposed a Generic Scalable BIM&S Framework using the IFC standard, DSMs generated with a MDA approach, RISE middleware, and 3D visualization. We developed a tool for extracting information from IFC, building DSMs, and constructing the initial simulation files. Our case study uses a Cell-DEVS model of the evacuation process of a multi-floor building, using Autodesk Revit, BimServer.org, CD++, RISE, and Autodesk 3ds Max. The study shows that this kind of system can enable designers to extract information automatically from IFC into a specific simulation model, and run the simulation remotely through web services. Finally, designers can visualize the 3D simulation results in a BIM authoring tool to make further decisions or plan the next design iteration. Some future directions for this work are to use MDA model transformation techniques to automatically find mappings to provide a one-stop workflow to automate the entire proposed process.

References

Ahmed, A., Wainer, G., and Mahmoud, S. 2010. Integrating Building Information Modeling & Cell-DEVS Simulation. In Proceedings of SimAUD 2010. Orlando, FL

Al-Zoubi, K., and Wainer, G. 2010. Distributed Simulation using RESTful Interoperability Simulation Environment (RISE) Middleware. Intelligence-Based Systems Engineering, pages 129–157.

Beetz, J., Berlo, L.V., Laat, R.D., and Bonsma, P. 2011. Advances in the Development and Application of an Open Source Model Server for Building Information. In Proceedings of the CIP W78 conference, Nice.

Duboc, L., Leiter, E., and Rosenblum, D. 2012. Systematic Elaboration of Scalability Requirements through Goal-Obstacle Analysis. IEEE transactions on software engineering

Eastman, C., Teicholz, P., Sacks, R., and Liston, K. 2008. BIM Handbook. Wiley & Sons.

Fu, C., Aouad, G., Lee, A., M-Ponting, A., and Wu., S. 2006. IFC model viewer to support nD model application. 2006 Automation in Construction, 15 (6), pp. 178-185.

Hensen, J. L. M. 2002. Simulation for performance based building and systems design: some issues and solution directions. In Proc. of 6th Int. Conf. on Design and Decision Support Systems in Architecture and Urban Planning, TUE, NL.

Hetherington, R., Laney, R., Peake, S., and Oldham, D. 2011. Integrated Building Design, Information And Simulation Modelling: The Need For A New Hierarchy. In: Building Simulation 2011, Sydney, Australia. November 2011.

Hitchcock, R. J., and Wong, J. 2011. Transforming Ifc Architectural View Bims for Energy Simulation: 2011. Proceedings of Building Simulation.

Jeong, Y.S., Eastman, C.M., Sacks, R., and Kaner, I. 2009. Benchmark tests for BIM data exchanges of precast concrete. 2009 Automation in Construction, 18 (4), pp. 469-484.

Jiang, Y., Ming, J., Wu, D., Yen, J., Mitra, P., Messner, J. I., and Leicht, R. 2012. Bim Server Requirements to Support the Energy Efficient Building Lifecycle. In 2012 ASCE in civil engineering.

Lipman, R.R. 2010. Developing Coverage Analysis For Ifc Files. Proceedings of the CIB W78 2010: 27th International Conference.

Malinowsky, B., and Kastner, W. 2010. Integrating Process Communication in Building Information Models with IFC and LON. 8th IEEE International Workshop on Factory Communication Systems.

Ribault, J., and Wainer, G. 2012. Simulation process In the Cloud For Emergency Planning. 12th IEEE/ACM International Symposium on Cluster, Cloud and Grid Computing.

Roman, D., Morin, B., Wang, S. and Berre, A. J. 2010. A Model-driven Approach to Interoperability in B2B Data Exchange. Advanced results in MDI/SOA innovation Workshop, MDI.

Sanchez, P., Barreda, J., & Ocon, J. 2008. Integration of domain-specific models into a MDA framework for time-critical embedded systems. In Intelligent Solutions in Embedded Systems, pp. 1-15. IEEE.

Wainer., G. 2009. Discrete-event Modeling and Simulation: a Practitioner's Approach. CRC/Taylor & Francis.

Wainer, G., Al-Zoubi, K., Dalle, O., Mittal, S., Martín, J., Sarjoughian, H., Zeigler, B.P. 2010. Standardizing DEVS Simulation Middleware. Ch. 18, Discrete-Event Modeling and Simulation: Theory and Applications. Eds G. Wainer, P. Mosterman. CRC Press. Taylor & Francis.

Wang, S., Morin, B., Roman, D., and Berre, A.J. 2011. A Semi-automatic Model Transformation Approach for Semantic Interoperability. Proceedings of NATO Symposium & Workshop on Semantic & Domain Based Interoperability. Norway.

Wang, S., Schyndel, M.V., Wainer, G., Subashini, V., and Woodbury, R. 2012. DEVS-based Building Information Modeling And Simulation for Emergency Evacuation. Proceedings of the WSC. Germany. IEEE.

Won, J., and Lee, G. 2011. Algorithm for Efficiently Extracting IFC Building Elements from an IFC Building Model. In Proc. 2011 ASCE workshop on computing in civil engineering.

Zeigler, B.P., Praehofer, H., and Kim, T.G. 2000. Theory of Modeling and Simulation. Academic Press.

Evaluation of Indoor Climate in Low Energy Houses

Liesbeth Staepels[1], Griet Verbeeck[1], Staf Roels[2], Liesje Van Gelder[2], Geert Bauwens[2]

[1]PHL-ARCK Research Group, Department of Architecture,
PHL University College / Hasselt University
Agoralaan, gebouw E,
3590 Diepenbeek, Belgium
liesbeth.staepels@phl.be
griet.verbeeck@phl.be

[2] Division of Building Physics, Department of Civil Engineering,
KU Leuven
Kasteelpark Arenberg 40,
3001 Heverlee, Belgium
staf.roels@bwk.kuleuven.be
liesje.vangelder@bwk.kuleuven.be
geert.bauwens@bwk.kuleuven.be

Keywords: Low Energy, Comfort, Evaluation, Indoor Climate, Dwellings.

Abstract

The aim of the EU EPBD is to realize lower energy consumption in buildings, without neglecting the indoor climate, which can be specified as thermal comfort and indoor air quality. The research analysed 70 recently built dwellings in Flanders, Belgium, with standard execution ranging from low energy efficiency up to and including even energy positive houses. A monitoring campaign was set up to evaluate the indoor environment quality, during both the winter and summer periods.

Both in winter and summer, the temperature in the homes is mostly within comfort boundaries. However, in better insulated dwellings the mean temperature is generally somewhat higher and the deviation is smaller, whereas on warm days the temperature can rise uncomfortably in both living room and bedroom. CO_2 and humidity measurements show good to reasonably good indoor air quality, independently from the type of ventilation system.

1. INTRODUCTION

For the last couple of years, construction has evolved to include better insulation, so buildings consume less energy. The motivation for this trend includes awareness of global warming, exhaustibility of fossil fuels, increasing energy costs, etc.

In the EU, the obligations of the Kyoto Protocol regarding the reduction of energy use and CO_2 emissions resulted in the EU Energy Performance of Buildings Directive (EPBD 2002). This directive imposes requirements on the EU Member States concerning the energy performance of buildings. In 2010 this directive was recast to specify that by 2021 all new buildings have to be Nearly Zero Energy Buildings (Recast EPBD 2010).

In Flanders, Belgium, the EPBD was converted into the EPB legislation in 2006 (EPB now includes Energy Performance and Indoor Climate). Requirements were not only imposed on the energy performance of new buildings, but also on the indoor climate, by means of minimum ventilation rates and control of summer overheating risk. Since then, the requirements have been tightened on a regular basis, in anticipation of the 2021 target for Nearly Zero Energy Buildings. Some individuals, however, did not want to wait for this target and have already chosen to have their buildings perform better than the legal requirements. They have combined several building techniques, like high insulation values, heat pumps, heat recovery, etc., to reduce the energy use of their dwellings. A recent report by the Flemish Government shows that, since the introduction of the EPB legislation, there has been increasing voluntary action to meet energy performance levels beyond legal requirements (Flemisch Energy Agency 2012).

The realization of a better energy performance label for these dwellings makes it possible to study their real energy and comfort performance. Since the EPB legislation also requires a good indoor climate, it is useful to evaluate the comfort of these dwellings, both thermal comfort as well as indoor air quality. Different sources indicate that comfort might be a problem in these type of houses (Verbeeck, Carmans and Martens 2011; KULeuven 2009, 2011). For instance, Verbeeck, Carmans and Martens explain that summer comfort in low energy houses is an important focus

which should now be taken into account during the design of the dwelling to avoid overheating.

The results of this paper are part of a larger research project in which the robustness of the performance of low energy dwellings is studied. Through monitoring and simulations the sensitivity of low energy concepts is evaluated, with regard to their impact on both energy consumption and indoor comfort. The objectives of this research are to define guidelines to create high performance, comfortable and energy efficient dwellings.

In this paper the results of energy efficiency measures on the indoor climate are described. Section 2 presents the dwellings as well as a methodology for the evaluation of the indoor climate, for both thermal comfort and indoor air quality. Sections 3 and 4 present and discuss the main results of the monitoring campaign, for both winter and summer seasons. Finally, in Section 5, conclusions are formulated, together with some initial guidelines for good indoor climate in (very) low energy buildings.

2. METHODOLOGY

2.1. Description of the dwellings

For this research, 70 dwellings were selected, distributed over the Flemish territory. This selection included a wide variety of houses in terms of energy performance, but also in terms of construction methods, building types, installation types, etc. Most of the houses were recently built, mainly just before or after the implementation of the EPB regulation in 2006. Three dwellings were thoroughly renovated to the extent that they can be regarded as new buildings when investigating indoor climate or energy consumption.

With regard to typology: the selection consists of 45 detached, 24 semi-detached and 2 attached houses. 44 dwellings are massive constructions with brick cavity walls and 27 are wood frame constructions. The 3 ventilation types most frequently used in Flanders are represented: 14 dwellings have natural ventilation, 14 exhaust ventilation and 43 have balanced ventilation with heat recovery. With regard to the heating systems, gas boilers, heat pumps, wood boilers and local electrical heaters are represented.

In Flanders, the energy performance of a dwelling is expressed in terms of the insulation level (K-level) and the energy performance level (E-level). The insulation level gives an indication of the thermal losses of the building envelope, taking into account the overall mean insulation value (U-value) in addition to the compactness of the building (ratio of heated volume and overall heat loss area) and the heat loss through 2D and 3D component junctions. Well insulated dwellings have a lower K-level. K45 represents a mean U-value of 0.45W/m²K for a compactness of 1m. Most passive houses have an insulation level between K10 and K20. The E-level is a ratio of the primary energy consumption of a building, for standard climate and user behavior, to the calculated reference primary energy consumption, depending on the compactness of the building. For dwellings, the energy consumption for heating, cooling, domestic hot water, pumps and fans is considered, reduced by the energy production of renewable energy sources. The lower the E-level, the better the energy performance. Negative E-levels can be considered for energy positive dwellings, which produce more primary energy through PV solar panels than they consume on a yearly basis for heating, cooling, domestic hot water and ventilation. Near-zero energy, the aim for new buildings by 2021, is represented by a level of about E0. Figure 1 shows the distribution of the selected dwellings according to insulation level and energy performance level. The requirements since 2006 and the aim of near-zero energy (± E0) are also indicated.

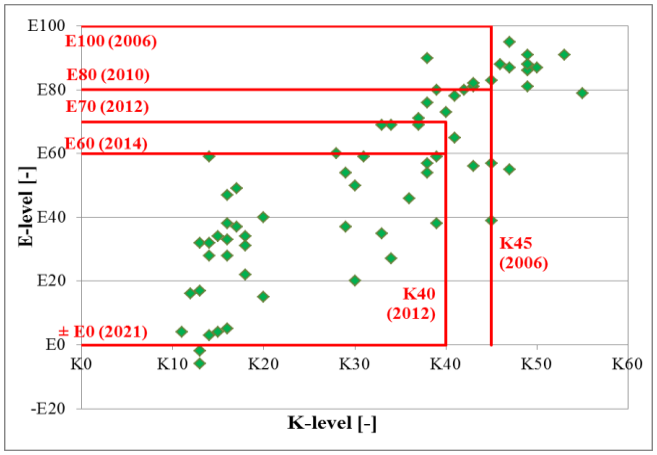

Figure 1. Distribution of the dwellings according to their insulation level (K) and energy performance level (E)

2.2. Monitoring campaign

In order to evaluate the quality of the indoor environment, a monitoring campaign was set up in each house over two periods each at least two weeks long: one in winter between November 2011 and April 2012, and the other in summer between June 2012 and September 2012. In

the living room, master bedroom and bathroom, indoor air temperature and relative humidity were measured every 15 minutes with an ONSET HOBO U12 logger. CO_2 concentration was also measured every 15 minutes with a Telaire 7001, coupled with a HOBO U12 logger. In winter, CO_2 concentration was monitored in most living rooms and some master bedrooms, whereas in summer these measurements were more focused on the master bedrooms and in some living rooms. For a reference to the outdoor climate, measurements of temperature, vapor pressure and solar radiation were taken from one central location in Flanders and were used for all dwellings.

2.3. Evaluation criteria for thermal comfort

Thermal comfort was evaluated by the mean indoor air temperature and the standard deviation in the living room and master bedroom. For the period in summer, the maximum indoor temperature during occupation was also verified.

Comfort boundaries are derived from ISO 7730 (ISO 2005). This standard describes limits for operative temperature. Since the dwellings being considered are well insulated, the air temperature and operative temperature will be very close. In this research, upper and lower boundaries will therefore be set to evaluate indoor air temperature.

A weak point is that the ISO 7730 standard is developed for thermal comfort in the work environment. Different studies show that the experience of occupants in their own house diverges from that in their work environment (Karjalainen 2008, Hong et al. 2008). Especially while sleeping, the principle of heat exchange is different than assumed in the PMV-model, resulting in lower comfort temperatures (Leung and Ge 2012, Peeters et al. 2008). However, none of these studies define adjusted boundaries for thermal comfort in dwellings.

Therefore, the comfort boundaries for indoor air temperature in winter were set to 20°C-24°C for living rooms and 18°C-22°C for bedrooms. In summer, a comfort boundary of 23°C-26°C was set for both types of rooms.

2.4. Evaluation criteria for indoor air quality

A first method to evaluate the indoor air quality is by means of the CO_2 concentration. According to EN 13379, indoor air can be qualified in four levels (IDA1 to IDA4) based on the difference in CO_2 concentration of the indoor air ($c_{CO2,i}$) versus that of the outdoor air ($c_{CO2,e}$); see Table 1 (CEN 2007). Outdoor air contains about 350 to 400 ppm CO_2 (Liddament 1996). Based on the value of the indoor CO_2 concentration in several dwellings when not occupied, a general value of 350 ppm for the outdoor CO_2 concentration is used in the calculations. For good indoor air quality, the IDA1 or IDA2 levels should be aimed for.

	$c_{CO2,i} - c_{CO2,e}$ (ppm)	$c_{CO2,i}$ (ppm)	
IDA1	≤ 400	≤ 750	High IAQ
IDA2	400 – 600	≤ 950	Good IAQ
IDA3	600 – 1000	≤ 1350	Moderate IAQ
IDA4	≥ 1000	≥ 1350	Low IAQ

Table 1: Boundary conditions for the indoor air quality (IAQ) levels according to EN 13379.

Alternatively, the indoor air quality can be assessed by means of the internal humidity, according to the internal climate classes (ICC) defined in EN 13788 (CEN 2001). Table 2 shows the boundary conditions for the different classes (ICC1 to ICC5) for the vapor pressure difference between indoor and outdoor ($p_i - p_e$) as a function of the monthly mean external temperature θ_{em}. Additionally the typical corresponding building types are shown. In order to avoid problems of interstitial condensation and mold, level ICC3 or lower should be aimed for.

	$p_i - p_e$ (Pa)		
	$\theta_{em} < 0°C$	$0°C \leq \theta_{em} \leq 20°C$	Building types
ICC1	< 270	$< 270 – 13.5\ \theta_{em}$	Storage
ICC2	< 540	$< 540 – 27.0\ \theta_{em}$	Offices, shops
ICC3	< 810	$< 810 – 40.5\ \theta_{em}$	Buildings with low occupancy
ICC4	< 1080	$< 1080 – 54.0\ \theta_{em}$	Buildings with high occupancy
ICC5	≥ 1080	$\geq 1080 – 54.0\ \theta_{em}$	Special buildings, e.g. laundry, brewery, etc.

Table 2: Boundary conditions for the indoor climate classes according to EN 13788.

3. RESULTS

3.1. Winter period

3.1.1. Temperature

Figures 2 and 3 show the mean indoor air temperature and standard deviation for all living rooms and master bedrooms, as a function of the insulation level (K-level). Distinction has been made between the different types of ventilation. The green area represents the comfort zone.

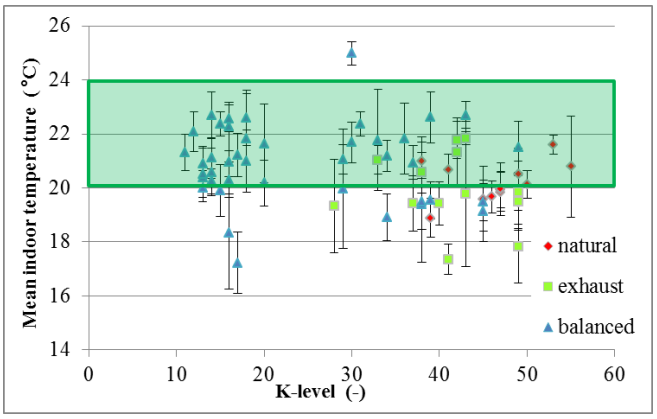

Figure 2. Mean indoor air temperature in winter period for all living rooms as a function of K-level and of the ventilation system

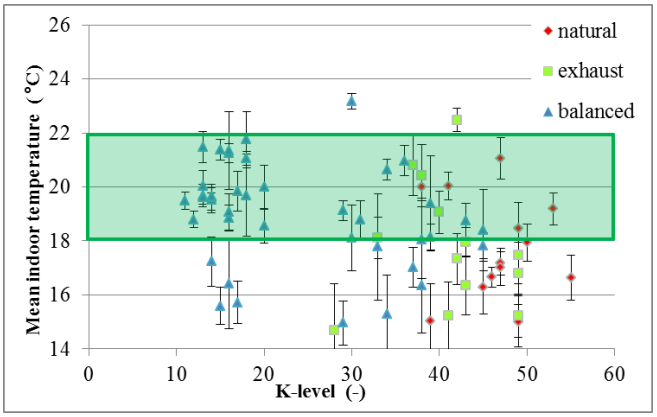

Figure 3. Mean indoor air temperature in winter period for all master bedrooms as a function of K- level and of the ventilation system

3.1.2. Indoor air quality

Figure 4 shows individual results for 50 living rooms of the cumulative percentage of time the CO_2 concentration is within a certain IDA class or better. As the periods when the living rooms were occupied is variable and inconsistent, the whole monitoring period is taken into account. Distinction is made between the ventilation systems.

In Figure 5, results of the indoor air quality in terms of vapor pressure differences between indoor and outdoor are given as a function of the ventilation system. Due to the limited monitoring period of 2 weeks, daily averaged vapor pressure differences are shown instead of monthly averaged. Each value for the vapor pressure difference of a dwelling is the volumetrically averaged value based on the measured vapor pressures in and the volumes of living room, master bedroom and bathroom.

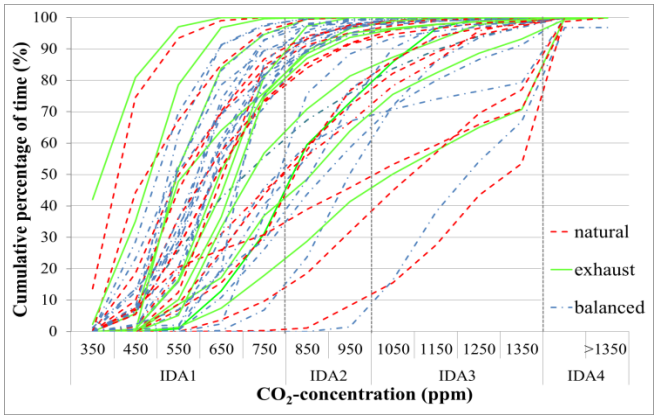

Figure 4. Cumulative percentage of time the CO_2 concentration in 50 living rooms is within an IDA class as a function of ventilation system

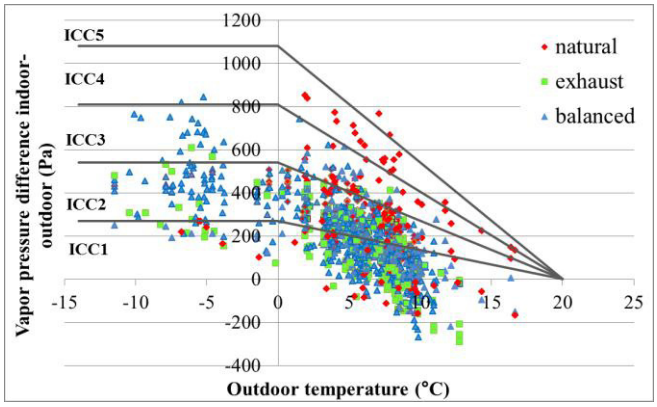

Figure 5. Daily averaged vapor pressure difference in all dwellings as a function of the daily averaged outdoor temperature and of the ventilation system in winter period

3.2. Summer period

3.2.1. Temperature

Figures 6 and 7 show the mean indoor air temperature and standard deviation in living rooms and master bedrooms as a function of K-level. The green zone represents the comfort zone.

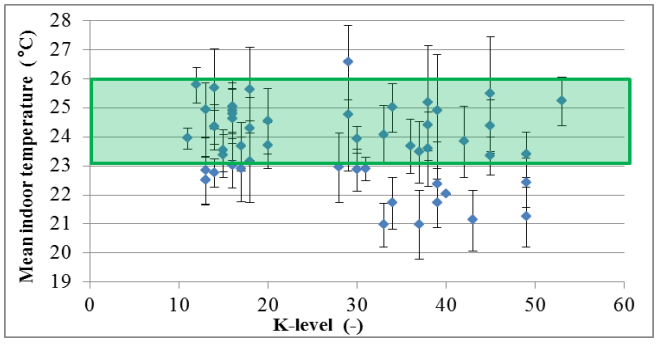

Figure 6. Mean indoor air temperature in summer period for all living rooms as a function of K-level .

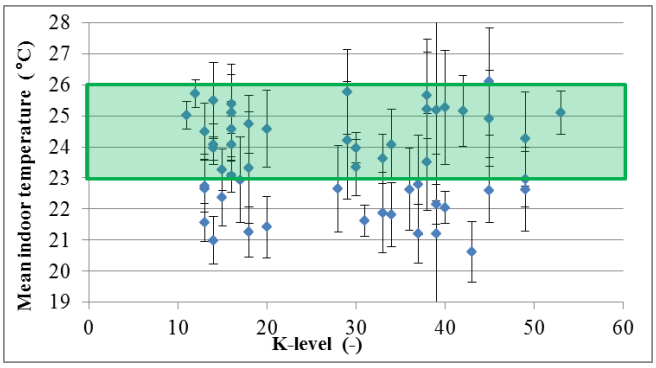

Figure 7. Mean indoor air temperature in summer period for all master bedrooms as a function of K-level .

Figures 8, 9 and 10 show the maximum indoor air temperature during the (possible) occupancy periods for respectively the living rooms, between 3 p.m. and 10 p.m., and the master bedrooms, between 10 p.m. and 7 a.m. These are presented as a function of the mean outdoor air temperature during the whole measurement period (in Figures 8 and 9) and as a function of the mean daily amount of radiation during the whole measurement period (in Figure 10). Difference is made for massive constructions versus wood frame constructions. In two dwellings, active cooling was used during the measurement period. The maximum indoor air temperature in these dwellings is indicated by a green circle. In one bedroom the logger was installed close to a classic model television. During the use of this apparatus, high local temperatures were measured, which do not refer to the general room temperature. The maximum indoor air temperature for this bedroom is marked by a red circle.

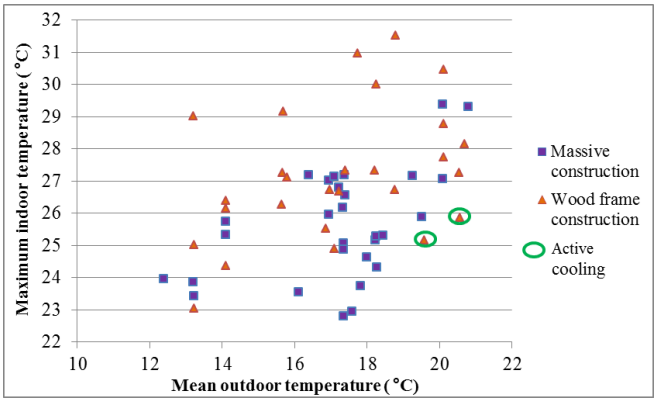

Figure 8. Maximum indoor air temperature in 56 living rooms during occupancy (between 3 p.m. and 10 p.m.) as a function of mean outdoor temperature over the whole monitoring period and the construction type.

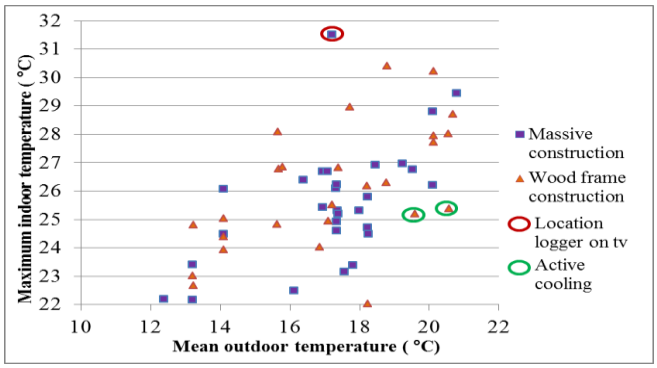

Figure 9. Maximum indoor air temperature in 55 bedrooms during occupancy (between 10 p.m. and 7 a.m.) as a function of mean outdoor temperature over the whole monitoring period and the construction type.

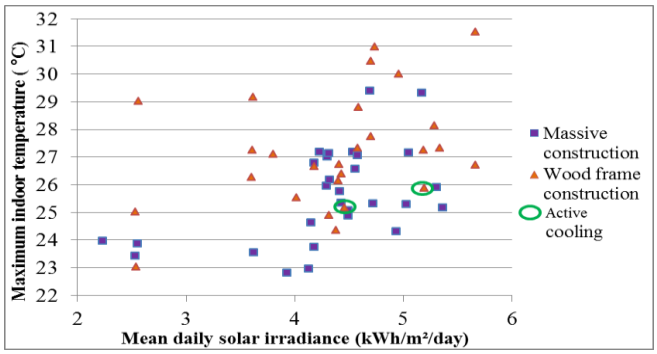

Figure 10. Maximum indoor air temperature in 56 living rooms during occupancy (between 3p.m. and 10 p.m.) as a function of mean daily solar irradiance of the whole monitoring period and the construction type.

3.2.2. Indoor air quality

Figure 11 shows the cumulative percentage of time the CO_2 concentration is within a certain IDA class or better in the master bedroom. To ensure the results in the bedrooms give a correct indication of the CO_2 concentration during occupancy, only the measurements during the night between 1 a.m. and 5 a.m. are taken into account.

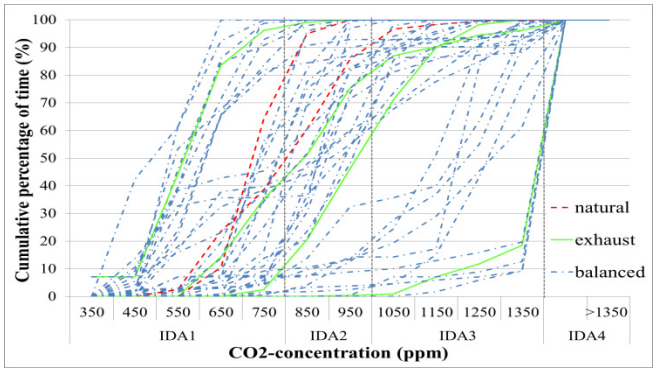

Figure 11. Cumulative percentage of time the CO2 concentration in 42 master bedrooms, during nighttime in summer, is within an IDA class as a function of the ventilation system

4. DISCUSSIONS

4.1. Temperature

As Figures 2 and 3 show, in approximately 60% of all living rooms and bedrooms the mean temperature is in the comfort zone during the winter period. In less than 40%, it is below the comfort temperature and in some rare cases it is above the comfort zone. Considering also the standard deviation, it can be concluded that most dwellings have a comfortable indoor air temperature during the entire measuring period. This is confirmed by the temperature trends of the individual dwellings where there is a small difference between the minimum and maximum temperatures.

For most dwellings where the mean indoor temperature in the living room is below the comfort zone, the standard deviation and individual trends show that during room occupancy periods, the indoor temperature is within the comfort zone, but outside these periods there is a (small) reduction in the temperature. Especially in dwellings with natural and exhaust ventilation, where cold outdoor air directly enters the room, limited heating periods result in low mean temperatures. In some cases, a low set temperature is the residents' choice, resulting in a low mean temperature and small standard deviation.

In the bedrooms, the indoor temperatures are more often below the lower comfort boundary. The standard deviations show that also during occupancy the temperature does not reach the comfort zone. The trends of the individual measurements show that often the bedrooms are not heated and that realization of thermal comfort in these rooms is considered less important.

Figures 2 and 3 show that in better insulated dwellings with a low K-level, the indoor temperature is generally higher and the standard deviation is smaller. For dwellings with a K-level below 25, there are merely a few where the mean indoor temperature in the living room is below 20°C. For dwellings with a K-level above 25, however, the lower mean indoor temperature affects half of the dwellings. This result is mostly due to the better insulation value of the houses, but is also influenced by the ventilation system. As shown in Figures 2 and 3, the well-insulated dwellings are all equipped with a balanced ventilation system with heat recovery. For the houses with higher K-level, it appears that the highest mean indoor temperature occurs when a balanced ventilation system is present. However, the ventilation system is not the only determining parameter for indoor temperature, as is shown by the fact that there are also dwellings equipped with a balanced ventilation system with heat recovery where the mean temperature is below 20°C in the living rooms. In these cases the lower mean temperature is influenced by the residents' settings of their desired temperature and length of heating period during the day.

During the research the influence of other parameters was also checked, such as the construction type (massive versus wood frame construction), the percentage of glazing as window to floor ratio, the type of heat production and heat distribution, etc. However, these parameters did not have a significant impact on the mean temperature during the heating season. It is important to notice that some of the well-insulated dwellings have a very limited heating capacity, for instance by means of a local, removable electrical heater. However, even this type of dwelling could easily realize thermal comfort in the winter period.

The results for thermal comfort in the summer period are shown in Figures 6 to 10. In this season, the indoor conditions are far more dependent on the outdoor climate, namely outdoor air temperature and solar irradiance. Since the measurements had to be spread over the season due to logistical reasons, all dwellings had different outdoor conditions, which makes a comparison between dwellings more difficult. In winter these differences are in most cases intercepted by the heating installation. In summer such compensation is not present, except for the two houses with active cooling.

Figures 6 and 7 show that the mean indoor air temperature is within the comfort zone for 64% of the living rooms and 58% of the bedrooms. For the other dwellings the mean temperature was below the comfort zone. Only in one dwelling is the mean temperature above the upper boundary. The measurement in this dwelling took place during a hot, sunny period.

However, the according standard deviations indicate that temperatures can increase highly. This is confirmed by Figures 8, 9 and 10, which present the maximum indoor air temperature during the occupancy periods in both living room and master bedroom. The influence of the outdoor climate is included by showing the indoor temperature as a

function of the mean outdoor air temperature or the mean daily solar irradiance during the measuring period. These figures show that in 55% of the living rooms and in 47% of the bedrooms the maximum indoor temperature rises above the upper comfort boundary of 26°C, even in periods when the outdoor climate is not extremely warm or sunny.

From Figures 8, 9 and 10 it is clear that the temperature in wood frame construction dwellings rises higher than in massive constructions. In the latter, the temperature remains within the comfort zone for a longer percentage of time. There was not a clear impact of the construction type on the mean temperature, but in wood frame constructions standard deviations were larger than in massive constructions.

With regard to the influence of percentage of glazing, orientation of living room and bedroom, and type of ventilation system, no significant impact could be found, either for the mean temperature or for the maximum temperature.

4.2. Indoor air quality

As shown in Figure 4, the CO_2 concentration in the living rooms during the winter period is reasonably good. For most dwellings, IDA3 or IDA4 is reached for only a limited amount of time. Attention has to be drawn to the fact that these results concern averages on the entire measuring period, whether the living rooms were occupied or not. The conclusions may therefore be somewhat too positive, as mainly the indoor air quality during occupation is of interest. However, in 32 of the 50 monitored living rooms IDA2 or better is reached during more than 90% of the time, so it might be expected that also during occupation the indoor air quality is satisfying.

The results in the bedrooms are less positive: at least 40% of the time CO_2 concentration reached IDA3, regardless of the type of ventilation system and more than 20% of the time IDA4 was reached in dwellings with mechanical ventilation (exhaust or balanced). Dwellings with natural ventilation seem to perform better, but caution is needed given the limited amount of monitored bedrooms with this type of ventilation system.

As the results of Figure 5 show, the internal humidity level is good. In most of the dwellings the vapor pressure differences between indoors and outdoors are below category ICC4 and most of the days even below category ICC3. Especially with mechanical ventilation indoor air quality, equivalence to buildings with low occupancy is realized. One dwelling with a couple of days of high indoor humidity influences the results for natural ventilation.

The measurements for CO_2 concentration in the summer period show even better results in the living rooms. Especially with natural ventilation, IDA2 or better is reached, but here also caution is needed since there were only two living rooms monitored. Figure 11 shows that in 31 of the 42 monitored bedrooms the indoor air quality is high or good for more than 60% of the time (IDA2 or better). In these 31 dwellings, all types of ventilation systems are represented. In the other 11 bedrooms, however, the indoor air quality is moderate or low for a large part of the time. These cases stem from dwellings with a mechanical ventilation system (exhaust or balanced), but considering the limited number of monitored dwellings with a natural or exhaust ventilation system, here also caution is needed.

During the summer period, the vapor pressure indoors is often lower than outdoors, due to humidity absorption by walls, furniture, etc. In some of the bedrooms it can be noticed that during the occupancy period at night a high CO_2 concentration is accompanied by a high humidity. However, this high humidity is cleared out during the daytime, so no problems of mold and interstitial condensation are expected. In general, good results for indoor air quality in terms of internal humidity are reached in all dwellings, with all types of ventilation systems.

Combining the information about the moderate to low indoor air quality in bedrooms and the high temperatures that can occur during the summer period, it can be concluded that in some dwellings with balanced ventilation, the occupants do not take advantage of the opportunity of opening windows during night. This extra ventilation could support or even replace the ventilation system and remove the surplus CO_2 and humidity. It could also bring in cooler outdoor air to reduce the temperature, since in Belgium outdoor temperature easily drops below 20°C on hot days and even below 15°C on cooler days in summer. Considering the temperature difference with the maximum indoor temperatures in the bedrooms during nighttime, as presented in Figure 9, there is a great potential for natural night cooling.

5. CONCLUSION

In preparation for the requirement that, starting from 2021, all new buildings have to be Nearly Zero Energy Buildings, this research evaluated the in situ performance of a range of low energy dwellings. In this paper, the performance especially of thermal comfort and of indoor air quality has been evaluated.

Results concerning the indoor air temperature during the winter period show that the mean temperature lies within or close under the comfort boundaries and that the standard deviation is rather small. This effect is even stronger for well-insulated dwellings. Thermal comfort in winter can therefore definitely be realized in low energy houses. The comfort is even better because temperature reduction outside the heating periods is very limited. A balanced ventilation system with heat recovery supports this comfort, but in less insulated dwellings the effect is partially overruled by the residents' choices of set temperature and length of heating period.

In general the thermal comfort in summer is good. The mean indoor air temperatures are within the comfort boundaries. The maximum temperatures, however, can rise quite high, both in living rooms and bedrooms. Especially wood frame constructions are sensitive for this, although this type of dwelling also cools down faster. To facilitate this cooling down, it is important to make optimal use of opening windows, especially for night ventilation in bedrooms regardless of the type of ventilation installed.

The indoor air quality is reasonably good in almost every dwelling, independent of the type of ventilation system. Only in a number of bedrooms the CO_2 concentration, and to a lesser extent the humidity, can rise to a moderate or low indoor air quality. In summer the opening of windows can also provide a solution for this.

Acknowledgements

This research is funded by IWT, the Flemish governmental Institute for Science and Technology within the TETRA research program and according to the rules of the IWT-TETRA research program co-financed by 25 organizations and companies related to the building sector.

References

CEN EUROPEAN COMMITTEE FOR STANDARDIZATION 2007, EN 13779 Ventilation for non-residential buildings – Performance requirements for ventilation and room-conditioning systems.

CEN EUROPEAN COMMITTEE FOR STANDARDIZATION 2001, EN 13788 Hygrothermal calculation procedure of building components (internal surface temperature to avoid critical surface humidity and interstitial condensation)

EPBD, Directive 2002/91/EC of the European Parliament and of the Council of 16 December 2002 on the energy performance of buildings.

FLEMISH ENERGY AGENCY 2012 EPB in figures 2006-2011. Report with figures on the energy performance regulation – Procedures and results, geometrical and energetic characteristics of the Flemish building stock – period 2006-2011. (in Dutch)

HONG, S.H., GILBERTSON, J., ORESZCZYN, T., GREEN, G., RIDLEY, I., THE WARM FRONT STUDY GROUP 2008. A field study of thermal comfort in low-income dwellings in England before and after energy efficient refurbishment, Building and Environment, 44 (2009), p. 1228 – 1236.

ISO INTERNATIONAL STANDARD 2005, ISO 7730 Ergonomics of the thermal environment – Analytical determination and interpretation of thermal comfort using calculation of the PMV and PPD indices and local thermal comfort criteria.

KARJALAINEN, S. 2008. Thermal comfort and use of thermostats in Finnish homes and offices, Building and Environment, 44 (2009), p. 1237 – 1245.

K.U.LEUVEN, DEPARTEMENT BUILDING PHYICS SECTION, Rapport 2009/11, Monitoring Massief-passief woning te Bottelaere. (in Dutch)

LEUNG, C., GE, H. 2012. Sleep thermal comfort and the energy saving potential due to reduced indoor operative temperature during sleep, Building and Environment, 59 (2013), p. 91 – 98.

LIDDAMENT, M. W. 1996. A guide to energy efficient ventilation, Air Infiltration and Ventilation Centre

PEETERS, L., DE DEAR, R., HENSEN, J., D'HAESELEER, W. 2008. Thermal comfort in residential buildings: comfort values and scales for building energy simulation, Applied Energy, 86 (2009), p. 772 – 780.

Recast EPBD, Directive 2010/31/EU of the European Parliament and of the Council of 19 May 2010 on the recast of the energy performance of buildings.

VERBEECK, G., CARMANS, W., AND MARTENS, V. 2011 Theory versus practice of energy and comfort in 4 low energy houses in Belgium.

HubPod: Integrating Acoustic Simulation in Architectural Design Workflows

Brady Peters[1], Jane Burry[2], Nicholas Williams[2], and Daniel Davis[2]

[1]Royal Danish Academy of Fine Arts
Philip de Langes Allé 10
1435 Copenhagen, Denmark
brady.peters@kadk.dk

[2]Royal Melbourne Institute of Technology
GPO Box 2476
Melbourne, Victoria 3001, Australia
jane.burry@rmit.edu.au

Keywords: Acoustic Simulation, Design Workflows, Sound Scattering, Digital Fabrication.

Abstract

This paper reports on research that seeks to integrate acoustic simulation into an architectural design workflow. The goal of this research is to develop rapid and accessible workflows for architects that allow them not only to tune the acoustic performance of designs at the scale of the room, but also at the level of the geometry and materiality of the surface. The project that serves as the test case is the HubPod, a semi-enclosed meeting room situated within an open working environment. As this study builds on previous research which investigates the acoustic properties of hyperboloid surface geometry, the main drivers for design were both the acoustic performance as well as the complex geometric and fabrication constraints involved with setting out and constructing the hyperboloid geometry. This paper focusses specifically on the integration of the acoustic simulation. Four design workflows were developed: two of these allowed for the investigation of the acoustic performance of the room using acoustic simulation software; the other two allowed for the measurement and visualisation of the acoustic performance of the surface using custom-written scripts to calculate and visualise sound scattering. This paper will present some of the data produced by these simulations, and reflect on the value of the different workflows and simulation methods to this architecture project.

1. INTRODUCTION

Meeting rooms are communication spaces and therefore should be designed for optimal speech intelligibility. Meeting rooms are commonly small, relatively square, and are often sparsely furnished. Many times, the only acoustically absorbing surface is the ceiling. These characteristics can lead to poor acoustic performance. Small, square rooms with hard surfaces develop resonances between parallel reflecting surfaces. (Long 2006) These resonances cause certain frequencies to be amplified which are annoying and decrease speech comprehension. A second problem is flutter echoes, that is, sounds that persist locally due to multiple reflections between parallel, concave, or chevroned wall surfaces. (Long 2006) A third problem is that uneven distribution of acoustic absorption causes acoustic absorbing material to work at less than optimal performance, thereby increasing the reverberation time (Nagata 2009). A low reverberation time and signal-to-noise ratio is important to achieve good speech intelligibility (Bradley 1986). However, it is critical to have strong early reflections of sound as well; simply striving for a low reverberation time will decrease the speech intelligibility (Bradley 2009).

The HubPod is a prototype meeting room. It is designed to have excellent acoustic performance as a meeting room and to improve the acoustic performance of the open working environment in which it is situated. The HubPod seeks to create an acoustically better meeting room through three specific features: a non-rectangular overall geometry and non-parallel wall surfaces to reduce resonances, a highly articulated interior surface to provide significant sound scattering and reduce flutter echoes, and a balance of materials adjusted to control acoustic absorption therefore producing a space without echoes or resonances but which also does not sound ‘dead’. This set of design criteria led the team to a scheme for an aggregate structure composed of different 'cells'. These cells could then be assigned different types of material, they would have a complex geometric profile to create sound scattering, and the cells would be brought together in non-rectangular formation; see Figure 1.

The surface geometry of the cells is derived from a hyperboloid of one-sheet. Previous research has demonstrated that aggregate structures composed of this geometry produce sound scattering surfaces (Burry et al. 2011).

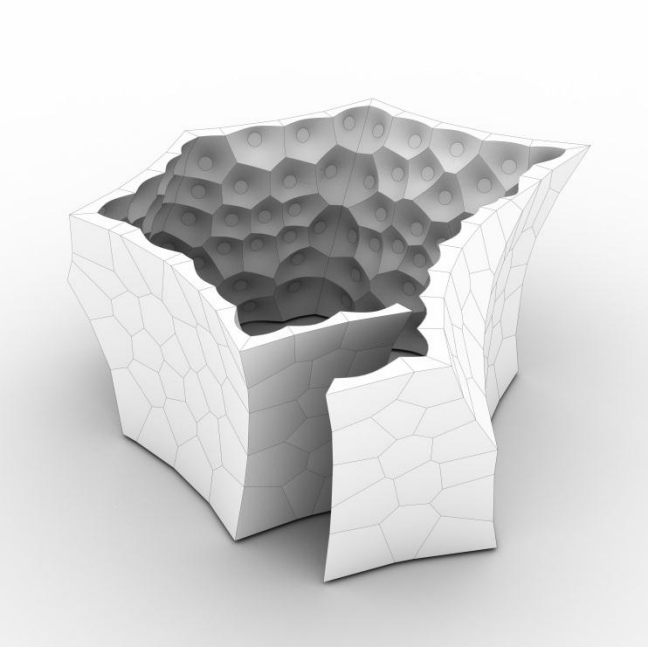

Figure 1. The HubPod: 3-D visualisation.

One of the aims of the HubPod research project is the creation of a series of flexible digital design workflows that would allow for many design decisions to be deferred until late in the design process. The hypothesis is that as the complexities involved in the geometry and fabrication would be encoded into the logics of a computational design system, there would then be more time to explore design options and develop a better meeting room. In terms of the acoustic research, as the design workflow was implemented digitally, this gave the opportunity for the digital acoustic simulation to be used and integrated. Acoustic performance was a primary consideration and this integration would allow the design to become performance-driven. As such, one of the goals of the HubPod research project was the development of rapid and accessible workflows for architects that would allow them to tune the acoustic performance of the HubPod design. Specifically, this research project sought to integrate digital acoustic simulation at the scale of the room and at the level of the geometry and materiality of the surface.

Currently, architects and architecture students are taught to use Sabine's formula to measure acoustic performance. However, while this approach is certainly accessible, it is not very fast, nor does it apply for many cases. The Sabine formula does not work for rooms that have odd shapes or unevenly distributed material (Rindel 2010), it only calculates a single parameter, reverberation time, and it does not give a spatial response. To study parameters beyond reverberation time, to study different room shapes with potentially uneven distributions of materials, and to gain an understanding of the spatial distribution of performance, acoustic simulation software must be used (Peters 2010). Therefore, acoustic simulation software was used as a primary means of measuring acoustic performance. However, there were a few obstacles with using acoustic simulation software, and so other workflows were also developed. First, the acoustic simulation software is a separate piece of software and so not fully integrated into the digital workflow, so another workflow had to be included using a plug-in to the architecture design software that allowed for the calculation of acoustic performance within the design environment. Second, sound scattering performance cannot be predicted using acoustic simulation software; therefore, two different digital techniques were developed to calculate, and visualise, the acoustic performance of the complex surface geometry of the HubPod, and integrate this performance testing into the architectural design workflow.

2. DEVELOPING ARCHITECTURAL DESIGN WORKFLOWS

Digital workflows have been developed for the rapid generation of design proposals of the HubPod. The simulation of the acoustic performance of each proposal used both off-the-shelf acoustic software as well as custom scripts. While the acoustic simulation is the focus of this paper, the digital workflows that generated the hyperboloid geometry were a critical part of this process as these provided the framework into which the simulation routines needed to be situated. These workflows needed to consider what data was needed by the different acoustic simulations, and how the calculated performance could then re-inform the geometry and material of the HubPod.

2.1. GEOMETRY AND FABRICATION CONSTRAINTS

Several key decisions drove the definition and constraint of the design space of the project. The geometry of the hyperboloid of one-sheet was a fundamental research driver. A circular hyperboloid of revolution, rather than elliptical, was selected for this project. The circular hyperboloid has the known geometric property that the intersection of any two common hyperboloids results in a planar curve where these hyperboloids are oriented equidistant from and aligned to a common point; see Figure 2. In other terms, both hyperboloids are oriented normal to and lie on a sphere. This results in a complex geometric surface that produces sound scattering.

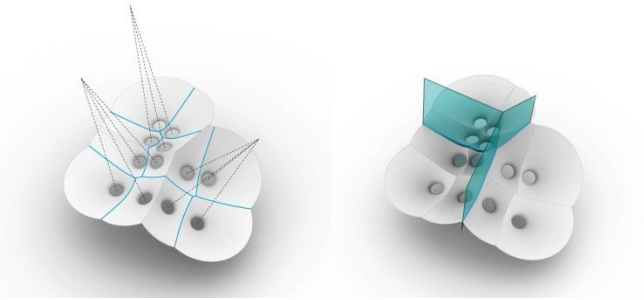

Figure 2. The proposed geometric rules to ensure planar intersection curves between hyperboloids: (left) intersection curves of spheres on a common sphere and (right) mirroring planes at the transition from one sphere to another.

It was hence resolved that the overall form of the HubPod would be comprised of a series of intersecting spheres of a common radius. Using these spheres as set out geometry, hyperboloids could be distributed in any configuration with guaranteed planarity of intersection curves, Two geometric 'families' were identified as the space for design exploration of the overall form and a series of opportunities and constraints identified in the subsequent arrangement of hyperboloid geometry; see Figure 3. These strategies create overall room shapes that deviate from the regular, square format of meeting rooms, thus reducing the chance of resonances and flutter echoes.

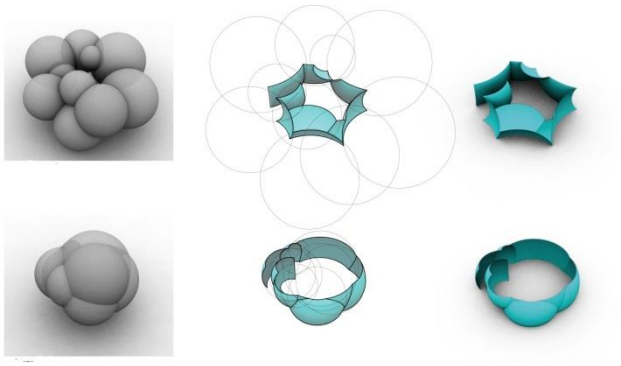

Figure 3. The two design families chosen: the geometry of alternate Boolean union and difference of sphere.

2.2. DIGITAL MATERIALS

Each hyperboloid defines one 'cell'. The importance of the planar intersections between hyperboloids can be explained by a second decision, this one related to the fabrication strategy. This extended a previous strategy in which a series of 'cells' were created, each a hybrid component with one hyperboloid face (Burry et al. 2011). The 'cells' proposed for the HubPod were comprised of a timber frame supporting a hyperboloid and a planar face on opposite sides; see Figure 4. These cells meet with simple bolted connections to be assembled as the larger whole of the Pod. The acoustic importance of this strategy is that the materials of these faces could be varied allowing the acoustic performance of the interior or exterior of the space to be tuned. The hyperboloid faces are made from plexiglass, spun metal, or a hardened, acoustic-absorbing felt. The planar faces are made from plexiglass or hardened, acoustic-absorbing felt. The acoustic absorption and scattering coefficients of the materials were necessary for the digital simulations.

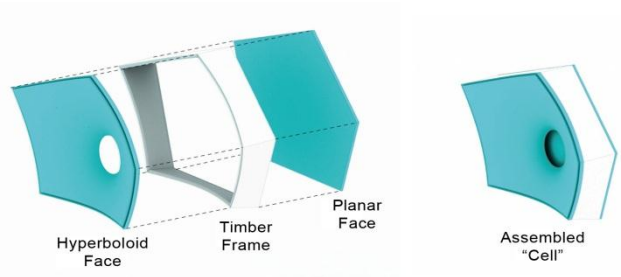

Figure 4. Materials in the Fabrication Strategy and Material Definition in Acoustic Simulation.

2.3. DIGITAL DESIGN WORKFLOW

A set of parametric models were developed which allowed the designers to independently address the overall form, the surface patterning and material distribution for a proposed design. These were created using Grasshopper, a parametric modelling plugin for McNeel Rhinoceros 4.0. The output of each model could be used for tests with various acoustic simulations; see Figure 5.

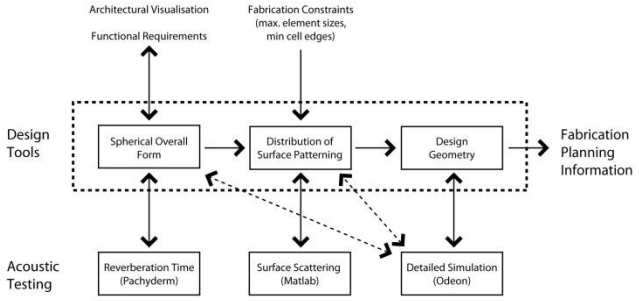

Figure 5. The scope of design tools and their interactions with acoustic simulation software.

2.4. ACOUSTIC SIMULATION OF THE ROOM

To understand the acoustic performance of an interior space, geometrical acoustic simulation is the currently accepted method (Vorlander 2008). Many acoustic simulation software packages now provide valid results (Bork 2006); however, when compared to architectural design software most of these software packages have limited abilities to actually create geometry. Therefore, the geometry is created in architectural design software, then exported, and imported into the simulation software. This workflow, titled 'Parallel modelling and simulation', requires knowledge of how acoustic simulation works as this impacts the way in which we draw the geometry as architects. Odeon, the simulation software used in this workflow, requires simplified geometry. It was found that the geometry should be triangulated and that it was not necessary to have extensive surface detail. As the materiality of the individual surfaces is critical, it is important to put the geometric entities on different levels (or layers) in the architectural design software according to their acoustic performance. This makes it easier to assign the correct material in acoustic simulation software. A DXF file with triangulated geometry is exported from the CAD software and imported into the simulation software. Once this process is set up, the generation and analysis of design options is simple and relatively quick. The time it takes to run a simulation is much longer than it takes to export the data from the design software and import it into the simulation software. This workflow was used to do all of the detailed acoustic analyses of the HubPod and its surrounding spaces. As an example, the speech transmission index (STI), or degree of intelligibility, was calculated. This was used as a measure of the degree to which sounds are disturbing from one point to another. The more clearly one understands meaning in sounds, the more disturbing it is. The results are shown in Figure 6.

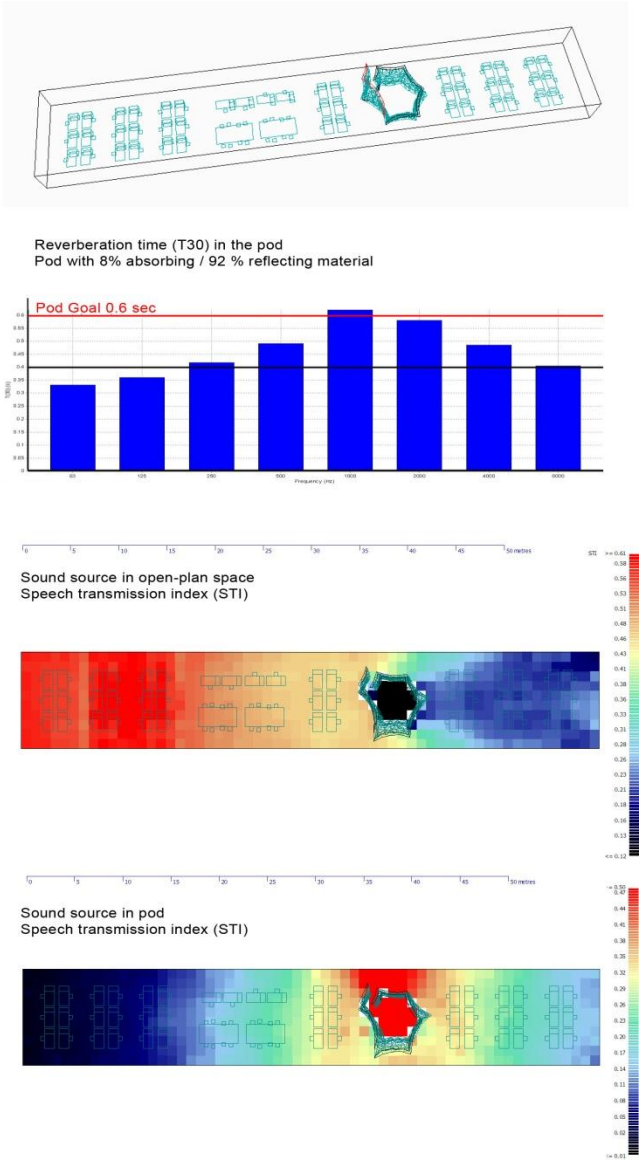

Figure 6. Geometry imported into Odeon acoustic simulation software, Calculated reverberation time inside of HubPod, STI calculated with sound source outside (above), and inside (below), the HubPod.

This workflow, to create geometry in one software and analyse in another, allows for specialist software to be used and gives potentially a great deal of information about an option. However, this workflow is limited in terms of feedback into the design process. The results from the acoustic simulation software cannot be fed into a computational optimisation loop with the geometry and/or material modification abilities of the generating scripts in the design software. The workflow, as it is not fully integrated, is also not appropriate as a sketch tool; it does not allow for a quick analysis of many different options.

The second workflow used to integrate acoustic performance in the HubPod is to use an analysis program that runs internally within the digital design environment. The software used here was the Pachyderm software which runs as a plug-in to McNeel Rhinoceros 4.0. (van der Harten 2013) In this workflow, titled 'Integrated modelling and simulation', both the geometry and the analysis happen simultaneously within the same software without the need to translate the data between systems. This decreases the time necessary to make sure that data is compatible and reduces errors introduced in the translation process. It was not the aim of this research project to validate or compare these particular analysis software tools, but to develop new workflows to integrate sound into the architectural design process; however, a quick check indicated that the analysis done using Pachyderm was consistent with the results from Odeon. It was also discovered that the calculation times for Pachyderm took longer than Odeon; unfortunately, this meant that speed gained through integrating the analysis in the design software was lost due to an extended calculation time. One reason for this is that Odeon was developed in such a way that all octaves are handled using a single round of ray-tracing, whereas in Pachyderm, each octave band is handled by an independent round of ray-tracing. The approach in Pachyderm allows the user to specify frequency-dependent scattering coefficients. A suggestion for the development of Pachyderm would be to build in an option where only one round of ray tracing is performed to provide a way to calculate fast and efficient sketch solutions. Pachyderm was a useful tool to calculate many different acoustic parameters, although in this experiment we focused on the calculation of reverberation time; however, Odeon was a useful tool to calculate STI and produced spatial distributions of the different acoustic parameters. It must be emphasized that these observations on these particular analysis software tools do not reflect on this design workflow in general, but did impact this specific implementation of it. Because of Pachyderm's ease-of-use and availability, this workflow was used as part of the teaching component of the HubPod project. This workflow allowed a class of architects and architecture students to engage with the acoustic performance of this complex structure and begin to play creatively with sound and space. An example of the results that were produced was a study conducted by a group of students of different room shapes, see Figure 7. This study showed that, when considering only room shape, an overall convex form for the HubPod had the lowest reverberation time.

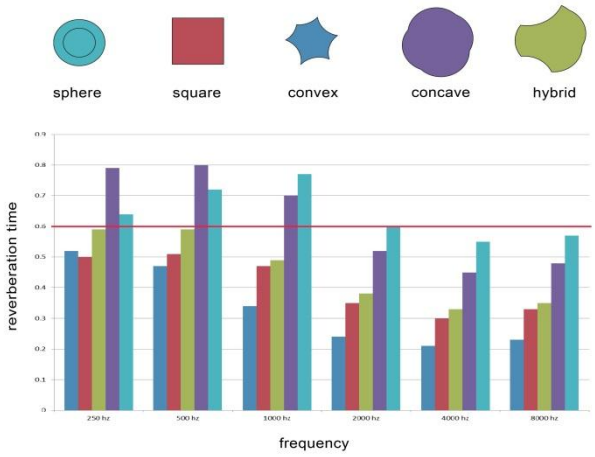

Figure 7. Comparison of five different room shapes using Pachyderm and their calculated reverberation times.

2.5. ACOUSTIC SIMULATION OF THE SURFACE

In the last decade there has been an increased interest in the characterization of sound scattering. (Cox 2009) It has been shown that the correct modelling of sound scattering is necessary for the accuracy of geometric room acoustic models. (Vorlander 1995) There has also been increased understanding on how important sound scattering is for the acoustic performance of a space. It has been suggested that one of the reasons that traditional concert halls sound better than modern halls is because of the greater degree of surface detail that occurred at a variety of scales to provide sound scattering across a range of frequencies. (Cox and D'Antonio 2003) Therefore, in recent years, there has been the development of a standard measure for sound scattering. (Vorlander and Mommertz 2000)

While most acoustic simulation software packages include the effects of sound scattering, few actually allow

for the measurement of the acoustic properties of complex geometric surfaces. So, given that the HubPod has a complex geometric surface, and the sound scattering performance of this surface is a crucial part of the design, how can the acoustic performance of this surface be predicted? Previous research has developed a digital / physical design workflow for integrating architectural parametric modelling with rapid prototyping and laboratory measurements of sound scattering coefficients. (Peters 2010) In a further experiment, this workflow was then successfully used to measure the acoustic performance of different hyperboloid structures. (Burry et al. 2011) While this research demonstrated that this workflow works, its disadvantages were that it takes considerable time for each iteration (days) due to the time it takes to rapid prototype a model and then measure it in a laboratory, and there are still outstanding issues with the process in terms of achieving accurate and reliable results (Peters 2010, Choi and Jeong 2008). Therefore, for the HubPod, we looked to develop a purely digital design workflow to obtain the scattering coefficient from surface geometries.

Unlike geometric acoustics, where sound is abstracted as a vector, to model sound waves themselves a numerical modelling algorithm must be used. Boundary Element Modelling (BEM) is an accepted way to model sound waves and calculate various acoustic parameters associated with the wave equation. (Cox 2009) Here in the HubPod project we used the OpenBEM library, an open-source library of Boundary Element Modelling algorithms. A script written in Matlab used this library and calculated the scattering coefficient from a 2D section. Therefore, to get feedback on the acoustic performance of the hyperboloid surface of the HubPod, first a section was taken through the geometry generated by the digital design workflow, then a custom script in the architecture software analysed this section and created a text definition of the geometry for input into Matlab, which then finally calculated the scattering coefficient; see Figure 8.

Figure 8. Workflow 3: BEM calculation of sound scattering coefficient - Rhino to Microstation to Microstation VBA to Text file to Matlab.

This workflow calculated the scattering coefficients for several different design options. It was used to decide the density of the hyperboloid cells, and to determine whether it was necessary to introduce variety in the well-depth of the hyperboloids (it was not). The workflow and measurement procedure have only been validated against previous results by the author and not against established models. The results were useful in two distinct ways in the design process: first, to compare between options for surface geometries, and second, to use the calculated scattering coefficient in acoustic simulation software to get more accurate results. The sound scattering coefficient used in Odeon is a single number taken at 707 Hz, see Figure 9.

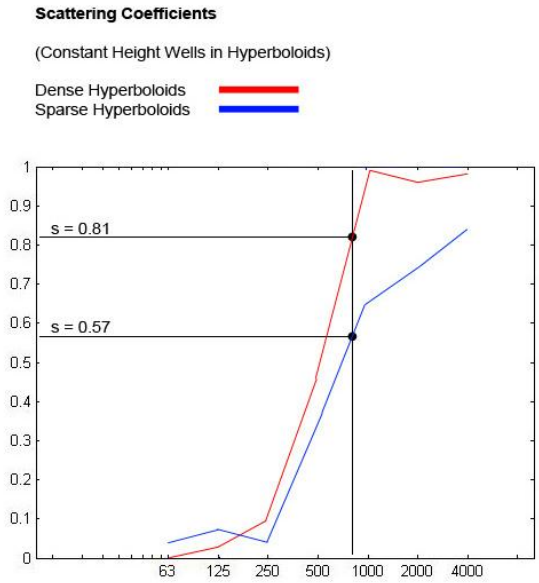

Figure 9. BEM Calculation of scattering coefficients for sparse and dense configurations of hyperboloids. The single scattering value required by Odeon (measured at 707Hz) is noted.

Another algorithm that can be used to calculate sound waves is the finite-difference time-domain (FDTD) scheme (Cox 2009). FDTD is now used for many types of simulations, including calculation of sound scattering coefficients (Redondo 2009). For the fourth workflow, the FDTD algorithm was implemented in the Processing language to create visualizations of sound scattering. In this design workflow the geometry created in the architectural design software is processed using a custom script to produce a discretized grid of points mapping the space and geometry of the surfaces. This grid, captured in a text file, is then imported into Processing which then produces visualizations; see Figure 10.

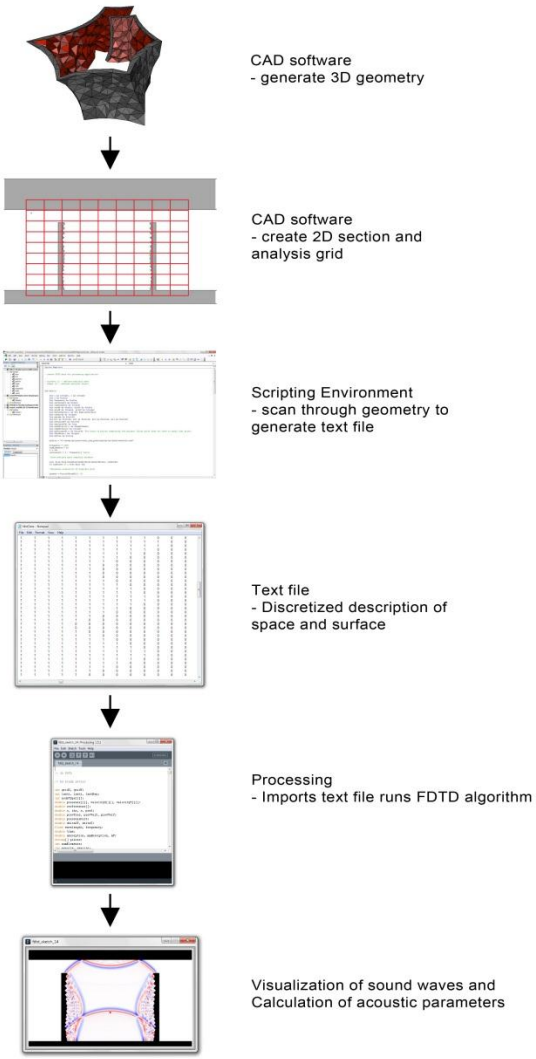

Figure 10. Workflow 4: Visualisation of sound scattering - Rhino to Microstation to Microstation VBA to Text File to Processing.

The current implementation does not yet calculate the scattering coefficient, but is used for creating images and videos. It has been previously shown that this visualization technique produces very effective results that allow an intuitive comprehension of acoustic phenomena in rooms—as a way to compare options, and to see the diffusion of the sound energy as a result of different geometries (Yokota, Sakamoto and Tachibana 2002). Several screenshots from two different animations are shown in Figure 11 and show how the sound energy is diffused to a greater degree with the hyperboloid surface.

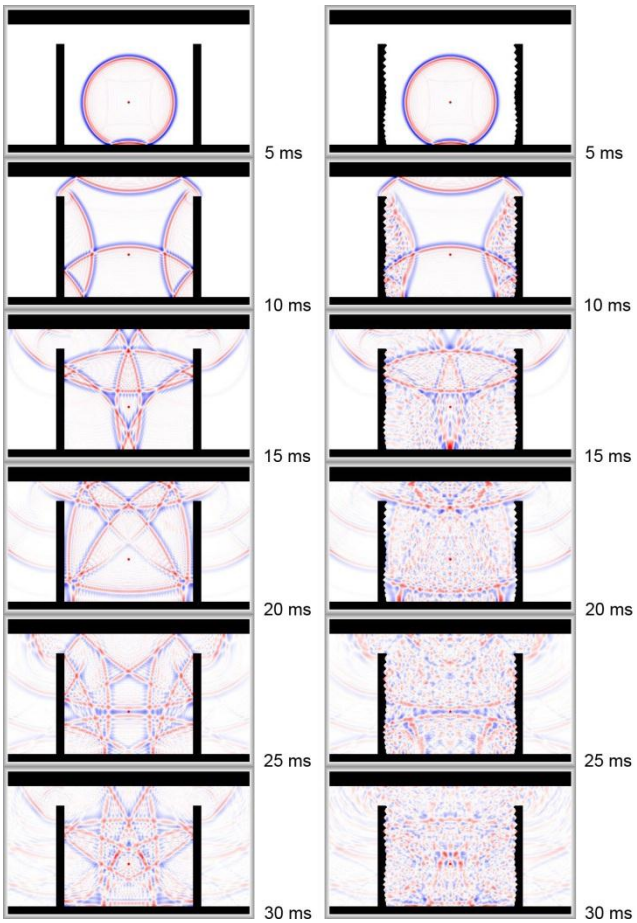

Figure 11. Visualisation of sound waves in a meeting room with a) flat walls on the left, and b) walls composed of hyperboloids on the right.

3. CONCLUSIONS

A broad conclusion from the project is that there is a need for more software that allows architects to measure acoustic performance and design for sound. As computational techniques and parametric tools now allow architects to see the potential for including acoustic performance as a design driver, there is an increased interest by architects to create spaces and surfaces that can define sound in a more specific way. However, while there are some great acoustic simulation software packages for acoustic engineering, there is no fully-featured acoustic design software for architects. This research project suggests four different ways in which these new software packages might integrate with an architect's workflow: as separate acoustic analysis/design software; as an integrated plug-in for design software; as a plug-in or separate software to calculate the acoustic performance of materials; and, as a tool for the creation of visualisations of acoustic performance.

In this project, the use of separate software for acoustic simulation still provided the most useful results, though these did not include information on the sound scattering performance. The integration of acoustic performance analysis in architectural software is a benefit as it allows for the testing of ideas quickly. This integration of analysis gives the potential to set up iterative optimisation processes that could be linked to the generative design tools. However, the feedback from the software used for this project could be more detailed and displayed in a more visual format. There is a specific need for a design tool that measures the acoustic performance of complex surfaces. Architects are more interested in creating these types of surfaces and more interested in having these surfaces be performance-driven. The method of calculating sound scattering by using BEM digitally appears to be faster and more inexpensive than the previously examined process of using rapid prototype models. The FDTD algorithm provided a way to visualise sound. This provided a deeper understanding on how the complex geometry affected the sound waves and complemented the measurement of the sound scattering coefficient. The HubPod project developed and tested four specific workflows for integrating acoustic performance into architectural design. While these are not proposed to be answers to all design situations, they do point to several general approaches that could be developed further to provide sound design tools for architects.

The HubPod project, the design of a prototype for a meeting room, gave the opportunity to develop a series of digital design workflows for the definition of a structure based on an aggregate of cells composed of hyperboloids. The workflows developed to integrate acoustic performance into the design process allowed for the design of a meeting room that met the design criteria. The project is currently under construction and will be acoustically tested when finished.

Acknowledgements

We gratefully acknowledge the assistance of Arthur van der Harten who not only wrote the Matlab script for calculating the scattering coefficient but is the creator of the open-source acoustic analysis software Pachyderm.

References

BORK, I. 2005. 'Report on the 3rd Round Robin on Room Acoustical Computer Simulation.' in Acta Acustica United with Acustica, Vol. 91 pp 740-763.

BRADLEY, J. 1986. 'Speech Intelligibility Studies in Classrooms' in Journal of the Acoustical Society of America Vol 80 No 3.

BRADLEY, J. 2009. ' A New Look at Acoustical Criteria for Classrooms.' in Inter-Noise Proceedings.

BURRY, J, DAVIS, D, PETERS, B, AYRES, P, KLEIN, J, PENA DE LEON, A, BURRY, M. 2011. 'Modelling Hyperboloid Scattering: The challenge of simulating, fabricating, and measuring.' in Design Modelling Symposium Proceedings, Berlin.

CHOI, YJ. AND JEONG, DU. 2008, 'Some Issues in Measurement of the Random-Incidence Scattering Coefficients in a Reverberation Room', in Acta Acustica United with Acustica, Vol. 94, pp. 769-773.

COX, T. AND D'ANTONIO, P. 2003. 'Engineering Art: The science of concert hall acoustics.' Interdisciplinary Science Reviews, 2003, Vol. 28, No. 2.

COX, T. AND D'ANTONIO, P. 2009. Acoustic Absorbers and Diffusers: Theory, design and application, London, Taylor & Francis.

LONG, M. 2006, Architectural Acoustics, Burlington, Elsevier.

NAGATA, M. 2009. 'The Effects of Diffusion on Room Acoustics,' in Nagata Acoustics Newsletter No. 259.

PETERS, B. 2010. 'Acoustic Performance as a Design Driver: Sound Simulation and Parametric Modeling using SmartGeometry,' in International Journal of Architectural Computing, No 3, Vol 8.

PETERS, B. AND OLESEN, T. 2010. 'Integrating Sound Scattering Measurements in the Design of Complex Architectural Surfaces: Informing a parametric design strategy with acoustic measurements from rapid prototype scale models.' in eCAADe Proceedings.

REDONDO, J, PICO, R, AVIS, M, COX, T, 2009. 'Prediction of the Random-Incidence Scattering Coefficient Using a FDTD Scheme' in Acta Acustica with Acustica, Vol 95.

RINDEL J, 2010. 'Room Acoustic Prediction Modelling,' in Encontra da Sociedade Brasileira de Acustica.

VAN DER HARTEN A. 2013 (in press). 'Pachyderm Acoustical Simulation Towards Open-Source Sound Analysis,' in Architectural Design No. 222.

VORLANDER, M. 2008. Auralization. Springer.

VORLANDER, M. 1995. 'International Round Robin on Acoustical Computer Simulations.' in 15th International Congress on Acoustics Trondheim, Norway.

VORLANDER, M. AND MOMMERTZ, E. 2000, 'Definition and measurement of random-incidence scattering coefficients', in *Applied Acoustics*, 60, pp. 187-199.

YOKOTA, T, SAKAMOTO, S, AND TACHIBANA, H, 2002. 'Visualization of sound propagation and scattering in rooms,' in Acoustic Science and Technology Vol 23 No 1.

Session IX

Data Mining using ANN for Finding the Effects of Building Structure on Thermal Comfort Parameters 223
Lubaid Ahmed, Abdolreza Abhari
Ryerson University

A Generalized Event Driven Framework for Building Occupancy 227
Gandherva Gunathilak, Aiswarya Prasannakumar, Negin Nazarian, Homa Naeimi
Indian Institute of Technology Hyderabad, University of California San Diego

Simulation for Planning Passenger and Freight Transportation System Projects 231
Beth C. Kulick
TranSystems Corporation

Preliminary Results of Model Predictive Control of Shading Systems 235
Brent Huchuk, William O'Brien, Cynthia A. Cruickshank
Carleton University

Data Mining Using ANN for Finding the Effects of Building Structure on Thermal Comfort Parameters

Lubaid Ahmed, Abdolreza Abhari

Department of Computer Science
Ryerson University
350 Victoria Street, Toronto, Ontario, Canada
lubaid@scs.ryerson.ca

Department of Computer Science
Ryerson University
350 Victoria Street, Toronto, Ontario, Canada
aabhari@scs.ryerson.ca

Keywords: Data Mining, Classification, Artificial Neural Network, Automatic Building Design, Thermal Comfort, Wireless Sensor Networks.

Abstract

The main objective of this work is to use an Artificial Neural Network (ANN) for data mining in the thermal comfort data of building environment datasets collected through a wireless sensor network. Currently there are many research activities trying to use data mining methods to find data patterns in machine-generated data (i.e., "big data"). The data collected in this work is composed of temperature, humidity and air flow values collected from the 4th floor of an educational building. The main goal of this research is to find the effects of building structure design on the collected parameters. This will help to answer questions regarding how to change the structure design and examine its effects on a building's thermal comfort parameters.

1. INTRODUCTION

Searching large data sets with the goal of discovering new patterns in the data sets is called "data mining". Data mining uses sophisticated mathematical algorithms to predict or detect different hidden patterns in datasets. In this work we used Artificial Neural Network (ANN) for doing approximation, which is one of the data mining approaches.

We have trained ANN, by learning the datasets, to approximate temperature and airflow for different locations in a building. Therefore, our work is similar to regression analysis but because of the complexity of the model it was done by ANN. Using ANN in data mining can also be for the purpose of classification. A "classification model" determines that any given data or sample belongs to a particular predefined class. The C4.5 Weka classification model was used to develop relevant classification rules (Gao et al. 2010).

The main differences between classification analysis and regression analysis are:

- if the target (dependent) variable that should be predicted is continuous (numeric), then regression analysis is used
- if the target variable is categorical with discrete (unordered) values, then classification analysis is used.

Thermal comfort is the temperature, humidity and other conditions which occupants experience in a building. The Predicted Mean Vote (PMV) index measures the mean response with regard to the thermal comfort of the people living in the building (Fanger, 1970). Thermal comfort is dependent on human activities, insulation material, mean radiant temperature, humidity, air temperature, and velocity of indoor air (Atthajariyaku, 2004). In this work we only focused on using data mining for three thermal comfort parameters, as will be explained below.

2. DATA COLLECTION USING WIRELESS SENSOR NETWORK

An educational building called Eric Panil Hall (EPH) of Ryerson University was selected for this research. Construction of the building was completed in the mid-1970s. Both static and dynamic attributes were measured. The following dynamic attributes were collected using sensors: air velocity, temperature and humidity, from different locations in

the hallway of the 4th floor of EPH. The static attributes are the distance between each sensor location and nearest window, elevator, ventilator and stairs on both the left and right hand sides of the sensor. Figure 1 shows a floor map with location of the sensors and structural parameters of the 4th floor of the EPH building.

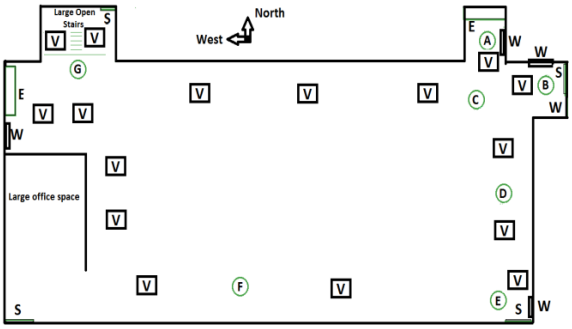

Figure 1: Sensor locations (in circle), vents (V), windows (W), stairs (S) and elevators (E) for both data collection phases.

The data collection process had two phases covering two distinct time periods. Wireless Sensor Network (WSN) nodes were used, each node consisting of one or more sensors. In Phase 1, these nodes were placed in different locations along the southern and eastern hallways. Sensor placements can be seen in Figure 1. In Phase 2, WSN nodes were deployed in the northern and western hallways. At the end of both data collection phases, data denoting the values for sensor locations on the 4th floor of the EPH building was stored in a file and then transferred to the database server. This building covers approximately 3144 m^2. Because of the small number of sensors and short data collection period, we collected data only for corridors at this stage.

3. DATA MINING USING ANN

3.1 Artificial Neural Network Design

In our research we used approximation as the data mining method. We used ANN for finding the relation between building structure and thermal comfort data to be able to do predictions based on approximation. The ANN was implemented using MATLAB software. A three-layer feed-forward network with sigmoid hidden neurons containing 10 neuron and linear output neurons was used, which could fit multi-dimensional data mapping. The ANN model was then trained by using the Levenberg-Marquardt backpropagation function. This function is used to train, validate and test datasets collected by WSN nodes. As shown in Figure 2, the ANN design consists of three layers. W is weight and b is bias parameters for each neuron. All layers have neurons; these neurons are interconnected with each other.

Input Layer: The number of neurons depends on the number of inputs/variables. If there are 8 variables/inputs, then 8 nodes are present in the input layer of the ANN model.

Hidden Layer: There can be more than one layer; each layer has multiple neurons. We used 10 neurons. The number of neurons is adjusted using trial and error method, until the best performance for ANN is achieved.

Output Layer: This layer depends on the number of outputs required; in our case 1 output, so 1 neuron is present in the output layer.

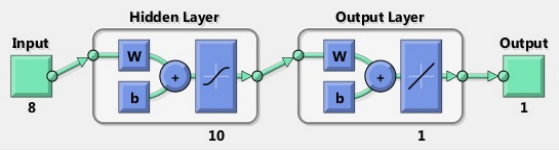

Figure 2: Three-Layer Feed Forward ANN.

3.2 Methodology

First we analysed the collected data to find any correlation between the dynamic parameters. This is explained below.

3.2.1 Data Analysis

By analysing the data we found that for air velocity, there are clearly regions where the velocity of air drops and remains constant. Within the same time interval, the temperature is observed to rise until air velocity increases and then temperature begins to drop. At a longer time scale of 6.11 days, regions which have this decline in air velocity and corresponding rise in temperature become quite apparent. In actuality, the mean air velocity of 0.46 m/s deviates only by about ±0.13 m/s from the mean for the whole collection of data.. The temperature measurements have a mean of 22.3°C and deviate by only ±0.41°C. The mean relative humidity as a percentage was 61.22%, with a deviation of ±5.86%.

The periodicity of each environmental variable is evident from data, which depicts quantities for air velocity, humidity and temperature observed at the B, E and G node locations, respectiÂvely.

Location	Closest Structural Component to Sensor (in meters)								Sensor data for 2 months (mean)		
	Elevator		Stairs		Window		Vent		Temp. ºC	R. Hum. %	A.Vel. cm/s
	Right	Left	Right	Left	Right	Left	Right	Left			
A	3.2	56	13	51	1.22	8	8	10	-	-	27
B	14	60	2.44	45	2.13	3.96	1.83	10	22.76	57.88	31
C	10	51	11	44	8	12	6	7	23.36	-	-
D	32	82	18	25	24	16	7	12	24.53	-	-
E	11	50	2.13	41	1.83	40	1.83	9	21.92	58.09	31
F	59	65	27	67	28	58	9	11	23.47	-	20
G	5.33	69	7.62	57	6.71	57	1.83	5.5	21.87	63.43	21

Table 1: Shows distance between sensor location and specific building component.

We have noted the periodic nature of air velocity and temperature in the data. The increase in temperature is matched by a decrease in air velocity at the node locations. Lastly, the rise and fall of temperature along with air velocity is likely an indication of the automatic cooling system increasing and decreasing air flow to maintain a certain temperature.

By analyzing the temperature over the whole collection of data, we concluded that the thermal comfort level on the 4th floor is in an expected metric range stated by Humphreys and Nicol (1998). The details of how we analyzed the thermal comfort with respect to temperature data can be read in our previous paper (Behboudi, 2012). Our collected data shows the lack of a linear correlation between relative humidity and temperature, as there are no discernible relationships between the two quantities. Though no relationship could be established between humidity and the other variables, the decrease and increase in humidity over a large time scale also suggests periodicity in the fluctuation of humidity to a certain degree. The data showed that the period of oscillation for humidity is larger than the period of oscillation for air velocity and temperature.

The large variations in relative humidity perhaps indicate a lack of measures to control the moisture in the air near the node locations. The effects of external weather may also be an important factor in determining the moisture content of internal air in the locations of the WSN nodes.

There are two types of attributes for each sensor location: namely static and dynamic. Static attributes are the physical distance between the sensor and nearest structural property, shown in Table 1. Dynamic attributes are temperature, relative humidity, and air velocity, which were sampled every minute for 2 months. After cleansing the data, we used 6 days of samples for this work. We used structural parameters as inputs, in the order shown in Table 1, starting from the right elevator and ending at the left vent. Temperature and air flow were used as output (one at a time) for the time that had both of them as shown in Table 1 and is related to date of Sept. 19, 2011 to Sept. 30, 2011.

3.2.2 Experimental Results

For this research activity, first we focussed on the temperature data for which we had the most number of sensors. Data was collected from 7 different locations on the 4th floor of the building. The employed ANN had 8 inputs of distance to structural parameters and 1 output. Accuracy of the ANN model was calculated using mean square error (MSE); if the MSE is close to zero, the results are said to be best. The following results are based on static attributes for all sensors. ANN was trained using 5 days of data samples from all locations, and validated separately for all locations. After many trials and errors, we arrived at the best performance for ANN.

Loc.	Temperature (mean)		Air Velocity (mean)	
	Measured	Predicted	Measured	Predicted
B	23.06	22.53	30.81	25.24
C	23.89	23.88	-	-
D	25.12	25.11	-	-
E	22.54	22.53	51.21	51.28
F	23.85	22.87	19.59	19.64
G	22.05	22.03	19.56	25.20

Table 2: Shows the averages of temperature and air velocity for validation day.

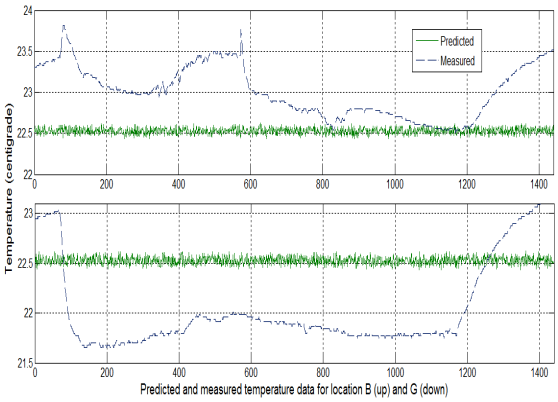

Figure 3: Predicted and measured temperature data for locations B and G.

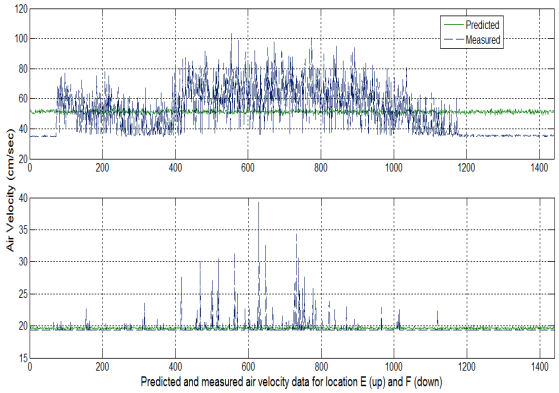

Figure 4: Predicted and measured air flow data for locations E and F.

By looking at both measured and predicted temperatures we observed that in the measured data, ventilators were causing fluctuations. For each location these fluctuations are less pronounced in the predicted data compared to the measured data because of the collective samples used for training ANN. We did the training for 8640 samples from 6 temperature sensor locations. We only collected the temperature data samples for locations B to G (excluding location A). We repeated the same design for ANN to approximate air flow. The training for air flow was done using 5760 samples from four locations. Both temperature and air flow were validated with one day of data from all sensor locations (1440 samples). The results can be seen in Table 2, and Figures 3 and 4. ANN can approximate the mean values of temperature and air flow with good precision.

4. CONCLUSION

Data mining using an artificial neural network appeared to be an effective tool for this work. Although we need to collect more data on structural parameters, we could approximate the temperature and air flow by using available structural parameters. A future software outcome of this research will allow us to answer the question: if we change static attributes (for example distance from a location to ventilator, to windows, etc), how much will the thermal comfort level of that building location change accordingly? The results of this research are very promising and will provide an excellent platform for building software to simulate the effects of changing the structural parameters of a building on its thermal comfort parameters.

In our long-term plan of research, we aim to collect different structural characteristics of several buildings, along with their thermal dynamic characteristics. We will use collected data from different buildings and train our ANN design (by the same data mining technique). With varied datasets from multiple buildings, the ANN can learn the relationship between different structural properties and the thermal dynamics of different indoor environments.

Acknowledgement

The authors thank the Natural Sciences and Engineering Research Council of Canada for support to initiate this research. We also thank our industrial partner Autodesk Canada Inc. for technical support.

References

Atthajariyakul, S., Leephakpreeda, T.: 2005, Neural computing thermal comfort index for HVAC systems. Energy Conversion and Management, Vol. 46, Issue 15-16.

Behboudi, N., Butt, F., Abhari, A., 2012, Automatic building design with ANNs and GA, SimAUD, Orlando, Florida, US, Video of data visualization at www.scs.ryerson.ca/~aabhari

Gao, Y., Tumwesigye, E., Cahill, B., Menzel, K.; 2010, Using Data Mining in Optimisation of Building Energy Consumption and Thermal Comfort Management, 2nd International conference on Software Engineering and Data Mining (SEDM).

Humphreys, M.A. and Nicol, J.F., 1998 Understanding the Adaptive Approach to Thermal Comfort, ASHRAE Technical Data Bulletin Vol. 14 (1) Field studies of thermal comfort and adaptation (ed. Geschwiler M et al) American Society of Heating Refrigeration and Air-Conditioning Engineers, Atlanta, USA.

P.O. Fanger: 1970, Thermal Comfort: Analysis and Applications in Environmental Engineering, McGraw-Hill, New York.

Climate Data Online http://climate.weatheroffice.gc.ca/climateData/canada_e.html, 2012. [Online; accessed 18-January-2013].

A Generalized Event Driven Framework for Building Occupancy

Gandherva Gunathilak[1], Aiswarya Prasannakumar[1], Negin Nazarian[2], Homa Naeimi[2]

[1]Indian Institute of Technology Hyderabad
Department of Computer Science and Engineering
|Yeddumailaram, Andhra Pradesh, India
cs11m06@iith.ac.in, cs11m08@iith.ac.in

[2]University of California, San Diego
Department of Mechanical and Aerospace Engineering
9500 Gilman Dr., San Diego, CA 92093
nenazari@ucsd.edu, hnaeimi@ucsd.edu

Keywords: Building Occupancy, Event-Driven Model, Agent-Based Model, Occupant Presence, Energy Simulation, Event-Driven Model.

Abstract

Building occupancy is very important for building energy simulation and research; however, generating an occupancy model that is closer to the real world occupancy patterns is a very challenging task. In this paper, we have proposed a generalized event driven framework for the simulation of building occupancy. Real humans work together in groups and their presence is affected by events. So, the proposed model incorporates the concept of events and groups. Unlike the existing building occupancy models which were based on a Markov chain, the proposed framework is fully event-driven and group-based, which makes it closer to reality. The proposed model develops a generalized framework which will be able to simulate the occupancy patterns for any building, be it an office, a lab or even a house.

1. INTRODUCTION

Building simulation tools are critical in designing buildings with higher energy efficiency, higher thermal comfort, higher safety, etc. In these simulations, human occupancy patterns in the building play a significant role because humans continuously interact with the building to increase their personal comfort. For instance, the occupants use appliances that use various forms of energy. Humans also emit heat, water vapour, pollutants, etc. If the building occupancy model is able to generate granular and realistic data, then the energy simulation tools can predict building energy consumption with higher accuracy. Therefore, a model capable of reproducing real building occupancy patterns is of great importance.

Initially, building occupancy was represented by using deterministic methods. There are existing mathematical models which were proposed by [Wang et al. 2005], [Page et al. 2007], [Liao et al. 2011] and [Chuang et al. 2011]. These existing models are based on a Markov chain or a probabilistic distribution. However, to develop a realistic model, parameters that affect the occupancy of real humans need to be included in the model. The disadvantages of the existing models are (a) Most of the existing models are mainly based on a Markov chain or a probabilistic distribution which makes the model less realistic. A Markov chain can capture the stochastic components of the building occupancy; however it fails to capture the deterministic component of the building occupancy. Therefore these models may result in non-realistic simulation. (b) Most of the existing models are developed based on the office environment, so these models can simulate realistic occupancy patterns only for the office environment. (c) The existing models will generate similar patterns for different buildings; thereby, they fail to simulate the occupancy of each building uniquely. (d) In the existing models, all the users are treated equally and simulated in the same fashion. But the building occupancy of real humans will be different depending on their personal profile. (e) The existing agent-based models can only simulate a fixed number of users. The number of users being simulated cannot be changed dynamically.

In the present work, two such real world parameters are included. They are events and groups. The presence and absence of real humans in a building is affected by events which happen every day. An employee who is working in an office environment enters the office building at 9:00 a.m. in the morning because the work event starts and he exits the office building at 6:00 p.m.

because the work event ends. Real humans work and interact together as groups. Humans can have a group event such as a group meeting or a group get together that will affect the occupancy pattern for every member of the group. The proposed event-driven framework only considers building occupancy and it cannot generate the occupant movement in the building. (For occupant movement, the readers may refer to the two models by [Liao et al. 2011] and [Chuang et al. 2011].)

2. PROPOSED FRAMEWORK

The proposed framework is a fully event driven framework where every change is caused by an occurrence of an event. The occupants may also enter and exit without any reason; this can be captured by randomised events or by using a probabilistic distribution/Markov chain as in the case of the existing models.

The proposed model is also agent based; it consists of agents, who have a set of behaviours. These agents mimic the behaviour of humans. But, the difference between the existing agent-based models and proposed framework is that the existing agent-based models always simulate a constant number of agents, which is given to the model in the form of initial input. However, the proposed framework can simulate additional users whenever necessary.

In this framework, events are categorised as follows:

(a) **Deterministic or Probabilistic:** Deterministic events are events which are bound to happen over a day (lunch breaks, meetings, and so on). Probabilistic events may or may not occur over a day (accidents, sick leave, and so on).

(b) **Personal or Global:** Personal events affect only a particular individual (sick leave, personal holiday, accident, and so on). Global events affect everyone in the building (natural disasters, power failures, riots, war, and so on).

One of the main advantages of the proposed framework is that it can capture and trace the occupancy for every user in a unique manner. For example, in the office environment the occupancy pattern of the CEO and an employee will never be similar because of their personal profile. But, all the existing models will generate the same occupancy pattern for different occupants. Therefore, in the existing models, the individual user occupancy pattern is very hard to capture. However, in the proposed framework the occupancy pattern of every user can be uniquely simulated and captured, thereby making the simulation closer to reality.

The framework supports two types of users: internal users and external users. The internal users are regular users of the building; these users are simulated at every time instant by the simulator. This concept is similar to the work done by [Page et al. 2007] and [Liao et al. 2011]. Each internal user may be a member of several groups. The external users are not regular users of the building, but they are forced to come into the building because of an event. The event that forces a non-regular user to come inside the building is called an external event. External events are global events that affect everyone in the building. For example, a fire alarm is an external event will cause fire fighters to come inside the building. The fire fighters are the external users who come inside the building for the duration of the external event.

3. ALGORITHM

3.1. Input and Output

There are four input lists to the algorithm:

(a) Group information list, which contains the information about the groups and the number of occupants belonging to each group.

(b) User profile list, which contains information about internal users who need to be simulated uniquely; it also contains information about the events from which the user is exempted.

All the users in the two above-mentioned lists are simulated as internal users.

(c) Deterministic events list, which contains the information about the deterministic events. It contains the following fields: event name, event id, event starting time frame, duration, whether it's global or not, priority and other metadata.

(d) Probabilistic events list, which contains the information about the probabilistic events. It contains the following information: event name, event id, probability of occurrence, expected duration, whether it's global or not, priority and other metadata.

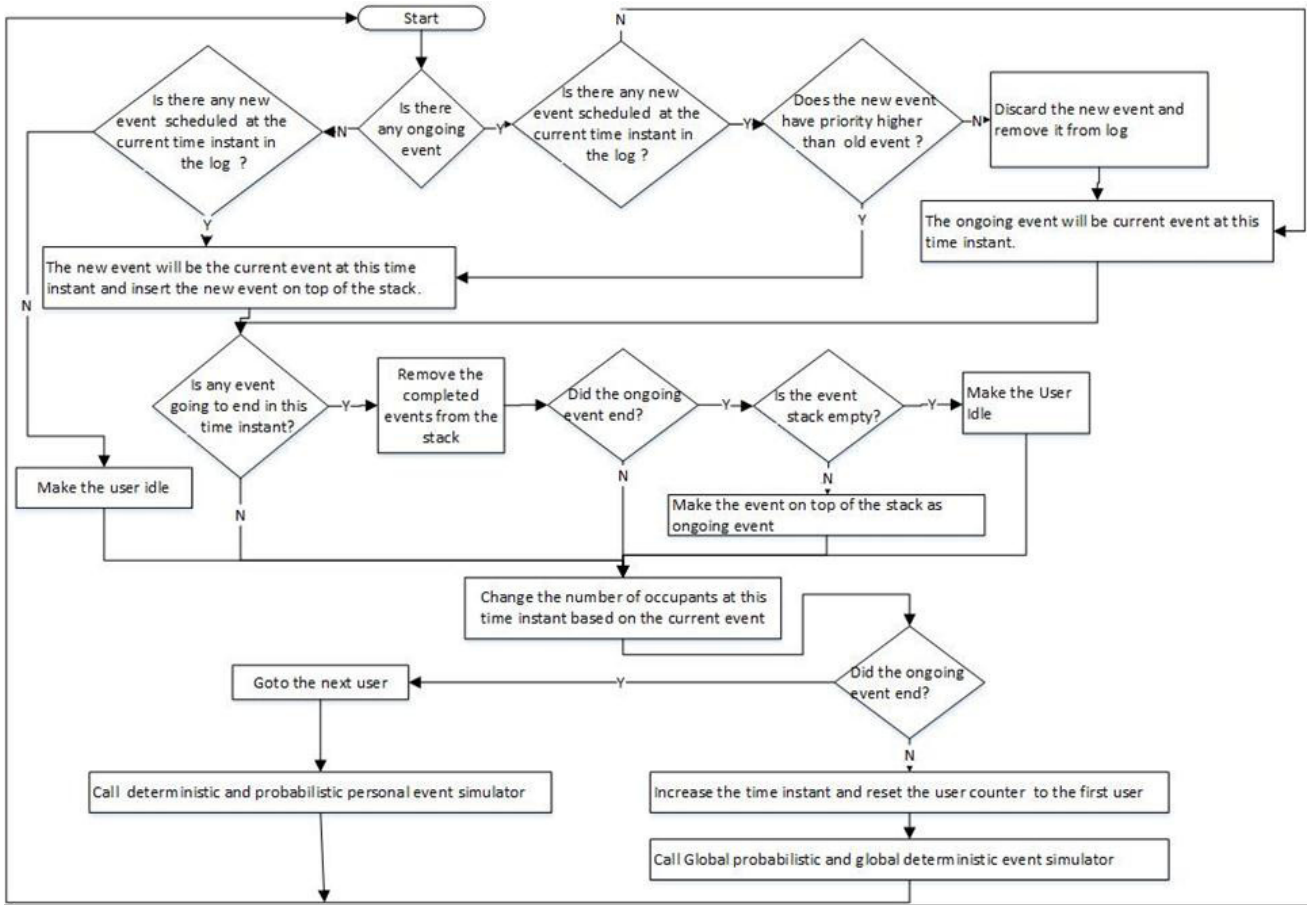

Figure 1. Main Algorithm

There are two outputs from the algorithm:

(a) User log, which contains the information about the events in which the user is involved. There is a separate log for every user.

(b) The building occupancy list, which contains the number of users present in the building at every time instant.

3.2. Main Algorithm

The main algorithm (Figure 1) simulates the activity of every user for the current time instant and then it proceeds to do the same for the next time instant. The main algorithm also calls the event schedulers. The event schedulers schedule the events using the inputs given in the events list. More than one event can be activated at a given time instant, so the event with the highest priority will be selected as the on-going event for this time instant. The other event is stored in the event stack and it will be resumed once the higher priority event has ended. The main algorithm generates the building occupancy list and it edits the user log generated by the event schedulers.

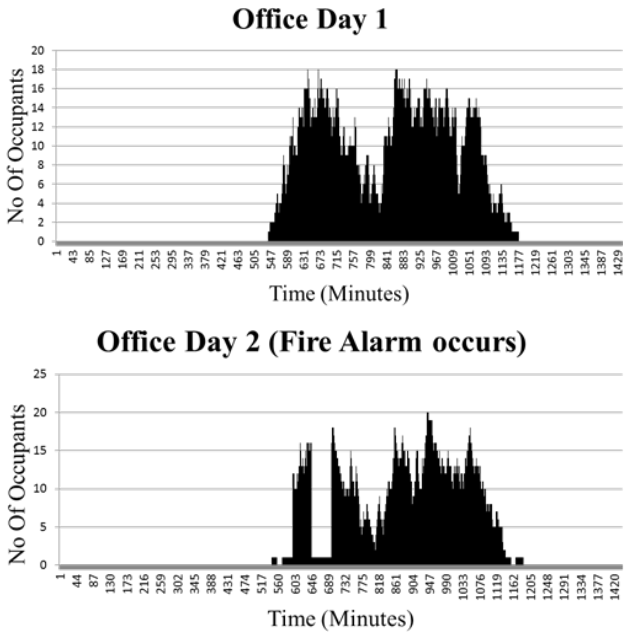

Figure 2. (Top) Office Day 1. (Bottom) Office Day 2.

```
faculty is coming in at 531 because of lab visit event
faculty is coming out because the eventlab visit ended at 572
faculty is coming in at 590 because of Internal project meeting event
faculty is coming out because the eventInternal project meeting ended at 625
faculty is coming in at 635 because of lab visit event
faculty is coming out because the eventlab visit ended at 650
faculty is exempted from the event networks lab meeting at 660
faculty is coming in at 690 because of cse faculty meeting event
faculty is coming out because the eventcse faculty meeting ended at 721
faculty is coming in at 929 because of lab visit event
faculty is coming out because the eventlab visit ended at 969
faculty is coming in at 1022 because of student meeting event
faculty is coming out because the eventstudent meeting ended at 1038
faculty is coming in at 1195 because of lab visit event
faculty is coming out because the eventlab visit ended at 1233
```

Figure 3. User Log for Network Faculty in the Lab Environment

4. PRELIMINARY RESULTS

A MATLAB script was used to implement the algorithm and analyse the results. We used this script to simulate the building occupancy pattern for two scenarios.

(a) Scenario 1: Office environment

The office environment had three groups. Twenty one internal users were simulated. There were three probabilistic events, three deterministic events and one external event. A fire alarm event was triggered on day 2 (Figure 2) from 10:30 a.m. to 11:20 a.m. which caused all the users to go out. During this event, the building was only occupied by fire fighters who were external users.

(b) Scenario 2: Lab environment (Computer lab).

The Lab environment had nine groups, such as bachelor, master, or doctorate students; faculty; research groups; etc. A total of thirty internal users were simulated. Among those thirty users we maintained user profiles for five users so that they could be simulated uniquely. We simulated nine probabilistic events and eight deterministic events. There was a sudden increase in the lab occupancy on Day 1 (Figure 4) from 2:30 p.m. to 4:30 p.m. because of the lab session event of a group of undergraduate students. The user log for the network faculty is shown in Figure 3.

5. CONCLUSION AND FUTURE WORK

In this paper, we have proposed a generic event-driven framework for building occupancy. The results of the simulation of an office and a lab environment were shown. It was found that this framework can capture sudden peaks in occupancy (for example, because of a lab session in the lab environment) and a sudden drop in occupancy (for example, because of a fire alarm in the office environment). This generic framework can be used to predict the occupancy pattern of any building when providing proper input. Also, many new concepts like events, user profile management and groups are proposed in the current framework. These new entities are not only confined to the building occupancy model, but they can also be used in many other topics of research concerning building energy simulation. In the future, we plan to compare our model with real building occupancy patterns.

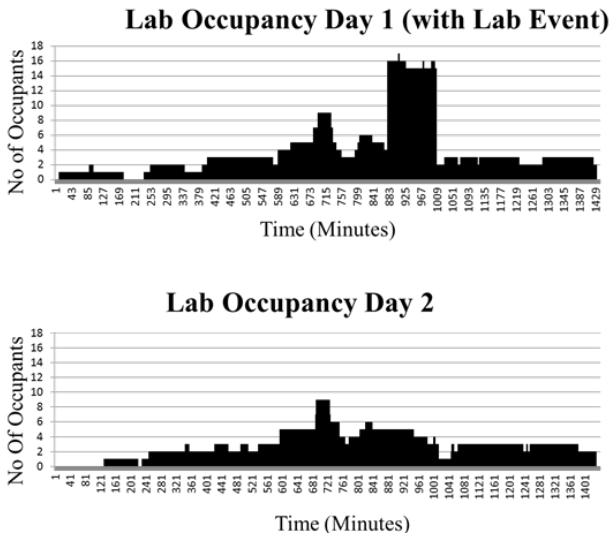

Figure 4. (Top) Lab Day 1. (Bottom) Lab Day 2.

Acknowledgements

The authors would like to thank M V Panduranga Rao, Assistant professor and Mukesh Kumar Giluka, Phd Scholar from IIT Hyderabad for their support and valuable reviews on our work.

References

Chuang Wang, Da Yan, Yi Jiang (2011). A novel approach for building occupancy simulation. BUILD SIMUL, 4: 149–167

Liao C, Lin Y, Barooah P (2011). Agent-based and graphical modelling of building occupancy. Journal of Building Performance Simulation, doi: 10.1080/19401493.2010.531143.

Page J, Robinson D, Morel N, Scartezzini JL (2008). A generalized stochastic model for the simulation of occupant presence. Energy and Buildings, 40, 83 − 98.

Wang D, Federspiel CC, Rubinstein F (2005). Modeling occupancy in single person offices. Energy and Buildings, 37: 121 – 126

Simulation for Planning Passenger and Freight Transportation System Projects

Beth C. Kulick

TranSystems Corporation
12555 High Bluff Dr., Suite 210
San Diego, CA 92130
bckulick@transystems.com

Keywords: Operations Planning, Operations Analysis, Infrastructure Capacity Planning, Value Engineering, Master Planning, Transportation Corridor Planning.

Abstract

Transportation projects are complex systems that involve many stakeholders and multiple goals, including sustainability. Simulation modeling provides a unique and flexible framework to assist with concept development, stakeholder consensus building, and public approval during environmental impact reviews. Modeling provides the ability to quantify concept performance differences between alternatives and demonstrate that a concept provides operational sustainability for each of the stakeholders and modal flows. We present three case studies to help elucidate the complexities involved and to show how modeling and simulation have been employed in these infrastructure projects.

1. INTRODUCTION

Transportation projects, such as those for maritime ports, airports, passenger rail and freight rail are typically large investments and they can be a complex system that includes multiple modes, new technologies, operating concepts, and operators. These projects are initiated by metropolitan planning organizations, city port authorities, and statewide department of transportation agencies and others. Architectural or engineering services firms are often contracted to assist with the project planning steps. The planning processes include evaluating and ranking alternatives with subjective and quantitative criteria. Additionally, as projects evolve, there is a need to gain stakeholder approval and conduct environmental impact reviews. Simulation modeling provides a unique and flexible framework to assist with concept development, stakeholder consensus building, and public approval during environmental impact reviews. Modeling provides the ability to quantify concept performance differences between alternatives and demonstrate that a concept provides operational sustainability for each of the stakeholders and modal flows. This paper describes several transportation planning projects and how simulation modeling can provide quantitative performance metrics to support the planning processes that enable the project to move towards advanced design and engineering stages.

2. CAPACITY PLANNING FOR PORT OF LONG BEACH, CALIFORNIA

The Port of Long Beach and Port of Los Angeles are both located in the San Pedro Bay in Southern California and the cargo volumes moved through this area are the largest in North America. These ports generate significant truck and rail traffic and must operate very close to high population areas and business centers. The ports are a significant source of regional jobs and business and there are numerous public and private infrastructure investments that have been built and are being planned. The environmental sensitivity of new transportation projects within this area receives significant public review and the environmental reporting process is important for obtaining project approval by the cities in order to move forward into final engineering and construction.

Simulation has been an important part of the rail system planning process at the San Pedro Bay Ports. In particular, the Port of Long Beach (POLB) has been using simulation to assist with planning efforts to determine the type of facilities needed and to determine the size needed to support future volume projections. A multi-phase modeling effort was implemented to support the project planning for a major new rail facility at POLB.

First, a model was built to quickly screen the concepts and alternatives that were being originally considered by

port planning. Within a few weeks, a high level model was developed and used to determine that the acreage at the proposed site must all be dedicated to direct intermodal rail support (containers loaded directly on rail cars at the docks) rather than other alternatives for truck transfer of containers.

With this result, and as a second modeling phase, the planning team could now focus on how a direct intermodal rail support facility would need to be designed. The site is constrained and there were concerns that this facility would not provide the capacity without the need for operating changes from the rail roads or marine terminal operators. A more detailed model was built to explore specific track configurations and included planning variables to test the impact of operating rules and policies. For example, the model was able to demonstrate to stakeholders that the tracks for this new facility would have to be shared based on dynamic needs within the port, or else the facility would not be able to sustain operations. The modeling was critical for gaining stakeholder approval and consensus for the project. The following screen capture shows the scope of the model and an animated dashboard of real-time intermodal activity at the Port.

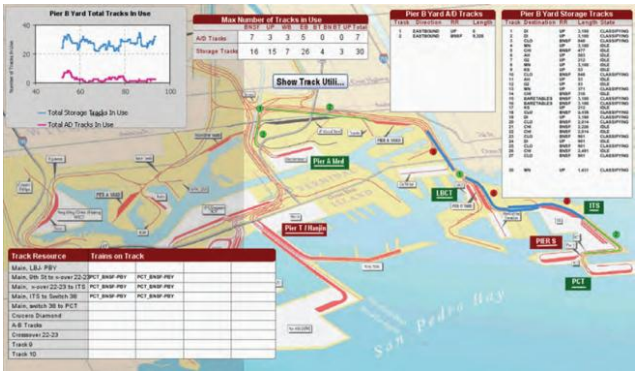

Figure 1: Port of Long Beach Rail Status Dashboard

Other modeling phases were conducted to gain quantitative information for the environmental reporting. A series of model runs were made to quantify air quality impacts, and the reporting includes the amount of time that train engines are moving cars. It is possible to get useful reports of estimated pollution based on tonnage carried, miles traveled, and so on.

The modeling is still important for POLB. More recent concerns have led POLB to use the model to evaluate whether other projects by Port of Los Angeles and others can effectively coexist in the Port network without sacrificing capacity plans.

3. MODELING FOR PASSENGER RAIL FOR RAMSEY COUNTY MINNESOTA

Ramsey County Regional Rail Authority (RCRRA) conducted a regional study (Collins and Rogers 2012) to look at potential area improvements related to implementing new high-speed corridor passenger trains. Specifically, RCRRA has future plans to improve the St. Paul-area passenger rail service by adding a new "Red Rock Commuter" service. In addition, Ramsey County is planning infrastructure improvements to support higher speed Amtrak passenger rail service associated with the reopening of St. Paul Union Depot.

Figure 2: Model Interface for Ramsey County Analysis

Currently, this area is highly utilized by several major freight railroads including BNSF, Canadian Pacific (CP), and Union Pacific (UP). There are a number of freight terminals in the area and the corridor freight traffic in this area is expected to grow. Amongst railroad carriers, there is a big concern that the addition of more passenger rail traffic in this area will further increase freight train congestion delays.

Simulation modeling was used to study the potential infrastructure improvements designed to support additional passenger rail service, such as new Red Rock commuter trains and increased Amtrak intercity and Higher Speed Rail, without impacting the significant (and growing) freight operations in Ramsey County. Using current and projected freight volumes, the model was used to evaluate several infrastructure options with and without additional passenger rail activity. The scope of the modeled area is shown in Figure 3.

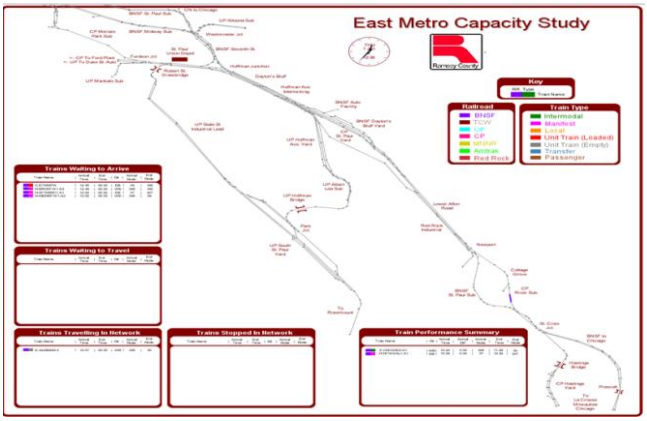

Figure 3: Ramsey County Freight and Passenger Corridor

The modeling team used a flexible modeling approach for this planning level project. Modeling tools were used that enable rapid configuration of rail corridors and is flexible to test changes as they evolve during the planning process. Our approach allows for changes (operating or infrastructure) to be included in the analysis to explore tradeoffs to address constraints as they are identified. It is often found that the tradeoffs identified through the simulation process are the ones that reduce infrastructure, and the modeling assists with consensus building among competing stakeholders.

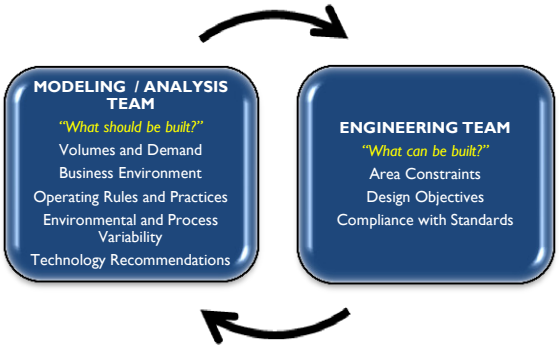

Figure 4: Analysis Iterations between Design and Modeling

The analysis was framed to show how freight level service is impacted with the addition of new passenger service. This enabled RCCRA planning to provide a fact-based demonstration to the railroads of what level of infrastructure change is really needed to support the new passenger volumes.

The modeling was able to show how some stakeholder initiatives would not provide a solution that equally benefited all operators. Based on this information, new alternatives were tested to ensure that there was a more equitable situation across all operators.

After performing analysis across a final set of options, the modeling was able to show the resulting speed differences for new passenger service and infrastructure improvement. The model was able to show that several of the proposed options all showed satisfactory level of service to the area operations. The costs and environmental difficulty to implement the options varied significantly.

With this modeling effort, Ramsey County was able to make well-informed, data-driven planning decisions with the best interest of all parties involved. The following chart shows a horizontal line of performance that must be achieved to gain stakeholder approval. The bars on this chart show how the proposed options (as simulated) meet or exceed this level.

Figure 5: Performance Results between Scenarios

4. MODELING TO SUPPORT SAN JOSE AIRPORT PLANNING AND DESIGN

The San Jose Airport was undergoing major upgrades to better serve its user base. A planning and design study was initiated to determine what facilities would be needed to transfer passengers between the main air terminals to supporting ground transportation facilities including a consolidated rental car facility. The new system would need to support pedestrians and bus transfers between terminals and a multiple floor rental car facility.

Modeling was used to make sure the components of this new system would have the needed capacity to support the peak volumes for both arriving and departing passengers. Each airport has its own unique dynamic of passenger flow—the San Jose airport has its peak arrival patterns on

Monday mornings and its peak departure patterns on Thursday or Friday afternoon. Also, the type of passengers at these times is typically for business. The attributes of the typical business user, where there is an average of 1.2 persons per rental car transaction, and other details needed to be analyzed to determine bus and facility capacity requirements.

Using data that characterized the demand profile of the user base of San Jose airport, modeling was used to determine the size of facilities needed. The modeling was first used to determine the size of the bus fleet and operating requirements to service the peak customer arrivals and departures. A set of proposed bus schedules was tested to determine the size and frequency of service to the terminal areas to maintain an optimal level of passenger service and avoid congestion at curb areas. The ability of the airport roadways and curb queuing positions to accommodate the rate of bus flow was a part of the modeling. Pedestrian flow modeling was also performed, where the dynamics of people moving and waiting with bags was analyzed to determine the amount of queue space needed on curbs.

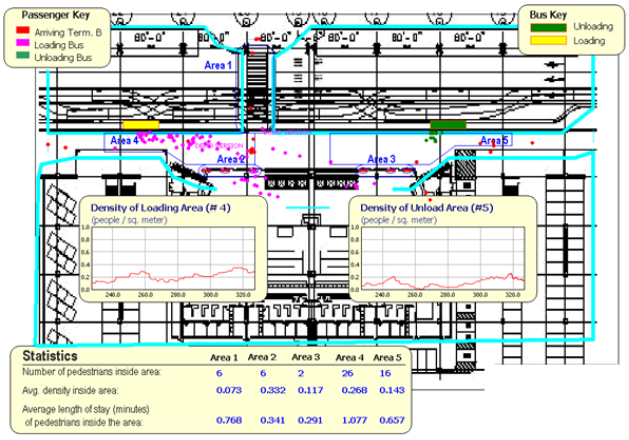

Figure 6: Passenger Flow within Airport Facility

This model was extended into a model of the six-floor rental car facility. It included the pedestrian flow as passengers move into and out of the buses. The modeling was used to refine the building architecture to ensure there was a fluid connection between the bus transfers and the entrance to the facility from the curb.

A critical design of this facility relies on the ability of the elevator system to take the passengers to the various floors. Each of the floors was being operated by different rental car companies, and the expected volume share of passengers was included in the modeling. The operators each had their own vision of whether the elevators should be shared or dedicated to floors. The modeling was able to show that the most efficient operation was to share elevators across all floors and it was able to prove that fewer elevators were needed than originally planned.

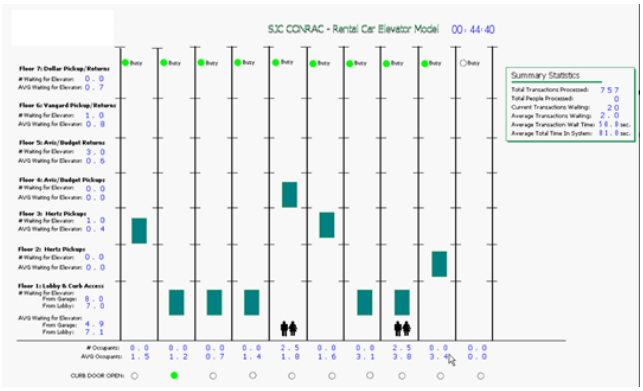

Figure 7: Model to Demonstrate Elevator System Performance

5. CONCLUSION

Simulation modeling has long been a technique for analyzing many industrial processes and operations. Increasingly, simulation modeling is becoming an important part of major infrastructure planning decisions. As plans need to achieve higher volumes and new facilities developed to transfer freight or people across multiple modes, it is becoming more important to take a systems view of facilities and operations to ensure they all work together. Simulation modeling can encompass pedestrian flows, complex rail operations, and other aspects of transportation planning and design. The ability of simulation to ensure that facilities are adequately sized for growth and to validate the amount of infrastructure that is really needed to support volume or service projections make it a powerful part of the planning process.

References

COLLINS, D., ROGERS, M. (2012). Developing Capacity Improvements to Increase Freight and Passenger Rail Performance. In *Proceedings of the AREMA 2012 Annual Conference & Exposition*. The American Railway Engineering and Maintenance-of-Way Association.

KULICK, B.C. (2011). Operations Analysis using Simulation Modeling to Evaluate Capacity Requirements for Direct Intermodal Rail Facilities at the Port of Long Beach. In *Proceedings of the AREMA 2011 Annual Conference*. The American Railway Engineering and Maintenance-of-Way Association.

Preliminary Results of Model Predictive Control of Shading Systems.

Brent Huchuk[1], William O'Brien[2], and Cynthia A. Cruickshank[3]

[1]Carleton University
1125 Colonel By Dr,
Ottawa, Ontario, Canada, K1S 5B6
brent_huchuk@carleton.ca

[2] Carleton University
1125 Colonel By Dr,
Ottawa, Ontario, Canada, K1S 5B6
Liam_OBrien@carleton.ca

[3] Carleton University
1125 Colonel By Dr,
Ottawa, Ontario, Canada, K1S 5B6
ccruicks@mae.carleton.ca

Keywords: Shades, Model Predictive Control, Reactive Control, Energy Management System.

Abstract

Shades in buildings are widely installed and are an effective technique for managing solar gains and occupant comfort. A model of a typical office space located in Ottawa, Ontario has been created and the model was developed for analysis under variable conditions. Analysis has resulted in the generation of an advanced reactive system facilitated by the use of the energy management system (EMS) built within EnergyPlus, along with a predictive control system optimized for minimizing the energy demand by the office space. The approach to optimization is done through the use of a basic model predictive control facilitated by the use of MATLAB (Mathworks 2011) and EnergyPlus (DOE 2012). The predictive system at this stage is delivering reductions of 5% during shoulder season over its reactive counterpart, but this work is still on-going.

1. INTRODUCTION

Window shading systems are installed in most commercial and residential buildings in some variation. Very rarely are these systems automatically or optimally controlled. The shade's position and movement is often determined by a user (or users) and is a function of the level of light, presence of glare, occupant position relative to the window, or previously determined position preferences (Reinhart and Voss 2003). The optimal control of blinds is known to be able to reduce utility loads by 10-30% while increasing the time occupants are able to spend with a maximized view of the outside (Lee et al. 1998). The fundamental problem with manual shades is that people use them to alleviate discomfort (glare) but then they rarely re-open them and meanwhile rely on electric lighting (O'Brien et al. 2012). Due to the added cost and complication of motorized shading controls, the adoption of advanced shading technology has been slow outside of niche markets and advanced applications.

The increased availability and capability of dynamic computer simulation techniques to model a building's performance provides a possible strategy for finding the ideal balance between the often-conflicting benefits of modern design and occupant comfort.

1.1. Background

Numerous studies have examined the effects of shading on the utility load of buildings and the role that occupant interaction with the shades has on loads. Groups have attempted to ascertain patterns and control strategies that better mimic and model the usage of the shades by the occupants in order to better understand and predict a building's energy performance (May-Ostendrop et al. 2010, Rijal et al. 2008). Much of the recent work investigating different methods of building control and their subsequent effects has been based on the utilization of model predictive control (MPC). Model predictive control is an advanced technique for optimizing control by predicting model behavior for a short period of time in advance and applying a cost function, which is to be minimized. Its adoption in building sciences has been because of MPC's ability to extract benefits from systems through slow reaction to changing variables (Ma et al. 2010, Ma et al. 2011, Corbin et al. 2012, May-Ostendrop et al. 2010). These authors all attempt to use MPC for building optimization, but their approach and factors are highly varied. The major differences include the approach to developing the building model. Some utilize simplified models (Oldewurtel et al. 2012, Ma et al. 2010), while others rely on complex simulation tools (May-Ostendrop et al. 2010). The other major difference lies in which functions are used for optimization; i.e., whether cost, the amount of energy, or other quantifiable costs were used.

The use of shades has long been known as an effective means of controlling glare, which affects occupant comfort, while allowing for occupants to access views and natural light. Recently there has been a change in thinking regarding the level of daylight that occupants require, along with an increased motivation for using daylight and solar

gains as a method of reducing the overall utility demand of the space (Tzempelikos and Athienitis 2007). In order to effectively manage solar gains, control must not be limited to only a reactive system (i.e., a system that acts once a condition has changed). Due to the thermal storage and, consequently, the delay in thermal effects a predictive system that can act proactively on a space is required.

1.2. Motivation

Past studies have focused on the ability of a system to be optimized in terms of overall cost either by minimizing the loads or by making informed decisions in advance. This allowed alternative and less energy-demanding solutions to be utilized (Oldewurtel et al. 2012). Investigation into the potential of MPC as an actual means of control often overlooks the complex aspects of whether or not occupants will be satisfied with these sorts of systems: ultimately their interaction will be what determines whether or not a method will actually will be able to achieve the intended benefit.

2. APPROACH

The research approach used to date when studying MPC has relied on two major components: (1) an accurate model and (2) an efficient control technique. Work was started on the modelling of an existing office space that would be readily available later for measurement and experimentation of control strategies derived from its model. Using SketchUp (Trimble, 2012), a geometrical model (see Figure 1) was designed for a west-facing office with a shading extrusion similar to what is used for the Delta Controls Lab found on Carleton University's campus in central Ottawa, Ontario.

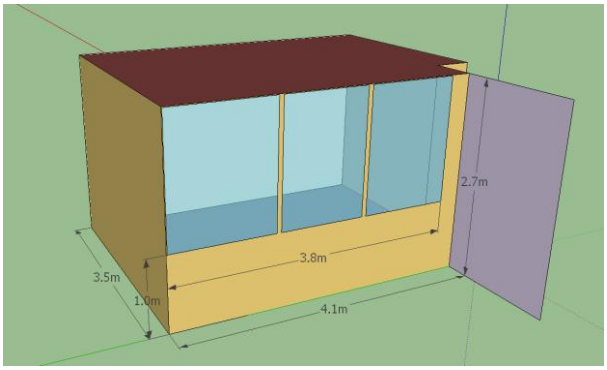

Figure 1. SketchUp model of the typical office space used in simulations.

The model uses constructions for a common building in zone 6 given by OpenStudio (NREL 2012). The window system was altered to better reflect the actual windows of the office based on preliminary measurements of their performance.

This geometry was used as the basis for configuring an input for an EnergyPlus IDF file. The effectiveness of shades was initially investigated using an ideal loads HVAC system with interior walls treated adiabatically (for simplicity), a zone sensible heat capacity multiplier to account for room contents, and a scheduled temperature and light profiles standard to EnergyPlus, derived from ASHRAE standard 90.1 (ASHRAE 2010). For the reactive system, the parameters included in the investigation were exterior temperature and incident solar energy on the surface. The shades were a binary system and could only be considered as fully open or fully closed. Using MATLAB as a call manager to EnergyPlus, a data analysis system and a file writer, a brute force approach was used with all combinations for threshold values, with shades only deployed when both setpoints were exceeded. Values from 0^oC to 30^oC (in $1C^o$ increments) for the exterior temperature and 0 W/m^2 to 1000 W/m^2 (in 50 W/m^2 increments) for incident energy were run in an annual simulation to determine which combinations resulted in minimum total utility loads (heating, cooling and lighting). The results from the analysis were considered the best set points for a reactive-based system. Based off of these results, the set points were concluded to be at 15^oC and 150 W/m^2.

The reactive system was added through the EMS that is imbedded within EnergyPlus. Through EMS the user has the ability to write and include custom pieces of code. Of particular use is its ability to create custom sensors and actuate systems used in the model. The system of interest to be actuated here was the shades. Using EMS allowed the number of adjustments to be limited to only once per hour in order to match the limitations of the input schedule used by the predictive system. The EMS controls were used to actuate the shades to close at night, determined as a period when no solar energy was incident on the window's surface. The inclusion of this condition was based on the idea that in a commercial application the building would most likely have been scheduled to have the blinds closed during the night in order to conserve heat at night in winter.

2.1.1. 24-hour prediction horizon with single hour based analysis

The predictive system was facilitated using MATLAB to run the simulation through DOS commands as well as to write to a file that was used as a schedule for the EnergyPlus input. MATLAB ran an EnergyPlus simulation for a given number of days (not including warm-up periods) with the shades both open and closed in the first hour. MATLAB imported these results from the exported comma separated value (CSV) file and determined which circumstance gave the minimum load for the first hour and assigned this value to a shade position schedule file that EnergyPlus imports every time it is called. This process was repeated for every hour during the time period in question. This initial scheme came with two major flaws. First, the utility minimums have

no discretion of what the comfort or the internal conditions are like. For example, the system would suggest closing the blinds for the majority of the time and rely on artificial lighting. Secondly, the limitation of only using single hour analysis was that though minimal hourly loads were taken into consideration, the true benefits of predictive simulation were left being unutilized, namely that preconditioning and use of the thermal lag of the space was not being investigated. As a result of this, there were times at which the reactive control-based system was out-preforming the predictive system through sets of circumstances in the daily weather profiles.

2.1.2. 24-hour prediction horizon with multiple hour based analysis

In order to correct and develop a more effective control strategy, both aforementioned limitations were corrected. It was concluded that a second condition needed to be introduced and the basic metric for this was the amount of energy used by the space with the inclusion of the lighting energy. In order to make the system utilize more benefit from MPC, a variable length 'floating window' was included. In this configuration every possible shade combination was investigated over a floating window of N hours in order to determine the minimum utility load over the duration of the window. Instead of two simulations per hour, the system looked at 2^N simulations. The results of a sensitivity analysis showed that with only the two possible shade positions the effectiveness of a floating window length diminished after five hours for simulations run during different months of the year. Results for a day of simulations in both September and June can be found in Figure 2. The data illustrates that the total utility load (heating, cooling and lighting) decreases as the length of the floating window increases. A six hour window was selected, as a longer window provided minimal decrease to the loads.

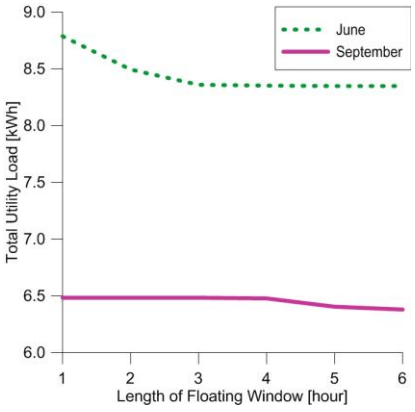

Figure 2. Results from simulations for the month of June and September using different floating window lengths.

The results from simulations for the month of September, which is typically considered a shoulder season (i.e., not predominantly a cooling or heating season), are shown in Figure 3.

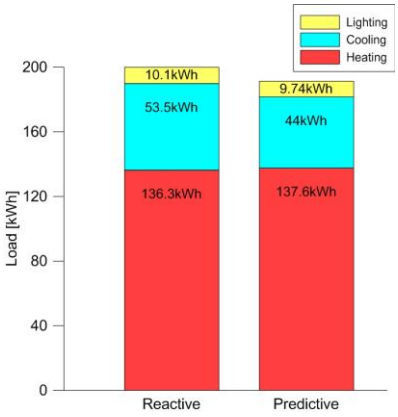

Figure 3. Results from simulations for the month of September using Ottawa weather.

A shoulder season was selected because of its particularly large temperature swings during the day, when overheating is particularly problematic. The results show a savings of approximately 5% from the reactive controls described previously. The reactive control alone would represent a significant increase when compared to the manual intervention typically relied upon as a control. The energy savings come from a 20% decrease in the cooling loads; however these reductions came with an increased use of heating and lighting. These results agree with the trend found when investigating the optimal set points for the reactive control. That analysis had indicated that this particular model was cooling dominated in terms of loads and would be where most savings could be extracted.

When the shading decisions are compared, the increased lighting and heating can be explained by the predictive system making decisions proactively that prevented the use of cooling energy later in the day. The remedy to prevent this overheating was the closing of shades earlier in the day, which would create more energy usage in both electric lighting and heating for a short duration. A future extension to these results would be the inclusion of a weighting factor to the three forms of energy usage, since often some are electric grid based, while others are natural gas or steam generated. This means either additional monetary costs or environmental costs could be considered.

3. DISCUSSION

The work to date is a starting point for future investigation. The latest iterations of predictive analysis have shown, like other studies had previously, that MPC is a possible method for decreasing the utility load required by a zone even over an optimal reactively controlled system.

It should be noted that the results of this study are unique to the office geometry and model. For example, as the thermal properties of the office change and more or less thermal mass is introduced, the lag in conditions will increase and decrease respectively, which will change the appropriate length of the floating window. Similarly, if the office had a different window to wall ratio, different window construction (such as low-e coating), or faced a different orientation the amount of solar gain would change, as would its effect on the office space.

When examining the shading position (open or closed) that the predictive system recommends, it is possible to find conditions that the reactive system does not account for. In particular, the predictive system would trigger before the reactive system would be able to, in order to delay overheating conditions and limit the effect of overheating. During the night, the system is able to identify the temperature decrease and exploit it to precool the structure. The extended window is able to determine if the precooling is an advantageous technique, considering at the same time the potential increase in the energy required to condition the space when the building begins to be heated for occupied periods.

4. CONCLUSION

This work confirms the initial conclusion that MPC is a possible solution for advanced control in buildings. Initial research shows that this simplified approach would be able to reduce the amount of energy used for an office. Much of this work shows effectiveness in principle, but elements are not optimally conditioned in many ways. In particular, the current methodology does not take into account occupant comfort within the zone or the potential interaction of the occupants with the shades based on their preferences. Further, the ability for these systems to be incorporated into real world settings along with the feasibility of this work needs to be investigated.

Acknowledgments

The authors would like to acknowledge the support of the Natural Sciences and Engineering Research Council of Canada.

References

AMERICAN SOCIETY OF HEATING, REFRIGERATING AND AIR-CONDITIONING ENGINEERS (ASHRAE). 2010. ASHRAE 90.1-2010 Standard-Energy Standard for Buildings Except Low-Rise Residential Buildings. ASHRAE, Inc.

CORBIN, C.D, HENZE, G.P, AND MAY-OSTENDORP, P, AND SALSBURY, T. 2012. A model predictive control optimization environment for real-time commercial building application. Journal of Building Performance Simulation. iFirst Article. 1-16.

DEPARTMENT OF ENERGY (DOE). 2012. EnergyPlus. V7.2.0.

LEE, E.S, DIBARTOLOMEO, D.L, AND SELKOWITZ, S.E. 1998. Thermal and daylighting performance of an automated venetian blind and lighting system in a full-scale private office. 29. 47- 63.

MA,Y, BORELLI, F, HENCEY, B, COFFEY, B, BENGEA, S, AND HAVES, P. 2010. Model predictive control for the operation of building cooling systems. Innovative Smart Grid Technologies. 5106 - 5111.

MA, J, QIN, S.J, LI, B, AND SALSBURY, T. 2011. Economic model predictive control for building systems. 2010 American Control Conference.

MAY-OSTENDORP, P, HENZE, G.P, CORBIN, C.D, RAJAGOPALAN, B, AND FELSMANN, C. 2010. Model-predicitve control of mixed-mode buildings with rule extraction. Building and Environment. 46. 428- 437.

MATHWORKS. 2011. MATLAB. 2011a.

OLDEWURTEL, F, PARISIO, A, JONES, C.N, GYALISTRAS, D, GWERDER, M, STAUCH, V, LEHMANN, B, AND MORARI, M. 2012. Use of model predictive control and weather forecasts for energy efficient building climate control. Energy and Buildings. 45. 15- 27.

NATIONAL RENEWABLE ENERGY LABORATORY (NREL). 2012. OpenStudio. V0.10.

O'BRIEN, W, KAPSIS, K AND ATHIENITIS, A.K. 2012. Manually-operated window shade patterns in office buildings: a critical review. Building and Environment. Available online 16 October 2012, http://www.sciencedirect.com/science/article/pii/S0360132312002685.

REINHART, C.F, AND VOSS, K. 2003. Monitoring manual control of electric lighting and blinds. Lighting Research and Technology. 35. 243-260.

RIJAL, H.B, TUOHY, P, HUMPHREYS, M.A, SAMUEL, A, AND CLARKE, J. 2008. Development of an adaptive window-opening algorithms to predict the thermal comfort, energy use and overheating in buildings. Jounral of Building Performance Simulation. 1. 17- 30.

TRIMBLE. 2012. SketchUp 8.

TZEMPELIKOS, A, AND ATHIENITIS, A,K. 2007. The impact of shading design on building cooling and lighting demand. Solar Energy. 81. 369-382.

Presenting Author Biographies

Abdolreza Abhari

Dr. Abdolreza Abhari is an Associate Professor in the Department of Computer Science at Ryerson University in Toronto, Canada. He obtained his Ph.D. in computer science from Carleton University in Ottawa, Canada (2003). Prior to that he received his M.Sc. in information systems and his B.Sc. in computer engineering from Sharif University of Technology in Tehran (1992 and 1989 respectively). He has worked as a system consultant for industrial and research institutions in Iran, the Netherlands, Germany and Canada. Dr. Abhari's research interests are in the areas of web mining, modeling and simulation, distributed systems (focusing on sensor networks and their applications in building design), data mining, database and network systems, and soft computing. He is the editor of five books and has published more than 50 papers in peer reviewed journals and conferences. He is the member of ACM, SIGSIM ,BISC and SCS scientific organizations and has been the general chair of several international symposiums and conferences.

Simon Breslav

Simon Breslav is a research scientist with Autodesk Research, which he joined in mid-2010 after completing a M.Sc. in Computer Science (with a focus in Computer Graphics) at the University of Toronto, and a Bachelor of Computer Science in 2006 at the University of Michigan. As part of the Autodesk Environment and Ergonomic Research group, Simon is working on Building Performance and Simulation Projects. His current research interests include Information Visualization, Computer Vision, and Human Computer Interaction. Before joining Autodesk, Mr. Breslav worked at Thomson Reuters and held internships at the Adobe Creative Technology Lab and Auryn Animation Studio. Originally from Riga, Latvia, Simon enjoys spending his free time making comics, meditating, watching movies and smiling.

Nathan Brown

Nathan Brown is a LEED Accredited Professional with a Master of Architecture and a Master of Science in Architecture from the University of California, Berkeley, and an undergraduate degree from Yale University. As an Associate at Loisos + Ubbelohde, he brings a broad range of technical research and design experience to his work designing dashboard interfaces to display building performance data. Nathan recently won an AIA/COTE research scholarship to analyze the actual energy performance of projects that have won the Top Ten Green Projects award. His previous work experience includes developing data visualizations using script-generated graphics for the Center for the Built Environment. Mr. Brown currently lectures at the California College for the Arts and won the UC Berkeley Department of Architecture's outstanding GSI award in 2010.

José A. Candanedo

José A. Candanedo is a postdoctoral fellow in the Buildings Group at CanmetENERGY-Varennes (Natural Resources Canada). José obtained his Ph.D. degree at Concordia University (Montréal) in 2011. His Ph.D. research focused on control strategies for net-zero energy solar homes. José also holds an M.Eng. from McGill University and a Bachelor's degree from the Technological University of Panama (1999). His academic interests include building-integration of renewable energy technologies, system identification, modeling complexity in building simulation, thermal energy storage, predictive control strategies, and load management in high-performance buildings.

Angelos Chronis

Angelos Chronis is a Design Systems Analyst in the Applied Research + Development group at Foster + Partners, and teaches at the Bartlett School of Graduate Studies of University College London. He holds a diploma in Architecture from the University of Patras, Greece and an M. Sc. with distinction in Adaptive Architecture and Computation from the Bartlett School of Graduate Studies, UCL, London. He is a registered Architect in Greece. Angelos has published papers in international conferences and journals, including the SimAUD symposium, at which he has received an "Outstanding Paper" award in 2011 and the eCAADe conference, at which his paper was selected for publication in the International Journal of Automation in Construction. Angelos's main research interest is the integration of simulation environments and performance optimization methods in the architectural process, particularly in the field of computational fluid dynamics.

Susannah Dickinson

Susannah Dickinson is an architect and Assistant Professor at the University of Arizona. Her work explores the relationship that computational design and fabrication processes can have in the development of more ecologically responsive environments. This stems from a background largely gained through years of professional experience in the offices of Frank O. Gehry, Los Angeles and SHoP Architects, New York. She is currently on the board of directors of ACADIA (Association for Computer Aided Design in Architecture).

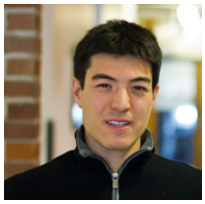

Rhys Goldstein

Rhys Goldstein is a Simulation Researcher at Autodesk Research in Toronto, Canada. His work combines building information modeling (BIM) with sensor data and simulation to help predict and ultimately reduce energy consumption in buildings. Rhys received the best paper award at the 2010 IBPSA-USA Conference for a new method to simulate the behavior of building occupants. He is currently investigating the use of open standards like the Industry Foundation Classes (IFC), as well as modeling conventions like the Discrete Event System Specification (DEVS), to help researchers collaborate in the development of simulation software. Rhys received a B.A.Sc. in Engineering Physics at the University of British Columbia in 2003, and a M.A.Sc. in Biomedical Engineering at Carleton University in 2009. His master's thesis was on the simulation of small-scale deformable biological structures, an example being vesicle clusters that self-assemble inside nerve cells. Rhys also worked in mineral exploration for several years, leading geophysical surveys in Tasmania, Cyprus, Oman, and many sites in North America.

Tianzhen Hong

Dr. Tianzhen Hong is a Research Scientist with the Simulation Research Group of Lawrence Berkeley National Laboratory. He is also a registered mechanical engineer with the state of California and a LEED accredited professional with USGBC. His research focuses on building performance modeling and simulation methods of design, operation, maintenance, and human behavior to achieve low energy buildings and sustainable urban systems. He is a key developer of EnergyPlus, the chief developer and product manager of VisualDOE version 4.0, and the founding developer of DeST (former BTP). Dr. Hong is leading a research area to study building energy monitoring, integrated design, and human behavior under the U.S. – China Clean Energy Research Center for Building Energy Efficiency. He received his B.Eng., M.Eng. and Ph.D. in HVACR from Tsinghua University, China, and has co-authored more than 70 journal articles, conference papers, and technical reports.

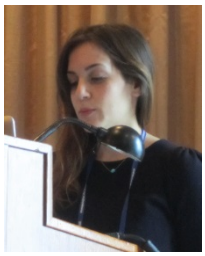

Chrysanthi (Sandy) Karagkouni

Sandy Karagkouni is an architect holding a Diploma in Architectural Engineering from Aristotle University of Thessaloniki, in Greece. She has recently completed an M.Sc. in Adaptive Architecture and Computation at the Bartlett School of Graduate Studies, UCL, London.

Zak Kostura

Zak Kostura is a practicing structural engineer with Arup, a global multidisciplinary engineering firm. He has worked on the design of high rise buildings in Europe and the Middle East, and specializes in structures with unique geometry that require detailed computational analysis. A graduate engineer of the department of Civil and Environmental Engineering at the Massachusetts Institute of Technology, Zak has broad experience with many aspects of building design, including architecture, civil and structural engineering and sustainability. He is an associate editor of the CTBUH Journal, a regular publication that explores the many aspects of tall building design. As a writer, Zak attempts to illustrate the inextricable link between contemporary urban design and its broader societal context.

Beth Kulick

Beth Kulick has been applying simulation modeling and analysis techniques on a wide range of supply chain and transportation projects for over 25 years. Her current focus is to use modeling to assist with analyzing transportation projects that may include rail, trucks, and multiple modes. This modeling assists clients in making informed decisions for infrastructure improvements and determining if a combination of operating or physical changes will assist in creating sustainable solutions. Beth has significant expertise in applying these techniques for complex environments such as ports and multimodal systems.

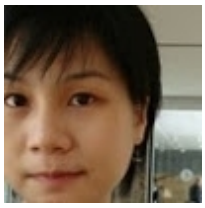

Shih-Hsin (Eve) Lin

Shih-Hsin (a.k.a. Eve) Lin hails originally from Taipei, Taiwan. At the National Taiwan University she acquired her Bachelor's degree in Civil Engineering and her Master's degree in Construction Engineering & Management. With an interest in sustainable design sparked by her professional and academic experiences, Eve went on to earn a second Master's degree at the University of Southern California School of Architecture in Building Science. During her studies at USC, Eve concentrated on emerging technology related to building energy simulation—technology that pushes the boundaries of accepted best practices for sustainable design. Eve is currently a Ph.D. in Architecture candidate at USC, focusing on design technology and energy performance feedback.

Negin Nazarian

Negin Nazarian is currently pursuing her Ph.D. in Mechanical Engineering at University of California, San Diego. She is a research assistant at Urban Energy Lab, where she works on Computation Fluid Dynamics (CFD) simulations of urban environments to study building energy and Urban Heat Island (UHI) implications. Negin's work is focused on analyzing heat transfer and flow fields in the urban canopy, and studying building Convective Heat Transfer Coefficients (CHTC). Negin also received her Master of Science degree from UC San Diego (2012) and her B.Sc. in Mechanical Engineering from University of Tehran, Iran (2011).

Paul Nicholas

Paul Nicholas holds a Ph.D. in Architecture from RMIT University, Melbourne, Australia, and joined the Center for Information Technology and Architecture (CITA) as an adjunct professor in 2011. Paul's particular interest is in computational approaches that support interdependent design and thinking by establishing new and different links between architecture and other fields. Having previously worked at Arup Melbourne from 2005 and Edaw London from 2009, his current research explores the idea that composites, or designed materials, necessitate new relationships between material behavior and digital representation. Paul co-founded the design practice *mesne* in 2005, and has exhibited in recent Beijing and Venice Biennales.

Liam O'Brien

Liam (William) O'Brien, Ph.D., is an Assistant Professor and Program Advisor for Carleton University's new Architectural Conservation and Sustainability Engineering program. He is researching design processes and energy simulation for high-performance solar buildings. Current research initiatives include studying the effect of occupant behaviour on building energy performance, the control of HVAC equipment in both residential and commercial buildings to improve occupant comfort and energy use, and occupant control of window shades. In addition, he has provided consultation for twelve building projects from Canada to Uganda. Dr. O'Brien has written for over twenty conference and journal publications. He is heavily involved in the building design and research community: he is the Faculty Advisor for the Carleton Solar Decathlon team and ASHRAE student chapter, Vice President of the Canadian Chapter of the International Building Performance Simulation Association (IBPSA-Canada), and a board member on the Canada Green Building Council (Ottawa Chapter Emerging Green Builders). He has organized multiple academic conferences, including chairing SimAUD 2013, and numerous educational workshops aimed at graduate students and professionals.

Hiroshi Ota

Hiroshi Ota has been lecturer since 2009 at the Institute of Industrial Science, University of Tokyo. His research topics include the role of architecture in urban regeneration, and the development of a network simulation model for the process of regeneration. As an architect, Hiroshi co-founded the design firm Design Neuob, with projects including "Guest House in Kugahara" (2003), "AGC Studio" (2010), and "Shirakawa Public Toilet" (2011). Hiroshi's artistic endeavors include "PopulouSCAPE" (2005)—a visualization of the world's urban populations—and the urban intervention projects of "Picnopolis" (2008-) by Tokyo Picnic Club.

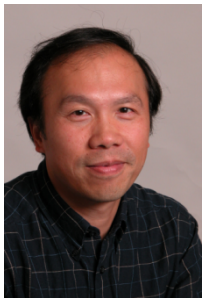

Chengzhi Peng

Chengzhi Peng holds B.Arch, M.Sc. and Ph.D. degrees in Architecture and Computer Aided Architectural Design. He is Senior Lecturer at the School of Architecture, University of Sheffield, UK, where he researches and teaches architectural and urban design computing. In the past three years, Chengzhi and his Ph.D. student Amr Elwan have been developing the Climate Change Conscious Urban Neighbourhood Design (C3UND) framework, investigating how a next generation environmental modeling platform may be realized to support interactive climate change conscious urban neighbourhood design.

Brady Peters

Brady Peters is an architect and researcher specializing in the application of computer programming and digital fabrication in the design process. As an Associate Partner at Foster + Partners, he has designed many buildings with complex geometry using parametric modeling and performance simulation techniques. Currently a PhD fellow, Brady's research develops computational methods to integrate sound into the architectural design process. He is the co-editor of an upcoming issue of the "Architectural Design" (AD) journal on computational design in architectural practice and is the co-editor of "Inside Smartgeometry," which reflects on the first 10 years of the Smartgeometry organization and conferences.

Liesbeth Staepels

Liesbeth Staepels, researcher at the PHL University College, achieved her Master's Degree in Civil Engineering in 2002 from the Catholic University of Leuven, Belgium. From 2002 until 2011 she worked in some of the largest consulting and engineering firms in Belgium, where she specialized in HVAC systems and sustainable buildings. From 2008 until 2011 she combined this role with a part-time teaching assignment at the Department of Arts and Architecture at the PHL University College in Diepenbeek (Belgium). Since 2011, Liesbeth has been working at PHL on a research project funded by the Institute for the Promotion of Innovation through Science and Technology in Flanders (IWT-Vlaanderen). Her research focuses on the real performance and economic feasibility of low-energy dwellings.

Todor Stojanovski

Todor Stojanovski graduated in architecture in Macedonia and has an M.Sc in built environments from KTH Royal Institute of Technology, Stockholm, Sweden. He is currently a Ph.D. candidate in the division for Traffic and Logistics at KTH, where he researches BRT (Bus Rapid Transit) and TOD (Transit-Oriented Development). Todor's professional interests include cities and public transportation, urban morphology and public transport infrastructures, urban design and planning, sustainability and the future of cities.

Ming Tang

Ming Tang, LEED AP, is Assistant Professor at the School of Architecture and Interior Design, University of Cincinnati. He is founding partner of Tang & Yang Architects, which has won numerous design awards. He holds a Master of Architecture degree, a Master of Art degree in Digital Media and Technology, and a Master of Fine Art degree in Interactive and Game Design. His multi-disciplinary research includes parametric design, digital fabrication, building information modeling, performance driven design, digital computation, virtual reality, algorithms and programming, GIS simulation, mathematical form, interactive design and visual effects. His forthcoming book, *Parametric Building Design with Autodesk Maya*, will be published by Routledge in 2014.

Tassia Helena Teixeira Marques

Tassia Helena Teixeira Marques graduated from the University of Sao Paulo, School of Engineering of Sao Carlos in 2010, and is now a Master´s student at University of Sao Paulo, Architecture and Urban Planning Institute of Sao Carlos. Tassia is developing research on the influence of thermal properties of the opaque envelope on the thermal performance of social housing in Sao Carlos, SP, under the coordination of Professor Dr. Karin Maria Soares Chvatal. This research is supported by FAPESP (Sao Paulo Research Foundation). Tassia has particular specialty in Environmental Comfort and Thermal Performance Simulation of Buildings and Energy Efficiency.

Theodoros Themistocleous

Theodoros Themistocleous is an Architect-Engineer (NTUA Greece), Urban Designer (MArch UD, Bartlett, UCL) and Computational Designer (MSc AAC, Bartlett, UCL) who has distinguished recognition in several architectural competitions. His latest interests are focused around kinetic architecture and the development of methodologies for digital driven design, fabrication and control of kinetic systems, and he is currently researching the development and application of soft kinetic systems in architecture. Theodoros is using algorithmic procedures to develop fabricated (SLS 3D printed) material systems with inscribed behaviors able to pneumatically actuate to predefined forms.

Michael van der Laan

Michael van der Laan is a Research Associate at the University of British Columbia and a Design Consultant with expertise on building/city information modeling, performance simulation, and sustainable design. His research focuses on how digital tools are used early in the design process. Specifically, how data-rich 3D models are used in decisions that impact the long-term sustainability of a project (such as affordability, energy, daylight, and comfort).

Simin Wang

Simin Wang uses his strong computational design skills and digital scripting ability to tackle the design process by identifying opportunities to investigate and implement new ideas, technologies, and material. Simin was part of the design team at Jenny Sabin Studio for the MyThread Pavilion (commissioned by Nike FlyKnit Collective), where he participated in all phases of architectural design, from concept development, to prototyping, to final construction. Simin is currently working on a theater and atrium space design project at Peking University in China, and his design of a vacation house complex in Xinjiang province, China, is scheduled to begin construction late June, 2013. As a research assistant in the Jenny Sabin Lab at Cornell AAP, Simin is part of the eSkin project supported by the National Science Foundation. Through this project he has developed a digital tool palette to simulate the unique behavior of eSkin material.

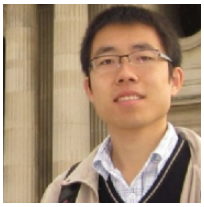

Sixuan Wang

Sixuan Wang is a Ph.D. Candidate in Electrical and Computer Engineering at the Ottawa-Carleton Institute for Electrical and Computer Engineering (OCIECE), Carleton University, Canada. He obtained his M.Eng. (2011) from Harbin Institute of Technology, China and M.Sc. (2012) from the University of Bordeaux, France. Sixuan's widespread academic experience includes Modeling & Simulation, Software Engineering, Distributed Systems, Web Services and Cloud Computing. He also participated in various scientific and industrial projects, including 6 months' research in the NSERC Engage project (Integrating Building Information Modeling and DEVS Remote Simulation) with Autodesk Research on Toronto (2012, Canada), 8 months R&D in the European REMICS project (REuse and Migration of legacy applications to Interoperable Cloud Services) within SINTEF institute (2011, Norway), and 1 year R&D in the EOMS project (Electrical Operation Maintenance System) within Bright Oceans Corporation (2008, China). His current research interests are web-based/distributed simulation, discrete-event systems, middleware and cloud services.

Ji Zhang

Ji Zhang is currently a post-doctoral Research Fellow at the Centre for Sustainable Asian Cities in the School of Design and Environment at the National University of Singapore. He is involved in studies on sustainability of the built environment and in research projects investigating the relationship between density, urban form, and environmental performance in high-density urban contexts through computer simulation and perception survey in areas such as daylight availability, solar access, view, outdoor air movement, and so on. Ji holds a PhD degree in Architecture from the National University of Singapore and a professional Master's degree in Architecture from the South China University of Technology.

Organizers

General Chair

Liam O'Brien
Assistant Professor, Department of Civil and Environmental Engineering, Carleton University

Co-Chair

Azam Khan
Head, Environment and Ergonomics Research Group, Autodesk Research

Program Committee

Marilyne Andersen
Associate Professor, School of Architecture, Civil and Environmental Engineering, École Polytechnique Fédérale de Lausanne

Ian Beausoleil-Morrison
Associate Professor, Mechanical and Aerospace Engineering, Carleton University

Nancy Clark Brown
Senior Manager, Autodesk Education

Michael Glueck
Research Scientist, Autodesk Research

Ted Kesik
Associate Professor, Faculty of Architecture, Landscape, and Design, University of Toronto

Christoph Reinhart
Associate Professor, School of Architecture and Planning, Massachusetts Institute of Technology

Gabriel Wainer
Associate Professor, Department of Systems and Computer Engineering, Carleton University

Scientific Committee

Marilyne Andersen
EPFL

Shady Attia
EPFL

Ramtin Attar
Autodesk Research

Ian Beausoleil-Morrison
Carleton University

Simon Breslav
Autodesk Research

Jose Candanedo
Natural Resources Canada

Yi-Chao Chen
Concordia University

Nancy Clark Brown
Autodesk

Alan Fung
Ryerson University

David Gerber
University of Southern California

Michael Glueck
Autodesk Research

Rhys Goldstein
Autodesk Research

Eric Gordon
Consultant in Urban Design

H. Burak Gunay
Carleton University

Brent Huchuk
Carleton University

Nathaniel Jones
Cornell University

Costa Kapsis
Concordia University

Ted Kesik
University of Toronto

Ata Khan
Carleton University

Azam Khan
Autodesk Research

Phylroy Lopez
Natural Resources Canada

Lira Nikolovska
Autodesk

Liam O'Brien
Carleton University

Briana Paige Kemery
Carleton University

Christoph Reinhart
MIT

Andrew Rice
Cambridge University

Leanne Robinson
Arctic Energy Alliance

Siobhan Rockcastle
EPFL

Greg Schleusner
HOK

Lukas Swan
Dalhousie University

Gabriel Wainer
Carleton University

Sponsors

Sponsored by

In co-operation with

Cover Image Credits

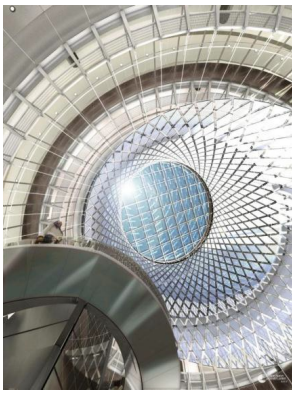

Modeling, Analysis and Simulation of a Form-Found Civic Sculpture for Lower Manhattan

Zak Kostura, Erin Morrow, Ben Urick

Arup, Texas Advanced Computing Center

End-node Approach for Pedestrian Flow Simulation

Hiroshi Ota

University of Tokyo

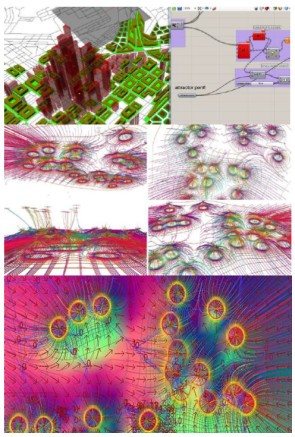

From Statistical to Diagrammatic: Geo-spatial and Time-based Data Visualization through Parametric Modeling

Ming Tang, Chris Auffrey, Mingming Lu

University of Cincinnati

Integrated Design in the Simulation Process

Martha Tsigkari, Angelos Chronis, Sam Conrad Joyce, Adam Davis, Shuai Feng, Francis Aish

Foster + Partners

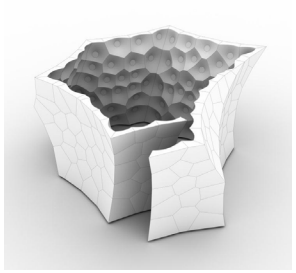

HubPod: Integrating Acoustic Simulation in Architectural Design Workflows

Brady Peters, Jane Burry, Nicholas Williams, Daniel Davis

Royal Danish Academy of Fine Arts, Royal Melbourne Institute of Technology

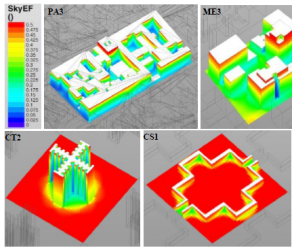

A Study of the Relationship between Urban Form and Environmental Performance for Three Urban Block Typologies in Paris

Ji Zhang

National University of Singapore

Designing-In Performance: Towards Cloud Based Simulation and Multidisciplinary Design Solution Space Search

Shih-Hsin (Eve) Lin, David Jason Gerber

University of Southern California

Isomorphic City: A Customizable Future Scenario

Susannah Dickinson, David Gonzalez, Kyle Szostek

University of Arizona

Author Index

A
Abhari , Abdolreza 223
Ahmed, Lubaid 223
Aish, Francis 153
Auffrey, Chris 147

B
Bauwens, Geert 205
Breslav, Simon 93
Brown, Nathan 57
Burry, Jane 213

C
Candanedo, José. A. 163
Chronis, Angelos 23, 31, 41, 153
Chvatal , Karin M. S. 49
Cruickshank , Cynthia A. 235

D
Davis, Adam 153
Davis, Daniel 213
Dickinson, Susannah 183
Doherty, Ben 93

E
Elwan, Amr F 169

F
Feng, Shuai 153
Freire, Victor 75

G
gen Schieck, Ava Fatah 41
Gengnagel, Christoph 15
Gerber, David Jason 139
Girling, Cynthia 191
Glynn, Ruairi 23
Goldstein, Rhys 93, 197
Gonzalez, David 183
Gunathilak, Gandherva 227
Gunay, Huseyin Burak 101

H
Hong, Tianzhen 179
Huchuk, Brent 235

J
Joyce, Sam Conrad 153

K
Karagkouni, Chrysanthi (Sandy) 41
Kellet, Ron 191
Khan, Azam 93, 197
Kostura, Zak 67
Kulick , Beth C. 231

L
Lafuente Hernández, Elisa 15
Lin, Shih-Hsin (Eve) 139
Loisos, George 57
Lucia, Andrew 7
Lu, Mingming 147

M
Marques, Tassia H. T. 49
Morrow, Erin 67

N
Naeimi, Homa 227
Nazarian, Negin 227
Nicholas, Paul 15

O
O'Brien, William (Liam) 85,235
Ota, Hiroshi 129

P
Pang, Xiufeng 179
Paradis, Éric 163
Peng, Chengzhi 169
Peters, Brady 213
Piette, Mary Ann 179
Philip, Santosh 57
Prasannakumar, Aiswarya 227

R
Roels, Staf 205
Rumery, Dan 93

S
Sabin, Jenny E. 7
Santiago, Ibone 57
Senbel, Maged 191
Sher, Elite 23
Staepels, Liesbeth 205
Stojanovski, Todor 111
Stylianou, Meli 163
Su , Tao 191
Szostek , Kyle 183

T
Tang, Ming 147
Theodoros, Themistocleous 31
Tsigkari, Martha 41, 153

U
Ubbelohde, M. Susan 57
Urick, Ben 67

V
van der Laan, Michael 191
Van Gelder, Liesje 205
Verbeeck, Griet 205

W
Wainer, Gabriel 75
Wang, Simin 7
Wang, Sixuan 75, 197
Williams, Nicholas 213

Z
Zhang, Ji 119

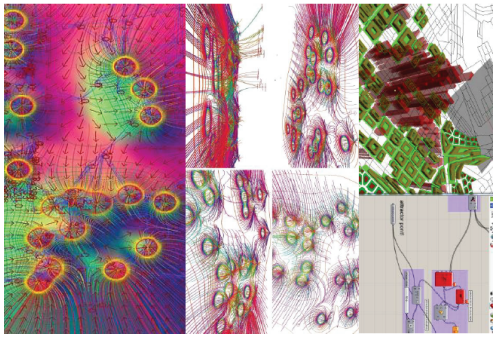

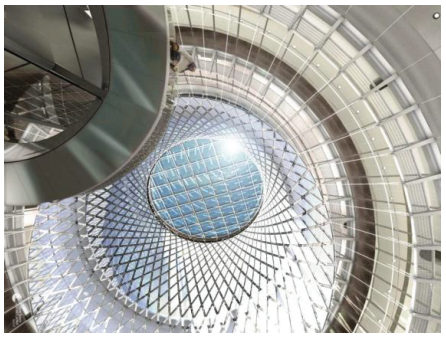
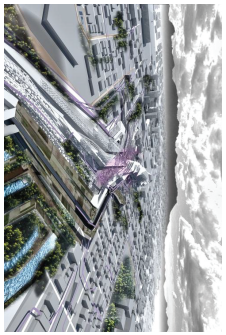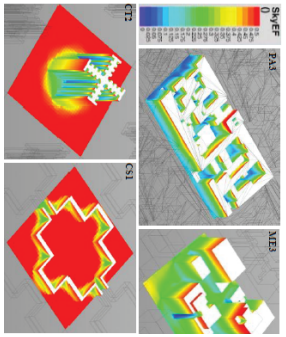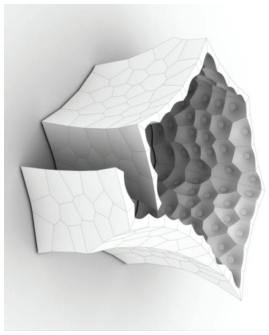
Symposium on Simulation for Architecture and Urban Design
2013